

NO-2214 957

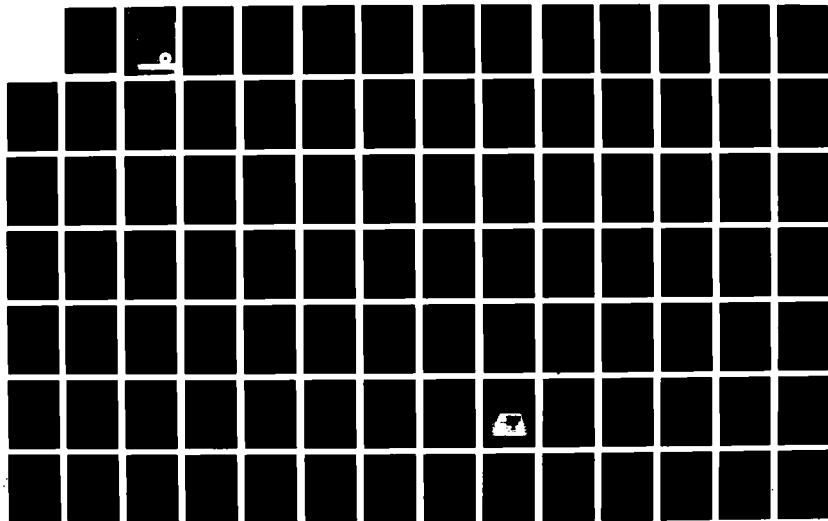
STATE OF THE ART OF PAVEMENT RESPONSE MONITORING
SYSTEMS FOR ROADS AND AIR... (U) COLD REGIONS RESEARCH AND
ENGINEERING LAB HANNOVER NH V JANOO ET AL. SEP 89
CRREL-SR-89-23

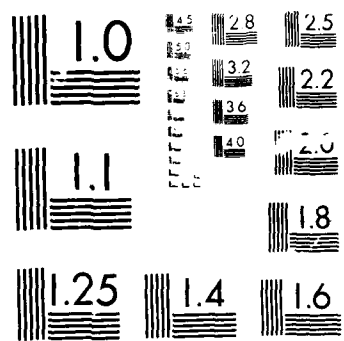
173

UNCLASSIFIED

F/B 13/2

ML





AD-A214 957

DTIC FILE COPY

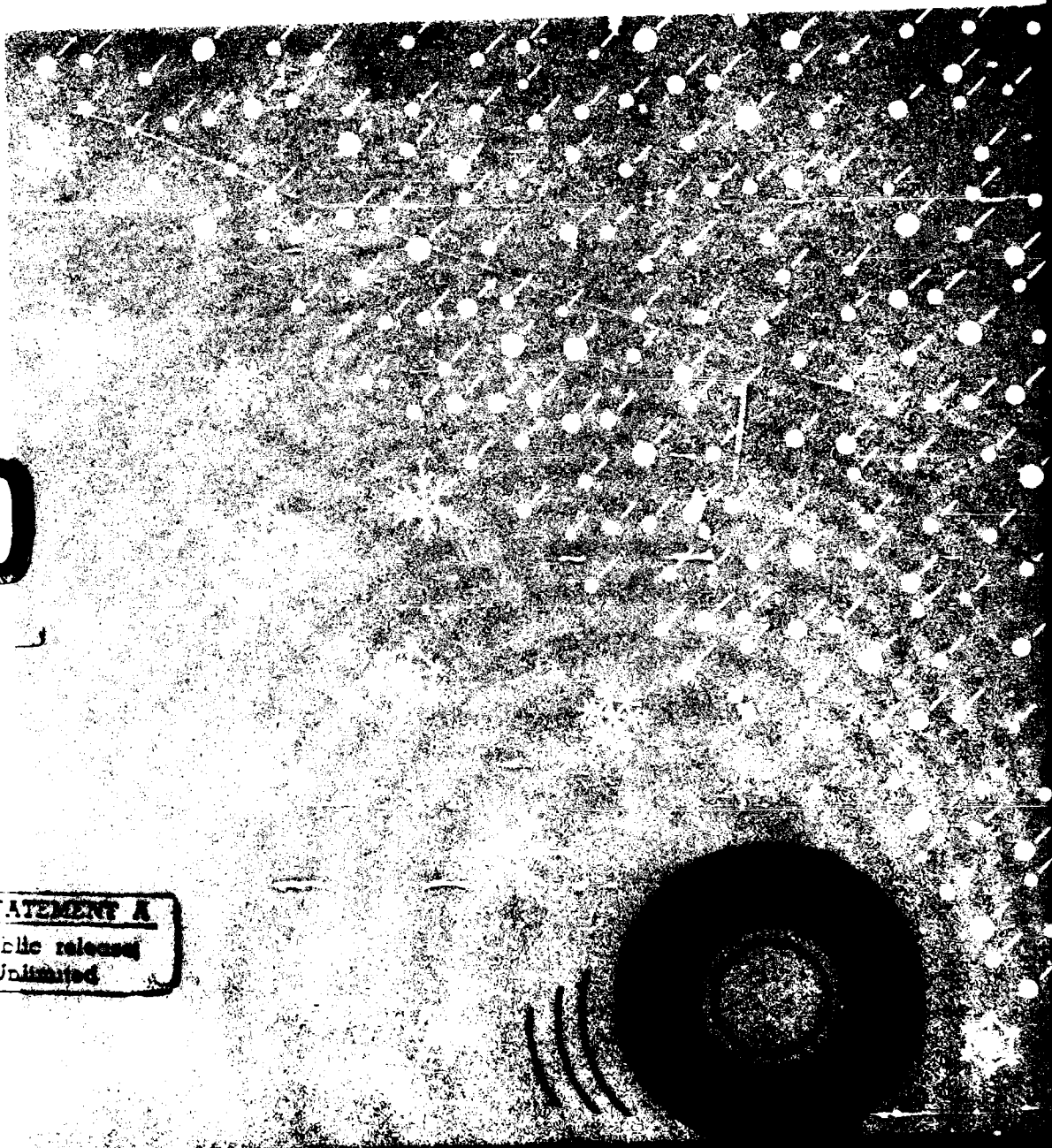
(4)



US Army Corps
of Engineers

Cold Regions Research &
Engineering Laboratory

State of the Art of Pavement Response Monitoring Systems for Roads and Airfields

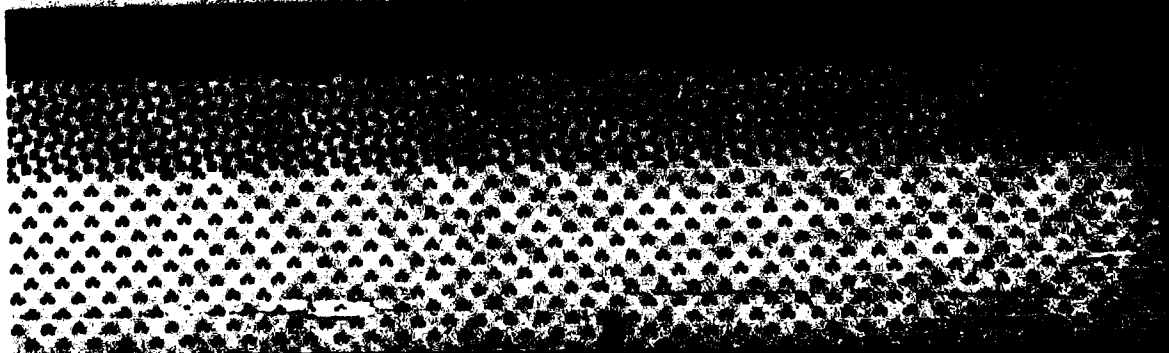


DTIC
S D
DEC 05 1989
D
CS

DISTRIBUTION STATEMENT A

Approved for public release
Distribution Unlimited

Special Report 89-23



Symposium

**State of the Art of
Pavement Response Monitoring Systems
for Roads and Airfields**

6-9 March 1989
West Lebanon, New Hampshire, U.S.A.

Vincent Janoo and Robert Eaton, Editors
September 1989

Sponsored by
U.S. Army Cold Regions Research and
Engineering Laboratory
Hanover, New Hampshire
CRREL Special Report 89-23

89 12 01 224

PREFACE

The First International Symposium on the State of the Art of Pavement Response Monitoring Systems for Roads and Airfields was held at the Cold Regions Research and Engineering Laboratory in Hanover, New Hampshire, U.S.A., in March 1989.

The theme of this symposium was the current state of the art of instrumentation of pavement structures subjected to varying thermal and moisture regimes.

The symposium was divided into nine sessions. With the exception of the first and last, each session was devoted to a particular measurement. These measurements included moisture content, temperature and load deformation. One session was devoted to nondestructive testing in cold regions. The last session was devoted to past and current field instrumentation studies. The interest shown in this symposium clearly demonstrates the importance attached to instrumentation of pavement structures by the pavement engineering profession all over the world.

A subcommittee was formed at this meeting to discuss the need for future conferences on this topic. The committee agreed that meetings should be held every two years. The Second International Conference on Pavement Instrumentation is thus being planned for the Fall of 1991.

We wish to thank the invited speakers and participants for making this symposium a success. We also thank all the many CRREL personnel, and Sidney Gerard of Science and Technology Corporation, who helped support this effort.

Vincent Janoo
Robert Eaton

Accession For	
NTIS CRA&I	<input checked="" type="checkbox"/>
DTIC TAB	<input type="checkbox"/>
Unannounced	<input type="checkbox"/>
Justification	
By <i>per ch</i>	
Distribution	
Availability Codes	
Dist	Availability Codes
<i>A-1</i>	

CONTENTS

Preface	iii
Attendees	vi
Session 1: Introduction	1
Instrumentation and pavement design, <i>T.D. White</i>	2
Impact of environment on pavement response and performance, <i>L.H. Irwin</i>	9
Monitoring pavement performance in seasonal frost areas, <i>R.L. Berg</i>	10
Instrumentation needs—SHRP's view, <i>L.H. Irwin and A. Pelzner</i>	20
Session 2: In-Situ Moisture and Drainage Measurements	23
Soil suction monitoring for roads and airfields, <i>D.G. Fredlund</i>	24
Measurement of in-situ pore pressures, <i>J.B. Sellers</i>	40
In-situ measurement of soil water content in the presence of freezing/thawing conditions, <i>J.L. Nieber and J.M. Baker</i>	45
In-situ permeability measurements, <i>L.K. Moulton</i>	63
Experimental project no. 12: Concrete pavement drainage rehabilitation, <i>R.C. Kelly</i>	74
Session 3: In-Situ Temperature Measurements	77
Temperature and thaw depth monitoring of pavement structures, <i>D.C. Esch</i>	78
Determination of frost penetration by soil resistivity measurements, <i>R.T. Atkins</i>	87
Thermocouple and thermistor temperature measurement systems, <i>R. Briggs</i>	101
A simple and economical thermal conductivity measurement system, <i>R.T. Atkins</i>	108
Session 4: Data Acquisition and Management	117
Information management—State of the art: The SHRP LTPP experience, <i>D.B. Clarke and R.A. Margiotta</i>	118
High speed data acquisition system for PCC pavement testing, <i>P.A. Okamoto</i>	128
Data acquisition: First the FERF then the world, <i>K.V. Knuth</i>	136
Cold regions weather data systems, <i>R.E. Bates and S. Gerard</i>	139
Session 5: Load Deformation Measurements	147
State-of-the-art stress, strain and deflection measurements, <i>P. Ullidtz and H.J. Ertman Larsen</i>	148
In situ stress measurements, <i>F.T. Selig</i>	162
Pavement design with the pavement pressuremeter, <i>J.-L. Briaud and P.J. Cosentino</i> ..	170
Monitoring pavement responses to traffic loads, <i>J.T. Christison</i>	180
Use of the multidepth deflectometer for deflection measurements, <i>T. Scullion and A.J. Bush III</i>	186
Session 6: NDT in Cold Regions	197
NDT in cold regions: A review of the state-of-the-art of deflection testing, <i>N.F. Coetzee and R.G. Hicks</i>	198
Applicability of spectral-analysis-of-surface-waves method in determining moduli of pavements, <i>S. Nazarian</i>	210
Alaska's experiences with non-destructive testing, <i>B. Connor</i>	226
Experience with nondestructive testing of two instrumented airfield pavements in Manitoba, Canada, <i>G.V. Ganapathy</i>	234

Session 7: Load Deformation Measurements	267
Applications of field instrumentation and performance monitoring of rigid pavements, <i>R.S. Rollings and D.W. Pittman</i>	268
In-situ strain measurements in hot-mix asphalt pavements, <i>D.A. Anderson and P.E. Sebaaly</i>	278
Iowa Department of Transportation weigh-in-motion, <i>B. McCall</i>	286
SHRP prototype procedures for calibrating falling weight deflectometers, <i>C.A. Richter and L.H. Irwin</i>	296
Iowa Department of Transportation pavement instrumentation, <i>R. Dankbar</i>	304
 Session 8: Correlation Between Field and Lab Results	 309
A direct comparison of nondestructive, laboratory, and in situ testing, <i>M. Anderson and D.A. Timian</i>	310
Resilient modulus determination for frost conditions, <i>E.J. Chamberlain, D.M. Cole and G.F. Durell</i>	320
Backcalculation of layer moduli and runway overlay design: U.S. Coast Guard Air Station, Kodiak, Alaska, <i>T.S. Vinson, H. Zhou, R. Alexander and R.G. Hicks</i>	334
Variability of pavement layer moduli from NDT measurements, <i>G.R. Rada, W. Uddin and M.W. Witzak</i>	346
 Session 9: Field Instrumentation Case Studies	 359
Minnesota cold regions pavement test facility, <i>D.E. Newcomb, R.O. Wolters and S. Lund</i>	360
Full scale pavement test: International joint research, <i>A.-G. Dumont and R. Addis</i>	370
Case studies in application of pavement instrumentation, <i>R.A. Bentsen and A.J. Bush III</i>	376
Experience of pavement instrumentation at TRRL, <i>R.R. Addis</i>	385
Construction of fully instrumented test pavements in North Carolina, <i>R.N. Stubstad, N.P. Khosla and W.W. Wynn</i>	394

ATTENDEES

R. R. Addis
Transport &
Road Research Laboratory
Old Workingham Road, Crowthorne
Berkshire, RG11 6AU
United Kingdom
44 344-77-241 (Fax 44-344-770556)

Mary Adolph
US Army Corps of Engineers
215 No. 17th St.
Omaha, Nebraska 68102
402-221-4306

David L. Allen
Kentucky Transportation Center
University of Kentucky
108 Transportation Research Bldg.
Lexington, Kentucky 40506-0043
606-257-45-1 (Fax 606-257-3342)

Al Allen
Applied Measurements, Inc.
P.O. Box 316 / 77 Great Rd.
Acton, Massachusetts 01720
617-263-2776

Wendy L. Allen
USACRREL
72 Lyme Road
Hanover, New Hampshire 03755-1290
603-646-4290 (Fax 603-646-4278)

Mark Anderson
Applied Research Associates, Inc.
P.O. Box 40128
Tyndall AFB, Florida 32403-0128
904-286-5703 (Fax 904-286-5717)

Colin Ashmore
Hodges Transportation, Inc.
P.O. Box 234
Carson City, Nevada 89702
702-882-3261 (Fax 702-882-3261)

Ronald Atkins
USACRREL
72 Lyme Road
Hanover, New Hampshire 03755-1290
603-646-4245 (Fax 603-646-4278)

Robert W. Ballew
Maine D.O.T.
Division of Aeronautics
Augusta State Airport
Augusta, Maine 04333
207-289-3119

Robert B. Barton
J.H. McNamara, Inc.
308 N. Harvard Street
Alston, Massachusetts 02134
617-782-3350

Ross A. Bentsen
USAE Waterways Experiment Station
P.O. Box 631
Vicksburg, Mississippi 39180
601-634-2991 (Fax 601-634-3139)

Richard L. Berg
USACRREL
72 Lyme Road
Hanover, New Hampshire 03755-1290
603-646-4207 (Fax 603-646-4278)

Egbert Beuving
Netherlands Pavement Consultants
P.O. Box 83
NL 3870 CB Hoevelaken
The Netherlands
3495-36344 (Fax 3495-36517)

Sue Bigl
USACRREL
72 Lyme Road
Hanover, New Hampshire 03755-1290
603-646-4475 (Fax 603-646-4278)

Andrew Bodocsi
University of Cincinnati
ML 71
Cincinnati, Ohio
513-556-3696

Jean-Louis Briaud
Civil Engineering
Texas A&M University
College Station, Texas 77843-3136
409-845-3795

Richard Briggs
Alaska DOT & PS
2301 Peger Road
Fairbanks, Alaska 99709

Randall W. Brown
HQ Air Force Engineering
and Services Center
HQ AFESC/DEMP
Tyndall AFB, Florida 32403
904-283-6337

Peter P. Canisius
Bundesanstalt fuer Strassenwesen
Bruderstrasse 53
D - 5060 Bergisch Gladbach 1
Federal Republic of Germany
+49(2204)43-700 (Fax +49(2204)43-833)

Ed Chamberlain
USACRREL
72 Lyme Road
Hanover, New Hampshire 03755-1290
603-646-4236 (Fax 603-646-4278)

Len Chase
Alberta Research Council
P.O. Box 8330, Postal Station F
Edmonton, Alberta T6H 5X2
Canada
403-450-5257

David Clarke
SAIC
800 Oak Ridge Tpk.
Oak Ridge, Tennessee 37831
615-482-9031 (Fax 615-482-6828)

Nick Coetzee
Dynatec
P.O. Box 71
Ojai, California 93023
805-646-2230

William Connor
Alaska DOT & PS
2301 Peger Road
Fairbanks, Alaska 99709

Edel R. Cortez
USACRREL
72 Lyme Road
Hanover, New Hampshire 03755-1290
603-646-4301

Steven L. Cumbaa
Louisiana Department of Transporta-
tion and Development
4101 Gourrier Ave.
Baton Rouge, Louisiana 7080
504-767-9106 (Fax 504-767-9108)

Roman Dankbar
Iowa Department of Transportation
800 Lincoln Way
Ames, Iowa 50010
515-239-1190 (Fax 515-239-1639)

Guy Dore
R-SHRP
1765 Blv. St. Laurent
Ottawa, Ontario
Canada
306-966-5336

John Dunncliff
8 Adams St.
Lexington, Massachusetts 02173
617-862-3175

D. L. Fredlund
Dept. of Civil Engineering
University of Saskatchewan
Saskatoon, Saskatchewan S7N 0W0
Canada
306-966-5336

Robert Eaton
USACRREL
72 Lyme Road
Hanover, New Hampshire 03755-1290
603-646-4207 (Fax 603-646-4278)

William F. Edwards
Ohio Department of Transportation
25 S. Front St.
Columbus, Ohio 43215
614-466-2916

Larry G. Eftefield
Caterpillar, Inc.
Technical Center, P.O. Box 1875
Peoria, Illinois 61656-1875
309-578-3977 (Fax 309-578-4277)

Tahar Elkorchi
Worcester Polytech. Inst.
100 Institute Rd.
Worcester, Massachusetts 01609
508-831-5518

Dave Esch
Alaska DOT & PS
2301 Peger Road
Fairbanks, Alaska 99709

Gani V. Ganapathy
Public Works Canada
(Air Transportation)
333 Main St. 8th Floor; P.O. Box 8550
Winnipeg, Manitoba R3C0P6
Canada
204-983-8613 (Fax 204-983-7338)

Donald Garfield
USACRREL
72 Lyme Road
Hanover, New Hampshire 03755-1290
603-646-4246 (Fax 603-646-4278)

Sid Gerard
STC
Route 120
Hanover, New Hampshire 03755
603-643-1472

Wilbur M. Haas
Michigan Technological University
Houghton, Michigan 49931
906-487-2572 (Fax 906-487-2943)

William O. Hadley
Louisiana Tech University
323 Old Wire Road
Ruston, Louisiana 71270
318-257-4410

David Hein
Dynatest Limited/Jegel/Paumatic
52 Ashwarren Road
Downsview, Ontario M3J 1Z5
Canada
416-630-1072 (Fax 416-630-7045)

Dennis R. Hiltunen
Penn State University
212 Sackett Building
University Park, Pennsylvania 16802
814-863-2936

Gregg C. Hoge
USACRREL
72 Lyme Road
Hanover, New Hampshire 03755-1290
603-646-4502 (Fax 603-646-4278)

Tim Horner
N. Dakota State Highway Dept.
600 E. Boulevard Ave.
Bismarck, North Dakota 58505-0700
701-224-2611

Stuart W. Hudson
ARE, Inc.
2600 Dellano Lane
Austin, Texas
512-327-3520

Lynne Irwin
Cornell Local Roads Program
Cornell University, Riley-Robb Hall
Ithaca, New York 14853
607-255-8465

Vincent Janoo
USACRREL
72 Lyme Road
Hanover, New Hampshire 03755-1290
603-646-4207 (Fax 603-646-4278)

John Kalafut
USACRREL
72 Lyme Road
Hanover, New Hampshire 03755-1290
603-646-4234

Maureen Kestler
USACRREL
72 Lyme Road
Hanover, NH 03755-1290
603-646-4335

Wala E. I. Kogali
University of Alberta
Department of Civil Engineering
Edmonton, Alberta T6G 2G7
Canada
403-492-2795 (Fax 403-492-0249)

Hegeon Kwun
Southwest Research Institute
6220 Culebra Road
San Antonio, TX 78284
512-522-2076 (Fax 684-4822)

K. Wayne Lee
University of Rhode Island
Dept of Civil Engineering
Kingston, RI 02881
401-792-2695 (Fax 789-3878)

Lewis Link
USACRREL
72 Lyme Road
Hanover, NH 03755-1290
603-646-4201 (Fax 603-646-4278)

Paul Los
FHWA
400 7th St., SW
Washington, DC 20590
202-366-4668

Steven M. Lund
Minnesota Dept. of Transportation
Transportation Building Room B-9
St. Paul, MN 55155
612-296-4878

Eugene Marvin
USACRREL
72 Lyme Road
Hanover, NH 03755-1290
603-646-4405 (Fax 603-646-4278)

Bill McCall
Iowa Department of Transportation
800 Lincoln Way
Ames, Iowa 50010
515-239-1682 (Fax 515-239-1682)

Issam Minkarah
University of Cincinnati
ML 71
Cincinnati, Ohio
513-556-3696

Melvin W. Morgan
Maine Dept. of Transportation
P.O. Box 1208
Bangor, Maine 04401
207-941-4522

Lyle K. Moulton, Chairman
Department of Civil Engineering
West Virginia University
Morgantown, W. Virginia 26506-6101
304-293-7110 (Fax 304-293-5024)

Soheil Nazarian
Dept. of Civil Engineering
The University of Texas-El Paso
El Paso, Texas 79968

John Neiber
Dept. of Agriculture Engineering
University of Minnesota
1390 Eckles Avenue
St. Paul, Minnesota 55108

David E. Newcomb
University of Minnesota
500 Pillsbury Drive, SE
Minneapolis, Minnesota 55455
612-626-0531

Col Charles Nichols
USACRREL
72 Lyme Road
Hanover, New Hampshire 03755-1290
603-646-4200 (Fax 603-646-4278)

William E. Oakes
Christman Associates
Manager of Engineering
19 North Main Street
P.O. Box 325
Chester, Connecticut 06412
203-526-4359

Paul Okamoto
CTL
5420 Old Orchard Road
Skokie, Illinois 60077-4321
312-965-7500

Stewart Osgood
Metcalf and Eddy
P.O. Box 4043
Woburn, Massachusetts 01888

J. H. L. Palmer
Institute for Research in Construction
National Research Council of Canada
Ottawa, Ontario K1A 0R6
Canada
613-993-3787 (Fax 613-954-5984)

Andrian Pelzner
SHRP
818 Connecticut Avenue, NW
4th Floor
Washington, D.C. 20006
202-334-3774

Claude J. Phene II
Agwatronics, Inc.
P.O. Box 2807
1420 W. 11th Street
Merced, California 95344

David W. Pittman
USACE Waterways Experiment
Station
P.O. Box 631
Vicksburg, Mississippi 39180
601-634-3066

Charles A. Pryor
National Stone Association
1415 Elliot Place, NW
Washington, D.C. 20007

William Quinn
USACRREL
72 Lyme Road
Hanover, New Hampshire 03755-1290
603-646-4471 (Fax 603-646-4278)

Conzalo Rada
Pavement Consultancy Service
4700 Berwyn House Road, Suite 202
College Park, Maryland 20740
301-345-7716

Cheryl Allen Richter
SHRP
818 Connecticut Ave NW, 4th Floor
Washington, D.C. 20006
202-334-1430 (Fax 202-223-2875)

A. J. Roberto, Jr.
USACRREL
72 Lyme Road
Hanover, New Hampshire 03755-1290
603-646-4240 (Fax 603-646-4278)

Reynaldo Roque
Penn State University
Civil Engineering Department
212 Sackett Bldg.
University Park, Pennsylvania 16802
814-865-31-1 (Fax 865-3039)

Marg Rutherford
Dept. of Civil Engineering
Seattle University
Seattle, Washington 98122
206-296-5526

Larry A. Scofield
Arizona Dept. of Transportation
College of Engineering - ERC, Rm. 405
Arizona State University
Tempe, Arizona 85287
602-965-3544

Thomas Scullion
Texas Transportation Institute
The Texas A&M University
College Station, Texas 77843-3135

Ernest T. Selig
University of Massachusetts
Amherst, Massachusetts 01003
413-545-2862

Barry Sellers
Geokon, Inc.
48 Spencer Road
Lebanon, New Hampshire 03766
603-448-1562

James D. Shinn II
Applied Research Assoc., Inc.
Box 1204 Waterman Road
S. Royalton, Vermont 05068
802-763-8348 (Fax 802-763-8283)

Sally Shoop
USACRREL
72 Lyme Road
Hanover, New Hampshire 03755-1290
603-646-4100 (Fax 603-646-4278)

Rebecca Smith
ARE, Inc.
6811 Kenilworth Ave #316
Riverdale, Maryland 20737
301-277-2400 (Fax 301-864-6624)

O. J. Svec
Institute for Research in Construction
National Research Council of Canada
Ottawa, Ontario K1A 0R6
Canada
613-993-3806 (Fax 613-954-5984)

Jaime Tamarit
Centro De Estudios Y Experimentacion De O.P.
Alfonso XII, No. 3
28014 Madrid
Spain
2790605 (Fax 2280354)

Myron Tanner
Campbell Scientific, Inc.
P.O. Box 551
Logan, Utah 84321
801-753-2342 (Fax 801-752-3268)

Gus Tarakji
San Francisco St. University
415-338-1851

Helen Tetteh-Wayoe
Research and Development
Alberta Transportation and Utilities
First Floor, Twin Atria Building
4999 - 98 Avenue
Edmonton, Alberta T6B 2X3
Canada
403-422-2750

Mang Tia
University of Florida
Dept. of Civil Engineering, Weil Hall
Gainesville, Florida 32611
904-392-6784 (Fax 904-392-9673)

David A. Timian
Applied Research Associates, Inc.
P.O. Box 40128
Tyndall AFB, Florida 32403-0128
904-286-5703 (Fax 286-5717)

Waheed Uddin
TRDF
6811 Kenilworth Ave
Riverdale, Maryland 20904
1-800-456-8733

Per Ullidtz
Dynatest
P.O. Box 71
Ojai, California 93023
805-646-2230

George E. Veyera
University of Rhode Island
Dept. of Civil Engineering
Kingston, Rhode Island 02835
401-792-2684 (Fax 789-3878)

Ted S. Vinson
Dept of Civil Engineering
Oregon State University
Corvallis, Oregon 97331
503-754-3494

Wayne Winn
Dynatest
P.O. Box 71
Ojai, California 93023

Tom White
Dept. of Civil Engineering
Purdue University
West Lafayette, Indiana 47907
317-494-2215

Session 1:
Introduction

Instrumentation and Pavement Design

Thomas D. White

Purdue University

ABSTRACT

Pavement Instrumentation, although proven to be of great benefit in understanding pavement response and in setting design criteria, has not been applied routinely. There may be several reasons for the infrequent use of instrumentation. For example, early instrumentation was difficult to install and sensitive to installation and use. The failure rate required significant redundancy. Installation, maintenance, data collection and data reduction were expensive. Therefore, benefits compared to costs were considered marginal. Analytical methods were considered in many cases adequate to estimate pavement responses due to the effects of load, climate and materials, etc. In a number of cases (the problems of data reduction and analysis overwhelmed researchers. As a result, manual techniques were often relied upon to obtain results. These data often have been filed without complete analysis.

Starting in about 1985 several U.S. Highways agencies initiated research projects with pavement instrumentation. These projects included modern instrumentation and data acquisition systems. More importantly there was an awareness of a need for planning and commitment to develop the software for data reduction and analysis. The instrumentation utilized has proven to be more reliable and standard software can mitigate the data reduction and analysis effort.

Limited pavement response data are showing significant results. A better understanding is being gained as to the type of pavement response that can be expected which can have an impact on design.

INTRODUCTION

There are several significant benefits that can result from the use of instrumentation data in developing design procedures. Perhaps the most important is better understanding of the response phenomenon of pavement systems. Existing analytical procedures have proven to be beneficial in interpolating and in some cases extrapolating pavement response and materials properties for design and evaluation. However, enough data on pavement response mechanisms exist for researchers to know that the existing analytical models do not adequately represent many of the subtleties of pavement response phenomenon. These subtle phenomenon represent the true opportunity to understanding pavement mechanics and therefore pavement design and performance.

In addition to better understanding pavement mechanics, pavement response data represents an opportunity to validate analytical models as well as to calibrate model response variables. The validation and calibration process must include adequate instrumentation data to reflect the possible distribution of the

magnitude of response variables (i.e. deflection, strain, etc.) Use of unique values of response variables to set design criteria is not realistic. It is only through use of response variable distributions that satisfactory design criteria can be set. A reasonably broad based pavement instrumentation data set is needed to define the response variable distributions. With such a data set design criteria can be adopted for a desired reliability level.

There is a need to continue the current interest in pavement instrumentation. Involvement of staff at all levels of an organization will insure acceptance and support for needed technology to better design and manage large pavement systems. Technology will be relied on increasingly as a result of reduced staff and resources while the workload and demand for resources increases. The technology that can be utilized today for data collection is at the point of being a tool for the pavement engineer to apply rather than a discipline to be learned.

Pavement Instrumentation Guidelines

Guidelines for pavement instrumentation were prepared by White (1) as part of an assessment of instrumentation experience within agencies responsible for pavements. The assessment was conducted to support planning for the Strategic Highway Research Program (SHRP) as well as planning for a Federal Highway Administration (FHWA) experimental demonstration project on pavement instrumentation. The assessment contrasted observational and physical response data that could be measured by instrumentation.

Understanding long term pavement performance (LTPP) is a primary component of the SHRP program. Results of the study are to be nationally relevant. Experimental designs have been developed for the major performance factors for various types of pavement (i.e. subgrade, pavement type, thickness, climate, traffic, etc). The experimental design is primarily directed toward making measurements and observations on in-service pavements. Once the data is collected the significance of the factors as well as the interactions among factors can be examined. With the significance of data established equations

can be developed as predictive design equations or as distress calibration functions for empirical-mechanistic design procedures.

In addition to the observational data, consideration was given to the benefit of specific pavement response data. Physical response data provides a direct measure for a number of factors influencing pavement performance. Table 1 lists candidate pavement physical response.

Table 1 Potential Pavement Response Data

- * Load Induced
 - Deflections and Deformations
 - Strains
 - Stresses
 - Pore Pressures
- * Environmental Effects
 - Temperature
 - Frost Penetration
 - Moisture
- * Other
 - Density
 - Volume of Water (Subdrainage)
 - Material Changes

A number of studies are possible based on the above type of data. For example, studies can be made of load equivalency; rigid pavement features such as dowel size and location, wider pavements and tied shoulders and flexible pavement features such as thickness, aggregate base and tire pressure.

Suggestions are offered by White as to the planning, application and scope of pavement instrumentation data. Table 2 indicates some factors to be considered in planning for pavement instrumentations. An important point is that data acquisition, storage and reduction should also be considered.

Pavement instrumentation will provide data on what are defined as responsive attributes of the pavements materials, structural components and special features. The attributes include deflection, and deformation, strain, stress and pore pressure. Attribute data may be desired for the elements of a rigid pavement listed in Table 3.

Table 2 Instrumentation Planning Factors

1. Theory (linear, non-linear, visco-elastic)
2. Responsive Attributes (deflection, strain, stress)
3. Pavement Features (load transfer, layer equivalency)
4. Contributory Factors (loads, climate)
5. Background Data (in situ material properties and potential changes in those properties)
6. Pavement Condition (roughness, distress)
7. Instrumentation (sensors, replications, security)
8. Data Handling (collection, reduction, storage)
9. Training (installation, operation)

Table 3 Candidate Rigid Pavement Elements for Instrumentation

1. Slabs
 - a. Edge
 - b. Corner
 - c. Center
 - d. Interaction (Joint-Vertical, Horizontal)
2. Reinforcement
 - a. Dowels
 - b. Ties
 - c. Temperature Steel
 - d. Prestress Tendons
3. Base
4. Subgrade
5. Layer Interfaces

Similarly, attribute data may be desired for the elements of a flexible pavement as listed Table 4.

Table 4 Candidate Flexible Pavement Elements for Instrumentation

1. Surface
2. Base
3. Subbase
4. Subgrade
5. Layer Interfaces
6. Lateral Interfaces (Shoulders)

Instrumentation may also have application to obtaining other significant data. The categories of other significant data are attribute support data, background data and pavement condition data. Attribute support data includes magnitude, amount and character

of traffic, tire pressures and position of loading. Background data refers to certain data that establishes the state of the various layer materials at the time instrumentation data is collected. This information would also be desirable at various times during the life of the instrumentation and at the time any failure in the immediate area of the instrumentation occurs. Background data that may be desirable includes: in situ California Bearing Ratio (CBR), plate bearing, moisture/density and surface load-deflection data. Pavement condition data is important in defining the type of distress that occurs. Accumulation of distress establishes the rate of pavement deterioration and provides a scale of performance.

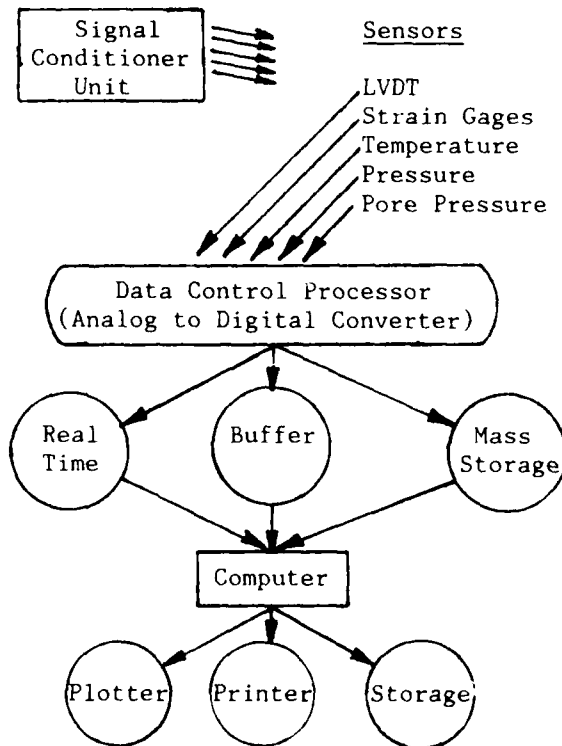
There are a number of practical considerations related to instrumentation application. The type of sensors and installation techniques are important with respect to costs, time of installation, reliability and replication.

Redundancy suggests multiple gages which would compensate for failure of one or more sensors or gage installations and would insure data at a given location and feature. Replication on the other hand refers to multiple instrumented sites at which there may be a redundancy of several sensors. Replication is considered because measurements will vary even though test sites and the instrumentation are supposed to be similar. Accounting for the variability in measurements will enhance the statistical significance of the data.

Data acquisition systems are evolving rapidly both from a hardware and software stand point. Based on current technology, Figure 1 suggests components required to collect pavement instrumentation data. Signal conditioning and data control processors are available from several sources and more options are available in a single unit. The schematic in Figure 1 presents a choice of computer communication and a choice of output from the computer. The actual structure of the system has some flexibility.

The summary of the instrumentation guide by White suggests several factors important to successful pavement instrumentation. In addition, several opportunities are mentioned for more efficient and effective instrumentation data

collection as a result of evolving technology. To minimize the impact of sensor or installation failure quality instruments and materials are required. However, care and experience with installation are the two factors that will reduce gage failure to an acceptable level. An agency should involve an instrumentation engineer in the planning and execution processes.



Note: each channel should be sampled at a minimum rate of 500 cps

Figure 1 Schematic of a Data Collection and Handling System

Current Data Processors have eliminated many of the steps in processing and analyzing data and are designed to communicate directly with storage mediums or computers. However, there still appears to be a need for software to specifically address pavement data.

Estimates of costs that were presented for sensors and installation were nominal. It was pointed out that costs not addressed were data handling costs, including hardware and labor costs during the data collection and subsequent analysis. These costs will be substantial.

Instrumentation and data acquisition systems based on new technology will provide an opportunity for more and better pavement response data. Of particular interest is the concept of a package of instrumentation that would function at a remote site, self calibrate and transmit data telemetrically.

A word of caution was offered about expectation for real pavement data. There is a real potential for differences in measured pavement responses when compared to theoretically predicted responses. There may also be great variability in the measure values. Replication of instrumentation can help to quantify the variability.

Pavement Design

A discussion of approaches and the critical factors in pavement design is warranted prior to considering the application of instrumentation in the process.

As part of the discussion a general description of pavement design is offered as: Conceiving the form of a pavement system, selecting materials and proportioning layers to satisfy structural or functional requirements. Within this general description a number of design procedures have developed. There exists design procedures that fall into the categories in Table 5.

Table 5 Design Procedure Categories

1. Standard Sections
2. Functional
3. Empirical
4. Mechanistic - Empirical
5. Mechanistic

Adoption of standard sections is not uncommon. Two widely spaced examples of the uses of standard sections are California and Germany. The reason for adopting standard sections vary somewhat. California (2) feels that for certain traffic and applications a specific section will provide the best level of service. Pavement drainage is a major component of their standard sections. In Germany, a catalogue of pavement structures has been developed (3). The thickness is dependent on the number of trucks of a certain weight.

An obvious example of a functional

design procedure is the American Association of State Highway and Transportation Officials (AASHTO) design procedure (2). This well documented procedure is based on providing a level of functional serviceability.

Essentially, the above standard section approaches are empirical design procedures because the standard sections adopted have been observed to provide an adequate level of performance. However, specific empirical design procedures have been developed based on observation, test experience or limiting criteria. An example of a limiting criteria that has been used in design procedures is surface deflection. The U.S. Army Corps of Engineers CBR-Thickness design procedure (3) is based on the performance of pavement test sections and theoretical interpolation and in some cases extrapolation of the observed performance data. Ultimately, prototype pavement performance was factored into the results. The test and observation process categorizes this procedure as an empirical design procedure. This categorization should not detract from the method because it is one of the more widely used design procedures in the world. There are a number of factors related to the development of the CBR - thickness design procedure that are important to understanding pavement performance. However, these factors will not be discussed in this paper.

The interpolation and extrapolation of performance by theory in developing the CBR-Thickness procedure places the method close to being a mechanistic-empirical design procedure. However, the method uses theory to calibrate observed performance data. While mechanistic-empirical design procedure are based on using the observational data to calibrate/validate mechanistic models. Although there are limitations of the mechanistic models their primary benefit is in representing pavement section geometry as well as utilizing more rational material properties. Measured pavement prototype response along with observed performance are needed to adequately calibrate/validate design procedures. This calibration/validation step in general compensates for ignorance as mentioned above in the discussion of pavement response phenomenon. A mechanistic design procedure would involve use of an analytical model and a

priori material properties. Pavement design is more than one inclement of technology away from an ultimate mechanistic procedure.

Pavement Performance

An adequate pavement design is expected to accommodate critical events; survive the applied loads without structural failure and provide a desired level of performance. The most significant critical event affecting pavement performance is spring thaw 4). Satisfying each of these pavement performance components requires pavement thickness. For example, thickness is required to survive loads applied during spring thaw. Thickness is also required to control structural deterioration. Similarly, thickness is required for long term performance and addresses the overall uncertainty in achieving the desired performance.

Performance can imply failure. Unfortunately, pavement failure is not well defined. Definitions of failure have involved limits of measured response such as the elastic deflection and permanent deformation, measures of serviceability such as roughness and observations of distress such as cracking and patching. Actual failure may be structural, functional, material or a combination.

Measured pavement response through instrumentation will have many benefits as previously mentioned. However, the physical attribute data collected through instrumentation may not clearly register the effect of time or traffic.

Physical attributed data remain reasonably constant up to some point at which the pavement system begins to deteriorate rapidly. At this time one significant component to the pavement has failed or several less significant components fail and the effect is that the pavement system can no longer perform its intended function. The lack of change in the physical attributes with time or accumulation of traffic highlights distress as the second category of pavement response. Increase in severity and extent of distress occurs over a period of time or with accumulation of traffic. As a result, distress accumulation provides a time scale for pavement performance. An equally important contribution of distress response

is that it identifies the mechanisms of the pavement system failure.

By way of additional contrast between physical and distress attributes distress type, extent and severity is a broad measure or a macro performance indicator. On the other hand, deflection, strain or distress is a point specific or micro indicator of pavement performance. Both types of performance indicators should be represented by a distribution rather than a unique values. The ideas of a distributive representation refers to a composite expected value and measure of dispersion. The macro indicator, distress, could be reasonably uniform within a given pavement length but would vary between comparable pavements or areas of pavements. On the other hand, deflection, strain, etc. will vary from point to point in the same pavement as well as between comparable pavements and condition of test. The amount of variability of micro response type performance indicator data collected from real pavement may be a surprise to some pavement engineers and researchers that analyze ideal pavement sections with a mechanistic model and with assumed unique material properties.

Interpretation of Testing

Pavement designs may differ because of fundamental differences in the mode of testing from which data was obtained to develop the design procedures. Two modes of testing that have been used are accelerated and prototype. Accelerated testing involves testing over a limited period of time and in a manner to accentuated failure. This mode of testing might not include the breath of distresses found in a prototype pavement. In addition, materials are often limited and traffic is controlled. Very importantly the effect of climate cycles is minimized. Prototype testing would include climatic effects but loading would occur as a mixed traffic stream. However, determining prototype pavement performance would require long term observation and testing.

The rate of pavement loading may be classified as static or dynamic. It is important to know the rate of loading on which a given design criteria is based.

The AASHO Road Test was basically a dynamic loading test and the results are

biased to this test condition. For instance, although dynamic vehicle loads may be measured to be higher than static loads, as long as the pavement and material response remain rate of loading dependent, the pavement deflections and strains as indicators of fatigue and rutting will be less under dynamic loading than static or slowly moving loads. Field data has been presented from a number of studies showing that as the rate of loading increases, i.e. vehicle speed, the deflection and strain decrease (5,6). Figure 2 shows the effect of speed on deflection. The effect of static and slower traffic is apparent on uphill grades, intersections and where heavy vehicles frequently stop. Use of a static model to analyze results of field test conducted with loads moving at highway speeds inherently result in criteria that have been calibrated for dynamic loading. It is likely that criteria so developed do not reflect the worst case of static and slowly moving loads. In addition, material quality specified as a result of dynamic load performance may not be valid for slow moving loads.

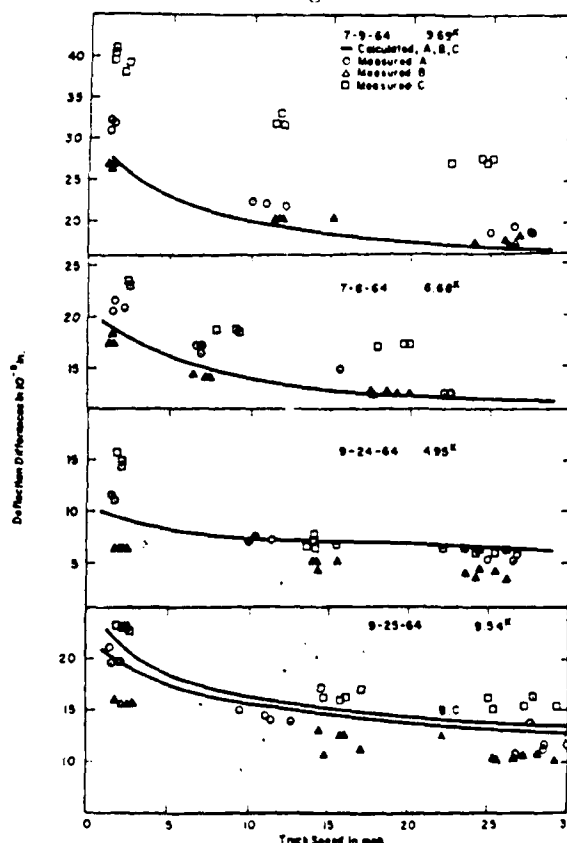


Figure 2 Effect of Speed on Deflection (5)

Essentially, analysis and criteria need to be compatible or the analysis procedure needs to be able to translate between the static and dynamic cases.

Non-Load Factor Instrumentation

A number of factors other than load will affect pavement response. Instrumentation can provide a measure of these associated responses. Candidate factors are temperature, frost penetration, moisture, solar radiation and various material physical property changes. These factors affect pavement response in various way. For example material strength may be lowered or increased which could modify the interaction with loading.

SUMMARY

A number of important points can be highlighted concerning the application of instrumentation to evolving better pavement design methods.

- * Continued development of pavement design will require instrumentation data as a major component.
- * Physical responses recorded by instrumentation and observational data can complement each other.
- * Planning ahead for instrumentation and data reduction will increase effectiveness and utilization of such data in the design process.
- * More opportunities exist for use of modern instrumentation in pavement research.
- * There are many applications and benefits to be realized for instrumentation.
- * Instrumentation can provide data for establishing limiting pavement response criteria.
- * Through instrumentation load equivalency can be scaled and extended.
- * Feature effectiveness can be evaluated with the use of instrumentation (i.e. Rigid pavements: dowel location, wider lanes and tied shoulders; flexible pavements, layer thickness, aggregate base and drainage).
- * Performance data can be complemented and extended by instrumentation.

Other than instrumentation can be used to validate mechanistic models.

Instrumentation will provide data for better conceptualization of pavement response.

The opportunity to use instrumentation along with the data will require training experience.

REFERENCES

1. "Report 100: Pavement Instrumentation and the Instrumentation Plan for Flexible and Rigid Pavements," TRB-AASHTO, Demonstrations of Instrumentation, Federal Highway Administration, Washington, D.C., December 1965.
2. Discussion with CALTRANS STAFF
3. Gooding, Francis, "Experiences and New Developments in Concrete Road Construction in the Federal Republic of Germany," 4th International Conference on Concrete Pavement Design and Rehabilitation, Purdue University, West Lafayette, IN, April 18-20, 1989.
4. AASHTO guide for design of Pavement Structures, American Association of State Highway and Transportation Officials, 1986.
5. "Development of CBR Flexible Pavement Design Methods for Airfields," A Symposium, ASCE Transactions, June, Vol. 115.
6. Gopal, B. G. and White, T.D., "The AASHTO Flexible Pavement Design: current status," accepted for publication in Transportation Research Record, Transportation Research Board, National Academy of Sciences.
7. Horn, W.D. and Ledbetter, R.H., "Pavement Response to Aircraft Landing Loads, Volume 1, Instrumentation Systems and Testing Programs," Technical Report S-75-11, USAF Waterways Experiment Station, Vicksburg, Ms, June 1975.
8. Colburn, B.S., "Pavement Deformations from Laboratory Tests and Field Theory," Second International Conference on the Structural Design of Asphalt Pavements, Ann Arbor, MI, August 1976, pp. 664-708.

IMPACT OF ENVIRONMENT ON PAVEMENT RESPONSE AND PERFORMANCE

Lynne H. Irwin Director
Cornell University Local Roads Program
Ithaca, New York

ABSTRACT

One of the remaining "frontiers" in pavement research involves developing an understanding which will lead to predictive models regarding the effect of environment on pavement response and performance. The environment that is of concern is both above and beneath the pavement. It is driven by the seasonal changes in the weather.

Freezing air temperatures result in the penetration of a frozen zone beneath the pavement. When the pore moisture freezes the modulus of elasticity and the strength of the materials increase significantly. As a result, the pavement response to wheel loads and tire pressures changes. The loss of pavement performance due to heavy wheel loads is relatively minimal during the frozen season.

Winter is followed by spring. In the frost belt and also in more temperate climates, subsurface materials have increased moisture contents, in a zone of limited depth beneath the pavement. Materials become weak, and heavy vehicle loads take a tremendous toll on pavement life during this time of the year.

In a subtle fashion, evaporation begins to exceed precipitation from day to

day, and the pavements begin to gain strength as the granular materials gradually lose moisture. Modest changes can have a big impact on pavement response.

These patterns are repeated from year to year, and yet each year is different, as patterns of temperature, rainfall and drought vary. Roads in close proximity to one another, perhaps even intersecting, differ in their response to environmental changes due to the fact that they are built of different materials.

Methods for pavement design and pavement evaluation do not specifically include environmental effects in their models. Today we see "lumped parameters," such as Regional Factor, or a Soil Support Value, or a Materials Coefficient, which gloss over or ignore important factors which we know influence the response and performance of our pavements.

This paper will report on a series of studies that have been conducted by the Cornell Local Roads Program in an effort to add to our knowledge of this intriguing frontier. We feel that it is far too early to develop the needed models, but perhaps the work will help to suggest ways to further pursue the topic.

MONITORING PAVEMENT PERFORMANCE IN SEASONAL FROST AREAS

Richard L. Berg U.S. Army Cold Regions Research
and Engineering Laboratory
Hanover, N.H.

ABSTRACT

As pavement design and evaluation procedures become increasingly complex, additional instrumentation and more frequent observations may be necessary to provide the data required to verify and refine these more sophisticated procedures. This additional instrumentation may be increased numbers of previously used devices or more sophisticated equipment to measure parameters we have not monitored in the past. For example, we have measured subsurface temperatures and frost heave at the pavement surface for years. Within about the last 10 years we have also measured in-situ moisture contents versus depth and time, but an inexpensive and universal device for making these measurements is not yet available.

In this paper, I discuss measurements we currently make, measurements we plan to make in the next few years, and measurements we would like to make but have not because the necessary equipment is not available.

INTRODUCTION

Federal government agencies such as the U.S. Army Corps of Engineers, the U.S. Air Force, the Federal Aviation Administration and the Federal Highway Administration have all developed, or

are in the process of developing, mechanistic pavement design methods to replace the empirical methods currently used. The mechanistic methods generally require more detailed information of the material properties than previously used. The mechanistic methods also provide more detailed output during the design process. For example, vertical and horizontal stresses and strains can be computed at various depths and distances from the imposed loads for a given design.

The Cold Regions Research and Engineering Laboratory (CRREL) is developing detailed models of freezing and thawing of pavement systems as part of our research studies. These models allow us to compute frost heave and frost penetration versus time, as well as temperatures and pore water pressures (or moisture contents) with time and depth. These models are being incorporated into the pavement design procedures as illustrated in Figure 1.

To verify the design of pavements using the new procedures, measurements of several parameters must be made at various depths and times. The measurements are then compared with computed values to determine the correlations and to suggest where, or if, refinements are necessary.

In the remainder of this paper, I briefly review the mechanistic pavement design method we are developing for

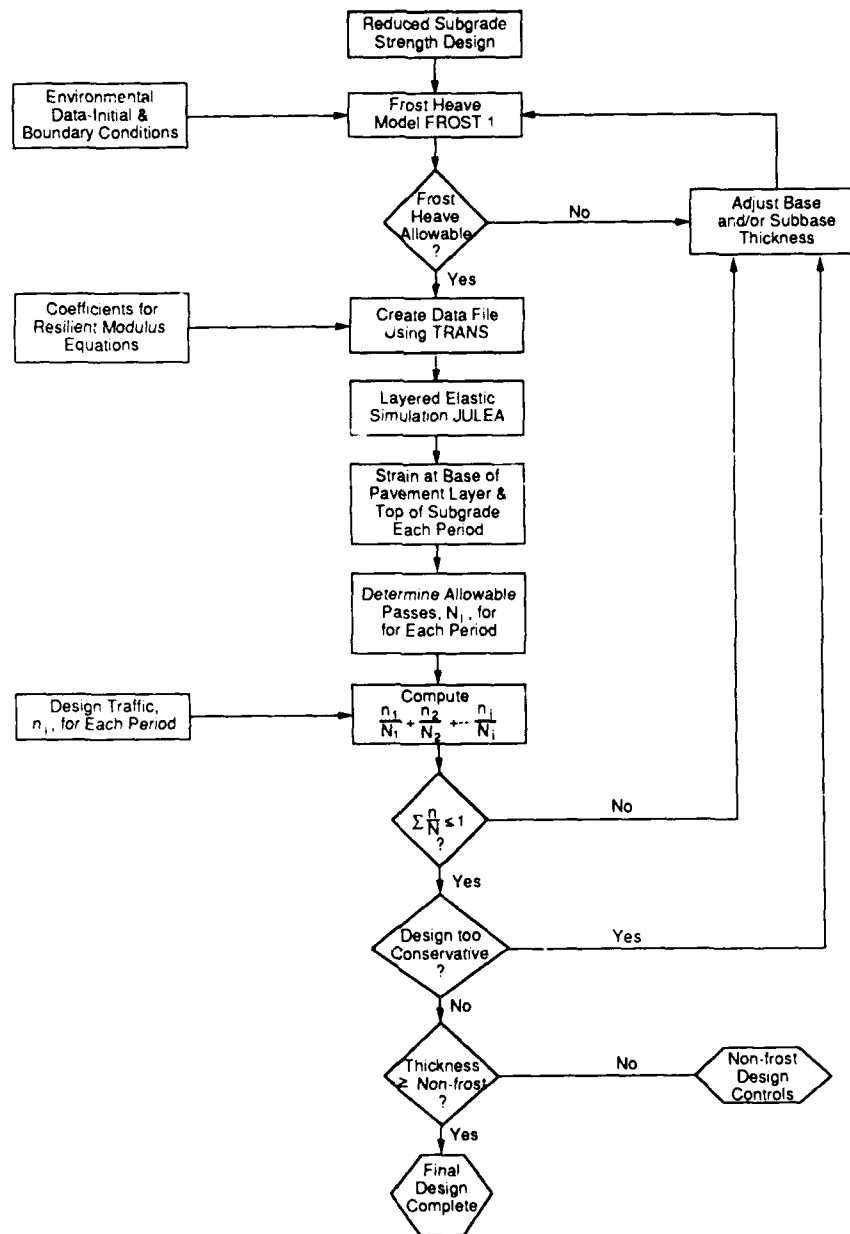


Figure 1. Proposed Corps of Engineers design procedure for pavements in cold regions.

the Army and the Air Force. Then I review the types of instrumentation we currently use to characterize pavement performance in seasonal frost areas and additional types of instrumentation which must be installed to provide the necessary information for the new design method. Some types of instrumentation must be refined to provide the necessary data or to increase the instrument's longevity when installed in pavements.

CURRENT AND PAST INSTRUMENTATION

Temperature Sensors

We have used these devices for years to monitor subsurface temperatures and to determine frost and thaw penetration depths with time.

Thermocouples are the devices we have used most frequently. Several types of thermocouples are available, as shown in Table 1, but we nearly

Table 1. Common thermocouples and application factors. (From *Measurements and Control*, Issue 123, June 1987, p. 251. Measurements and Data Corporation, Pittsburgh, Pa.

ISA CODE	CONDUCTOR		TEMPERATURE RANGE °F	LIMITS OF ERROR		APPLICATION NOTES	SEEBECK COEFFICIENT	
	POSITIVE	NEGATIVE		STANDARD	SPECIAL		μV/°C	μV/°F
E	Chromel	Constantan	32 to 600 632 to 1600	±3°F ±1/2%	—	Highest output of common thermocouples	62	34
J	Iron	Constantan	32 to 530 530 to 1400	±4°F ±3/4%	±2°F ±3.8%	Reducing atmosphere recommended	51	28
T	Copper	Constantan	-300 to -75 -150 to -75 -75 to +200 200 to 700	— ±2% ±1-1/2°F ±3/4%	±1% ±1% ±3/4°F ±3.8%	Excellent in oxidizing and reducing atmosphere within its temperature range	40	22
K	Chromel (Trade name, Hoskins)	Alumel	32 to 530 530 to 2300	±4°F ±3/4%	±2°F ±3.8%	For oxidizing atmosphere	40	22
S	Platinum 10% Rhodium	Platinum	32 to 1000 1000 to 2700	±5°F ±1/2%	±2.5°F ±1/4%	Laboratory standard, highly reproducible	7	4
R	Platinum 13% Rhodium	Platinum	32 to 1000 1000 to 2700	±5°F ±1/2%	±2.5°F ±1/4%	Oxidizing atmosphere recommended	7	4

always use those fabricated from copper and constantan wires (type T). As illustrated in Table 1, this type of thermocouple has the lowest limits of error and greatest sensitivity in the temperature range of interest to us: -60°F to +140 °F. Copper-constantan thermocouples provide about 22μV/°F of output at 32 °F. This sensitivity increases above 32 °F and decreases below 32°F. Individual pairs of wires (one copper wire and one constantan wire) are sometimes used, but we often purchase cables containing 12,16 or 24 pairs of wires depending on the number of sensors we plan to use in one vertical profile. Several wire diameters are available, but we generally use number 18 or 22 AWG. The standard-quality wire is accurate to ±1.5 °F, and special-quality wire is accurate to ±0.75 °F. We generally purchase the special-quality material, but its cost is about 50% greater than the standard-quality wire.

Several types of devices are available to monitor thermocouples; most of the newer devices display temperatures directly, but some provide microvolt displays. The former instruments must be used only with the specific thermocouple type they are designed for. The latter instruments require the use of conversion tables or equations to obtain temperatures. Single-channel and multiple-recording-type instruments are available, and they may be powered by either batteries or "line" voltage.

The major problem with thermocouples is that their accuracy is lower than most other temperature sensors, and as a result, indicated frost and thaw depths often vary substantially. This is especially true in the spring when temperatures are near the freezing point, and a variation of 0.1 or 0.2°F can result in errors from six inches up to a foot or more in frost or thaw depths.

We have often used thermistors to measure temperatures also. Most of the recently developed battery-powered recorders will accept thermistor inputs. Some of the recorders require fabrication of external interfacing circuits, but others have "built-in" circuits for certain types of thermistors. Several types of thermistors have been used, ranging in size from a "fly speck" to a few tenths of an inch in length. The user must choose thermistors to suit the need. Care must be taken to obtain devices which are rugged enough to withstand some physical abuse and are not altered by the moist environment in which they will be used. "Iso-curve" thermistors are available, but they are more expensive than those with individual calibrations. The iso-curve thermistors possess the same calibration, within a specified accuracy. This accuracy may be 0.1°F or less.

Recorders and manually operated devices available to monitor thermistors may be battery operated or powered by "line" voltage. Thermistors may be fab-

Table 2. Comparison of electrical temperature-sensing techniques. (From *Measurements and Control*, Issue 122, April 1987, p. 269. Measurements and Data Corporation, Pittsburgh, Pa.)

	RTD	THERMISTOR	THERMOCOUPLE
Accuracy*	0.01 to 0.1°F	0.1 to 1°F	1 to 10°F
Stability*	Less than 0.1% drift in 5 yrs	0.2°F drift/year	1° drift/year
Sensitivity*	0.1 to 10 ohms/°F	50 to 500 ohms/°F	50 to 50 μ volts/°F
Range	-420 to 1600°F	-150° to 550°F	-300 to 3100°F
Output	1 to 6V	1 to 3V	0 to 60mV
Power (100-ohm load)	4×10^{-2} watt	8×10^{-1} watt	2×10^{-7} watt
Features	Greatest accuracy over wide range, greatest stability	Greatest sensitivity	Greatest economy, highest range

*Varies with range and point on scale.

multi-conductor cables similar to thermocouples. Several thermistors can share one common lead wire, which results in a smaller wire bundle for multiple sensors. Thermistors are generally much more accurate and more repeatable than thermocouples, so they are often preferable to thermocouples in thawing conditions when the temperature is nearly isothermal. Thermistor circuits also have a higher output voltage than thermocouples when operated near 32°F and are therefore less susceptible to electrical noise problems.

Other types of temperature sensors are also available, such as diodes, RTDs, and liquid-in-glass thermometers. Table 2 compares characteristics of the three types of temperature sensors most commonly used in field installations.

Surface Elevations

Surface elevations are taken at marked locations several times in the fall, winter and spring. Elevations in

the summer or fall are used as references, and the difference between the reference elevation and the current elevation at a particular point is the total frost heave on that date. These surveys are the "standard" elevation surveys using engineer's rod and level equipment. Conventional benchmarks may be moved by frost action in the winter and spring; therefore, a reference point unaffected by frost heave must be installed. A "frost-free" benchmark (Figure 2) is necessary to preclude this type of problem. The benchmark must be identified so that it can be readily located beneath snow and located so that it will not be struck or disturbed by snow removal equipment. On an operational roadway or airport, traffic control is necessary for safety of the survey crew as well as the traveling public. We normally use a two-person survey crew with a conventional engineer's level and rod. We have also used a rotating laser level, an automatically reading rod and a one-person

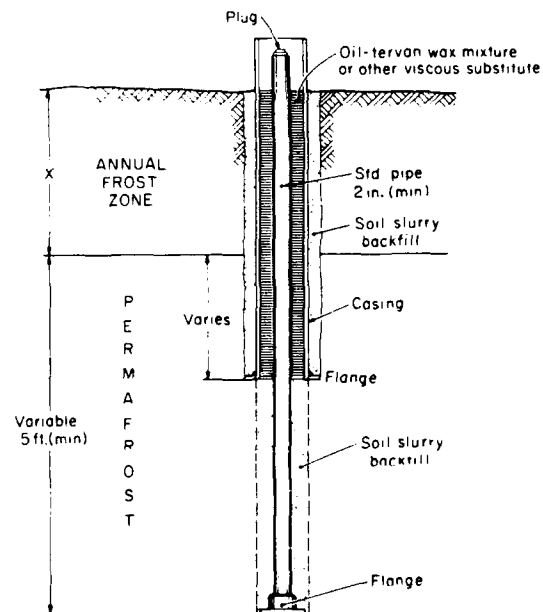


Figure 2. Recommended permanent benchmark. In seasonal frost areas the depth below the annual frost zone should be two to three times the thickness of the annual frost zone. (From Linell and Lobacz, 1980.)

crew. This is very slow because one person must work the rod as well as record the data. A two-person crew is generally preferable.

Water Table Elevation

Water table elevations are generally obtained using a conventional water well. Often we have used the water well as a frost-free benchmark for the elevation surveys. If the water table is near the ground surface or if frost penetrates beneath the protective casing (Figure 2), the water well may be moved by frost heave. If the water well is to be used as a benchmark, it should be installed to a depth of about three times the estimated depth of frost penetration beneath the road or airfield where the snow is cleared. If the water well is not used for a benchmark, its top elevation should be determined during each survey. We have used both steel pipes and plastic pipes for the well. We have generally read the water level using a string, a float and a ruler. This device is simple and inexpensive, but several more elaborate devices are also available. One problem occasionally encountered is that the water in the upper part of the well may freeze; then the water table is lowered, but this may not be noticed because of ice in the system. A pressure transducer could be lowered to the bottom of the well and may provide a true reading if the water table receded even though the surface was frozen. We have not used this technique.

Soil Moisture Content

Several types of soil moisture sensors are available, and others are under development. The general problem with these devices is that they do not function correctly for a long period of time; they seldom operate for more than three or four winters. Table 3 reviews several types of equipment, the range of applicability and the advantages and disadvantages of each type. Neiber (1989) discusses the performance of these devices in more detail.

Most of the studies we have con-

ducted involved no materials finer than silts; as a result, tensiometers (Figure 3) have generally been used in our work. Since they are subjected to freezing and thawing, we fill them with a nontoxic antifreeze to preclude breakage of the ceramic tip or the dial gage. Occasionally the ceramic tip is pulled away from the remainder of the device due to frost heave. When this occurs, the tensiometer must be replaced as it cannot be repaired. Tensiometers must be calibrated in each soil by developing a moisture characteristic curve in the laboratory. The laboratory test must be conducted at the same density as the soil exists in the field. The moisture characteristic curve is highly dependent on the soil density, and it exhibits hysteresis between wetting and drying cycles. Despite these problems we have used tensiometers extensively with satisfactory results. We have sometimes replaced the dial gages with pressure transducers and connected them to recording equipment. The tensiometers generally cost less than \$100 each, but when a pressure transducer is added the price can be increased by 50% or more.

We installed thermocouple psychrometers in one test section at CRREL. The soil was a low-plasticity clay installed slightly above its optimum moisture content and too near saturation for the devices to operate properly. The calibration procedure is complex and time-consuming. They can be monitored manually or automatically, but the system for automatic monitoring is relatively expensive. We believe that psychrometers will be used very little in freezing and thawing soils because the environment is generally too wet to allow for adequate sensitivity of the devices.

Nuclear devices have also been used to monitor moisture changes. We have used surface moisture/density gages during construction and depth probes after construction. The nuclear access tubes are left in place and must be sealed to prevent condensation and the influx of water from the surface. Nuclear probes sample the moisture content over a large volume of soil, and

Table 3. Major technical limitations of in-situ soil moisture sensor systems. (From U.S. Army, 1989.)

<i>Sensor type</i>	<i>Disadvantages and comments</i>
Neutron scatter	<p><i>Disadvantages</i></p> <ol style="list-style-type: none"> 1. Poor resolution (max resolution about 6 in.). 2. Influenced by physical-chemical soil properties. 3. Surface measurements can be inaccurate. 4. Access tube installation difficult in soils that contain fragments. <p><i>Comments</i></p> <ol style="list-style-type: none"> 1. Measures moisture regardless of state. 2. Reasonable accuracy and precision. 3. Insensitive to temperature change. 4. Rapid response time (seconds). 5. Employable in most soils. 6. Senses a wide range of moisture level.
Resistivity 0.5 to 15 bars*	<p><i>Disadvantages</i></p> <ol style="list-style-type: none"> 1. Influenced by soil salinity. 2. Temperature dependant. 3. Low overall accuracy, moderate precision. 4. Exhibits hysteresis between wetting and drying. <p><i>Comments</i></p> <ol style="list-style-type: none"> 1. Moderate response time (minutes). 2. Employable in most soils.
Capacitance Wide range (function of specific sensor)*	<p><i>Disadvantages</i></p> <ol style="list-style-type: none"> 1. Influenced somewhat by soil texture, density and salinity. <p><i>Comments</i></p> <ol style="list-style-type: none"> 1. High accuracy and high precision. 2. Rapid response time (seconds). 3. Under correct operation can distinguish water from ice.
Tensiometric 0.1 to 0.9 bars*	<p><i>Disadvantages</i></p> <ol style="list-style-type: none"> 1. Not useful in many dry soils. 2. Exhibits hysteresis between wetting and drying. 3. Difficult to implant probe in soils that contain fragments. <p><i>Comments</i></p> <ol style="list-style-type: none"> 1. Moderate response time (minutes). 2. High accuracy and precision. 3. Useful under conditions near saturation. 4. Adaptable to low temperatures.
Thermocouple psychrometer 1.0 to -80 bars* ⁺	<p><i>Disadvantages</i></p> <ol style="list-style-type: none"> 1. Corroded by acidic soils. 2. Sensor thermal gradients may give bad readings. 3. Often of low precision. <p><i>Comments</i></p> <ol style="list-style-type: none"> 1. Wide range of sensitivity. 2. High accuracy. 3. Relatively insensitive to temperature changes. 4. Insensitive to changes in bulk density. 5. Relatively long response time (hours).

the volume is inversely proportional to the amount of water in the system. The nuclear probe must be calibrated for each soil, and a large volume of soil is necessary for the calibration. Since the devices sample moisture over a large volume, they cannot readily detect moisture changes near boundaries. Another problem with these devices is that they are relatively expensive to

purchase, on the order of \$5000; however, one device can be used to monitor several sites. The devices must be operated manually.

Other equipment has also been used or will be used. "Coleman" and "Bouyoucos" blocks were developed for agricultural applications more than 30 years ago. They detect gross changes in moisture contents and do not survive

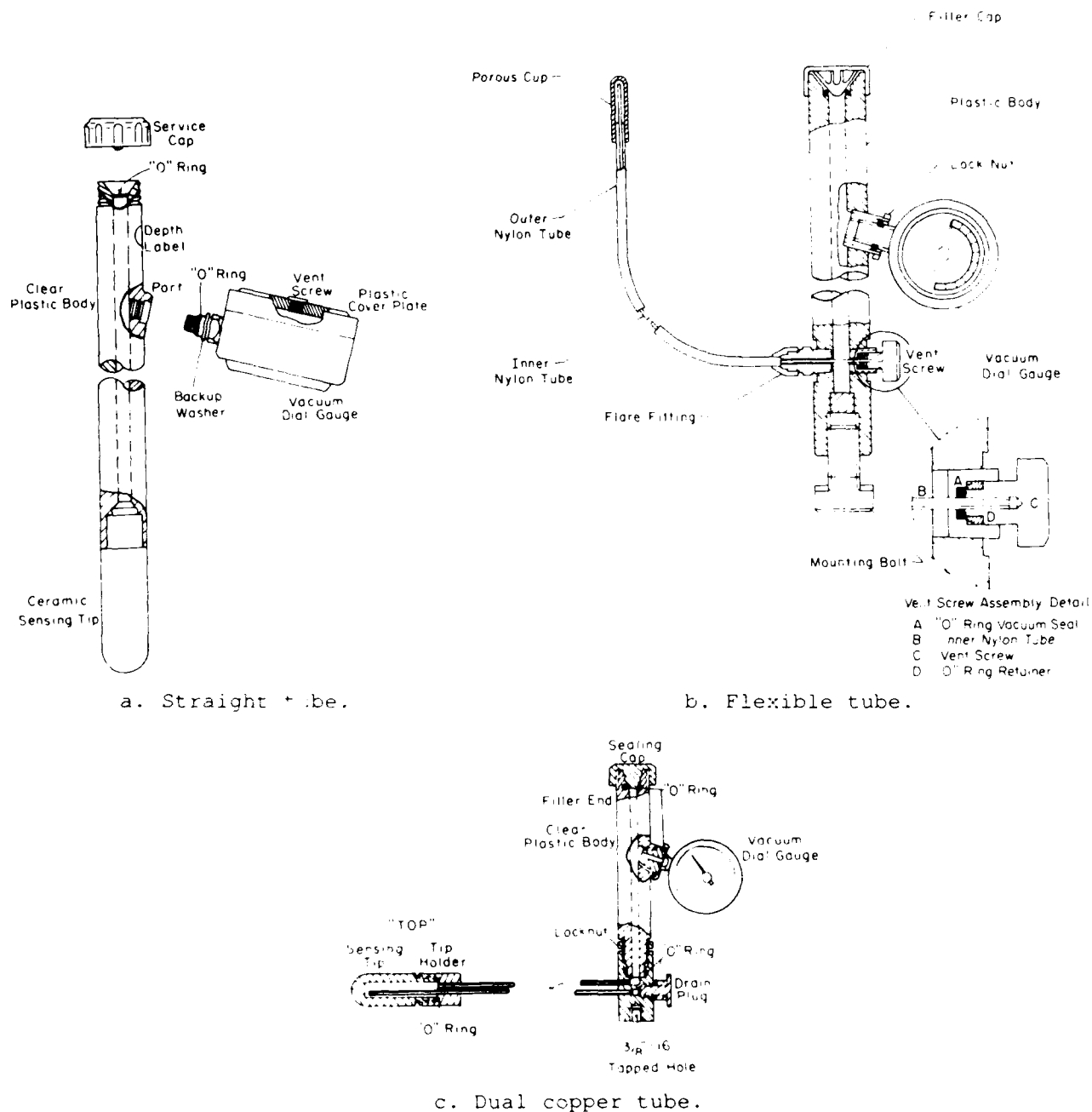


Figure 3. Three tensiometer models in use at CRREL. (From Ingersoll, 1981.)

for a long time. More recent devices are discussed by Neiber (1989) and Fredlund (1989) at this symposium. Some of them look very promising.

Subsurface Movement

These measurements have occasionally been made to determine the vertical distribution of frost heave in a pave-

ment system. We have used conventional settlement plates similar to those used in dams or other types of embankments. We have also used devices based on magnetic sensors or other similar systems. The various systems have performed acceptably but have not been widely used. All of the devices are monitored manually. We are investigating recently developed equipment for this applica-

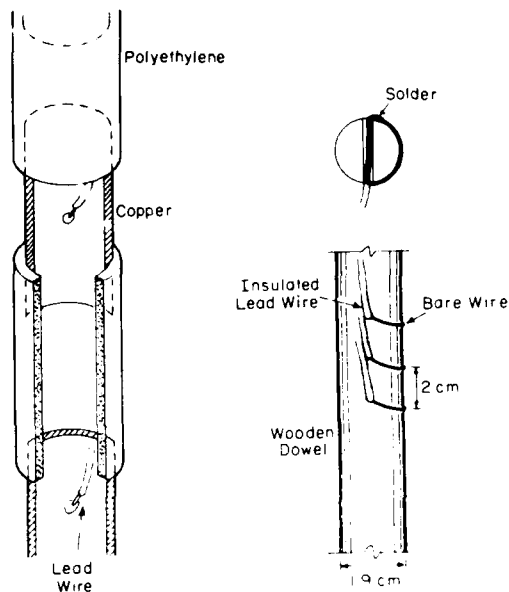


Figure 4. Initial (left) and second-generation resistivity probes. (From Atkins, 1979.)

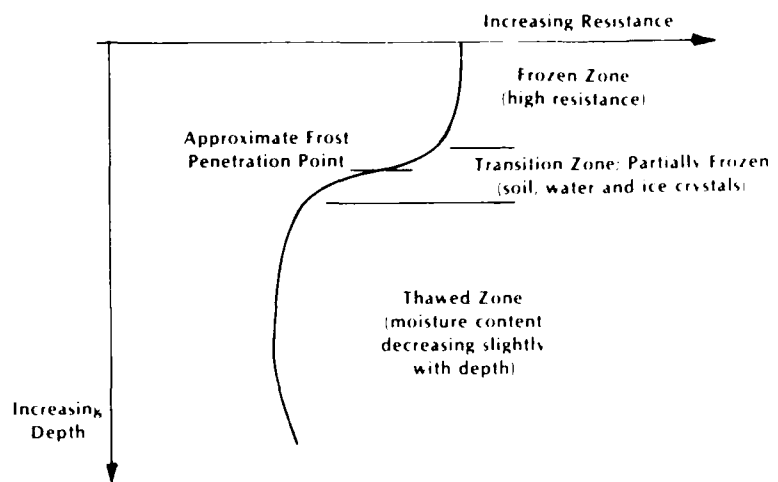


Figure 5. Typical resistance vs depth curve. (From Atkins, 1979.)

tion also. A major problem with all of these devices is to accurately measure movement without affecting the soil properties, moisture content and thermal regime around the sensor.

Electrical Resistivity Gages

These gages are often installed to aid in defining frozen and thawed layers. They are especially useful in delineating frozen and thawed boundaries when temperatures are nearly isothermal, as frequently happens in the spring, or when clayey soils are present. Figure 4 is a sketch of an electrical resistivity gage which was fabricated at CRREL. Figure 5 is a typical set of observations from a vertically installed gage. Note the large change in resistance from the frozen to the thawed states. This large difference allows the boundaries between frozen and thawed materials to be located quite accurately. These gages are not commercially available, but they can be easily fabricated by "in-house forces" or specified for a contractor.

Figure 6 is a schematic of a combined electrical resistivity gage and temperature assembly. Either thermis-

tors or thermocouples could be used in the temperature assembly. The combined system has the advantage that one will always know where the resistivity electrodes are relative to the temperature sensors and vice versa. If they are not in the same assembly, differential frost heave could cause changes in relative positions of the temperature and resistivity sensors with time.

EQUIPMENT NEEDS

To develop more accurate mechanistic design methods using cumulative damage concepts, it is extremely important that we develop a better understanding of the annual moisture and temperature variations within the pavement system and the influence of these variations on pavement strength, performance and life. We can monitor temperatures with the desired accuracy and frequency. If properly selected, assembled and installed, the temperature sensors will provide reliable data for 20 years or more. Moisture measurements are a problem, however. A sensor must be usable in the wide variety of materials placed in pavement systems. That sensor must

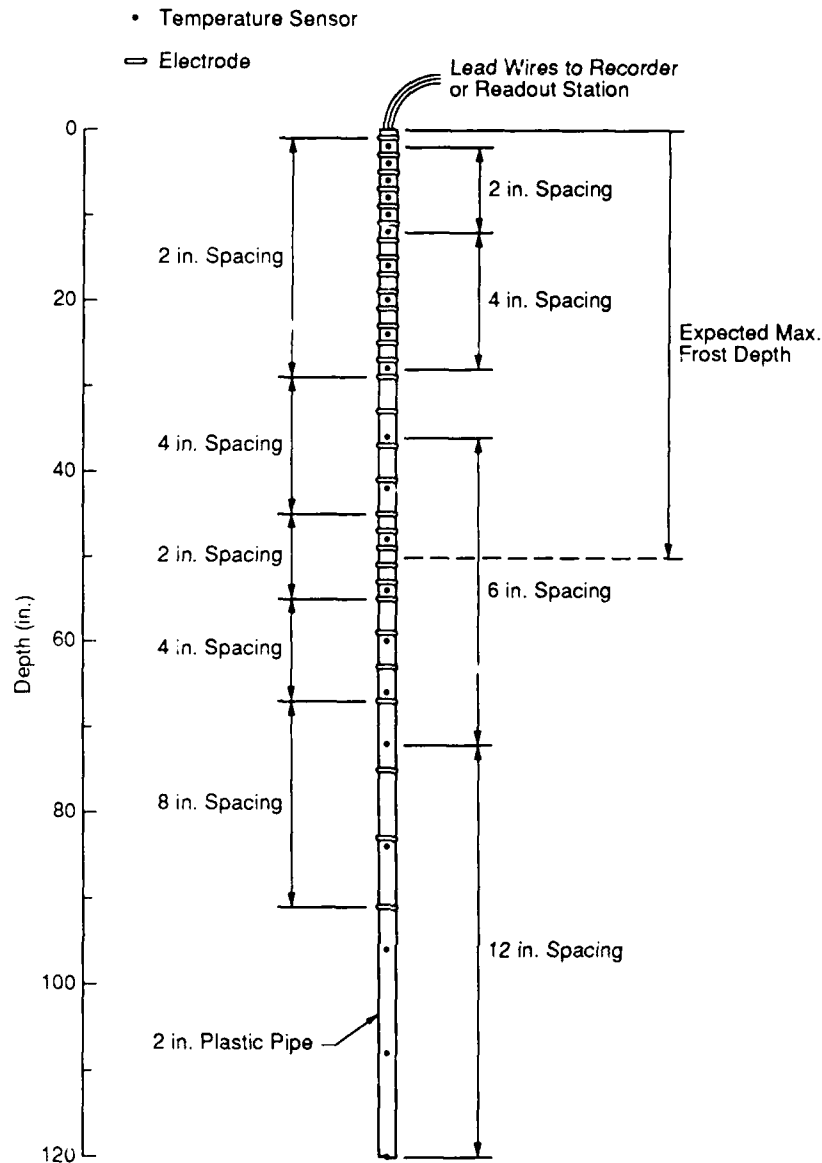


Figure 6. Schematic of a typical combined temperature and electrical resistivity assembly.

also provide valid data over 10-20 years. Papers by Neiber (1989) and Fredlund (1989) at this symposium may provide information on new equipment for this purpose.

We have not successfully measured in-situ stresses and strains in pavement layers and unbound material layers in pavement systems in seasonal frost areas. However, both Anderson and Sebaaly (1989) and Christison (1989) discuss this type of measurement for bound layers. The two primary problems in developing this equipment are: (a) the

pavement system may move a few inches due to frost heave, but movements due to traffic loadings may be only a few hundredths of an inch or less; and (b) the modulus of the soil-water system may change two to four orders of magnitude between its frozen state and its thawed and saturated state. The modulus of asphalt-bound layers also varies with temperature, but substantially less than the underlying soils subjected to freezing and thawing.

In the last few years, a few states (Illinois, Iowa, Minnesota, North Caro-

lina and Pennsylvania) have installed, or soon will install, equipment as part of FHWA Experimental Project 621 entitled "Pavement Instrumentation." Information from these studies will provide experiences with different types of gages and their installation procedures. These installations will also provide data concerning the reliability and longevity of the sensors. According to papers by Selig (1989), Ullidtz and Ertman Larson (1989) and Christison (1989) at this symposium and other recent publications, suitable devices may now be available or are currently under final development.

REFERENCES

Atkins, R.F. (1979) Determination of frost penetration by soil resistivity measurements. USA CRREL Special Report 79-22, Hanover, N.H.

Anderson, D.A. and P.E. Sebaaly (1989) In-situ strain measurements in hot-mix asphalt pavements. In *Proceedings of the Symposium on the State of the Art of Pavement Response Monitoring Systems for Roads and Airfields*, this volume.

Christison, J.T. (1989) Monitoring pavement responses to traffic loads. In *Proceedings of the Symposium on the State of the Art of Pavement Response Monitoring Systems for Roads and Airfields*, this volume.

Fredlund, D.G. (1989) Soil suction monitoring for roads and airfields. In *Proceedings of the Symposium on the*

State of the Art of Pavement Response Monitoring Systems for Roads and Airfields, this volume.

Ingersoll, J.E. (1981), Laboratory and field use of soil tensiometers above and below 0°C. USA CRREL Special Report 81-7, Hanover, N.H.

Linell, K.A. and E.F. Lobacz (1980) Design and construction of foundations in areas of deep seasonal frost and permafrost. USA CRREL Special Report 80-34, Hanover, N.H.

Neiber, J.L. (1989) In-situ measurement of soil water content in the presence of freezing/thawing conditions. In *Proceedings of the Symposium on the State of the Art of Pavement Response Monitoring Systems for Roads and Airfields*, this volume.

Selig, E.T. (1989) In-situ stress measurements. In *Proceedings of the Symposium on the State of the Art of Pavement Response Monitoring Systems for Roads and Airfields*, this volume.

Ullidtz, P. and H.J. Ertman Larson (1989) State-of-the-art: stress, strain and deflection measurements. In *Proceedings of the Symposium on the State of the Art of Pavement Response Monitoring Systems for Roads and Airfields*, this volume.

U.S. Army (1989) Selection of methods for soil moisture measurement, Engineer Technical Letter (draft), U.S. Army Corps of Engineers.

INSTRUMENTATION NEEDS - SHRP'S VIEW

Dr. Lynne H. Irwin Formerly Senior
Staff Engineer*

Adrian Pelzner Senior Staff
Engineer
Strategic Highway
Research Program
Washington, DC

The Strategic Highway Research Program (SHRP) may be expected to be a consumer of some of the developments in pavement instrumentation that will be discussed at this conference. We want to use instrumentation to do pavement research. For us, the urgency with which we are pursuing our mission prevents us from using pavements to do instrumentation research.

Our main use of pavement instrumentation will be in the Specific Pavement Studies (SPS) program in our Long-Term Pavement Performance (LTPP) research. There, for example, we may measure pavement strain and other parameters pursuant to determining structural coefficients for asphalt and concrete pavements.

In SPS we also plan to investigate how seasonal changes in the environment affect pavement performance. We refer to this as our Environmental Studies project. It will involve making many surface and subsurface measurements of key variables such as temperature,

* Dr. Irwin was on sabbatical leave with SHRP during January-December 1988. He is currently Associate Professor and Director, Cornell University Local Roads Program, Ithaca, NY.

moisture, modulus, and strain, and observing how these parameters change at various intervals of time. We expect that these studies will be conducted in a variety of different climate zones, incorporating many different types of subgrade and base course materials. We are still actively formulating our plans for this project, but we expect to be heavily influenced by such factors as cost, various practical considerations and what is possible, as reported at this conference, as well as other sources of instrumentation information.

We have many questions about pavement instrumentation. How durable is it? Will it last as long as we need it to? Will it report consistent results? Most importantly, we are concerned about whether it actually measures what it purports to. From nuclear meters to stress cells, it is evident that these are questions that must be answered before we can put instrumentation to work in our research.

We hope to find answers to some of these questions at this conference. Thus, while we are here with a "shopping list" like many others, we are also here as a supportive partner. We look forward to using the fruits of your labors in our research.

SHRP PAVEMENT RESEARCH STUDIES

Most pavement researchers have a clear understanding of the SHRP plans for the LTPP studies. Thus I will provide only a very limited overview, along with an update on some key dimensions of the program.

General Pavement Studies (GPS)

The GPS project is underway. We have taken delivery on four Dynatest Falling Weight deflectometers. Their initial calibrations and comparisons have been done. Production FWD testing has begun.

We expect to receive delivery on several key pieces of performance measurement equipment within a few weeks. Meanwhile, GPS site selection is nearly completed, and the drilling and sampling of the selected sites is taking place.

The purpose of the GPS studies is to observe the change in pavement performance due to traffic on selected

sections of the existing highway system. State highway departments across the United States have nominated test sites for the study. Many foreign countries, including Canada and many others worldwide, are cooperating in this project.

In the United States as of February 7, 1989, 768 GPS test sites have been verified and incorporated in the study. Ultimately we expect the number of sites will be approximately 800.

Each site will be 500 feet long. It is our goal to measure pavement roughness about once per year using a profilometer. The pavement distress will be photographed every year or two. The structural performance of every site will be determined at least once using the falling weight deflectometer. Through drilling and sampling, followed by extensive laboratory testing, the important properties of each pavement layer, including the subgrade, will be determined.

All of the data will be placed in a database to be managed by the Transportation Research Board. The data will be available to pavement researchers and to all who would choose to use it.

Specific Pavement Studies (SPS)

Plans for the SPS projects are being finalized. SPS will consist of a limited number of newly constructed pavements, strategically located around the country, which will be specially built for specific research purposes.

Some of the objectives of this research, will be to determine the validity of various structural coefficients for both asphalt and concrete pavements and how they affect pavement performance, to assess the effect of various levels of subsurface drainage on pavement performance, and to determine how maintenance practices affect pavement performance.

To achieve the full potential of these studies in terms of the information that they can yield, will take fifteen to twenty years after construction. Since SHRP is expected to cease operations in 1993, we expect that the states which host the SPS test sites will continue to make the needed observations. Provisions will be made for inclusion of the SPS data in the aforementioned database. It is in the SPS projects that we expect to

have the greatest need for pavement instrumentation. To log traffic data, weigh-in-motion equipment will be installed at all SPS sites. For the structural research there certainly is a potential to use subsurface strain instrumentation and measurements.

Environmental Pavement Studies

One instrumentation-intensive research area, and a corollary part of the SPS projects, is what we refer to as our Environmental Studies project. We plan to investigate how seasonal variations in the environment (i.e., temperature, humidity, evaporation, precipitation, etc.) affect pavement performance.

Our objective will be to relate various independent variables, such as moisture content, permeability, density, and modulus of elasticity to the dependent performance variables such as roughness, rutting, cracking and distress. How to correctly account for seasonal changes in pavement materials properties, and how to predict such changes, are of particular interest.

It appears likely that the Environmental Studies can be incorporated into other SPS projects, and for the most part separate pavement test sections will not be necessary.

Among the many measurements that we might wish to make above and beneath the pavement are the following. All of these measurements would be made throughout the year.

- * weather - site specific weather data such as temperature, humidity, wind, precipitation, and possibly evaporation and/or solar insolation
- * pavement temperature - temperature at various depths from very near the surface to five feet or more deep
- * frost penetration - in freezing climates, a record of the depth of freezing and thawing beneath the pavement surface
- * moisture content - of granular materials in the base, subbase, and subgrade layers

- * soil moisture tension - suction in the partially saturated granular layers
- * water table elevation - depth to the free water surface
- * density - in situ density of various layers, or a measure of overburden pressure at various depths
- * stress - vertical and horizontal pressure at various depths beneath the surface due to wheel loads
- * strain - vertical and horizontal deformation at various depths beneath the surface due to wheel loads
- * permanent deformation - rutting, including vertical and horizontal movement at various depths beneath the surface
- * modulus of elasticity - in situ modulus of various layers, determined either by instrumentation, or by back-calculation from non-destructive testing on the pavement surface

INFORMATION NEEDS

We need to make our choices carefully always keeping in mind costs and cost effectiveness. Due to the long-term nature of our pavement studies, instrumentation durability is a foremost concern. Devices which last only a year or two are costly in the framework of a twenty-year study. There is also a danger that the act of removing and replacing non-durable instrumentation will destroy the pavement structure and invalidate the measurements.

In choosing our instrumentation we must also be confident that it measures what we want it to. Limitations in the state-of-the-art for certain types of instrumentation are very severe. Some devices return a "number", but SHRP must be sure that the number is real. The ability to calibrate the instrumentation, and to verify periodically, while the instrument is in place, that the calibration is unchanged, is highly desirable.

Our intent is to use instrumentation to do pavement research. We must rely on the work of others who have already used pavements to do instrumentation research. Fortunately, we can do so. The agenda for this conference closely parallels the range of our needs. We hope to begin to find answers to many of our questions here.

We appreciate the timeliness of this conference. We are enthusiastic about the prospects for making significant strides in our quest to make better, longer-lasting pavements. The data from our pavement instrumentation will be an important element of our pavement performance studies.

We are here to listen and to learn.

**Session 2:
In-Situ Moisture and
Drainage Measurements**

SOIL SUCTION MONITORING FOR ROADS AND AIRFIELDS

D.G. Fredlund

Professor of Civil Engineering
University of Saskatchewan
Saskatoon, Saskatchewan
CANADA S7N 0W0

ABSTRACT

The measurement of negative pore-water pressure is central to the study of compacted soil behavior. Negative pore-water pressures are as important to understanding compacted soil behavior as positive pore-water pressures are to understanding saturated soil behavior. However, there are serious difficulties associated with the measurement of pore-water pressures which are highly negative.

Negative pore-water pressures, u_w , are generally referenced to the pore-air pressure, u_a , and called the matric suction component of suction (i.e., $(u_a - u_w)$). The salts in the pore fluid give rise to a second component of suction; namely, the osmotic suction, ψ_o . A combination of the two components of suction are referred to as total suction. All three soil suction terms can be described within one theoretical context using Kelvin's equation. The soil suction terms are described in terms of the thermodynamics of the air immediately adjacent to the air-water interface.

This research paper first presents the theory of soil suction measurements and then describes several devices which can be used for the measurement of soil suction insitu and in the laboratory. Emphasis is placed on recent technological developments which show promise for geotechnical practice. In

particular, the use of thermal conductivity sensors to indirectly measure matric suction is discussed.

Typical soil suction measurements on a wide range of soils are presented. The advantages, disadvantages, and range of measurement are discussed for each suction device. The emphasis is on obtaining insitu suction measurements. Procedures that can be used for the insitu measurements are described. In general, the paper is intended to give a state-of-development in the measurement of soil suction.

INTRODUCTION

The long term performance of a highway is strongly influenced by the subgrade soil conditions. However, generally the properties of the subgrade are given minimal consideration in the design of a highway structure. This is due to the difficulties associated with assessing the stress state and the physical properties of compacted soils. Consequently, the subgrade is usually characterized in an empirical manner. The resulting design procedure for the pavement structure is quite different from more theoretical procedures commonly used for classical soil mechanics problems.

The empirical approach to pavement structure design is largely the result of difficulties related to measuring the stress state in subgrade soils (Fredlund and Rahardjo, 1987). The pore-water pressures of a newly compacted subgrade

are negative relative to atmospheric conditions.

Negative pore-water pressures result in an increase in strength of the subgrade soil. With time, the negative pore-water pressures in a subgrade soil can change as a result of microclimatic changes in the vicinity of the pavement structure. Most pavement structures cannot perform satisfactorily unless the pore-water pressures in the subgrade remain somewhat negative. When the pore-water pressure is referenced to the pore-air pressure, the resulting term (i.e., matric suction) is used as one of the stress state variables to describe the state of the soil.

This paper presents the theory related to the components and the measurements of soil suction. A summary is then given of recent experiences in measuring soil suction. The emphasis is on measuring insitu soil suction. An attempt is made to provide a theoretical context for understanding the components of soil suction and then discussing devices which show the greatest promise for use in geotechnical engineering.

THEORY AND COMPONENTS OF SOIL SUCTION

Each of the components of suction has an effect on the partial water vapor pressure at the air-water interface (Fredlund and Rahardjo, 1988). Therefore, a thermodynamic context forms a theoretical basis for understanding the components of suction. Soil suction can be related to partial water vapor pressure through the use of Kelvin's equation.

$$\psi = - \frac{RT}{v_{wo} \omega_v} \ln \frac{\bar{u}_v}{\bar{u}_{vo}} \quad [1]$$

where:

- ψ = suction (kPa)
- R = universal (molar) gas constant (i.e., 8.31432 J/(mol K))
- T = absolute temperature (i.e., $T = (273.16 + t^\circ)(K)$)
- t° = temperature ($^\circ C$)
- v_{wo} = specific volume of water or the inverse of water density (i.e., $1/\rho_w$) (m^3/kg)
- ρ_w = water density (i.e., 998 kg/m^3 at $t^\circ = 20^\circ C$)
- ω_v = molecular mass of water vapor (i.e., 18.016 $kg/kmol$)

\bar{u}_v = partial pressure of pore-water vapor (kPa)

\bar{u}_{vo} = saturation pressure of pure water vapor over a flat surface at the same temperature (kPa)

If we select a reference temperature of $20^\circ C$, the constants in Equation [1] give a value of 134,950 kPa. Equation [1] can now be written to give a fixed relationship between suction in kilopascals and relative vapor pressure.

$$\psi = - 134,950 \ln \bar{u}_v / \bar{u}_{vo} \quad [2]$$

Equation [1] shows that the reference state for quantifying the components of suction is the vapor pressure above a flat surface of pure water (i.e., water with no salts or impurities) (Figure 1). The term \bar{u}_v / \bar{u}_{vo} is called relative humidity, RH (%).

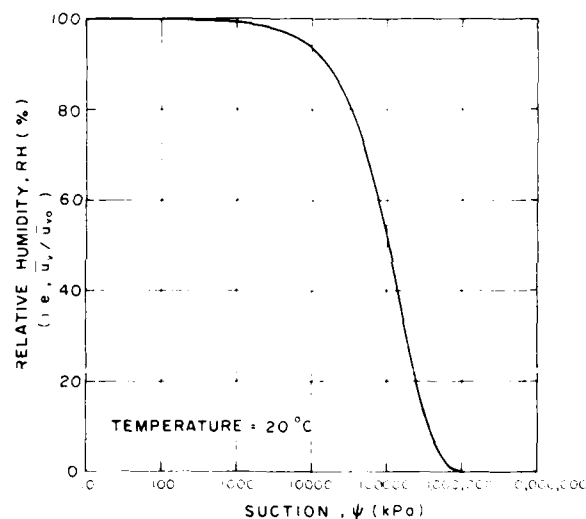


Fig. 1 Relationship Between Relative Humidity and Soil Suction

Figure 1 shows a plot of Equation [2]. It can be noted that a slight reduction in relative humidity results in extremely high suctions. For example, a relative humidity of 94.24% corresponds to a suction of 8000 kPa. The range of suctions of interest in geotechnical engineering will correspond to high relative humidities.

Any phenomenon which results in a reduction in the partial vapor pressure causes a reduction in the relative humidity at the air water interface, and consequently, gives rise to soil

suction. Two phenomena are known to produce a reduction in partial vapor pressure; namely, the presence of a curved surface (i.e., a meniscus) and the presence of salts in the water (Figure 2).

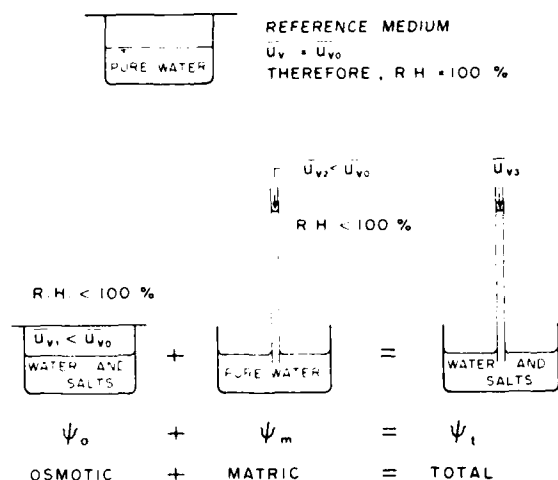


Fig. 2 Illustration of Phenomena Giving Rise to a Reduction in Partial Vapor Pressure

The reduction in partial vapor pressure caused by a curved (i.e., concave) water surface can be visualized using a capillary tube. The water vapor pressure or the relative humidity decreases as the radius of curvature of the water surface decreases. At the same time, the radius of curvature is inversely proportional to the difference between the air and water pressures across the surface (i.e., $(u_a - u_w)$). The $(u_a - u_w)$ term is called the matric suction; where: u_a is pore-air pressure

and u_w is pore-water pressure. This means that one component of the total suction is matric suction and it causes a reduction in the relative humidity at the air-water interface.

The pore-water in a soil generally contains dissolved salts (i.e., a solvent). The partial vapor pressure over a flat surface of solvent is less than the vapor pressure over a flat surface of pure water. In other words, the relative humidity decreases with increasing dissolved salts in the pore-water in the soil. The decrease in relative humidity due to the presence of dissolved salts in the pore-water is referred to as the osmotic suction. In summary, total suction, ψ_t , can be considered as the sum of the matric suction and the osmotic suction.

$$\psi_t = (u_a - u_w) + \psi_o \quad [3]$$

Table 1 shows typical matric, osmotic and total suction values for two soils which commonly form the subgrade for roads built in the province of Saskatchewan, Canada (Krahn and Fredlund, 1972). The Regina Clay is a highly plastic, inorganic clay with a liquid limit of 78% and a plastic limit of 31%. The glacial till has a liquid limit of 34% and a plastic limit of 17%. Suction values are given for soils compacted to standard AASHTO conditions with the water contents at optimum and 2 percent below optimum. The relationship between the suction components along with their significance to subgrade performance are discussed later in this paper.

Figure 3 shows experimental data illustrating that the matric plus the

Table 1

Typical Suction Values for Compacted Soils

Soil Type	Water Content (%)	Matric Suction	Osmotic Suction	Total Suction
Regina Clay	30.6 (optimum)	273	187	460
$\gamma_{max} = 87.9$ PCF	28.6	354	202	556
Glacial Till	15.6 (optimum)	310	290	600
$\gamma_{max} = 122.5$ PCF	13.6	556	293	849

osmotic components of suction do indeed equal the total suction of the soil. The data presented is for Regina Clay specimens compacted under Standard AASHTO conditions at various initial water contents. Each of the soil suction values were measured independently.

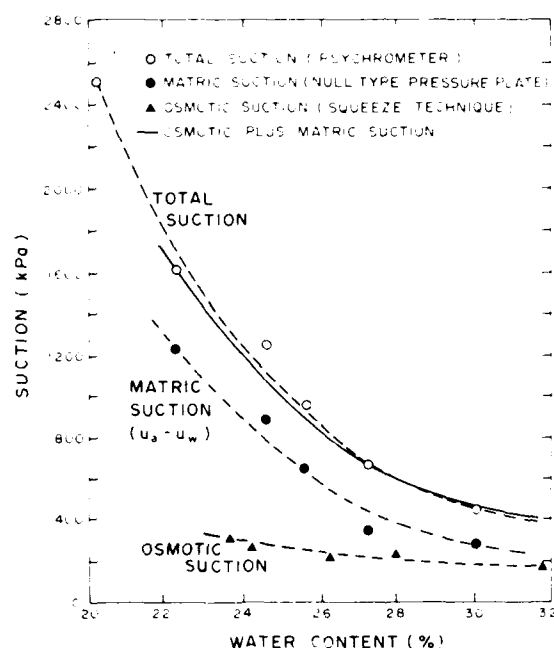


Fig. 3 Total, Matric, and Osmotic Suction for Regina Clay (From Krahn and Fredlund, 1972)

The role of osmotic suction has commonly been associated more with unsaturated soils than with saturated soils. In reality, dissolved salts are present in both saturated and unsaturated soils. Therefore, the role of osmotic suction bears similarly upon the behavior of both saturated and unsaturated soils. Changes in osmotic suction due to changes in salt content will affect the mechanical behavior of a soil. However, osmotic suction changes are not generally taken into account in an analysis for either saturated or unsaturated soils if their changes have been simulated during the laboratory measurement of soil properties. Therefore, it is generally the matric suction component which is of interest in geotechnical engineering.

Natural microclimatic processes such as precipitation and evaporation (and evapotranspiration) impose a flux condition at the ground surface. The net flux can be viewed as subsequently pro-

ducing changes in the matric suction within the soil profile. The changes occur as a result of the movement of water through the soil.

If the engineer is primarily interested in measuring and/or predicting changes in matric suction, the question could be asked, "Why should the engineer be interested in measuring osmotic or total suction?" Osmotic and total suction are truly of secondary interest from the standpoint of analysing most engineering problems. However, these components may be of interest for the following reasons:

- 1) There are situations where the interest is only in the change of matric suction. Since osmotic suction remains relatively constant over a considerable water content range, a change in total suction would be approximately equal to a change in matric suction.
- 2) For certain suction ranges, it might be easier to measure total suction than matric suction. Therefore, by measuring total suction and subtracting the osmotic suction, it is possible to obtain the matric suction.

Another way to visualize the predominant importance of matric suction is by realizing that the engineer is primarily interested in knowing the negative pore-water pressure in the soil. In general, the negative pore-water pressure is numerically equal to the matric suction since the pore-air pressure is atmospheric. Volume change, shear strength, and seepage analyses all require an understanding of the pore-water pressure. In this sense, saturated and unsaturated soil mechanics analyses are similar. The difficulty in directly measuring highly negative pore-water pressures gives rise to the study of soil suction measurements.

DEVICES USED TO MEASURE SOIL SUCTION

Several devices commonly used for measuring soil suction are listed in Table 2. Also shown are their range of applicability and comments related to their performance.

MATRIC SUCTION MEASUREMENTS

Matric suction measurements are of greatest importance in geotechnical engineering. All three of the devices

Table 2
Devices for Measuring Suction

Name of device	Suction component measured	Range (kPa)	Comments
Null type pressure plate	Matric	0 to 500	Range for measurement is a function of the air entry value of the ceramic disc.
Tensiometers	Negative pore-water pressures or matric suction when pore-air pressure is atmospheric	0 to ~ 90	Difficulties with cavitation and air diffusion through ceramic cup
Thermal conductivity sensors	Matric	0 to ~ 400+	Indirect measurement on a porous ceramic sensor
Psychrometers	Total	100* to ~ 8,000	Constant temperature environment required
Filter paper	Total	(Entire range)	May measure matric suction when in contact with moist soil
Pore fluid squeezer	Osmotic	(No limit)	Used in conjunction with a psychrometer or electrical conductivity measurement

*Controlled temperature environment to $\pm 0.001^\circ\text{C}$

mentioned in Table 2 can be used in the laboratory. The thermal conductivity sensors give an indirect measure of matric suction. Considerable research is presently underway on these sensors, and they show promise for use in geotechnical engineering. Each of the devices is discussed below.

Null Type Pressure Plate

Null Type Pressure Plates utilize the axis-translation technique and can measure matric suction over a wide range. The axis-translation was developed and used by Hilf in the late 1940's to measure negative pore-water pressures less than zero absolute pressure (Hilf, 1948). This apparatus has been used for over 30 years to

measure suctions in the laboratory. However, there is still little information in the literature on the use of this technique (Bocking and Fredlund, 1980).

Figure 4 shows a schematic layout of a Null Type Pressure Plate apparatus. It is also necessary for the apparatus to have a flushing system to remove air bubbles from below the high air-entry disc in order to keep the compartment above the transducer saturated with water. Also shown are some numbers illustrating how a highly negative pore-water pressure can be measured using this apparatus.

Let us suppose that a soil specimen has an initial pore-water pressure of -250 kPa when it is placed on the (saturated) high air entry disc. The

specimen will immediately attempt to draw water up through the ceramic disc causing the pressure transducer to start registering a negative value. The cover is quickly placed on the top of the device, and the air pressure in the chamber is increased until there is no further tendency for the movement of water through the high air entry disc. At equilibrium, the chamber air pressure may be 255 kPa while the water compartment may register 5 kPa. Therefore, the matric suction of the soil is 250 kPa.

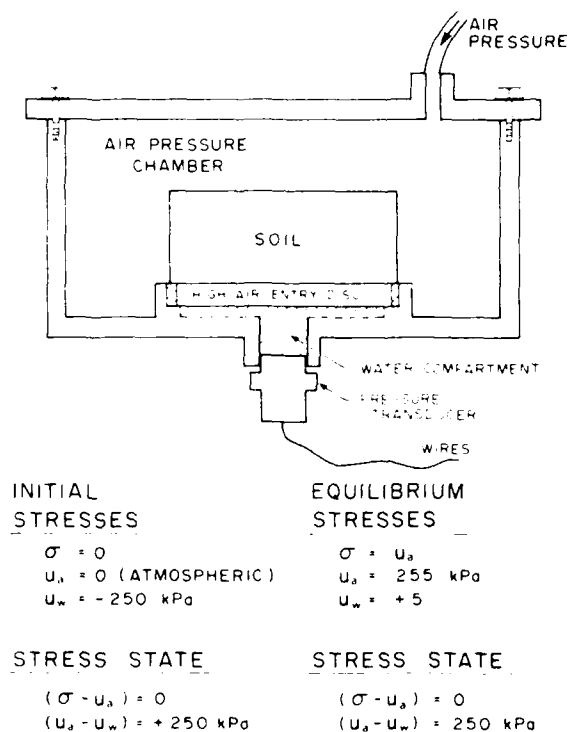


Fig. 4 Schematic of a Null Type Pressure Plate Apparatus for Measuring Matric Suction

Several typical Null Type Pressure Plate results on Regina Clay are shown in Figure 5. The response time is a function of the permeability characteristics of the high air entry disc and the soil. For the test data shown, the high air entry disc was 0.125 inches in thickness. Some air diffused through the water in the disc as was evident by air slowly accumulating below the high air entry disc. As a result, the suction measurements show a slight drop after about 12 hours. Thicker high air entry discs (i.e., 0.250 or 0.275

inches) generally function in a superior manner.

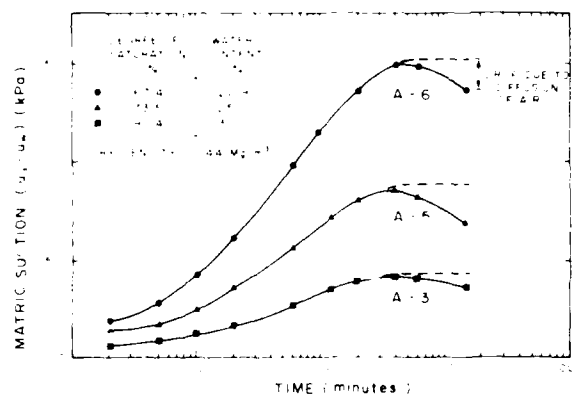


Fig. 5 Development of Matric Suction in Statically Compacted Regina Clay (From Pufahl, 1970)

The range over which soil suctions can be measured is a function of the air entry value of the ceramic discs. The air entry discs are generally purchased from Soilmoisture Equipment Corporation, Santa Barbara, California, to the specifications desired. Permeability and air entry values for standard ceramic discs available from Soilmoisture Equipment Corporation are shown in Table 3.

Tensiometers

A tensiometer measures the negative pore-water pressure in a soil. The tensiometer consists of a porous ceramic, high air-entry cup connected to a pressure measuring device through a small bore capillary tube. The tube and the cup are filled with deaired water. The cup can be inserted into a precored hole until there is good contact with the soil. After equilibrium has been achieved, the water in the tensiometer will have the same negative pressure as the pore-water in the soil. The water pressure that can be measured in a tensiometer is limited to approximately negative 90 kPa due to the possibility of cavitation of the water in the tensiometer. The measured negative pore-water pressure is numerically equal to the matric suction when the pore-air pressure is atmospheric (i.e., u_a equals to zero gauge pressure). When the pore-air pressure is greater than atmospheric pressure (i.e., axis-

Table 3

Summary of the Properties of High air Entry Ceramic Discs*

Type of Ceramic	Bubbling Pressure (kPa)	Permeability (cm/sec)	Radius of largest Pore (cm)
1/2 Bar	48 - 62	3.17×10^{-5}	2.6×10^{-4}
1 Bar (low flow)	137 - 206	3.5×10^{-7}	8.5×10^{-5}
1 Bar (high flow)	130 - 192	8.8×10^{-6}	8.8×10^{-5}
2 Bar	240 - 309	1.76×10^{-7}	5.3×10^{-5}
3 Bar	316 - 481	1.76×10^{-7}	3.7×10^{-5}
5 Bar	> 550	1.23×10^{-7}	2.7×10^{-5}
15 Bar	> 1510	2.64×10^{-7}	0.96×10^{-5}

*Results computed from data published by Soilmoisture Equipment Corporation

translation) the tensiometer reading can be added to the pore-air pressure reading to give the matric suction of the soil. The measured matric suction must not exceed the air entry value of the ceramic cup. The osmotic component of soil suction will not be measured by tensiometers since soluble salts are free to flow through the porous cup.

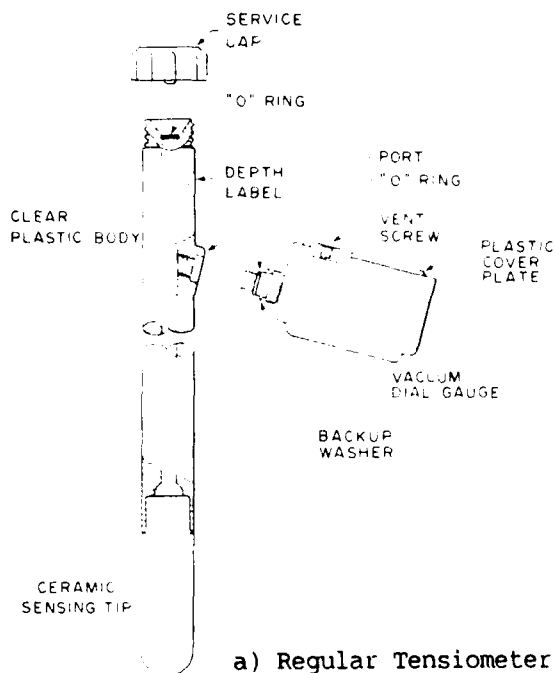
There are several types of tensiometers available from Soilmoisture Equipment Corporation, Santa Barbara, California, U.S.A. Figure 6 shows two types of tensiometers. Slow diffusion of air through the high air entry cup is a problem common to all tensiometers. As air diffuses through the water in the ceramic cup, the pressure being read on the gauge slowly increases towards zero (i.e., atmospheric pressure). The coaxial leads shown on some of the tensiometers are provided for the purpose of flushing the diffused air (or services the tensiometers). Usually this procedure is required on a daily basis and it is sometimes difficult to get an accurate suction measurement because of the water moving from the tensiometer into the soil.

The Quick Draw tensiometer has proven to be a particularly useful portable tensiometer to rapidly measure negative pore-water pressures (Figure 7). The water in the tensiometer is subjected to tension for only a

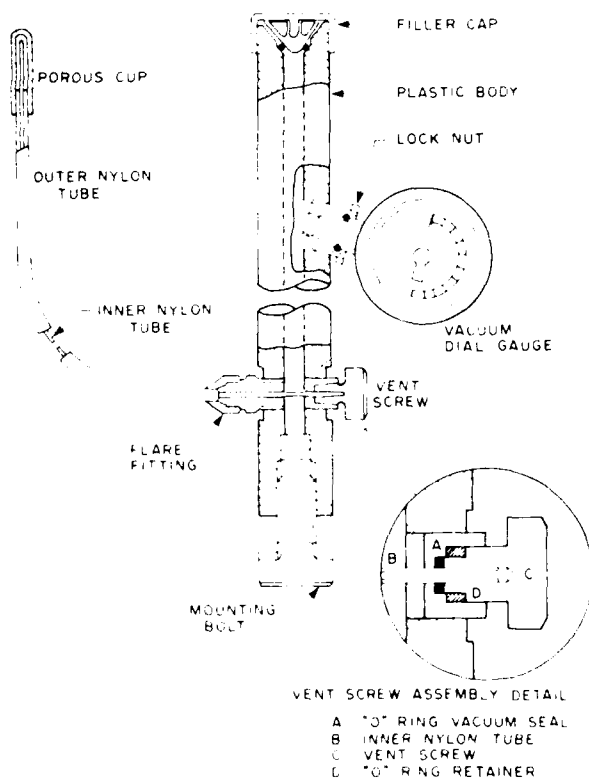
short period of time during each measurement. Therefore, air diffusion through the ceramic cup with time is minimized. The Quick Draw tensiometer can repeatedly measure pore-water pressures approaching minus one atmosphere when it has been properly serviced. When it is not in use, the probe is maintained saturated in a carrying case which has water saturated cotton surrounding the ceramic cup. Figure 8 illustrates the distribution of matric suction along a trench excavated perpendicular to a railway embankment in British Columbia, Canada. The embankment soil consisted predominantly of unsaturated silt. The negative pore-water pressures were measured on the sidewalls of the trench using a Quick Draw tensiometer.

Thermal Conductivity Sensors

A thermal conductivity sensor indirectly measures the matric suction in a soil. The sensor consists of a porous ceramic block containing a temperature sensing element and a miniature heater. Measurements are made by inserting the sensor into a pre-drilled hole in the soil and allowing the matric suction in the ceramic block to come to equilibrium with the matric suction in the soil. The equilibrium matric suction is related to the water content



a) Regular Tensiometer



b) Small Tip Tensiometer with Coaxial Tubing

Fig. 6 Two Tensiometer Models Manufactured by Soilmoisture Corporation, Santa Barbara, California

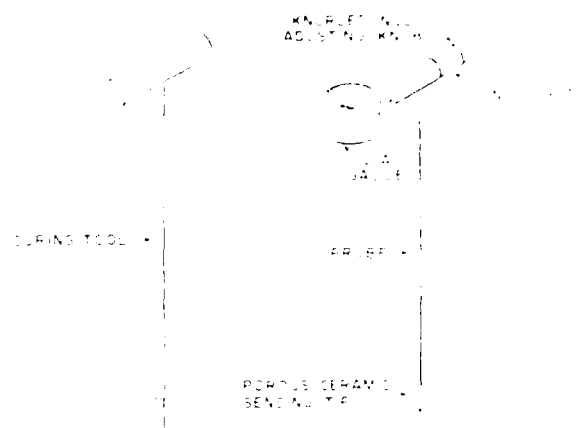


Fig. 7 "Quick Draw" Tensiometer from Soilmoisture Equipment Corporation

in the porous block. The amount of water in the porous block affects the rate of heat dissipation within the block. Therefore, the water content in the porous block can be measured indirectly by measuring the heat dissipation of the block. This is accomplished by generating a controlled amount of heat at the center of the porous block and measuring the temperature rise at the same point after a fixed period of time. More heat will be dissipated throughout the block with increasing water content in the block. The undissipated heat causes a temperature rise that is inversely proportional to the water content in the porous block. As a result, the measured temperature rise can be calibrated to measure the matric suction in the soil.

The thermal conductivity sensor calibration can be conducted using a pressure plate apparatus. A pressure plate set up for calibrating the sensor

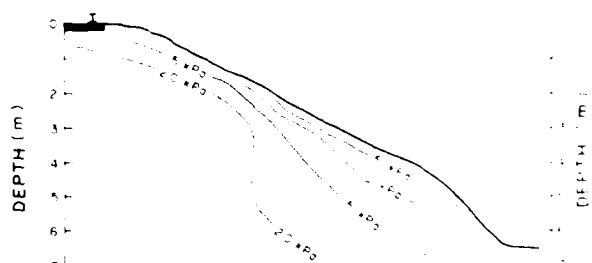
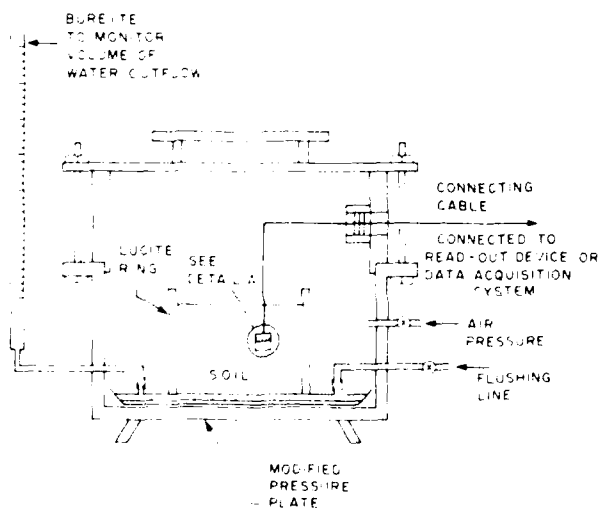


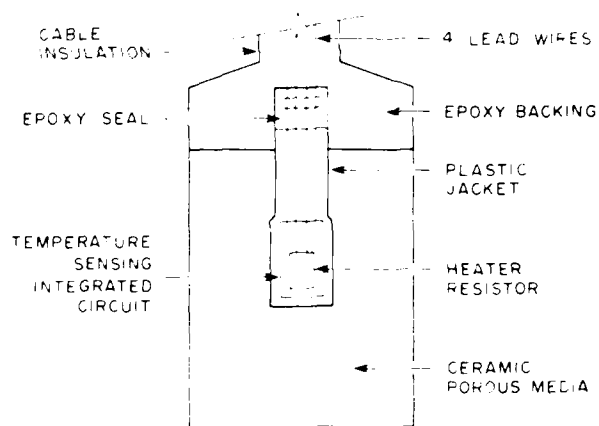
Fig. 8 Matric Suction Contours along a Railway Embankment (From Krahn, Fredlund, and Klassen, 1987)

is shown in Figure 9 together with a cross-section of a sensor. The height of the pressure chamber was increased in order to provide several circular holes along the chamber wall. The holes are used to connect several sensors to the read-out device or data acquisition system. Several sensors are first installed in a soil mixture which is placed on the pressure plate. A desired matric suction, $(u_a - u_w)$, is then applied to the soil mixture by applying an air pressure, u_a , and maintaining a zero water pressure below the ceramic disc. The pore-water will flow out from the soil mixture and collect in a volume change indicator. The water outflow will cease when equilibrium is attained. During calibration, the pressure plate setup is contained within a temperature controlled box. The response of each sensor is monitored periodically until equilibrium is achieved. The reading at equilibrium is used in the calibration of the sensor. The above procedure is repeated for various applied matric suctions to provide a calibration curve (Fredlund and Wong, 1989).

A thorough calibration study on AGWA-II thermal conductivity sensors has been completed recently at the University of Saskatchewan, Canada (Wong and Ho, 1987). The AGWA-II sensors used in the study were manufactured by Agwatronics Incorporated, Merced, California, U.S.A. Typical results indicate a non-linear calibration curve



a) Modified Pressure Plate Apparatus



b) Cross-section of Sensor

Fig. 9 Pressure Plate Setup for Calibrating Thermal Conductivity Sensors (From Wong and Ho, 1987)

which may be approximated by a bilinear curve as illustrated in Figure 10. The breaking point of the calibration curve was found to be around 175 kPa. It has been found that relatively accurate measurements of matric suctions can be expected from the AGWA-II sensor in the range of 0 to 175 kPa. Matric suction measurements above 175 kPa correspond to a steeper calibration curve with a lower sensitivity. In general, the sensors also produced consistent and stable output with time. There were, however, situations where difficulties were encountered with the sensors and these are described by Wong et al (1989).

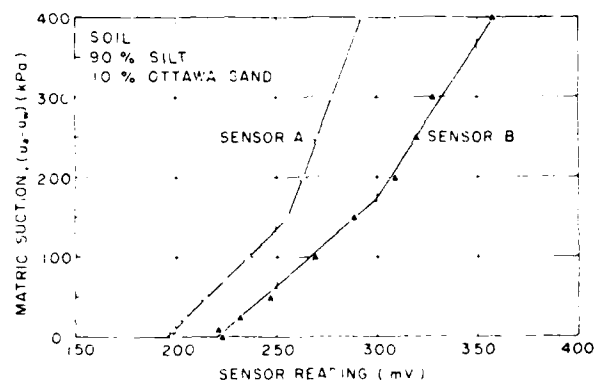


Fig. 10 Calibration Curves for Two AGWA-II Thermal Conductivity Sensors from Agwatronics Incorporated (From Wong and Ho, 1987)

The AGWA-II thermal conductivity sensors have been used for laboratory measurements of matric suction on numerous soils. Figure 11 shows the results on a highly plastic clay from Sceptre, Saskatchewan, Canada. The measurements were performed using two sensors. One sensor was initially saturated while the other sensor was initially dry. The responses of both sensors were monitored immediately and at various elapsed times after their installation. The results indicate that the equilibrium time required for the initially dry sensor is less than the equilibrium time for the initially saturated sensor. The initially dry sensor required about 4 days to equilibrate, whereas the initially wet sensor required about 16 days.

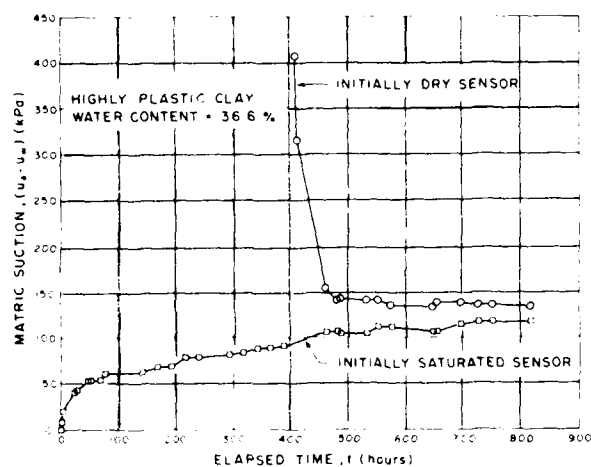


Fig. 11 Laboratory Measurements of Matric Suction Using the AGWA-II Thermal Conductivity Sensors

The results from several other laboratory tests using the AGWA-II sensors are shown on the following figures. The results shown in Figures 12, 13 and 14 were from samples of highly plastic Regina Clay. The samples were from below the floor slab of Darke Hall in Regina, Saskatchewan and were supplied by Clifton Associates, Regina. In each case initially wet and dry sensors were placed in opposite ends of undisturbed, 3 and 1/2 inch diameter shelly tube samples. The equilibrium suctions for both sensors in each sample are similar. The measured matric suctions show a direct relationship to their natural water content.

On another study, a large number of undisturbed samples were taken from the

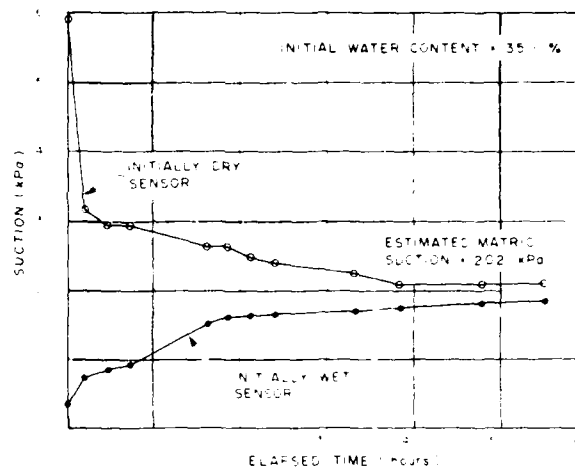


Fig. 12 Matric Suction Measurements on Regina Clay from a Depth of 0.52 Metres

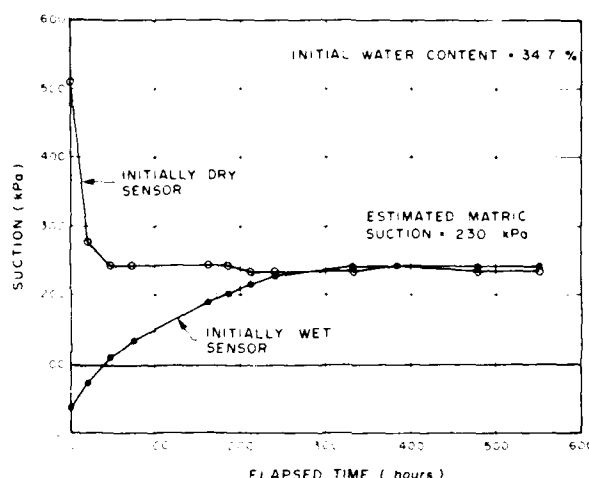


Fig. 13 Matric Suction Measurement on Regina Clay from a Depth of 4.65 Metres

Lake Agassiz clay below the railway in Winnipeg, Manitoba. The results were corrected for the effect of overburden unloading during sampling and then plotted as negative pore-water pressures in Figure 15. The average matric suction was 99 kPa in the upper 4 meters. The suction then decreased to zero at 5 and 1/2 meters, the depth at which the groundwater table was measured in the field. The samples were from a number of boreholes along a section of the railway and do not necessarily depict the variation that may be found in single boreholes.

The AGWA-II sensors have also been used for measuring matric suction in a highway test track with a controlled

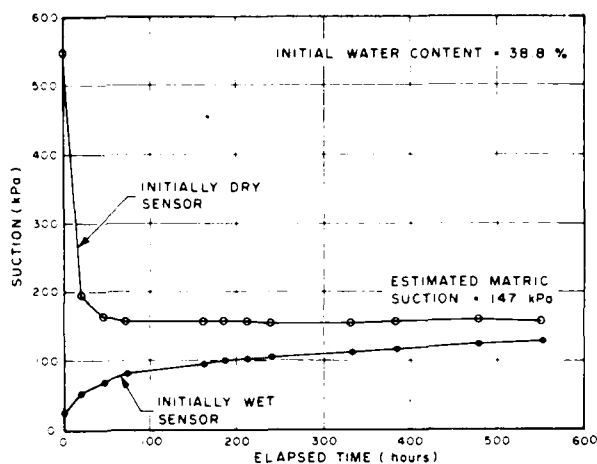


Fig. 14 Matric Suction Measurement on Regina Clay from a Depth of 1.03 Metres

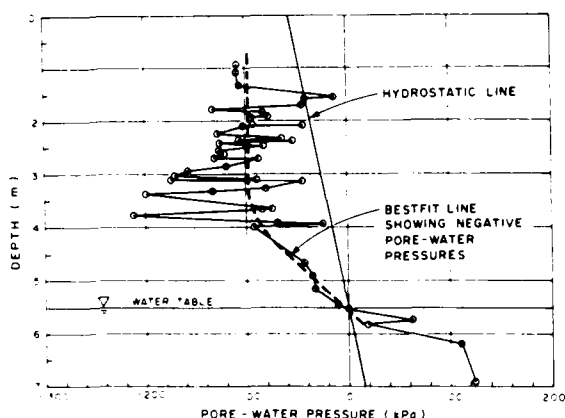


Fig. 15 Negative Pore-water Pressure Data for Undistributed Samples from Lake Agassiz Clay near Winnipeg (Clifton, Lam and Sattler, 1988)

environment (i.e., controlled temperature and humidity). Typical results on a glacial till subgrade are presented in Figure 16. The measured matric suctions are constant with time and the water contents show a reasonable decrease in matric suction with respect to depth and water content.

TOTAL SUCTION MEASUREMENTS

Two techniques have been used to measure the total suction in a soil; namely, the use of psychrometers and filter paper.

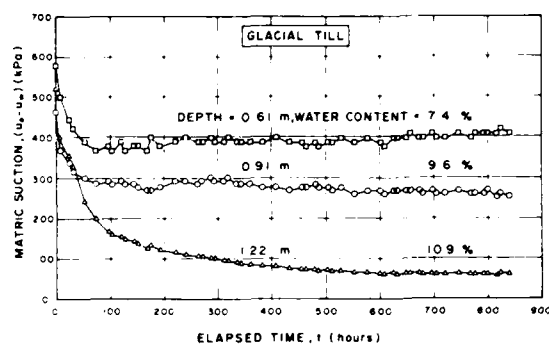
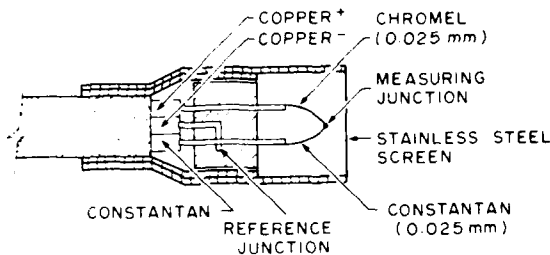


Fig. 16 Field Measurements of Matric Suction Using the AGWA-II Thermal Conductivity Sensors under Controlled Environments

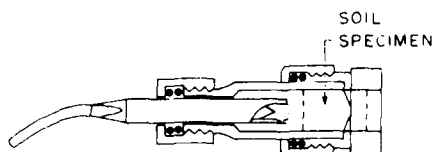
PSYCHROMETERS

Thermocouple psychrometers are used to measure the total suction in a soil by measuring the relative humidity, RH, in the soil. Total suction is related to relative humidity in accordance with Equation 1. Details of the thermocouple psychrometer are shown in Figure 17a. The measurements of total suction are conducted by placing a soil specimen in a small chamber together with the psychrometer (Figure 17b). The relative humidity is then measured after equilibrium is attained between the air near the psychrometer and the pore-air in the soil. Equilibrium at relative humidities approaching 100 percent are difficult to obtain since the slightest lowering of temperature may cause condensation of water vapor. The lower limit of total suction measurements using a psychrometer is approximately 100 kPa under a controlled temperature environment. At 100 kPa, a controlled temperature environment of $\pm 0.001^\circ\text{C}$ is required in order to measure total suctions to an accuracy of 10 kPa (Krahn and Fredlund, 1972). The thermocouple psychrometer is capable of measuring total suctions up to 8000 kPa (Edil and Motan, 1984). Therefore, psychrometers can be used for measuring high suctions in soils from arid regions. In situ measurements of total suctions using psychrometers are not recommended because of significant temperature fluctuations which occur in the field. However, laboratory measurements can be conducted in a controlled temperature environment using undisturbed soil specimens from the field. The specimens should not be covered with hot wax

following sampling, since temperature changes alter the relative humidity in the soil. Figure 18 illustrates measurements of total suctions on soil samples from various depths at a location near Regina, Saskatchewan, Canada.



a) Thermocouple Psychrometer Details



b) Chamber with Soils Specimen and Psychrometer

Fig. 17 Details of Thermocouple Psychrometer Manufactured by J.R.D. Merrill Specialty Equipment, Logan, Utah, U.S.A.

Filter Paper

Theoretically, the filter paper method can be used to measure the total or matric suction of a soil. The method is based on the assumption that a filter paper can come to equilibrium (i.e., with respect to water flow) with a soil having a specific suction. The equilibrium can be reached by water exchange between the soil and the filter paper in a liquid or vapor form. When a dry filter paper is placed in contact with a soil specimen, moisture flow takes place from the soil to the paper until equilibrium is achieved (Figure 19). When a dry filter is suspended above a soil specimen (i.e., no contact with the soil) the vapor flow of water should occur from the soil to the paper until equilibrium is obtained (Figure 19). Having established equilibrium con-

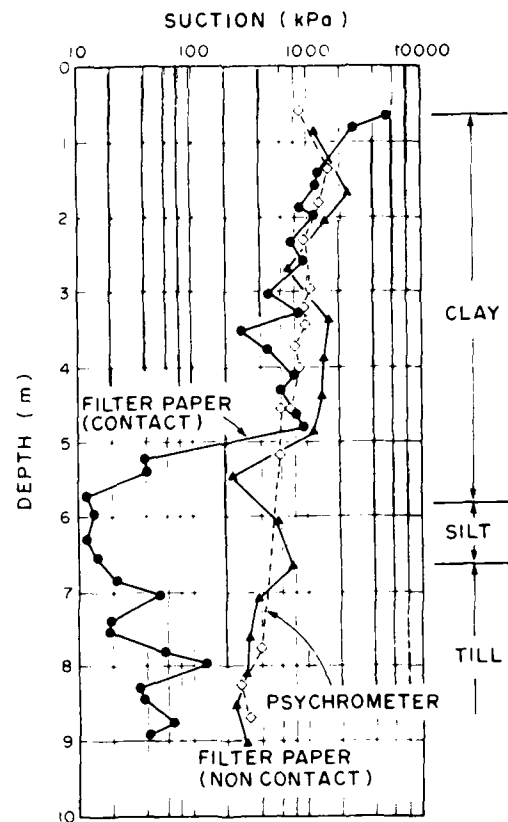


Fig. 18 Suction Profile Versus Depth Obtained Using Thermocouple Psychrometers and the Filter Paper Method (From van der Raadt, Fredlund, Clifton, Klassen and Jubien, 1987)

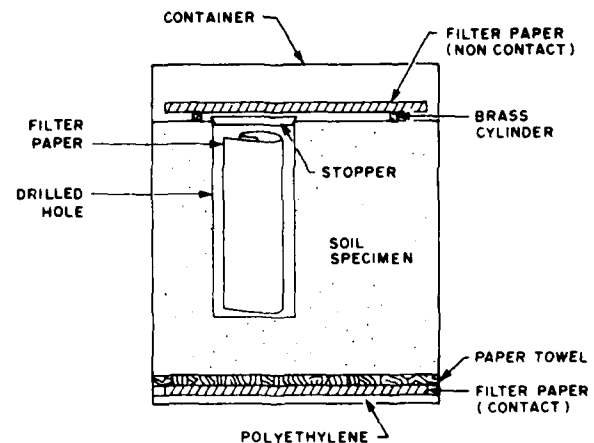


Fig. 19 Contact and Non-contact Filter Paper Method for Measuring Matric and Total Suctions, respectively (From Al-Khafaf and Hanks, 1974)

ditions, the water content in the filter paper can be measured. The filter paper water content is related to a suction value through use of the filter paper calibration curve as illustrated in Figure 20. Theoretically, the equilibrium water content of the filter paper corresponds to the soil matric suction when the paper is placed in contact with the soil and liquid flow occurs. On the other hand, the equilibrium water content of the filter paper corresponds to the total suction of the soil if the paper is not in contact with the soil and only vapor flow occurs. The filter paper method can be used to measure almost the entire range of suctions.

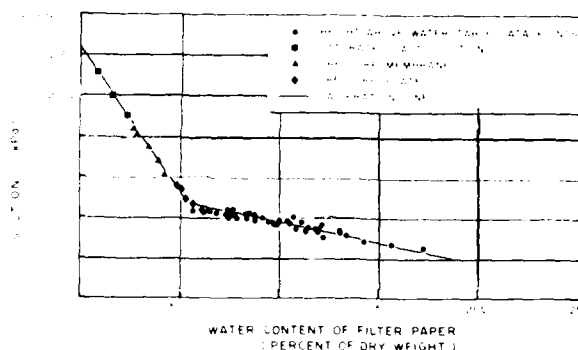


Fig. 20 A Typical Calibration Curve for Filter Paper (From McQueen and Miller, 1968)

A comparison between the results of suction measurements using filter papers and psychrometers is shown in Figure 18. The results from the non-contact filter paper agreed closely with the psychrometer results indicating that total suction was measured.

However, the contact filter paper did not exhibit consistent results with respect to depth. This is believed to be due to poor contact between the filter paper and the soil specimen that resulted in the total suction being measured instead of the matric suction (i.e., in the depth range of 0 to 5 m in Figure 18).

In other words, it is difficult to ensure good contact between the soil and the filter paper. For this reason, total suction will generally be measured when using the filter paper technique.

Figure 21 shows the results of filter paper measurements of total suction on a highly plastic clay from Eston, Saskatchewan (Ching and Fredlund,

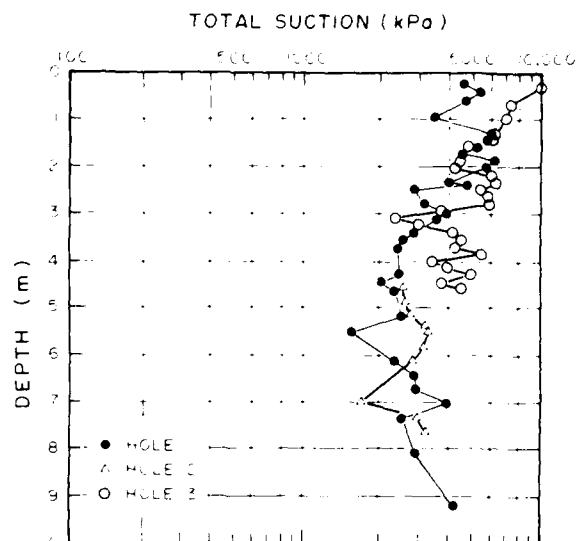


Fig. 21 Total Suction Profile for Eston Clay Using the Filter Paper Technique

1984). While augering 3 boreholes, water content samples were taken at about 1 foot (0.3 m) intervals. Three filter papers were included in each glass, water content container and specimens were allowed to equilibrate for one week. The measured suction on the highly swelling clay ranged from 2000 to 6000 kPa. Although there is no direct confirmation of these measurements, they appear to be reasonable for the Eston Clay deposit.

It may be possible to use the filter paper technique for insitu measurements of (total) suction. A proposed scheme for measuring suctions in subgrade soils is shown in Figure 22. The filter papers would be left in-place for about one week and then removed for the measurement of its water content. New filter papers could then be installed and allowed to equalize for another week. Although this scheme has not been used to-date, it appears to have possibilities as a low cost, approximate technique to evaluate suction.

It should be emphasized that the filter paper technique is highly user dependent and great care must be taken in measuring the water content of the filter paper. The balance must be able to weigh to the nearest 0.0001 gram. Each dry filter paper weighs about 0.52 grams and at a water content of 30%, the weight of water in the filter paper would be 0.16 grams.

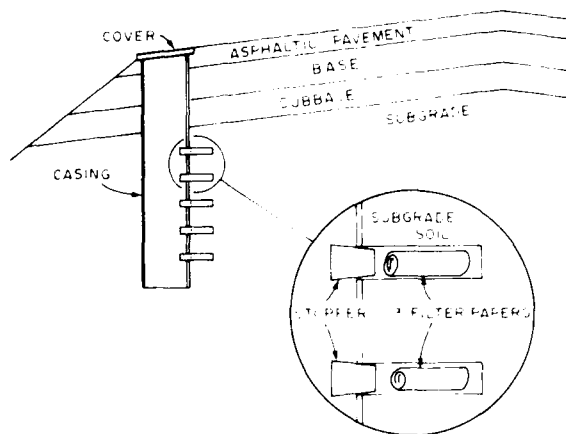


Fig. 22 Proposed Scheme Using Filter Papers to Measure Total Suction

In general, the filter paper appears to provide more of an indication of the suction magnitude in the soil rather than an absolute value. Further research may lead to improvements in the technique.

OSMOTIC SUCTION MEASUREMENTS

Several procedures can be used to measure the osmotic suction of the soil. For example, it is possible to add distilled water to a soil until the soil is in a fluid condition, then drain off some effluent, measure its conductivity and linearly extrapolate the osmotic suction back to the natural water content conditions. This is known as the saturation extract procedure. Although the procedure is simple, it does not yield an accurate measurement of the osmotic suction but this procedure, likewise, gives poor results. It is the pore fluid squeezer technique that has proven to give reasonable measurements of matric suction.

Pore Fluid Squeezer

The osmotic suction of a soil can be determined by measuring the electrical conductivity of pore-water from the soil. Pure water has a low electrical conductivity in comparison to the pore-water that contains dissolved salts. Therefore, the electrical conductivity of the pore-water from the soil can be used to indicate the total concentration of dissolved salts which is related to

the osmotic suction of the soil. The pore-water in the soil can be extracted using a pore fluid squeezer which consists of a heavy-walled cylinder and piston squeezer (Figure 23). The electrical resistivity (or electrical conductivity) of the pore-water is then measured. A calibration curve (Figure 24) can be used to relate the electrical conductivity to the osmotic pressure of the soil.

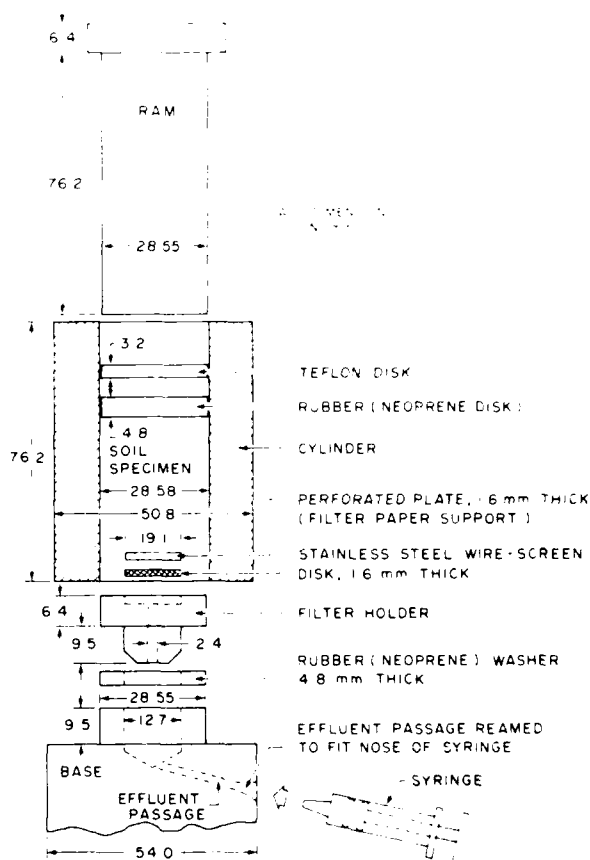


Fig. 23 Pore Fluid Squeezer (From Manheim, 1966)

SUMMARY

Several devices for measuring total, matric, and osmotic suctions have been described in this paper. Techniques and limitations associated with each device are outlined. More research is required on the measurement of suction. However, it is now possible to measure the components of soil suction for engineering projects. The best procedures and devices vary, depending primarily upon the range of suction being measured and the accuracy required.

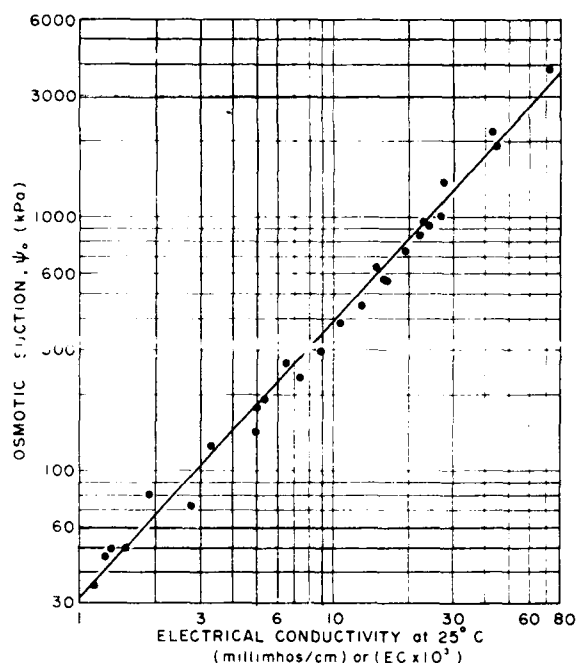


Fig. 24 Osmotic Pressure Versus Electrical Conductivity Relationship for Pore-water Containing Mixtures of Dissolved Salts (From USDA Agricultural Handbook No. 60, 1950)

REFERENCES

- Al-Khafaf, S. and R.J. Hanks. (1974). "Evaluation of the filter paper method for estimating soil water potential". *Soil Sci.* 117, pp. 194-199.
- Bocking, K.A. and Fredlund, D.G. (1980). "Limitations of the Axis-Translation Technique", *Proc. of the 4th Int. Conf. on Expansive Soils*, Vol. I, pp. 117-135.
- Ching, R.K.H. and Fredlund, D.G. (1984). "A Small Saskatchewan Town Copes with Swelling Clay Problems", *Proc. of the Fifth International Conference on Expansive Soils*, Adelaide, South Australia, May 21-23, pp. 306-310.
- Clifton, A.W., Lam, L.W. and Sattler, P.J. (1988). "Embankment Instability, Investigation and Analysis, Emerson Subdivision, Winnipeg, Manitoba", A Report to Canadian Pacific Railways Ltd., Prepared by Clifton Associates Ltd. and the University of Saskatchewan Geotechnical Group, July, 29 p.
- Edil, T.B. and Motan, S.E. (1979). "Soil-Water Potential and Resilient Behavior of Subgrade Soils", *Transportation Research Record* 705, TRB, National Research Council, Washington, D.C., pp. 54-63.
- Fredlund, D.G. and Wong, D.K.H. (1989). "Calibration of Thermal Conductivity Sensors for Measuring Soil Suction", *ASTM Geotechnical Testing Journal* (In Press).
- Fredlund, D.G. and Rahardjo, H. (1988). "State-of-Development in the Measurement of Soil Suction", *Proc. of the International Conference on Engineering Problems on Regional Soils*, Beijing, China, Aug. 11-15, 1988, pp. 582-588.
- Fredlund, D.G. and Rahardjo, H. (1987). "Soil Mechanics Principles for Highway Engineering in Arid Regions", *Transportation Research Record* 1137, Soil Mechanics Considerations in Arid and Semiarid Areas, Transportation Research Board, pp. 1-11.
- Hilf, J.W. (1948). "Estimating Construction Pore Pressures in Rolled Earth Dams", *Second Int. Conf. on Soil Mech. and Fdn. Eng.*, Rotterdam, Vol. III, pp. 234-240.
- Krahn, J., D.G. Fredlund, and M.J. Klassen. (1987). "The effect of soil suction on slope stability at Notch Hill". *Proc. 40th Can. Geotech. Conf.*, Regina, Saskatchewan.
- Krahn, J. and Fredlund, D.G., (1972). "On Total, Matric and Osmotic Suction", *Soil Science*, Vol. 114, No. 5, pp. 339-348.
- Manheim, F.T. (1966). "A hydraulic squeezer for obtaining interstitial water from consolidated and unconsolidated sediment". *U.S. Geol. Survey Prof. Paper* 550-C, pp. 256-261.
- McQueen, I.S. and R.F. Miller. (1968). "Calibration and evaluation of a wide range method of measuring moisture stress". *J. Soil Sci.* Vol. 106, No. 3, pp. 225-231.
- Phene, C.J., G.J. Hoffman and S.L. Rawlins. (1971). "Measuring soil matric potential in situ by sensing heat dissipation within a porous body: I. Theory and Sensor Construction. II.

Experimental Results". Soil Sci. Soc. Amer. Proc. 35, pp. 225-229.

Pufahl, D.E. (1970). "Evaluation of Effective Stress Components in Non-Saturated Soils", M.Sc. Thesis, University of Saskatchewan, Saskatoon, Canada.

U.S.D.A. Agricultural Handbook No. 60. (1950). "Diagnosis and improvement of saline and alkali soils".

van der Raadt, P., D.G. Fredlund, A.W. Clifton, M.J. Klassen and W.E. Jubien. (1987). "Soil suction measurement at several sites in western Canada." Transportation Research Record 1137, Soil Mechanics Considerations in Arid and Semiarid Areas, Transportation Research Board, pp. 24-35.

Wong, D.K.H. and A. Ho, (1987). "An evaluation of a thermal conductivity sensor for the measurement of soil matric suction". Internal Report, Dept. of Civil Engineering, University of Saskatchewan, Saskatoon, Saskatchewan, Canada.

Wong, D.K.H., Fredlund, D.G., Imre, E. and Putz G. (1989). "Evaluation of AGWA-II Thermal Conductivity Sensors for Soil Suction Measurements", presented to Transportation Research Board, Washington, D.C., January.

MEASUREMENT OF IN-SITU PORE PRESSURES

J.B. Sellers

President, Geokon, Inc.

ABSTRACT

Excess pore water pressures can be the cause of instability in soils.

In freezing and thawing ground, ice dams may be formed which impede the free drainage of the soils and create unstable conditions.

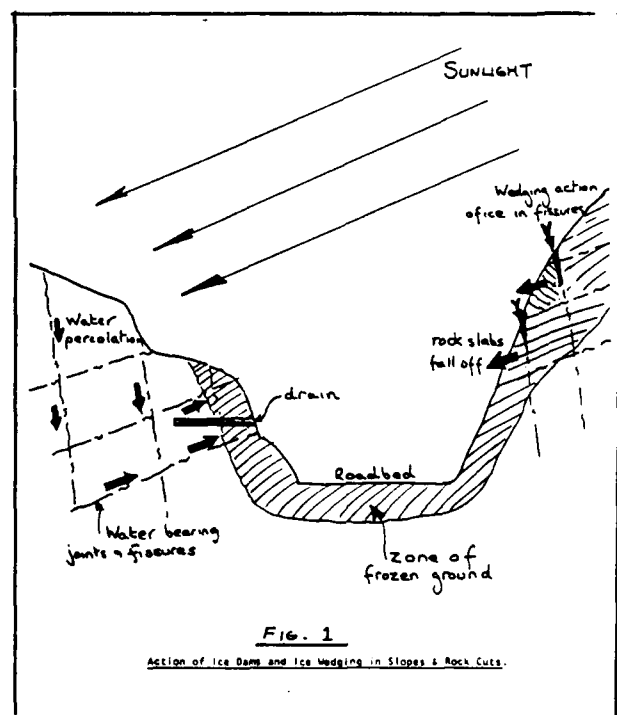
Observation wells and standpipe piezometers in conjunction with simple dipmeters are useful in monitoring the level of the local water table. In-situ pore pressures, at particular locations, can be measured using piezometers operating with either pneumatic, vibrating wire or electrical strain gage type transducers.

Care must be taken to ensure that measured pore water pressures are not influenced by the type of piezometer selected, nor by the type of filter stone, nor the method of installation. Steps should be taken to ensure that piezometers are not damaged by the freezing process. Certain types of piezometers are more suitable for automatic data acquisition.

1. Introduction

Soil stability is markedly influenced by pore water pressures; the effect being to reduce the cohesive strength, according to the well-known Coulomb formula, by reducing the effective stress between adjacent soil particles. This effect is enhanced in freezing and thawing cycles by the presence of ice dams which prevent free drainage of the ground water. In hilly terrain, ground water pressures may build up to dangerous levels behind ice

dams. (Fig. 1.)



2. Ground Water Regime

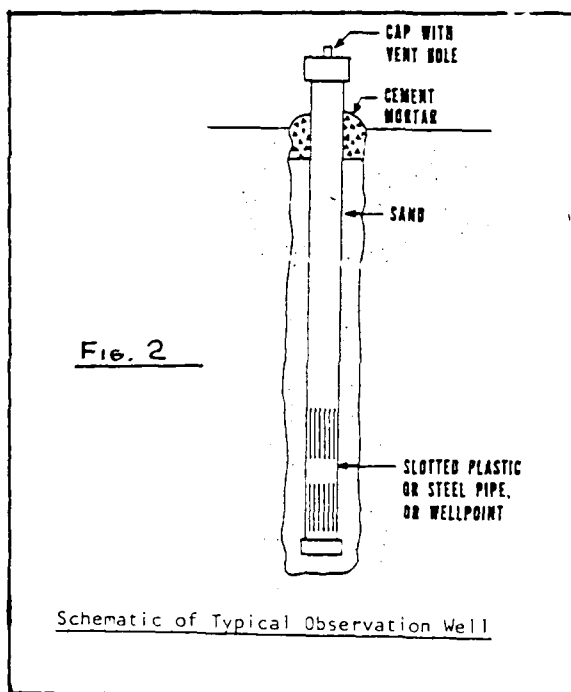
It is often useful to measure the

prevailing ground water levels in the surrounding locality since this will give a knowledge of ground water flow patterns and will provide a base against which to compare pore pressures at specific locations.

Observation wells and open standpipe piezometers are often selected for this purpose on account of their inherent simplicity and reliability.

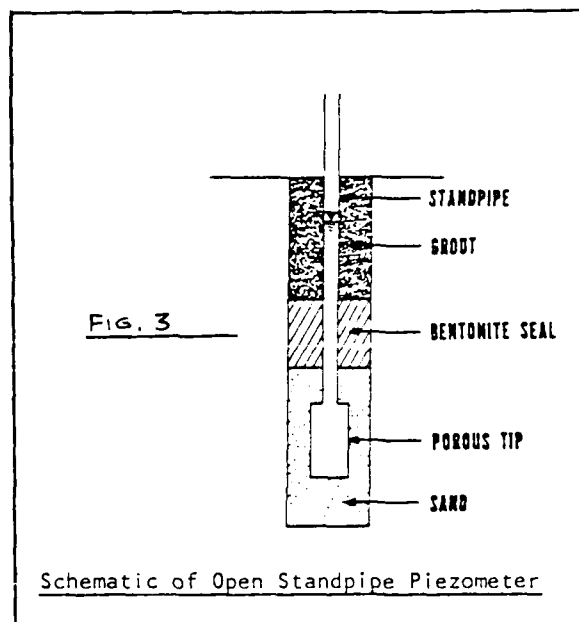
2.1 Observation Wells

Wells, i.e., unsealed boreholes, (Fig. 2) are not recommended since they only work well in continuously permeable strata. Elsewhere, they can connect otherwise isolated ground water regimes and disturb the normal drainage patterns.



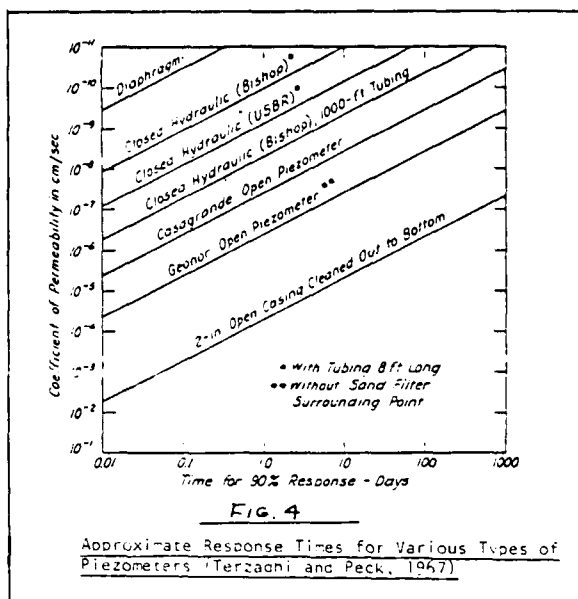
2.2 Open Standpipe Piezometers

Use PVC or ABS pipes (flush coupled) with a porous filter at the bottom to allow water to enter (Fig. 3). The standpipe is sealed into the borehole using bentonite pellets or grout so that the pore water pressure is measured only in the ground immediately opposite the sand zone around the filter.



Open standpipe piezometers are very reliable, but suffer from some disadvantages: a) they are susceptible to freezing and may require the use of oil or antifreeze if they are to be kept open during cold weather, b) they require a somewhat laborious, manual readout procedure, using a dipmeter and c) they have a long hydrostatic time lag in soils of low permeability.

This last consideration is important: all piezometers require flow of pore water to or from the device before the pressure changes can be sensed. A diaphragm type piezometer whether pneumatic, vibrating wire or electrical requires only very small flows sufficient only to depress the diaphragm by a few thousandths of an inch, whereas an open tube standpipe would require much greater amounts to raise or lower the water level inside the pipe. The time required to reach equilibrium with open tube types can be very long (Fig. 4).



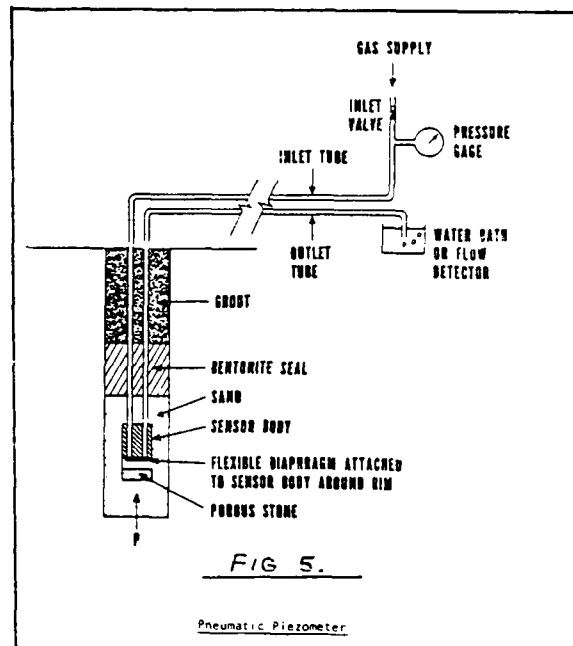
3. Pore Water Pressures

These are best measured by means of diaphragm type devices which have small hydrodynamic time lags and are better able to follow rapidly fluctuating pore pressures. These devices are installed in a manner which isolates them in the zone to be monitored using watertight seals usually made from bentonite but occasionally by means of inflatable packers.

3.1 Pneumatic Piezometers

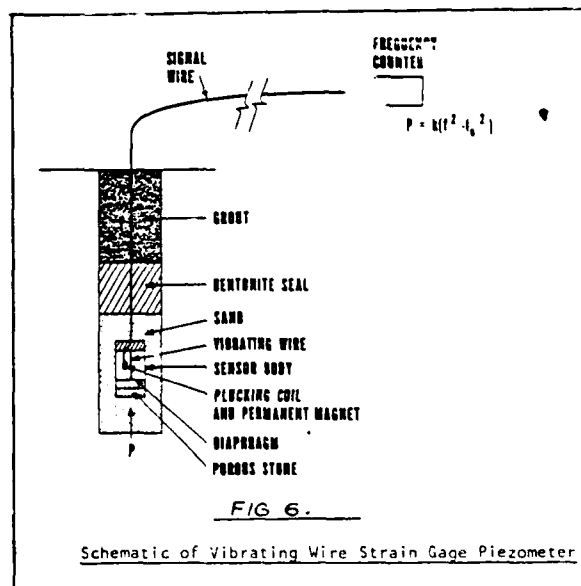
Various styles of pneumatic piezometers exist. The basic principle calls for the pore water pressure to hold a check valve either closed or open (Fig. 5). Pressure is applied to the other side of the check valve by means of a compressed gas. At the point of equalization between the pressure in the gas and the pore water pressure, the check valve opens or closes, allowing or preventing gas flow in the system. When this occurs, the gas pressure is read by means of a pressure gage or pressure transducer. Advantages of this type lie in an ability to resist freezing and in not being susceptible to lightning damage. Disadvantages are a somewhat cumbersome read-out process which is not easily adapted to automatic data acquisition systems (ADAS). Also, tubes leading to the piezometer tip can become clogged, pinched or water-logged and with big tube lengths,

pressure losses in the lines can become significant. They cannot easily measure negative pore water pressures, and are not suitable for dynamic measurements.



3.2 Vibrating Wire Piezometers

Pore pressures act on a diaphragm the deflection of which is measured by means of a vibrating wire (Fig. 6).



The resonant frequency of vibration of the

wire alters as the water pressure changes. The sensor is actually a mechanical one, i.e., a length of tensioned music wire, and this gives the device its excellent long-term stability. Another advantage accrues from the fact that the output is a frequency which is easily transmitted over long cables and is not easily degraded by ingress of moisture. The readout is rapid and is adaptable to ADAS systems capable of handling frequencies and supplying the correct excitation input to the sensor. Disadvantages are a susceptibility to lightning damage. Also, they are unsuitable for the measurement of rapid dynamic changes since the readout procedure requires a length of time (several milliseconds) to measure the frequency. They can be damaged by freezing if precautions are not taken. Where diaphragm style piezometers are used to measure very small pore pressure changes accurately, it will be necessary to compensate for barometric pressure changes. This can be done in two ways, either a second transducer can be used to read barometric pressures only, and readings used to apply a correction, or the inside of the piezometer can be vented to the atmosphere by means of a fine tube inside the cable.

3.3 Electrical Piezometers

Pore water pressures cause deflections of a diaphragm to which electrical strain gages are attached. Resistance changes in the strain gages alter the voltage output from a Wheatstone Bridge network. Advantages are a rapid response time making them suitable for dynamic measurements. Disadvantages are a susceptibility to freezing, lightning, barometric pressure changes and to cable effects caused by long cables and moisture penetration. In recent years the Druck pore pressure transducer has achieved some prominence and a reputation for high accuracy.

4. Installation Procedures

4.1 Boreholes

Most piezometers are installed in boreholes and a variety of methods are in use. [Dunnicliff] The intent is to create a sand zone immediately around the piezometer tip and to seal this zone by filling the rest of the borehole with bentonite, either in pellet form

or in the form of bentonite cement grout. Several piezometers can be installed in one borehole but the procedure requires great skill to avoid interconnections between the various zones.

4.2 Fills

Piezometer installations in fills often requires protection from construction equipment, particularly the cable which may be placed in trenches and back-filled around with fine grained material. Care and attention must be paid to every part of the cable (or tubing) and particularly to those parts which could be affected by differential soil movements. Migration of water along the trenches can be prevented by bentonite plugs.

4.3 Soft Ground

In soft ground it may be possible to push the piezometer directly into the ground. For this purpose, the piezometer housing is provided with a point and has a thread to couple it to either drill rods or water pipe. The act of pushing the piezometer into the ground may cause high pressures at the piezometer tip so it is wise to read diaphragm type piezometers during installations and allow time for excess pressures to dissipate should they build up during installation.

5. Automatic Data Acquisition System (ADAS)

All dataloggers are easily connected to electrical style piezometers with voltage excitation and output. Several dataloggers are on the market which can also be connected to vibrating wire types. In all cases, it is very important to include lightning protection as part of the package. Pneumatic piezometers can be connected to ADAS via pressure transducers but the need for a constant and reliable compressed gas source can be a problem.

Conclusion

In-situ pore pressure can be measured in a variety of ways. When choosing a device or technique consideration should be given to such things as hydrostatic time lag, susceptibility to freezing, lightning and barometric pressure changes, ease of readout, adaptability to ADAS.

Installation procedures should be carefully observed to avoid damage to

cables/tubes and to avoid leakage paths.

Ref.

Dunnicliffe, J. - Geotechnical
Instrumentation for Monitoring of Field
Performance. John Wiley 577 pp.

In-situ Measurement of Soil Water Content in the Presence
of Freezing/Thawing Conditions

John L. Nieber, Department of Agricultural Engineering
University of Minnesota

John M. Baker, Department of Soil Science, USDA-ARS
University of Minnesota

ABSTRACT

Numerous methods are available for in-situ measurement of soil water content. These methods include techniques that either measure soil water content directly or measure soil matric potential and then infer soil water content. Methods available for measuring soil matric potential include tensiometry, electrical resistance, thermocouple psychrometry, and thermal diffusivity. Methods available for direct measurement of soil water content include neutron scattering, gamma attenuation, x-ray attenuation, nuclear magnetic resonance, time domain reflectometry, and thermal conductivity. The principles underlying the various soil water measurement methods are presented. Problems associated with measuring soil water content under freezing/thawing conditions are emphasized.

INTRODUCTION

Soil water is important in numerous physical processes of the environment. For instance, it is important in determining surface runoff generation, ground water recharge, the freezing/thawing rate of soils, and deformation of soils under load. The movement of soil water and the status of soil water content can be predicted using mathematical models. However, to develop and/or test these models, in-situ soil water content must be measured.

Soil water is usually quantified according to one of the following definitions:

θ_w = weight basis water content,

θ_v = volume basis water content,

$\theta_v = \theta_w \rho_d$, and

ρ_d = dry bulk density of the soil.

These definitions apply specifically to soil materials that do not undergo significant volume changes over time. Thus these definitions do not apply to soils with high shrink/swell potential. For soils having high shrink/swell potential the

following definition for soil water content is often used (Philip, 1969a,b).

$$\theta = (1 + e) \theta_v \quad (1)$$

where θ is the moisture ratio defined as the volume of water per volume of soil particles; and e is the void ratio, defined as the volume of voids per volume of soil particles.

Numerous methods for measuring soil water content are available, including one direct method and numerous indirect methods. The indirect methods include those that yield soil water content directly, and those that yield soil matric potential from which soil water content is inferred.

The purpose of this paper is to comprehensively review the various methods for measuring soil water content. The accuracy of the various methods and their performance when the soil is in a partially or completely frozen condition are given emphasis.

The description of individual methods is brief since cited references are given that provide additional details. Detailed descriptions of the principles underlying various methods and the materials and procedures for implementing various methods are provided by Klute (1986).

SOIL WATER MEASUREMENT METHODS

Methods for measuring soil water content can be categorized as providing either a direct or an indirect measure of soil water content. The only method for acquiring a direct measure of soil water content is the gravimetric method. Indirect methods can be put into two categories. In one category the soil water content is obtained by measuring a property directly related to soil water content.

This category includes the methods of neutron scattering, gamma attenuation, x-ray attenuation, nuclear magnetic resonance, time domain reflectometry, and thermal conductivity. In the other category the soil matric potential is measured and then the soil water content is inferred from the soil matric potential value.

Direct Methods

The only direct method of measuring soil water content is the gravimetric method. This involves the collection of a sample of soil and measuring sample weight and volume before and after drying of the sample. Water content with this method can be expressed either on a weight or a volume basis. Determination of the volume basis of soil water content requires that the dry bulk density of the soil be known.

The collection of the soil sample for the gravimetric method is simple if the dry bulk density of the sample does not have to be determined. However, if the dry bulk density is needed the volume of the sample has to be measured. To determine this volume requires that great care be exercised to avoid compression of the soil sample during sampling. A number of sampling methods available to avoid sample compression are described by Blake and Hartge (1986).

The gravimetric method is the most accurate method for determining soil water content. However, it is destructive, which prevents repeated sampling of the same area over time. This aspect greatly restricts use of the gravimetric method for monitoring soil water content beneath pavements. Because of this its use for monitoring soil water content beneath pavements is limited to the

calibration and validation of other methods for measuring soil water content.

Indirect Methods

With indirect methods of soil water content measurement, soil water content is determined by measuring properties related to soil water content. Indirect methods can be placed into two categories. In Category I the soil water content is uniquely related to the property being measured. These methods provide more of a "direct" measure of soil water content than methods belonging to Category II. In Category II the soil matric potential is measured and then soil water content is inferred based on the relationship between soil matric potential and soil water content. Since this relationship is not necessarily unique, Category II methods will not provide as "direct" a measure of soil water content as Category I methods.

Soil water content determination methods belonging to the two categories will be described in the following

subsections. Category I methods will be described under the heading "soil water content". Category II methods will be described under the heading "soil matric potential".

Soil Water Content

Neutron scattering. The neutron scattering method is based on the phenomenon of the slowing of fast neutrons by hydrogen atoms. In this phenomenon, some of the neutrons emitted by a radioactive source collide with hydrogen atoms in the soil surrounding the radioactive source. In the collision, a neutron is slowed, or thermalized. Fast neutrons colliding with other types of atoms are also slowed, but hydrogen is particularly efficient at slowing fast neutrons. The problem then becomes one of detecting and counting the number of neutrons that are slowed and relating this number to the amount of water present in the soil.

The neutron scattering method is implemented with a neutron probe device as illustrated in Figure 1.

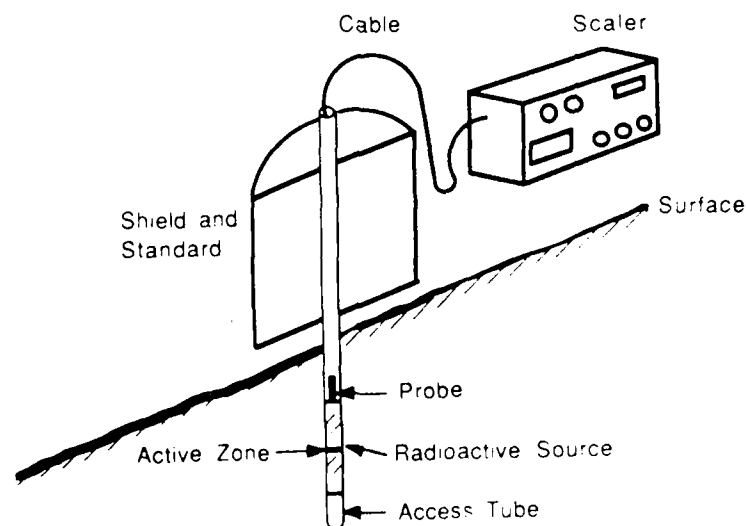


Figure 1. Configuration for the neutron probe.

Usually an access tube is placed in the soil to maintain ready access to the soil profile. The probe contains a radioactive source, usually americium-241/beryllium. Above the source is a tube filled with a boron trifluoride gas. Some of the fast neutrons emitted by the radioactive source are slowed by collisions with hydrogen atoms in the soil surrounding the source. Thermalized neutrons passing into the gas filled tube collide with the boron trifluoride molecules, releasing an alpha particle. The alpha particle is attracted to a negative high-voltage electrode in the detector, and the resulting electrical pulse is counted by a logging instrument. Only thermalized neutrons will produce this electric pulse upon collision with the boron trifluoride molecules.

Since hydrogen atoms in the soil are primarily associated with water molecules, the higher the water content of the soil, the larger will be the number of thermalized neutrons counted by the instrument. However, the neutron probe senses the relative number of hydrogen atoms present in the soil, whether these atoms are associated with water molecules or not.

Some soils have large amounts of hydrogen atoms which are not associated with water molecules. Organic soils are a good example of this type of soil.

Atoms such as beryllium, carbon, nitrogen, oxygen, and fluorine have appreciable efficiency at neutron thermalization, although hydrogen is much more efficient. Atoms with thermalization efficiencies significantly greater than hydrogen include cadmium, boron, lithium, and chlorine.

The neutron probe should be calibrated for each soil where

it is used. The calibration is based on the determination of water content by the gravimetric method when the access tubes are installed. The calibration accounts for indigenous hydrogen atoms present in the soil not associated with water molecules, and for other elements present that affect neutron thermalization. The calibration equation for a neutron probe is linear:

$$\theta_v = A + B (CT/SC) \quad (2)$$

where CT and SC are the count rate and standard count, respectively, of the neutron probe, and A and B are calibration coefficients. The standard count is taken when the source and detector are enclosed in the shield standard illustrated in Figure 1.

The neutron probe measures the soil water content in a spherical region surrounding the source and detector. This sphere has a radius of about 16 cm for conditions near saturation, and about 70 cm radius for near dry conditions (Van Bavel et al., 1956). Regardless of the water content, the neutron probe provides an average value over a fairly large volume. The instrument is, therefore, not adequate when high-resolution of the soil water profile is needed, or when a measurement near a boundary, such as near the subgrade/pavement interface, is needed.

The neutron method works whether the water in the soil is frozen or liquid. The hydrogen atoms in frozen water are detected in the same way as they are in liquid water. Thus, the neutron probe provides a measure of the total water, sum of the frozen and unfrozen volumes, present in the soil.

Gamma attenuation. The gamma attenuation method of soil water measurement is based on the phenomenon of gamma photon absorption by the solid and liquid mass composing the soil. A gamma photon passing through a soil mass will collide with solid or liquid materials or will pass without collision. The higher the density of the soil material, or the higher the soil water content of the soil, the greater the chance that a photon will collide with either solid or liquid materials. For a given dry bulk density of soil, the number of photons passing without collision through a soil mass increases as the soil water content is reduced.

The instrument for implementing the gamma attenuation method is illustrated in Figure 2. The method requires the use of two parallel access tubes. The radioactive source, usually Cesium 137, emits gamma photons and is placed in one of the access tubes. The other access tube contains a photon

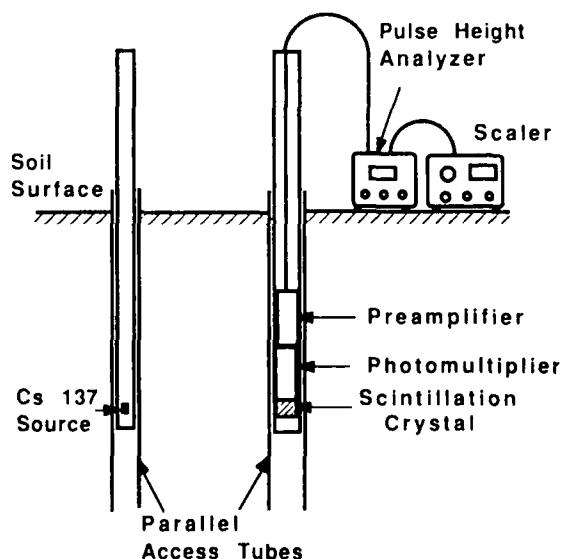


Figure 2. Configuration for the gamma probe.

detector, which consists of electronics and a crystal placed at the same level as the radioactive source. A typical crystal is thallium-activated sodium iodide. When the crystal is struck by a gamma photon a light pulse is produced, which is detected by a photodetector.

The theoretical equation describing the relationship between soil water content and the number of unattenuated photons is given by

$$\theta_v = \frac{\ln\left(\frac{I}{I_0}\right) + X\mu_s\rho_d}{-X\mu_w} \quad (3)$$

where I and I_0 are the count rate and standard count rate of the instrument respectively, X is the distance between the source and the detector, and μ_w and μ_s are the photon attenuation coefficients for water and soil solids.

According to equation (3), using the method requires knowledge of the attenuation coefficients of soil solids and of water, the dry bulk density of the soil, and the value of I_0 . The attenuation coefficients μ_s and μ_w were reported by Van Bavel et al. (1985) to be $0.058 \text{ cm}^2/\text{gm}$ and $0.053 \text{ cm}^2/\text{gm}$ respectively. Values reported by other researchers vary from these values over a 50% range and demonstrate the need to determine these attenuation coefficients for each instrument. The value of I_0 has to be determined for each instrument and must be adjusted to account for the decay of the radioactive source, based on its half-life. Typical values of I_0 for commercially available field instruments are on the order of a 200,000 to 300,000 counts per minute. The dry bulk density of the soil can be determined gravimetrically using standard methods or by using the

procedure described by Van Bavel et al. (1985).

The gamma attenuation method can be used for measuring detailed profiles of soil water content. With current instruments suitable for the field, soil water content can be resolved at about 1 cm depths. Also soil water content can be measured fairly close to boundaries, such as at the interface between a subgrade and the pavement. Measurements made right at the boundary must be interpreted carefully because of photon scattering and escape at the boundary.

If two radioactive sources with distinct energy characteristics are used, the gamma attenuation method can simultaneously measure the dry bulk density water content of the soil. Each source has a unique set of attenuation coefficients for equation (3). The two equations are thereby independent and can be solved simultaneously for dry bulk density and soil water content. This type of instrument is limited to the laboratory because of the high energy levels required of the radioactive sources. For reasons of practicality, the dual-energy technique cannot be used in the field.

Like the neutron probe device, the gamma attenuation device provides a measure of the total water present in the soil. It does not distinguish between frozen and unfrozen soil water.

X-ray attenuation. The method of x-ray attenuation operates on the same principle as the gamma attenuation method. An x-ray source and an x-ray detector are located on opposite sides of an object. The strength of the x-ray beam passing through the object is measured by the detector. The strength of the beam after passing through the object

relative to the strength of the beam at the source is related to the attenuation properties of the object. For a particular type of material, the amount of attenuation is related to the bulk density of the material. The attenuation equation for x-rays has the same form as that given in equation (3) for the gamma attenuation method.

In a CAT (Computer Aided Tomographic) scanner, the x-ray source emits a thin, fan shaped beam. A bank of detectors, opposite the source from the object, measure the strength of the beam passing through the object. Multiple views of the object are obtained by rotating the source and detectors around the object and making measurements at discrete angular positions. The data from these multiple views are used to calculate the attenuation of the x-ray beam in discrete volumes or pixels of the object. The attenuation in each pixel is related to the bulk density of the material in the pixel. CAT scanner machines are now available to provide spatial resolution on the submillimeter scale.

CAT scanners were originally developed for use in medicine to detect tumors and other benign/malignant features in the human body. The typical scanner is doughnut shaped with the x-ray source and detectors located on the inside circumference of the doughnut. A patient is placed on a table that conveys the patient through the doughnut. The table stops at discrete positions for each scan. The resulting set of scans are used to produce two-dimensional images of cross-sections of the patient's body at each of the discrete positions.

In recent years CAT scanners have found applications in many scientific areas including the soil sciences. For scanning of

soils a soil column is placed on the conveyor table and scans of the column are taken at discrete positions. Pixel values obtained in each scan are related to the wet bulk density of the soil contained in each pixel. If the soil sample is dry, then the pixel values provide an image of the distribution of dry bulk density at discrete locations along the soil column. The application of CAT scanner technology to the determination of the dry bulk density distribution in soil columns was first presented by Petrovic et al. (1982). An example application to the determination of the water content distribution in soil columns is presented by Crestana et al. (1985).

When using the x-ray attenuation technique, it is essential that the operator be shielded by lead or leaded glass to prevent exposure to x-ray emissions. For this reason the x-ray attenuation method is restricted to laboratory applications.

Nuclear magnetic resonance. The nuclear magnetic resonance (NMR) technique was originally developed to determine the molecular structure of substances. In recent years it has been extensively applied in medical imaging technology. It can also be used to measure water content of various materials, including soils. The technique is reasonably safe because it does not use radioactive substances or high energy particle bombardment. The major danger associated with the instrument is that very strong magnets are used and care has to be taken when working near loose steel objects.

The NMR technique is based on the principle of measuring the change in spin orientation of atoms when the atoms are placed in a static magnetic

field with a pulsed oscillating magnetic field acting orthogonal to the static field (Gadian, 1982; Zientara and Neuringer, 1988; and Paetzold et al., 1985). Specific atoms respond to the oscillating magnetic field at a specific frequency of oscillation. Hydrogen is the atom best detected by the NMR technique because of its simple atomic structure. Hydrogen associated with different substances can be identified because of the differences in bonding orientation in the substances. The difference between hydrogen associated with ice, liquid capillary water, and liquid water bonded tightly to clay surfaces can be detected.

The main component of a conventional NMR instrument is a hollow cylinder formed by magnets. The sample is placed inside the cylinder. Medical NMR units have this form and the patient lies inside the cylinder while measurements are made. This cylindrical configuration facilitates the acquisition of high-resolution three-dimensional images of the sample.

An NMR instrument for rapid measurement of soil water content in the field has been described by Paetzold et al. (1985). This instrument uses a flat configuration for the magnets in contrast to the cylindrically shaped magnets used in conventional NMR instruments. A loss in accuracy occurs with this flat configuration because the static magnetic field produced is not spatially uniform as it is in the cylindrical configuration. The instrument can simultaneously measure soil water contents at various specified depths. With the instrument mounted on the back of a vehicle, and soil water measurements can be acquired at speeds up to 10.5 mph.

Time domain reflectometry. Time-domain reflectometry (TDR) is a relatively new and promising method for measuring soil water content. The change in the apparent dielectric permittivity of soil is the measured property that is related to volumetric water content. Principal advantages of TDR are that it is insensitive to the effects of temperature, salinity, and bulk density (Topp et al., 1980), which distinguishes it from earlier instruments for measuring soil water content based on changes in soil electrical properties. Furthermore, Topp et al. (1980) found that a single empirical calibration equation applies to a wide variety of soils.

The principle of operation is described in detail by Topp et al. (1980) and Ledieu et al. (1986); an overview of practical application of TDR is given by Topp and Davis (1985). The method uses equipment developed for testing coaxial cables in the telecommunications industry. The TDR unit contains a pulse generator, a sampler that produces a low frequency facsimile of the high frequency output, and an oscilloscope that displays the sampler output. Electromagnetic pulses containing a spectrum of frequencies in the 1 MHz to 1 GHz range are sent down a transmission line that terminates in a parallel pair of steel waveguides embedded in the soil. Any change in impedance along the waveguides causes a partial reflection of the pulse and this reflection is visible on the oscilloscope trace. Thus there is a partial reflection where the waveguides enter the soil, and the remainder is reflected at the end of the waveguides. The travel time of the pulse between these points can be measured on the oscilloscope trace and it is a function of

the relative permittivity of the soil surrounding the waveguides. Relative permittivity is in turn a strong function of the water content, since the relative permittivity of air, dry soil, and water are approximately 1, 4 and 80, respectively.

Figure 3 illustrates the results of a simple test of the method in which the water content of a 20 liter container of Hubbard sand was varied from air dry to near saturation, and measured by gravimetric and TDR methods. Figure 4 illustrates two of the oscilloscope traces from that test, one in dry soil ($\theta_v = 0.016$), and the other in wet soil ($\theta_v = 0.305$). The system can be used in a reasonably small volume of soil, because for typical waveguides spaced 50 mm apart the spatial sensitivity is largely confined to a quasi-elliptical area of approximately 1000 mm² surrounding the waveguide axis (a much limited sensitivity extends to perhaps 4000 mm²), with no significant variation in sensitivity along the length of the waveguides (Baker and Lascano, 1989). The band of influence is narrow, approximately 30-40 mm, in the plane oriented transverse to the waveguides, so the depth resolution of horizontally placed waveguides is nearly as good as that obtained with gamma attenuation.

An important factor in northern climates is that the dielectric constant of ice is approximately 4, very near that of dry soil. Thus freezing of soil affects the apparent dielectric constant of the soil in the same way as drying, so that in partially frozen soils TDR measures unfrozen water content only (Patterson and Smith, 1981; Stein and Kane, 1983). Consequently, simultaneous measurement at a given site with TDR and with a method such as neutron

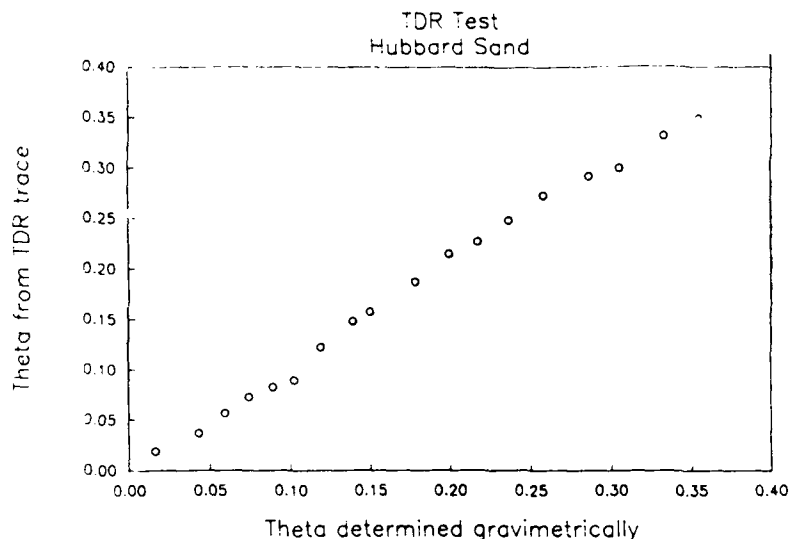


Figure 3. TDR oscilloscope traces in Hubbard sand at two different water contents. The traces are superimposed so that the initial reflections (where the waveguides enter the soil) coincide. The arrows indicate that reflection and the respective final reflections from the end of the waveguides.

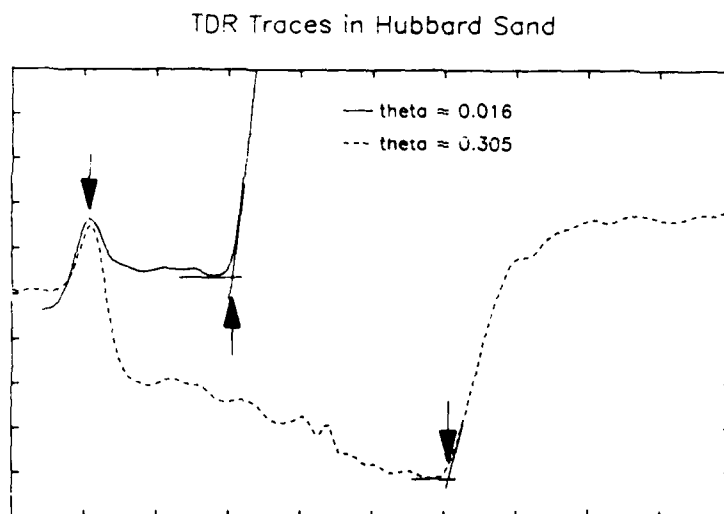
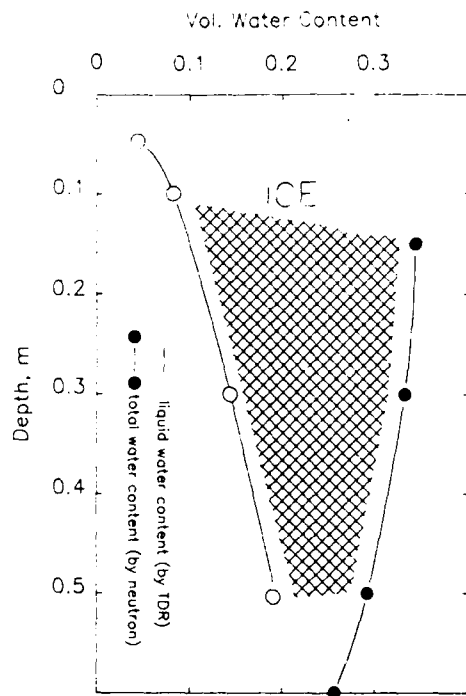


Figure 4. A comparison of volumetric water content obtained with TDR against water content determined from knowledge of initial water content and amount of water added.

scattering or gamma attenuation, that measures the total amount of water present, allows the determination of the ice content of the soil (Figure 5)

The relatively high cost of time-domain reflectometers, approximately \$7000, and

concern about the performance of electrical methods of soil water measurement have probably slowed acceptance of TDR. However, the accuracy of the method, its safety relative to that of nuclear methods, its spatial resolution, and the



Rosemount, MN
February 13, 1989

Figure 5. Profiles of liquid water content ((by TDR) and total water content (by neutron scattering) in Waukegan silt loam. Soil temperatures at the time were -8.1, -5.3, -3.9, and -3.2 degrees Celsius at 0.05, 0.1, 0.3, and 0.5 m, respectively.

successful results obtained by numerous independent research groups suggests that its use will increase considerably in the future.

Thermal conductivity method. The thermal conductivity of a soil is dependent on the soil water content as illustrated in Figure 6. The principle of the thermal conductivity method (De Vries, 1952) is to measure the rate of temperature rise at a point in a soil caused by a heating element placed at that point. This rate of temperature rise is related to the thermal conductivity of the soil, which is related to the soil water content.

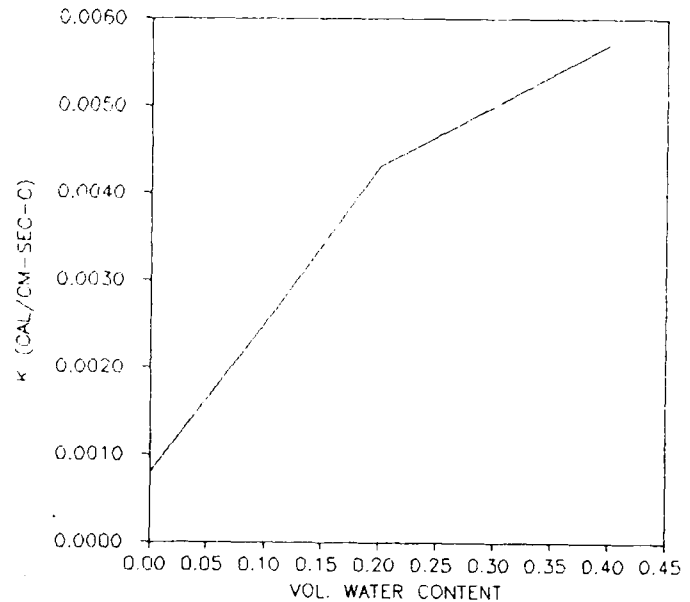


Figure 6. Illustration of the relationship between thermal conductivity and water content.

With the thermal conductivity method a cylindrical probe, usually a glass capillary tube, containing a heating wire is inserted into the soil. An electrical current is applied to the heating wire and the rise in temperature in the cylinder is measured with a thermocouple or thermister placed adjacent to the probe. The relationship between the temperature of the cylinder and time is given by

$$T - T_0 = (q_h / 4\pi K) (C + \ln t) \quad (4)$$

where T is the temperature at time t , T_0 is the initial temperature, K is the thermal conductivity, q_h is the heat generated per unit time per unit length of the heating wire, t is time, and C is a constant. A plot of T versus

the logarithm of time allows the determination of the thermal conductivity.

To use this method the relationship between thermal conductivity and soil water content for the soil of interest must be determined, either in the laboratory or in the field. With this relationship and thermal conductivity measurements, and the soil water content can be determined for the soil in-situ. Since the thermal conductivity of the soil is sensitive to the dry bulk density of the soil, the K versus θ_v relationship should be determined for the soil at the same dry bulk density as that in the in-situ condition.

Soil Matric Potential

Tensiometry. The tensiometric technique provides a direct measurement of the matric potential of a soil. The fundamental unit of a tensiometer is a porous membrane which provides the interface between a water-filled pressure sensing tube and the soil. The porous membrane is semipermeable in that it allows the passage of water but prevents the passage of soil air. Conventionally

the porous membrane is cup shaped and made of ceramic material. Fritted glass or porous steel materials can also be used. In some instances, especially for laboratory applications, a flat membrane is more convenient than a cup shaped membrane.

The configuration for a typical field tensiometer unit is illustrated in Figure 7. The water inside of the tensiometer unit is continuous with the water in the soil pores so that the pressure in the soil is transmitted to the water inside the tensiometer. Various ways for measuring the pressure inside the tensiometer unit are illustrated in Figure

7. Mercury manometry and electronic pressure transducers connected through a tube are the conventional methodology as seen in the right hand tensiometer configuration. This configuration requires a substantial effort to maintain the water column in the connecting tube and the pressure transducers (mercury manometer or electronic pressure transducer).

A more recent development is the configuration shown to the left in Figure 7. Here, the pressure in the air space above the water level in the

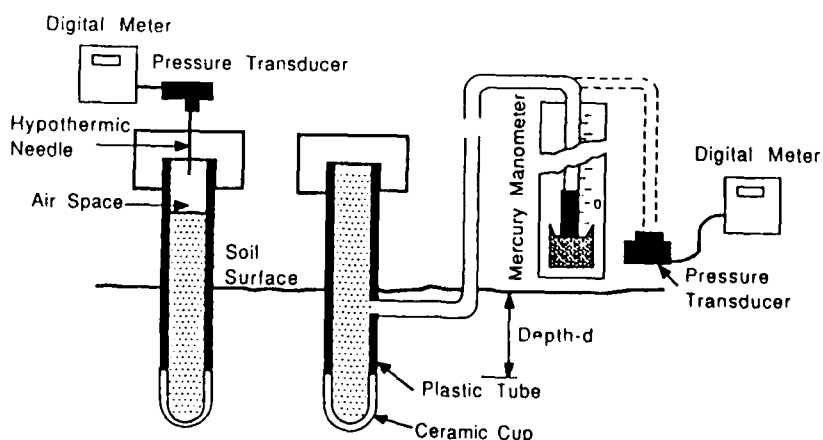


Figure 7. Example tensiometer/pressure transducer configurations.

tensiometer tube is measured with an electronic pressure transducer (Marthaler et al., 1983). Since the pressure of the air in the air space is in equilibrium with the pressure in the underlying water column, this air pressure can be used to determine the soil matric potential. An advantage of this approach is the ease of maintenance of the tensiometer.

Electrical resistance blocks. The matric potential in fabricated porous materials placed in a soil come to equilibrium with the matric potential of the soil in contact with that material. If two electrodes are imbedded into the fabricated material, the electrical resistance between the electrodes depends on the water content of the porous material. The electrical resistance of the porous material decreases and the water content of the material increases. If the relationship between electrical resistance and matric potential of the material is determined, the material imbedded in soil can be used to measure soil matric potential based solely on a resistance measurement.

Various types of electrical resistance blocks have been developed over the years. The major difference between the earlier types of blocks was the type of material used to form the porous matrix. The first type of resistance blocks were made from gypsum and are called gypsum blocks. Typically gypsum blocks are either cylindrical or prismatic in shape.

The second generation of resistance block was made of nylon. Generally these blocks are rectangular in shape and relatively thin. The nylon material is generally encased in a perforated plastic or stainless steel casing to provide strength to the nylon matrix. The advantage of the

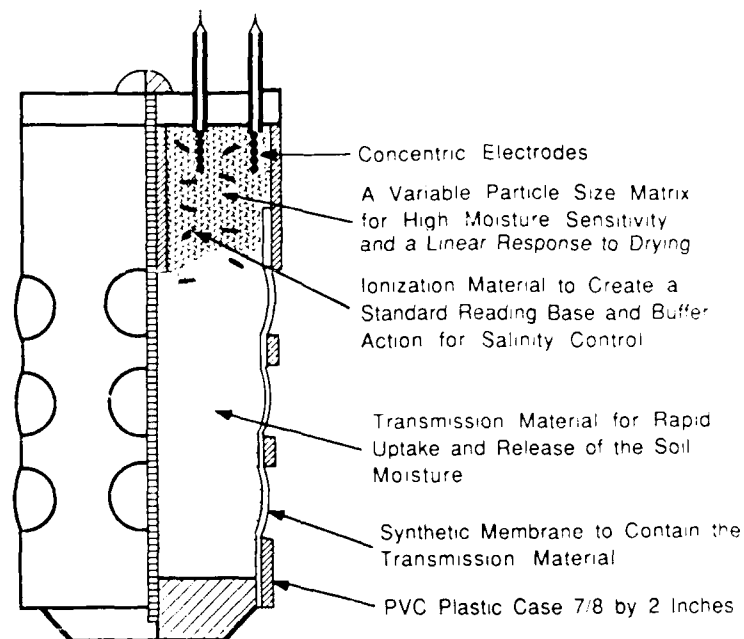
nylon block is the ease with which they can be inserted into a soil because of the thin dimension.

Problems associated with using the gypsum or nylon block sensors have been the degradation of the porous materials over time, and the sensitivity of the resistivity to the salinity of the soil water. Neither of these blocks have a built-in means for offsetting the influence of soil salinity.

The newest type of electrical resistance block is the WATERMARK BLOCK (Armstrong et al., 1985). An illustration of this type of block is presented in Figure 8. The body of the block is composed of a perforated plastic tube. The electrodes are placed into a porous matrix that provides adequate sensitivity even when the soil is near saturation. In addition, the block contains a chemical buffer to offset the influence of soil salinity on resistance.

Electric resistance sensors are sensitive to changes in the amount of water contained in the porous matrix due to the ions dissolved in the water. Freezing of the surrounding soil freezes the water in the porous matrix and results in a large rise in the electrical resistance. This rise is caused by the exclusion of dissolved ions from the water upon freezing. The electrical resistance of ice is very similar to that of distilled/deionized water.

Because of the large rise in electrical resistance upon freezing, electrical resistance blocks can track the freezing/thawing front in soils (Wilin et al., 1972). This information could be useful in correlating pavement strength/deflection to the status of freezing of the subgrade materials.



Watermark Sensor

Figure 8. Configuration for the WATERMARK electrical resistance block.

Heat dissipation blocks. The rate of dissipation of heat in the fabricated porous material is related to the water content of the material, because the thermal conductivity and heat capacitance of the material are each functions of the water content. If this rate of heat dissipation is measured, the matric potential of the material can be determined based on a laboratory calibration. The matric potential of the surrounding soil will then be known.

Figure 9 illustrates a heat dissipation block. Usually the porous matrix is composed of ceramic material although other porous materials can be used.

In the operation of heat dissipation blocks, a heat pulse is applied at the center of the block. The temperature at the center of the block is monitored during the period beginning at heating initiation and ending with heating cessation. Since the thermal

diffusivity, the ratio of thermal conductivity to heat capacitance, is a function of the water content of the block, the water content of the block can be determined from the temperature change during heating. The relationship between matric potential and water content for the block is known from laboratory calibration, so the matric potential for the block can be determined from the water content measurement. From the assumption of equilibrium of matric potentials, the matric potential of the surrounding soil will also be known.

The thermal diffusivity of the soil surrounding the block may differ significantly from that for the block. If the heat pulse reaches the block/soil interface, the temperature readings may be significantly affected. Therefore the block should be large enough so that the heat pulse remains in the block

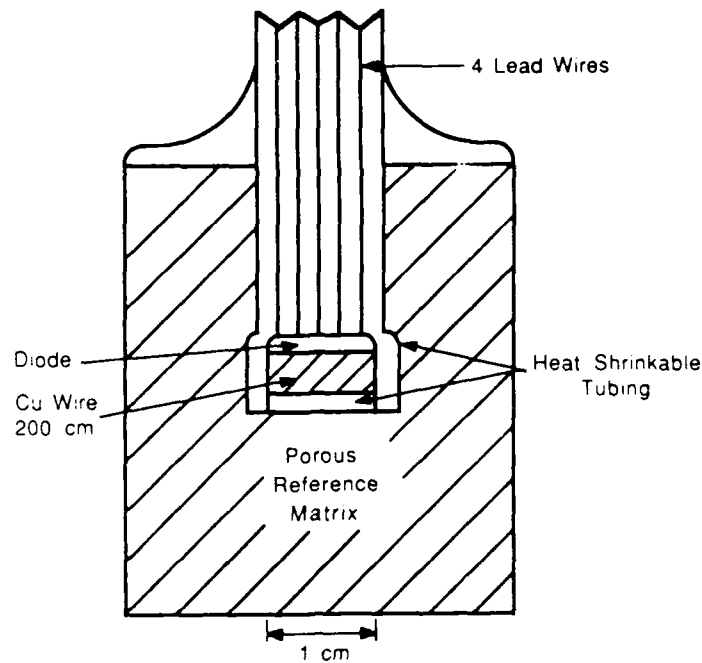


Figure 9. Configuration for a heat dissipation block.

during the period of temperature measurement.

Thermocouple psychrometry. The method of thermocouple psychrometry for measuring soil water potential is based on the assumption of equilibrium between the soil water potential in the liquid phase and the partial pressure of the water vapor in the soil air near the liquid-air interface. By measuring the partial pressure of the water vapor in the soil air the water potential at that point is calculated from the equilibrium equation

$$\Psi = \frac{RT}{m g} \ln \left(\frac{p}{p_0} \right) \quad (5)$$

where Ψ is the water potential of the liquid water, p is the water vapor pressure in equilibrium with the liquid water, p_0 is the saturation

water vapor pressure at the temperature of the liquid water, R is the ideal gas constant, T is the temperature of the liquid water, g is the acceleration of gravity, and m is the molecular weight of water. According to equation (5), as the soil water potential decreases (soil becomes drier) the partial pressure of the water vapor in the soil air decreases. Significant reductions in this partial pressure do not begin to occur until the soil matric potential drops below about 10 bars, as illustrated in Figure 10. Even at soil matric potentials as low as 100 bars, the relative humidity of the soil atmosphere is still above 90%.

The thermocouple psychrometer is used to measure the partial pressure of the water vapor in the soil. An illustration of the typical configuration of a thermocouple psychrometer for field use is presented in Figure 11. The unit is composed of a porous

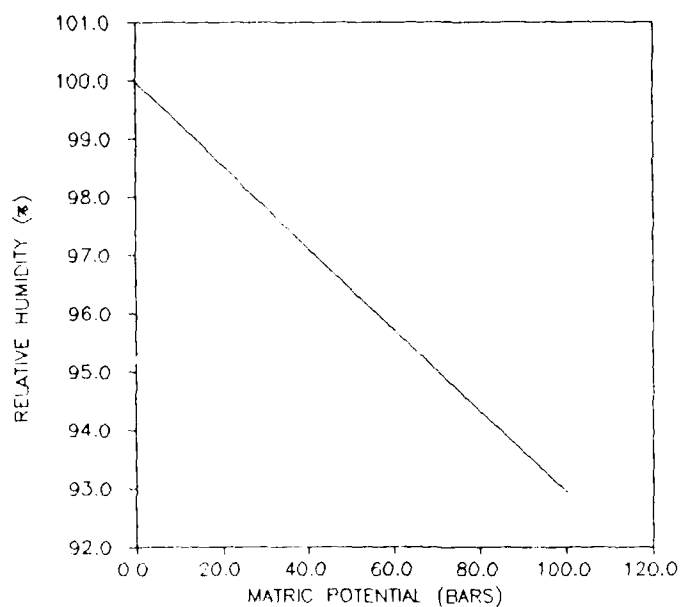


Figure 10. Relationship between relative humidity of soil air and soil matric potential.

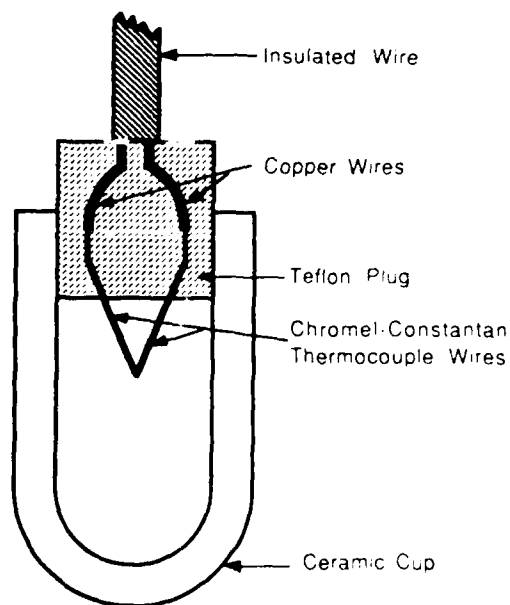


Figure 11. Configuration of a thermocouple psychrometer.

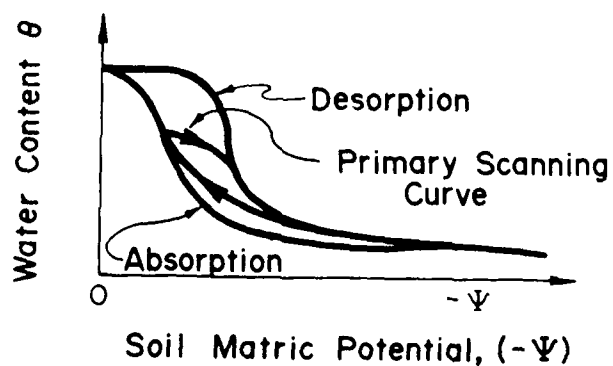


Figure 12. Relationship between water content and soil matric potential illustrating capillary hysteresis.

ceramic cup with thermocouple wire junction contained inside.

In one type of configuration the temperature at the thermocouple junction is measured with the junction in a dry state. A current is then passed through the junction in the direction required to cool it and cause moisture condensation on the junction. The temperature of the junction is then measured again to produce a depression of the temperature. The partial pressure of the soil air water vapor can then be determined from this temperature depression.

DISCUSSION

The principles of operation of a number of soil water measuring techniques have been described in the above sections. The accuracy and application limits of these soil water measuring techniques are summarized in Table 1.

The direct method is the most accurate of the methods available. The level of accuracy achievable with this method is dependent only on the level of care exercised in

handling the soil sample, and the accuracy of the weighing scales used.

Among the indirect methods of soil water content determination the methods in Category I are the most accurate. The reason that the methods in Category I are more accurate than the methods in Category II is based on the fact that Category I methods measure soil water content as the primary dependent variable, whereas Category II methods measure soil matric potential as the primary dependent variable and then infer soil water content.

The major problem with using soil matric potential in determining soil water content is the nonuniqueness of the soil water characteristic curve. An example form of the soil water characteristic is illustrated in Figure 12. The nonunique relationship is a result of the phenomenon called capillary hysteresis. This relationship means that the soil water content at a given soil matric potential depends on the wetting and drying history of the soil. Therefore, unless one knows the wetting and drying history of a

Table 1. Summary of capabilities of soil water measurement methods.

Method	Field Technique (2)	Destructive (2)	Matric Potential Range (Bars)	Error		Potential For Frozen Soil Measurement
				Matric Potential (Bars)	Water Content (%)	
Gravimetric	yes	yes	< 0	±0.05	± 0.1	yes
Neutron	yes	no	< 0	±0.05	± 2.0	yes w/TDR
Gamma	yes	no	< 0	±0.05	± 1.0	yes w/TDR
X-ray	no	no	< 0	±0.05	± 1.0	no
NMR	yes	no	< 0	±0.05	± 1.0	yes
TDR	yes	no	< 0	±0.05	± 1.3	yes w/Neutron on Gamma
Thermal						
conductivity	yes	no	< 0	±0.05	± 5.0	no
Tensiometry	yes	no	> -0.8	±0.001	±100.0	no
Electrical						
resistance	yes	no	> -2.0	±0.01	±100.0	somewhat
Heat						
dissipation	yes	no	> -5.0	±0.01	±100.0	no
Thermocouple						
psychrometry	yes	no	< 10.0	±0.5	± 0.5	no

soil, it is not possible to determine the soil water content from the soil matric potential alone.

The amount of error associated with using soil matric potential alone in determining soil water content depends on the width of the hysteresis loop in the soil water characteristic. This width depends on the textural properties of the soil. Some soils have a fairly narrow hysteresis loop, whereas others have a wide loop.

Category II methods can be used to measure soil matric potential quite accurately as seen in Table 1. However, the inference of soil water content from a soil matric potential measurement cannot be made with nearly as much confidence.

Significant errors exist for Category I methods when the soil matric potential is to be determined. With Category I methods the soil water content is measured, and to obtain soil matric potential it is necessary to use the soil water characteristic curve. Due to capillary hysteresis, large errors in soil matric potential determination can result.

Among the soil water content determination methods described, the TDR method supplemented with either neutron scattering or gamma attenuation appears to offer the best opportunity for determination of liquid water content and ice content of a partially or fully frozen soil. The neutron scattering and gamma attenuation methods each provide a measure of the total water content (liquid water plus ice) of the soil. The TDR method provides a measure of the liquid water content.

The electrical resistance block appears to offer an opportunity to track the depth of freezing in a soil profile. This can be done using frost tubes, but it might be preferable in some instances to

monitor the depth of freezing from a remote location. Electrical resistance blocks are highly sensitive to the phase of the water present in the block porous matrix. When freezing of the water in the porous matrix occurs, the electrical resistance of the block increases sharply.

No single method is obvious choice for all situations. Rather, it is necessary to weigh their strengths and weaknesses to fit the desired objective.

ACKNOWLEDGEMENTS

Published as Paper No. 16,892 of the scientific journal series of the Minnesota Agricultural Experiment Station on research conducted under Minnesota Agricultural Experiment Station Project No. 12-048. Financial support from the Minnesota Department of Transportation contributed to the development of this manuscript through Basic Agreement No. 64408.

REFERENCES

- Armstrong, C.F., J.T. Ligon, and S.J. Thomson, 1985. Calibration of WATERMARK Model 200 soil moisture sensor, Paper No. 85-2077, American Society of Agricultural Engineers, St. Joseph, MI.
- Baker, J.M., and R.J. Lascano, 1989. The spatial sensitivity of time-domain reflectometry, Soil Sci. (in press).
- Blake, G.R. and K.H. Hartge, 1986. Bulk Density, IN: Methods of Soil Analysis, Part 1: Physical and Mineralogical Methods, Agronomy Series No. 9, Second Edition, American Society of Agronomy.

Crestana, S., S. Mascarenhas, and R.S. Pozzi-Mucelli, 1985. Static and dynamic three-dimensional studies of water in soil using computed tomographic scanning, *Soil Sci.*, 140:326-332.

De Vries, D.A., 1952. A nonstationary method of determining thermal conductivity of soil in situ, *Soil Sci.*, 73:83-89.

Gadian, D.G., 1982. Nuclear Magnetic Resonance and its Application to Living Systems, Oxford University Press, New York.

IRROMETER, 1989

Klute, A. (ed.), 1986. Methods of Soil Analysis, Part 1: Physical and Mineralogical Methods, Agronomy Series No. 9, Second Edition, American Society of Agronomy.

Ledieu, J., P. De Ridder, P. De Clerck, and S. Dautrebande, 1986. A method of measuring soil moisture by time-domain reflectometry, *J. Hydrol.*, 88:319-328.

Marthaler, H.P., W. Vogelsanger, F. Richard, and P.J. Wierenga, 1983. A pressure transducer for field tensiometers, *Soil Sci. Soc. Am. J.*, 47(4):624-627.

Paetzold, R.F., G.A. Matzkanin, and A. De Los Santos, 1985. Surface soil water content measurement using pulsed nuclear magnetic resonance techniques, *Soil Sci. Soc. Am. Jour.*, 49(3):537-540.

Patterson, D.E. and M.W. Smith, 1981. The measurement of unfrozen water content by time-domain reflectometry: results from laboratory tests, *Can. Geotech. J.*, 18:131-144.

Petrovic, A.M., J.E. Siebert, and P.E. Rieke, 1982. Soil bulk density in three

dimensions by computed tomographic scanning, *Soil Sci. Soc. Am. Jour.*, 46(3):445-450.

Philip, J.R., 1969a. Moisture equilibrium in the vertical in swelling soils, I. Basic theory, *Aust. Jour. Soil Res.*, 7:99-120.

Philip, J.R., 1969b. Moisture equilibrium in the vertical in swelling soils, II. Applications, *Aust. Jour. Soil Res.*, 7:121-141.

Stein, J. and D.L. Kane, 1983. Monitoring the unfrozen water content of soil and snow using time domain reflectometry, *Water Resour. Res.*, 19:1573-1584.

Topp, G.C., J.L. Davis, and A.P. Annan, 1980. Electromagnetic determination of soil water content: measurements in coaxial transmission lines, *Water Resour. Res.*, 16:574-582.

Topp, G.C. and J.L. Davis, 1985. Time-domain reflectometry (TDR) and its application to irrigation scheduling. IN: D. Hillel (ed.), *Advances in Irrigation*, v. 3, pp 107-127. Academic Press.

Van Bavel, C.H.M., N. Underwood, and R.W. Swanson, 1956. Soil moisture measurement by neutron moderation, *Soil Sci.*, 82:29-41.

Van Bavel, C.H.M., R.J. Lascano, and J.M. Baker, 1985. Calibrating two-probe gamma-gauge densitometers, *Soil Sci.*, 140(5):393-395.

Wilin, B.O., W.P. MacConnell, and L.F. Michelson, 1972. Reliable and inexpensive soil frost gage, *Agon. J.*, 64:804-841.

Zientara, G.P. and L.J. Neuringer, 1988. Medical imaging for the 21st century, *Perspective in Computing*, 8(1):14-25.

IN SITU PERMEABILITY MEASUREMENTS

By
Lyle K. Moulton
Chairman
Department of Civil Engineering
West Virginia University

ABSTRACT

A broad range of techniques and equipment for the measurement of the in situ permeability of soils and aggregates is summarized, and the applicability of these methods to the field determination of the permeability of base and subbase courses is discussed. The development of a prototype in situ test device, designated as the field permeability testing device (FPTD), for the determination of the permeability of pavement base and subbase courses, is described and discussed. This project was completed at West Virginia University under the sponsorship of the Federal Highway Administration (FHWA). It involved an extensive program of laboratory and field testing of the equipment. Following the completion of this contract, the FHWA refined the equipment and made it available for additional field use by various highway agencies over a period of several years. The results of these practical applications of the FPTD are presented and discussed. Limited international adoption and use of the equipment is also described.

The advantages and limitations of the FPTD are discussed. It is concluded that this equipment has considerable potential for practical field use. The device permits the consideration in design of the saturated hydraulic conductivity (permeability) of bases and subbases and also permits the development of construction specifications for the permeability of these materials, since it makes available a mechanism for the evaluation and control of permeability during construction.

INTRODUCTION

Many of the problems associated with the unsatisfactory performance of pavement systems are attributable to excess moisture in the subgrade and the structural section of the pavement. Recognizing this situation, many agencies specify that granular bases and subbases have outlets that drain water from the pavement section as quickly as possible. However, the base and subbase layers are not always

permeable enough to prevent damage to the pavement under saturated conditions and normal traffic loads (1,2).

As part of the effort to develop effective subsurface drainage systems for pavements, rational procedures have been developed for estimating the amount of water that enters the pavement section and designing the drainage layers to rapidly remove this water (1,2). The principal material property required to use these procedures is the coefficient of permeability. Minimum coefficients of permeability must be specified to meet design requirements of the drainage system. Existing laboratory testing methods can be used to determine the permeability coefficients of candidate drainage layer materials, and these values can be compared with the design requirements. Although these laboratory methods are well known and quite reliable, relatively small variations in gradation and density, such as those normally encountered in construction, can produce large changes in the coefficient of permeability (2-5). Thus, the field permeabilities of these materials can differ from the values determined in the laboratory. Therefore, the coefficients of permeability of base, subbase and subgrade materials should be determined in situ. Proven methods for such determination must be available before the coefficient of permeability can be routinely specified in construction contracts to control materials and construction practices.

Recognizing this need, the Federal Highway Administration (FHWA) contracted for the development of a test apparatus and procedure for determining the in situ permeability of highway base, subbase and subgrade materials. The investigation included (a) the evaluation of existing methods of in situ permeability determination and their suitability for determining the permeability of base, subbase and subgrade layers, (b) the laboratory evaluation of the developed method, and (c) the field testing and evaluation of the most promising technique.

Throughout the course of this work, several very important factors regarding the nature of the problem and the required operating characteristics of the prototype FPTD were given special consideration

1. The flow or seepage domain in pavement structural systems consists of layered, nonhomogeneous, anisotropic media. A determination of the coefficient of permeability (saturated hydraulic conductivity) in the transverse or longitudinal direction (while keeping in mind that the vertical permeability influences the amount of surface water that infiltrates the pavement structural section) is of primary concern in designing the drainage of these layers. The overriding influence of the horizontal flow limits the usefulness of techniques that measure only vertical permeability

2. The prototype FPTD should measure the coefficients of permeability of individual layers ranging in thickness from 3 inches (76.2 mm) to 18 inches (457.2 mm), with coefficients of permeability ranging from 10^{-4} cm/sec to 10 cm/sec, under a variety of boundary conditions. These boundary conditions included both initially saturated and unsaturated layers as well as underlying layers that were either more or less permeable than the layer being evaluated

3. The measurement technique adopted should be non-destructive or disturb the layer being evaluated as little as possible

4. The prototype FPTD must be simple to operate and be rugged and durable for field use.

5. The device should measure the coefficient of permeability within a factor of 2 of the true permeability 90 per cent of the time

SUITABILITY OF EXISTING METHODS

A detailed review of the literature dealing with the in situ determination of the coefficient of permeability was conducted. A review of these papers showed that the existing methods could be grouped into a relatively small number of categories as shown in Table 1. It became clear from the summary presented in Table 1 that most of the methods for in situ permeability determination do not satisfy one or more of the performance criteria outlined above, and therefore, are not directly applicable to the in situ determination of the permeability of pavement bases and subbases. For this reason, and for the sake of brevity, no attempt has been made here to present details of the

Table 1. Summary of Literature Review - In Situ Determination of Permeability

Test Method	Applicability w/Respect to GWT	Direction of Measured Perm.	Relative Disturbance	Major Limitations on Applicability of Method	Applicability to Base and Subbase
1. Individual Boreholes and Wells					
(a) Uncased					
(1) Packer Tests	Below GWT	Horizontal	High	Requires Rock or Cemented Soil	Poor
(2) Pumping Tests	Below GWT	Primarily Horizontal	High	Below GWT, Costly	Poor
(3) Auger Hole Method	Below GWT	Combined-Horiz. & Vert.	High	Requires Unstrat. Soil, below GWT	Poor
(4) Shallow Well Pump in (well piezometer, dry auger hole)	Above GWT	Primarily Horizontal	High	Water Quant., Equipment, Time	Poor
(b) Partially Cased					
(1) Piezometer Method	Below GWT	Varies-Depends on L/D	High	N.G. in Rocky Soils, Below GWT	Poor
(2) Well Point Method	Below GWT	Varies-Depends on L/D	High	N.G. in Rocky Soils, Below GWT	Poor
(c) Fully Cased	Below GWT	Combined-Horiz. & Vert.	High	N.G. in Rocky Soils, Below GWT	Poor
2. Multiple Well Systems					
(a) Pumping Tests w/ Observation Wells	Below GWT	Primarily Horizontal	High	Below Groundwater Table	Poor
(b) Two Well System w/one pumped into the Other	Below GWT	Primarily Horizontal	Low to High ^(d)	Equipment, Time, Hole Clogging	Fair to Poor ^(d)
(c) Four Well System	Below GWT	Primarily Horizontal	Low to High ^(d)	Equipment, Time	Fair to Poor ^(d)
3. Infiltrimeters					
(a) Single Tube (Ring)	Above GWT	Combined-Vert. & Horiz.	Medium	Req. Unstrat. Soil, N.G. in C. Grav.	Poor
(b) Cylinder Permeameter	Above GWT	Vertical	High	Time, Equip., N.G. in C. Grav.	Poor
(c) Double Tube	Above GWT	Vert. w/Isotropic Soil ^(b)	High	Time, Equip., N.G. in C. Grav.	Poor
(d) Gradient Intake	Above GWT	Vertical	High	Install., Equip., N.G. in C. Grav.	Poor
(e) Seepage Meter	Below GWT	Vertical (Indirect)	High	Exist. of External Flow Cond.	Poor
4. Air Entry Permeameter	Above GWT	Vertical	Medium	Lim. to Rel. Dry Soils, Installation	Fair
5. Spherically Symmetric Flow To/ From Spherical Cavity	(a)	Combined-Horiz. & Vert.	High	Install., N.G. in C. Grain Soils	Poor
6. Short Cell Apparatus	Below GWT	Combined-Horiz. & Vert.	High	Req. Adit or Tunnel for Install.	Poor
7. Measurement of Seepage From Test Pools	Above GWT	Primarily Vertical	Very High	Disturbance, Equip., Time	Poor
8. Shoulder Perm. Test w/Elec. Probes	Above or Below GWT	Primarily Horizontal ^(c)	Low to Medium ^(d)	Lack of Applicable Theory	Presently Fair-Good to Excellent in Future

(a) Above and below GWT. (b) Combined Vert. & Horiz. w/ Anisotropic Soil. (c) Actual Coeff. of Permeability, not Indirect. (d) Method gives relative measure of permeability. (d) Depends on hole diameter and spacing

various test methods, including analytical considerations, equipment, procedures, etc. A complete listing of the numerous publications, describing the various methods presented in Table 1, is included in References (6) and (17).

However, it was found that the circulation technique, involving two and four well systems (7-10), would be worthy of further consideration relative to the in situ determination of the permeability of pavement bases and subbases. Unfortunately, a detailed mathematical analysis (verified by electrical analog) showed that some of the measurements required in this technique were neither reliable nor practical (6).

It was also found that the concept embodied in the shoulder permeability test method, suggested by Maytin (11), had some promise. This concept suggested that the change in soil conductivity, associated with the flow of pore water with a salt concentration different than that of the natural pore water, might be an effective means of measuring the seepage velocity between two points and, thus, lead to a direct application of Darcy's law for determination of permeability. Indeed, it was found that this principle had been used by Szily (12) in the study of the permeability of undisturbed sand samples and by Bouwer and Rice (13) and by Denisov (14) in the determination of the velocity of flow between two points in a natural soil deposit. Wenzel (15) even referred to the development of this method by Slitchter as described in a paper (16) published as early as 1902. This method, referred to henceforth as the velocity technique, formed the basis for the development of the prototype FPTD.

THE VELOCITY TECHNIQUE

Fundamental Considerations

As noted above, the velocity technique involved the direct application of Darcy's Law, which can be stated as follows:

$$v = ki$$

where v is the discharge velocity, k is the coefficient of permeability (in units of velocity), and i is the dimensionless hydraulic gradient. This hydraulic gradient, i , can be expressed in finite difference form as

$$i = \frac{\Delta h}{L}$$

where Δh is the loss of the total head between two points on a flow path (streamline) in the flow domain, and L is the distance measured along the flow path between these two points. Furthermore, the discharge velocity, v , can be expressed as

$$v = n v_p$$

where v_p is the seepage velocity (i.e., the actual average velocity of flow within the pores of the soil), n is the porosity

of the soil. Thus, Darcy's Law can be rewritten and solved for the coefficient of permeability, k , to give

$$k = \frac{n v_p}{\Delta h / L}$$

Further development of the velocity technique required: (a) a method for the establishment of saturated steady state flow within the layer of base or subbase to be evaluated; (b) a method for measuring the average seepage velocity, v_p , along a flow path between two points, a known distance, L , apart; (c) a method for determining the head loss, Δh , between these two points, and a method for determining the in situ porosity, n , of the base or subbase being evaluated.

Development of the Technique

Theoretical and experimental studies were conducted to provide the equipment and procedures necessary for the development of a practical in situ permeability measurement system based on the velocity technique. Relative to the critical items cited above for the development of the technique, the following conclusions were reached:

1. Saturated steady state flow could be established by injecting water under constant head through a perforated injection tube located in the center of a circular plate. Flow net studies, conducted using electric analogs, showed that the flow pattern and, thus, the configuration of the streamlines and equipotential lines could be controlled by regulating the plate diameter and injection depth relative to the existing boundary conditions, i.e., the base and subbase layer thickness and their relative permeabilities. Ideally, it was desired to create a flow pattern such that the streamlines, within a certain zone in the top layer (i.e., the one being evaluated), would be essentially parallel to the surface. Flow net studies showed that this condition could best be achieved by injection of the water over the full depth of the layer when it is underlain by an impervious stratum or one of much lower permeability. It was also discovered that full depth injection is not absolutely necessary under these boundary conditions in order to establish a sizeable zone of essentially horizontal flow.

2. Electrical conductivity could be utilized for measurement of seepage velocity. In this scheme, once saturated steady state flow has been established, a quantity of electrolyte solution is introduced through the injection tube, and electric conductivity probes are used to time the rate of flow between two selected points on a streamline. Of the conductivity measurements investigated, a system that consisted of a two wire probe and a microammeter was judged to be the simplest, most effective, and most economical for both laboratory and field use.

3. Two possible methods were considered for determining the head loss, Δh , between the velocity measuring probes

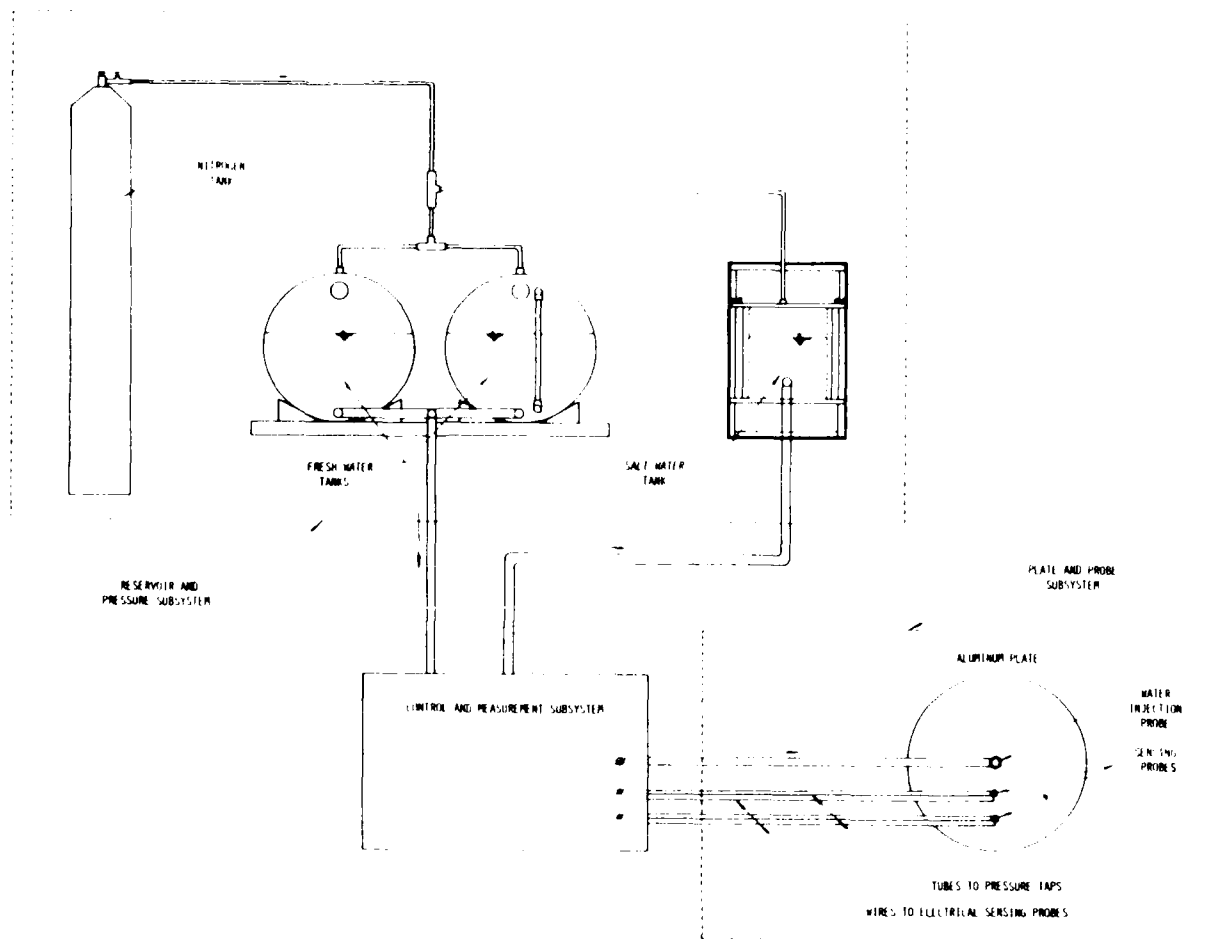


Figure 1. Schematic Diagram of FPTD and Its Subsystems

in the flow domain: (a) the analytical (mathematical) evaluation of the head loss between the two points as a function of the measured flow rate and the total head loss through the system, and (b) the direct measurement of the head loss between the two points. It was found that the analytical solution required a knowledge of the ratio of the permeabilities of the various layers of the flow domain. Therefore, it was decided that the head loss, Δh , would be determined by direct measurement of the fluid pressures at the ends of the electric conductivity probes. Either a manometer or a differential pressure gage (DPG) could be utilized for the measurement.

4. Using measured values of the dry density (ρ_d) and the specific gravity of solids (G_s) of the soil, the porosity (n) could be calculated using the expression

$$n = 1 - \frac{\rho_d}{G_s \rho_w}$$

The basic features of the principal components of the field permeability test device are illustrated schematically in

Figure 1. As indicated in the figure, the pressure taps were incorporated into the electric conductivity probes. The electric conductivity probes were subsequently modified so that both the wire ends and the pressure taps were placed in the sides rather than the ends of the probes.

Preliminary Laboratory Studies

The accuracy and reliability of the technique were studied initially by placing electric conductivity/pressure probes in the side of a modified constant head permeability test device, and then comparing the coefficient of permeability values based on the velocity technique and the conventional constant head method. In addition to assisting in verification of the viability of the velocity technique, two significant observations were made as a result of these studies, viz:

1. Some error is introduced into the velocity determination, because of the effects of hydrodynamic dispersion and diffusion of the salt solution. Thus, the apparent velocity of flow between the two probes, as measured by the initiation of conductivity change, was slightly higher than the actual

average velocity of flow as determined in the constant head permeameter. It was found, however, that the magnitude of this error was time dependent and could be minimized by using a combination of probe spacing and hydraulic gradient that permitted the test to be run in the shortest possible time.

2. It was also found that, of all the electrolyte solutions tested, the best results were achieved using an ammonium chloride (NH_4Cl) solution consisting of 25 milligrams of ammonium chloride in 100 milliliters of water.

A substantial amount of data was accumulated using the two wire electric probe with pressure tap system installed in the modified constant head permeameter. The resulting data are summarized in Figure 2 which shows the comparison between the coefficient of permeability (k_p) measured with the modified constant head device, and that determined with the velocity technique (k_p) using the two wire electrical probe system. As can be seen in Figure 2,

the velocity technique produced a very good approximation to the results obtained with the constant head permeameter, although it did produce a slight over-prediction of the coefficient of permeability because of the dispersion and diffusion phenomena discussed previously. Even with this problem, almost all of the data fell within the 95 percent confidence limit band and thus confirmed the viability of the velocity technique for in situ permeability measurements.

Before fully developing the prototype field permeability test device (FPTD), a preliminary device was tested in a large laboratory cell system especially fabricated for this research investigation (6.17). This system permitted the direct determination of coefficient of permeability values for simulated base and subbase courses under saturated horizontal sheet flow conditions. In addition, since the individual cells had a plan area of 5 feet by 5 feet (1.5 m x 1.5 m), in situ measurements could be made using a preliminary version of the prototype FPTD. A limited test series

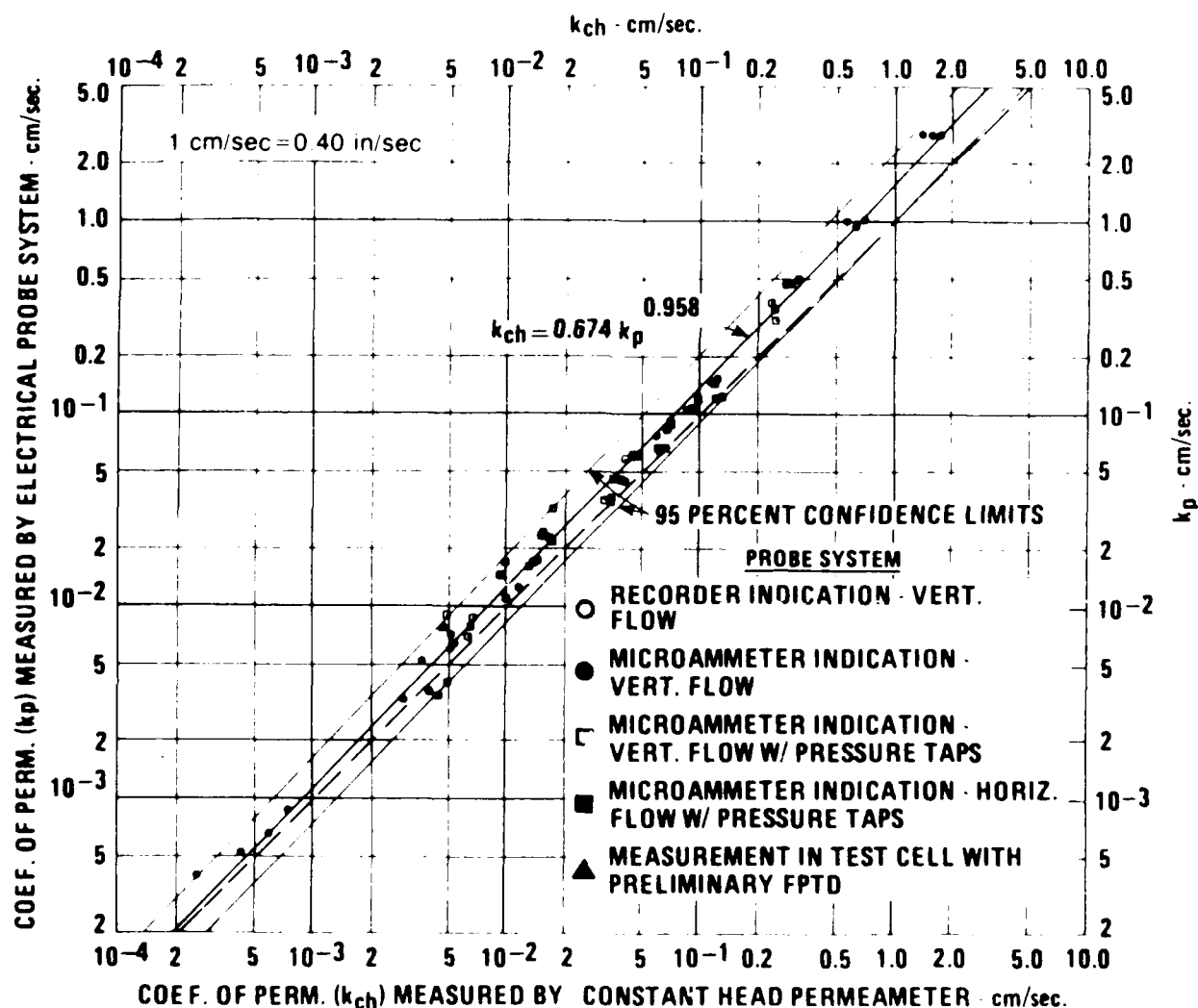


Figure 2. Comparison Between Coefficients of Permeability Measured With Modified Constant Head Device and Two Wire Electrical Probe System

with the preliminary device yielded excellent results, as shown in Figure 2.

DEVELOPMENT AND EVALUATION OF THE PROTOTYPE FPTD

The remainder of the project was devoted to completing the development of the prototype FPTD, evaluating the accuracy and reliability of the method, and establishing the suitability of the equipment for field use. As might be expected, the device underwent a number of evolutionary changes and modifications as the laboratory and field evaluation programs progressed. The laboratory testing program was especially extensive, utilizing the test cell system to establish the quantitative effects of varying certain test parameters as well as the accuracy and reliability of the method.

Description of the FPTD

The prototype device consisted of three major subsystems as shown in Figure 1: (a) the reservoir and pressure subsystem; (b) the control and measurement subsystem; and (c) the plate and probe subsystem.

The reservoir and pressure subsystem consists of the freshwater supply tanks, a saltwater supply tank, and a pressure source. The freshwater supply tanks provide the water for saturating the base or subbase and establishing

steady state flow during permeability testing. The saltwater supply tank provides the electrolyte solution that initiates the conductivity change. The pressure source, which maintains the gas pressure of the system, is a regulated nitrogen gas cylinder. For field use, the reservoir and pressure subsystem were mounted in the rear of a West Virginia University (WVU) mobile research vehicle.

The control and measurement subsystem consists of the hydraulic controls, the electric sensing system and the pressure sensing system (Figure 3). The hydraulic controls can shut off the water supply or precisely regulate the flow of either freshwater or saltwater (electrolyte) to the water injection probe. The two electric sensing circuits provide an adjustable response to the conductivity change that occurs as the electrolyte solution passes the electrodes in the sensing probes. The pressure sensing system consists of a differential manometer that determines the head difference between the pressure taps in the sensing probes.

The plate and probe subsystem consists of the horizontal plate, water injection probe, and sensing probes (Figure 1). The 18 inch (457.2 mm) diameter aluminum plate is equipped with a central port through which the water injection probe is inserted and with radially located ports through which the sensing probes are inserted. To minimize the amount of piping at the interface between the plate and the base or subbase, the plate was machined with annular projections on its bottom surface.

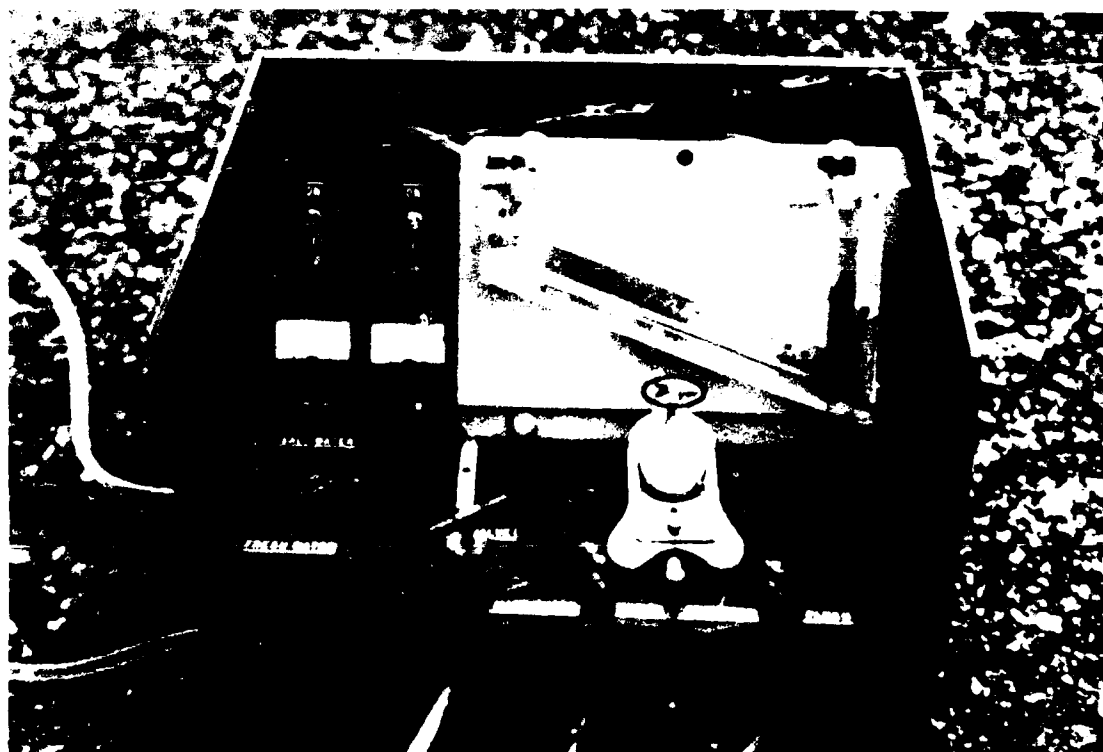


FIGURE 3. Close-up view of Control and Measurement Subsystem

The water injection probe consists of closed end tubing with holes located at regular intervals along its length. During testing, the probe is oriented so that these holes point in the direction of the row of plate ports, that is, in the direction of testing.

The sensing probes were constructed of stainless steel tubing with a brass tip. The tip contains four ports to permit access of water to the manometer for head measurement. A two-wire electrode is brought down through the sensing probe and secured in the tip. Both the water injection probes and the sensing probes were made in various lengths to suit the geometry of the test situation.

Laboratory Evaluation of the FPTD

The principal objectives of this component of the investigation were to evaluate performance of the prototype FPTD for a variety of materials as well as physical and hydraulic boundary conditions.

The materials to be tested were selected more on the basis of permeability than their suitability as base or sub-base. On this basis, six different materials were selected or blended to produce permeabilities between 10^{-4} and 10^{-6} cm/sec (0.4×10^{-4} and 4 in/sec).

Physically, the boundary conditions were varied by using either a homogeneous or layered system with different layer thicknesses. The physical location of impermeable, moderately permeable, and very permeable materials was varied within the layered system. The location of the free water surface was varied relative to the position of the layer being tested. In addition, the effects of FPTD test parameters, such as direction of testing, plate size, probe location, and probe spacing, on permeability coefficients were evaluated in the laboratory.

The test results indicated that neither layer thickness nor water table depth significantly affected the measured coefficient of permeability, as long as saturated steady state flow was established before testing. Similarly, if the underlying material was either impervious or moderately permeable, it did not significantly influence the results. However, some problems were encountered in obtaining reliable measurements when the underlying layer had a permeability over 100 times that of the layer being tested. In this case, the bulk of the flow was found to move abruptly downward and then horizontally through the very pervious layer. Other tests, however, showed that permeability measurements of a layer that is above a much more permeable layer are reliable if a condition of steady state saturated flow is maintained in both layers.

The evaluation of the influence of the direction of testing showed, as expected, that some materials exhibited considerable variations, whereas others showed only small differences. These results suggest that considerable anisotropy might exist, particularly under field conditions,

where placement and compaction of bases and subbases might not be as uniform as in the laboratory test cells. Consequently, in actual practice, it would be desirable to perform tests in orthogonal directions at a given test location and then take the permeability as the geometric mean of the results.

The influence of the plate size, the depth of the water injection probe, and the depth, location and spacing of the sensing probes are interrelated. Ideally, these parameters should be controlled to produce a zone of essentially horizontal flow, so that the tips of the sensing probes can be located on a single streamline. It was found that plate size can be held constant if the depth of the water injection probe and the depth and location of the sensing probes are properly controlled. Therefore, the 12 inch (304.8 mm) diameter plate was selected for most of the laboratory and field tests. For layers 12 inches (304.8 mm) thick or less, full depth penetration of the water injection was required. For layers from 12 to 18 inches (304.8 to 457.2 mm) thick, a 12 inch (304.8 mm) penetration depth was found to be satisfactory. For layers less than 12 inches (304.8 mm) thick, placing the tips of the sensing probes at the center of the layer proved satisfactory. For layer thicknesses exceeding 12 inches (304.8 mm), the sensing probe depth should not exceed 6 inches (152.4 mm). However, for layer thicknesses exceeding 12 inches (304.8 mm), it is desirable to make measurements at several depths and average the results. Although the results of tests to determine the influence of sensing probe location were somewhat erratic, they tended to show that the best results were produced with 2 inch (50.8 mm) and 3 inch (76.2 mm) spacing, with the interior probe located within the center third of the plate, that is, within 3 inches (76.2 mm) of the center. This was particularly true when a layer of highly permeable material is under the layer being tested.

The overall accuracy of the FPTD and the reproducibility of the results achieved were evaluated by comparing coefficients of permeability measured by the FPTD, k_{FPTD} , with the coefficients of permeability for the same materials measured in the test cells, k_{TC} , using steady sheet flow. The data from these 430 test results are shown in Figure 4. On the average, the FPTD produced results very close to those measured by the test cell technique (solid line in Figure 4), with only a slight tendency for underprediction in the low permeability range and a very slight tendency for overprediction in the high range. Figure 4 was prepared using the data from all 430 test results that were obtained during the laboratory evaluation of the FPTD. The shaded area in Figure 4 represents the zone where the data would fall if the FPTD measured the coefficient of permeability within a factor of 2 of the true value. If all of the data are considered, then only 22 percent of the data fall within the shaded zone. However, an examination of some of the test data can be questioned, including data not even with what proved to be unsatisfactory locations or spacings of the sensing probes. Of these data, approximately 14 percent of the total, then 31.8 percent of the test data, fall within the shaded zone. Thus,

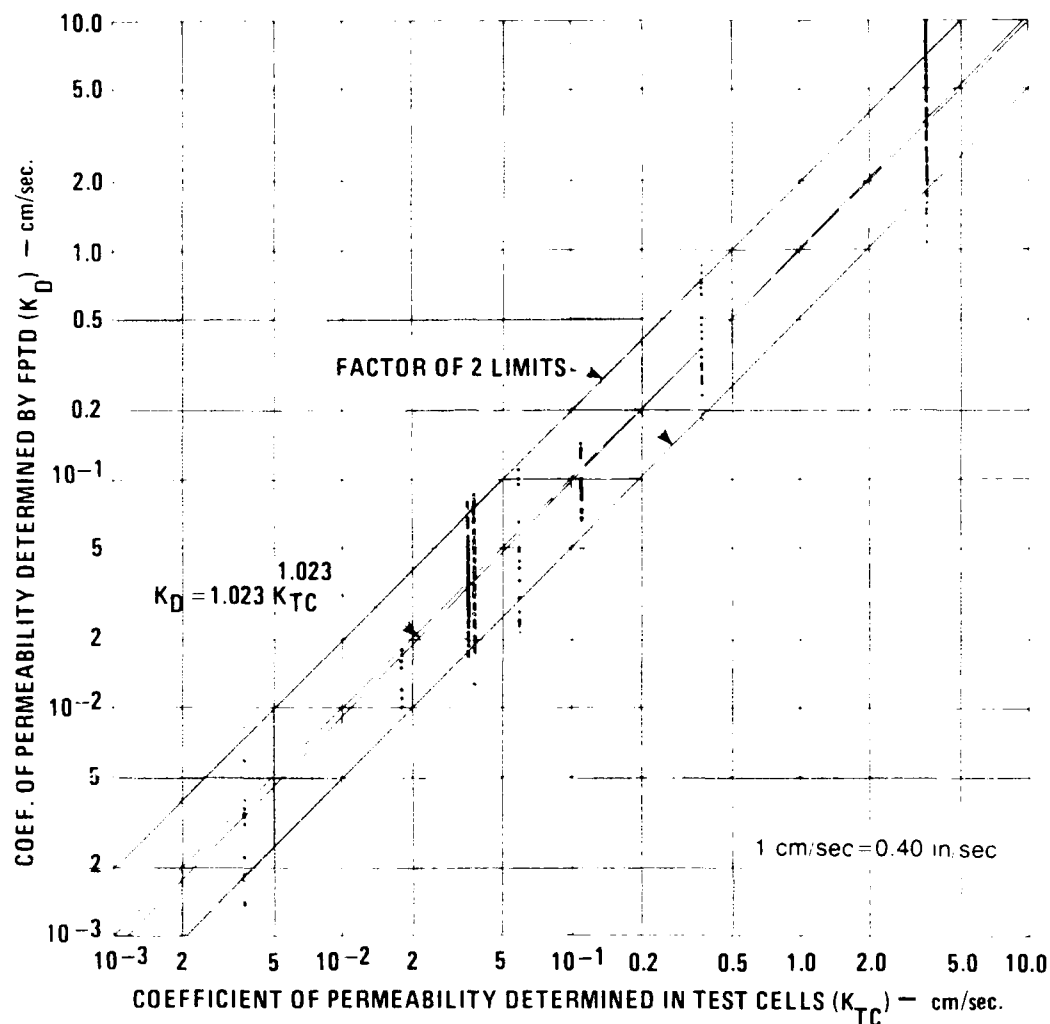


Figure 4 Comparison Between Permeability Determined In Test Cells and Permeability Measured By FPTD

the prototype FPTD satisfied the requirement that it measure the coefficient of permeability within a factor of 2 of the true value 90 percent of the time

Field Evaluation of the FPTD

The performance of the FPTD was evaluated under actual field conditions. The field testing program consisted of investigations at 18 test sections in 13 locations in 8 States (Kentucky, Maryland, Michigan, North Carolina, Ohio, Pennsylvania, Tennessee, and West Virginia). Almost all of the test sections consisted of a single base or subbase layer overlying an impervious subgrade. Samples were collected at each test location and returned to the WVU laboratories for physical properties and permeability testing. In addition, field nuclear moisture density determinations were made at each test location. These tests were conducted to calculate the in situ porosity of the layer and provide the target dry density values for the laboratory permeability tests.

The FPTD performed satisfactorily in the field on all but 3 of the 18 test sections. In two tests, the flow rate required to maintain steady state flow in the base exceeded the flow capability of the FPTD. Laboratory time-lag permeameter tests (3) on these materials revealed average permeability coefficients near the proposed upper limit of the operating range of the equipment. The third failure occurred on a dense graded aggregate base that had a laboratory permeability coefficient near the lower operating limit of the equipment. In all three failures excessive piping at the plate base course interface was found to be one of the limiting conditions. As a result, the annular serrations previously noted were machined into the base of the plate in an attempt to develop a better interfacial seal. Although subsequent performance improved, none of the remaining test sections exhibited particularly high or low permeability values so the interfacial seal was not tested under either extreme. It was also noted that a better interfacial seal could be achieved on freshly compacted

material than on bases or subbases that had been in place and under traffic for some time.

Although the comparison of field test results with those on samples, that had been returned to the laboratory for preparation of permeability test specimens, were not particularly good, it was recognized that there are certain inherent problems in comparing field and laboratory test results. There may be differences in dry density (porosity), differences in direction of fluid flow, and differences in fabric (particle orientation). The laboratory evaluation (discussed above) on carefully controlled samples established that the prototype FPTD could produce consistent and accurate results over a relatively wide range of material types and boundary conditions.

The field evaluation program conducted by the Department of Civil Engineering at West Virginia University did identify potential minor problems with the equipment, demonstrate its ruggedness and durability, and assist in developing a systematic test procedure. The program also identified possible refinements to improve equipment portability and operation. The sensing probes were the only components that presented problems during field testing, but the probes are inexpensive and easy to replace when failures occur.

SUBSEQUENT FIELD EVALUATIONS OF FPTD

Following the completion of the West Virginia University contract with FHWA, at the end of May, 1979, the prototype FPTD was turned over to the Federal Highway Administration for further development and testing. The equipment was rebuilt at the FHWA Fairbank Research Station, and a program of field testing was initiated. Although the prototype FPTD was repackaged by FHWA, the equipment and all its subsystems were basically unchanged. Thus, at this stage, the system was still considered to be the first generation of the FPTD.

The FHWA subsequently contracted with various state highway agencies to evaluate the equipment in the field in what might be considered typical applications in their states. These evaluations took place between the Fall of 1980 and the Spring of 1981 and included tests performed by Dames & Moore (18), the Pennsylvania DOT (19), the West Virginia DOH (20), the State of Washington DOT (21), and the State of Florida DOT (22). The Dames & Moore tests were an unofficial evaluation, conducted by Mr. John Wallace, a Dames & Moore Project Manager, who had been a WVU Graduate Research Assistant assigned to the development of the FPTD.

Field tests on the First Generation FPTD

The tests conducted by Dames & Moore (18) were designed to evaluate anisotropy of base and subbase layers in a project in New Mexico. Although the equipment performed satisfactorily in this application and

demonstrated that there can be substantial differences between the vertical and horizontal permeabilities of compacted base and subbase layers, there was no real effort made to evaluate the equipment under a variety of conditions it might be expected to encounter in actual practice.

The first detailed testing of the equipment was made by the Pennsylvania DOT under contract with FHWA (19). In this study, very detailed testing was conducted on 5 different base and subbase materials. A complete evaluation of the equipment was conducted with generally satisfactory results. Although it was concluded that the equipment was theoretically sound and would provide reproducible results at the same location, it was found that the first generation FPTD was not ready for routine use by ordinary engineering technicians. It was found, however, that experienced engineering technicians, who understood the operation of the equipment, could produce a satisfactory test result in about 30 minutes. A series of recommendations for improvements to the equipment was also provided by Penn. DOT.

The FPTD was then evaluated by the West Virginia DOH (20) under contract with FHWA. Although the statistical data collected as part of this evaluation seemed to indicate that the device performed its intended purpose satisfactorily, considerable difficulty was encountered with the equipment at some locations. In fact, for the 28 locations where the equipment was evaluated, valid test results could only be produced at 20 locations. It was also concluded in West Virginia that the equipment was not yet ready for routine field use. Several suggestions for improvements in the electrodes and manometer system of the equipment were also provided by the WVDOH.

The next series of evaluations were performed by the State of Washington DOT (21), also under contract with FHWA. Although various problems were encountered in assembling and keeping the FPTD operational, once operational, reasonable results were obtained for most of the 20 tests that were performed. However, it was found that it was difficult to obtain consistent and reasonable results in a slow draining silty sand material. Some problems were also encountered with piping along the plate-base course interface. Recommendations for improving the equipment, especially its ease of use and reliability, were provided.

Finally, a very comprehensive series of tests were conducted by the State of Florida DOT (22). Unfortunately, the most common base and subbase courses in Florida have coefficients of permeability that are at or below the lower limit of applicability of the FPTD. Thus, substantial problems were encountered with piping at the plate-base course interface, if the water injection pressure was raised in an effort to achieve saturation and steady state flow in a short time. In an effort to overcome this problem, a layer of Bentonite was used between the plate and the layer being tested. This was apparently successful in minimizing the

piping problem, but the testing times, i.e., an average of 7.5 hours per test, that had to be used were very large compared to the testing times used successfully in other states.

Field Tests on the Second Generation FPTD

Following the first series of field evaluations, described above, the FHWA redesigned and rebuilt the FPTD during 1982 in response to the many suggestions provided by the testing agencies. Although the basic concept was not changed, the manometer and other system hardware was replaced to make the FPTD more compact and more durable. These changes included a new timer mechanism which employed an automatic triggering when the salt solution contacts the probe tip, the addition of the triggering device itself, which provided adjustable compensation for the natural conductivity of the fresh water and the soil, a modification to the plate to provide deeper annular projections to result in less tendency for piping, and replacement of the manometer by a pressure transducer. In early 1983, highway agencies were again invited to enter into contract with the FHWA to conduct new evaluations of the second generation of the FPTD. This new series of tests were conducted in West Virginia, New York and Florida.

The test on the second generation FPTD, conducted by the West Virginia DOH (23), proved the equipment to be satisfactory for its intended purpose. Although some minor changes in the equipment were recommended, it was concluded that the revised equipment was substantially better than the previous version. The criticisms were considered to be minor and more in the realm of convenience and durability than actual subsystem redesign, as was the case with the earlier version. Although piping beneath the plate was not a problem at the WV test sites, bentonite was used as a sealant at one site as required by the contract with FHWA. This procedure appeared to work satisfactorily.

Unfortunately, all of the attempts by the New York State DOT (24) to use the second generation FPTD were unsuccessful, because of an equipment malfunction. They could not get the upstream sensing probe to give an indication of when the slug of salt solution passed by, although the downstream sensing probe apparently worked satisfactorily. Thus, the testing was concluded and the equipment was returned to FHWA.

The final series of tests on the second generation FPTD were conducted by the State of Florida DOT (25). It was concluded that the second generation FPTD benefited considerably from the modifications in design and construction, and it was possible to reduce the average testing time over what had been required during the earlier evaluation tests. Nevertheless, there was still a problem in developing saturation and steady state flow in the relatively low permeability base and subbase materials normally used in Florida. Although it was judged that the redesigned FPTD would work satisfactorily in the soils for which it was

designed, its productive use in Florida would be limited because of the low permeability base and subbase materials commonly used.

THE NEW ZEALAND EXPERIENCE

In 1984, the Geomechanics Section of the Central Laboratories of the Ministry of Works and Development in New Zealand began development of a FPTD, based upon that developed by Moulton and Seals (6,17) at West Virginia University for FHWA. Although based upon the same principles, the FPTD developed at the Central Laboratories was slightly different (26). The sealing plate was square and utilized concentric rubber O-rings to seal the bearing surface between the probes and the plate perimeter. In addition, a sand-bentonite paste was spread over the rings completely filling the gaps between them. This was found to provide a satisfactory seal, even when very high water injection pressures were used. Both the sensing probes and the manometer used were slightly different than in the original version of the FPTD, but the major difference was that the detection of the passage of the salt water between probes was by measurement of the change in capacitance between the dual wire electrodes in each probe.

Both laboratory and field tests of the equipment have shown that the device is capable of measuring the coefficient of permeability over a wide range of values. According to McLarin and Bartholomeusz (26), it was believed that the equipment had been evaluated to the point where it could be used with confidence to establish order of magnitude permeabilities at a range of sites of interest to the National Roads Board of New Zealand.

CONCLUSIONS

Although, clearly, based upon the evaluations conducted to date, both in the United States and in New Zealand, the FPTD needs further development and testing in order to become completely operational for routine field use, this equipment has considerable potential for practical field use. The device permits the consideration in design of the saturated hydraulic conductivity (permeability) of bases and subbases and also permits the development of construction specifications for the permeability of these materials, since it makes available a mechanism for the evaluation and control of permeability during construction.

REFERENCES

1. Cedergren, H.R., Arman, J.A., and O'Brien, K.H., Development of Guidelines for the Design of Subsurface Drainage Systems for Highway Pavement, Structural Sections Report No. FHWA RD 73-14, Federal Highway Administration, Washington, D.C., February 1973.
2. Moulton, L.K., Highway Subdrainage Manual, Report No. FHWA TS 80-224, Federal Highway Administration, Washington, D.C., February 1980.

3. Barber, W.S., and Sawyer, C.L., Highway Subdrainage Public Roads, Vol. 26, No. 12, February, 1952, pp 251-256
4. Smith, T.W., Cedergren, H.R., and Reyner, C.A., Permeable Materials for Highway Drainage, Highway Research Record No. 68, Highway Research Board, 1964
5. Strohm, W.E., Nettles, E.H., and Calhoun, C.C., Jr., "Study of Drainage Characteristics of Base Course Materials", Highway Research Record No. 203, Highway Research Board, 1967, pp. 8-28.
6. Moulton, L.K., and Seals, R.K., Determination of the In Situ Permeability of Base and Subbase Courses, Final Report, Report No. FHWA-RD-79-88, Federal Highway Administration, Washington, D.C., May, 1979
7. Childs, E.C., Measurement of Hydraulic Permeability of Saturated Soil In Situ I. Principles of a Proposed Method, Proceedings, Royal Society (London), Vol. 215, 1952, pp 525-535
8. Childs, E.C., Measurement of Hydraulic Permeability of Saturated Soil In Situ II, Proceedings, Royal Society (London), Vol. 216, 1953, pp 72-89
9. Kirkham, D., Measurement of the Hydraulic Conductivity of Soil in Place, Special Technical Publication No. 163, American Society for Testing and Materials, 1955, pp 80-97.
10. Snell, A.W., and Van Schilfgaarde, J., Four Well Method of Measuring Hydraulic Conductivity of the Soil, Transactions, American Society of Agricultural Engineers, Vol. 7, 1965, pp 83-87.
11. Maytin, I.L., A New Field Test for Highway Shoulder Permeability, Proceedings, Highway Research Board, Washington, D.C., Vol. 41, 1962, pp. 109-124
12. Szily, J., "Permeability Device for Sand Samples, Proceedings, First International Conference of Soil Mechanics and Foundation Engineering, Cambridge, Mass., Vol. III, 1936, pp. D-24 to D-26
13. Bouwer, H., and Rice, R.C., Journal, Irrigation and Drainage Division, American Society of Civil Engineers, IR4, December, 1968, pp.481-492.
14. Denisov, N. Ya., The Concept of the Percolation Coefficient and the Methods of its Determination, Selected Sections from Engineering Geology and Hydrogeology (Moscow), Israel Prog. for Sci. Trans., 1960, pp. 9-66
15. Wenzel, L.K., Methods for Determining Permeability of Water Bearing Materials, Water Supply Paper No. 887, U.S. Geological Survey, 1942, pp 20-50, 71-117
16. Slitchter, C.S., The Motion of Groundwater, U.S. Geological Survey Water Supply Paper No. 67, 1902, pp. 48
17. Moulton, L.K., and Seals, R.K., In Situ Determination of Permeability of Bases and Subbases, Phase I, Interim Report, Report No. FHWA-RD-78-21, Federal Highway Administration, Washington, D.C., December, 1977, 104 pp.
18. Wallace, J.F., Project Manager, Dames & Moore, Letter to Jerome R. Blystone, Federal Highway Administration, November 26, 1980, Unpublished
19. Hoffman, G.L., In-Situ Permeability of Bases (FPTD), Report No. PA 80-11, Submitted to Federal Highway Administration by Pennsylvania DOT, Harrisburg, PA, April 1981, Unpublished
20. Baldwin, J.S., and Jarvis, J.G., In Situ Permeability of Bases, Report No. DOT FH 11-89-47, Submitted to Federal Highway Administration by West Virginia DOH, Charleston, WV, October, 1981, Unpublished
21. Jackson, N.C., In-Situ Permeability of Bases, Report No. DOT-FH-11-8007, Submitted to Federal Highway Administration by State of Washington DOT, Olympia, Washington, December, 1981, Unpublished
22. Ho, R.K.H., and Cogdill, L.L., Evaluation of Field Permeability Testing Device, Submitted to Federal Highway Administration by State of Florida DOT, Gainesville, Florida, February 10, 1982, Unpublished.
23. Jarvis, J.G., and Sovick, G.P., III, In-Situ Permeability of Bases (Phase 2), Submitted to Federal Highway Administration by West Virginia DOH, Charleston, WV, August, 1985, Unpublished
24. Bender, T.J., An Evaluation of the Field Permeability Testing Device, Submitted to the Federal Highway Administration by the New York State DOT, Albany, NY, 1986, Unpublished
25. Ho, R.K.H., Webb, T.B., and Cogdill, L.L., Field Trials of In-Situ Permeability Device, Submitted to Federal Highway Administration by State of Florida DOT, Gainesville, Florida, May, 1986, Unpublished
26. McLarin, M., and Bartholomeusz, W.G., The Field Permeability Testing Device, Report 2/85/5, Central Laboratories MWD, Lower Hutt, New Zealand, 1985, 32 pp

EXPERIMENTAL PROJECT NO. 12:
CONCRETE PAVEMENT DRAINAGE REHABILITATION

Robert C. Kelly

Federal Highway Administration
Experimental Projects Branch

INTRODUCTION

The pavement structural section is the most costly element of the highway system. Its premature failure is of major concern. Among the reasons cited for pavement failures, inadequate base drainage has been identified as a nationwide problem, particularly for concrete pavements. Although States do design pavements with base drainage in mind, many States have had to use different remedial pavement drainage techniques. Pavement drainage rehabilitation techniques fall into two categories: (1) techniques to seal the pavement to prevent surface water infiltration, and (2) techniques to remove water once it has entered the pavement system.

There are differences of opinion as to whether the various remedial pavement drainage techniques work and their effectiveness. These differences occur because there is a lack of good documentation to substantiate the various opinions and because of the many variables that affect pavement drainage. Therefore, there is a need to evaluate these pavement drainage approaches. This project primarily investigated the effectiveness of retrofit longitudinal edgedrain systems.

OBJECTIVES

The objectives are to evaluate and clearly document the effectiveness of retrofit longitudinal edgedrains in removing water that has entered the

pavement system. A secondary objective will be to evaluate various nondestructive methods for inspecting and evaluating pavement drainage systems. The ultimate objective of the project is for the FHWA to be in a better position to provide guidance to States on the performance and design of longitudinal edgedrain systems.

SCOPE

FHWA field personnel have canvassed their regions to identify projects 3-10 years old that will demonstrate the effect of retrofit edgedrains. Extensive reviews of candidate projects were conducted, and ten States (Alabama, Arkansas, California, Illinois, Minnesota, New York, North Carolina, Oregon, West Virginia, and Wyoming) were selected for detailed study and instrumentation. An attempt will be made to compare the test sites with adjacent control sections where no edgedrains were installed.

The Office of Surface Water of the U.S. Geological Survey (USGS) is assisting with instrumentation and data collection. Rainfall and runoff from the drainage system will be measured by a dual tipping bucket gauge to determine the response of the system to storm events. Druck pressure transducers and Delbhorst soil moisture blocks will be installed in the pavement section to measure moisture and saturation conditions under the pavement. At several sites, additional moisture readings will be taken by a neutron probe to verify readings from other instrument sensors.

Surface permeability readings will

also be made. Readings at the pavement/cement-treated base and the cement-treated base/subbase interfaces as well as deep within the subbase will be recorded using a constant head permeameter. Attempts will be made to use dye injection to trace flow at the pavement/cement-treated base interface.

The instrument configuration plan is shown in Figure 1. Data will be collected and stored in a data logger installed in an instrument house at the site. The USGS will retrieve and analyze the data on a monthly basis.

In addition to the instrumentation, the condition of the existing edgedrains will be examined by excavating "post mortem" inspection pits. Condition of the edgedrain pipe, backfill and filter fabric will be evaluated for clogging, erosion of fines, and other evidence of performance. Visual surveys of the pavement will be

made periodically as well as measurements of faulting and pavement slab deflection.

CURRENT STATUS

Test instrumentation sites have been installed on I-65 near Greenville, Alabama. Different types of instruments are being evaluated and installation techniques refined. The remaining States will be instrumented in the Spring of 1989. North Carolina is scheduled for instrumentation in late March.

An FHWA draft state-of-the-art report on concrete pavement drainage rehabilitation has been distributed for comment within FHWA. Since site installations will be monitored for a minimum of one year, followed by "post mortem" inspections, the final report for this project will probably not be available until early 1991.

**Session 3:
In-Situ Temperature
Measurements**

TEMPERATURE AND THAW DEPTH MONITORING OF PAVEMENT STRUCTURES

David C. Esch, P.E. State of Alaska Department of Transportation

Pavement surface and subsurface temperatures may be measured with a variety of sensors. True surface temperatures can be measured only by temporarily installing contact thermometers, thermocouples, or thermistors, or by use of a non-contact infra-red radiation sensing thermometer. In practice, the actual surface "skin" temperature is less meaningful than the temperature at the mid-point of the pavement layer, which may be used to estimate the pavement's mechanical properties and to determine the mean-annual pavement surface temperature.

Beneath the pavement layer, temperatures are generally observed primarily to determine the frozen or unfrozen state of the granular layers of the pavement structure and the subgrade soils. For this purpose, thermocouples and the thermistors are the sensors of common choice, although mechanical recorders and even strings of thermometers have been used for this purpose.

The location of the freezing or thawing front may be inferred from the plotting and interpretation of subsurface temperatures at various depths, or may be measured directly from "frost tubes". An alternative method discussed herein is the use of the TDR probe method to measure indirectly the unfrozen moisture content of the soil. This procedure may resolve the dilemmas which can result from the fact that soil at 0°C may be either in the frozen or thawed states.

This presentation discusses the practical considerations, the design, installation, monitoring, and interpretation of temperature and frost

depth monitoring systems for roads and airfields, based on 35 years of field experience in Alaska.

Introduction

In selecting equipment and measurement methods for determining temperatures and depths of freezing and thawing in pavement structures the engineer should first focus on the purpose of making the measurements and then on the required frequency and precision of the data. Since the mechanical properties of asphalt-bound pavement layers are strongly temperature dependent, research analyses of the field performance of pavement structures may require knowledge of the hourly, daily, and annual variations in pavement and treated base layer temperatures. In these shallow layers, the accuracy of the individual temperature observation probably needs to be no better than 1-3°C, but data recording becomes essential in view of the rapid temperature changes which occur. Greater accuracy in recorded measurements of near-surface temperatures is required only when the data will be used for thermal heat-flow analyses or for studies of air to surface temperature relationships, or for forecasting the formation of road surface ice. Mechanical properties of unbound soil layers are not generally considered to be temperature dependent in the temperature range above 0°C, but these properties change greatly between the "frozen" and "thawed" states. From examination of the pavement distress versus age plots from the AASHTO Road Test, it is apparent that most of the damage occurred during the brief period of springtime thaw-weakening. For this reason the location of

the freeze-thaw interfaces becomes extremely critical in the analysis of pavement performance at specific times during the freezing and thawing seasons. Temperature measurement accuracy should approach or exceed 0.2°C at these times. In addition, the Engineer must consider the fact that frozen and unfrozen soils can both exist at temperatures between 0° and -2°C , depending on porewater salt contents, clay mineralogical effects, and hysteresis effects. At these times, proper analysis and interpretation of temperature data becomes essential in inferring the locations of the freeze-thaw interfaces. The use of supplemental data from devices such as frost-tubes and time-domain-reflectometer (TDR) probes becomes very helpful in location of freeze-thaw interfaces. Other thaw depth detection procedures such as soil resistance measurements or unfrozen moisture measurements by the TDR method (Kane, 1987) should also be considered for use in conjunction with or in lieu of soil temperature measurements. This may be particularly critical where heavy roadway salting is used and salt infiltration into the pavement structure is likely.

Information used in preparation for this paper came from the literature, and from instrumentation and monitoring experience on more than twenty road and airfield pavement and subgrade temperature measurement sites in Alaska. The first of these sites were instrumented in 1953, when five Alaskan roadway sites on permafrost subgrades had thermistor cables installed along with remote "Bourdon tube" chart recorders for measuring subsurface and "surface" temperatures. The history and theory of temperature measurements in solids has been well reported elsewhere (See References) and the focus herein will be kept on the practical problems and questions which relate to field monitoring of road and airfield embankments.

Methods of Temperature Measurement

Thermometers are broadly defined as temperature measuring instruments devised to indicate their own temperature based on physical changes, and designed to be inserted into areas where the adjacent temperature is desired. The most common of these is the liquid-in-glass thermometer. Miller (1985) discusses the use of mercury-glass thermometers by a Dr. Williams to measure soil temperatures in Vermont in 1789. Mercury thermometers are still in common use in China to measure soil near-surface and subsurface temperatures, particularly for studies involving foundations on permafrost.

Since the establishment of the International Temperature Scales and refinement of the liquid-in-glass thermometer, many other procedures for the measurement of temperature have been developed. Baker et al. (1975) provides a good discussion of six types of thermometers and also of "radiation pyrometers" which are non-contact temperature indication devices. For temperature measurements in pavements and in soils, the temperature range of concern is from -50 to $+60^{\circ}\text{C}$. Consideration should be given to several devices suitable for use over this range of temperatures; listed and described as follows:

Radiation Pyrometers

These devices, sometimes termed "infrared thermometers" are available from several manufacturers, and provide acceptably accurate measurements of pavement surface temperatures ($\pm 2^{\circ}\text{C}$) when operated within the manufacturer's recommended temperature range. Their primary use is in control of asphalt pavement mix compaction, to observe field cooling rates, and also for approximate observations of pavement temperatures during field deflection testing in conjunction with Benkelman Beam, falling weight deflectometer (FWD), or cyclic load test methods (Dynaflect & Roadrater). Typically available equipment with a sensitivity of about 1°C is available in the cost range of \$300 to \$900. Some units allow adjustment for the emissivity of the pavement surface and can be calibrated in the field if the actual surface temperature is measured by more precise methods. Infrared thermometers do not appear to be well suited for continuous recording of surface temperatures under field conditions. These units do allow almost instantaneous measurements when manually operated, by simply pointing the sensor at the surface in question and observing the readout. As such, they have a definite place in the field of pavement temperature measurements.

Bourdon Thermometers

Bourdon thermometers typically consist of a rather large $1/4$ " to 1" diameter bulb section filled with a liquid; a gas and liquid (vapor pressure type), or a pure gas. The changes in temperature at the bulb result in changes of volume of the liquid or in pressure of the gas filling the bulb. These changes are sensed by a bourdon tube, and indicated by a connected rotating pointer, or used to activate a pen-arm on a chart recorder. By proper design these units can be fabricated to read over any specified temperature range, with the sen-

sitivity being a function of temperature range. They have the added advantage that the connecting tubing between the temperature sensing bulb and the bourdon tube readout may be 100 feet or more in length. They are ideally suited for 7 to 31 day chart recorders which can be driven by battery power or by key-wound clock mechanisms. Accuracy of 1° - 2°C is provided and calibration checks may be easily made by inserting the bulb in an ice-water bath. The previously mentioned temperature recorders first purchased and installed at Alaskan roadway sites in 1953, have been used periodically at various field sites over a 30 year period. For simplified continuous mechanical recording of near-surface pavement temperatures, the bourdon thermometer may still merit consideration for monitoring of pavement layer temperatures.

Installation of bourdon thermometers is best done by placing a rigid plastic or metal access casing at the desired depth beneath the pavement surface during construction. Typically, a casing is placed just beneath the final pavement layer. The access casing then allows the temperature sensing bulb to be inserted beneath the desired location and removed as necessary for periodic calibration checks.

Liquid-in-Glass Thermometers

The primary use of these simple temperature measurement devices in pavement studies is for the observation of pavement layer internal temperatures during non-destructive (FWD, etc.) field testing. The proper analysis of pavement responses to test loadings by the "back-calculation" of layer elastic properties requires a reasonable estimation of the average pavement layer temperatures; or better yet, of the temperatures at the top, middle, and bottom of the asphalt-bound layers. These temperatures may be measured by punching or drilling a small hole to the desired depth, filling it with a conducting fluid, and inserting a partial-immersion type thermometer. The precision of such thermometers can be almost any level desired, depending on the functional range of the thermometer used. The principal disadvantages of glass thermometers for subsurface observations are the several minute waiting time required for stabilization of temperatures, and the fact that the access holes or tubing, and heat conduction along the thermometer, may in themselves change slightly the indicated temperatures. For use in measuring pavement temperatures, a "partial immersion" glass thermometer, or a small metal bourdon thermometer of the one-piece type

having a rotating pointer on the dial face are the preferred types.

Electrical Resistance Thermometers (RTDs)

The electrical resistance of a wrapped coil of platinum wire has been found to increase nearly linearly with temperature over a wide temperature range (Fig. 1). Precisely prepared and calibrated platinum resistance thermometers are generally regarded as the most accurate and reliable laboratory measurement system for the temperature range of -200 to $+1177^{\circ}\text{F}$. However, the relatively large size ($0.1"$ to $0.3" \times 1"$) of the sensors, their slow rate of temperature change versus time, their small change in resistance with temperature (0.4 to 2 ohms/ $^{\circ}\text{C}$), and the high costs of RTD sensors ($\$75$ - $\$150$) have generally led to a preference for other types of sensors for field use. A second type of thermally sensitive electrical resistor, termed the "thermistor", is currently favored for precise temperature measurements in the vicinity of 0°C , as discussed below.

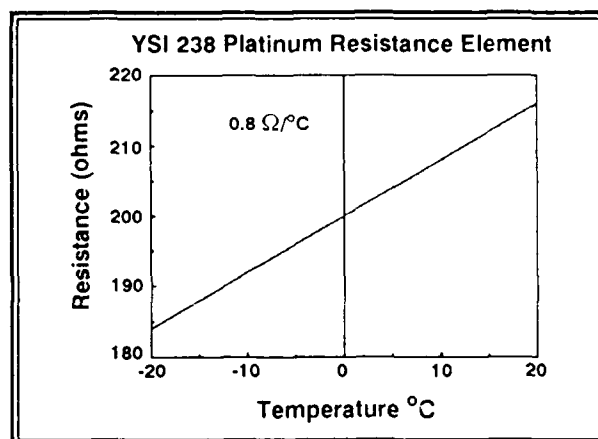


Fig. 1. Typical Platinum Resistance Thermometer (RTD), resistance versus temperature plot.

Thermistors

Thermistors, named for **THERM**ally sensitive res**ISTORS**, generally have an inverse and very non-linear relationship between resistance and temperature. Their primary attribute is their large change in resistance with temperature. A commonly used type varies by roughly 500 ohms per $^{\circ}\text{C}$ in the vicinity of 0°C (Fig. 2), allowing for easy measurement of temperatures with a, low-cost, portable ohm-meters or an appropriate recording device.

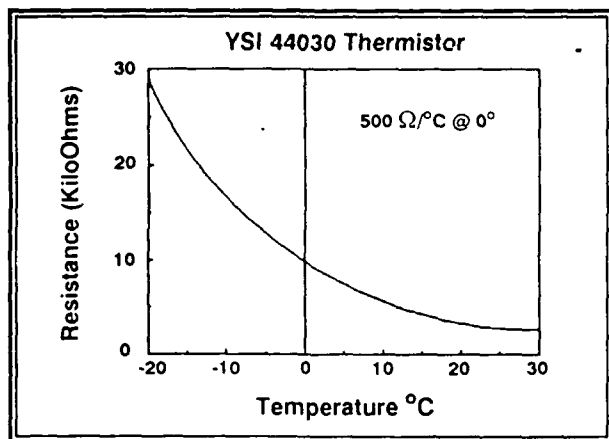


Fig. 2. Typical plot of resistance versus temperature for a common thermistor type.

Thermistors are manufactured by compressing and sintering powdered metal oxides to form small beads or discs. Lead wires are connected to opposing sides, and the thermistors are then encapsulated in glass or epoxy for moisture resistance.

The first temperature measurement cables installed at Alaskan permafrost roadway sites in 1953 utilized thermistor discs which were about 1/2 inch in diameter. The resistance versus temperature relationships of these early thermistors were all individualistic, and separate calibration equations had to be used for each. In addition, the stability of temperature versus resistance calibrations over time were in doubt, and these early cables were removed and re-calibrated after about 5 years in service. Significant changes in calibration were noted. Thermistors installed at Alaskan sites at Fairhill (1979) and at Gardiner Creek (1983) have also presented long-term drift problems, as evidenced by different indicated temperature-time trends from adjacent deep thermistors (Fig. 3 and 4). The drift in thermistor calibrations over time is generally attributed to the development of micro-cracks in the sintered thermistor pellet. This cracking is intensified by periodic overheating or temperature cycling.

In recent years, new manufacturing procedures for thermistors have improved their consistency, durability, and interchangeability. Sorted and matched thermistors may be purchased to provide interchangeability from 0.2°C to better than 0.05°C , so that a single temperature-resistance equation may be used for all sensors in a given cable.

The concern over stability in soil burial, in spite of careful preparation and sealing efforts aimed to exclude moisture, remains as the major

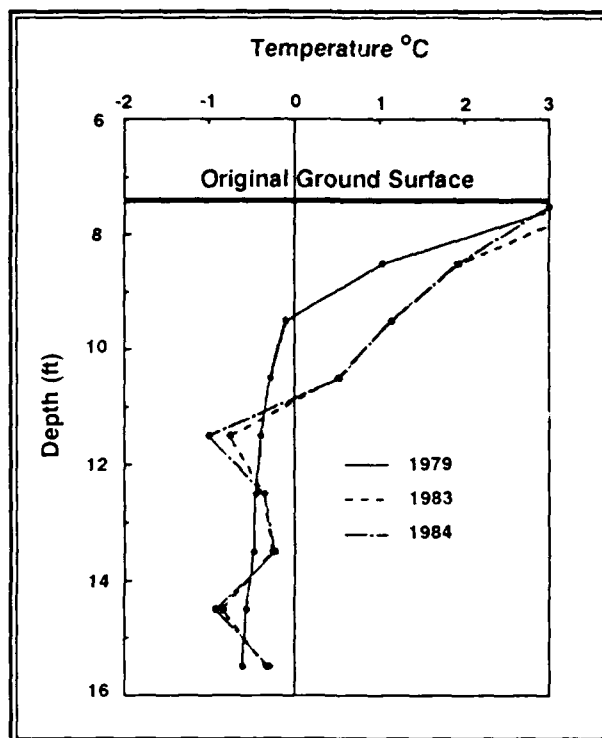


Fig. 3. Temperature versus depth plots in September for same thermistor string in first (1979), fourth, and fifth years. Indicates drift of calibrations on thermistors at 11.5 and 14.5 ft. depths.

objection to use of thermistors for long-term soil burial. In some pavement installations, one would like the sensors to remain stable and useable for periods of 20 years or more. One alternative approach is to install access casings through the pavement surface, and to progressively lower a single thermistor probe for logging temperatures at selected depths. Though time-consuming and disruptive to traffic, this procedure provides very high accuracy if the access tube is kept small and filled with a fluid such as glycol or oil. It minimizes the installation costs, allows the periodic re-calibration of the thermistor probe, and may be ideal when infrequent thaw depth data is needed at the lowest possible cost.

Thermocouples

Thermocouples are simply electrical junctions of two wires made of dissimilar metals, and function based on "Seebeck-effect" voltages generated by the heating or cooling of a two-metal junction. The basic thermocouple measurement circuit must consist of a pair of thermocouple junctions (Fig. 5) with the voltage measured being characteristic of the wire materials used and indicating the difference in temperature between the two junctions (Fig. 6). When the reference

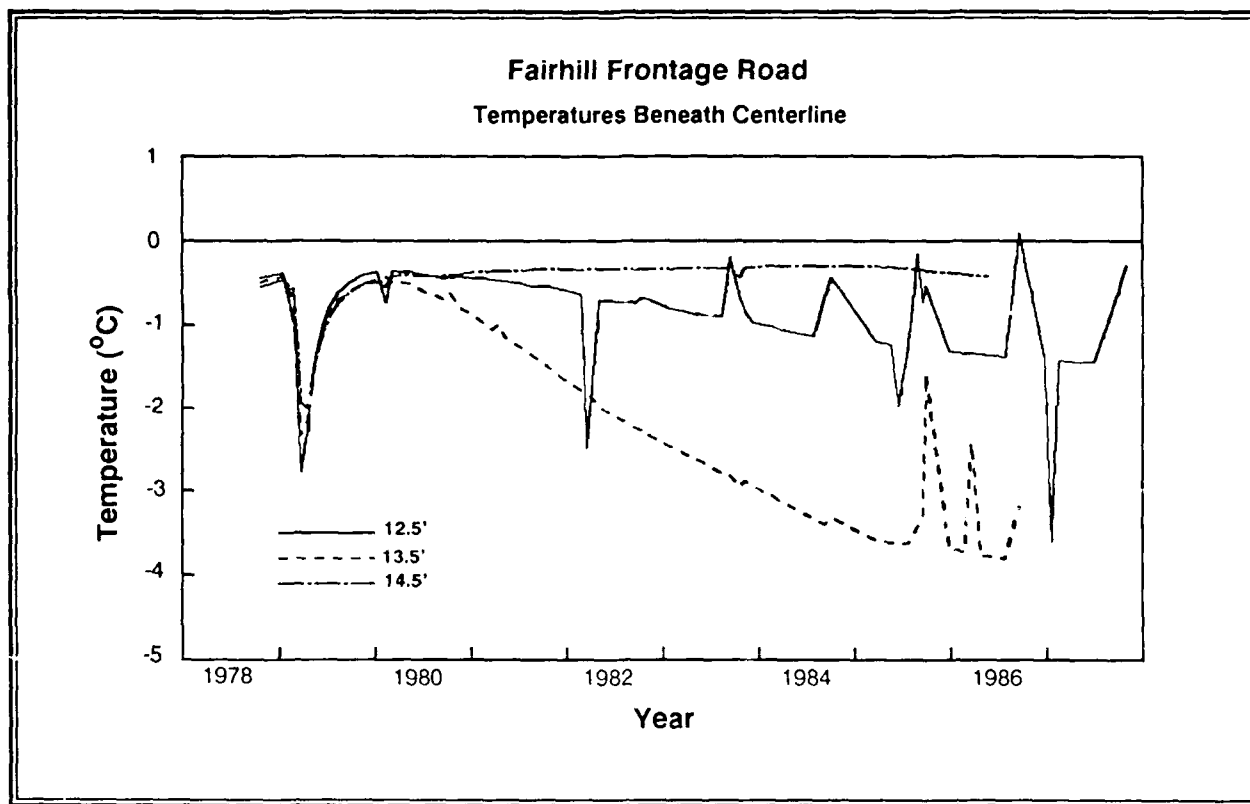


Fig. 4. Temperature versus time plots of stable (-14.5 ft.) and adjacent drifting (-12.5 & -13.5 ft.) thermistors.

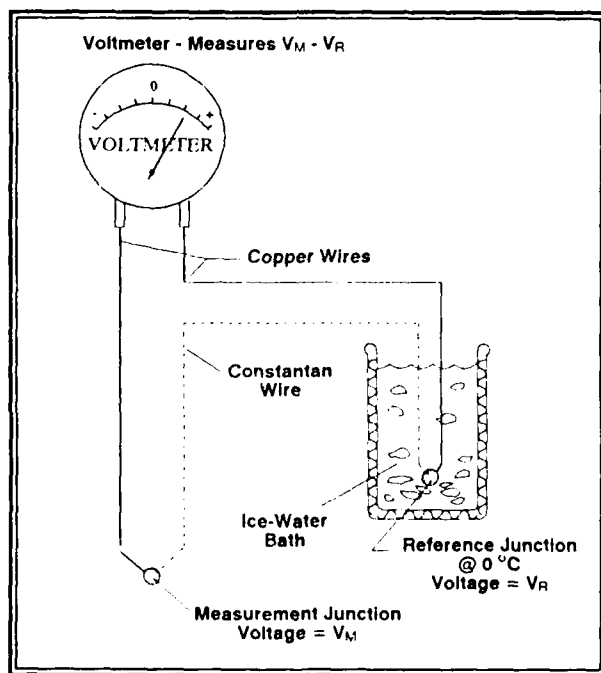


Fig. 5. Typical Type T thermocouple measurement circuit.

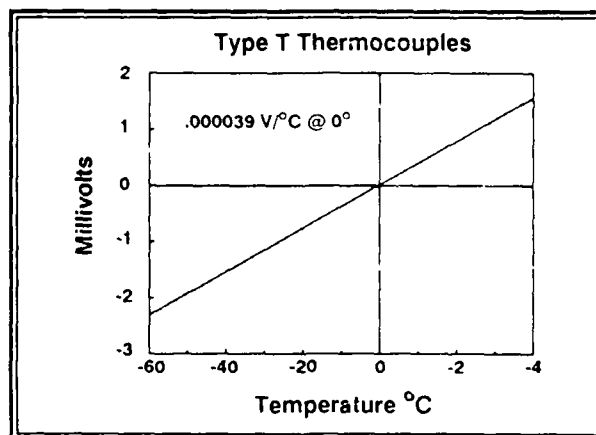


Fig. 6. Millivolt ($\text{V} \times 10^{-3}$) output of Copper - Constantan or Type T thermocouples relative to reference junction in ice bath at 0°C .

junction temperature is known, as 0°C in an ice bath, the measurement junction temperature can be calculated from standard tables. Many different wire materials may be used. In practice, for temperature measurements in soils the thermocouple materials of choice are copper and constantan (an alloy of copper and nickel), and are designated as "Type T" thermocouples. The accuracy standards for Type T thermocouples are much higher at 0°C and below, than the limits for other thermocouple types. "Special Type T" thermocouple wire, produced to vary by no more than $+0.4^{\circ}\text{C}$ from the standard Type T thermocouple tables, is generally used. This wire offers twice the accuracy of "standard wire". In practice, a string of thermocouples assembled from the same wire lot will generally agree within $\pm 0.1^{\circ}\text{C}$ in the vicinity of 0° , the critical temperature for freeze-thaw determinations. Ideally the reference junction thermocouple should also be made of the same wire lot, or else the calibration of the reference junction should be checked by placing both the temperature measurement and reference junction thermocouples in properly prepared ice-baths.

Field Instrumentation

Thermocouple circuitry and readout equipment in use by the Alaska Department of Transportation and Public Facilities is discussed in detail in the paper by R. Briggs, also presented at this symposium. In brief summary, separate thermocouple wire pairs are wrapped together in cables and brought out to jack panels or 2 pole copper-constantan rotary switches. Thermocouple junctions are twisted and soldered or made with crimp-on "Quik-Tips"™, and then coated for waterproofing. Field readout devices are typically high-resolution (1 micro-volt) portable Volt-Ohm meters. The reference junction temperature is maintained at 0°C by a carefully prepared ice-bath (Fig. 7). In practice, most errors in field readings have been traced to improperly prepared or maintained ice baths or to temperature gradient effects on measurement equipment exposed to low air temperatures ($t^{\circ}\text{C}$). The ice-bath related problems can be avoided by careful ice bath preparation, making certain that the "thermos" flask contains no more water than necessary to fill the voids between the ice particles, and that the reference junction is kept near the mid-point of the ice bath. If any drift in voltage readings occurs when the ice bath is agitated, the stability of the ice bath is at fault and more ice must be added. Temperature effects on meters may be avoided by keeping them well insulated, and allowing sufficient warmup time. Taking readings from

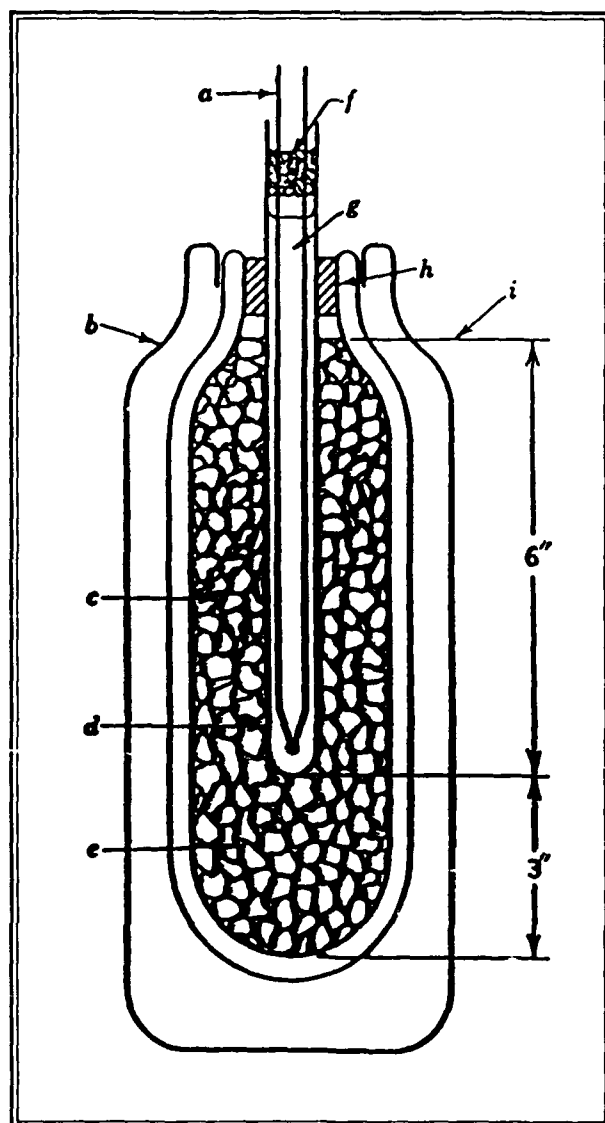


Fig. 7. Detail of recommended ice bath reference for thermocouple measurements.

- a. Thermocouple wire with insulating coating extending well below the surface
- b. Dewar ("Thermos") Flask
- c. Crushed, pea-size ice extending to bottom
- d. 1/4" diameter glass tube
- e. Distilled or de-ionized water filling spaces between ice granules
- f. Cotton plug
- g. Silicone oil or acid-free kerosene
- h. Rubber stopper
- i. Water level

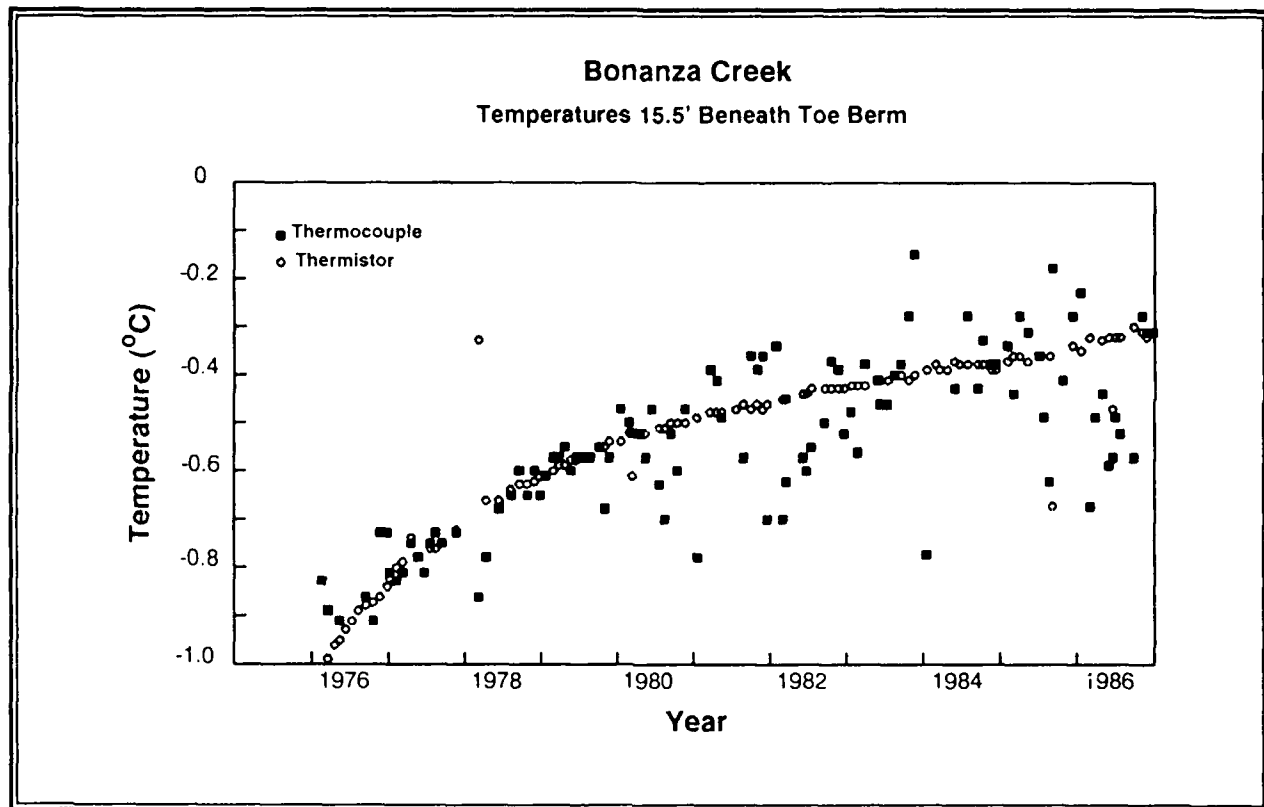


Fig. 8. Comparison of temperature data from paired thermocouples and thermistors at Bonanza Creek test site (from R. Briggs).

a warm vehicle or other shelter is preferable in winter.

Field Installation Procedures

Direct soil burial or placement in 3/4" or 1" plastic tubing are methods both in common use. When placed near the surface or in areas with high thermal gradients such as around buried insulation layers, direct soil burial is preferred. Where significant frost-heaving is expected, care is required in design and installation to assure that sensors are not progressively pulled out of position by frost action forces. Access caps or ports placed in the pavement commonly give problems from intrusion of water and dirt, and complete burial of cables beneath the pavement, extending laterally to a remote readout box is always preferred. In practice, deep borings are backfilled around the cables using rock chips or dried mortar sand up to a depth of 4 to 5 feet from the surface, above which native soils are placed and properly compacted.

Field Accuracy Expectations

The anticipated field "consistency" of deep (-20 to -30 ft) subsurface temperatures as indicated by monthly readings of thermistors is about

.02°C or better, which requires field repeatability to 10 ohms or better. The short-term (1-3 yr) accuracy of thermistors is considered to be very good. Most deeply buried thermistors placed in permanently frozen or "permafrost" soils have been stable or have not drifted more than 0.5°C over periods of up to 15 years. However, some thermistors have drifted by as much as 4°C after 10 years in service, in spite of efforts to seal them against moisture. For long-term service, thermocouples have proven superior, although the month to month repeatability of deep thermocouples is only expected to be 0.3°C or better (Fig. 8).

No significant long-term drift has been noted on thermocouples which have been in service as long as 20 years, as judged by observed temperature versus depth plots of many vertical strings of 12 thermocouples each.

Thaw Depth Determinations

The accurate location of the top and bottom of seasonal frost layers from subsurface temperature data requires some judgement, coupled with a consideration of heat flow theory. Changes in the position of frozen/thawed inter-

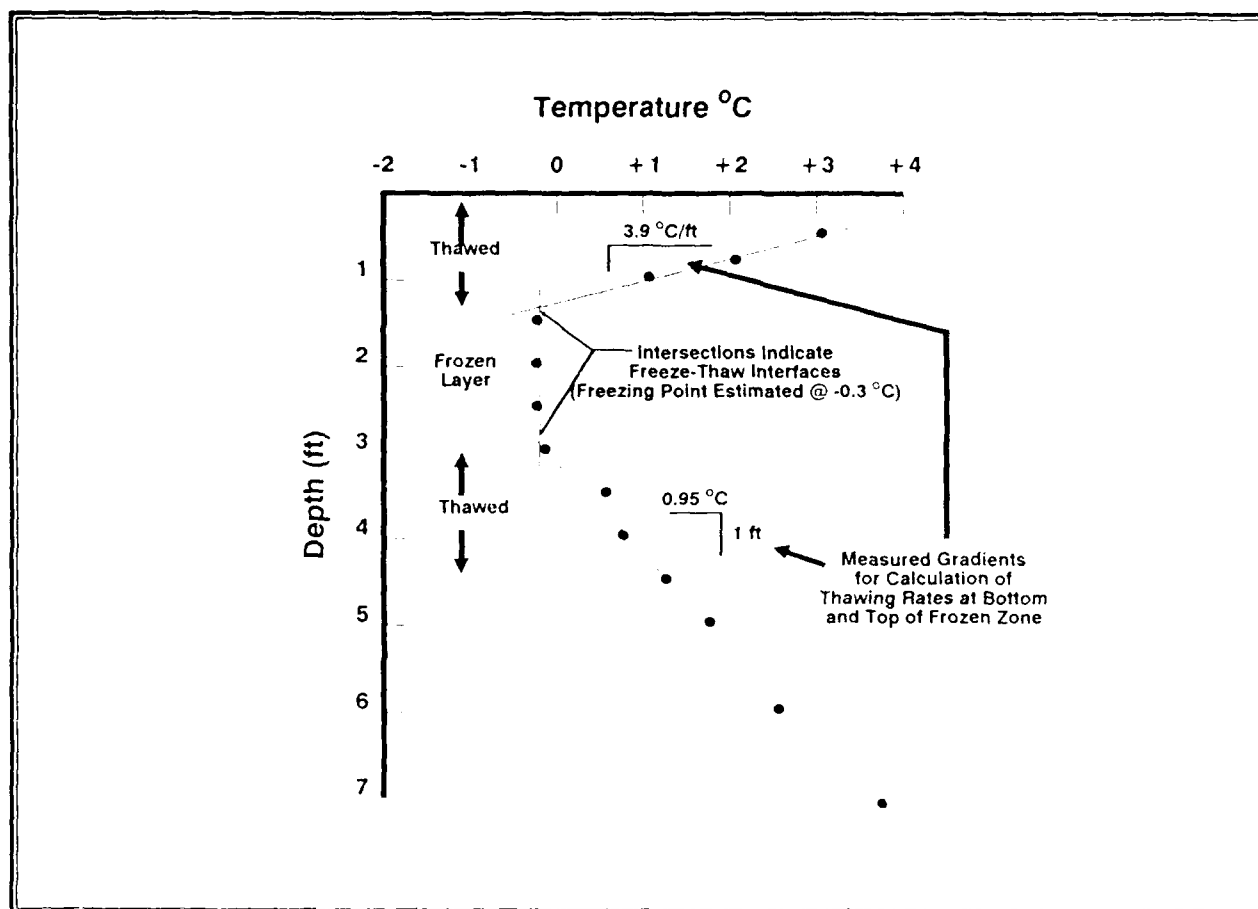


Fig. 9. Procedure used to determine depths of freeze-thaw interfaces from subsurface temperature data points.

faces require that the heat of fusion of the soil moisture must be removed or added at the interface, resulting in an appropriate change in the frost depth. The rate of change of the frost depth can be calculated from surface and subsurface temperature data. From a knowledge of the soil densities and moisture contents and a plot of temperatures versus depth, the positions of the top and bottom of the frozen layer and the rates of change of these positions may both be determined. Accurate interpretations require, however, that temperature data be obtained after several days of freezing or thawing weather, when the surface layers are at temperatures well below or above the freezing point. At times, all subsurface temperatures may be found to be very close to the phase change temperature, and accurate thaw-depth interpretations then become much more difficult or impossible to make.

The procedure for thaw depth determinations should be applicable without the need to know the actual freezing point of the porewater. Thaw-depth determinations are generally made as shown by Figure 9, based on an adequate number

of temperature versus depth data points obtained from vertical strings of 12 to 16 thermocouples or thermistors. In this procedure, straight lines are drawn through the two or three data points just above or below the suspected location of the freeze-thaw interfaces, and the interfaces are determined by the intersection of these lines. If temperatures are accurate, the freezing point depression may also be determined, as well as the hourly rates of freezing and/or thawing.

Economic Considerations

The current costs of sensors, wire, and readout devices for thermocouples, thermistors, and RTDs are shown by Table I. Costs not shown which could not be quantified but must be considered, are these for fabrication and calibration checks.

Thermocouples require little preparation time and are so similar in output when made from the same wire lot that no calibration checks are needed. However, quality 2-pole thermocouple switches or plug panels are moderately expensive,

Table 1. Temperature Equipment and Sensor Costs.

Sensor Type	Sensor	Unit Costs	
		Wire/50'	Meter
Thermocouple	\$0.05	\$20.00	\$900
Thermistor	\$25.00	\$12.00	\$370
Platinum RTD	\$75.00	\$15.00	\$900
TDR Probe	\$20.00	\$10.00	\$4600

ranging from \$8.00 to \$18.00 per thermocouple connection.

Thermistors require extreme care in attachment of the leads and in sealing against moisture. Overheating during soldering, rough handling, or excessive resistive heating will destroy thermistor beads. Calibrations of completed thermistors must be checked at 0°C to assure consistency prior to installation. Switches for thermistors are relatively low in cost, at about \$1.00 to \$2.00 per thermistor.

Table II. Temperature Measurement System Considerations and Types Installed by Alaska DOT&PF.

<u>Ideal System for Temperature Measurements</u>	
Low Cost	
Zero Drift	
Extreme Accuracy	
No Operator Sensitivity	
Simple to Log Data	
Extreme Durability	
<u>Use in Alaska (DOT&PF) Practice</u>	
Thermistors	1953 - 59
Thermocouples	1960 - 73
Combined System	1974 - 78
RTDs	1979 - 80
Thermistors	1979 - 85
Today (1989)	Combined Systems

Platinum RTDs are more durable than thermistors, but calibrations should again be checked after fabrication, and care must be taken in preparing and insulating the lead wires. Readout equipment for RTDs must be capable of greater precision than for thermistors, as readings are required to .01 ohm.

Summary of Temperature Sensor Use in Alaska - Past and Future

The history of sensor choice and use in Alaskan highway study site monitoring is shown by Table II. It can be seen that the favored sensor type has vacillated between thermistors and thermocouples. RTDs were also successfully used at one 2-year study site, but no long-term experience is available.

Where low-cost information is required only on annual maximum depths of freezing and thawing beneath roadways, recent installations by the DOT&PF have involved the installation of plastic pipe casings, which allow logging of temperatures versus depth using a single thermistor probe. For future installations requiring temperature measurement cables we will strongly consider the use of several RTDs in conjunction with many thermocouples, to provide a stable long-term temperature measurement system.

References & Bibliography

ASTM, "Manual on Use of Thermocouples in Temperature Measurement", ASTM Publication 470B, (1981).

Baker, H.D., Ryder, E.A. and Baker, N.H., "Temperature Measurement in Engineering", Omega Engineering, Inc., Stamford, CT, (1975).

Kane, D.L., "Soil Moisture Monitoring Under Pavement Structures Using Time Domain Reflectometry", Alaska Department of Transportation and Public Facilities Statewide Research Report AK-RD-87-08, (1987).

Miller, D.L., "Temperature Monitoring/Ground Thermometry", in ASCE Monograph Thermal Design Considerations in Frozen Ground Engineering pp. 53-71, (1985).

Osterkamp, T.E., "Temperature Measurements in Permafrost", Alaska Department of Transportation and Public Facilities Statewide Research Report AK-RD-85-11, (1984).

DETERMINATION OF FROST PENETRATION BY SOIL RESISTIVITY MEASUREMENTS

Ronald T. Atkins
U.S. Army Cold Regions Research and Engineering Laboratory
Hanover, New Hampshire 03755

ABSTRACT

Because of freezing point depression and isothermal springtime conditions, frost penetration measurements using temperature-sensing devices can become unreliable. In recognition of this problem two frost penetration sensors that depend on changes in soil resistivity were tested. Tests were conducted on a parking area with an asphalt-concrete surface where salt was periodically applied as part of snow removal operations. For comparison, data were obtained from a resistivity probe, a thermocouple probe and a thermistor probe. Results indicated that measuring temperature to determine frost penetration can lead to large errors under some conditions, for instance, when salt has been applied or when frost is coming out of the ground in spring. The resistivity probe performed reliably

during the entire measurement program. Conclusions from this study indicate that resistivity probes have definite advantages that should be considered when future frost penetration measurement programs are designed.

INTRODUCTION

A widely used method for determining frost penetration into the ground during winter relies on measuring temperature as a function of depth. This method assumes that temperatures below 0.0°C indicate frozen soil. Figure 1 is a typical plot of temperature vs depth for Hanover, N.H., in midwinter. It shows that frost has penetrated to a depth of 74 cm.

However, frost penetration determinations under roadbeds that rely on temperature measurements have two disadvantages:

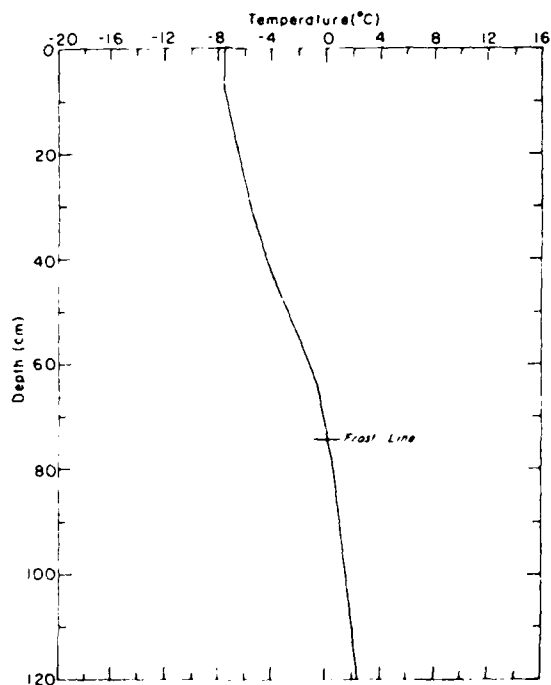


Figure 1. Typical temperature vs depth curve during winter months.

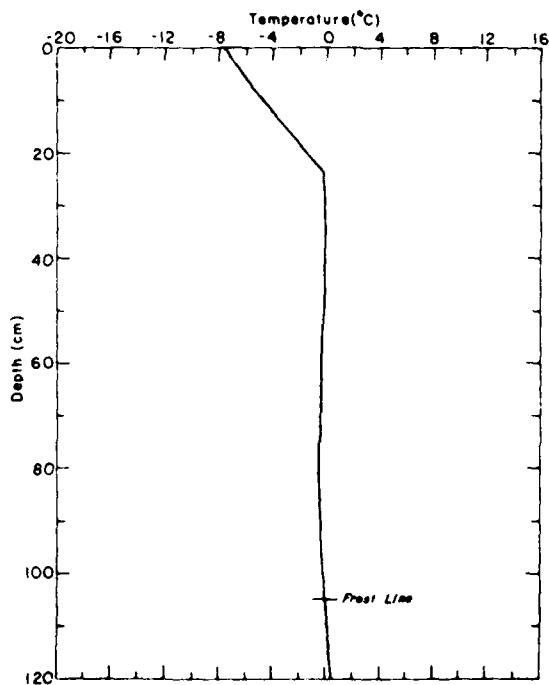


Figure 2. Typical temperature vs depth curve during springtime conditions.

1. Salts or other impurities in the soil/water system depress the freezing point below 0.0°C .

2. During spring thaw, subsurface temperatures often become nearly isothermal at 0.0°C (see Fig. 2), making it difficult to establish the frost line.

The problem of freezing point depression can be partially solved by taking soil samples and measuring their actual freezing temperature. But even then the nonhomogeneity of the soil plus the changing springtime groundwater conditions may cause uncertainties to remain. The problem is further complicated by the requirement that the temperature measurements be very accurate. For instance, in Figure 1 an uncertainty of $\pm 0.25^{\circ}\text{C}$ (typical for a thermocouple measurement) would lead to a frost depth uncertainty of approximately 5 cm. The same $\pm 0.25^{\circ}\text{C}$ uncertainty under the springtime conditions of Figure 2 would lead to a frost depth uncertainty of approximately 40 cm.

The desire to make frost penetration determinations independent of temperature measurements has led to the development and use of a series of soil resistivity probes. This paper describes two of the probes developed, gives the results of the initial test program, and makes recommendations for future work.

THEORETICAL CONSIDERATIONS

Distilled water has a relatively high volumetric resistivity, on the order of several hundred megohms. However, for water containing even small concentrations of impurities, such as is normally found

in soils, the volumetric resistivity drops to values typically around 20,000 ohms. If this groundwater is then frozen, the mobility of the charge carrier becomes severely restricted so that the volumetric resistivity rises abruptly. Typical volumetric resistivities for frozen groundwater are greater than 100,000 ohms and often may be as high as several megohms (1 megohm = 1,000,000 ohms).

Since the electrical resistance of soil moisture rises sharply when the water freezes, the state of subsurface water can be determined by taking resistance measurements. The sensing surfaces can be fixed plates, bare wires or nearly any type of electrical conductor. The spacing between these surfaces is not critical but must be held uniform. Also, good contact must be maintained between the surfaces and soil. Under these conditions the resistance between the sensing surfaces (as sensed by an external circuit) can be determined by a composite resistivity term consisting of several parameters. For instance, the value will depend, in part, on the resistivity of the soil itself, the resistivity of the water, the percent moisture content, the resistivity of any ice crystals present and the contact resistance between the soil and the surfaces of the sensor plates.

The volumetric resistivity of dry bulk soils is normally very high, on the order of several megohms. Therefore, soil resistivity does not play much of a part in determining subsurface soil resistance. On the other hand, the resistivity of the groundwater is relatively small, so if it is present to any appreciable extent it

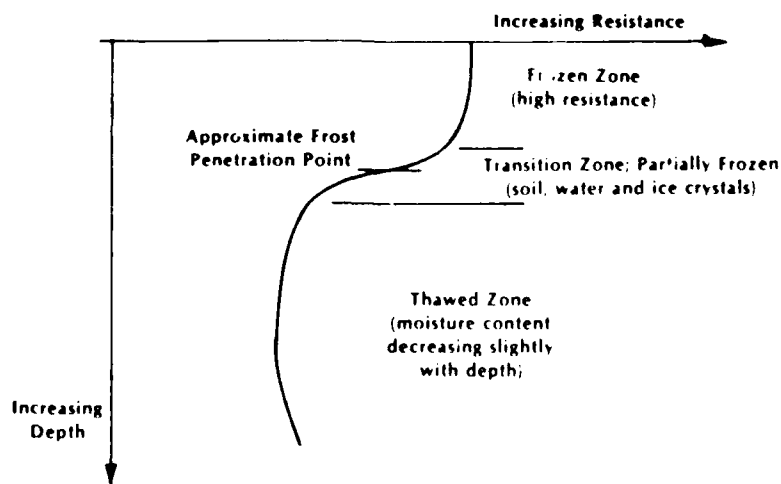


Figure 3. Typical resistance vs depth curve.

NO. 124-501

STATE OF THE ART OF PAVEMENT RECONSTRUCTION
SYSTEMS FOR ROADS AND AIR (U) COLD REGIONS RESEARCH AND
ENGINEERING LAB HANNOVER NH V JANOO ET AL. SEP 89

UNCLASSIFIED

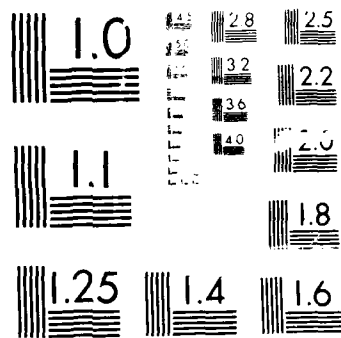
CRREL-SR-89-23

F/B 13/2

ML

17

18



will be the primary factor in determining the resistivity of the soil/water system. As this groundwater begins to form ice crystals and finally freezes, the resistance, as read by an external circuit, will increase in relative proportion to the number of ice crystals formed. This process will continue until the resistance finally becomes stable at some large ohmic value determined by the resistivity of the soil-ice mixture. Figure 3 shows this situation schematically for typical conditions in an area where frost action is in progress.

No absolute resistance measurements are necessary to determine frost penetration by this method since it is the shape of the resistance vs depth curve that is important. Nevertheless, it is necessary to consider the method for making the external resistance measurements.

If direct current resistance measurements are used, the groundwater will almost certainly become polarized, leading to erratic, non-repeatable and misleading resistance measurements. Therefore, resistance measurements cannot be made with volt-ohmmeters, digital multimeters, DC bridges, or other commercially available resistance measuring devices which use a direct current voltage source.

Since an alternating current source reverses its polarity each half cycle, it avoids the groundwater polarization problem. With a low frequency AC source, impedance readings due to cable and sensor capacitances can also be avoided. And if a frequency below 60 Hz is used, possible errors due to line frequency and all its harmonics can be filtered out if necessary. Therefore, a low frequency AC resistance measurement is one method for frost penetration determination using soil resistivity measurements. It is also possible to make resistance measurements at higher frequencies (1000 Hz or more) and filter 60-Hz pickup with a high-pass filter. Both methods have been used successfully. However, this paper reports results using the low frequency (45-Hz) measurement system.

SENSORS

Two types of probe assemblies have been used. The initial probe assembly was fabricated using pieces of copper tubing as the sensing surfaces and pieces of polyethylene tubing as an insulator and

spacer. The complete probe was made by alternately telescoping together pieces of copper tubing 3.2 cm long and pieces of polyethylene tubing 3.8 cm long. Diameters were chosen so that the outside diameter of the copper tubing (2.2 cm) was a twist fit for the inside diameter of the polyethylene tubing. The exposed sections of each piece of copper tubing were placed 5 cm apart along a total length of 105 cm. Individual lead wires (no. 22 AWG with polyvinyl insulation) were soldered to the inside of each copper piece and led up the inside of the "pipe" during assembly. Each sensing surface exposed approximately 3.5 cm² to the soil.

A principal design consideration for the initial probe was providing a large surface to make adequate contact with the soil. Preliminary tests showed that for fine silts a much smaller surface area would suffice. Therefore, a much simpler probe was designed for subsequent tests. This second probe was much easier to fabricate and performed equally as well as the first.

The second generation probe was a wooden dowel 1.9 cm in diameter, in various lengths up to 100 cm. At 2-cm intervals along the entire length of the dowel 1.0-mm holes were drilled diametrically through the dowel. An insulated, solid no. 22 wire was inserted through each drilled hole. The insulation was

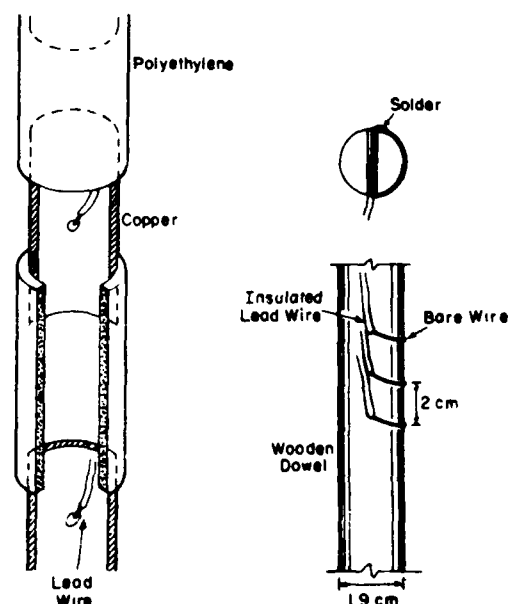


Figure 4. Initial (left) and second generation resistivity probes.

then stripped off the wire so that the bared section could be wrapped tightly around the circumference of the dowel and soldered back upon itself. This type of probe exposed an area of approximately 1.0 cm² to the soil. Both probes are shown in Figure 4.

The individual lead wires for the sensing surfaces were brought out to terminal strips at a readout station. The wires were connected sequentially to the terminal strips and readings were taken in order between leads 1 and 2, 2 and 3, 3 and 4, etc., for the entire length of the probe. Leads up to 30 m long were used.

MEASUREMENT EQUIPMENT

Two methods were used to measure soil resistance. Initially a commercially available oscillator and digital multimeter were used. Both of these units were operated from 110-V, 60-Hz line power. Later in the test program a battery-operated system consisting of a Wien-

bridge oscillator and a battery-operated digital multimeter were used in order to demonstrate the feasibility of taking field measurements.

As discussed previously, it is not necessary to make completely accurate resistance measurements in order to determine frost penetration. The shape of the resistance vs depth curve alone provides the necessary information. Therefore, the actual readings taken were the voltage drop across the unknown soil resistances as compared to the voltage drop across a 1.0-megohm resistor (Fig. 5). The circuit diagram for the Wien-bridge oscillator is shown in Figure 6. Under this arrangement the voltage was read and plotted directly with no intermediate calculations required. A typical plot is shown in Figure 7.

The operating frequency was 45 Hz. This frequency was about at the lower limit for the AC voltage ranges of the digital multimeters. At 45 Hz the line frequency could be filtered out and errors due to capacitive effects avoided. The normal operating voltage was 3 V, peak to peak.

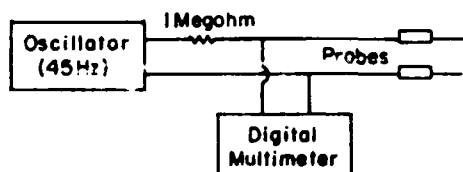


Figure 5. Voltage-ratio circuit for resistivity measurements.

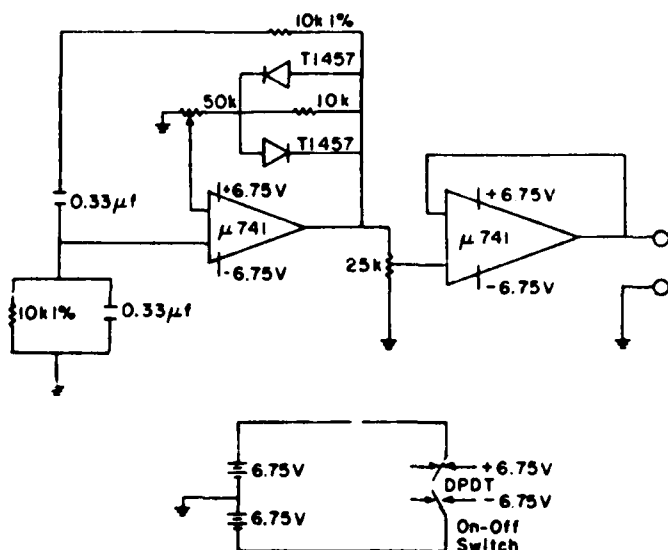


Figure 6. Wien-bridge oscillator circuit for battery-operated measurements.

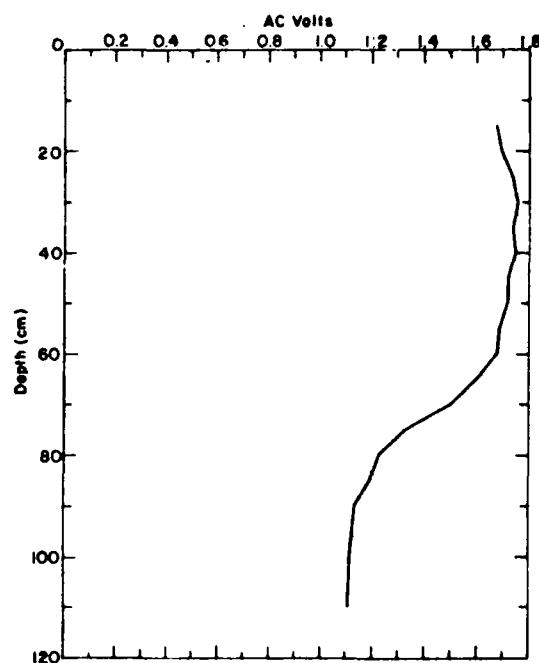


Figure 7. Typical voltage (resistance) vs depth curve during winter season.

TEST PROGRAM

The copper ring probe was tested from January to April as part of a program evaluating several methods for detecting frost penetration, including a thermistor probe and a thermocouple probe. The site selected was an asphalt-concrete-surface parking lot at CRREL in Hanover, New Hampshire. This area was kept plowed free of snow and therefore experienced significant frost penetration.

As described earlier, the resistivity probe was 105 cm long with sensing surfaces spaced every 5 cm. The thermocouple and thermistor probes were 120 cm long with their 12 temperature sensors spaced 10 cm apart along their length. The thermistor and thermocouple probes were placed vertically in the ground with their top sensor at the surface. The resistivity probe was placed in the ground so that the midpoint between its top two sensing surfaces was 15 cm below ground level. Therefore, all probes were capable of reading frost penetration to a depth of 120 cm. All three probes were carefully installed and backfilled to ensure good contact with the soil. (Earlier tests had shown that installation was extremely important if reliable, reproducible measurements were to be obtained.) Asphaltic concrete patching material was used to reseal the drill holes. The test leads from all three probes were buried 15

cm under the surface and led to the readout station inside the main CRREL building approximately 15 m away. Readings were taken on each probe three times a week from January to April.

ANALYSIS OF DATA

Although it is not necessary to show all the data obtained for the period mid-January to mid-April in order to evaluate the performance of the resistivity gauge, a reasonable sampling is presented in Appendix A. These curves demonstrate how the gauge reacted to significant changes in ground frost and show that the measurements were repeatable from week to week. Comparable data for the thermocouple and thermistor gauges are shown in Appendices B and C. All of these data were used to compile a seasonal graph for each gauge (Fig. 8).

All gauges showed solid freezing down to 75 cm in mid-January. But beginning on 31 January the resistivity gauge began to show a thawed zone from 15 to 25 cm. Neither the thermistor gauge nor the thermocouple gauge indicated this thawing, i.e. both indicated temperatures below 0°C. Subsequent measurements indicated that this discrepancy was real, continuous, and repeatable with respect to each of the three gauges.

This disagreement highlighted the real value of the resistivity gauge. An

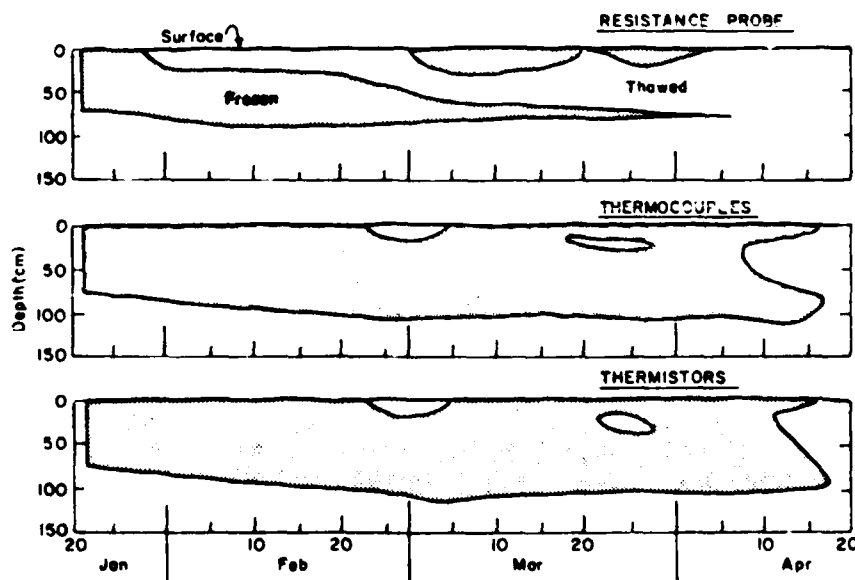


Figure 8. Seasonal frost penetration as seen by a thermistor, a thermocouple, and a resistivity probe.

explanation for the discrepancy was sought, and it was found that a mixture of sand and salt had been put down during snow removal operations on 29 January. The salt had combined with surface meltwater and lowered its freezing point. The salty meltwater had then filtered down through the cracks in the asphalt concrete into the soil, thawing the soil as it went. As a result, the resistivity gauge "saw" highly conductive salt water, which was correctly read as a thawed condition, while the temperature gauges saw below-freezing temperatures, which led to the incorrect conclusion of frozen conditions. This situation continued through most of February, with the saline meltwater slowly penetrating into the frozen soil beneath it.

On 24 February the weather turned warmer, bringing substantial amounts of relatively salt-free meltwater onto the surface and slightly beneath it. This meltwater raised surface temperatures above the freezing point so that the temperature gauges began to indicate thawing near the surface. At this point in the season all three gauges agreed that thawing had occurred. However, only the resistivity gauge showed that the effects of the salt water had caused thaw to a

considerable depth. The resistivity gauge also showed that the warm surface water of 24 February had accelerated the rate at which the thawed zone was penetrating into the frozen soil.

On 5 March all gauges indicated that freezing had once again taken place at the surface (refreezing of the salt-free surface water). The resistivity gauge was readily interpreted as showing a thawed zone between two frozen zones. The temperature data are somewhat difficult to interpret, with the thermistor gauge showing an isothermal condition while the thermocouple gauge showed solid frost down to 104 cm. In fact, from this point on, interpretation of the temperature gauges became somewhat uncertain, with clearly defined frost limits almost impossible to determine. The resistivity gauge, on the other hand, continued to show the position of the frost lines with no ambiguity, right up to the point where the ground became completely frost-free.

The success of this initial test program led to the use of resistivity type frost gauges in several laboratory and field test programs that still are in progress today. For example, these gauges are often installed as a routine part of the CRREL FERF research instrumentation

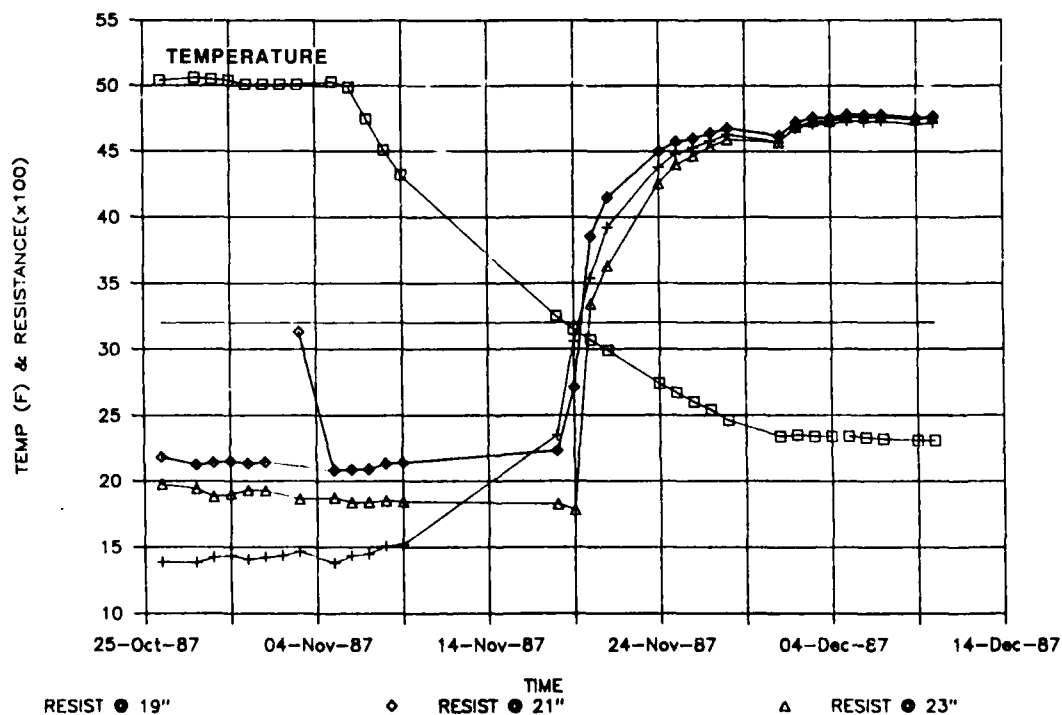


Figure 9. Temperature (at 22-in. depth) vs resistance: FERF test, frost entering soil.

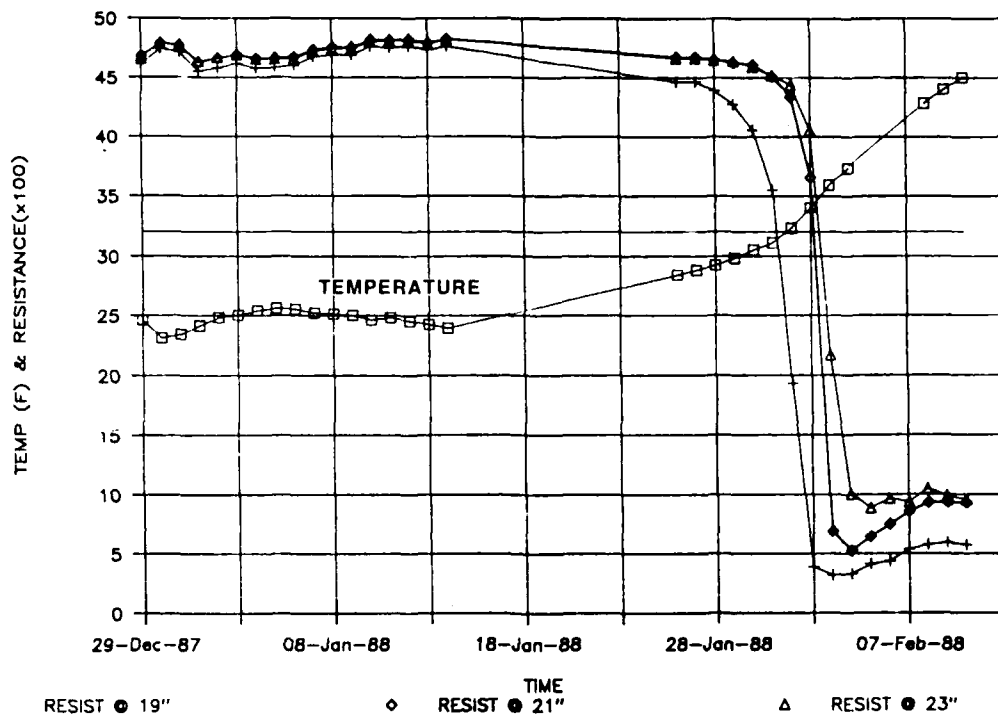


Figure 10. Temperature (at 22-in. depth) vs resistance: FERF test, frost leaving soil.

systems. Examples of frost entering and leaving a FERF test section are shown in Figures 9 and 10. Freezing and thawing was induced by freeze panels so that the dates are merely to show elapsed time and are not related to seasonal weather conditions. Resistivity gages were also installed under the runway in Jackman, Maine, as part of that pavement monitoring instrumentation program. For these programs the simpler wooden dowel gauges were used. These gauges gave curves similar to the ones in this report. The AC resistivity gauges described in this paper have been successfully interfaced to data logging systems; however, it requires a large number of data channels for such an arrangement. These gauges have also been used in conjunction with a computer which calculated the frost depth directly and stored this number.

CONCLUSIONS, RECOMMENDATIONS AND COMMENTS

The initial evaluation of the frost resistivity gauge plus experience gained with further use have led to the following conclusions:

1. An AC resistivity gauge can accurately and reliably determine frost penetration.

2. The AC resistivity gauge is superior to temperature measurement gauges for determining the presence of frost under spring thawing conditions.

3. The use of temperature measurement gauges to determine frost depths under asphalt concrete surfaces will lead to erroneous results if salt is used as part of a snow removal program. The practical result of this conclusion is that it is highly likely that highways and runways that are treated with salt for snow removal or ice control will almost certainly be thaw weakened for a major portion of the winter season, not just the spring.

Test results and conclusions indicate that the following recommendations are appropriate for future frost measurements programs:

1. The use of both temperature and resistivity gauges is definitely advisable since, in general, one type complements and increases the confidence level of the other in determining maximum frost depth, as for example in Figure 8.

2. Other frost detection methods such as frost tubes should not necessarily be totally excluded in favor of resistivity or temperature gauges in any frost measurement program.

3. In some instances, such as when chemicals are added to the soil/water system, the primary measurement tool for determining frost penetration and thawing should be the resistivity gauge.

4. Readout techniques can be automated by several different design

methods. However, normally the frost depth is changing so slowly that a manual measurement once a week is sufficient. One exception to this is if salt is applied so that rapid melting occurs and needs to be monitored.

5. The gauges described here are simple and inexpensive. There is little need for further investigations into minimum area for a sensing surface or for optimum spacing between these sensing surfaces.

APPENDIX A: RESISTANCE GAUGE DATA.

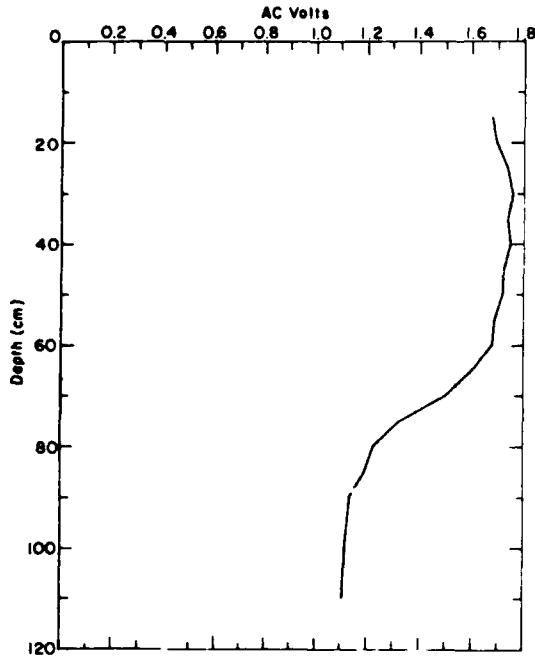


Figure A1. 22 Jan 1975.

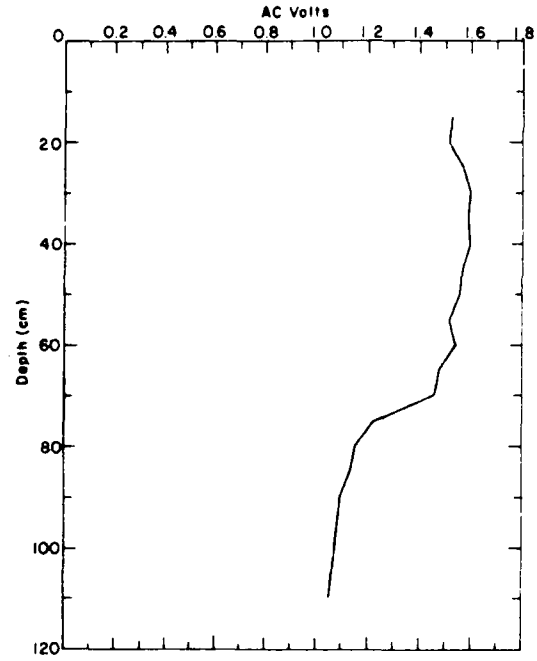


Figure A2. 29 Jan 1975.

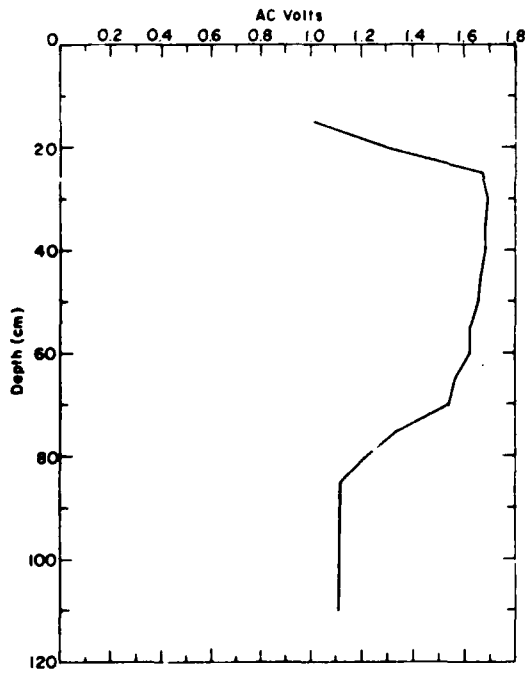


Figure A3. 31 Jan 1975.

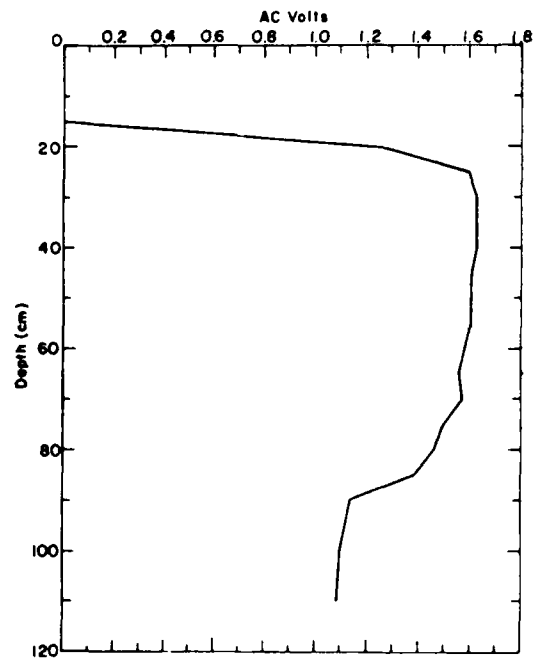


Figure A4. 7 Feb 1975.

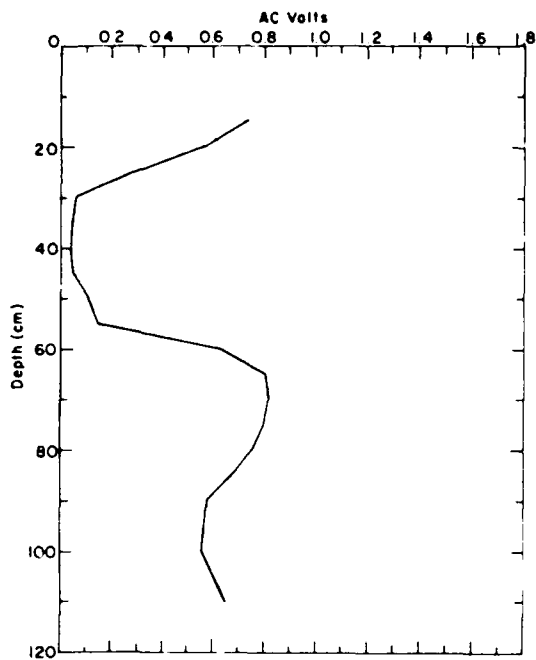


Figure A5. 5 Mar 1975.

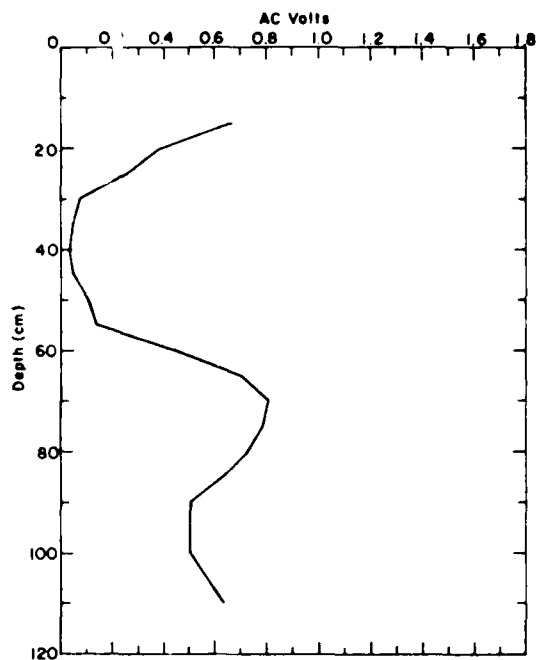


Figure A6. 10 Mar 1975.

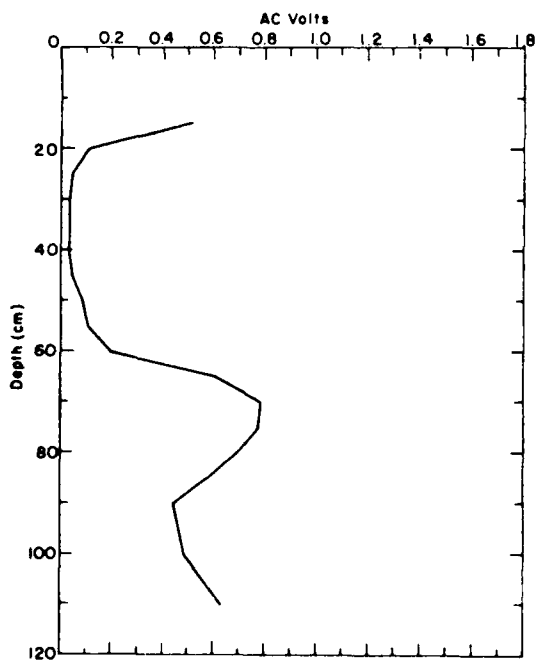


Figure A7. 17 Mar 1975.

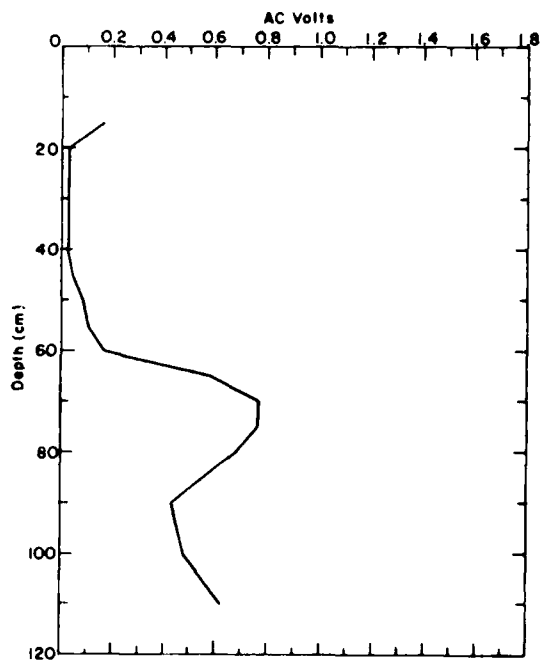


Figure A8. 19 Mar 1975.

APPENDIX B: THERMOCOUPLE DATA.

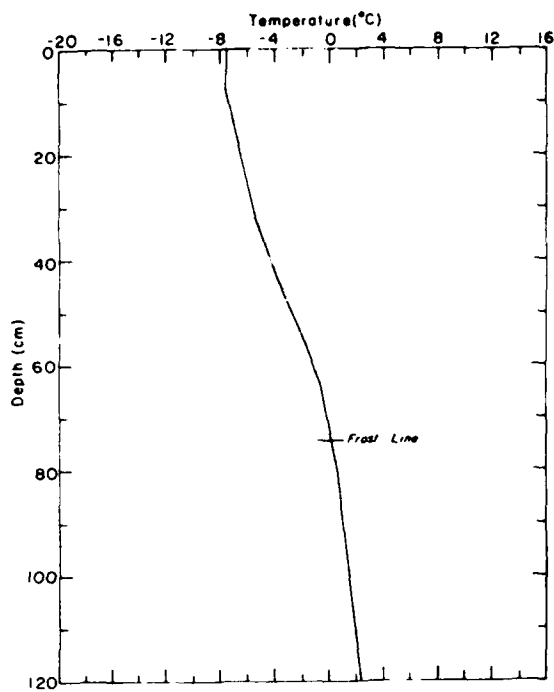


Figure B1. 22 Jan 1975.

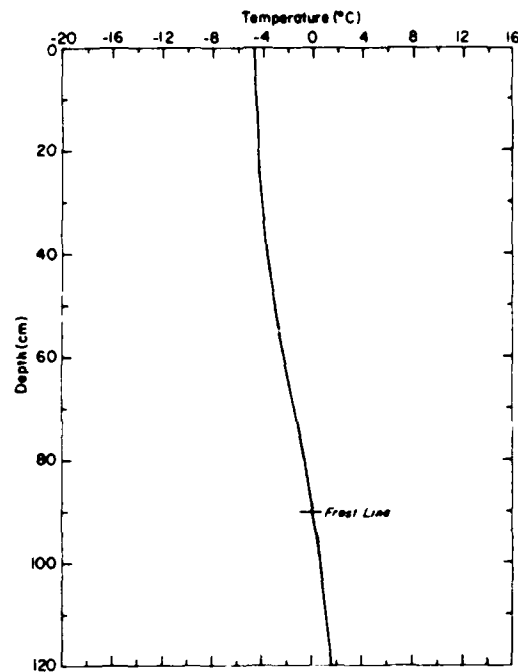


Figure B2. 7 Feb 1975.

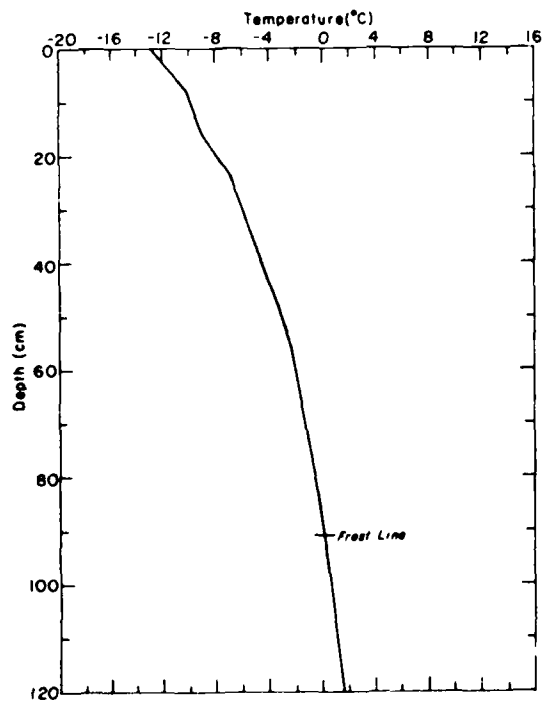


Figure B3. 10 Feb 1975.

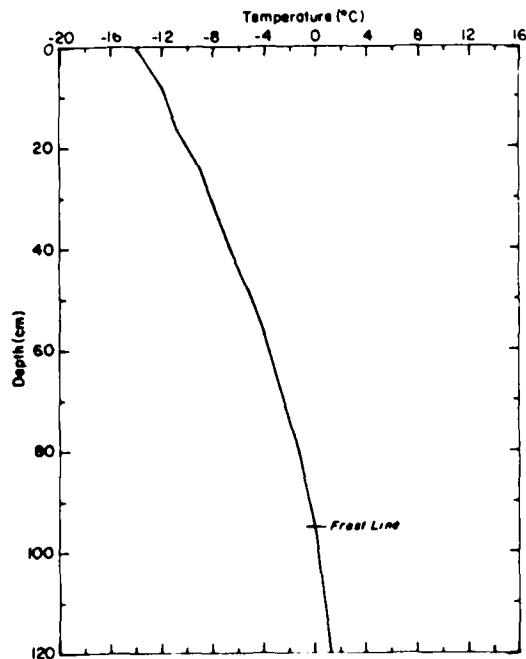


Figure B4. 14 Feb 1975.

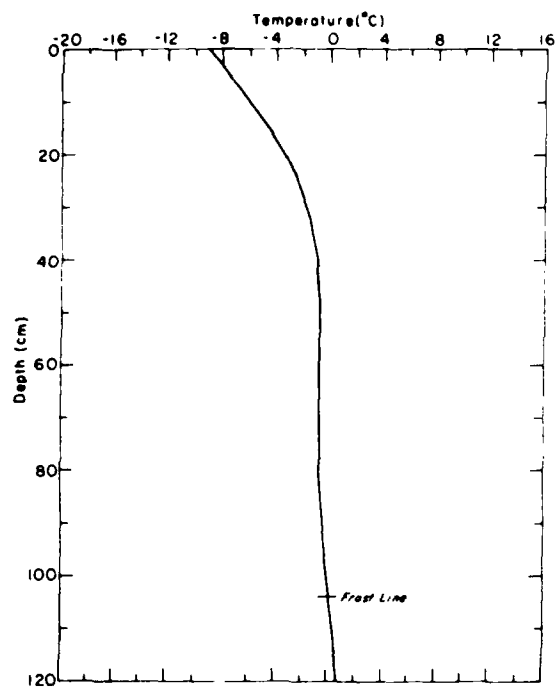


Figure B5. 5 Mar 1975.

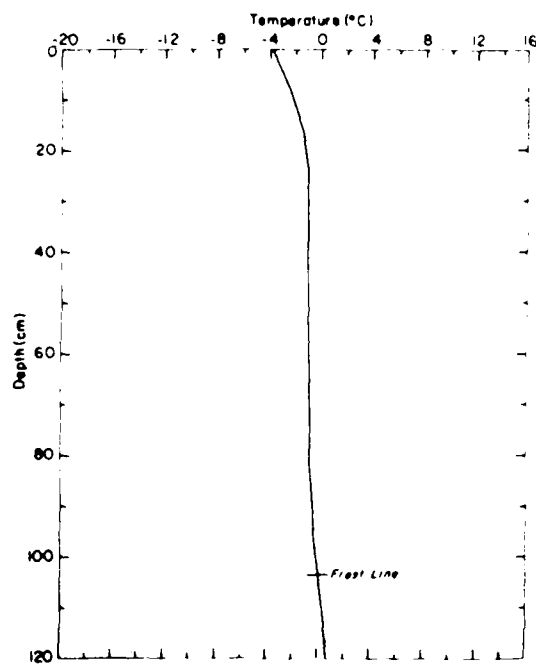


Figure B6. 17 Mar 1975.

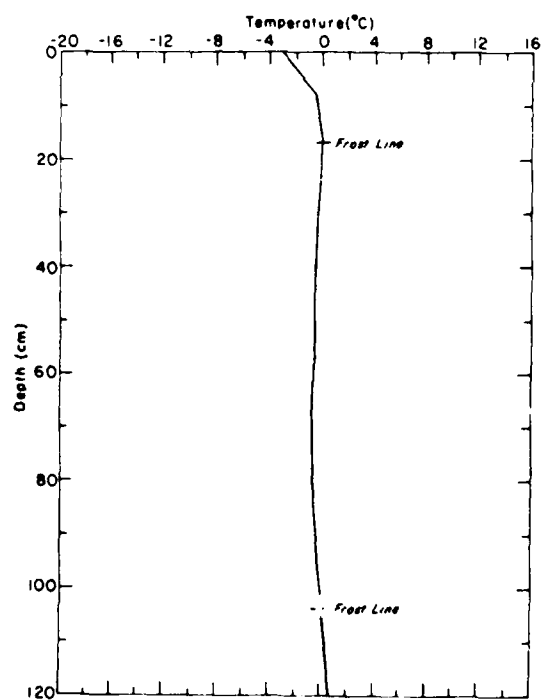


Figure B7. 21 Mar 1975.

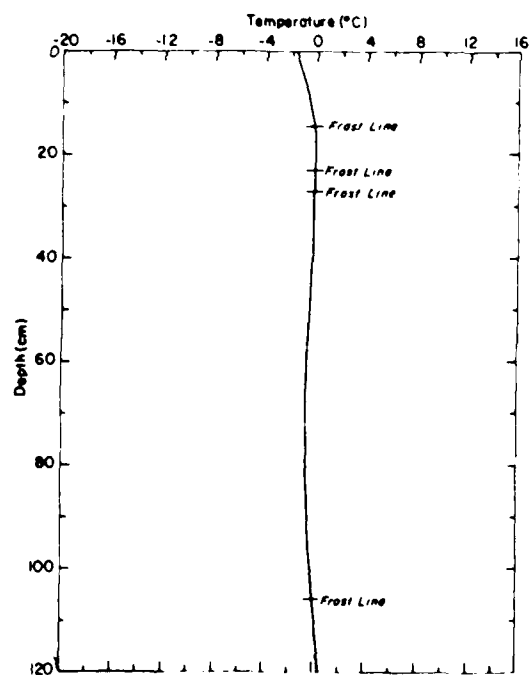


Figure B8. 24 Mar 1975.

APPENDIX C: THERMISTOR DATA.

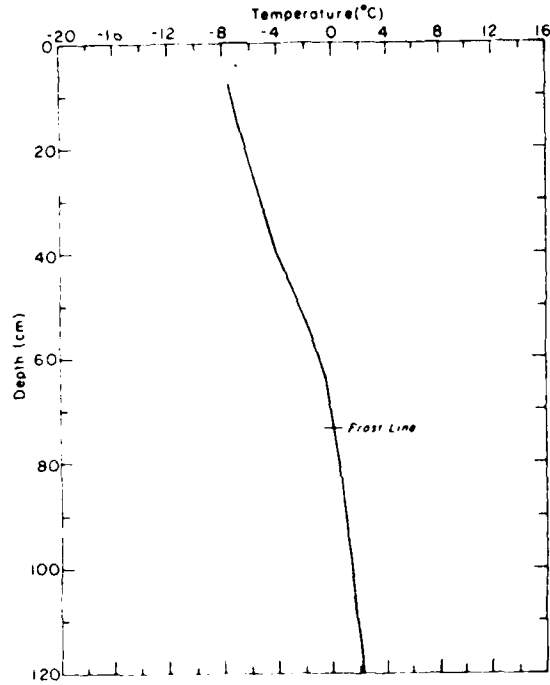


Figure C1. 22 Jan 1975.

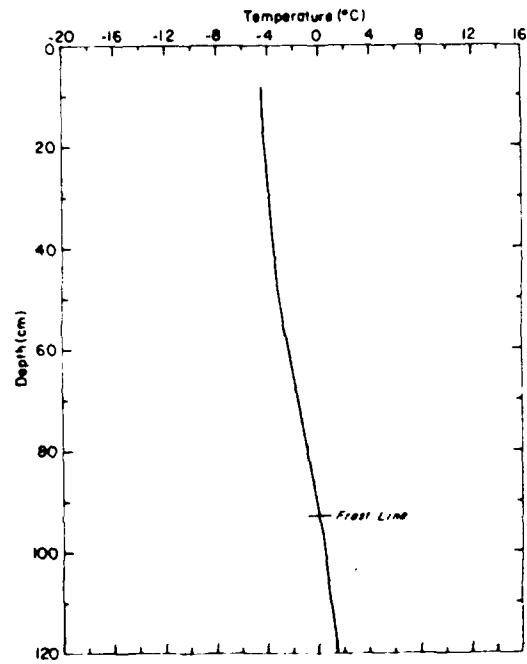


Figure C2. 7 Feb 1975.

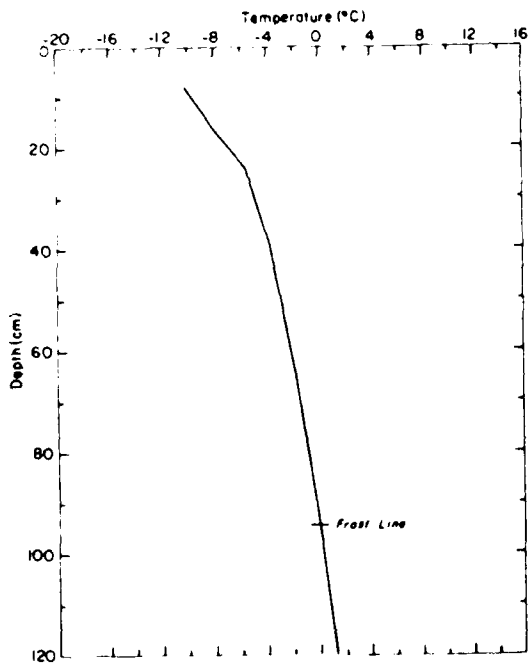


Figure C3. 10 Feb 1975.

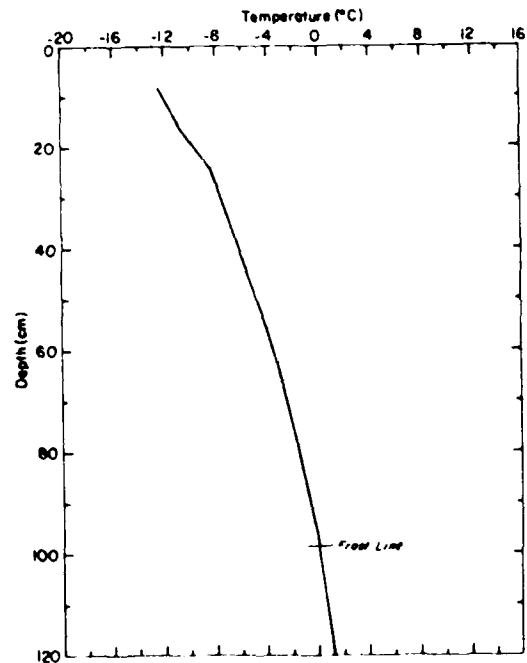


Figure C4. 14 Feb 1975.

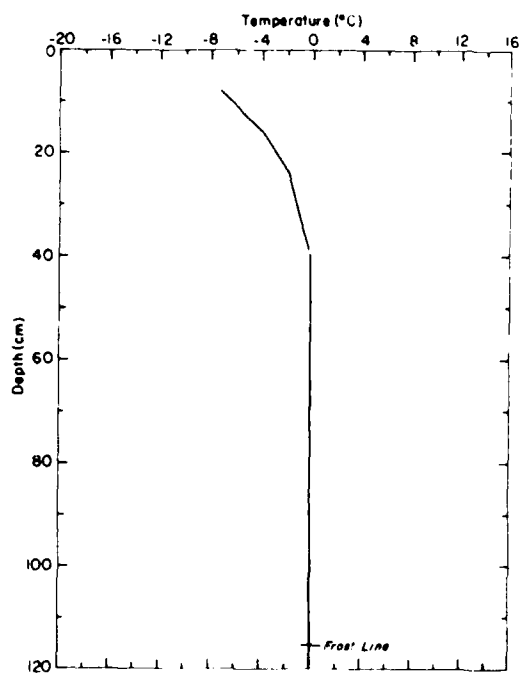


Figure C5. 5 Mar 1975.

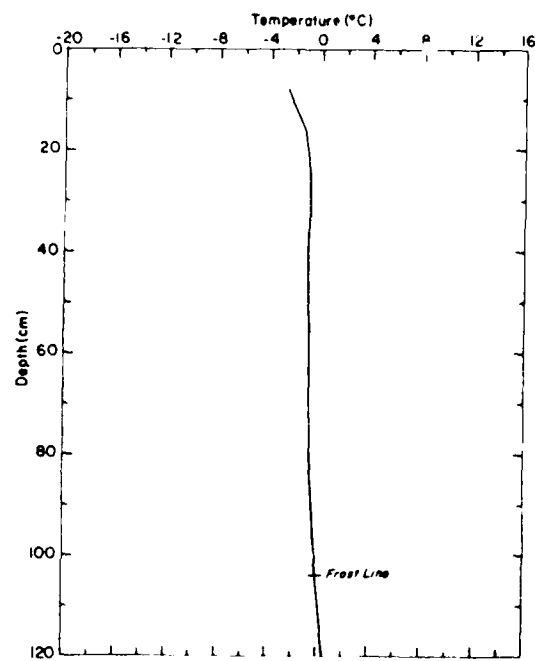


Figure C6. 17 Mar 1975.

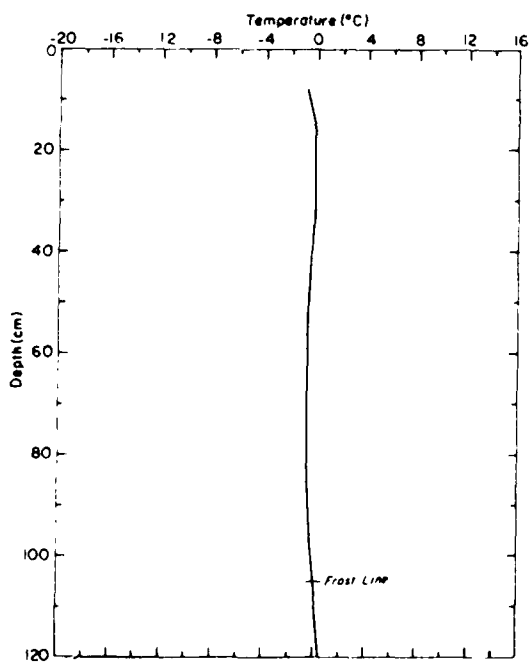


Figure C7. 21 Mar 1975.

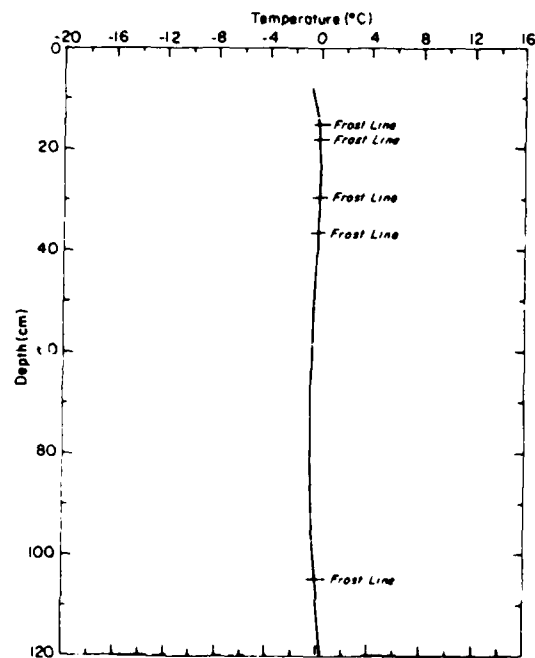


Figure C8. 24 Mar 1975.

THERMOCOUPLE AND THERMISTOR TEMPERATURE MEASUREMENT SYSTEMS

Richard Briggs, C.E.T., Electronics Technician, State of Alaska Department of Transportation

ABSTRACT

The accurate measurement of subsurface temperatures using thermocouples and thermistors requires the proper selection of sensors. It also requires the use of good practice in fabrication of sensors into cables, the selection of suitable connectors, switching systems, and readout devices for use under the particular field conditions at the sites to be monitored. Electrical quantities measured in the field are converted into units of temperature with tables or equations based on empirical data.

Based strictly on cost and durability considerations, thermocouples would be the sensor of choice. However, the problems of obtaining reliable measurements of field potentials as small as one microvolt, and the problems of achieving a stable reference voltage under varying field temperatures, often lead to the use of thermistors because of their greater temperature sensitivity and the greater reliability of field measurements.

Temperature measurements may be made manually during site visits, recorded on tape or microchips by small battery-powered data loggers, or relayed to the office via phone lines or packet radio. The author's personal experience with these systems and the benefits, precautions, and problems thereof, will be presented and discussed in this paper.

INTRODUCTION

With an average annual air temperature of -3.5°C and extremes that range over 90°C , the thermal regime of roadbeds and pavements in Interior Alaska is of critical importance in determining their structural response. Many years of experience in making field measurements using manual and automated methods have narrowed the selection of temperature transducers to thermocouples and thermistors (See the paper by D. Esch, also presented at this symposium). Accurate and repeatable measurements are necessary as only a fraction of a degree C can make a significant difference in interpreting how the roadway may be responding to stresses.

This paper will focus on techniques found to minimize errors that occur in field data collection and reduction. Although a 'how-to' treatment is beyond the scope of this forum, it is hoped that engineers and technicians will find this information useful in implementing thermal data acquisition systems.

THERMOCOUPLES

Fabrication

Type T with special limits of error is the wire of choice for State of Alaska Department of Transportation and Public Facilities

(ADOT&PF) Statewide Research. Smaller wire gauges such as 22-24 AWG are used in vertical and horizontal strings to minimize heat flow along conductors which can upset the thermal equilibrium of the soil being measured. Wire and jacket insulation must be moisture-proof, abrasion resistant, and have a low coefficient of friction. Nylon would be the best choice here and fabric the worst.

Always use wire from the same spool or lot. Cut the wire to length and tape it to the floor one wire at a time. At least two wire markers should be placed on each end to ensure that no mix-ups can occur while the wires are bundled into strings. Junctions are now soldered or crimped in place, coated with ScotchkoteTM and protected with heat-shrink tubing. Wrap the string with tape or spirally cut polyethylene tubing for mechanical protection. The string is now ready for installation in a trench or hole.

Manual readings of temperature require selection of a low thermal double pole switch. Thermocouple switches utilize selected alloys to minimize thermal electromotive force (EMF). They are also somewhat massive to equalize the temperature across the switch body. The switch

and a type T panel jack must be installed on a panel and housed in a rainproof enclosure. Currently, ADOT&PF is using BD-5 telephone housekeeping closures; however, any type of rainproof box will do, provided it is large enough to allow good wiring practice and avoid a 'rat's nest'.

Measurements

Manual thermocouple measurements require an ice bath for highest accuracy. Two thermocouples are connected in a series-bucking configuration so that the constantan wires are joined together, leaving the copper wires to be connected to the meter inputs (See Fig. 1). The thermoelectric voltage produced is proportional to the difference in temperature between the two junctions. Since the ice bath is at 0°C, a positive voltage would indicate an above freezing temperature and a negative reading below freezing.

The ice bath can be constructed from a Dewar flask or vacuum bottle. If a stainless steel vacuum bottle is selected, then the reference junction must be insulated electrically from the ice and water mixture to avoid ground loops and resulting

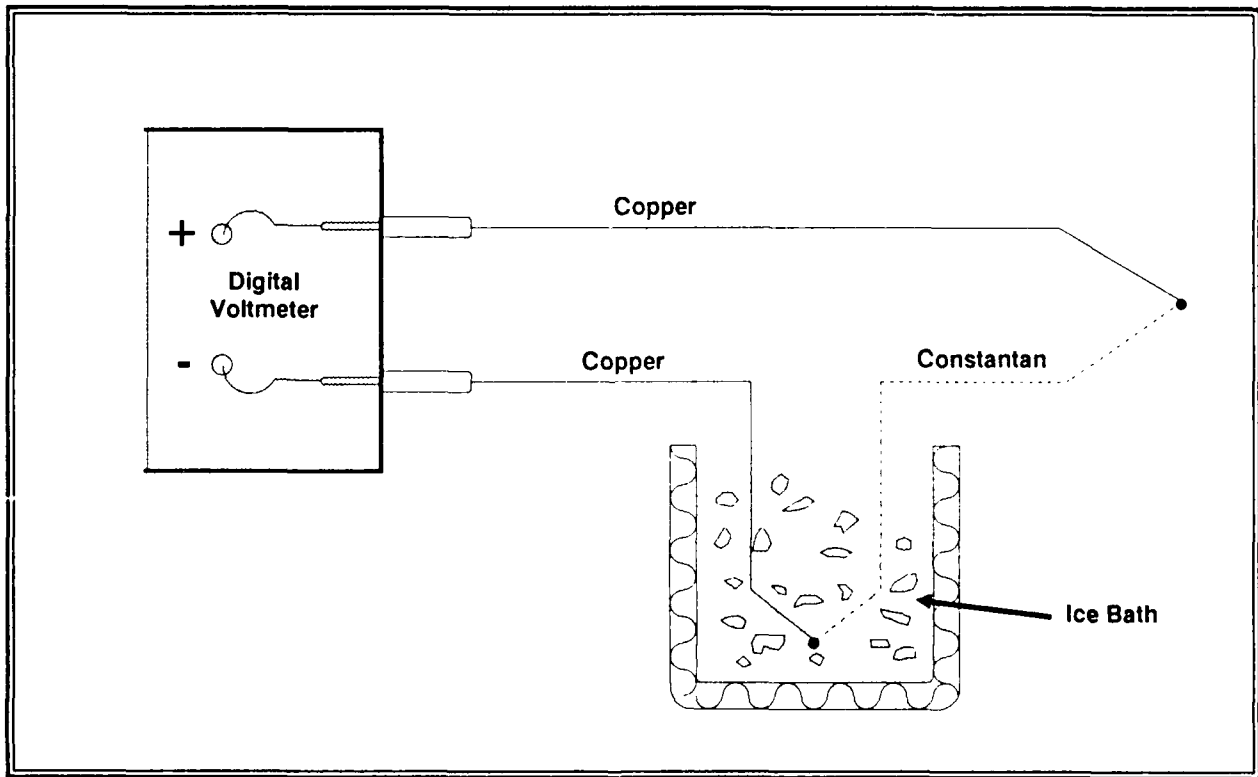


Fig. 1. Circuit design for reading of thermocouples.

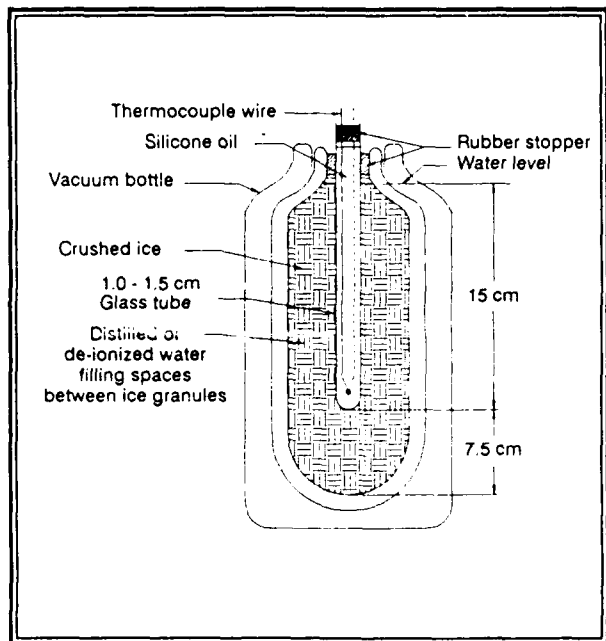


Fig. 2. Design of reference junction ice bath.

electrical noise. A test tube filled with kerosene or silicone oil works well and enhances the thermal stability of the reference junction (See Fig. 2).

The ice bath itself is preferably made with distilled, deionized water; although tap water in most locations will introduce errors less than $.01^{\circ}\text{C}$. Shaved or pea-sized ice is packed into the container until it is full, then water is added until the spaces between the ice are filled. Let the bath stabilize for a quarter hour and then pack more ice into the flask to ensure that the mixture extends to the very bottom.

At this point the reference junction assembly may be inserted 15 cm or more into the slush, being careful not to break the test tube. In 15 to 20 minutes the bath will be ready to use.

Although thermocouple thermometers with internal references designed to eliminate the ice bath have been available for several years, ADOT&PF Statewide Research has found their accuracy to be inadequate under field conditions. The meter in use at this time is a Hewlett-Packard 3468A. It is a battery powered, 5 1/2 digit DMM with one microvolt resolution, outstanding stability and accuracy, and the ability to be remotely programmed. Other instrument manufacturers produce similar equipment. Two design features of the HP-3468A that may not be readily apparent are the thermal gradient-minimized circuit board

design and the auto-zero feature which causes the meter to make two measurements for every reading compensating for thermal EMFs generated within the meter.

Twenty minutes before readings are to be taken, the meter is plugged into the ice bath and an HP-41 calculator, slipped into an insulated bag, and turned on. The HP-41 acts as a remote display for the meter and may even be used to convert the thermocouple voltage into $^{\circ}\text{C}$, reducing the chances of an unskilled operator selecting the wrong function on the meter or misinterpreting the display. The following is a sample program listing:

HP-41 Program 1.

```

01 LBL"TC"
02 REMOTE
03 "F1R1Z1"
04 OUTA
05 IND
06 1 E6
07 *
08 END

```

This program places the meter in remote control mode, brings the most recent voltage reading into the HP-41's X register, and displays the result in microvolts. Another program may interact with the operator, store readings in extended memory, or use time alarms to log data.

After inserting the type T panel plug into the panel jack in the field station, the voltmeter display must be watched for drift caused by a thermal gradient across the connectors. If the reading is stable, proceed to collect the data. Switched systems should be checked a second time to confirm that less than 2 microvolts of drift have occurred since the first reading was taken.

Raw data in microvolts may be stored in a hand held computer or written down on a form. Archiving the data in microvolts is recommended as it is much easier to account for operator and systematic errors at a later date. An advantage of computer aided testing is that both the thermoelectric voltage and the temperature may be displayed at the same time, giving the operator confidence and assisting with troubleshooting if necessary.

Voltage to Temperature Conversion

NBS Monograph 125 contains computer generated tables and equations for converting a thermoelectric voltage into temperature over the temperature range of a type T thermocouple, -270 to 400°C. Higher accuracies may be obtained by using the raw voltages given in Table 8.3.2 of the monograph over the temperature range of interest in a third degree polynomial curve fit program. The power series polynomial is of the form,

$$T = a_0 + a_1E + a_2E^2 + a_3E^3 \quad (1)$$

where T is the temperature in degrees C, E is the voltage in microvolts and a_0 , a_1 , a_2 and a_3 are the constants derived from the curve fit.

Table 1 shows the coefficients calculated by an HP-85 computer to cover -50 to 50°C.

Table 1.

	BELOW ZERO	ABOVE ZERO
a_0	-3.15971796E-4	-2.80607794E-3
a_1	2.58090450E-2	2.58446730E-2
a_2	-7.47693928E-7	-6.52482306E-7
a_3	9.73827161E-11	1.24873605E-11

It is important to note that this fit degrades rapidly outside of the -50 to 50°C range; however within these limits the curve agrees with the NBS data to better than .01°C.

Since eq(1) runs slowly in a computer, the nested form will save execution time:

$$T = a_0 + E(a_1 + E(a_2 + a_3E)) \quad (2)$$

HP-41 program 2 may be merged with program 1 or used on its own to calculate temperature from a microvolt value stored in the X register. The display will show both microvolts and °C.

HP-41 Program 2.

```

08 LBL "CONV"      29 *
09 STO 00          30 -6.52482E-7
10 X=0?           31 +
11 GTO 02          32 RCL 00
12 X>0?           33 *
13 GTO 01          34 2.58447E-2
14 9.73827E-11     35 +
15 *              36 RCL 00
16 -7.47694E-7     37 *
17 +              38 -2.80608E-3
18 RCL 00          39 +
19 *              40 LBL 02
20 2.5809E-2       41 CLA
21 +              42 FIX 0
22 RCL 00          43 ARCL 00
23 *              44 "|="
24 -3.15972E-3     45 FIX 2
25 +              46 ARCL X
26 GTO 02          47 "| C"
27 LBL 01          48 AVIEW
28 1.24874E-11     49 END

```

THERMISTORS

Fabrication

Although thermistors are easier to measure than thermocouples, they are sensitive to moisture, thermal cycling, and aging. Glass bead encapsulated thermistors in the 2252 to 10,000 ohm range (@25 °C) with .1°C interchangeability are used by ADOT&PF Research. They have shown better stability with time than the epoxy encapsulated bead type.

The following method of fabrication has been used for five years and has shown good results, but only the passage of time will tell how effective it is over longer periods.

Wire for thermistors that will be buried should be rated for this application. A high density polyethylene jacket is considered sufficient mechanical protection. Insulation for the inner conductors may be polyethylene or polypropylene. Polyvinyl chloride (PVC) should be avoided because of its high dielectric absorption.

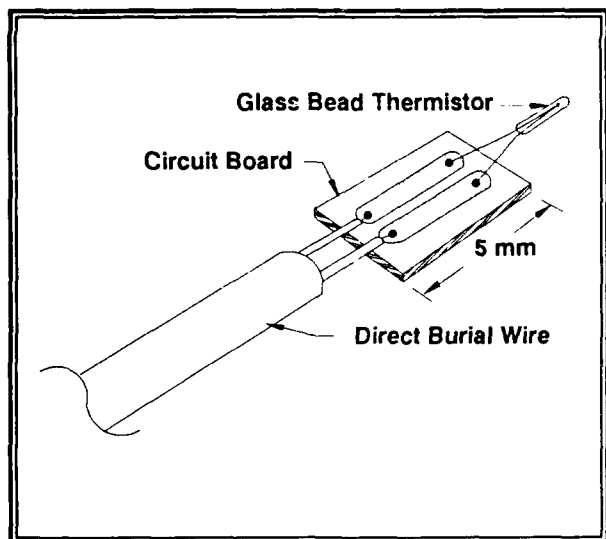


Fig. 3. Thermistor fabrication (not to scale).

Thermal and mechanical stress during the assembly process may be reduced by first soldering the relatively heavy cable to a strain gauge terminal or small printed circuit board (See Fig. 3). While soldering the thermistor use a heat sink and monitor its resistance so that the maximum working temperature is not exceeded. The assembly is then coated with a non-corrosive silicone rubber such as Dow 3140 RTV, set aside for 24 hours, and given a second coat. After curing is complete, a 10 cm piece of heat-shrink tubing (with glue) is installed, again paying close attention to the thermistor temperature rise with an ohmmeter. Several coats of Scotchkote (TM) complete the encapsulation.

Measurements

Thermistors, as thermally sensitive resistors, can be read with an ohmmeter. Ordinary switches and connectors are used for manual measurements and thermal EMFs will have a minimal effect on the meter. It is important to note that any current applied to the thermistor will cause it to dissipate some heat. The amount of power required for a 1°C rise in the thermistor is called the dissipation constant and is dimensioned in milliwatts per °C. Two constants are usually provided by the manufacturer; one with the thermistor in air and the other in well-stirred oil. It can be shown through Ohm's Law that a 2252 ohm thermistor at 0°C (7355 ohms) will have less than a .0002°C rise with 10 microamps applied and a 4

mW/°C dissipation constant. This error source, although insignificant, will increase a hundredfold for a tenfold increase in the applied current. Therefore, knowledge of the amount of current that an ohmmeter or signal conditioning device puts through the thermistor is necessary.

Resistance readings that take more than a few seconds to settle indicate instability of and possible damage to the thermistor. If the ohmmeter leads are reversed and the display shows a change of more than 5 ohms, the thermistor circuit is polarized and must be considered inoperative or out of calibration. The author believes that these symptoms are associated with improper encapsulation and the resulting migration of moisture into the thermistor body, although no questionable thermistor strings have been recovered and their moisture content ascertained. This opinion is based on knowledge of the encapsulation method used and the probable water content of the soil in which unstable thermistors have been found.

ADOT&PF uses the same meter for reading thermistors and thermocouples. Since most field sites are instrumented with both devices, the meter is switched between the volts and ohms functions with a user-defined key on the HP-41. Resistance readings are made with one ohm resolution at 10 microamps. Under program control the current is toggled on and off in a 1:10 duty cycle to minimize self-heating. Successive readings are compared so that the HP-41 can notify the operator when stability is reached.

Resistance to Temperature Conversion

Tables provided by the thermistor manufacturer may be used to convert field resistance data into temperature. As this requires linear interpolation to acquire fractional degrees, an equation that describes the characteristic curve of the thermistor can be solved by a computer for greater precision.

Negative coefficient thermistors used by ADOT&PF are best described by the Steinhart and Hart equation:

$$\frac{1}{T} = a + b(\ln R) + c(\ln R)^3 \quad (3)$$

where T = temperature in degrees Kelvin,

$\ln R$ = the natural logarithm of the resistance in ohms, and the coefficients a , b and c are derived from measurement. These coefficients may be obtained from the thermistor supplier or found by measuring the resistance at three temperatures and solving three simultaneous equations. The temperatures chosen for calibration should be at least 10 degrees apart and bracket the temperature of interest.

DATA LOGGERS

Although they are from the same family as strip chart recorders and FM instrumentation tape decks, data loggers distinguish themselves by their design as interrupt-driven, microprocessor run devices. In other words, an event such as a timer, voltage level, or a person pushing a button will tell the data logger to make a measurement. Depending on its complexity (and cost) the instrument may have non-volatile memory, multiple inputs, and the hardware and software to support a variety of sensors and telecommunications options.

Data loggers used for thermocouple measurements require an isothermal block on the input terminals for accurate performance. The isothermal block is combined with a thermistor, RTD or solid-state temperature sensor to replace the ice bath reference. A possible source of error in such a system would be the temperature gradient between the input terminal and sensor, which is difficult to quantify. ADOT&PF Research evaluated several isothermal block thermocouple systems and has found them inaccurate at the extreme low temperatures encountered during Alaskan winters. Even low power CMOS circuitry can produce enough heat to make a substantial gradient at -50°C .

A precision voltage or current source is required for most data loggers which are used with thermistors. If a voltage source is used, then a low temperature coefficient resistor which is equal to the thermistor resistance at mid-temperature is placed in series with the thermistor in a half-bridge configuration. The applied voltage is limited so that the power dissipated in the thermistor will not cause an error-producing amount of self heating. The voltage drop across the thermistor will be proportional to its resistance. Constant current sources are easier to deal with. The current is set

to a non-self heating level and the resulting voltage drop is measured across the thermistor. If decade currents are selected, i.e., 10 microamps, resistance calculation is as simple as moving a decimal point.

Thermal data from soils and pavements should be scanned at two minute intervals to yield minimum, average, and maximum values, which are output to final storage on an hourly basis. Temperatures move slowly in these structures and more frequent scanning is unnecessary; deep sensors may require no more than daily readings. Data should be stored in the raw form to ease troubleshooting and avoid tedious backcalculation if systematic errors become known.

Final storage may be a portable cassette drive, solid state storage module, printer, modem or radio frequency telemetry to a personal computer. The value of a modem or telemetry link to the office cannot be overestimated. ADOT&PF installed a solar powered data acquisition system in 1985 that featured a line-powered modem which enables communication with the data logger. By mid-December, the system battery was at a low state of charge. Thanks to the modem, ADOT&PF was able to assess the problem and modify the data logger program to reduce power consumption without making a 600 mile trip.

WORK IN PROGRESS

ADOT&PF has purchased and installed five temperature probes manufactured by Measurement Research Corporation of Gig Harbor, WA. These probes use epoxy encapsulated thermistors spaced at intervals along their 1.2 meter length. A hand-held readout is connected to the probe through a four wire cable, with the switching circuitry located in the probe itself. As the display is configured to show the thermistor's number and temperature, an unskilled person may operate it. Temperature data will be acquired this spring and compared to Falling Weight Deflectometer data in an attempt to correlate the depth of thaw with pavement deflections.

Since two of the probes are located in remote areas away from phone lines, a packet radio network will be developed to link the probes to the office. Packet systems allow digital data to be transmitted from several stations on the same

channel. Collision avoidance, message passing (digipeater), and error recovery are part of the packet protocol. Each station has a unique address and may pass messages or data on to stations beyond the radio horizon of the originating station. This system will enable ADOT&PF to place load restrictions as they are needed and reduce their duration.

BIBLIOGRAPHY

American Society for Testing and Materials, 1981, "Manual on the Use of Thermocouples in Temperature Measurement", STP 470B, ASTM Committee E-20 Philadelphia, PA.

Baker, H.D., Ryder, E.A. and Baker, N.H., 1953, 1975, "Temperature Measurement in Engineering", Omega Press, Stamford, CT.

Flora, M., 1982, "Basic Concepts of Thermistors for Thermometry", Yellow Springs Instrument Co., Inc., Yellow Springs, OH.

Hewlett Packard, 1980, "Practical Temperature Measurements", AN-290, Hewlett Packard, Palo Alto, CA.

Keithley, J.F., Yeager, J.R., and Erdman, R.J., 1984, "Low Level Measurements", Keithley Instruments, Inc., Cleveland, OH.

NBS Monograph 125, 1974, "Thermocouple Reference Tables Based on the IPTS-68", National Bureau of Standards, USGPO, Washington, DC.

Osterkamp, T.E., 1984, "Temperature Measurements in Permafrost", State of Alaska Department of Transportation and Public Facilities Statewide Research Report AK-RD-85-11, Fairbanks, AK.

Roberts, T.D., Merritt, R.P., and Kokjer, K.J., 1981, "Low Data Rate Digital Transmission Techniques for Alaskan Applications", State of Alaska Department of Transportation and Public Facilities Statewide Research Report AK-RD-80-06, Fairbanks, AK.

Trautman, J.P. and DesJardin, L.A., 1983, "A Portable, Low Cost, High-Performance Digital Multimeter for the HP-IL", Hewlett Packard Journal (February, 1983), Hewlett Packard, Palo Alto, CA.

Zarling, J.P., Kinney, T., McGilivray, R., and Briggs, R., 1986, "Data Logger Evaluation", State of Alaska Department of Transportation and Public Facilities Statewide Research Report AK-RD-86-21, Fairbanks, AK.

A SIMPLE AND ECONOMICAL THERMAL CONDUCTIVITY MEASUREMENT SYSTEM

Ronald T. Atkins

U.S. Army Cold Regions Research and Engineering Laboratory
Hanover, New Hampshire 03755-1290

ABSTRACT

This report describes a recently patented method for using commercially available thermistors to make in-situ thermal conductivity measurements with commonly available electronic equipment such as digital voltmeters. The emphasis is on the use of a single thermistor to measure the thermal conductivity of soils. Calibration techniques are explained and examples provided. Limits on this technique are discussed, including measurement range, material grain size, the amount of material needed for a valid measurement, and temperature stability. Specific examples of the use of this technique are provided for thermal conductivity measurements of soils, building materials, and the sludges in a sewage treatment plant. Data analysis is provided including a statistical approach to finding the thermal conductivity in large volumes of material.

1. INTRODUCTION

The original intent of the work described in this report was to develop a method for measuring point thermal conductivities¹ that used inexpensive sensors

¹ Throughout this report thermal conductivity measurements are reported in calories per square centimeter per centimeter per second per degree Celsius (or cal/cm-sec-°C). To convert these values to BTU per square foot per inch per hour per degree Fahrenheit (BTU/ft²/in./hr/°F) divide by 3.44×10^{-4} .

that were readily available from commercial sources, required no specialized instruments, would give reasonably accurate measurements of thermal conductivities, could be checked using readily available "standard materials," and would be field operable.² Specific restrictions on the use of this method for thermal conductivity measurements are that (1) there must be sufficient material to ensure that measurements are taken in a large volume compared to the volume of the thermistor, (2) the material must have a reasonably uniform temperature distribution and be relatively stable in temperature during the measurement interval (about 10 minutes), and (3) the grain size of the material must be small enough to ensure that intimate thermal contact is maintained over the entire surface of the thermistor.

Examples of materials for which this thermal conductivity measurement technique is appropriate are fine-grained soils, building materials such as polystyrene, gel-like materials such as silicone grease, and fiberglass insulations.

2. THEORY

Assume that a thermistor is a perfect sphere embedded in a material such as is shown in Figure 1. When the thermistor's semiconductor bead is heated slightly

² This measurement technique was awarded a U.S. Patent (Patent 4,522,512) on 11 June 1985.

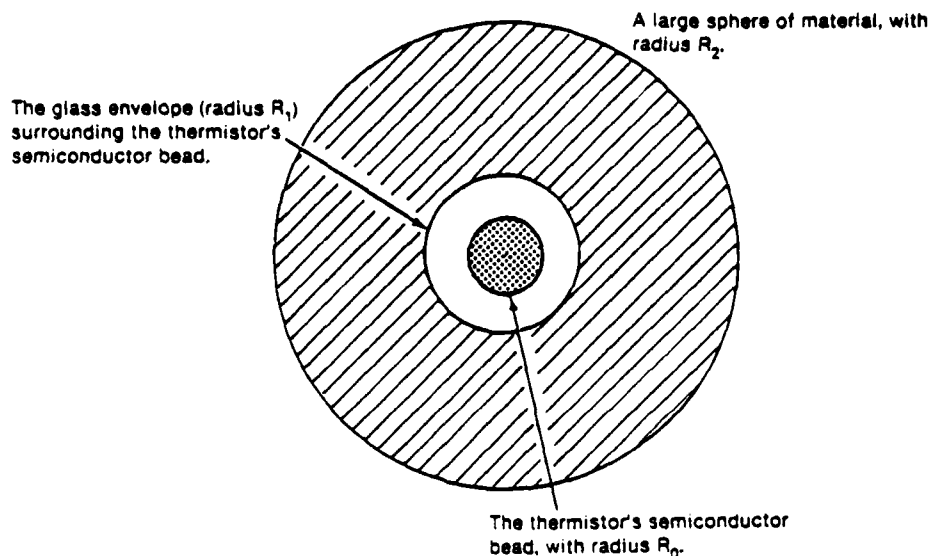


Figure 1.

(electrically) the steady-state heat flow equation³ into the glass envelope is

$$Q = K_t \sqrt{A_0 A_1} \frac{T_0 - T_1}{R_1 - R_0} \quad (1)$$

where

- Q = thermal energy being generated in the semiconductor bead
- K_t = thermal conductivity of the glass envelope of the thermistor
- A_0 = surface area of the semiconductor sphere
- A_1 = surface area of the glass sphere
- T_1 = surface temperature of the glass sphere
- T_0 = surface temperature of the semiconductor bead
- R_0 = radius of the semiconductor bead (sphere)
- R_1 = radius of the glass bead (sphere)

Since the surface area of a sphere is $4\pi R^2$, eq 1 can be written as

$$Q = K_t 4\pi (T_0 - T_1) \frac{R_1 R_0}{R_1 - R_0} \quad (2)$$

If the sphere of test material is assumed to completely surround the glass sphere of the thermistor, then at steady state the

thermal energy flowing into the glass bead can be assumed to flow on into the material, so that

$$Q = K_m 4\pi (T_1 - T_2) \frac{R_2 R_1}{R_2 - R_1} \quad (3)$$

where

- K_m = thermal conductivity of the material
- T_2 = temperature of the surface of the sphere of material
- R_2 = radius of the sphere of material.

Solving eq 3 for the thermal conductivity of the material, K_m :

$$K_m = \frac{Q}{4\pi (T_1 - T_2)} \left[\frac{1}{R_1} - \frac{1}{R_2} \right]$$

If the volume of material is so large that the radius R_2 can be assumed to be infinite with respect to R_0 and R_1 :

$$K_m = \frac{Q}{4\pi R_1 (T_1 - T_2)} \quad (4)$$

This equation can be used to find the thermal conductivity of the material provided a means can be found to find a value for T_1 (the surface temperature of the glass envelope). This means is provided by eq 2, which, when solved for T_1 , gives:

$$T_1 = T_0 - \frac{Q (R_1 R_0)}{K_t 4\pi R_0 R_1}$$

³ See any standard heat transfer textbook (e.g. Kreith, 1961).

When the thermistor is heated, the value of Q can be found by:

$$Q = 0.2389 I^2 R_{\text{hot}}$$

where

I = current in the thermistor

R_{hot} = resistance of the thermistor when it is heated

Q = heat flow in calories per second.

In theory, then, a thermistor can be used to measure the thermal conductivity of a bulk material by using the following three equations:

$$Q = 0.2389 I^2 R_{\text{hot}}$$

$$T_1 = T_0 - \frac{Q (R_1 - R_0)}{K_t 4\pi R_0 R_1}$$

$$K_m = \frac{Q}{4\pi R_1 (T_1 - T_2)}$$

For any given thermistor and material, the values of R_0 , R_1 and K_t will all be constants. Therefore, the second equation can be written as

$$T_1 = T_0 - AQ \quad \text{where} \quad A = \frac{R_1 - R_0}{4\pi K_t R_0 R_1}$$

This equation can then be substituted in the third equation so that

$$K_m = \frac{BQ}{T_0 - AQ - T_2} \quad \text{where} \quad B = \frac{1}{4\pi R_1}$$

or

$$K_m [(T_0 - T_2) - AQ] = BQ \quad (5)$$

This equation can be used to calibrate a thermistor that can then be used to measure the thermal conductivity of a material. All that is needed is to solve for A and B by using two materials whose thermal conductivities are known and measuring the Q , T_0 and T_2 associated with those materials.

T_2 is the "unheated" temperature of the material and is found by measuring the temperature of the material before heating the thermistor, using standard thermistor-temperature measurement techniques. T_0 is found by measuring the heater current to the thermistor and the voltage across it. This is simplified to just a voltage measurement if a known constant current is

used to heat the thermistor. Since both the current and the voltage of the heated thermistor are known, its resistance is known (by Ohm's law) and, therefore, the temperature, T_0 , of the semiconductor bead. Q is the heater current times the voltage across the thermistor times 0.2389:

$$Q = 0.2389 I \cdot V$$

or, by Ohm's law,

$$Q = 0.2389 I^2 R$$

The complete technique for using a thermistor to measure bulk thermal conductivity is therefore as follows.

I. Calibrate:

1. Measure Q , T_0 and T_2 for the thermistor in each of two materials whose thermal conductivity is known.

2. Use these values to solve for A and B in the equation:

$$K_m [(T_0 - T_2) - AQ] = BQ \quad (6)$$

(using standard two equation-two unknowns techniques).

II. Measure:

1. With A and B known, place the thermistor in an unknown material and measure Q , T_0 , and T_2 .

2. Calculate the thermal conductivity using:

$$K_m = \frac{BQ}{(T_0 - T_2) - AQ} \quad (7)$$

All measurements must be taken during a thermally steady-state condition. This condition is determined by monitoring the voltage across the thermistor. When the voltage is steady, the thermal conditions are in steady state.

This technique measures thermal conductivity at a single point. To obtain an average value for the thermal conductivity of a nonhomogeneous material, statistically valid sampling techniques must be used.

3. MEASUREMENT PROCEDURES

The thermistors used in the measurements described in this report were Fenwal

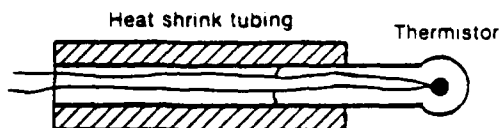


Figure 2.

GB32P101-T. Earlier tests used similar glass bead thermistors manufactured by Victory Engineering Corporation. Any glass bead thermistor is suitable, including double bead thermistors that match a known curve. When selecting a thermistor, some care must be taken to ensure the glass diameter is large compared to the grain size of the material being tested (i.e. that there is good thermal coupling between the thermistor and the material). To make it easier to insert the thermistor into a test material, a piece of dual-wall heat-shrink tubing can be shrunk onto the thermistor's glass bead extension to form a convenient probe (Fig. 2).

A number of different circuit configurations are possible (Fig. 3). No matter which circuit is used, they all do the same thing; namely, provide a small current to read the lower ("cold") temperature and then a larger current to heat the thermistor and at the same time read the higher ("hot") temperature. Typical lower temperature currents are 30 to 70 μA and typical higher temperature currents are 2 to 5 mA.

For the lower temperature reading it is necessary to know the current in the thermistor and the voltage across the thermistor so that the thermistor resistance can be determined. The lower temperature is then found using standard thermistor-temperature measuring techniques (discussed briefly in the following section).

At the higher temperature, the energy being applied is calculated, as well as the temperature itself. Since the current in the thermistor and the voltage across

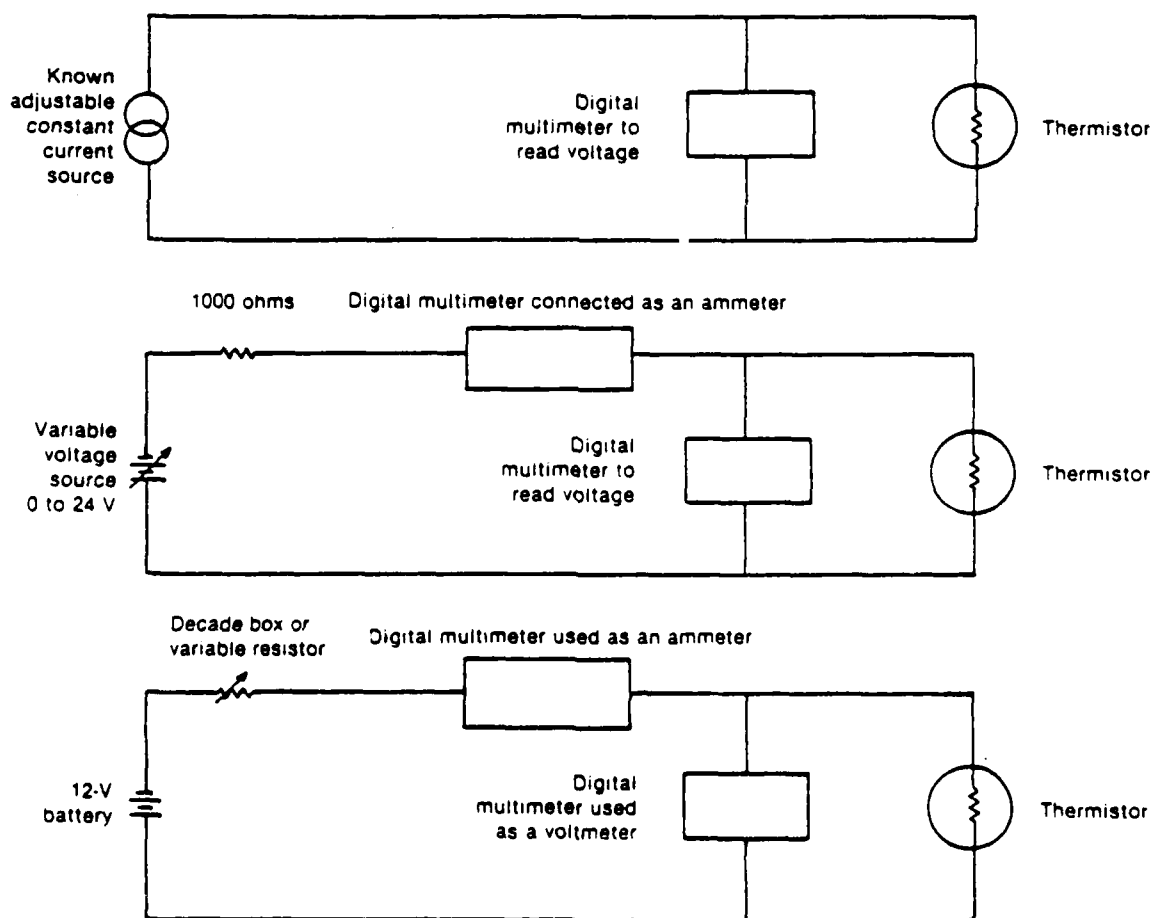


Figure 3.

it are known, $Q = 0.2389 I \cdot V$ is the energy flow in calories per second.

3.1 Typical Measurement

The step-by-step procedure for a typical measurement is as follows:

1. Insert the thermistor in the test material and connect the electrical circuit.

2. Apply a small, lower-temperature current, for instance, $40 \mu A$.

3. Observe the voltage across the thermistor; when it becomes steady (a change of only 1 or 2 mV/min), record the voltage and the current. These two values are then used to calculate the thermistor's resistance and, hence, the lower temperature.

4. Apply a heater current, typically 3 mA. Note the time when this current is applied.

5. Observe the voltage across the thermistor; when it becomes steady, record the current and voltage. Typically, at room temperature, it takes from 5 to 10 minutes for the temperature to stabilize. The time interval over which the heater current was applied should also be recorded.

6. Calculate the higher temperature and the thermal energy, Q , being dissipated in the sample.

7. Reapply the lower-temperature current and wait the same time interval over which the heater current was applied.⁴ Record the current and voltage and calculate the lower temperature again.

8. Average the two lower temperatures.

9. Calculate the thermal conductivity of the test material using:

$$K_m = \frac{B Q}{(T_{\text{hot}} - T_{\text{cold}}) - A Q}$$

The calibration process is exactly the same as above except that K_m is known for the two calibration materials and the values of A and B are calculated using

⁴ The assumption here is that the sample is changing temperature slowly and that the "hot" reading should be taken equidistant in time between the two "cold" readings to account for this temperature change.

the two equations-two unknowns method. Typical calibration materials are:

Water: $K_m = 1.43 \times 10^{-3} \text{ cal/cm-sec-}^\circ\text{C}$

Silicone oil: $K_m = 0.30 \times 10^{-3} \text{ cal/cm-sec-}^\circ\text{C}$

3.2 Example: Test Material: Dry Fairbanks Silt

Time	I	V
0845	30 μA	0.06982 V
0850	3 mA	5.254 V
0855	30 μA	0.06966 V

First lower temperature:

$$R = \frac{0.06982}{30 \times 10^{-6}} = 2327.3 \text{ ohms}$$

lower temperature: 21.19°C .

Higher temperature:

$$R = \frac{5.254}{3 \times 10^{-3}} = 1751.3 \text{ ohms}$$

higher temperature = 28.51°C .

2nd lower temperature:

$$R = \frac{0.06966}{3 \times 10^{-3}} = 2322.0 \text{ ohms}$$

lower temperature = 21.25°C .

Average lower temperature:

$$\frac{21.19 + 21.25}{2} = 21.22^\circ\text{C}$$

$$Q = 0.2389 \times 3 \times 10^{-3} \times 5.254 = 3.7655 \text{ mcal/sec.}$$

From eq 7 with $A=792.3573$; $B=0.36003$

$$K_m = \frac{0.36003 \times 3.7655 \times 10^{-3}}{[(28.51 - 21.22) - 792.3573 \times 3.7655 \times 10^{-3}]} = 0.315 \times 10^{-3} \text{ cal/cm-sec-}^\circ\text{C}$$

or

$$K_m = \frac{0.315 \times 10^{-3}}{3.44 \times 10^{-4}} = 0.916 \text{ BTU/ft}^2\text{/in./hr/}^\circ\text{F.}$$

If this had been a calibration process, the procedure would have been exactly the same except the value of K_m would have been known (for instance, using distilled water). By using two "standard" materials whose K_m 's are known, the values for A and

B for a particular thermistor could then be calculated.

3.3 Thermistor thermometry

There are several methods of converting a thermistor's resistance to temperature. The method used for this report was to purchase thermistors calibrated at three temperature points: -38°C, 0.01°C and +40°C. These three known points were then used to generate resistance-temperature tables in 0.1°C increments from -40°C to +40°C using the Steinhart equation:

$$\frac{1}{T_{\text{abs}}} = C_1 + C_2 \ln R + C_3 (\ln R)^3$$

where T_{abs} is the absolute temperature in kelvins (K), R is the resistance (in ohms) of the thermistor, and C_1 , C_2 and C_3 are constants which may be determined by using the three calibration points supplied with each thermistor. For the resistance temperature tables, K is usually converted to °C by subtracting 273.15.

Once the values for C_1 , C_2 and C_3 have been found, it is often convenient to program a small hand-held calculator to solve the Steinhart equation so that resistance values can be converted to temperature without bothering to look them up in a table.

3.4 Typical results

To demonstrate the use of this technique, two measurement programs were conducted, one on Fairbanks silt and one on typical building insulation. Typical data for these two test programs are shown below.

Table 1. Calibration data for one of the three thermistors.

Standard	$Q \times 10^{-3}$	T(hot)°C	T(cold)°C
water	4.2880	26.82	22.30
water	4.2952	26.78	22.25
silicone oil	3.6967	30.72	23.08
silicone oil	3.6931	30.75	23.12

For water:

$$K_m = 1.43 \times 10^{-3} \text{ cal/cm-sec-}^\circ\text{C at } 23^\circ\text{C}$$

For silicone:

$$K_m = 0.3 \times 10^{-3} \text{ cal/cm-sec-}^\circ\text{C at } 23^\circ\text{C}$$

3.4.1 Fairbanks silt

The calibrations for the tests on Fairbanks silt are illustrated in Table 1. All tests were run with a low-temperature current of 30 μ A and a high-temperature current of 3 mA. The calibration constants for the thermistor were obtained by calculating an A and B for each possible combination of raw calibration data and then averaging these values:

A	B
785.2716	0.38443
785.4557	0.38417
785.9818	0.38422
<u>786.1658</u>	<u>0.38395</u>

$$\bar{A} = 785.7187 \quad \bar{B} = 0.38419$$

$$K_m = \frac{0.38419}{[T(\text{hot}) - T(\text{cold})] - 785.7187 Q}$$

3.4.2 Test Data

Measurements were taken at three soil moisture content; 3%, 17% and 26%. Four measurements were taken for each soil moisture content. The results are illustrated in Table 2.

Table 2. Results of the tests on Fairbanks silt.

$Q \times 10^{-3}$	T(hot)	T(cold)	$K_m \times 10^{-3}$
<u>3% Moisture Content</u>			
3.7598	30.28	22.87	0.325
3.7734	30.18	22.95	0.340
3.7670	30.23	23.09	0.346
3.7670	30.23	23.15	<u>0.351</u>
Average =			0.340
Standard Deviation =			0.011
<u>17% Moisture Content</u>			
4.3862	26.23	21.63	1.448
3.3812	26.27	21.65	1.430
4.3697	26.33	21.73	1.431
4.3661	26.36	21.73	<u>1.404</u>
Average =			1.428
Standard Deviation =			0.018
<u>26% Moisture Content</u>			
4.4184	26.05	21.70	1.929
4.4012	26.15	21.86	2.037
4.3991	26.16	21.86	2.002
4.3798	26.27	21.98	<u>1.964</u>
Average =			1.983
Standard Deviation =			0.047

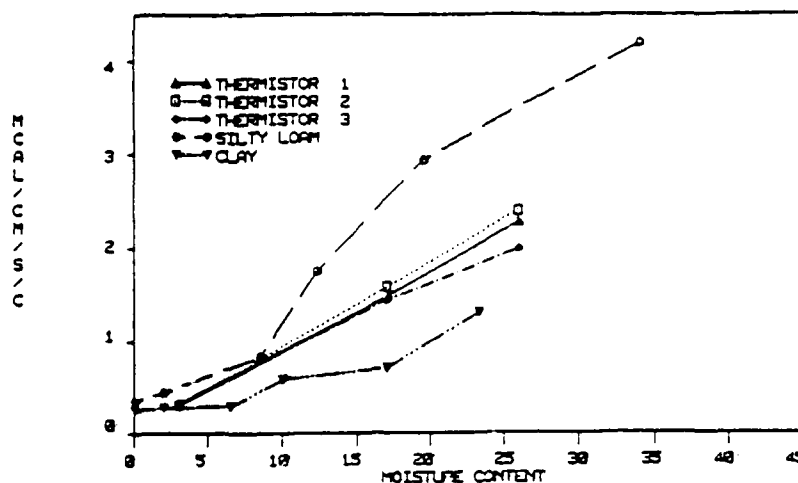


Figure 4.

Each data set was examined statistically to ensure that every specific measurement should be included in the results as a valid number. The technique used was the "outlier detection" method described by Abernathy and Thompson (1973).

These results are in agreement with those of other researchers (Fig. 4) who have measured the thermal conductivity of Fairbanks silts at various soil moisture contents (Farouki, 1931).

3.4.3 Insulation Material

These tests were not conducted by the author so only the results are reported, as received by the author (Table 3).

These tests were conducted by measuring the thermal conductivity at 1/4-in. intervals through the 2-in. test batts of insulation and averaging these values for a total figure for the batt. At the same time a total value for the batt was

Table 3. Results of the tests on 2-in. blue foam insulation.

Depth (in.)	K_m ($\frac{\text{BTU-in.}}{\text{hr ft}^2 \text{ } ^\circ\text{F}}$)		
<u>Sample 4-3</u>			
1/4	0.317	$K_{\text{ave}} = 0.610 \frac{\text{BTU-in.}}{\text{hr ft}^2 \text{ } ^\circ\text{F}}$	$K_{\text{hot box}} = 0.622$
1/2	0.320		
3/4	0.551		
1	0.746	$s = 0.221$	% water by volume = 20.9%
1 1/4	0.730	wt = 298.93 g	% water by weight = 752%
1 1/2	0.885		
1 3/4	0.709		
<u>Sample 4-4</u>			
1/4	0.329	$K_{\text{ave}} = 0.537 \frac{\text{BTU-in.}}{\text{hr ft}^2 \text{ } ^\circ\text{F}}$	$K_{\text{hot box}} = 0.591$
1/2	0.841		
3/4	0.660		
1	0.860	$s = 0.255$	$K_{\text{hot box}} = 0.541$
1 1/4	0.516		% water by volume = 16.7%
1 1/2	0.277		% water by weight = 621%
1 3/4	0.276		

obtained using the guarded hot box technique. As can be seen, the hot box reading and the average value using this thermistor method agree quite closely. The reason the thermistor readings increase as they proceed through the sample is that moisture was purposely introduced on one side of the sample for several hours prior to these measurements in order to determine (1) how much moisture was absorbed by the insulation batt, (2) to what depth the moisture had penetrated, and (3) how much the thermal insulation of the batt had deteriorated as a result of the moisture absorption.

4. DISCUSSION OF RESULTS

The results reported here demonstrate the use of a technique that meets the requirements as stated in the Introduction. Two measurement programs were reported, one where relatively high thermal conductivities were measured (soil) and one where low conductivities were measured (insulation). In each case the results were compared to typical values obtained by other researchers using different measurement techniques. The results are in general agreement in both cases; however, the emphasis here is to describe the measurement technique. The accuracy comparisons do not have a great deal of meaning since sampling techniques were used. The point measurement technique does have some unique characteristics for certain applications, such as profiling insulations that have absorbed moisture, or monitoring building insulations to detect moisture penetration.

The calibration materials used for all the measurements in this report were distilled water and silicone oil. The thermal conductivity for water at 25°C was obtained from a physics handbook. The silicone oil's conductivity was obtained from the manufacturer's specification sheets. The manufacturer warns that the data given are average values. However, a review of thermal conductivity tables shows that nearly all machine oils have a thermal conductivity of approximately 0.3×10^{-3} cal/cm-sec-°C.

The use of water and silicone oil as calibrating standards will certainly have some small error due to convective cooling of the thermistor. This error is dis-

cussed in some detail in the thermal conductivity literature. Generally, the errors are dismissed as "acceptable" (less than 10% error) if the temperature difference between the sensor and the test material is small, i.e. 10°C or less. On the other hand, a temperature of 5°C or more is necessary to make an accurate measurement. To stay within these temperature boundaries, it is necessary to choose the heater current with a little discretion. In general, low-conductivity materials will require only 2 or 3 mA while high conductivity materials will need 4 or 5 mA to achieve an acceptable temperature difference.

This measurement technique will ultimately result in the destruction of the thermistors since they were not designed to be heating devices. However, if care is taken to never exceed 40°C when heating the thermistor, a minimum of 40 tests can be expected. With five thermistors available, the average tests per thermistor were 70, and two were used for over 100 tests before failing. A good rule-of-thumb test to see if a thermistor is still giving correct temperatures is to place the thermistor in a constant-temperature environment (such as an ice bath) and take forward and reversed readings. If the difference between the forward and reverse readings is more than 4 or 5 ohms, the thermistor is likely unstable and should be discarded.

5. CONCLUSIONS AND RECOMMENDATIONS

This method can be used to determine thermal conductivities that are reasonably close to, or below, the values for the calibration standards. However, for bulk materials it is imperative that statistically valid sampling techniques be used.

The test results in this report do not guarantee accurate measurements much above the thermal conductivity of water (1.43×10^{-3} cal/sec-cm-°C). Although no tests were conducted, there is a high probability that the useful measurement range could be extended to higher conductivity materials by using higher-conductivity standards. Heat conductive compounds could probably be used as higher conductivity standards, although there might be some problems in accurately determining their thermal conductivity.

6. REFERENCES

- Abernathy, R.B. and J.W. Thompson, 1973: Handbook, Uncertainty in Gas Turbine Measurements, Air Force Handbook AEDC-TR-73-5, Engine Test Facility, Arnold Engineering Development Center, Air Force Systems Command.
- Farouki, O.T., 1981: Thermal Properties of Soils, U.S. Army Cold Regions Research and Engineering Laboratory, Hanover, New Hampshire, CRREL Monograph 81-1.
- Kreith, Frank, 1961: Principles of Heat Transfer, Fourth Printing, International Textbook Company, Scranton.

**Session 4:
Data Acquisition
and Management**

INFORMATION MANAGEMENT-STATE OF THE ART
THE SHRP LTPP EXPERIENCE

David B. Clarke
Richard A. Margiotta

Science Applications International Corp.
The University of Tennessee, Knoxville

The Long-Term Pavement Performance (LTPP) project is a major component of the Strategic Highway Research Program (SHRP). This 20-year effort is the most intensive evaluation of pavement performance since the American Association of State Highway Officials (AASHTO) Road Test in the early 1960s. Over 700 in-service general pavement sections (GPS) throughout the United States and Canada have been selected to date for the LTPP effort. An additional 200-300 specific pavement sections (SPS) will be constructed or modified to evaluate different pavement designs and maintenance treatments. Throughout the life of the project, SHRP will collect data for each section on material properties, environmental conditions, traffic, maintenance and rehabilitation, surface condition, and pavement response. Many of these measurements will use state-of-the-art techniques.

Based upon the AASHTO experience, SHRP recognized that LTPP would produce a tremendous volume of data. To maintain these data in a form readily accessible to the research community, SHRP is developing a sophisticated information management system (IMS). The IMS is based upon the OKACLE relational data base management system. The data base is distributed across several hardware platforms; a VAX computer serves as the primary data retrieval machine. This paper describes in detail the structure and functions of the LTPP IMS.

INTRODUCTION

In any project, information storage and retrieval is an important consideration. The computer, of course, offers exceptional capabilities in these areas and use of the computer to manage research data is routine. Techniques for managing these data, however, have been steadily increasing in sophistication. Ten years ago, most data were stored in flat files. Today, powerful data base management systems (DBMS) are available on personal computers, and the flat file format is not common. Data base management systems are without question tremendously flexible tools for data manipulation and storage.

Unfortunately, as projects increase in size and scope, their data management needs often grow beyond the capabilities of a basic DBMS. Large projects may have numerous hardware platforms, complicated data structures, multiple data bases, many types of data, and many sources of data. The relationships between the data may be complex and dynamic.

Information management systems are designed to meet these requirements and provide a high degree of integration among the various types and classes of data. The IMS concept is more of an approach to data management than a specific type of software or hardware. Information management systems may consist of numerous data bases, hardware

platforms, and applications. The important thing is that the IMS provides a seamless, integrated view of the data from which the user may draw any desired relationships.

This paper discusses the Information Management System (IMS) now under development for the Strategic Highway Research Program's (SHRP) Long-Term Pavement Performance (LTPP) project. The LTPP objective is to generate data that will allow a more comprehensive understanding of pavement performance under actual operating conditions on in-service highways. Using these data, researchers will be able to improve pavement design and maintenance methods. SHRP has designed a number of LTPP experiments from which a tremendous volume of data will flow. Under current plans, however, analysis of pavement performance using these data will be conducted by the research community. The IMS will be used to validate and store the data, and to serve as a conduit for its dissemination.

BACKGROUND

In comparison to other disciplines, transportation research has historically been severely underfunded. In the early 1980s, the emerging infrastructure crisis prompted substantial public and private mobilization of resources in several areas. The Surface Transportation Act of 1982 doubled Federal fuel taxes to help pay for increased highway maintenance and reconstruction activities. Several special studies of the infrastructure problem were also initiated. The most notable of these was the Strategic Transportation Research Study (STRS). STRS's mission was to determine the scope of research necessary to address problems and shortcomings in materials and techniques used in standard highway practice. STRS recommended a program of intense study in six high-priority research areas. These areas were chosen based upon the criteria that the research results be economically significant and readily implementable.

Overview of SHRP

SHRP was founded to implement the STRS recommendations. The program is

not comprehensive, nor does it replace on-going Federal and state highway research efforts. Rather, it focuses attention on the identified high-priority topics. Funding for SHRP comes from the Surface Transportation and Uniform Relocation Act of 1987, which allocates the program one-quarter of one percent of the state apportioned Federal highway aid. To achieve its goals, SHRP will spend \$150 million dollars over a 5-year period. This funding level accounts for about 25 percent of the current U.S. highway research and development (R&D).

Four technical research areas (TRA) comprise the SHRP program: Long-Term Pavement Performance, Asphalt, Concrete and Structures, and Highway Operations. These choices were made based upon the STRS recommendations. LTPP is investigating pavement design and maintenance methods. The Asphalt TRA is investigating the effect of asphaltic materials properties on pavement service life. The Concrete and Structures program has two functions: 1) to develop improved concrete materials and construction methods and 2) to develop better means for controlling corrosion in steel-reinforced concrete structures. Finally, the Highway Operations TRA is investigating improved ice and snow control, as well as materials and equipment for highway maintenance. The IMS is a component of LTPP, although other TRAs will provide some data to the system.

The LTPP Program

The fundamental relationships used in pavement design were developed nearly 30 years ago at the AASHTO Road Test. These relationships have been criticized for failure to account for many exogenous factors, including soil types, maintenance and construction practices, composition of materials, long-term loads, and climatic effects. Such issues can only be addressed with a controlled, in-depth, long-range field experiment using highway segments representing a wide variety of conditions.

LTPP was designed to rectify the perceived deficiencies of the Road Test and to improve the current state of knowledge. The stated objectives of the LTPP program are to:

- 1) Evaluate existing design methods;
- 2) Develop improved design methods and strategies for the rehabilitation of existing pavements;
- 3) Develop improved design equations for new and reconstructed pavements;
- 4) Determine the effects on pavement distress and performance of loading, environment, material properties and variability, construction quality, and maintenance levels;
- 5) Determine the effects of specific design features on pavement performance; and
- 6) Establish a national long-term pavement data base to support the above objectives and future research needs.

To accomplish these objectives, SHRP has designed two sets of pavement studies: general pavement studies (GPS) and specific special studies (SPS). These studies will collect data on in-service pavement sections throughout the country for a 20-year period. Sections for both studies are 151.5 meters (500 feet) long by one lane in width.

General Pavement Studies. The GPS sections, of which there are currently about 800 scattered throughout the 50 states, Puerto Rico, and the Canadian provinces, are the main focus of the LTPP program. These are existing in-service segments which will be monitored in detail throughout the life of the project. During GPS, eight specific types of pavements will be studied:

- 1) Asphalt Cement (AC) on granular base;
- 2) AC on bound base;
- 3) Jointed plain portland cement concrete (PCC);
- 4) Jointed reinforced PCC;
- 4) Continuously reinforced PCC;
- 5) AC overlay of AC;
- 6) AC overlay of PCC; and
- 7) Unbonded PCC overlay of PCC.

For each of these studies, the factorial matrix contains a number of variables considered to exert an influence on pavement condition. Factors selected vary depending upon the study type. For experiment 7 above, for example, the factors examined are moisture,

temperature, subgrade type, traffic rate, existing pavement type, overlay stiffness, and overlay thickness. Each of these factors are, of course, divided into ranges for classification purposes.

Candidate GPS sections are nominated by state highway authorities. LTPP selects sections for use in the project based upon an exhaustive set of criteria and the results of field validation. Selection of sections is, to a degree, continuing; LTPP would like to have at least 1,000.

Specific Pavement Studies. The SPS sections will be a mixture of modified existing and specially constructed sections which will be used to study in detail a more limited range of factors. GPS sections may move to the SPS as they undergo normal rehabilitation.

Wherever possible, SPS sections will be located in proximity to GPS sections. This simplifies data collection, since some GPS section data, such as traffic levels, will apply to the SPS section. In addition, it will facilitate the testing and observation of the SPS section, since crews will be in the area to perform these actions for the GPS section.

Other TRAs will use SPS sections in their experiments. The maintenance cost effectiveness portion of the Highway Operations TRA will, for example, apply different treatments to SPS sections and evaluate the effectiveness of these treatments. In these experiments, a number of SPS sections will be located around an SPS section.

History of the IMS Project

The designers of the LTPP project realized early on that the research would generate immense volumes of data. Unlike SHRP, which has a 5-year life, LTPP has a 20-year data collection horizon. After SHRP expires, the state highway agencies will continue to provide data to the system. This long lifetime means that the IMS must be carefully designed, since it will no doubt span quantum leaps in the state of the art for computer technology, materials testing, and highway instrumentation.

Because it is a key component of LTPP, planning for the IMS was begun during SHRP's interim phase. The

Federal Highway Administration (FHWA) sponsored a study to evaluate the LTPP plans and prepare preliminary design criteria for the proposed LTPP IMS. This effort, conducted by Coe-Truman Technologies, Inc., resulted in a document called the Implementation Plan. The Implementation Plan recommended a basic hardware and software architecture for the IMS, and computed such parameters as mass storage requirements.

Based upon the recommendations of the report, SHRP decided that each of its four regional offices would serve as data collection nodes for the IMS. Each office would have a small IMS to collect and validate data gathered for the region. These data would then be forwarded to a national IMS for storage and dissemination to the research community. To provide continuity over the 20 year LTPP data collection process, SHRP selected the Transportation Research Board (TRB) to operate this central system.

In the Fall 1987 program announcement, SHRP requested proposals for development of the IMS. SHRP specified the following objectives for an essentially turnkey project:

- 1) Implementation of the national IMS and four regional IMS nodes;
- 2) Installation of the national IMS at TRB;
- 3) Installation of the four regional nodes;
- 4) Installation of necessary interface and quality control subsystems between the regional offices and existing SHRP and contractor offices;
- 5) Provision of documentation and training to allow operation of the complete IMS by SHRP, TRB, and contractor staff;
- 6) Installation of interfaces between SHRP and contractor offices to allow flexible access to the data for a national analysis program; and
- 7) One year of maintenance support following system delivery.

The author's employer, Science Applications International Corporation (SAIC), responded and was eventually selected by SHRP to perform the job. At this time, development of the operational system is underway. Tasks

already completed include hardware/software selection and development of a pilot system. Following sections of this paper will discuss the project elements in detail.

LTPP DATA COLLECTION

The LTPP experiments will collect or generate a wide variety of data. These data are grouped into the following categories:

- 1) Inventory;
- 2) Maintenance;
- 3) Rehabilitation;
- 4) Traffic;
- 5) Materials testing;
- 6) Environmental; and
- 7) Monitoring.

For the most part, the four SHRP regional offices are coordinating the collection of data for the highway sections. Each of these offices has responsibility for the sections in a number of states. Data providers include state highway agencies (SHA), field sampling and testing contractors, the regional staff, and selected external data systems.

Inventory

The inventory data consists of information on the history and current status of the pavement section. Included is basic information to identify the section, such as the highway, milepost and station, section type, responsible agency, etc. Inventory data also describes the geometric details of the section and its materials properties. Finally, it contains information on the historical costs of construction and maintenance.

State highway agencies provide inventory data to the SHRP regional offices. Using their records, the SHAs fill out detailed data collection forms for each of their sections. These forms are submitted to the regional offices, where they are presently being reviewed and entered into an interim data base. Upon completion of the IMS, the data will be transferred from this interim data base.

Inventory data collection is in progress. Experience to date has shown that the quality of inventory data varies widely. Some states have

extensive records; others do not. Then too, available data often pertain to an extensive project of several miles. An assumption of uniformity is necessary to use the data for a 151.5 meter (500 foot) section.

Maintenance

Data will be collected for a GPS section each time maintenance is performed. These data will consist of detailed information on treatment type and location, application methods, materials properties, and cost. LTPP is still defining its maintenance data fields and formats. Because of differences in the practices used by the states, the IMS must be able to accommodate a wide variety of maintenance data.

To help ensure that all maintenance actions are recorded, the states have agreed to control maintenance on the SHRP sections. When maintenance is to be performed, SHRP will be contacted. The regional staff will then coordinate with the state to collect the required data. Current plans are for the maintenance data to be submitted to the regions using data forms.

The maintenance cost effectiveness (MCE) study of the Highway Operations TRA is applying specific treatments to SPS sections. Their objective is to compare the effectiveness and performance of the treatments. MCE will collect extremely detailed information on these experiments. Unlike LTPP, MCE will have a very controlled set of maintenance actions, so data formats will be highly standardized. These data will be stored in the IMS.

Rehabilitation

LTPP will record data on rehabilitation activities which occur after section monitoring begins. Rehabilitation activities are considered to revise the construction details of the section.

The collected data will describe the time and type of rehabilitation, changes to the existing section layer structure, reconstruction methods, material and layer properties, and costs. SHRP is still developing data collection specifications for rehabilitation. Current plans are for

the SHAs to record data during rehabilitation activities and to forward these data to the SHRP on collection forms.

Traffic

LTPP plans to obtain traffic data for all sections. These traffic data will include both the historic activity prior to section monitoring and the actual traffic during monitoring. Information of interest includes average annual daily traffic (AADT), percent heavy trucks, distribution of traffic by vehicle category, and distribution and magnitude of axle loadings.

Historical traffic data will be collected from SHA records. Where count data are missing, "backcasting" and other estimation techniques will be used to generate values. The SHAs will provide data using both paper forms and computer files.

The plan for collecting data during the monitoring phase is still being finalized. It is SHRP's goal, however, to have automated continuous vehicle classification and weigh-in-motion systems at or near each GPS section. The SHAs would collect the data from these devices and forward it to SHRP on a specified basis. This would continue for the duration of the project. Should funding limitations preclude the installation of these devices, staff would conduct periodic counts using portable equipment and factor the results to an annualized level.

SHRP plans to maintain traffic data in both raw and summary forms. The raw data would be available on request; the IMS would normally contain only summary statistics.

Materials Testing

LTPP is preparing to start a field sampling and materials testing campaign which will cover all GPS sections. The purpose of this campaign is to examine the layer structure of the sections and to verify the material properties of the layers. These results should indicate the degree to which materials have deteriorated since construction.

During the field operation, crews will take various types of samples from the pavement layers immediately before and after the test section. The

location, type, and condition of these samples will be recorded in the IMS. The crews will also probe for rock and perform certain in situ tests, which the IMS will also capture.

At the laboratory, the samples will be subjected to a variety of tests. The results will also be transmitted to the IMS. The IMS will store the raw test data from the samples and aggregated values for the specific layers. At present the materials test data will be sent to SHRP on paper forms.

Environmental

Environmental data for sections will include rainfall, temperature, solar radiation, and freeze-thaw characteristics. The data will be summarized on a monthly and an annual basis. Specifics of the environmental data collection program are still being worked out. Various sources specializing in climate information, such as the National Climatic Data Center or the State Climatologist, will most likely provide the data in machine readable format.

The IMS may be required to calculate a representative value from several weather stations in proximity to a section. In this case, it will store both the raw station data and the derived values for the section.

Monitoring

The monitoring category is an extensive portion of the LTPP data collection. Monitoring data consists of the following categories:

- 1) Surface distress;
- 2) Transverse profile (rutting);
- 3) Deflection; and
- 4) Longitudinal profile.

Surface Distress and Transverse Profile. LTPP will use high speed photography to record images of the pavement surface. The equipment, produced by PASCO, USA, also provides transverse profile information. It is also possible in some cases that distress surveys will be conducted manually in the field. The MCE study is expected to use this procedure exclusively.

The PASCO photographs will be reduced using an as yet unselected

system. The data reduction specifications call for the user to be able to record distress types and severities for one foot square increments of the test section. The reduced data will be in machine readable form. The IMS will record all of the localized distress information and will have an aggregate summary for the section.

The PASCO equipment provides transverse profile data in machine readable format.

Deflection. Deflection data will be obtained using falling weight deflectometers (FWD). SHRP has purchased a fleet of four FWDs from Dynatest Consulting, Inc. Current plans are for FWD equipment to be operated over each GPS section twice during the first five year period. State owned FWDs may be used to provide supplementary information.

Deflection measurements will be made at numerous points within a section. At each test location, a number of drops will be conducted using various loading conditions. The exact number of total drops within a section varies according to the pavement type. The positioning of the deflection sensors may also vary.

For each drop site, the FWD will produce data sets containing test parameters, peak response values and load-deflection time-history information. The total amount of raw data for a test section ranges as high as 4.9 million characters. The Dynatest FWD places test data on IBM-PC format data diskettes.

During the deflection tests, a technician will record pavement layer temperatures at two locations within the section. Temperature sensors will be installed in the pavement for this purpose.

The IMS must take the FWD data files, filter them to extract necessary data, and load these data into tables. Raw time history data will be stored off-line. The test parameters, peak data, temperatures, and machine configuration are retained on-line. Summary data for the deflection tests may also be developed.

Longitudinal Profile. SHRP will record the longitudinal profile of the

pavement sections annually for the first five years. The main instrument to be used for this is the K.J. Law Profilometer. SHRP has purchased three of these devices. Use of the Face DIPstick is also being considered because of its flexibility.

The current profiling plan is to obtain measurements (elevation vs. longitudinal coordinate) at 15.24 cm (6 in.) intervals in both wheel paths. These data would be maintained in the IMS in raw form. Summary statistics, such as the International Roughness Index (IRI) would also be maintained for each test.

The K.J. Law profilometers use DEC PDP-11 minicomputers for data collection and reduction. These data can be transferred to the IMS on magnetic tape. The DIPstick stores data internally, but can download it through a serial port to the IMS.

IMS COMPONENTS

The overall IMS consists of five nodes. Each of the four LTPP offices has a regional IMS. The national IMS will be located at TRB in Washington, D.C. This distributed design resulted from an evaluation of the processing requirements for the system. The regional machines are primarily used for data collection and validation. Personnel in the regions have a working relationship with all of the data providers and the technical expertise to judge data quality. The national machine will be used for data storage and retrieval. It has the processing power to handle large queries and for statistical analysis of large data sets. Routine use of the national machine by the regions was judged impractical because of the communications expense.

Hardware

Hardware selection for the regional and national machines was based upon numerous criteria. The basic goals, however, were to be cost effective, maintain system compatibility, have sufficient power for the tasks at hand, and to have an upgrade path.

Regional IMS. The regional IMS

machines are Compaq personal computers with the following specifications:

- 1) 25-mHz 80386 microprocessor;
- 2) 5 megabytes (MB) of random access memory;
- 3) 300 MB of fixed disk storage;
- 4) 1 3-1/2 inch 1.44 MB microfloppy drive;
- 5) 1 5-1/4 inch 1.2 MB floppy drive;
- 6) High speed dot matrix printer;
- 7) 2400 baud telephone modem;
- 8) 120 MB streaming tape drive; and
- 9) Enhanced graphics display adapter and color display.

These machines were chosen after a detailed evaluation of regional requirements revealed that a single user system would be adequate. Since the regional centers will only be in place for 5 years, these systems needed only to be well supported during this time. The 80386 machines are currently the state of the art in personal computing. All regions have their computers in place.

MS-DOS version 3.31 is used on the regional machines. The version has been modified by Compaq to handle files and devices in excess of the normal 32 MB DOS limit. The system users wished to use DOS for two reasons: 1) to maintain compatibility with existing office equipment and software and 2) because they felt most familiar with it. The planned operating system upgrade path is to OS/2 and UNIX should capacity demands require multi-processing or multi-user operation. The machine was sized for four users in a UNIX configuration.

The regional machines have expansion slots allowing for the addition of additional peripheral device controllers, network adapters, or communications ports should the need be identified.

National IMS. The national machine is to be a Digital Equipment Corporation MicroVAX 3600 minicomputer. This computer has the following specifications:

- 1) CMOS implementation of VAX processor architecture;
- 2) 32 MB of random access memory;
- 3) Hardware floating point processor;
- 4) Ethernet adapter;
- 5) 622 MB of fixed disk storage;

- 6) 1600/6250 bpi 1/2 inch magnetic tape drive;
- 7) 296 MB cartridge tape drive;
- 8) Terminal server;
- 9) 2400 baud telephone modem;
- 10) High speed line printer; and
- 11) 4 gigabyte program address space using virtual memory.

SHRP required that the national machine support a multi-user, multi-processing operation, with the capacity for 10 simultaneous timesharing users. The VAX machine was selected because it met this performance criteria and had an excellent upgrade path. The VAX series are common in research settings, and a wide variety of software is available. The IMS VAX will run under the VAX/VMS operating system.

SHRP also decided to purchase an extra regional machine for the national center. The extra computer will be used for regional software development and data exchange between the regions and the national VAX. The two computers will be interconnected using DECnet software and a high-speed serial connection or an Ethernet LAN.

Support Software

SHRP specified the use of a relational data base management system for the IMS. Based upon the variety of data to be collected in the system, SAIC concurred with this. ORACLE was selected from the group of candidate products after an evaluation that included product capabilities, technical support, vendor stability, hardware support, and market share.

ORACLE uses the industry standard Structured Query Language (SQL). SQL offers an extremely powerful command set for data manipulation and data base maintenance. The ORACLE product also includes a host language interface, a form management package, a report writer, and a menu manager. Numerous third party products are also available for the DBMS.

ORACLE has compatible versions for both hardware platforms chosen for the IMS. This is important because the software is the glue which integrates the IMS hardware components. Having one software product for both machines simplifies software development and maintenance, helps to ensure data

compatibility, and eases training requirements.

The ORACLE product has so far met most of its advertising claims. Applications developed on the personal computer (PC) are being ported and executed without change on the VAX. Table structures and data are also portable. Some problems with memory management have been observed in the PC software, but a new version of the product promises improvement.

All non-ORACLE applications for the IMS are written in ANSI 'C'. This decision was made to further insure the portability of the system software. These applications are primarily filters for processing machine readable data.

Data Tables

The IMS contains many tables. These consist of several types: administrative, lookup, data, and utility.

Administrative tables are the highest level in the IMS data structure. They contain such information as experiment definitions, user access privileges, and valid section identifications. The IMS code uses these tables to direct many of its low level activities. Write access to these tables is only possible at the national center and is strictly controlled.

Lookup tables are lists used to validate data or to translate values. Their contents, too, are controlled by the national center.

Data tables contain the information collected by the study. These tables are logically related through various key structures. The highest level key in the IMS is the section key, which uniquely identifies an LTPP section. Other keys are added to identify as necessary to uniquely identify table records. Almost all contents of the data tables originate at the regional centers.

Utility tables are used in various processing steps. Certain reports use utility tables, for example, to store intermediate results. These tables are also used to pass results between applications.

Because much of the data collection plan is incomplete, table specifications are still being developed for the IMS. Even after

completion of the plan, many changes will be identified during the course of the program. One of the benefits of the relational data model is the ease with which the data tables can be altered.

Applications

IMS system users interact with the system almost exclusively through applications programs. Direct access to SQL will rarely be required, and then only for the system operator. The applications use the basic capabilities of the DBMS to perform complex actions, while providing an interface to guide and protect the user. IMS applications use uniform design criteria for user interface elements such as menus, forms, error handling, and help messages.

IMS applications currently consist of four types: utilities, data entry forms, query processors, and reports. When present on both IMS platforms, applications are, with minor exceptions, identical.

Utilities are applications designed to perform utilitarian chores such as DBMS housekeeping and preprocessing input data files. They generally require minimal interaction with the user beyond the specification of control parameters.

Data entry forms allow the user to add, modify, or delete data from a table or tables. These forms have extensive data validation and control logic installed to protect the IMS. A journailling system records transactions performed by the user.

Query processors allow the user to perform a "canned" query without resorting to SQL. Instead of entering a complicated series of SQL statements, the user need answer only a short set of questions. The query processors are designed to select the desired records in an efficient manner. Furthermore, they are compiled for maximum execution speed. The disadvantage of this method is, of course, a lack of flexibility. Still, experience shows that users often have a limited set of requests. SQL is still available to handle the ad hoc query. Outputs from query processors may be stored in new tables, fed to report programs, printed using SQL, or written to data files.

Reports are applications used to rearrange or reduce data. Most of the

reports developed for the IMS so far will be used for data validation and administrative purposes.

IMS OPERATION

Operation of the IMS is expected to begin in mid 1989. This section discusses some of the major operational activities.

Data Processing and Validation

With the exception of environmental data, all information for the IMS will flow into the regional nodes. Before attempting to enter data, the regional center staff will when possible perform a desk check and attempt to correct obvious errors. The data will then be entered, depending on its type, via a form application or utility. These applications perform an extensive number of range and logic checks. Depending upon the severity of errors, incoming records may be rejected. The regional center staff reviews these and makes the needed corrections.

After loading batches of data, the regional staff may run various reports to evaluate data trends and perform interrecord consistency checks. The staff will take action to remedy problems found during these analyses.

At selected intervals, the regional centers transmit their validated data to the national center. Records are selected for transmission via the journailling facility. All transactions since the last data transmission are selected. The data, along with the journal file, are written to cartridge tape and sent to the national center. The regional journal is then reinitialized.

Upon receipt of data from a region, the national center operator uses the journal file to update the national data base. The data are read using the 386 platform and transmitted via the communications data link to the VAX. New blocks of data are moved into a shadow data base, where the LTPP Technical Assistance Contractor will perform interregional quality checks. Any data found to have problems is referred back to the regions for correction. Only after data passes these tests is it moved into the actual

national data base and made available to the research community. The shadow data base concept is easily implemented using the security features of ORACLE.

System Updates

The general philosophy behind IMS updates is to keep tight control at the national center. This is necessary to prevent unauthorized changes from making data inconsistent or software incompatible.

System table updates are performed under the control of the national system operator. All changes to administrative and lookup tables are made on the national machine. Copies of the tables are then transmitted to the regions. Regional systems lack the utility applications for administrative table maintenance.

Software development and testing will also take place at the national center. Updates will be transmitted to the regions as necessary. The regions do not have the staff necessary for these activities; their primary responsibility is to handle the experiment. SHRP will, however, ensure that the national center operator is an information systems engineer trained in the use of the IMS hardware and software.

Disseminating Data

Requests for data will be served by the national center. The regions may provide selected data to their states as a courtesy, but the research community will only receive cleansed data from the national data base.

The mechanism for initiating requests has not yet been fully developed. It is expected, however, that researchers will contact SHRP or TRB to request information. The request will be turned over to the national center operator, who will select the necessary records and output them in the specified format. SHRP does not envision that requesters of the data will have direct access to the data base. It is possible that users may be allowed dial-in access to the national machine to make requests or download selected data.

No decision has been made regarding user charges for requested information.

The possibility of charging for data and processing time in similar fashion to numerous state and federal agencies has been discussed. The IMS can provide data on 1/2 inch magnetic tape and PC format floppy diskettes. The national machine can write 100, 200, 300, 400, 500, 600, 700, 800, 900, 1000 IBM standard label or non-labelled tape in ASCII or EBCDIC.

CONCLUSIONS

A great deal of planning and investment have gone into the LTPP IMS. SHRP clearly places a great deal of importance on the system. They have selected advanced hardware and software and integrated into a system designed to function for the duration of a long project. It is too early to make any claims about the performance of the system, or about the data collected. Much of the IMS development lies ahead of us. Still, it is unlikely that pavement researchers will have cause to complain about their ability to obtain LTPP data.

ACKNOWLEDGEMENTS

The project described in this paper was sponsored by SHRP. The author wishes to thank Mr. Chuck Niessner of FHWA and Mr. Heikki Jamsa of SHRP for their guidance on this project. He also extends his appreciation to Ms. Cheryl Hamberger for reviewing this paper and Ms. Shirley McGill for editorial assistance.

HIGH SPEED DATA ACQUISITION SYSTEM FOR PCC PAVEMENT TESTING

Paul A. Okamoto
Construction Technology Laboratories, Inc.
Skokie, Illinois 60077

ABSTRACT

Field testing of in-service rigid pavements allows them to be evaluated under actual traffic load and environmental conditions. Data commonly collected includes load induced strains, load induced deflections, and slab temperature gradients. Field instrumentation provides important data to confirm theoretical and experimental pavement response due to environmental conditions and applied loads. Together with laboratory and theoretical data, field testing data can be used to develop, and improve mechanistic thickness design methods, load equivalency factors, distress functions, and pavement construction procedures.

Construction Technology Laboratories, Inc. (CTL) uses a high speed computer-based data acquisition system installed in an instrumentation van. The system is capable of recording up to 64 channels of static or dynamic data. All channels are simultaneously sampled, recorded, and stored in digital form on either floppy or hard disks and/or analog form on an F1 tape recorder for later interpretation. Analog to digital conversion is selectable up to approximately 1000 samples per second per channel.

This paper describes rigid pavement response commonly collected during field testing, capabilities of CTL's high speed data acquisition system, and a recent case study.

INTRODUCTION

The Long Term Pavement Performance (LTPP) Strategic Highway Research Program (SHRP) Advisory Committee has concluded that data collection from in-service pavements is needed to develop future policies on pavement design, construction, and maintenance.(1)* Together with laboratory experimental and theoretical data, field testing can be used to validate, develop and improve mechanistic thickness design procedures, load equivalency factors, distress functions, and pavement construction procedures. With the exception of AASHO Road Test, other test track results, and accelerated loading test facilities there has been no concentrated effort to evaluate the performance of pavements under actual traffic and environmental conditions. Research of factors influencing pavement performance can be accomplished in part by condition surveys and data acquisition from in-service pavements.

This paper discusses types of instrumentation, field testing procedures, and use of high speed computer controlled dynamic data acquisition systems in research and testing of portland cement concrete (PCC) pavements. Data analysis, application of data acquisition, and advantages of computer-based systems are also addressed.

* Numbers in parentheses refer to references at end of paper

INSTRUMENTATION

Responses commonly collected when testing concrete pavements include load induced strain, load induced deflection, slab temperature gradients, and slab curl. Deflections and strains due to moving wheel loads are collected using high speed data acquisition systems capable of acquiring data in the range of 200 to 1000 samples per second per channel. Slab temperatures gradients, ambient air temperature, slab corner curl, and edge curl can be manually read or automatically acquired by computer control.

Strain

Strains in pavements are measured with electrical resistance strain gages cemented to the pavement surface or embedded in plastic concrete during construction. For rigid pavements gages are commonly placed midway between transverse joints or cracks along the pavement edge. Gages can also be placed along the diagonal at a slab corner or along transverse joints as shown in Figure 1. The magnitude of measured load induced strain along the diagonal and transverse joint is generally less than that produced along the edge. Gages can also be placed in the interior of the slab or along concrete shoulder edges. A minimum gage length of 2-1/2 times the maximum size aggregate should be selected to reflect average strain in the pavement material matrix. For concrete pavements the minimum gage length is typically 100 to 120 mm.

Bonded electrical resistance gages with polyimide film backings commonly used to measure pavement surface strain are advantageous due to their relatively low cost, easy application, and sensitivity to both static and dynamic strain. The maximum strain is assumed to be located at the top and bottom surface equal in magnitude but opposite in sign. Thus, a value of 20 millionths compressive strain (positive value) at the slab surface would imply a 20 millionths tensile strain at the slab bottom. Disadvantages of surface gages include the low durability in severe environments or traffic loadings even when mounted in recessed grooves.

Gages are bonded to the concrete surface as follows:

1. Grind a recess sufficient to

OUTSIDE LANE CONCRETE SHOULDER

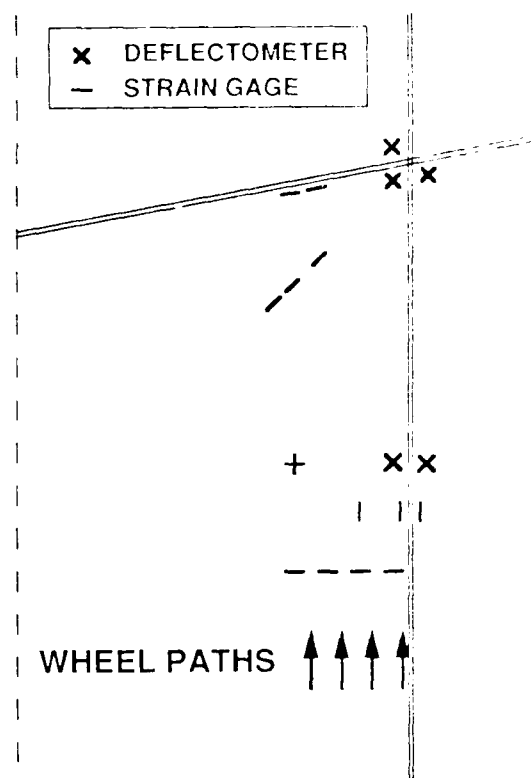


Figure 1 Instrumentation Layout

- remove the texture grooves in the pavement surface
2. Heat the concrete surface (when necessary) and clean the recess with acetone
3. Apply a thin coat of adhesive, place the gage in the adhesive and remove all air bubbles
4. Connect lead wires to the gage and run lead wires in recessed grooves to the pavement edge
5. Waterproof the gage
6. Fill gage and lead wire recesses with silicon rubber.

Several techniques have been used by CTL to embed strain gages in rigid pavement slabs for long term monitoring. One type of embedment gage consists of a wire strain gage sealed between two thin resin blocks. The blocks are commonly textured or coated with a coarse grit to provide bond with the concrete. The advantages

of using this type of gage is its relatively low cost, moistureproofing provided by resin blocks, excellent bond characteristics, and simplicity of installation. Disadvantages of using the resin block type of gage is that they may require corrections to values to compensate for temperature changes and require some care during installation.(2) A second type of embedment gage consists of approximately 1/4 to 1/2-in. temperature compensating strain gages welded to No. 3 or 4 size deformed reinforcement bars. Plates can also be welded to the ends of bars to ensure bond to the concrete. Strain in the concrete is transferred through the rebar to the strain gage. This type of gage has been successfully used to monitor stressing operations in prestressed pavements. Advantages of this gage include being a very rugged gage for placement in actual construction conditions and that they can be prefabricated prior to construction. Disadvantages include high fabrication costs and that gages have to be waterproofed. A third type of embedment gage used by CIL has been a Carlson Meter.(3) This type of gage is a strain sensor which is a long cylinder with an anchoring ring at each end to engage the surrounding concrete. This gage has been used to monitor stressing operations in prestressed pavements. Flexural strains can only be measured using this gage for very thick structural members. Within the brass cylinder two wound strain gage coils are supported by porcelain spools. As the ends of the meter move, one coil is stretched while the other one is shortened. Stretching causes an increase in wire resistance while shortening causes a reduction in resistance from which strain can be computed. Temperature can also be measured by measuring total resistance. This gage is considered very reliable and accurate for long term monitoring (prestressed pavements) but are relatively more expensive than other embedment gages.

If maximum dynamic tensile strain is of interest it may be cost-effective to use surface mounted gages and assume that strains at the slab bottom are equal in magnitude but opposite in sign. If long term monitoring of slab gradient strains are of interest, embedment gages must be used. Disadvantages include labor intensive installation of gages, installation

is generally done during construction only, and gages only start to provide reliable data when the concrete has gained approximately 25 to 50% of its ultimate strength. Long term performance and reliability has not conclusively been established by CIL to rate one embedment gage superior to another.

Embedment gages are installed in plastic concrete at various elevations during construction. A minimum of 25 mm (1 in.) concrete cover is recommended. Prior to construction, chair assemblies or frames must be made to hold gages at desired slab elevations. Gages also have to be placed during construction, positioned between the side forms and internal vibrators on the slipform pavers. Gages are often placed in boxouts secured to the subgrade which are removed after the slipform paver passes the instrumentation. Concrete has to be placed manually, consolidated, and finished in the boxed out areas around the instrumentation. Lead wires leading from the instrumentation to the shoulder are commonly fed through preplaced conduit in the subbase.

Other types or variations of the previously described embedment gages for concrete are also available. Weldable strain gages can also be placed on dowel bars at transverse joints to measure load induced strains.

Deflection

Load induced deflections are measured with resistance bridge deflectometers bolted to the concrete surface or mounted in core holes. These meters contain electrical resistance strain gages mounted on a metal strip bent into a circular arc and mounted in a cylindrical housing.(4) Readings are referenced to encased rods driven into the subgrade at a depth of 2 meters where no significant movement is assumed. As the deflectometer moves the metal strip arc changes its curvature producing resistance changes in the mounted strain gage from which displacement can be computed.

For concrete pavements deflections typically collected include corner, joint, and edge locations as shown in Figure 1. If the deflectometers are mounted in core holes, they can be located directly in the wheel path.

Warping and Curl Measurements

Soon after concrete is placed, drying shrinkage of the concrete begins. Drying shrinkage in a slab-on-grade occurs at a faster rate at the slab surface than at the slab bottom. In addition, because the subgrade and subbase may remain wet, the slab bottom remains relatively moist. Thus, total shrinkage at the bottom is less than at the top. This differential in shrinkage results in a lifting of the slab from the subbase at edges and corner. Movements of this type resulting from moisture differentials are referred to as warping. Over a period of time, the warping behavior is modified by creep effects. However, warping is almost never recoverable.

In addition to warping, a slab-on-grade is also subjected to curling. Curling is the change in the slab profile due to temperature differential between slab top and bottom. Curling is a daily phenomenon. Slabs are curled upward from their warped shape during the night when temperatures are low and curled downward from the warped shape during the midday period when temperatures are higher.

Pavement curl is measured with 0.001-in. indicators placed at the same locations as the deflectometers. Curl readings are referenced to the encased rods driven in the subgrade. Curl readings are manually taken approximately once or twice an hour.

Temperature Measurements

Changes in pavement temperature are measured with copper-constantan thermocouples placed at the surface of the concrete pavement and at the bottom of the pavement in areas where the concrete is removed at deflectometer locations. Thermocouples are inexpensive, reliable, operate over a very large temperature range, and respond rapidly to changes in temperature.

To measure temperature gradients in the slab, thermocouples can be placed in small diameter holes drilled to different depths. Temperature gradients can also be measured by casting thermocouples at varying elevations in concrete blocks and placing the blocks in the subbase adjacent to the pavement at least 12 hours prior to field testing.

Air temperature is monitored with a thermocouple shielded from the direct

sun. Readings are read either manually or computer controlled at intervals of 15 to 60 minutes

DATA ACQUISITION

Construction Technology Laboratories' data acquisition control system is a high speed computer based system designed for laboratory and field projects. A micro-computer is utilized not just for data analysis but integrated into the signal conditioning, acquisition control, storage, collection, reduction, and presentation of data. The computer based acquisition system is controlled with software developed by CTL. The system is used for monitoring and recording dynamic data. Applications of high speed data acquisition include pavement response due to moving loads, track response due to train loadings, and wind or vibration movement of a structure.

For pavement instrumentation a data acquisition system is comprised of the instrumentation, signal conditioners, recording systems, and a method of reducing, analyzing, and presenting the data. Instrumentation can include strain gages, displacement transducers, thermistors, load cells, or accelerometers. Signal conditioners provide excitation voltage, signal amplification, and electrical signal balance for each channel. The recording system obtains and stores either the continuous direct analog signal response or is discretely digitized. Once data are converted to engineering units it can be reduced, analyzed, and presented either manually or aided by computer.

Signal Conditioning

With CTL's high speed data acquisition system the signal conditioners are computer program controlled. The system is capable of recording 64 channels of static or dynamic data. Primary signal conditioning is provided by a 48 channel signal conditioner model. Each channel is equipped with

1. Individual signal conditioner
2. Selectable constant voltage or current excitation
3. Switch for 1/4, 1/2, or full bridge
4. Preset excitation and signal filtering

5. Computer or manual control zero electrical offset adjustment, shunt calibration, and selectable signal gain amplifier ranges

Additional signal conditioning is provided by standard and specially designed conditioners developed for particular types of instrumentation. Signal conditioner settings are monitored and stored by the computer.

Analog to Digital Conversion

All channels are simultaneously sampled to avoid multiplexing operations and skewing of data and then stored in digital and/or analog form. Data input into analog to digital (A/D) converters are digitized at stored at user selectable rates in the range of 10 to 1000 samples per second per channel. To properly evaluate analog signals at least 10 digital points per cycle are required. Data for each channel are simultaneously sampled and digitized with individual converters.

Data Handling

Data can then be stored in either digital and/or analog form. When stored in analog form on a 14 channel magnetic tape recorder, the data are digitized and analyzed at a later date. For most applications data are digitized by the computer, converted into engineering units, and stored in floppy or hard disk data files. Maximum double buffer digital storage rate without losing data for 64 channels of data acquisition is approximately 20,000 samples per second. Slower data rates are typically stored on floppy disks while large amounts of continuous data obtained at high acquisition rates are stored on a hard disk.

Data Presentation

All system control and digitized data examination are done through the computer display terminal which has full alphanumeric and graphical capability. Program controlled inputs for setting up the signal conditioners, starting and stopping data acquisition, and data presentation are through the terminal. Data is quickly and easily reduced then typically presented in tabular and graphic form after acquisition. When necessary, crit-

ical data can be immediately reduced and presented on the display terminal for preliminary analysis and review before leaving the test site. All data presented on the display terminal can be printed immediately with a hard copy printer.

Data typically summarized in tables include minimum, maximum, and average (redundant gages) values for selected instrumentation. Dynamic data can also be plotted as a function of time as shown in Figure 2. The digitized data can also be converted to analog form with D/A converters for plotting on XY, X'Y', and oscillographic recorders.

Instrumentation Van

The high speed data acquisition system is housed in a self-contained instrumentation van as shown in Figure 3. The van serves as a mobile office and electronics shop for installing field instrumentation and transporting data acquisition equipment, shown in Figure 4, to the test site. If necessary the acquisition system can be placed on location in a building or on board another test vehicle (e.g. railcar). The field testing system is powered by one of two electrical generators housed in the van. The first provides power for the data-acquisition equipment while the second serves as a backup unit and as a separate power source for air conditioning, power tools, and other equipment.

The van is also equipped with a closed-circuit-video system for visually monitoring test conditions at remote locations. The video equipment includes two cameras, three monitors, recorder and player, special effects generator, and other accessories.

APPLICATION OF DATA ACQUISITION

A field testing program was conducted by CTL for the Minnesota Department of Transportation to evaluate the effect of frozen support on concrete pavement performance. Minnesota's concrete pavement design procedure did not consider frozen support conditions during winter months when strains and deflections are smaller. Since concrete pavement designs consider repeated application of traffic loading and fatigue damage, it should be possible to take advantage of frozen support con-

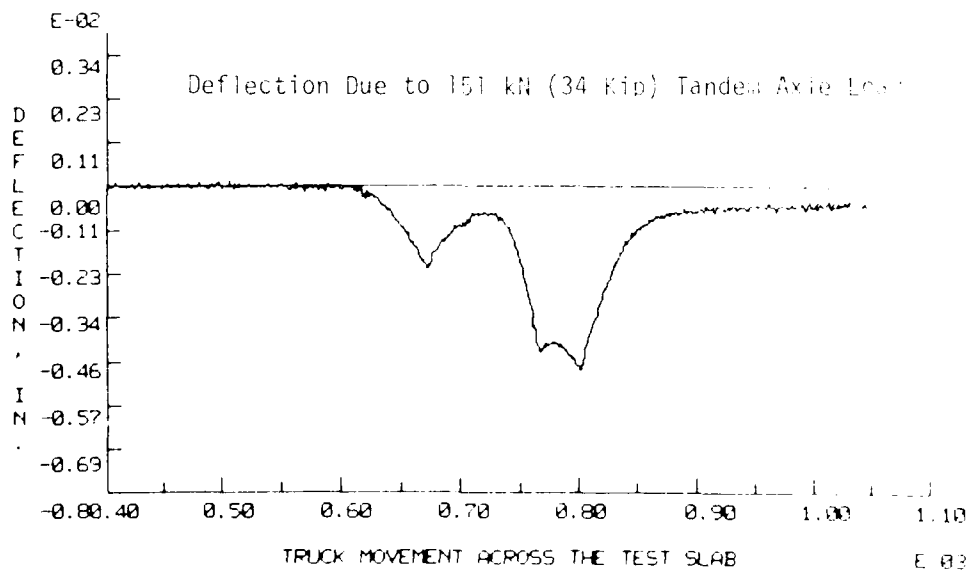
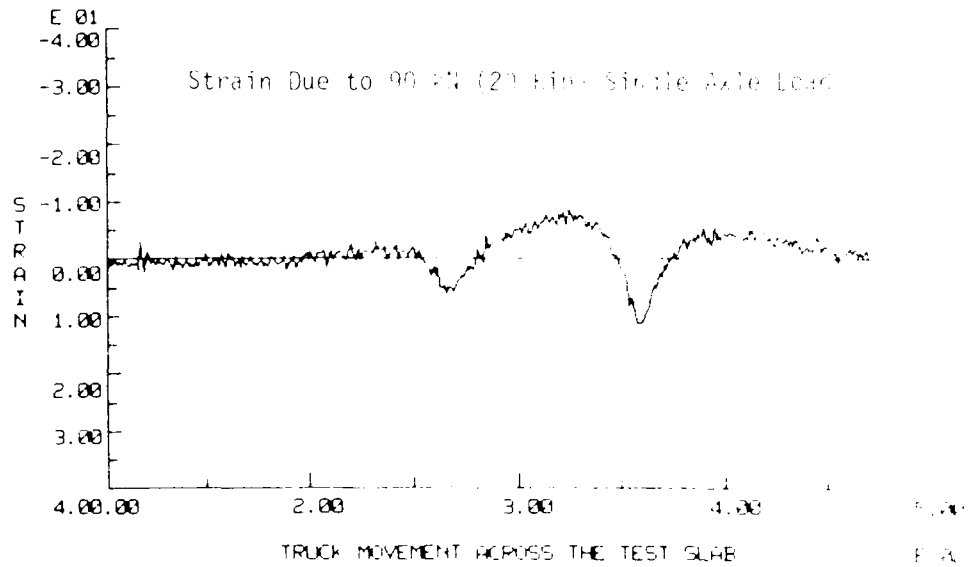


Figure 2 Plot of Strain and Deflection

ditions. Field testing was conducted during October 1982 when air temperatures were about 13°C (55°F) and February 1983 when air temperatures were about -4°C (25°F) to allow comparison of responses of pavement sections with a frozen support to the same sections when the support was not frozen.(5)

Field Testing

Ten sites at 5 different projects were instrumented and tested in both the inside and outside lanes. Dynamic pavement response due to 90 kN (20 kip) single-axle, 151 kN (34 kip) tandem-axle, 187 kN (42 kip) tandem-axle, and 187 kN



Figure 3 CTL's Instrumentation Van

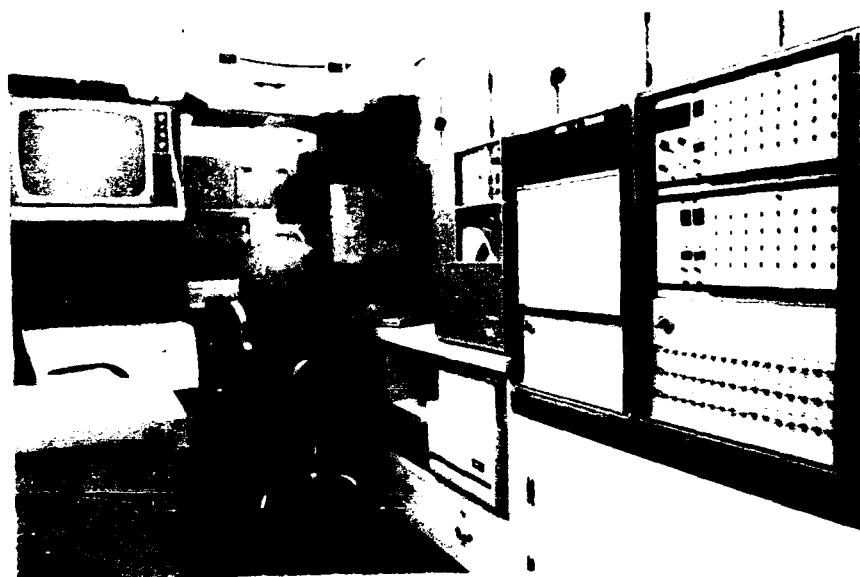


Figure 4 Data Acquisition Equipment

(42 kip) tridem-axle load trucks moving at creep speed were continuously measured at rates of approximately 200 points per second. Strains and deflections were measured due to multiple passes of moving loads at varying wheel paths of 50 to 960 mm (2 to 38 in.) from the pavement edge. Strains were measured in the edge (main-

line and shoulder), corner (diagonal), joint (transverse), and interior locations. Deflections were measured at edge (mainline and shoulder) and at corner (mainline) locations. Air temperature, concrete temperature (7 elevations), corner curl, and edge curl were periodically measured during load testing.

Testing was done during midday hours when the slabs were curled to their most downward profiles and no temperature corrections were necessary to compensate for curling effects on strain and deflection.

Data Analysis and Design Modifications

Deflection and strains measured during February were significantly less due than those measured in October due to frozen subgrade and subbase support. Edge deflections measured in February ranged from 15 to 25% of deflections measured during October. Similar to that measured at the edge, corner deflections in the winter were 5 to 15% of those measured in the fall. Edge strains in February generally ranged from 20 to 60% of those measured in October.

Based on measured pavement responses and AASHTO equivalence factors, new equivalence factors were developed for axle loads applied during the winter. The damaging effect of a single-axle or tandem-axle load applied in the winter is approximately 1/7th to 1/9th of that for the same axle load applied during the fall. If traffic is considered to be uniformly distributed over the 12-month period and if only 1/7th of the winter traffic is considered applicable, then only 79% of the total design value of the equivalent 80 kN (18 kip) single-axle loads need to be considered for thickness design.

SUMMARY

Field testing data together with laboratory and theoretical data can be used to develop and improve thickness design procedures, load equivalency factors, distress functions, and pavement construction procedures. To measure responses of moving loads a multi-channel computer-based data acquisition system capable of fast sampling rates is required. Data collection of in-service pavements will help shape future policies on pavement design, construction, and maintenance.

ACKNOWLEDGEMENTS

The opinions and findings expressed or implied in the paper are those of the author. They are not necessarily those

of Construction Technology Laboratories' parent company, the Portland Cement Association, or those of the Minnesota Department of Transportation.

REFERENCES

1. White, T. D., "Instrumentation for Flexible and Rigid Pavements," report to the Experimental Application and Evaluation Branch, Demonstration Projects Division, Federal Highway Administration, Washington, DC, December 1985.
2. Maffei, J. R., Burns, N. H., and McCullough, B. F., "Instrumentation and Behavior of Prestressed Concrete Pavements," Research Report 401-4 to the Texas State Department of Highways and Public Transportation, November 1986.
3. Tayabji, S. D., et al, "Instrumentation Plan for a Section of Prestressed Pavement Along U.S. 220, Blair County, Pennsylvania," report to Pennsylvania Department of Transportation, Harrisburg, Pennsylvania, June 1988.
4. Nowlen, W. J., "Techniques and Equipment for Field Testing of Pavements," Portland Cement Association Development Department Bulletin D83, 1964.
5. Ball, C. G., Tayabji, S. D., and Okamoto, P. A., "Effect of Frozen Support on Concrete Pavement Performance," report to Minnesota Department of Transportation, St. Paul, Minnesota, July 1983.

DATA ACQUISITION : FIRST THE FERF THEN THE WORLD

Kurt V. Knuth
USACRREL
Hanover, NH 03755

Abstract

A review of the measurement systems and the data collection techniques as applied to the laboratory, the Frost Effects Research Facility and finally the real world will be presented.

In the beginning there was the ruler, thermometer, pencil and paper. Then came electricity, motors, etc. till now there is the computer, fiber optics, lasers, ultrasound and the satellite. We will present the current as well as future data collection techniques for temperature, moisture content, pressure, stress, strain and displacement as used in the FERF and in remote sites.

Introduction

Humankind has been making measurements since probably cave dwelling days. Over 5000 years ago standards for measurements came into being. These were primarily for length and weights. Time was the next dimension to be "accurately" measured. One of the earliest hard copy of analog signals was in the field of physiology where a stylus would scrape carbon off of a "smoked drum" recorder, these date back over 175 years. With the advent

of electricity, the science of measurement moved ahead rapidly till now one can be recording real time data from an event halfway around the world.

We at the Cold Regions Research and Engineering Laboratory are primarily interested in measuring the effects of cold of most everything.

FERF

The Frost Effects Research Facility is a controlled environment for conducting cold-climate test. It is, in effect, a 29,000 square-foot refrigerator/freezer. The FERF is arguably the largest, most comprehensive facility of its kind in the world.

The FERF building is a steel-framed structure. It is 182 feet long and 102 feet wide and includes 12 test basins all 21 feet wide separated by wood and concrete bulkheads. The FERF is used for testing the effects of cold temperatures on pavements, soils, structures, vehicles, equipment and just about anything else that is affected by freezing weather and freeze/thaw cycles. Obviously these tests require widely different environments, and to ensure reliable results,

the temperature and moisture in each basin must be fully controllable.

Types of Measurements

The vast variety of experiments that occur within the FERF require a wide range of measurements: temperature, both above and below ground, humidity, moisture content, pressure, displacement, stress and strain to name most but not all of the parameters that are measured.

Temperature, our most widely measured parameter, is generally measured either by thermocouples or thermistors. Thermocouples are the easiest to install and read since most dataloggers have direct thermocouple inputs but require two leads for each measured point and a fairly heavy gauge wire if long runs are used. Also thermocouple accuracy is not as good as thermistors can be. Thermistors generally come as a probe and therefore is larger than a thermocouple, and is more expensive. On the positive side, thermistors, can be assembled into arrays with one lead per thermistor and one common resulting in a much smaller cable for the same number of measurement points. Thermistors do require an excitation voltage and normally a bridge circuit arrangement to read them.

Other means of measuring temperature are infrared and, just coming into its own, fiber optics, neither of which, depending on the application, are as accurate or as cost effective as thermocouples or thermistors. There is one commercial fiber optic temperature system that, while not originally designed for roadways, is being tested in roadways. This system, by York Technologies, is a distributed system that measures the temperature along the length of a 2000 meter fiber optic cable. There is a proposal to purchase one of the systems for CRREL.

Frost Heave

Currently underway is a project, by Berg, Janoo and others, to measure many of the parameters of frost heave. Among these are: total heave displacement, subsurface heave displacement, subsurface heave force at various depths, along with temperature and moisture content.

Employed in this experiment are some novel approaches such as using linear displacement transducers mounted on the bottom of the test pit and attached to plates at various depths to measure differential heave displacement. Also being used is a set of rods attached to the surface or subsurface inside of a tube attached to the base of the pit with magnets and magnetic sensors embedded in the rods and tubes respectively.

Force is being measured by a series of various length rods attached to the base of the pit with a plate on its top and strain gauges along its length. Total heave has been measured by placing a beam across the test section and measuring the distance from the beam to the surface along the length of the beam to create a transverse section of the test roadway. The beam is then moved and another set of measurements are taken. There are at present two proposals to modify the way this measurement is being done. Both involve a "car" riding on the beam attached to a computer and tracing the crown of the roadway either by an lvdt attached to a small wheel or with a ultrasonic transducer to measure the distance.

Moisture Content

The most commonly used soil moisture sensor is a gypsum block whose resistance is a function of moisture content. Presently there are two new sensors under development, one is a capacitance

probe under joint development with Dartmouth College, and the other is a fiber optic sensor being developed solely at CRREL.

Data Acquisition

The most common data collection instrument is the Kaye datalogger either with or without a ramp scanner. One such system presently has 70 temperature sensors but could hold as many as 700. In addition to the Kaye we also have a Hewlett Packard datalogger and by the time this is published a system from Campbell Scientific.

The Kaye system collects the data and either prints it on its built-in printer or stores it on magnetic tape. The tapes must then be collected and read into a computer for further analysis. The tape system for Shoop et. al. is being replaced by a dedicated computer system that will receive the data from the datalogger and do data reduction online with a printout of the previous days data waiting at the desk when personnel arrive in the morning. Carrying this a step further, a Kaye datalogger and a laptop computer with a modem have been installed in Alaska and sends weekly data directly to the principle investigators desk each weekend. As another example, the runway of the airport at Jackman Maine has been instrumented with about 75 temperature sensors, both thermistors and thermocouples, soil moisture blocks and some water depth sensors all connected to a Campbell CR21X datalogger. Since there is no power or phone at the site, the system is powered by rechargeable batteries and a solar panel. The data is sent from the site by a GOES satellite transmitter to a computer in Maryland from which we can download the data. CRREL presently has several satellite systems running at this time.

The trend in data acquisition at CRREL is toward the more

intelligent data collection devices and dedicated computer systems. While within the sensor world, we will always be using proven technology but also be testing and evaluating the leading edge of the latest in sensor technology.

References

Shoop, S. (1988) Research Plan and Experimental Design for the Study of Vehicle Mobility in Thawing Soils. USACRREL Internal Report #1001.

Shoop, S. (1988 in press) Experimental Research on Vehicle Mobility on Thawing Soils: Mobility test Basin and Preliminary Results. USACRREL Report #449.

Electronic Measurements and Instrumentation. Edited by Bernard M. Oliver and John M. Cage. McGraw-Hill Book Company 1971.

Berg, R., V. Janoo and others (project underway) Performance of Concrete Pavements During Freezing and Thawing.

Cold Regions Weather Data Systems

Roy E. Bates

U.S. Army Cold Regions Research
and Engineering Laboratory
Hanover, New Hampshire 03755

Sidney Gerard

Science and Technology Corporation
Hanover, New Hampshire 03755

1. ABSTRACT

The northern temperate climatic zones experience a varying scenario of winter environmental extremes of cold, icing, and precipitation, which severely influence people, equipment and operations. Even instruments used to measure cold and/or wet adverse environments may be incapable of operation if employed during severe cold weather. It is important to know the equipment's environmental restrictions and to evaluate the frequency and duration of disabling weather. In some instances, functional impairments persist after the causative meteorological conditions have subsided, e.g. glaze, rime and heavy snow and ice accumulation.

For over 25 years, CRREL has studied environmental conditions in winter weather. These efforts have concentrated on providing field-measured meteorological data and historical climatological data, as well as instrumentation support for many experiments conducted throughout cold regions of the Northern Hemisphere. These efforts have involved characterizing atmospheric conditions as well as surface conditions. Some of the measurements made are snow temperature profiles, depth of the snow on the ground with varying terrain and vegetation, temperature at the snow/ground interface, near-surface ground temperature and wind profiles, snow cover

properties, solar radiation, visibility and sky conditions.

Optimum field use of meteorological information requires that operable field-hardened and calibrated instrumentation be available to conduct field experiments. Field evaluations at CRREL indicate that minor modifications, readily accomplished by the manufacturer, may greatly improve severe-weather service of commonly available instruments, sensors and equipment.

2. INTRODUCTION

As environmental measurements are normally made in conjunction with pavement response monitoring systems, this paper is presented to provide a brief description of the various instrumentation packages used to gather atmospheric and background environmental data during field testing. The instrumentation discussed in this paper is not necessarily the best or the only equipment available. These are instruments CRREL currently has in inventory or ones that have been used in the past with success at cold region field experiment locations. The paper identifies instruments used to measure parameters of 1) the lower atmosphere, 2) air/snow interface temperature, and 3) the temperature profile of the snowpack and the underlying soil. Finally, the paper gives an

example summary of the computer-processed data and some data analyses.

3. ATMOSPHERIC INSTRUMENTATION

Table 1 summarizes the instrumentation used by CRREL to gather environmental data from the snow or ground interface up to 32 m in height. These instruments are normally mounted on towers that range from 4 to 32 m high. Table 1 presents the instrument, the parameter recorded, the type of sensor, the range of the data recorded as well as assessment of the accuracy of the instrument. Figure 1 depicts meteorological instrumentation mounted on a typical field tower. These particular sensors are located at the 8-m height on the instrument tower. The atmospheric parameters measured are normally those listed below:

1. Air Temperature
2. Dew Point
3. Relative Humidity
4. Wind Speed and Direction
5. Precipitation-Water Equivalent
6. Solar Radiation
7. Station Pressure

3.A. Air Temperature

CRREL has used several different instruments/sensors to measure and record air temperature. These instruments are:

1. General Eastern Model 650/612A
2. Vaisala HMP 122Y
3. Environmental Instrument Model 200 Dual Axis Probe
4. General Eastern System 1200 MPS
5. Rotronic MP-100F
6. Hygrothermograph Model 5-594

These instruments are presented in Table 1 with their measurement range capability and accuracy.

3.B. Dew Point

The general Eastern Model 650/612A or General Eastern System 1200 MPS is used to measure dew point.

3.C. Relative Humidity

Three instruments are currently being used to obtain relative humidity data. These are the 1) Vaisala HMP 112Y, 2) Rotronic MP-100F, and 3)



Figure 1. Instrumentation at center of tower (8 m), Camp Grayling, Michigan.

Table 1. Meteorological instruments.

Parameter	Instrument	Type of Sensor	Range	Accuracy
Ambient Temperature	General Eastern Model 650/612A	100 Ohm Platinum RTD (Linear)	-40° to +66°C	±0.1°
	Vaisala HMP 122Y	PT 100 element 1/3 DIN 43760	-40° to +66°C	±0.1°C at 20°C
	Environmental Instrument Model 200 Dual Axis Probe	Platinum RTD	-40° to +66°C	±0.1°C
	General Eastern System 1200 MPS	Platinum RTD	-100° to +350°C	±0.2°C
	Rotronic MP-100F	PT100 RTD	-50° to +150°C	±0.1°C @ 20°C to ±0.2°C
Dew Point	General Eastern Model 650/612A 1200 MPs	100 Ohm Platinum	-45° to +66°C	±0.1°C
Relative Humidity	Vaisala HMP 112Y	Humicap	0 to 100%	@ 20°C ±2% RH for 0 to 60% RH for 60% to 100%
	Rotronic MP-100F	Hygrometer Capacitive	0 to 100%	±1.5% @ 0-100% RH
Wind Speed and Wind Direction	Environmental Instrument Model 200 Dual Axis Probe	Two Static Pairs	0 to 102 M/S	±3%
		Heated Resistive Sensing Elements Mechanically Supported At Right Angles to Each Other	0-360°	±3°
Wind Speed and Wind Direction	Teledyne Geotech Wind System Model 101	Three-Cup	0-45 M/S	±1%
		Vane	0-540	±3%
Water Equivalent	Belfort Model 5915-12-20 cm Potentiometer Electronic Gage	Automatic Weighing	0-150 mm	±0.1 mm
Shortwave Solar Radiation (vertical and reflected)	Eppley Precision Solar (Pyranometer)	Radiometer	0.3 to 3 μ m	±1%
Infrared Longwave Radiation (vertical and reflected)	Eppley Precision Solar (Pyrgometer)	Radiometer	3 to 50 μ m	±3%
Station Pressure	Environment Instrument Model 200 Dual Axis Probe	Piezo Resistive Silicon Chip	630 MB 1080 MB	±2 MB
	Sierra-Misco Model 1520 Barometric Pressure Sensor	Multicell Aneroid	85-200 MB (600-1065 MB)	±0.5 MB Over any 100 MB Interval
Ambient Temperature	Hygrothermograph Model 5-5	Aged Bimetallic Strip	60 Adjustable	±1%
Relative Humidity	Hygrothermograph Model 5-594	Human Hair Bundles	0-100%	±0.1% 20 to 80% RH ±3% at Extremes

Hygrothermograph Model 5-594. In general, relative humidity data can be calculated from temperature and dew point data, but care should be taken, since slight inaccuracies in either type of data can lead to erroneous calculations.

3.D. Wind Speed and Direction

Currently CRREL is using two types of anemometers for measuring wind data. These are the Environmental Instrument Model 200 Dual Axis Probe and the Teledyne Geotech Wind System Model 101. The standard propeller or vane anemometers are susceptible to icing problems when used in high elevation areas such as the Mount Washington, New Hampshire, observatory, or where icing, glaze or riming occur frequently.

3.E. Precipitation-Water Equivalent

Measuring the amount of water-equivalent snowfall in real time is very difficult. CRREL is currently employing the Belfort Model 5915-12 20-cm Orifice Potentiometer Electronic Gage to gather water equivalent of falling snow. For measuring snow depth, snow depth stakes randomly placed over the measurement site will normally be sufficient. CRREL is now testing an acoustic snow depth gage for automatic recording of snow depth.

3.F. Solar Radiation

A critical environmental measurement is to establish the amount of incoming solar radiation from the sun as well as the amount of radiation being emitted back toward the sun. For electromagnetic wavelengths of 0.3 to 3.0 μ m, an Eppley Precision Solar (Pyranometer) Radiometer is used. For wavelengths of 3.0 to 50 μ m CRREL employs an Eppley Precision infrared (pyrgeometer) radiometer. These continuous daily measurements also give a good indication of cloud cover.

3.G. Station Pressure

For gathering continuous hourly atmospheric pressure data CRREL is currently using either the Environmental Instrument System Model 200 Dual Axis Probe or the Sierra-Misco Model 1520 Barometric Pressure Sensor.

4. GROUND/SNOW INTERFACE TEMPERATURE

The temperature of the snow/air interface (snow surfaces) for undisturbed snow covered terrain is extremely important for heat transfer and heat budget considerations. Measuring this temperature is extremely difficult and impossible under many conditions due to rapid surface flux, instability and turbulence. The apparent surface temperature is dependent on many factors such as the location (valley or hill), sunny or shaded area, in the open or in a tree-covered area, etc. CRREL uses three types of instruments to measure this parameter: 1) an inverted infrared Eppley Precision Solar (Pyranometer) radiometer as noted in 3.F, 2) thermistors, and 3) thermocouples. Another method which could be used, although not as accurate, would be to approximate or model the snow surface temperature from air temperatures measured in the first 2 m above the snow surface.

5. GROUND OR SNOW COVER TEMPERATURE PROFILES

Another important parameter that needs to be measured is the temperature profile below the surface of the snow or ground. In order to measure this parameter CRREL uses thermistors or thermocouples that are buried at various depths and in various grid configurations. These depths and configurations are determined by the particular application and research effort. Temperature profile measurements have been made at very shallow depths as well as up to 5 m below the surface.

6. DATA RECORDS AND ANALYSES

Oftentimes having the required instrumentation to measure meteorological parameters is only solving half the problem. Meteorological data are usually voluminous and time-consuming to analyze. In the recent past, collecting and summarizing these data manually was a monumental task if not insurmountable. CRREL has automated the data acquisition process for most of the instruments noted above. Figures 2 and 3 are hard copy examples of data gathered and produced by a data acquisition computer.

SOLAR RADIATION

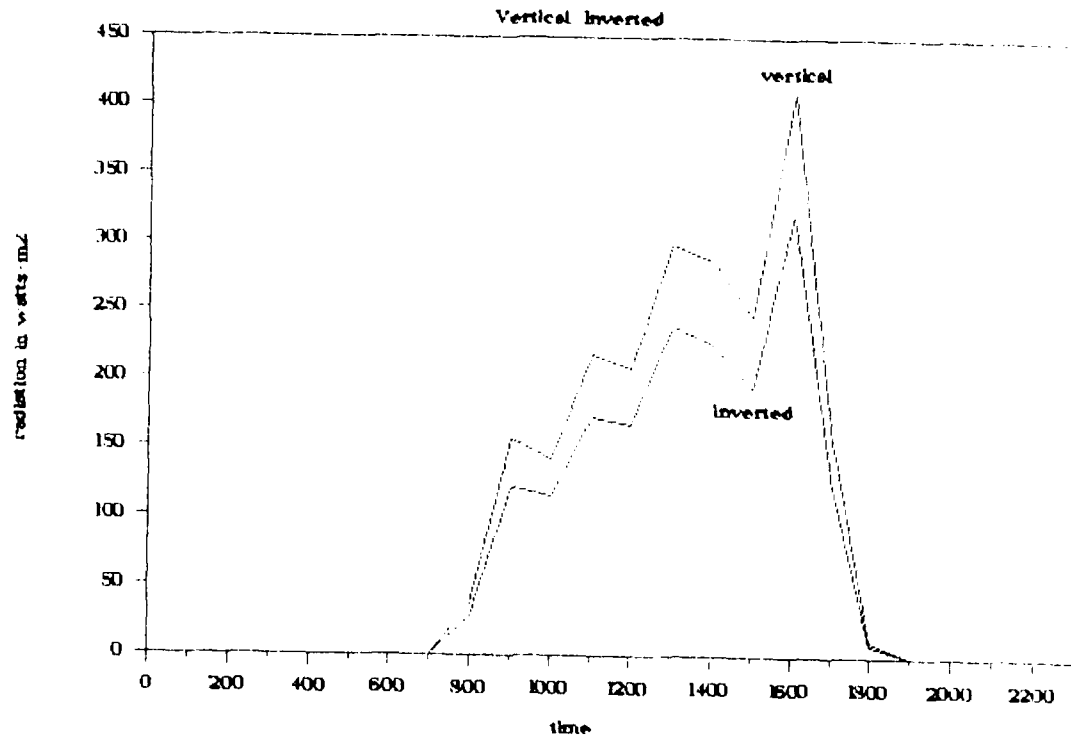


Figure 2. Typical solar radiation plots, Camp Grayling, Michigan, 2 March 1989 (see Table 2).

WIND DIRECTION

01 MARCH 1988

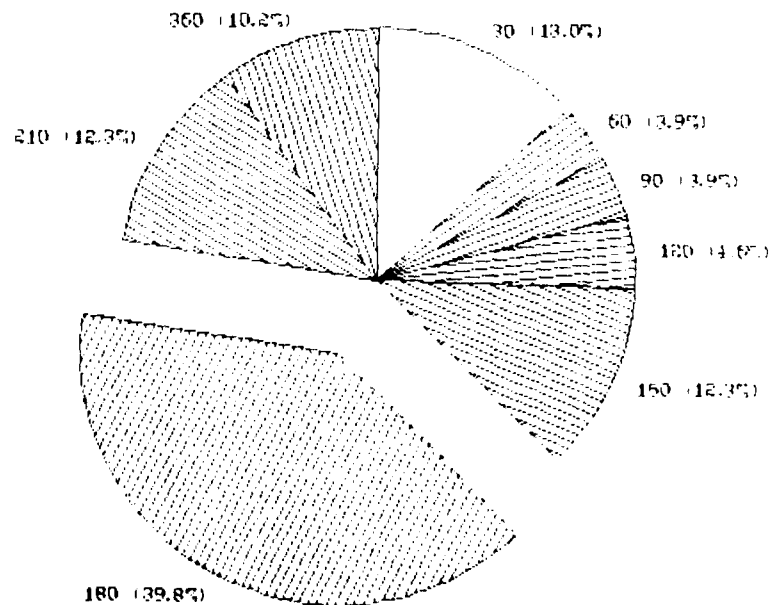


Figure 3. Typical wind direction plot, Camp Grayling, Michigan, 2 March 1989 (see Table 2).

Table 2. Meteorological data, Grayling, Michigan, 2 March 1989.

TIME	PRESS	WINDS		TEMP	DW/PT	RH	SOLAR	RAD	IR	RAD	PRCP
hhmm	mba	deg	spd	C	C	%	vert	invert	vert	invert	mm
0	964.3	187	3.6	-3.0	-3.0	100	0	0	287	285	29.3
100	963.6	202	2.7	-1.7	-2.1	97	0	0	291	289	29.3
200	963.3	213	3.3	-1.0	-2.0	93	0	0	295	292	29.3
300	963.0	216	2.0	-0.6	-1.3	95	0	0	299	293	29.3
400	962.9	227	1.4	-0.1	-0.9	94	0	0	302	296	29.3
500	963.1	291	0.6	0.2	-0.5	95	0	0	299	294	29.3
600	963.8	321	2.9	0.6	-0.8	90	0	0	298	298	25.3
700	964.4	338	2.9	-0.1	-1.2	92	0	0	297	295	29.5
800	965.7	337	4.8	-1.5	-3.3	88	38	29	281	288	29.5
900	967.0	323	4.7	-2.1	-5.2	79	156	121	254	282	29.5
1000	967.5	327	3.7	-2.6	-5.3	82	142	115	279	285	29.5
1100	968.6	333	4.5	-3.7	-6.5	81	218	173	272	283	29.5
1200	969.3	329	4.5	-4.2	-7.1	80	208	167	270	280	29.5
1300	970.0	315	4.7	-4.4	-7.4	80	299	239	273	282	29.5
1400	970.6	317	5.2	-4.7	-8.0	78	287	225	268	282	29.7
1500	970.9	316	4.9	-4.7	-8.2	76	247	193	267	281	29.7
1600	971.3	312	5.0	-4.6	-8.4	75	411	323	247	283	29.7
1700	971.9	330	5.0	-5.5	-8.3	81	156	123	259	274	29.8
1800	972.6	343	3.9	-6.3	-7.6	90	13	9	264	268	29.9
1900	973.5	340	3.5	-7.1	-8.3	91	0	0	248	263	29.9
2000	973.8	346	4.1	-7.9	-11.0	78	0	0	198	249	30.0
2100	974.3	344	3.1	-8.6	-11.3	81	0	0	197	244	30.0
2200	974.9	319	2.8	-8.7	-10.1	90	0	0	215	248	30.0
2300	975.4	331	3.5	-8.7	-10.0	90	0	0	250	258	30.0
MAX	975.4		9.1	0.6	-0.5	100			302	298	30.0
MIN	962.9		0.6	-8.7	-11.3	75			197	244	29.3
AVG	968.6	302	3.6	-3.8	-5.7	87			267	279	
TOTAL							2175	1717			0.7

Table 2 shows a daily summary of data gathered on a recent field experiment. These data and summaries are now processed in real time in the field and handed off to users as required.

7. SUMMARY

CRREL has developed an extensive capability to gather weather data in cold weather winter environments. This effort has been developed through long and extensive field experiment experience. Off-the-shelf instrumentation developed for use in temperate climates has to be modified and improved to satisfactorily function in cold regions. Organizations conducting field measurements in cold regions for the first time should make every attempt to contact CRREL or other comparable agencies for advice prior to taking instruments in the field. Cold regions weather data acquisition is more costly in terms of time, manpower and instrumentation.

8. SELECTED REFERENCES

Bates, R.E. (1987) "Meteorological System Performance in Icing Conditions," presented at Seventh Annual EOSAEL/TWI Conf., Dec 1986 (published proceedings April 1987).

Bates, R.E. and King, G.G. (1986) "Intensity of Snowfall at the Snow Experiments," presented at Sixth Annual EOSAEL/TWI Conference, December 1985 (published proceedings February 1986).

Bates, R.E. and O'Brien, H.W. (1985) "Meteorological and Snow Cover Measurements at Grayling, Michigan," Presented at 42nd Annual Meeting of Eastern Snow conference, June 1985 (published proceedings 1985).

Bates, R.E. and Govoni, J.W. (1984) Meteorological Instrumentation for Characterizing Atmospheric Icing. Second International Workshop on Atmospheric Icing of Structures. Trondheim, Norway.

Bates, R.E. (1984) Site-Specific Meteorology. Meteorological Section; Paper 2, SNOW-TWO/Smoke Week VI Data Report. (CRREL Special Report 84-20).

Bates, R.E. (1983) Chapter 2: Site-Specific and Synoptic Meteorology, SNOW-ONE-B Data Report. CRREL Special Report 83-16, June 1983.

Bates, R.E. (1982) The Northeast Snowstorm of 15-16 December 1981. Presented at Snow symposium II, Vol. 1, published March 1983. CRREL Special Report 83-4.

Bates, R.E. (1982) Meteorological Measurements, Snow-One at Camp Ethan Allen Training Center, VT. Snow Symposium 1, published by USACRREL, July 1982.

Bates, R.E. (1982) Section 3, Meteorology, SNOW-ONE-A Data Report. CRREL Special Report 82-6, pp. 43-180.

Bates, R.E. (1981) SNOW-ONE Preliminary Data Report, Section 3, Meteorology, pp. 24-221, CRREL Internal Report 715.

O'Brien, H.W., and Bates, R.E. (1980) Obscuration in the Cold Environment. Published in Proceedings of Smoke/Obscurants Symposium IV, 22-23 April 1980.

O'Brien, H.W. and Bates, R.E. (1982) Section 10, Snow-Cover Characterization. CRREL Special Report 82-6, pp. 554-578.

O'Brien, H.W. and Bates, R.E. (1984) Systems Operation Section Paper 4, Snow-Cover Characterization: SADARM Support SNOW/TWO/Smoke Week VI Data Report, CRREL Special Report (84-20).

Session 5:
Load Deformation
Measurements

STATE-OF-THE-ART
STRESS, STRAIN AND DEFLECTION MEASUREMENTS

P. Ullidtz, The Technical University of Denmark and
H.J. Ertman Larsen, The National Road Laboratory, Denmark

ABSTRACT

Pavements deteriorate under the combined action of loading and environmental effects, with the rate of disintegration or permanent deformation being related to the critical stresses and strains in the pavement layers. For areas with frost the highest rate of deteriorations is associated with the short periods of thaw, when the critical stresses or strains are largest.

To predict pavement performance for design or rehabilitation purposes the critical stresses or strains must be known. The paper first explains why the total pavement deflection is a poor substitute for stresses or strains and then discusses different means of determining the stresses and strains.

An indirect determination of the stresses and strains may be obtained by measuring the deflection basin under a known load, calculating the layer stiffnesses required to produce these deflections and then using the stiffnesses, adjusted for seasonal variations, to calculate the critical stresses and strains.

But how do these theoretical values compare to the actual stresses or strains in the materials? The only way to determine this is by measuring the stresses and strains. The last part of the paper

discusses some of the difficulties associated with monitoring the stresses and strains in pavement materials and some of the instruments recently developed for use in the Danish Road Testing Machine to overcome these difficulties. Some preliminary results, indicating that continuum mechanics may not work very well with granular materials, are also presented.

1. INTRODUCTION

All pavements deteriorate in time as a result of the combined action of loading and environmental effects. It is a reasonable assumption that the rate of deteriorations is related to the critical stresses or strains in the materials. For bituminous cement-bound materials the critical value may be the maximum tensile stressor strain in the layer, and for unbound materials it could be the maximum normal strain or the maximum shear stress in the layer. The strength of the materials is normally characterized by the permissible stresses or strains (normal or shear), or by relationships between damage rate and stress or strain level. For an asphalt concrete, for example, the permissible tensile strain for one million load applications could be the strain level that would result in 10% of the surface having class 2 cracking, after one million load applications.

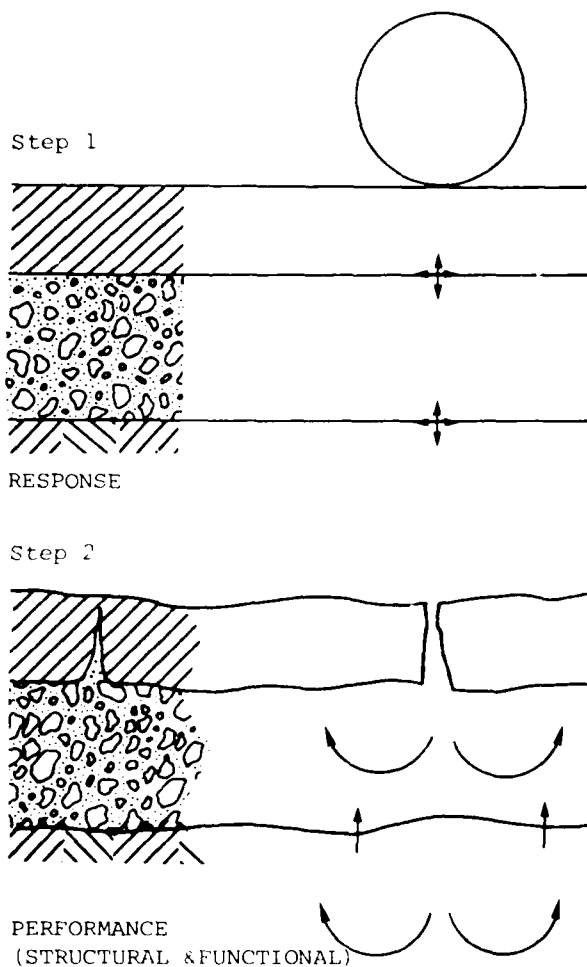


Fig. 1 Pavement response and pavement performance.

The common approach in engineering to design problems is to use a mathematical model to calculate the critical stresses or strains and then compare these to the permissible values (or, more recently, to calculate the increase in damage). This approach is also gaining a more widespread acceptance for pavement design purposes, under the label of "analytical-empirical" or "mechanistic-empirical" method, because it has some very important advantages over the purely empirical methods that have been commonly used for pavement design. A very important advantage is that the analytical part of the method is valid under any conditions of climate, loading, materials, etc., whereas empirical relationships can only be used under the conditions for which they were established. The two steps in the analytical-empirical method are illustrated in fig. 1 (P. Ullidtz, 1987).

1.1 Response and Performance

In step 1) a mathematical model is used to calculate the critical response. In most design procedures the horizontal, normal strain or stress at the bottom of bound materials, and the vertical, normal strain or stress at the top of the unbound materials, are considered to be critical. Some procedures use shear stress and some consider stresses or strains at other positions, caused by particular combinations of load and climatic effects.

The selection of critical stress or strain should, of course, be closely related to the type of pavement deterioration considered in step 2); in other words it should be a function of how the pavement performance is defined. Most design procedures use empirical relationships, 1) between cracking of the bound materials and the maximum tensile stress or strain in the layer, and 2) between permanent deformation (roughness or rutting) and the maximum compressive stress or strain in the unbound materials. To sum the damage caused by different combinations of load and climatic conditions Miner's law is normally used.

More sophisticated models like VESYS (Kenis, 1977) and MMOPP (P. Ullidtz, 1979) calculate the increase in damage and permanent deformation of the materials caused by the combined effects of loads, climate, the condition of the pavement, and of the materials.

1.2 Influence of Climate

Variations in climate affect the critical stresses or strains as well as the permissible values. The AASHO Road Test very clearly demonstrated the enormous effect of the spring thaw. Fig. 2 shows a typical performance of the flexible pavement study (duplicate sections). In the two periods of spring thaw there is a very sharp decrease in PSR. Superimposed on the test results are some simulations carried out with MMOPP. The simulations show a performance similar to the observed performance with respect to the importance of spring thaw.

Loop 6 5" AC + 6" Base + 12" Subbase
30 kips single

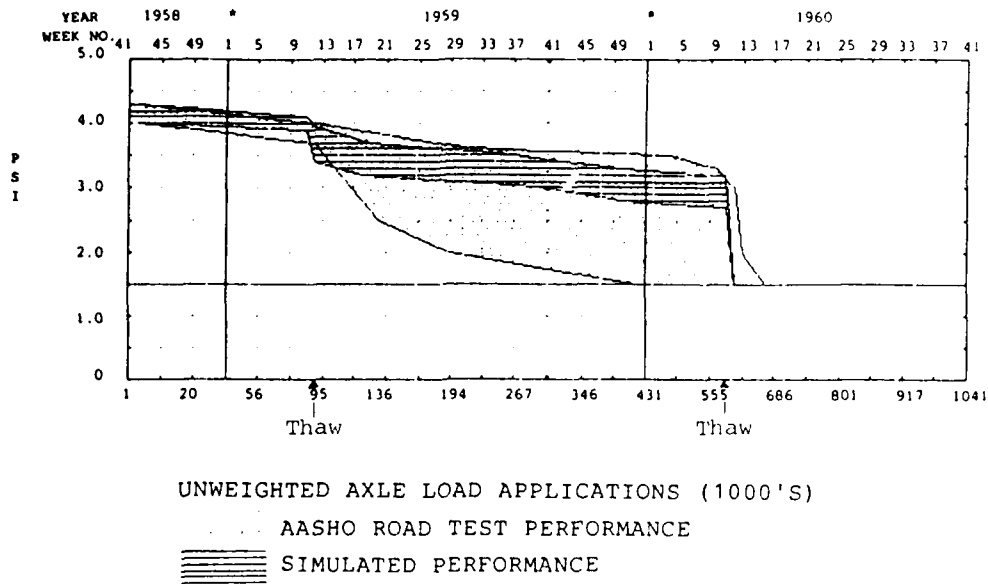


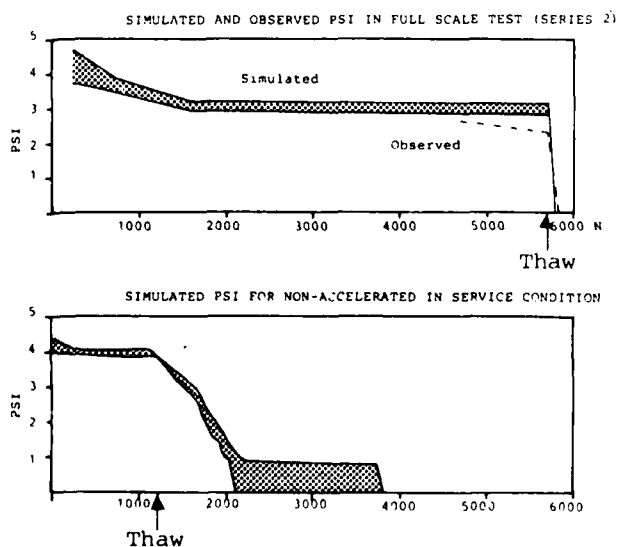
Fig. 2 AASHO Road Test example of spring thaw influence on performance.

Functional deterioration

Further evidence of the importance of frost/thaw is given in fig. 3, which shows the result of a full scale pavement test, carried out in the Danish Road Testing Machine (P. Ullidtz, 1982). The pavement failed during the first period of thaw, just like a large number of the AASHO Road Test Sections. An empirical interpretation of such a test, where the pavement fails in the first spring thaw period, is not possible, because almost any number of loads could have been applied before the thaw, without any measurable damage. Only if the rate of deterioration during the thaw can be related to the critical stresses or strains in the structure, can some valuable information be gained.

Structural deterioration

The functional deterioration (increase in roughness) during the thaw periods, in the two examples above, was quite obvious. Less obvious may be the structural deterioration in bitumen or cement bound materials (microcracking) that may occur during the thaw, but which will only later show as visible cracks. Structural deterioration may be detected with the Falling Weight



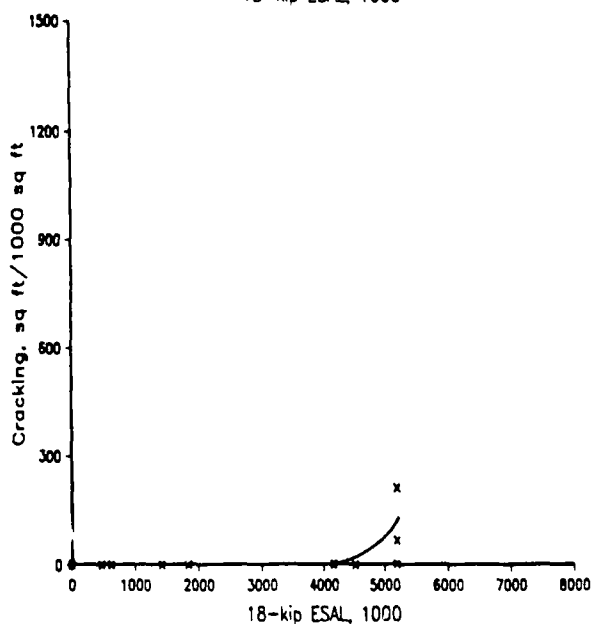
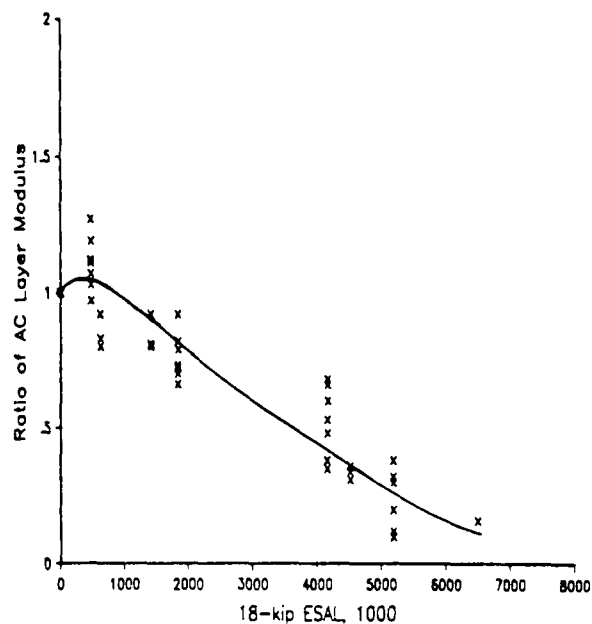


Fig. 4 Variation of ratio of AC layer modulus and AASHTO cracking as a function of 18-kip ESAL repetitions for lane 2 tests. (Sebaaly et. al., 1989).

Deflectometer (FWD). Microcracking of bound materials reduces the effective cross-sectional area, and therefore also the moduli of the material. This reduction in moduli may be calculated from FWD deflection data, provided that the deflections are measured sufficiently accurately and that a reasonably realistic mathematical model is used for the pavement structure (this is discussed further below).

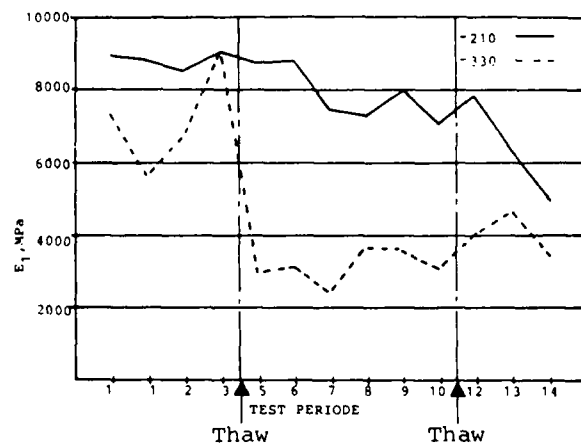


Fig. 5 Structural distress during thaw detected with the FWD.

An example of decreasing asphalt moduli, long before any cracking is observed, is given in fig. 4, from Sebaaly et al. (1989). The testing was carried out using the Federal Highway Administration (FHWA) Accelerated Loading Facility (ALF). Cracking was first observed when the moduli of the asphalt material had already dropped to about half its original value.

Another example of detecting structural damage with the FWD is shown in fig. 5 (P. Ullidtz, 1982). In this case the structural deterioration is directly related to a spring thaw period. The ordinate shows moduli at two points of a fly ash-cement-stabilized sand from the Danish Road Testing Machine (RTM). The abscissa shows the test periods. A sharp decrease in moduli occurred at one of the test points during the first spring thaw period and at the other point during the second spring thaw. It should be noted that no cracking was visible in the thin asphalt surfacing covering the stabilized material.

The FWD may be used to monitor the structural deterioration. For the more general purpose of establishing damage rate relationships (performance models), for functional as well as structural deterioration, it is necessary to measure the critical stresses or strains in the individual materials of the pavement structure.

1.3 Stresses and strains are needed

The purpose of the introduction was to demonstrate the need for determining the critical stresses or strains in pavement structures. During full scale testing or monitoring of long term pavement performance, the critical stresses or strains must be known in order to relate the performance to the strength characteristics of the individual pavement layers. For pavement design or rehabilitation the critical stresses or strains are needed in order to predict the performance.

The purpose was also to emphasize the importance of short, critical periods like the spring thaw. Short periods of extremely high temperatures may be equally critical. During such periods the stresses or strains must be monitored almost continuously, if they are to be related to the performance.

In the last part of the paper two methods of determining the stresses and strains will be discussed. The first is an indirect method, where the stresses or strains are calculated from the known layer stiffnesses, and the second is by direct measurement. The reason for presenting the "indirect" method before the "direct" method is that the "indirect" method is by far the most widely used. Much less effort has been devoted to direct measurement of stresses or strains. By choosing this order of presentation, the authors also hope to better illustrate the need for direct measurements, in order to verify the mathematical models used.

Before describing the different means of obtaining stresses and strains, however, the widespread use of deflections, as a substitute for stresses or strains, will be discussed.

2. WHY DEFLECTIONS SHOULD NOT BE USED DIRECTLY

When using one of the many methods for designing or evaluating pavements, by making use of a mathematical model to calculate the stresses or strains, it is necessary to determine the elastic (resilient) moduli of the pavement materials, in the laboratory or in situ, and then calculate the stresses or strains for the most important combinations of load and climate.

The procedure thus requires some measurements and a certain amount of calculation. If based on in situ measurements of deflection, it would be a little easier if the deflections could be used directly, rather than the stresses and strains. Deflection is a measure of the pavement response, as are stresses and strains, it may be tempting to assume that there is a good correlation between the different types of response (deflections versus stresses or strains). This, however, is not the case.

The difference between deflection on one side and stresses or strains on the other is quite evident already from Boussinesq's equations. Whereas deflections are inversely proportional to the depth beneath the surface, stresses and strains are inversely proportional to the square of the depth. How this affects the "correlation" between deflection and stress or strain may be illustrated by a simplified example:

Consider two pavements on different subgrades, as illustrated in fig. 6, that have deflections of d_1 and d_2 and strains at the top of the subgrade of e_1 and e_2 , under a given load. If the compression of the pavement layer is neglected (being small compared to the compression of the subgrade), then the deflections may be estimated from Boussinesq's equation:

$$d_1 = (1+\mu)(3-2\mu)P/(2\pi)/z_1/E_1, \text{ and} \quad (1)$$

$$d_2 = (1+\mu)(3-2\mu)P/(2\pi)/z_2/E_2 \quad (2)$$

where μ is Poisson's ratio

P is the load

z is the effective or equivalent depth to the subgrade, and

E is the moduli of the subgrade.

If the deflections were the same on the two pavements, i.e. $d_1 = d_2$, it follows that:

$$z_2 = (E_1/E_2)*z_1 \quad (3)$$

The strains at the top of the subgrade may be found from Boussinesq's equation:

$$e_1 = (1+\mu)(3-2\mu)P/(2\pi)/z_1^2/E_1, \text{ and} \quad (4)$$

$$e_2 = (1+\mu)(3-2\mu)P/(2\pi)/z_2^2/E_2 \quad (5)$$

Substituting (3) in (5) leads to:

$$e_2 = (E_2/E_1)*e_1 \quad (6)$$

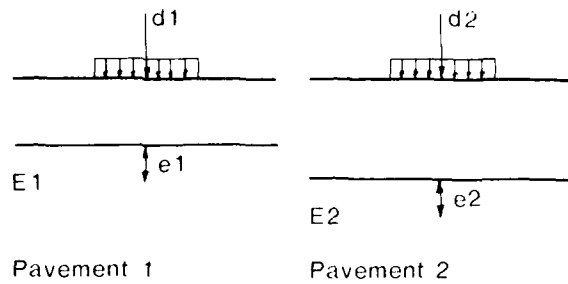


Fig. 6 Pavements with identical deflections may have different strains.

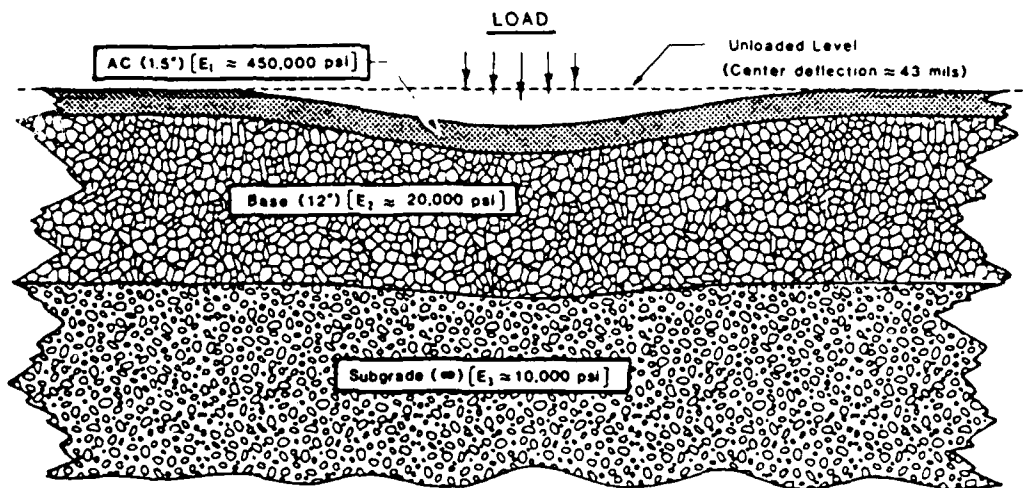


Fig. 7A Schematic representation of an unfrozen asphalt surfaced pavement under a 9000 lb load.

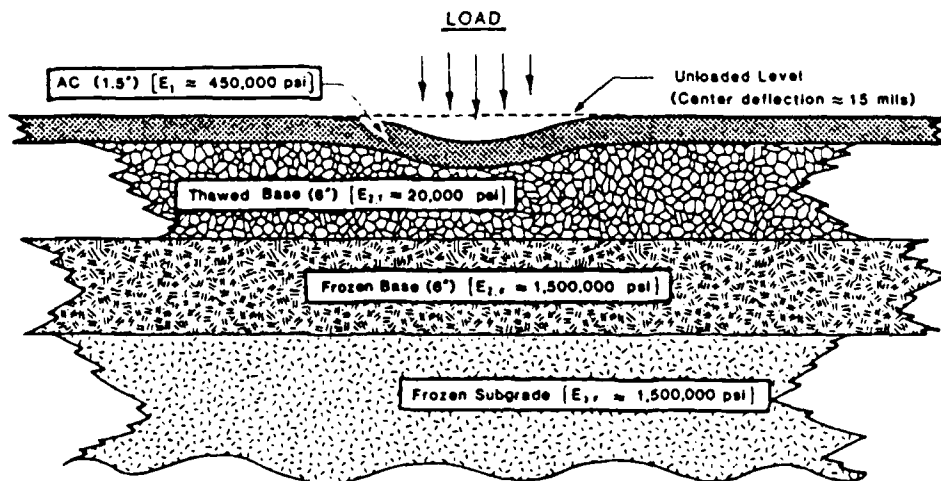


Fig. 7B Schematic representation of a partially frozen asphalt surfaced pavement under a 9000 lb load.

If $E_2 = 0.5 \cdot E_1$ then the subgrade strain in the second pavement will only be half of the strain value in the first pavement, even though the deflections were identical. If the 4th power law can be applied, this means that although the deflections indicate that the two pavements have the same bearing capacity, the second pavement will last 16 times longer than the first (with respect to traffic loading).

Another example, with particular reference to areas with frost, was given by Stubstad & Connor (1983).

The pavement shown in fig. 7A is unfrozen and in fig. 7B the same pavement section is shown but in a partially frozen state, after thaw has progressed 6" (150 mm) below the asphalt layer. The deflection of pavement 7A is three (3) times the deflection of pavement 7B, but nevertheless the horizontal strain at the bottom of the asphalt and the vertical strain at the top of the base are approximately equal.

These examples illustrate that it is necessary to make a little extra effort and calculate the stresses or strains, rather than just using the deflections. With the proliferation of micro computers this ought no longer be a problem.

3. INDIRECT DETERMINATION OF STRESSES AND STRAINS

Almost all presently used methods for calculating the stresses and strains in pavement structures are based on some version of elastic layer theory. In most cases all materials are assumed to be simple solid continua, homogeneous, isotropic, and linear elastic. Stresses and strains can then be determined if Young's moduli and Poisson's ratio are known for all materials. Some methods also permit anisotropic or non-linear elastic materials, requiring knowledge of some additional material characteristics.

Determining the elastic parameters from laboratory testing is extremely difficult because of the problems involved in reproducing the in situ conditions of the materials and getting the proper loading conditions. On existing pavement

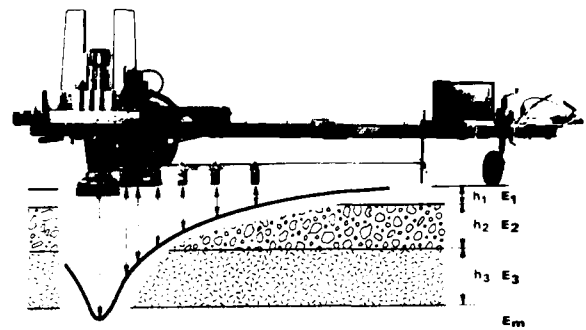


Fig. 8 Deflection basin under FWD (Ertman & Stubstad, 1982).

structures non-destructive, in situ testing is much to be preferred, bearing in mind that only pavement characteristics that have a significant influence on the surface response may be deduced.

For many years wave propagation methods have been used in an attempt to determine the elastic parameters of the pavement layers (the wave velocity being a function of these parameters). The main problem in using this method is that most pavement materials are non-linear elastic.

The stresses induced in the pavement materials during a wave propagation test are very small compared to the stresses under heavy traffic. The moduli derived from the wave velocities may, therefore, be very different from the moduli corresponding to design conditions.

Deflection testing has also been used for a long time to determine the structural condition of pavement systems. The deflections are measured at various distances from the load, and the layer moduli are then selected such that the theoretical deflection basin matches the measure basin, as illustrated in fig. 8 (H.J. Ertman & Stubstad, 1982).

In order to back-calculate the elastic parameters from the surface deflections, two conditions must be met. One is that the stresses in the structure must be close to the stresses caused by the design load, and the other that the deflections must be measured with a very high degree of accuracy, particularly at some distance from the load.

The need for the right stress level results, again, from the non-linearity of the materials. The need for very accurate deflection measurements is due to the large influence of the subgrade on the deflected shape. The subgrade moduli is determined from the deflections at some distance from the load, and these deflections are often very small, they may be as low as 20-30 μm (1 mil). Even a small error in the determination of the subgrade moduli will result in quite large errors in the determination of the layer moduli, because the layers above the subgrade only contribute some 20-30 % of the overall deflection, even at the centerline of the load. For the same reason any non-linearity of the subgrade or a rigid layer at shallow depth must also be considered in calculating the moduli.

With the FWD it is quite easy to use the indirect method to determine the stresses and strains and to monitor the effects of climatic conditions, number of load passages, ageing, etc. on the moduli as well as on the stresses and strains in the materials. But how close are these calculated stresses and strains to the actual stresses or strains in the materials? This, of course, is highly dependent upon how well the mathematical model of the pavement structure represents the actual characteristics of the materials and structure. With pavement materials tending to be non-continuous (particulate), non-homogeneous, anisotropic, viscous, plastic, visco-elastic, as well as highly variable in space and time, some doubt may be understandable.

4. DIRECT MEASUREMENT OF STRESSES AND STRAINS

The only way to find out how well a certain mathematical model predicts the stresses and strains is by comparing predicted values to measured values. When making such a comparison it is important that several types of pavement response (stress, strain, deflection) are compared, otherwise good agreement can always be obtained by selecting the appropriate elastic parameters.

Unfortunately, measuring stresses and strains in pavement structures is very difficult. Two major problems are 1) the calibration of the gauges, and 2) the durability of the gauges.

Rather than trying to cover the development of soil and pavement gauges - an impossible task anyway - the authors have selected to present some examples of instruments that have been used with the Danish Road Testing Machine (RTM), and of the attempts to overcome some of the difficulties encountered.

4.1 Soil pressure cells

Probably the most frequently used gauge for measuring dynamic soil stresses is the diaphragm cell. An example of a pressure cell used in some of the early experiments in the Danish RTM is shown in fig. 9. The principle of these transducers is that a pressure acting on the thin diaphragm of the cell will cause a deflection that can be transformed into an electrical signal by strain gauges cemented to the inside of the diaphragm (or a small LVDT (Linear Variable Differential Transformer) in some cases).

The cell in Fig. 9 was calibrated under hydrostatic pressure, but the signal produced by the cell, when it is embedded in a soil, is not necessarily identical to the signal it would produce under the corresponding hydrostatic pressure. The stiffness of the cell will be different from the stiffness of the surrounding soil, and this will change the stress field in the soil. This is very clearly illustrated in Fig. 10 (C. Busch & P. Ullidtz, 1978).

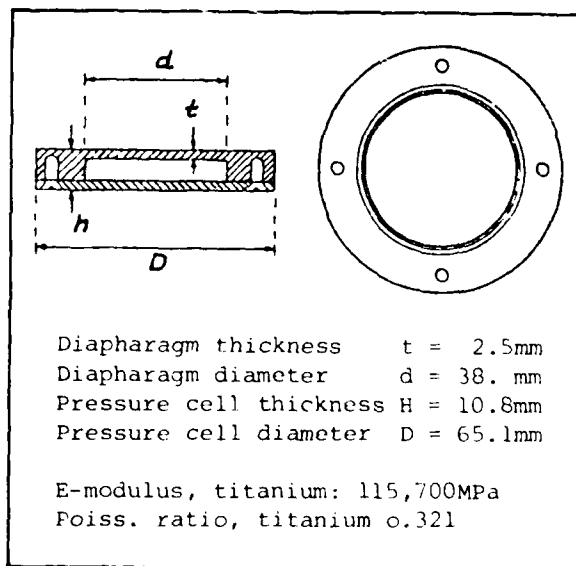


Fig. 9 Diaphragm soil pressure cell used in the early experiments in the Danish Road Testing Machine.

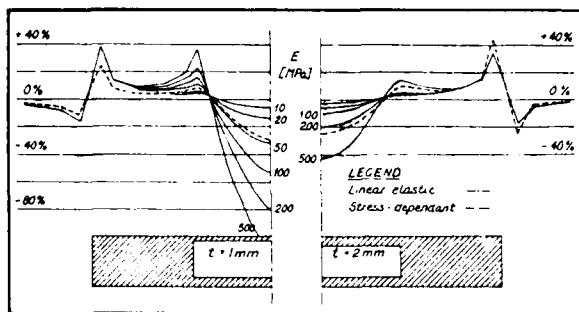


Fig. 10 Excess pressure on cel diaphragm for different soil modules.

The excess pressure in the plane of the cell diaphragm was calculated using a finite element program. The figure shows the excess pressure for different soil moduli and for two different cells. It can be seen that decreasing the soil moduli or increasing the diaphragm thickness "improves" the pressure distribution, confirming earlier results (Tory & Sparrow, 1966).

To overcome this calibration problem a new cell was developed. This cell has a double membrane, where the cavity between the membranes is filled with oil. The components of the cell are shown schematically in fig.11. The geometry of the cell has been improved by tapering the edges, to reduce the cross sensitivity and the stress concentrations at the edges, and the smooth surface has been abolished in favour of a rough surface, to ensure a better contact with the soil. This new gauge shows the same stress response when calibrated under hydrostatic pressure and in different soils.

Installation of the gauge is also likely to disturb the soil and thus the stress field. One technique which has proven successful has been to place a dummy gauge during compaction, and then replace it with the real gauge after compaction. Calibration of the gauges after installation, using an FWD fitted with a special hydraulic loading pad, has confirmed the calibration under hydrostatic pressure.

Even if the cells can be properly installed and calibrated the problems are not over. The environment of the cell is a very harsh one, and ensuring the durability of the cell is quite difficult.

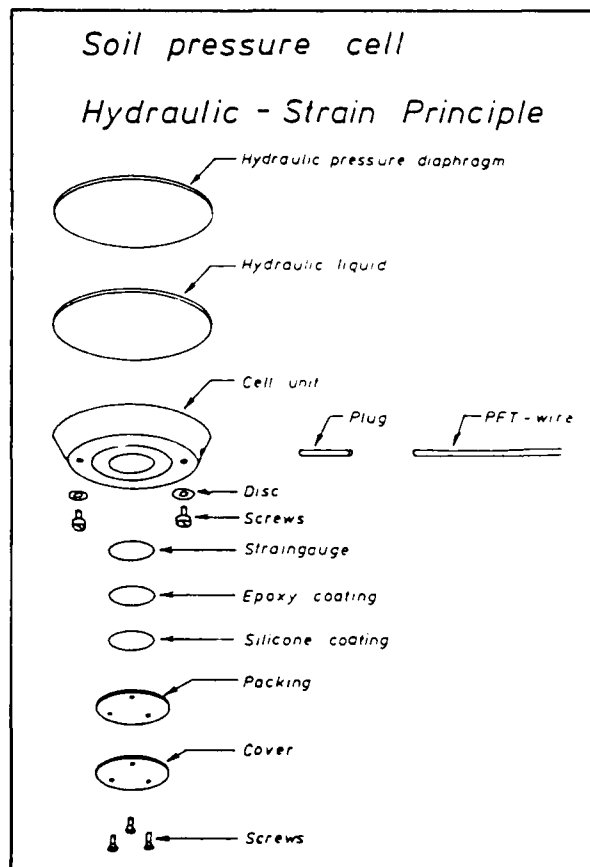


Fig. 11 Improved pressure gauge developed for the Danish RTM.

Early attempts at using gauges made of aluminum or brass were not successful, whereas titanium was found to be excellent. Still great care has to be taken to protect the electronics of the gauge against moisture. Some of the precautions taken are indicated in fig. 11.

4.2 Strain cells in unbound materials

Strains in unbound materials are mostly determined indirectly by measuring the differential displacement between two points (installing single wire strain gauges in granular materials is tricky though not impossible).

The differential deflection is normally measured by an LVDT or by measuring the changes in the mutual induction of two coils. An important advantage of the latter system is that the coils are not mechanically connected. A disadvantage is that moving metallic masses also induce a signal in the coils.

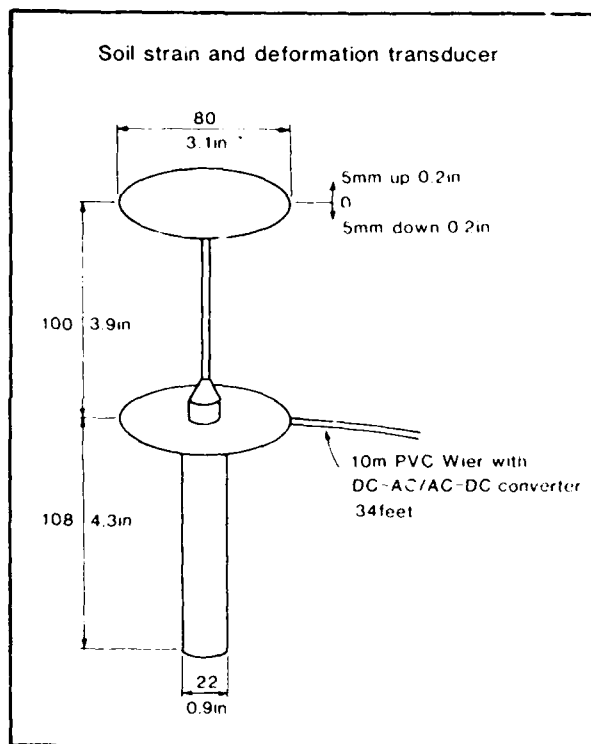


Fig. 12 Soil strain transducer.

GROUP	SCHEMATIC CONSTRUCTION	ASSEMBLY
1.1		FIXATION OF ANCHOR BARS IN THE LABORATORY
1.2		GAUGE USED TO SUPPORT AND FIXATION OF ANCHOR BARS IN THE LABORATORY
1.3		
2.1		FIXED ON MARSHALL SPECIMEN CUT TO 1/2 HEIGHT FIXED ON LABORATORY SPECIMEN
2.2		FIXED IN THE CENTER OF A LABORATORY SPECIMEN
2.3		FIXED IN A BLOCK OF SHEET ASPHALT
2.4		FIXED ON CORE TAKEN FROM THE PAVEMENT

Fig. 13 Asphalt straingauges employed at the international OECD experiment in Nardó.

In one experiment in the RTM the signal induced by the wheel trolley was found to be much larger than that caused by the strain. This effect of the trolley made the use of coil gauges impossible.

The strain cell presently used in the RTM is based on an LVDT, placed below the lower reference plate, as indicated in fig. 12. The cell may be used to measure resilient as well as permanent deformations. A procedure has been developed for installing the gauge with very little disturbance to the soil between the reference plates. The cell is made of stainless steel and is coated with epoxy to ensure good durability.

4.3 Strain gauges in bound materials

At the OECD International Experiment at Nardó (OECD, 1985) many different types of gauges for measuring strain in asphalt were tested. The gauge types are shown schematically in fig. 13. The strain gauge used in the RTM is based on the type 1.1 gauge in Fig. 13, but has been considerably improved with respect to durability.

When gauges are installed in the asphalt during construction they will be subjected to very high temperatures and to large mechanical impacts during compaction of the asphalt. After installation the major problem is damage caused by moisture, but the gauges may also suffer from fatigue before the asphalt does. In previous experiments in the RTM, where Kyowa type gauges have been used, none of the asphalt strain gauges have lasted for all of the experiment.

For this reason a new gauge was developed for the present experiment in the RTM. Some of the most important layers of this gauge are shown in fig. 14. The total number of layers in a cross section is 27. The gauge has been tested for more than two years in moist conditions in an asphalt specimen, and has been subjected to more than one million large strain repetitions and to several freeze/thaw cycles, without any damage to the gauge.

5. RESULTS FROM THE DANISH RTM

During autumn 1988 a new pavement was constructed and instrumented in the Danish RTM. The pavement is a traditional structure for light traffic, with 64 mm asphalt concrete, 130 mm basecourse gravel, and 390 mm subbase gravel on a moraine sand. 16 soil pressure cells, 16 soil strain transducers, and 12 asphalt strain gauges were installed as indicated in fig. 15. Two soil strain transducers in the subgrade were lost, probably because the cables were damaged during compaction control. In addition temperature gauges, soil suction gauges, tubes for nuclear density measurements, and water level gauges were installed.

The main purpose of the test is an attempt at quantifying the effect of water in the unbound materials. Loading tests will be carried out at different ground water levels, with simulated precipitation and (if time allows) with freeze/thaw cycles.

During construction of the pavement FWD testing was carried out on each layer, in addition to the standard quality testing. The FWD tests were done at 300 mm intervals (or closer) and the stresses and strains in the materials were measured simultaneously. The results of the last two test series, i.e. on top of the basecourse and on top of the asphalt, are discussed here.

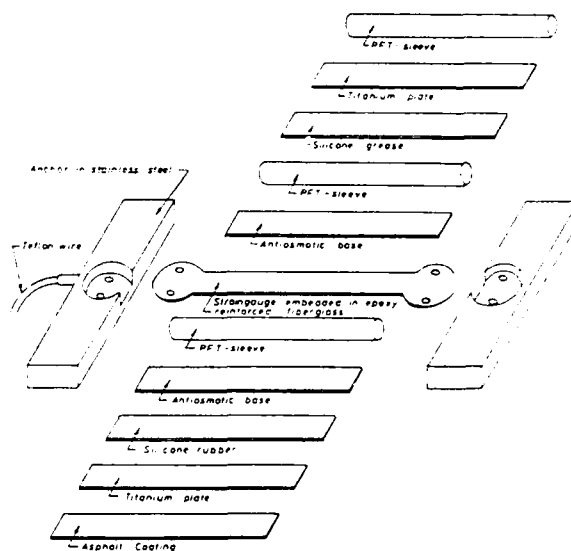


Fig. 14 High durability asphalt strain gauge.

Both stresses and strains showed standard deviations between 7% and 19% of the mean values (except for the subgrade strain where only two transducers were active). Variations of this magnitude are to be expected due to the variation in materials and in layer thicknesses.

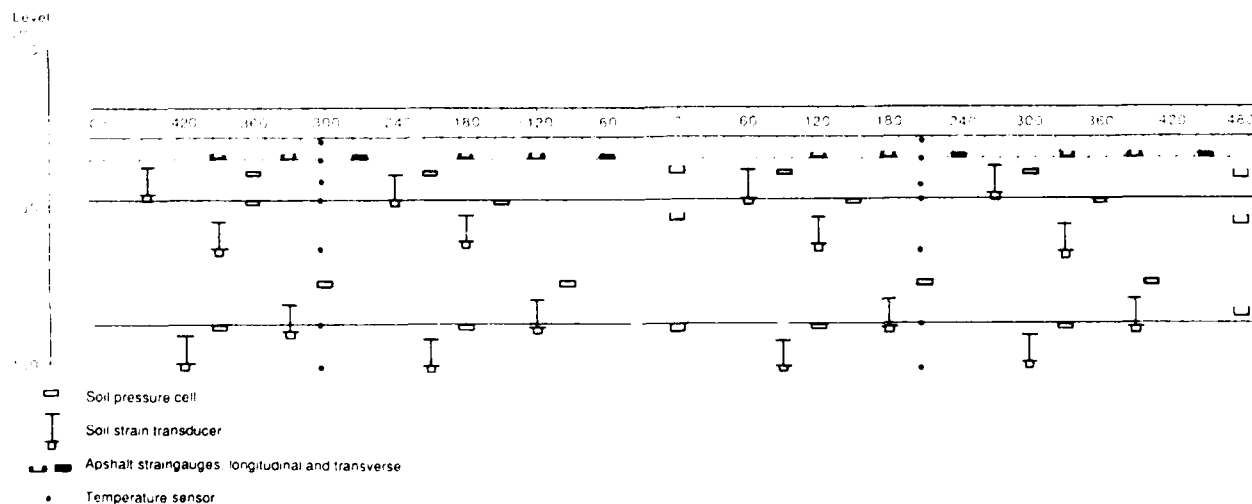


Fig. 15 Instrumentation of test pavement.

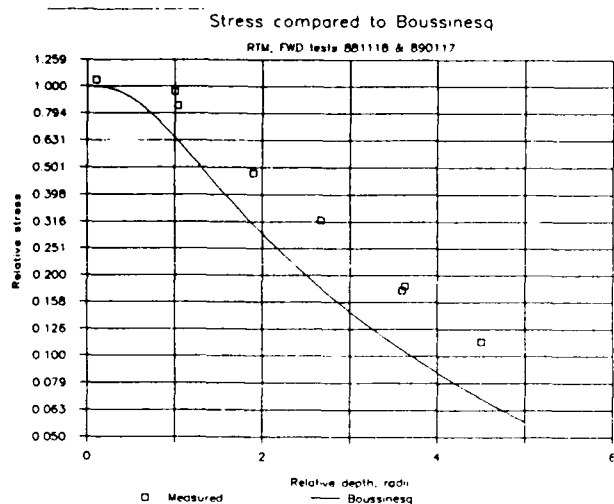


Fig. 16 Measured stress compared to Boussinesq's equation.

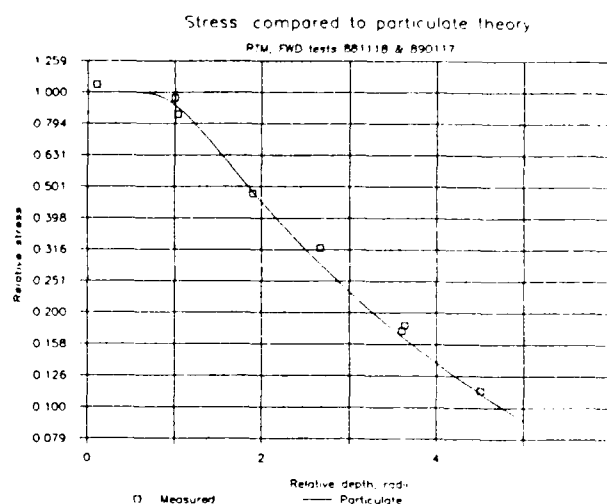


Fig. 18 Measured stress compared to particulate theory.

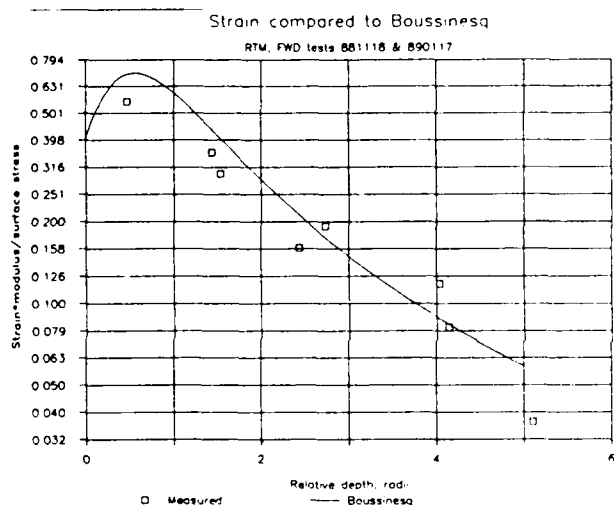


Fig. 17 Measured strain compared to Boussinesq's equation.

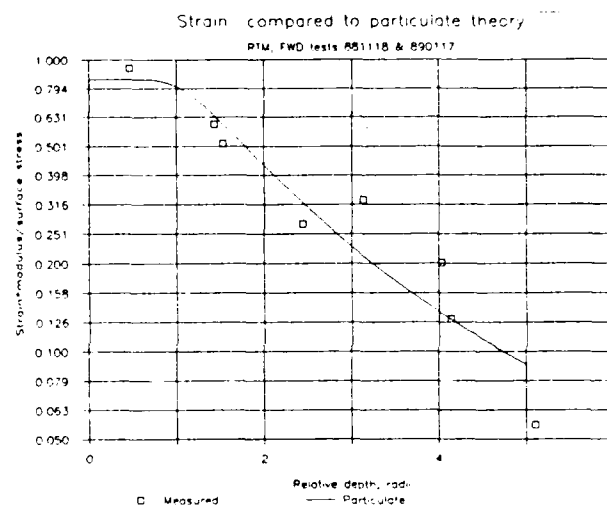


Fig. 19 Measured strain compared to particulate theory.

From the surface deflections during FWD testing the moduli of the layers were calculated using the ELMOD program (Dynatest, 1986). The moduli of the unbound materials (base, subbase and subgrade) were found to be almost identical, whether calculated from FWD tests on the base or on the asphalt. ELMOD indicated a depth to a rigid layer of 1570 mm (standard deviation 98 mm), quite close to the actual depth to the bottom of the concrete pit which is 1710 mm.

The layer moduli were then used with ELSYM 5 and, for some values, with ELMOD to calculate the stresses and strains,

and comparing these to the measured values. A Poisson's ratio of 0.35 was assumed for all materials. In the table below are given the ratio of calculated/measured values (c/m) for the FWD tests on top of the asphalt layer. If the agreement between calculated and measured value is perfect $c/m = 1$.

	ELSYM 5		ELMOD	
	Stress	Strain	Stress	Strain
Strain	c/m	c/m	c/m	c/m
Asphalt, long.	-	0.85	-	0.90
Basecourse	0.76	1.31	0.84	-
Subbase, top	0.61	1.28	0.70	-
Subbase, bottom	0.46	0.75	-	-
Subgrade	0.48	1.24	0.53	-

The most remarkable aspect of this comparison is that the calculated stresses are considerably below the measured values, particularly at large depths where the calculated stresses are only half of the measured values.

Better agreement is obtained if a simple combination of Odemark's method with Boussinesq's equations is used instead of elastic layer theory. In this simple combination only the thickness of the asphalt layer is transformed, based on the ratio of stiffness between asphalt and basecourse. Stresses and strains calculated using this method are compared to values measured during FWD tests on asphalt and on base course, in fig. 16 and 17. In this case the calculated stresses at the bottom of the subbase and at the top of the subgrade are approximately two thirds of the measured values.

If Boussinesq's equations are substituted by the equations for probabilistic stress distribution (Harr, 1977), with a coefficient of lateral stress of 0.21, the comparisons shown in fig. 18 and 19 are obtained. It should be noticed, however, that the coefficient of lateral stress was not determined experimentally, but was assumed. Experimental determination of the coefficient of lateral stress is very difficult. Unlike the other theoretical approaches, the probabilistic stress distribution does not assume that the materials are simple continua, but on the contrary that they are particulate. Here the agreement between measured and calculated stresses is almost perfect. For deflections and strains the agreement (or lack of agreement) is similar to the Boussinesq case.

6. CONCLUSION

In order to develop a fundamental understanding of how pavements deteriorate under the combined actions of loading and climatic effects, methods for determining the critical stresses and strains in the pavement materials must be available.

Instrumenting pavements with stress and strain cells is costly, and on existing structures it cannot be done without interference in the materials. In most cases the stresses and strains must, therefore, be determined by some indirect method, where 1) the surface deflections are measured under a known load, 2) a mathematical model is used to calculate the stiffnesses of the layers, and 3) the same mathematical model is used to calculate the stresses and/or strains from the stiffnesses.

But verification of the mathematical model must be done against actually measured stresses, strains, and deflections. Surface deflections can be measured accurately, but stresses and strains in the materials are difficult to measure. Several new gauges were recently installed in the Danish Road Testing Machine (RTM). These gauges, which are the result of twenty years development, are believed to be reliable. For the pressure cells this has been demonstrated through in situ calibration.

Results obtained from Falling Weight Deflectometer (FWD) tests during construction of the new pavement in the Danish RTM, have provided a strong indication that mathematical models assuming granular materials to be simple continua, do not satisfactorily predict the stress distribution in the materials. Calculated stresses may be less than half the measured values.

A good agreement between measured and calculated response may be obtained assuming probabilistic stress distribution in the granular materials. This, however, introduces one more parameter, the coefficient of lateral stress, which is very difficult to determine experimentally.

This result may not seriously affect the existing analytical - empirical (or mechanistic - empirical) methods of pavement evaluation. The empirical relationships used in these methods were derived using elastic layer theory, and the same theory must therefore be used to calculate the critical response. In addition to this, the inaccuracy in stress prediction is to some extent balanced out by a reverse inaccuracy in moduli.

From a more fundamental point of view, however, it is not satisfactory if the pavement response predicted by the mathematical model does not agree reasonably well with measured values (if the measured values are reliable). In the near future a number of full scale tests, Long Term Pavement Performance (LTPP) data etc. are to be interpreted, in order to develop performance models. Before investing too much effort in this, it would be desirable if more reliable response models could be established.

ACKNOWLEDGEMENT

The full scale experiments in the Danish Road Testing Machine are carried out in cooperation between the National Road Laboratory, the Danish Road Directorate, and the Institute of Roads, Traffic and Town Planning, the Technical University of Denmark, and are financially supported by the Danish Science Foundation.

REFERENCES

- Busch, C. & Ullidtz, P. "Laboratory Testing of a Full Scale Pavement", Report No. 19, The Institute of Roads, Traffic and Town Planning, The Technical University of Denmark, 1978.
- Dynatest "ELMOD - Users Manual", Dynatest Engineering A/S, 1986.
- Ertman Larsen, H.J. & Stubstad, R.N. "The Use of Non Destructive Testing in Flexible Pavement Rehabilitation Design", International Symposium on Bearing Capacity of Roads and Airfields, Trondheim 1982.
- Harr, M.E. "Mechanics of Particulate Media", McGraw-Hill International Book Company, 1977.
- Kenis, W.J. "Predicted Design Procedures- A Design Method for Flexible Pavements Using the VESYS Structural Subsystem", Fourth International Conference on the Structural Design of Asphalt Pavements. Ann Arbor 1977.
- OECD, "Strain Measurements in Bituminous Layers", Report prepared by the OECD/I4 Scientific Expert Group, OECD Transport Research, Swiss Federal Office of Highways, Berne 1985.
- Stubstad, R.N. & Connor, B. "Setting Highway Load Limits: A New Technique", The Northern Engineer, Vol. 15, No. 1, 1983.
- Tory, C. & Sparrow, R.W. "Behaviour of a Soil Mass under Dynamic Loading", Journal of the Soil Mechanics and Foundation Division, Proceedings of the American Society of Civil Engineers, 1966.
- Ullidtz, P. "A Fundamental Method for Prediction of Roughness, Rutting and Cracking of Pavements", Proceedings, Association of Asphalt Paving Technologists, Vol. 48, 1979.
- Ullidtz, P. "Predicting Pavement Response and Performance from Full Scale Testing", International Colloquium Full Scale Pavement Tests, Institut for Strassen-, Eisenbahn- und Felsbau, Eidgenössische Technische Hochschule, Zürich, Mitteilung 50, Zürich 1982.
- Ullidtz, P. "Pavement Analysis", Developments in Civil Engineering, 19, Elsevier 1987.

IN SITU STRESS MEASUREMENTS

by

Ernest T. Selig, Professor of Civil Engineering
University of Massachusetts
Amherst, MA 01003

ABSTRACT

Paper summarizes the considerations involved in measuring soil stresses within earth masses and at layer interfaces, as related to pavement systems. Presentation begins with measurement locations and reasons for interest in stress. Basic types of gages are described. Soil-gage interaction concepts are explained to illustrate the complications in stress measurement. Methods of gage installation and calibration are described. Indications are given of accuracy and precision in stress measurement. Finally considerations in gage selection are listed and recommended action given. Soil stress measurement is shown to be a challenging task with considerable uncertainty. Satisfactory results require suitable hardware, proper calibration and careful installation with replication of gages for each condition. This effort is justified when important reasons for knowing stress exist and when reasonable estimates can not be made by analytical means.

INTRODUCTION

This paper provides a review of in situ stress measurements using embedded gages. The emphasis is on applications to pavement systems. Only total stress will be considered. To obtain effective stress it is also necessary to determine pore water pressure. Techniques for pore pressure measurement are available,

but these are quite different than used for total stress (Ref. 1), and hence are beyond the scope of this paper. Also only normal stress will be considered. While measurement of shear stress is of interest, there is relatively little experience with this, and suitable gages generally are not available.

In situ total normal stress is inherently one of the most difficult parameters to measure accurately. This is so because the presence of the gage alters the soil stresses that would exist if the gage were not present. This compliance problem occurs because the gage has stiffness properties different from those of the soil, and the stress sensed by the gage is a function of the soil-gage interaction. This problem is further complicated by the alteration in soil conditions around the gage (embedment zone) associated with gage installation. Thus in situ stress measurements always have considerable uncertainty associated with them.

This paper will first consider the stress locations of interest in pavement systems. Basic types of gages will be described. Soil-gage interaction concepts are presented, followed by comments on installation and calibration. Then indications of accuracy and precision of in situ stress measurement are given. Finally factors to be considered in gage selection are summarized.

MEASUREMENT LOCATIONS

Potential locations of interest for stress measurement in a pavement system are shown in Fig. 1. The two general categories are: 1) at layer interfaces, and 2) within the layer masses. The second category has three subcategories: a) pavement material, b) compacted soil, and c) natural or undisturbed soil. Considering the compliance problem and placement effects, the order of increasing stress measurement uncertainty is probably as follows (1 least, 7 most):

Gage Location	Number
1. Pavement interface- σ_v	4,5
2. Soil layer interface- σ_v	10,11,15
3. Compacted soil- σ_v	8,13
4. Subgrade soil- σ_h	9,12,14,16
5. Granular base- σ_h	6,7
6. Pavement- σ_h, σ_v	1,2,3
7. Natural subgrade- σ_v	17

However details of specific situations could change this ranking.

In general applications, horizontal stress measurement is more uncertain than vertical; measurement in coarse-grained soils is more uncertain than in fine-grained soils; measurement of normal stress at interfaces is more certain than measurements within soil masses; stress measurements in the pavement are more difficult than in soil; the most reliable measurement is at the pavement-soil interface assuming that the gage sensing area can be large enough in relation to the soil particle size; and the most uncertain measurement is vertical stress in undisturbed soils away from the surface.

Within pavement (rigid or flexible) strains normally would be a more appropriate measurement than stress; thus stress gages would probably not be needed for locations 1-3. Locations 4 and 5 (preferably 4) would be useful for determining the extent of surface pressure reduction through the pavement. Locations 8, 10, 11, 13 and 15 would be used to determine vertical stress attenuation as a means of checking layer theory calculations. Deflection and/or strain measurements might be a preferred approach for this purpose, however. Little information is available on horizontal stresses in base and subgrade

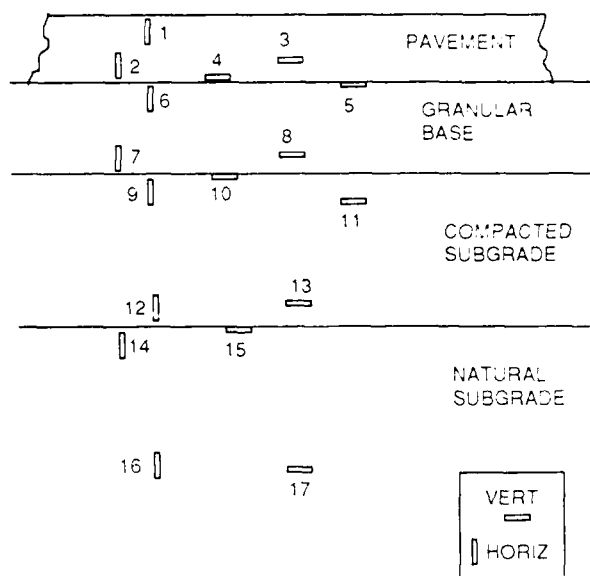


Fig. 1 Stress Measurement Locations

layers. Such measurements, particularly in the granular base, are needed to improve analytical models for predicting pavement performance. An example of the important role of these stresses in controlling permanent deformation is given in Ref. 2. Measurements deeper in the subgrade (locations 16 and 17) are probably not needed if the surface load induced stresses at these locations are small, because the geostatic stresses from the weight of pavement and compacted soil layers most likely can be estimated accurately enough.

TYPE OF GAGES

The soil stress gages, often called earth pressure cells, consist of a pressure sensor with a transducer to convert the pressure into a measurable signal. Different type of stress gages have been developed over the last 5 decades. Summaries of many of these are given in Refs. 3, 4 and 5.

The basic concepts defining the main types are illustrated in Fig. 2. All, but one, is thin in the direction of the measured normal stress compared to the transverse dimension. The one exception is a gage with the sensor housing projecting from the back of the gage body. In all cases soil pressure

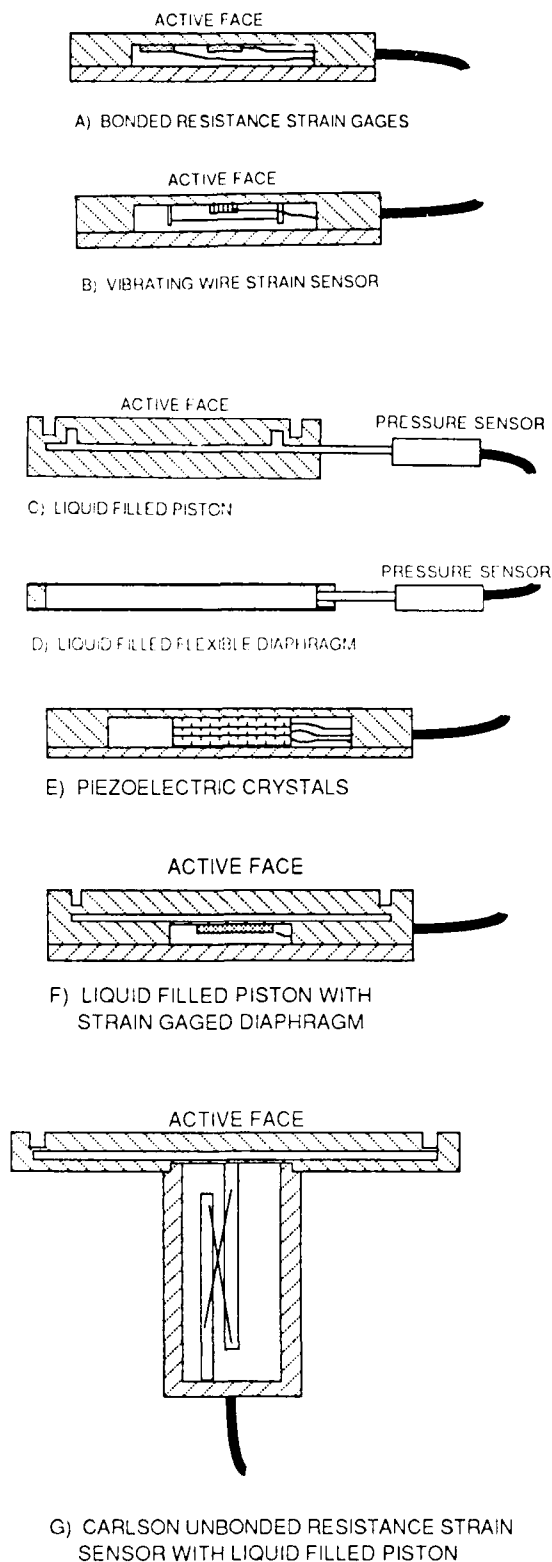


Fig. 2 Stress Gage Examples

is applied to either one or two active faces. The effect of the pressure is sensed by a variety of transducers. The proper choice depends on such considerations as overall gage size, rate of change of measured stress, data acquisition requirements, available readout equipment, and duration of use. The unbonded electrical resistance strain gage type has the longest record of reliable performance, which is an important factor to consider. However the large size and the configuration make it unsuitable for pavement applications.

The proper choice of gage type will depend on such factors as data acquisition requirements, rate of loading, stress location, gage size needed, durability and cost.

SOIL-GAGE INTERACTION

The difficulty in measuring soil stress with embedded gages can be understood by examining some basic concepts of soil-gage interaction. To do this consider the simplified case of a gage oriented to measure vertical stress in a semi-infinite soil mass (Fig. 3). Let P_0 be a uniform pressure applied to the entire soil surface. For simplicity neglect the soil unit weight so that P_0 is also the true average vertical soil stress at the gage location. Let P_m be the average normal soil pressure acting on the gage as determined from the gage output using fluid calibration. The reading error (or cell registration error) can then be expressed as:

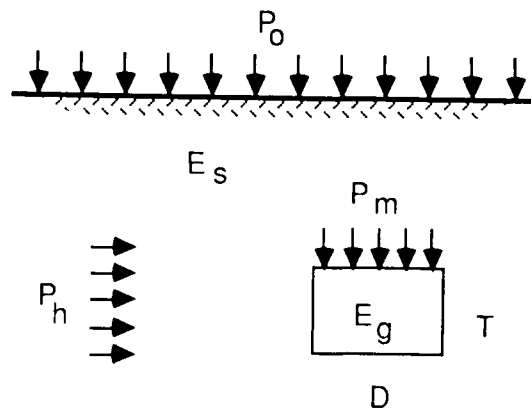


Fig. 3 Parameters for Soil-Gage Interaction

$$C_r = \frac{P_m - P_o}{P_o}$$

If $C_r = 0$ there is no error since $P_m = P_o$. A positive value of C_r means over-registration because the gage is giving too large a reading. Conversely a negative value of C_r means under-registration.

The value of C_r is a function of many factors including ratio of soil stiffness (Young's modulus) to gage compressibility (E_g/E_s), soil Poisson's ratio, ratio of gage thickness to diameter (T/D), deflection characteristics of sensing element, and ratio of soil stress transverse to the gage to the soil stress normal to the gage (P_h/P_o).

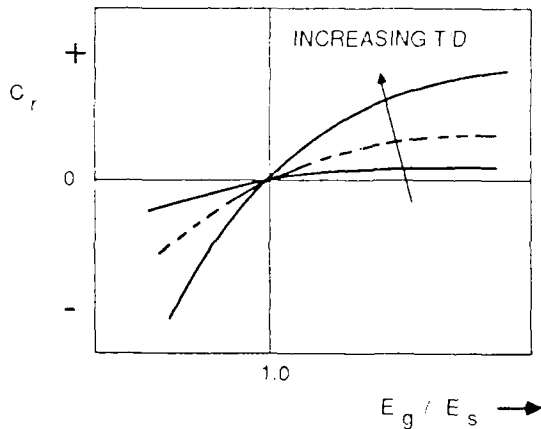


Fig. 4 Factors Affecting C_r

The effects of T/D and E_g/E_s are illustrated in Fig. 4. When E_g/E_s is unity, the error is zero, independent of T/D, but the rate of change of error with change in soil modulus is large. In fact the rate of change of error is largest for all cases in which $E_g \geq E_s$. Since the soil modulus is not constant, even if it is equal to the gage stiffness initially, this situation is not satisfactory because the calibration correction is undefinable. The best situation is to have a high gage to soil

stiffness ratio to minimize the change in error as soil stiffness changes. This permits the error to be determined by gage calibration in soil.

For any stiffness ratio, the error increases with increasing T/D ratio. Thus T/D should be as small as possible, considering such factors as the transducer requirements, fabrication limitations, and gage robustness.

It is clear from this example, that a gage optimally designed to measure the normal stress in one direction can not simultaneously measure the normal stress at 90 deg rotation, since the error in the transverse direction would then be maximized. Thus a triaxial gage in the form of a cube is unsuitable because it would have a significant error for all three orthogonal stresses.

The effect of transverse stress on the value of C_r has been illustrated by experiments and theoretical analysis (Refs. 4-6). Basically, as the ratio of P_h/P_o increases from a value less than 1.0 to a value greater than 1.0, the value of C_r decreases from a positive value to a negative value (i.e. from over-registration to under-registration). The magnitude of this trend is significantly influenced by the soil Poisson's ratio.

The soil stress distribution around embedded gages is illustrated in Fig. 5 for varying E_g/E_s and T/D ratios. Stress concentrations at the edges of the gage result in a non uniform soil pressure across the face of the gage. This distribution is a function of the mode of sensing element deflection. Thus, for example, a flexible diaphragm gage as a whole might have over-registration, but the sensing element might indicate under-registration because of pressure reduction in the center.

The soil-gage interaction effects for gages at the interface between the pavement and the soil are less complex than for gages fully embedded in the soil mass. Two situations are illustrated in Fig. 6, a gage placed on the structure surface so that it is fully projecting, and a gage recessed so that it is fully embedded in the structure. Theoretically the fully projecting case with a T/D ratio of K has an error, C_r , equal to that of a

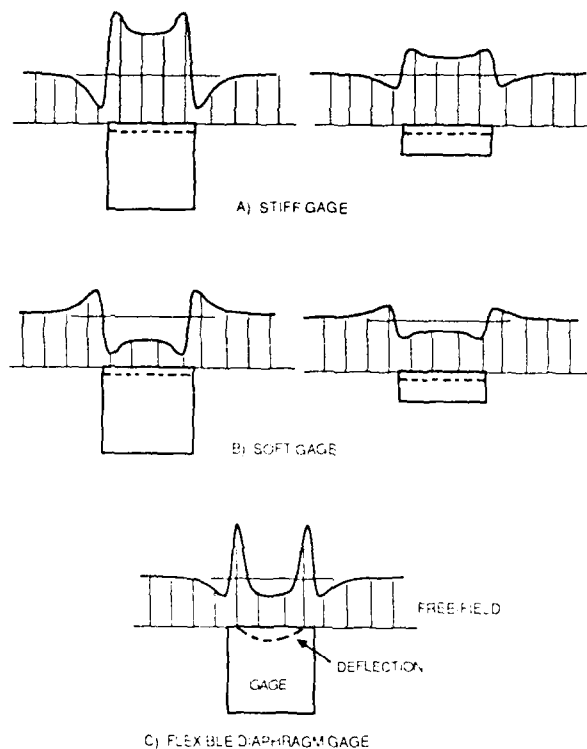


Fig. 5 Stress Distribution Around Embedded Gages

gage in the soil mass away from the structure that has a T/D ratio equal to $2K$.

The parameters for the fully embedded interface location are shown in Fig. 7 for the simple case of a uniformly deflecting sensing area. The error, C_r , is primarily a function of the deflection-diameter ratio, d/D , and the soil modulus, E_s , as shown in Fig. 8. Positive deflection, d , is away from the soil or in the active earth pressure direction. Negative deflection is toward the soil or in the passive direction. The passive direction causes over-registration and the active direction causes under-registration. Usually the gage sensing area deflects inward relative to the surface of the surrounding structure ($+d$). Hence C_r is usually negative and the gage under-registers. The error also increases with increasing soil stiffness, E_s .

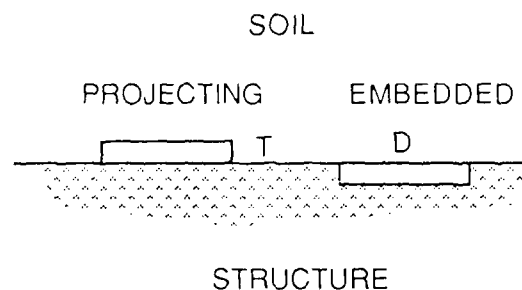


Fig. 6 Interface Gage Alternatives

GAGE INSTALLATION

A very significant factor influencing accuracy of stress measurement is the method of installation. An example of studies to investigate this effect is given in Ref. 7. Techniques must be developed for each application. Usually gage placement for measuring horizontal stresses is much more difficult than for measuring vertical stresses.

The alternatives may be divided into 3 general categories for gages within a soil mass: 1) excavating and recompacting the soil, 2) excavating the soil and backfilling with a sand bedding, and 3) excavating the soil and backfilling with grout. The first case is best with soft clays and fine sands.

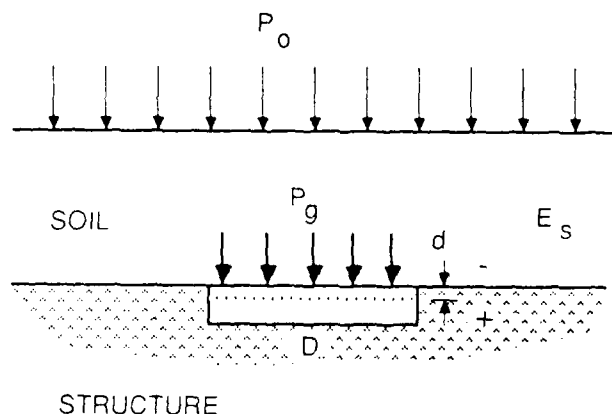


Fig. 7 Parameters for Interface Location

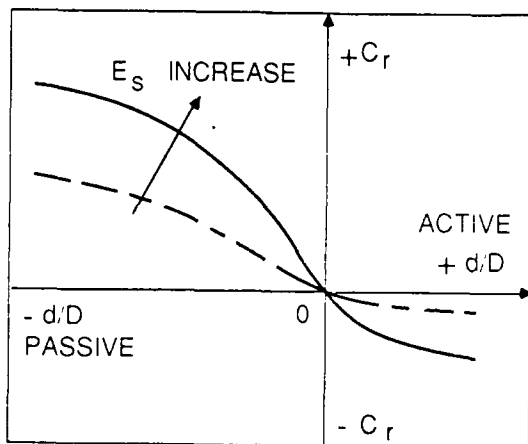


Fig. 8 Interface Gage Behavior

The second case is best with medium to stiff clays, and granular materials in general. The third method applies primarily to stiff, hard or very compact soils. In all cases the excavation should be done in a way that will achieve a flat surface adjacent to the gage, even if there is only one sensing face and this is directed away from the excavated soil surface.

For gages embedded in the pavement structure, grouting or forming the pavement around the gage are the most appropriate methods of placement. The grout should normally be selected to provide a stiffness similar to that of the surrounding structure.

The contribution of placement effects to registration error, C_r , must be estimated by analysis or calibration in soil under representative conditions. This is often difficult to accomplish. Also for consistency, the techniques should be repeatable from gage to gage.

Because of the important influence of placement methods on accuracy of stress measurement, the design of the gage and transducer housings should be done with ease of placement in mind. A flat, thin, cylindrical gage with only a cable or tubing projecting from the side is easiest to install in soil (Fig. 2A, B, E, F). Gages with a separate transducer housing (Fig. 2C and D) are more difficult to install. Gages with transducer housings on one face (Fig. 2G) are generally only suitable for use in a concrete mass or at the interface between a structure and soil.

GAGE CALIBRATION

Calibrations are needed to check gage performance and estimate values for C_r . The first step is to subject a gage to repeated cycles of fluid pressure applied to both faces (if a disk-shaped gage). Pressure can also be applied to the entire outer surface to determine whether side pressure affects the gage response. Fluid calibration is relatively easy to accomplish (Ref. 8). It provides information on the linearity, hysteresis, sensitivity (output per unit pressure change), resolution (smallest readable value), and precision (repeatability of reading) of the system including sensor, transducer, and readout. This is done without the complications caused by the soil and installation effects. The gage and readout, together and separately, should also be checked for effects of temperature variation.

The next step is to check the gage response in soil. The soil and placement conditions should simulate the field conditions as closely as possible. The two most common methods for accomplishing this use: 1) a large triaxial device (Ref. 4), or 2) a rigid-wall chamber with pressure applied to the soil surface (Refs. 7 and 8). Both are time consuming and expensive, and neither can fully achieve field simulation. However, if the results of such tests are not available for examination, these studies are necessary in order to judge the potential gage accuracy in soil.

The desired approach for best accuracy is to calibrate each gage in the field after placement. However, procedures for achieving this goal have not been demonstrated except in a few special cases. The most significant future contribution to stress measurement in soil would be the development of suitable field calibration methods.

ACCURACY AND PRECISION

Accuracy means the closeness of the measured stress to the true soil stress (that which would be present without the gage installed). Bias is the difference between the true value and the measured value. Precision is an indication of the repeatability or reproducibility of the stress measurement. Bias is a systematic error which can be reduced by

calibration, but generally not by replicate measurements. Precision represents random error which is reduced by averaging replicate measurements. For a stress measurement effort to be meaningful, the gage accuracy and precision both must be evaluated.

Information on accuracy and precision of stress measurements in soil is insufficient to draw firm conclusions. However in most cases the precision and accuracy of the gages and readouts under fluid pressure conditions are quite satisfactory. Even temperature effects can be adequately accounted for. By far the two biggest sources of error are caused by: 1) soil-gage interaction including installation effects, and 2) soil and construction variability from place to place.

The writer has observed coefficients of variation (standard deviation/mean) as high as 60% in field tests, although more likely values are $\pm 25\%$. The contribution of this variability due to placement has been reported to be ± 6 to 15% (Refs. 9-11). This represents low precision, and hence would require many replicate gage installations for the same conditions to diminish the imprecision to an acceptable level.

This variability is often thought (erroneously) to be bias or inaccuracy. With only one gage for measuring each condition, there is no way to tell whether the errors represent accuracy or precision. Analysis and soil calibration experiments do give an indication of potential bias, however. Values of -40% to $+80\%$ of the mean (under and over-registration, respectively) are clearly possible, and inaccuracies of 20% should be expected. Replications will not reduce this error -- only appropriate calibrations will reduce it.

CONSIDERATIONS IN GAGE SELECTION

A number of factors need to be considered in gage selection. This information comes from many sources, including references cited in this paper. The compiling of many of these effects in Ref. 6 was particularly helpful. A listing of the factors with a summary recommendations, emphasizing soil mass cases, is as follows:

1. Cell thickness to diameter ratio:
Use T/D ratio < 0.2 .

2. Gage to soil modulus ratio: Hard to measure, but keep as large as possible -- say > 5 to 10 .
3. Deflection to diameter ratio for clamped diaphragms: keep < 0.0005 .
4. Deflection to diameter ratio for uniform deflecting sensing areas: $K_{rep} < 0.00005$.
5. Edge stress concentration: Keep sensing area < 25 to 45% of total gage face area.
6. Ratio of sensing area diameter to soil mean particle size: Keep > 10 to 50 in vicinity of gage.
7. Transverse normal stress and shear stress: Prediction and control is uncertain. Evaluate by analysis and calibration.
8. Temperature sensitivity: Evaluate need to apply corrections.
9. Installability: Select geometry for satisfactory installation.
10. Gage mass density to soil mass density ratio: When very short (millisecond or smaller) loading times are involved, make close to 1.0 .
11. Frequency response: Transducer, gage body, and readout should be capable of responding at a rate at least 10 times faster than the rate of soil stress change.
12. Gage sensitivity to side pressure: Design to eliminate by isolation or by type and layout of transducer.
13. Robustness: Design to withstand handling and installation forces, as well as service overstress. Cable and transducer connections are particularly vulnerable.
14. Moisture: Seal gage and attached cable for anticipated water pressure conditions.

15. Durability: Select gage materials and coatings to prevent deterioration over required measurement period. Investigate potential drift over time. Develop corrective measures or means to recalibrate. For long term applications select gages with established records of satisfactory performance as either the primary or the back up system.

CONCLUSIONS

The starting point for planning soil stress measurements is to critically evaluate the reasons for the measurements, and where they would be located. Because of the errors involved with such measurements the reasons must be convincing to justify the high expense. Significant cost items are the necessary calibrations and essential replication of locations. A good understanding of the principles of soil-gage interaction and adherence to the guidelines in this paper will help in achieving acceptable results.

REFERENCES

1. Dunnicliff, John, Geotechnical Instrumentation for Monitoring Field Performance, Wiley, 1988.
2. Selig, E. T., "Tensile Zone Effects on Performance of Layered Systems," *Geotechnique*, Vol. 37, No. 3, 1987, pp. 247-254.
3. Selig, E. T., "A Review of Stress and Strain Measurement in Soil," *Proceedings, Symposium on Soil-Structure Interaction*, University of Arizona, Tucson, Arizona, Sept. 1964, pp. 155-171.
4. Hvorslev, M. J., "The Changeable Interaction between Soils and Pressure Cells; Tests and Reviews at the Waterways Experiment Station," *Technical Report S-76-7*, Waterways Experiment Station, Vicksburg, MS, June 1976.
5. Brown, S. F., "State-of-the-Art Report on Field Instrumentation for Pavement Experiments," *Transportation Research Record 640, Multiple Aspects of Soil Mechanics*, Transportation Research Board, Washington, D.C., 1977, pp. 13-28.
6. Weiler, W. A. and Kulhawy, F. H., "Factors Affecting Stress Cell Measurements in Soil," *Proceedings, ASCE, Journal of Geotechnical Engineering Division*, Vol. 108, No. GT12, Dec. 1982, pp. 1529-1549.
7. Hadala, P. F., "The Effect of Placement Method on the Response of Soil Stress Gages," *Technical Report No. 3-803*, Waterways Experiment Station, Vicksburg, MS, Nov. 1967.
8. Selig, E. T., "Soil Stress Gage Calibration," *ASTM Geotechnical Testing Journal*, Vol. 3, No. 4, Dec. 1980, pp. 153-158.
9. "Investigations of Pressures and Deflections for Flexible Pavements," *Report No. 4, Homogeneous Sand Test Section*, Waterways Experiment Station, Vicksburg, MS, Tech. Memo No. 3-323, December 1954.
10. "Stresses under Moving Vehicles - Wheeled Vehicles in Lean and Fat Clay, 1957," *Tech Report No. 3-545*, Waterways Experiment Station, Vicksburg, MS, May 1960.
11. Peattie, K. R. and Sparrow, R. W., "The Fundamental Action of Earth Pressure Cells," *J. Mech. and Phys. of Solids*, Vol. 2, 1954, pp. 141-155.

PAVEMENT DESIGN WITH THE PAVEMENT PRESSUREMETER

Jean-Louis Briaud
Paul J. Cosentino

Texas A&M University
Texas Tech University

INTRODUCTION

The pressuremeter test consists of drilling a hole and inserting in the open hole a cylindrical probe (Figure 1). Once at the testing depth the probe is inflated while recording the increase in pressure in the probe and the increase in volume of the probe. A test leads to the recording of a pressuremeter curve (Figure 1). Two of the parameters obtained from a pressuremeter curve are a soil modulus E and a limit pressure p_L . This test was developed by Menard in France in 1956 and has been used mostly for foundation design. In 1976 Briaud and Shields in Canada studied the possible application of the pressuremeter to airport pavement design. The sponsor was Transport Canada. Tests were performed and a design procedure was developed for airport pavements (Briaud, 1979, Briaud and Shields 1979, 1981, 1981a). In 1980, Briaud and Lytton in Texas studied the possible application of the pressuremeter to highway pavement design (Hung et al., 1981; Briaud et al., 1982, 1983). The sponsor was the Texas State Department of Highways and Public Transportation. Tests were performed and progress was made analytically on obtaining the small strain moduli from a pressuremeter test. In 1984, Briaud, Cosentino and Terry compared the pavement pressuremeter with the falling weight deflectometer and the cyclic triaxial test. The sponsor was the Federal Aviation Administration (FAA). Measurements and predictions were made for 3 airports (Briaud, et al., 1986, 1987). More recently Briaud, Morgan and Ross used the pavement pressuremeter for another highway related problem: the design of guard rail posts.

This article is a state-of-the-art on the use of the pressuremeter for pavement design with emphasis on the results obtained in the 1984 FAA study.

PAVEMENT DESIGN CONCEPTS

The pressuremeter has been used mainly for foundation design. The use of the pressuremeter in pavement design requires to acknowledge the differences which exist between pavements and foundations. In foundation ultimate bearing capacity is rarely considered because other design constraints, namely very small tolerable deflections, ensure that the factor of safety against bearing capacity failure is very large. Typical safety factors in foundations vary between 1.5 and 3; for most conventional pavements the safety factor is many times higher. In foundation engineering, movements of up to 25 mm (1 in.) can usually be tolerated while in pavements such differential movements would be disastrous for a plane trying to take off at 240 km/h (150 mph). In pavements, strains of less than 0.001 are taking place everytime the tire passes over the pavement. The tire pressure can be 200 kPa (30 psi) for a car, 550 kPa (80 psi) for a truck and up to 1700 kPa (250 psi) for a plane. Clearly, pavement design is a problem of limiting the deformations to very small tolerable values. Therefore the determination of layer moduli for very small strains becomes essential. Other differences with foundations are the fact that the stress level in the soil is lower for pavements and that the car, truck, or plane load the soil very rapidly but with a large number of repetitions. As a result the development of the pavement pressuremeter has focused on the determination of moduli as a function of strain, stress, rate of loading and cyclic loading.

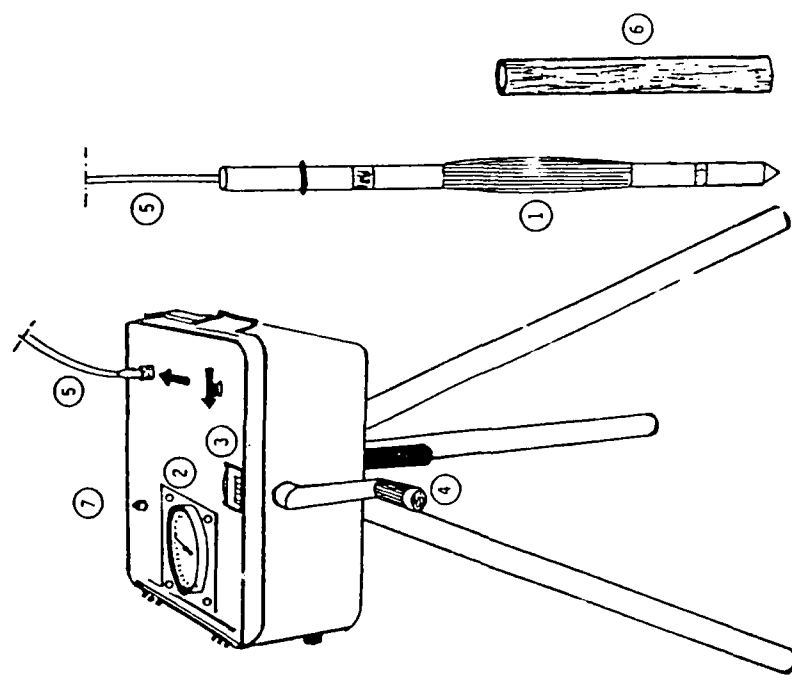


Fig. 2 Schematic of the latest Pavement Pressurimeter 1. Probe
2. Pressure gauge, 3. Displacement indicator, 4. Manual actuator, 5. Tubing,
6. Steel pipe for volume calibration, 7. Connection to water reservoir.

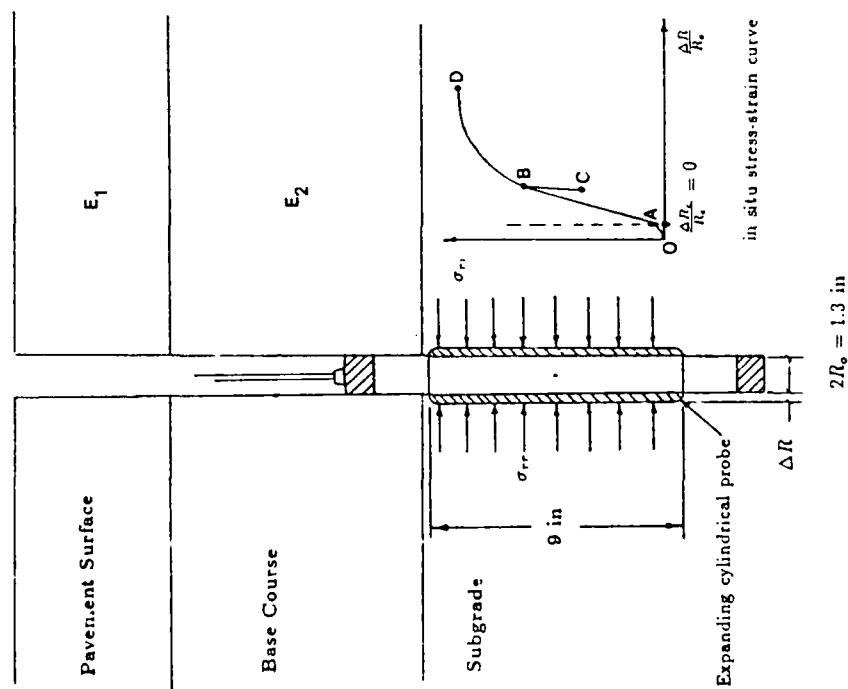


Fig. 1 Typical Pavement Pressurimeter Test and Pavement Cross Section

THE PAVEMENT PRESSUREMETER

The pavement pressuremeter was first developed for Transport Canada (Briaud, 1979). The unit was improved for the Texas Highway Department (Hung, et al., 1981). Rctest in 1984 made final improvements and commercialized the unit under the name of PENCEL. This unit consists of a small suitcase housing the central unit and of a probe and tubing (Figure 2). The probe is 35 mm (1.38 in.) in diameter and the inflatable part of the probe is 230 mm (9 in.) long. For new pavements the hole is made with a small flight auger 35 mm (1.38 in.) in diameter down to the testing depth. For the evaluation of existing pavements a 50 mm (2 in.) diameter hole is first open through the surface course. This is usually done with a concrete drill and the core can be used for determining the modulus of the surface course (asphalt or concrete). As a last resort the probe can be driven in place if it is not possible to prepare the hole with the flight auger; in this case conversion factors need to be applied to the moduli obtained (Briaud, et al., 1986).

The test itself consists of inflating the probe in a very specific sequence. The test lasts about 10 minutes so that in one hour, 4 to 5 tests in one hole can be performed by an experienced crew of two people. The pavement pressuremeter has advantages and drawbacks like other tests. It is compared on Table 1 to the falling weight deflectometer and the cyclic triaxial test. This table shows that the falling weight deflectometer is ideal for the rapid but crude evaluation of a large pavement area while the pavement pressuremeter is very well suited for a more in depth evaluation of a few specific zones. The very low cost of the pavement pressuremeter compared to the falling weight deflectometer makes it very attractive economically.

MODULUS AND LIMIT PRESSURE FROM THE PAVEMENT PRESSUREMETER

A modulus E can be obtained from an unload-reload loop on the pressuremeter curve (Figure 3). The equation is (Baguelin et al., 1978; Briaud, 1990):

$$E = (1 + \nu) (a_{r2} - a_{r1}) \frac{\left(1 + \frac{\Delta R}{R}\right)^2 + \left(1 + \frac{\Delta R}{R}\right)^2}{\left(1 + \frac{\Delta R}{R}\right)^2 - \left(1 + \frac{\Delta R}{R}\right)^2} \quad (1)$$

where ν is Poisson's ratio (to be estimated), ΔR and ΔR are the increases in probe radius for the two points considered, R is the radius of the deflated probe, a_{r1} and a_{r2} are the pressures against the wall of the borehole for the two points considered (Figure 3).

The limit pressure p_L can be obtained by manual extension of the pressuremeter curve to a value of $\Delta R/R_0$ equal to $0.41 + 1.41 (\Delta R_0/R_0)$ where ΔR_0 is the increase in probe radius when the probe comes in contact with the borehole wall. The limit pressure p_L is the pressure corresponding to this point on the $\Delta R/R_0$ axis (Figure 3).

CHART METHOD

There are essentially two sets of techniques to design a pavement, one is based on the use of charts, one is based on the use of computer programs modelling the pavement and subgrade as a multilayer system. In the chart method the subgrade is characterized by an average stiffness. The total thickness of pavement necessary is given in a chart as a function of this average stiffness and of the design vehicle for a given level of traffic. Such an approach was proposed by Briaud (1979) for the design and overlay of airport flexible pavements in Canada.

In this procedure the modulus was the reload modulus taken between points A and B on Figure 3. Note that in this case the pressure is brought back to the initial pressure before reinflating the probe. Moduli are obtained every 300 mm (1 ft) down to a depth of 1.5 m (5 ft). These five modulus values are averaged using an assumed but reasonable strain distribution under the wheel load (Briaud, 1979):

$$\frac{1}{E_{av}} = 0.01 \left(\frac{22.1}{E_1} + \frac{33.5}{E_2} + \frac{24.6}{E_3} + \frac{14.8}{E_4} + \frac{5}{E_5} \right) \quad (2)$$

where E_1 is the reload modulus obtained at the shallowest depth and E_2, E_3, E_4, E_5 are the reload moduli corresponding to the next four test depths (300 mm (1 ft) increment). The chart is presented in Figure 4. Note that an aircraft load rating (ALR) of 12 corresponds to a Boeing 747 while an ALR 1 is a very small private plane (Transport Canada, 1968).

LOAD RATING OF PAVEMENTS

It was mentioned earlier that the ultimate bearing capacity of a pavement is rarely of concern in the design. There are some exceptions to this statement. For example, a small airport may have a demand for some large aircraft landings or a secondary road may have a sudden increase in truck traffic due to construction on the main highway. In these cases it becomes necessary to rate the pavement for the maximum load that can be carried. The pavement pressuremeter is ideal in this case. The following equation is given to evaluate the tire pressure p_{max} which will lead to failure of the pavement by punching.

$$p_{max} = \frac{Plas}{A} + p_L \quad (3)$$

General Use	Falling Weight Deflectometer	Pressurimeter Test	Cyclic Triaxial Test
Range of Equipment Load or Test	\$50,000 Low	\$6,000 medium	\$50,000 high
Operator Versatility	medium	high	medium
Dependence of Use of Equipment	medium	medium	very complex
Time Required for Test	3 minutes	20 minutes	480 minutes
Time Required for Equipment Setup for Operation	1 hour	2 minutes	15 minutes (evacuate drill rig)
Cost Required	Surface Deflections When Investigation No	Stress/Strain Curve In Situ Yes	Stress/Strain Curve in Laboratory Difficult
Operator Skill Required	No	Complicated	Complicated
Operator Skill Required	Layer Moduli All Layer thicknesses Accurately known as a function of load level 5 cycles from Repeated Tests	Layer Moduli as Function of Stress, Strain, Cycles and Rate of Loading	Layer Moduli as Function of Stress, Strain, Cycles and Rate of Loading
Cost Rating of Parameters	Light Pavements Only	Yes	Yes
Check Parameter Parameters	No	Yes	Yes
Operator Skill Required	No	Disturbed (Useful for Ident- ification, Water Content . . .)	Undisturbed
Operator Skill Required	Yes	Yes	Yes
Operator Skill Required	Yes	Yes	Yes
Operator Skill Required	Yes	Yes	Yes

Table 1

Comparison of the Falling Weight Deflectometer, Pressurimeter and Cyclic Triaxial Tests for Pavement Design and Evaluation

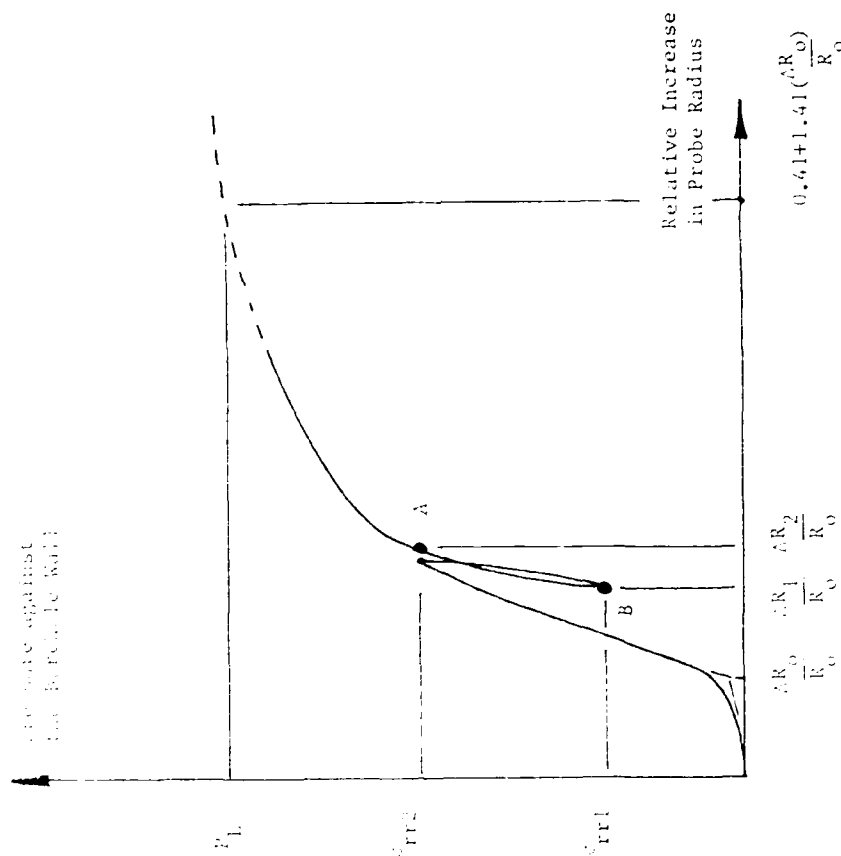


Fig. 3 A pressuremeter curve.

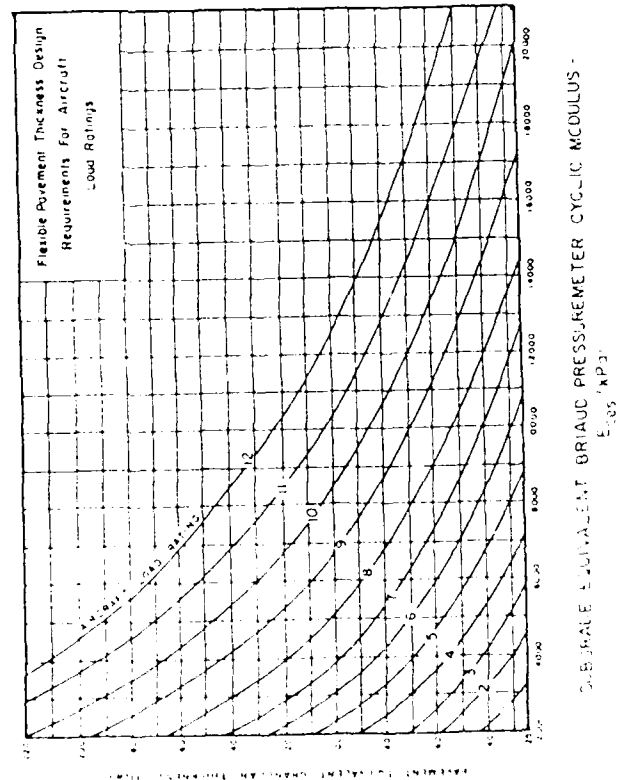


Fig. 4. Curves for the Design of Flexible Pavement using the Equivalent Pressuremeter.

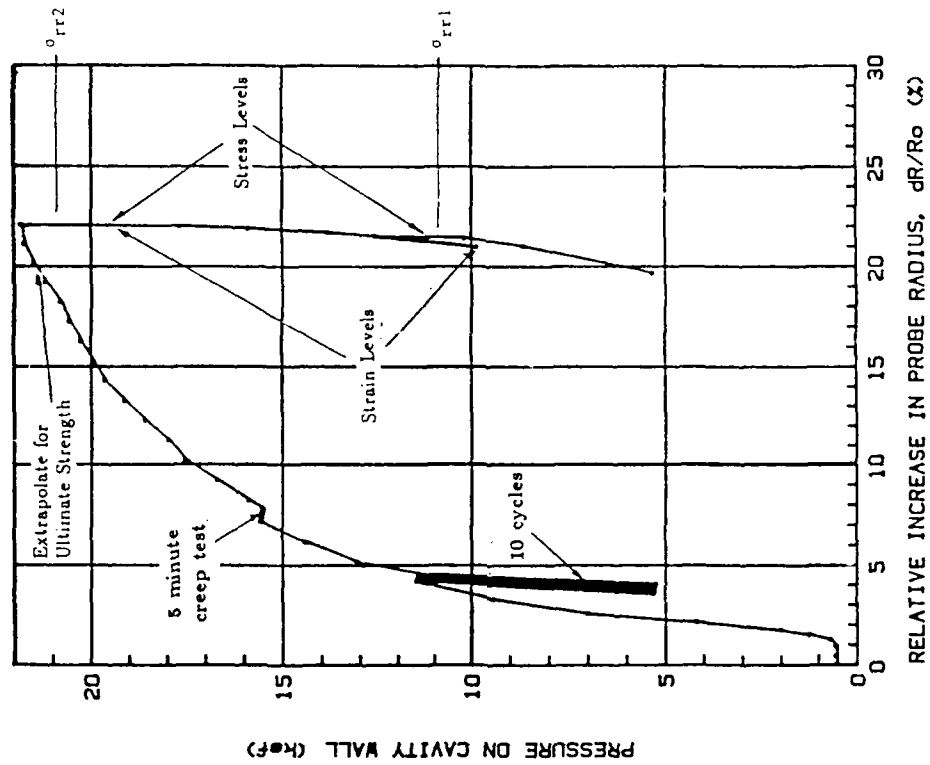


Fig. 5 Typical Airport Pressuremeter Results on Clays

where P and A are the perimeter and contact area of the tire imprint, t is the thickness of the surface course, s is the shear strength of the surface course material, α is a coefficient representing the condition of the surface course ($\alpha = 1$ for perfectly intact surface course, $\alpha = 0$ for full depth extreme cracking of the surface course), and p_L is the limit pressure of the first 300 mm (1 ft) of material below the surface course. This equation assumes that the surface course will shear vertically along the perimeter of the tire imprint and that the bearing capacity of the material below is equal to p_L . This bearing capacity comes from the experience gathered in foundation engineering (Briaud, 1990).

MODULUS AS A FUNCTION OF STRESS, STRAIN, RATE AND CYCLES

The soil modulus is influenced by many factors. The major influencing factors are the strain level, the stress level, the rate of loading and the number of cycles to which the soil is subjected. The influence of the stress level was studied by Janbu (1963). Janbu's work was followed by the work of Duncan and Chang (1970). The proposed model for the influence of the stress level is:

$$E_i = k \left(\frac{\sigma}{p_a} \right)^{n_s} \quad (4)$$

where E_i is the initial tangent modulus (strain = 0), σ is the mean normal effective stress, k is a unitless modulus number, p_a is the atmospheric pressure and n_s is the stress exponent.

Once the initial tangent modulus E_i has been determined, the influence of the strain level can be incorporated. This influence was studied by Kondner (1963) who proposed:

$$\frac{1}{E} = a + b\epsilon \quad (5)$$

where E is the secant modulus at a given strain ϵ , a and b are the strain influence parameters.

Once the modulus can be obtained for any stress and strain level, the influence of the rate of loading can be incorporated. Riggins (1981) proposed a rate effect model for undrained shear strength. It is extended here to moduli:

$$\frac{E_{t_1}}{E_{t_0}} = \left(\frac{t_1}{t_0} \right)^{n_r} \quad (6)$$

where E_{t_1} are secant moduli measured by loading the soil in times t_1 and t_0 respectively, and n_r is the rate exponent.

The effect of repetitive loading on the modulus is significant. Idriss et al. (1978) proposed the following model:

$$\frac{E_N}{E_1} = N^{-n_c} \quad (7)$$

where E_N and E_1 are the secant moduli to the top of the N th cycle and first cycle respectively and n_c is the cyclic exponent.

By regrouping all the influence factors it comes:

$$E = \frac{1}{k \left(\frac{\sigma}{p_a} \right)^{n_s} \cdot b\epsilon} \left(\frac{t_1}{t_0} \right)^{n_r} N^{-n_c} \quad (8)$$

This leaves 5 parameters to be determined: K, n_s, b, n_r, n_c . The following pavement pressuremeter test was developed in order to obtain those five parameters from one single test.

THE PAVEMENT PRESSUREMETER TEST

After the proper saturation and calibration of the equipment (ASTM D4719-87, Briaud et al. 1987, Briaud, 1990) the following inflation sequence is recommended for each test at a given depth (Figure 5):

1. Inflate the probe in equal volume increments each lasting 15 seconds. The volume increments should be 5 cm^3 ; this corresponds to 2.27% of the probe initial volume V_0 and to a $\Delta R/R_0$ of 1.13%. The field curve is obtained by recording the pressures and volumes at the end of each 15 seconds increment.
2. Ten cycles are performed near the end of the elastic or straight line portion of the curve where the pressure is p . The end of the straight line portion of the curve is determined during the test by recording the increase in volume Δv and the corresponding increase in pressure Δp . The end of the straight line is found when the ratio $\Delta p / \Delta v$ starts to decrease. Cycles are carried out between p and $1/2 p$. Each unloading step or reloading step lasts 15 seconds.
3. Once the cycles are completed, two or three 5 cm^3 volume increments are applied, and then a 5 minute creep test is conducted with pressure readings taken every 15 seconds.
4. Following the creep test, the expansion of the probe is completed to about 1.55 times its original volume (this requires an increase in probe volume of 120 cm^3) or until the limit of the pressure gage is reached.

5. At this point the probe is deflated using the following decrements, each lasting 15 seconds; 0.5, 1.0, 2.0, 5.0 and 10 cm³ down to one-half the maximum pressure (Figure 5).
6. Once this is reached, the probe is inflated by injecting 0.5 cm³ and then deflated by withdrawing 0.5 cm³ to complete the cycle. The test is completed by deflating the probe in 5 cm³ decrements.

OBTAINING MODULI FROM THE PAVEMENT PRESSUREMETER TEST CURVE

The parameters for the stress level model, k and n , can be obtained from the curve as follows. Upon deflation of the probe two moduli are calculated, E_1 over the first 0.5 cm³ of deflation, and E_2 over the deflation part of the small 0.5 cm³ loop midway through the deflation of the probe (E_1 and E_2 on Figure 6). The moduli E_1 and E_2 are calculated using equation 1; they correspond to the radial stress σ_{rr} and σ_{rr2} respectively. The stress σ_{rr2} is approximately 0.5 σ_{rr1} . It has been shown (Jamiolkoswky 1986, Briaud et al., 1987) that a reasonable estimate of the mean normal stress $\bar{\sigma}$ in the plastic zone around the pressuremeter is:

$$\bar{\sigma} = \frac{1}{3}(0.8\sigma_{rr} + \sigma_{ov}) \quad (9)$$

where σ_{rr} is the radial stress applied to the borehole wall and σ_{ov} is the vertical stress at rest at a depth corresponding to the midheight of the probe. In this manner $\bar{\sigma}_1$ is calculated for σ_{rr1} and $\bar{\sigma}_2$ for σ_{rr2} . Knowing $E_1, E_2, \bar{\sigma}_1$ and $\bar{\sigma}_2$, Equation 4 is used to backfigure k and n . Note that in Equation 4, $\bar{\sigma}, \sigma_{rr}, \sigma_{\theta\theta}$ are effective stresses while the pressuremeter gives total stresses. These total stresses can be used if the soil is unsaturated which is often the case for pavements. If the soil drains fast enough the pore pressures remain hydrostatic and can be taken into consideration. In saturated silts and clays traffic loading represents an undrained behavior of the soil where theoretically there is very little effect of the stress level on the modulus.

The parameters for the strain level model, a and b can be obtained from the curve as follows. Upon deflation of the probe two moduli are calculated, E_1 over the first 0.5 cm³ of deflation, and E_2 as a secant modulus between the point of first deflation and the point where the probe is first reinflated during the deflation of the probe (E_1 and E_2 on Figure 6). The moduli E_1 and E_2 are calculated using Equation 1; they correspond to the hoop strains $\epsilon_{\theta\theta 1}$ and

$\epsilon_{\theta\theta 2}$ respectively. Each of these strains is calculated between the two points A and B which define the slope of the modulus (Briaud, 1990):

$$\epsilon_{\theta\theta 1} = \frac{\Delta R_{rA}}{R_c} = \frac{\Delta R_{rB}}{R_c} \quad (10)$$

where R_c is the average cavity radius between A and B (Figure 3), ΔR_{rA} and ΔR_{rB} are the increase in cavity radius for points A and B respectively. The strains $\epsilon_{\theta\theta 1}$ and $\epsilon_{\theta\theta 2}$ are the hoop strains in the soil at the wall of the borehole for A and B. It has been shown (Jamiolkoswky, 1986; Briaud et al., 1987) that a reasonable estimate of the mean normal strain in the soil mass is:

$$\epsilon_{\theta\theta}(\text{mean}) = 0.32\epsilon_{\theta\theta}(\text{at the borehole wall}) \quad (11)$$

Knowing $E_1, E_2, \epsilon_{\theta\theta 1}(\text{mean})$ and $\epsilon_{\theta\theta 2}(\text{mean})$, Equation 5 is used to backfigure a and b .

The parameter for the rate effect model, n_r , can be obtained from the pressure holding test performed during the inflation of the probe after the cycles. The modulus E_1 and E_2 are calculated as the secant modulus to the points corresponding to elapse times t_1 and t_2 (E_{50} and E_{50} on Figure 6). The elapse times t_1 and t_2 are measured from the beginning of the pressure step. The time t_1 is taken as 1 minute and t_2 as 5 minutes. Knowing E_1, E_2, t_1, t_2 , Equation 6 is used to backcalculate n_r .

The parameter for the cyclic model, n_c , can be obtained from the series of cycles performed during the inflation part of the test. The modulus E_1 and E_2 are calculated as secant modulus to the points corresponding to the top of cycle 1 and 10 (E_0 and E_{10} on Figure 6). Knowing E_1, E_2, N_1 , and N_{10} , Equation 7 is used to backfigure n_c .

FIELD EXPERIMENTS

Tests were performed at 3 airports in Texas: College Station, San Antonio, and Possum Kingdom. The College Station pavement is made of 150 mm (6 in.) of reinforced concrete, 100 mm (4 in.) of granular base course underlain by a clay subgrade. The San Antonio pavement is made of 400 mm (16 in.) reinforced concrete, 200 mm (8 in.) of asphalt concrete, underlain by a very stiff clay. The Possum Kingdom airport is made of 50 mm (2 in.) of asphalt concrete, 50 mm (2 in.) of granular base underlain by dense sand.

Three types of tests were performed for each site: pressuremeter tests, cyclic triaxial tests and Falling Weight Deflectometer tests. The pressuremeter tests were performed every 300 mm (1 ft) down to 1.5 m (5 ft). Moduli were obtained as previously described. Samples were taken and placed in the triaxial cells, with great difficulty for the sand. Resilient moduli were obtained from the cyclic triaxial tests by following the established procedure (Barker and Brabston, 1975). The Falling Weight Deflectometer consists of dropping a weight on the pavement (Briaud et al., 1987). The impact force can vary from 7.5 kN (1500 lbs) to 120 kN (24000 lbs). Geophone data lead to the measurement of the pavement deflection under this dynamic load.

The moduli and moduli model parameters obtained from the pressuremeter and the cyclic triaxial tests were used in a multilayer elastic computer program in order to predict the deflection of the pavement under the FWD load. In each layer the modulus was chosen to correspond to the anticipated stress and strain level. For the concrete and asphalt layers the conventional modulus values were input. The deflections were predicted for the three airports and for each load level used in the FWD test. Comparisons with the measured deflections are presented on Figure 7. These comparisons showed that in sand the main factor influencing the modulus is the stress level while in clay it is the strain level.

CONCLUSIONS

The pavement pressuremeter was developed in 1976 and has been studied for over 10 years off and on. It is now ready for commercial use. It has been shown that it is inexpensive compared to the cyclic triaxial apparatus and the Falling Weight Deflectometer and that it can give the proper layer moduli to calculate small pavement deflections. Alternatively a chart approach can be used. Also the pavement pressuremeter can help in load rating light pavements.

REFERENCES

ASTM Standard D4719-87, "Standard Test Method for Pressuremeter Testing in Soils," *Annual Book of ASTM Standards*, Vol. 04.08, American Society for Testing and Materials, Philadelphia, 1988.
 Baguelin, F., Jezequel, J.F., Shields, D.H., *The Pressuremeter and Foundation Engineering*, TransTech Publications, Clausthal, Germany, 1978.
 Barker, W.R., Brabston, W.N., "Development of a Structural Design Procedure for Flexible Airport Pavements," *Report FAA-RD-74-199*, Federal Aviation Administration, Washington, 1975.
 Briaud, J.-L., "The Pressuremeter: Application to Pavement Design," Ph.D. dissertation, Civil Engineering, University of Ottawa, Canada, 1979.

Briaud, J.-L., *The Pressuremeter*, A. A. Balkema Publishers, Rotterdam, The Netherlands, 1990.
 Briaud, J.-L., Cosentino, P. J., and Terry, T. A., "Pressuremeter Moduli for Airport Pavement Design and Evaluation," *FAA Report DOT/FAA/PM-87/10*, Civil Engineering, Texas A&M University, College Station, Texas, 1987.
 Briaud, J.-L., Lytton, R. L., Hung, J. T., "Using a Pressuremeter for Pavement Design and Evaluation," *Int. Symp. on the Bearing Capacity of Roads and Airfields*, Civil Aviation Admin., Oslo, The Norwegian Institute of Technology, Trondheim, Norway, 1982.
 Briaud, J.-L., Lytton, R. L., Hung, J. T., "Obtaining Moduli from Cyclic Pressuremeter Tests," *ASCE Journal of the Geotechnical Engineering Division*, May 1983.
 Briaud, J.-L., Shields, D. H., "A Special Pressuremeter and Pressuremeter Test for Pavement Evaluation and Design," *ASTM Geotechnical Testing Journal*, Vol. 2, No. 3, pp. 143-151, 1979.
 Briaud, J.-L., Shields, D. H., "Pressuremeter Tests at Shallow Depth," *ASCE Journal of the Geotechnical Engineering Division*, Vol. 107, GT8, August 1981.
 Briaud, J.-L., Shields, D. H., "Use of the Pressuremeter Test to Predict Modulus and Strength of Pavement Layers," *Transportation Research Record, Layered Pavement Systems*, TRB 810, pp. 33-42, 1979.
 Briaud, J.-L., Terry, T. A., Cosentino, P. J., Tucker, L. M., and Lytton, R. L., "Influence of Stress, Strain, Creep and Cycles on Moduli from Preboring and Driven Pressuremeter," *Research Report 7035-1 to the Federal Aviation Administration*, Civil Engineering, Texas A&M University, College Station, Texas, 1986.
 Duncan, J.M., Chang, C.-Y., "Nonlinear Analysis of Stress and Strain in Soils," *ASCE Journal of the Soil Mechanics and Foundation Engineering Division*, Vol. 96, SM5, 1970.
 Hung, J.-T., Briaud, J.-L., Lytton, R.L., "Layer Equivalency Factors and Deformation Characteristics for Flexible Pavements," *Research Report 384-2A for the Texas Highway Department*, Civil Engineering, Texas A&M University, 1981.
 Idriss, I.M., Dobry, R., Sings, R.D., "Nonlinear Behavior of Soft Clays During Cyclic Loading," *ASCE Journal of the Geotechnical Engineering Division*, Vol. 104, GT12, 1978.
 Jamiolkovsky, M., personal communication, June 1986.
 Janbu, Nihmar, "Soil Compressibility as Determined by Oedometer and Triaxial Tests," *European Conf. on Soil Mech. and Found. Eng. Eng.*, Wiesbaden, Germany, Vol. 1, 1963.
 Kondner, R.L., "Hyperbolic Stress-Strain Response: Cohesive Soils," *ASCE Journal of the Soil Mechanics and Foundation Engineering Division*, Vol. 89, SM1, 1963.

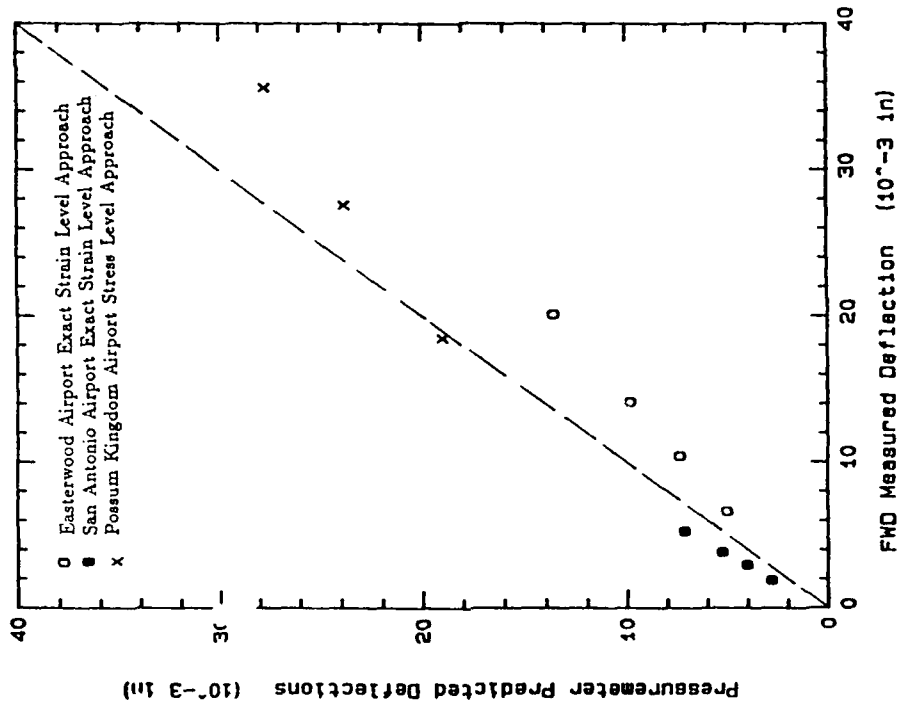


Fig. 7 PPMT Deflections vs FWD Deflections
Based on the Proposed Pressuremeter Approach for Each Subgrade

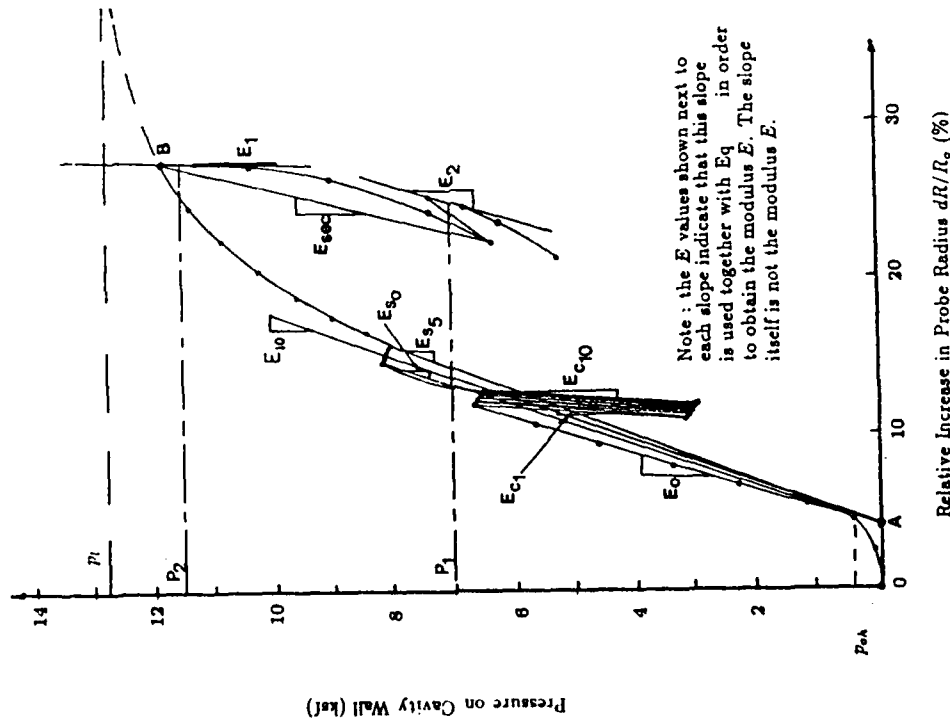


Fig. 8 Definitions for Airport PPMT Test

Riggins, M., "Viscoelastic Characteristics of Marine Sediments in Large Scale Simple Shear," Ph.D. dissertation, Civil Engineering, Texas A&M University, 1981.

Transport Canada, "Pavement Design and Rehabilitation," Manual AK-68-12, Ottawa, Canada, 1968.

MONITORING PAVEMENT RESPONSES TO TRAFFIC LOADS

J.T. Christison

Alberta Research Council

ABSTRACT

Instrumentation capable of recording strains and deflections under static and moving wheel loads has been installed in a number of pavement structures. Tests at the instrumented sites have yielded detailed pavement response measurements under a wide variety of traffic loading conditions and pavement temperatures. The paper presents an overview of the instrumentation. Installation procedures and the data acquisition system developed for monitoring the responses are described. Typical recorded pavement response profiles, together with results of preliminary analyses carried out to identify trends in the magnitude of asphaltic concrete-base layer interfacial tensile strains in different structures with variations in pavement temperature, are presented.

INTRODUCTION

In the early 1970's the Alberta Research Council, in cooperation with Alberta Transportation and Utilities, commenced development of instrumentation and a data acquisition system for monitoring structural responses of flexible pavements to traffic loads. The primary objective of this research effort was to obtain needed field information for assessing relative destructive effects of vehicle

axle loads and configurations on pavements. Following a number of field trials and equipment design modifications, an instrumented pavement test facility for recording traffic induced strains and deflections was successfully constructed in the summer of 1973 (Ref. 1). This facility, located approximately 30 km (18 mi) northwest of the City of Edmonton, has been followed by other local, national and international installations.

Referring to previously documented descriptions of the instrumented sites (Refs. 1,2,3,4,5), this paper presents a brief description of the transducers used to measure the pavement strains and deflections. Procedures for installing the instrumentation during construction of a new pavement structure and operational features of the data acquisition system and related peripherals are described. Pavement impact/vehicle load investigations carried out at Alberta test sites have yielded longitudinal asphaltic concrete-base layer interfacial strains produced by an 80 kN (18000 lb) single axle-dual tire load over a wide range of asphaltic concrete temperatures. Using these response measurements, preliminary analyses have been conducted to detect trends in the magnitude of in situ tensile strains with temperature. This paper summarizes results of these analyses.

PAVEMENT RESPONSE INSTRUMENTATION

The developed instrumentation consists of:

- i) sheet asphalt plates with embedded wire resistance strain gages, to measure the horizontal strains and,
- ii) surface-set linear variable differential transformer (DC-DT) assemblies, to measure total deflections.

The asphalt plates are laboratory prepared, 150 mm square by 12 mm thick, and consist of a mastic mix in which two - 120 ohm strain gages are embedded. The dual gauge configuration provides backup should failure occur on one gauge. The gauges can be positioned in any direction on the horizontal plane.

The primary component of a deflection transducer assembly is a commercially available linear variable differential transformer. A housing is fabricated to hold the coil of the transformer in a fixed position relative to the pavement surface. A deep set reference rod provides the zero datum for the transducer core.

Installation Procedures

General cross-sectional views of strain and deflection instrumentation installed in a full-depth asphalt pavement are shown in Figures 1 and 2, respectively. The triplicate configuration layout across the outer wheel path, shown in these figures, minimizes the number of test runs required to define maximum strains and deflections under a given loading.

The strain carriers are installed immediately prior to the application of subsequent pavement lifts. This decreases potential gauge damage due to construction traffic. When necessary the plates are protected by barricades and approximately a 25 mm covering of the base or surfacing material of the succeeding layer. Electrical connections for the differential transformers are set into the subgrade or base and referenced accurately. After paving, these locations are cored, a casing is installed to a depth of approximately 2.5 m into the subgrade, and a reference pipe having a minimum length of 3.5 m is driven to a reference depth of

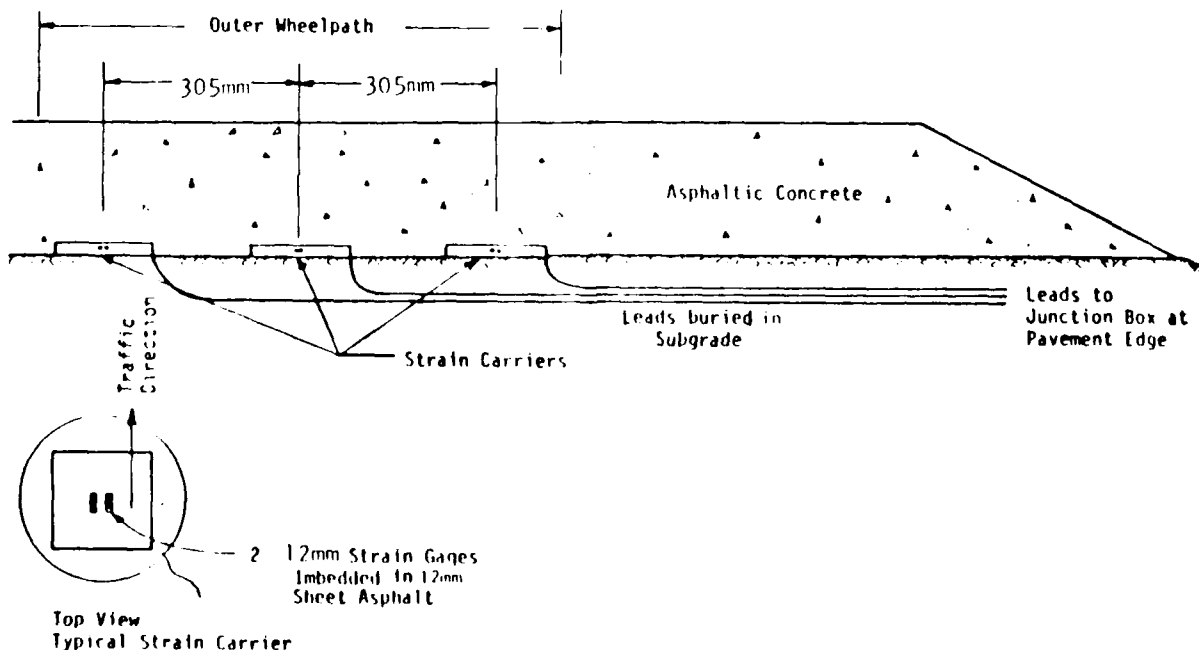


Figure 1 Strain Transducer Installation (Ref. 3)

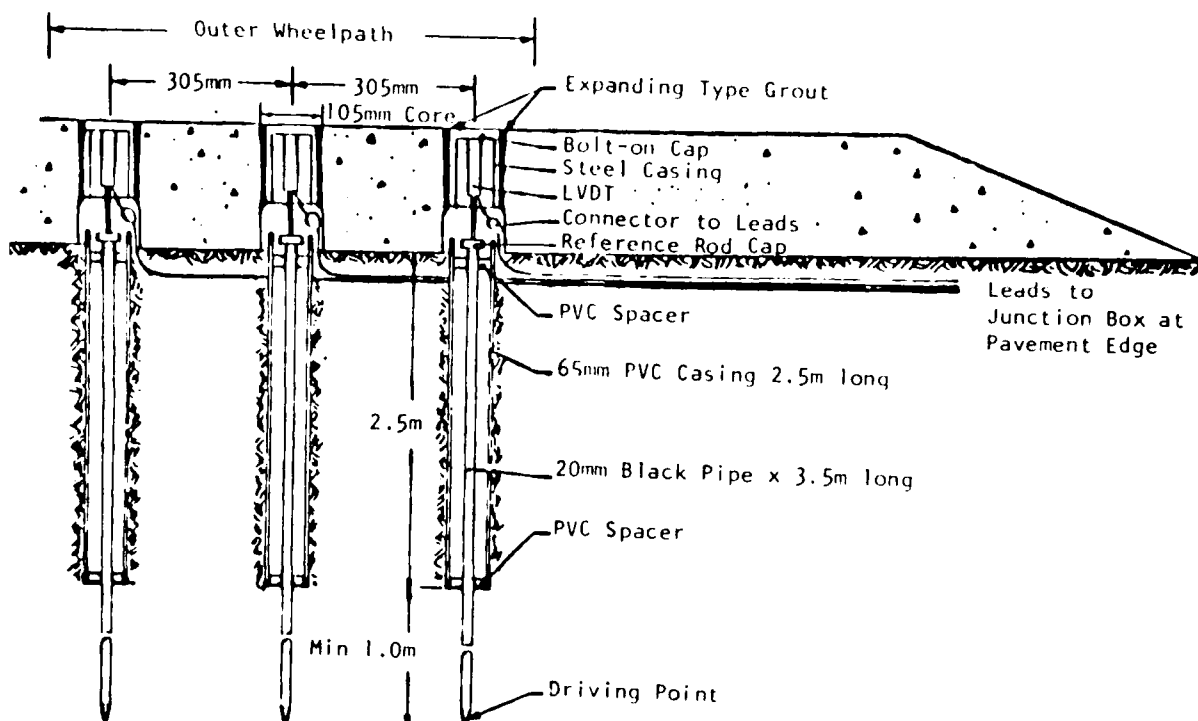


Figure 2 Deflection Transducer Installation (Ref. 3)

190 mm below the pavement surface. The space between the casing and subsoil is backfilled with sand and a 100 mm diameter steel casing, for housing the LVDT during testing, is placed flush with the pavement surface and grouted in place. A steel cap bolted to this casing provides waterproofing and access to the port for transducer installation. All control cables leading from the transducers are buried in the subgrade or base and are run to a junction box at the edge of the pavement surface for connection to the data acquisition system.

Service Life and Maintenance

Experience has shown that strain transducers surviving construction traffic usually remain operational for the service life of the pavement. (Transducers installed in 1973 at the original test site in Alberta are currently functioning although the highway has been rehabilitated and the site is no longer used as a test facility.)

The LVDTs and housings are removed from the pavement casings when not in use

and, therefore, maintenance of the LVDT units is limited to general cleaning. The permanently installed casings housing the deflection transducers are subjected to traffic and the environment. These factors can result in deterioration of the grout and subsequent movement of the casings. If this occurs, casing/asphalt concrete surface regrouting is required.

DATA ACQUISITION SYSTEM

The data acquisition system is designed to record stresses, strains and deformations under both static and moving, creep to + 120 km/hr, wheel loads. The system is developed around a (PDP11/24) digital computer with various peripherals and is housed in a van having a self contained power source for field operations. The peripherals include dual disks for system operation and mass storage, a signal condition system, real time clock which permits variable sampling rates and enables the time of each recorded event to be defined, video and a hard copy terminal and a digital plotter. The system is capable of addressing 16 channels in random or sequential order.

Operations of the acquisition system under moving wheel load conditions are generalized in Figure 3.

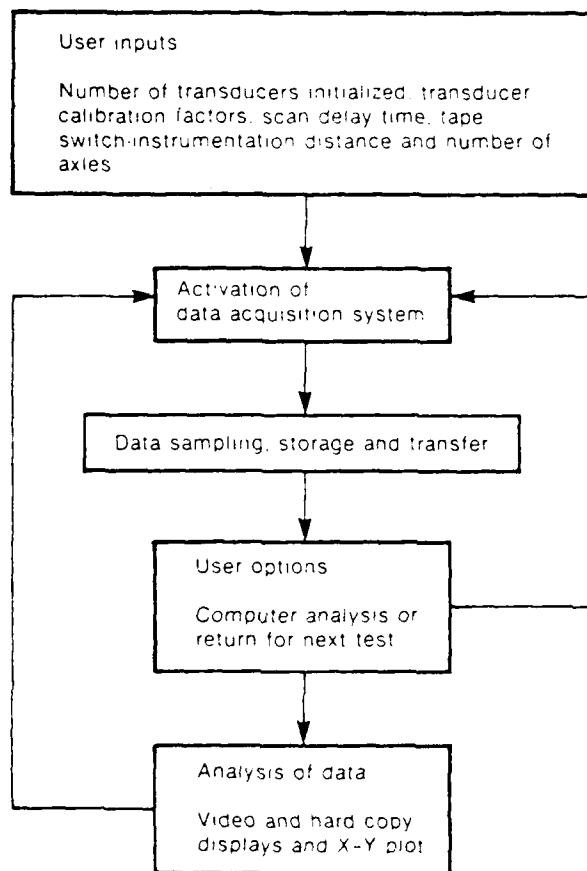


Figure 3 Operations of Data Acquisition System (Ref. 3)

The following presents a brief description of each of these operations.

User Inputs

The operator inputs via the video terminal the number of transducers being monitored, transducer calibration factors, a scan delay time, the distance from a tape switch position upstream of the instrumentation to the strain transducers and the number of axles on the oncoming vehicle. The calibration factors are used to convert the recorded voltage signals to engineering terms. The scan delay is the time interval between each cycle in which all transducers are monitored. The distance between the tape switch and strain transducers is used for vehicle velocity calculations.

Activation of Data Acquisition System

The acquisition system is activated when the first axle of the oncoming vehicle traverses the tape switch. (Activation can also be carried out by operator command.) At this time sampling of all designated transducers commences at a set scan rate and the preselected delay time.

Data Sampling, Storage and Transfer

Signals from transducers are multiplexed and converted from analog to digital at a rate of 50 usec/transducer. After the preselected delay time sampling continues. This sampling-delay time cycle is repeated until a selected buffer is filled. Data is then transferred to disk in sequential format.

User Options

The operator can select to perform an immediate computer analysis of the data or initialize the system for a subsequent test series. The latter option enables monitoring of on-line traffic.

Computer Analysis of Data

Data for the analysis routine is transferred from disk to memory and maximum and minimum readings recorded under each axle by each transducer are obtained by successive comparisons. These transducer outputs are then converted into engineering terms and their respective times from sequence initiation and vehicle velocity are determined. Velocity is calculated using the defined distance between the tape switch and the strain transducers and times of maximum strain response recorded under the leading axle of the vehicle. The recorded pavement responses, event times and vehicle velocity are displayed on the video terminal and, upon operator request, a hard copy image of the display is obtained.

In addition to video and hard copy displays, longitudinal profiles of individual transducer readings can be developed on the digital plotter. Typical examples of these real time profiles, showing deflections and strains monitored under a five axle tractor semitrailer, are presented in Figure 4.

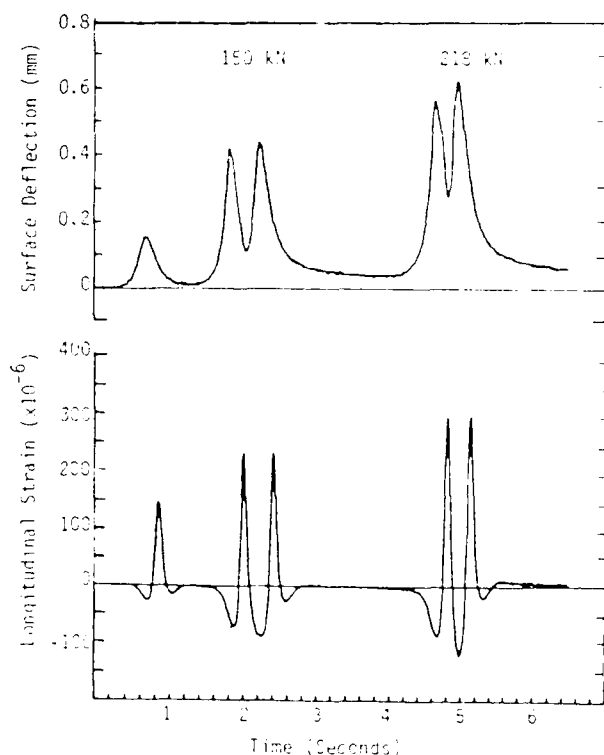


Figure 4 Typical Recorded Deflections and Strain Profiles

INFLUENCE OF TEMPERATURE ON PAVEMENT STRAINS

The testing procedure used to evaluate the relative destructive effects of axle loads and configurations on pavements is described in Refs. 3 and 4. Briefly, the procedure involves recording pavement response under both the test vehicle loading condition and an 80 kN (18000 lb) single axle-dual tire load of a Standard Benkelman Beam (Ref. 6) vehicle. Testing at Alberta sites has been carried out over a wide range of asphalt pavement temperatures. Using tensile strains produced by the standard 80 kN (18000 lb) load at vehicle velocities ranging from approximately 45 to 50 km/h (27 to 30 mph) at three instrumented sites, the following presents results of analyses carried out to detect trends in the magnitude of the tensile strains with variations in pavement temperature.

The three sites include a 280 mm full-depth asphalt pavement, an 140 mm asphalt concrete/170 mm cement stabilized granular base structure, and an 140 mm asphalt concrete/250 mm granular base structure. (The influence of asphaltic con-

crete temperature on interfacial tensile strains for the full-depth structure has been reported in Ref. 4.) The subgrade of each structure consists of a uniform, high plastic (CH) clay, with finished subgrade elevations at each site approximately 1.2 m (4 ft) above original ground. Longitudinal asphaltic concrete/subsurface interfacial tensile strains included in the analyses were recorded during summer and fall months when subgrade soils were unfrozen. Temperatures, at the time of testing, were recorded using thermocouples positioned at the surface, one-third and two-third depths, and the asphalt concrete-base layer interface in each structure. The average of the four temperature readings was used as the independent variable in the analyses. The minimum data population size available for analysis consisted of 30 average tensile strain measurements at pavement temperatures ranging from 8°C to 30°C (46°F to 86°F) for the cement stabilized base structure.

From regression analyses, the temperature/interfacial tensile strain trend for each of the three structures is shown in Figure 5.

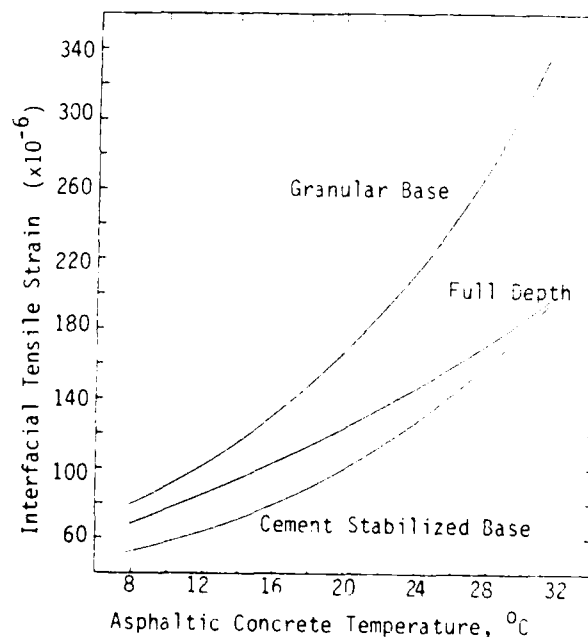


Figure 5 Asphaltic Concrete Temperature/Tensile Strain Trends

Interfacial tensile strains are highly dependent on temperature and for each struc-

ture increase by a factor of approximately three as average asphaltic concrete temperature increases from 10°C to 30°C (50°F to 86°F). At a given temperature, tensile strains are maximum in the untreated granular base structure and minimum in the cement stabilized base pavement. Based on the hypothesis that pavement distress such as asphaltic concrete fatigue is a function of the state of strain induced by traffic loads the field measurements reflect the importance of accurately incorporating the temperature dependency of highway construction materials in design and evaluation processes. Further pavement response analyses, incorporating additional pavement structures and encompassing a range of vehicle velocities, are ongoing.

SUMMARY

Instrumentation for recording structural responses of asphalt pavements to

REFERENCES

1. Shields, B.P., "Preliminary Report on Pavement Test Site: Alberta Secondary Road 794", Internal Report HTE/73/5, Alberta Cooperative Research Program, September, 1973.
2. Christison, J.T. and B.P. Shields, "Evaluation of the Relative Damaging Effect of Wide Base Tire Loads on Pavements", Proceedings of the Roads and Transportation Association of Canada, October 1980.
3. Christison, J.T., "In Situ Measurement of Pavement Behavior Under Load", Transportation Forum, Roads and Transportation Association of Canada, March 1985.
4. Christison, J.T., Anderson, K.O. and B.P. Shields, "In Situ Measurements of Strains and Deflections in a Full-Depth Asphaltic Concrete Pavement", Proceedings of the Association of Asphalt Paving Technologists, Vol. 47, pp. 398-430, 1978.
5. Christison, J.T., "Pavement Response to Heavy Vehicle Test Program: Part 1 - Data Summary Report, Vol. 8, Vehicle Weights and Dimensions Study, July 1986.
6. Pavement Design and Evaluation Committee (1959), "The CGRA Benkelman Beam Procedure", Canadian Good Roads Association, Ottawa, Technical Publication No. 12.

traffic loads has been developed and successfully installed in numerous structures. Tests carried out at instrumented facilities have provided detail information on the influence of traffic environmental and construction variables on the magnitude of pavement-base layer interfacial strains and pavement surface deflections. While extensively used to obtain quantitative assessments of the relative destructive effects of traffic loading conditions on pavements, the field measured responses are essential for verification of existing and/or development of improved overall pavement design and evaluation processes. Based on the hypothesis that pavement distress is a function of tensile strains induced by traffic, the developed pavement temperature-tensile strain trends for the three structures suggest that pavement distress is highly asphaltic concrete temperature and structure dependent.

NO 4214 987

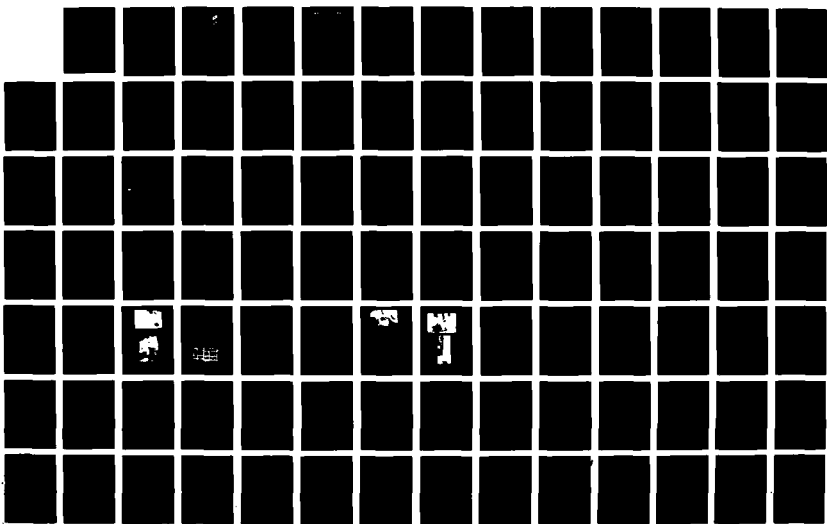
STATE OF THE ART OF PAVEMENT RESPONSE MONITORING
SYSTEMS FOR ROADS AND AIR... (U) COLD REGIONS RESEARCH AND
ENGINEERING LAB MANOVER IN V JANDO ET AL. SEP 89
CRREL-SR-89-23

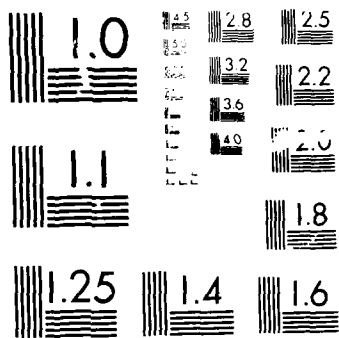
1/5

UNCLASSIFIED

F/8 13/2

NL





USE OF THE MULTIDEPTH DEFLECTOMETER FOR DEFLECTION MEASUREMENTS

Tom Scullion

Texas Transportation Institute
College Station, Texas

Al J. Bush III

Waterways Experiment Station
Vicksburg, Mississippi

ABSTRACT

The Multi-Depth Deflectometer (MDD) is an LVDT deflection measuring device which is retrofitted into pavement layers. A maximum of six MDD modules may be installed in a single 38mm (1.5 inch) diameter hole. The center core is attached to an anchor located approximately 2.1m (7 ft) below the pavement surface. Under the passage of a single load the MDD can be used to measure the depth deflection profile and the induced vertical compressive strains. After repeated loads the MDD can be used to measure the permanent deformations in each of the pavement layers.

In this paper the authors describe the MDD, the installation procedure and document observations made in full-scale experimental test pavements. These pavements were loaded with a Falling Weight Deflectometer (FWD) and trucks with different tire pressures 276 kPa and 758 kPa (40 psi and 110 psi). Analysis is included to illustrate how the MDD depth deflection profile can be used to backcalculate layer moduli. These moduli values are then compared with those backcalculated using the FWD surface deflections. Distinct tire pressure effects were noted in the measured vertical compressive strains, temperature effects were also identified.

A permanent MDD monitor site is under development in Texas which will include a flush mounted MDD together with low cost

weigh-in-motion and speed sensors. This will be able to identify the speed, weight and strains induced by each axle in the traffic stream. Another research activity is the mounting of an accelerometer on the center core which will monitor anchor movement.

The MDD's installed to-date have performed very well and they have the potential for becoming excellent tools for long term pavement monitoring.

INTRODUCTION

The Texas Transportation Institute (TTI) has been evaluating Multidepth Deflectometers (MDD) as pavement instrumentation tools since early 1988 (Scullion and Uzan, 1988). The system was developed in South Africa and has been used extensively as an integral part of their accelerated pavement loading program (Basson 1981, DeBeer 1988). The MDD is typically installed at the layer interfaces and is used to measure both the transient relative depth deflection profile and the permanent deformations in each layer. Figure 1 shows a schematic of a typical MDD which consists of modules with Linear Variable Differential Transformers (LVDTs).

The MDD modules are locked in position by turning the clamping nut which forces the steel balls outwards clamping them against the sides of the hole. The interconnecting rod is adjustable and

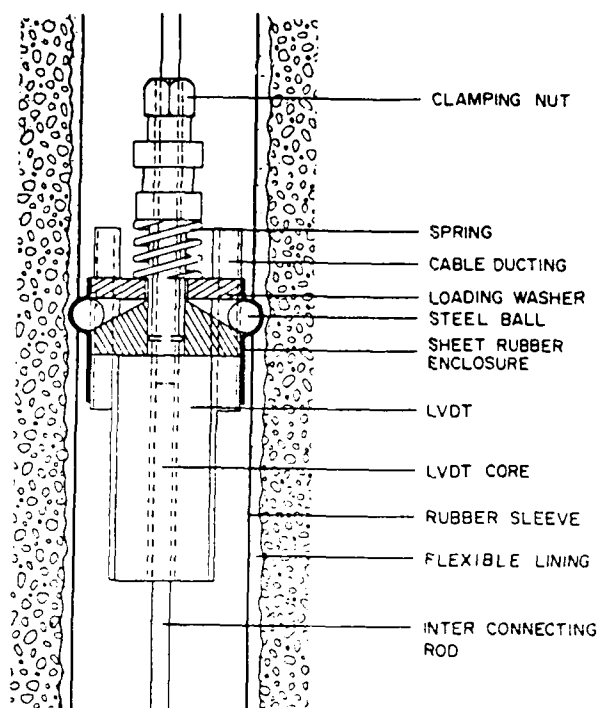


Figure 1. Components of a MDD Module.

contains LVDT cores at spacings which coincide with the module placement. A typical MDD installation is shown in Figure 2. In practice up to six modules may be placed in a single hole. The interconnecting rod is fixed to an anchor located at approximately 2.1m (7 ft) below the pavement surface. When data is being collected, a reinforced connector cable is attached which links to the data-capture system. When the MDD is not in use, a brass surface cap, which is flush with the surface, completely seals the hole.

Installation Procedure

In order for the MDD to operate effectively, special care has to be exercised in installing the unit. A percussion drill and a specially designed drilling rig are used to ensure a clean, vertical test hole. A 38mm (1.5 inch) diameter hole is drilled to a depth of approximately 2.1m (7 feet). The top 25mm (1-inch) of the pavement is drilled with a 64mm (2.5-inch) drilling bit for installation of the top cap. The hole is then lined with 2.5mm (0.1-inch) thick lining tube and the voids between the tube and the wall are filled with a rubber

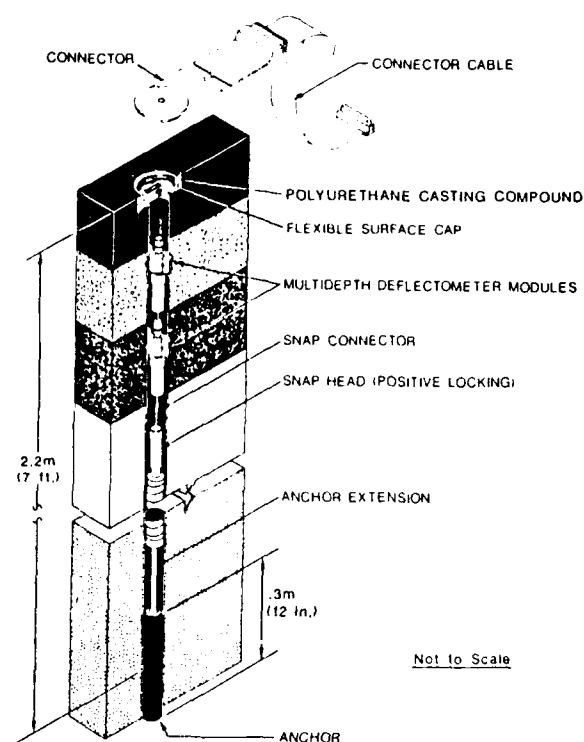


Figure 2. Pavement cross-section after MDD installation.

grout. The flexible lining tube provides waterproofing, a smooth surface and minimizes "cave-ins". The MDD anchorpin is locked in place using a fast setting cement/sand paste.

The MDD modules are installed into the correct predetermined position using an installation tool especially designed for the purpose. The module is guided to the correct position in the test hole and secured by turning the clamping nut at the top of the MDD module. Similarly all the other modules are installed. Once the modules are fixed in place, they are calibrated before use. The complete installation takes approximately 1 1/2 days. The hole is drilled, lined and the anchor is installed during the first day; the rubber grout needs approximately 12 hours to set (depending on the temperature). On the second day the MDD modules are installed and calibrated.

One of the major advantages of the MDD is that the modules can be extracted from the hole once testing is complete. With reference to Figure 2, the only parts of the system which cannot be extracted

are the anchor and hole lining. The MDD modules, center core, snap head connector and surface cap can be recovered for future use.

LVDT Selection

There are several factors which must be considered when selecting the appropriate LVDT. These include range, sealed vs. unsealed and type of LVDT. To date, both the E300 (range plus/minus 7.6mm or 0.30 inch) and E100 series LVDTs have been used. Typical MDD readings under FWD or Truck loadings and less than 2000 μ m (79 mils). Using the E300 series may require signal amplification, however they are easier to install and are recommended for long term testing. The E100 series may not require amplification, but are more difficult to install and can go out of range as the pavement deforms.

Hermetically sealed LVDT can be purchased and their use is recommended when long term monitoring > 1 year is to be performed. Unsealed units have been in operation for 12 months at the Texas A&M Research Annex without problem. The MDD hole is sealed so this prevents excessive moisture from entering, although condensation build up does occur. Unsealed units cost \$30 to \$40, the hermetically sealed units cost \$250 to \$350.

Only AC LVDT's have been used, although DC units are available. The AC units require external signal conditioning, whereas the DC units have the signal conditioner built in. Although the DC units would replace the expensive signal conditioner unit, little is known of their durability. The AC units are known to be extremely reliable.

Data Capture

TTI had developed a specialized data acquisition system for logging MDD pulses under Falling Weight Deflectometer and truck loads. A Compaq 386/20 microcomputer is used with a Data Translation circuit board, a sampling rate of 5000 reading per channel per second is used. Under FWD loading a 60 millisecond recording interval is used. Triggering has been automated based on a response of any of any sensor greater than a preset trigger level. The pretrigger

information, 100 data points, is stored and is included in the output record. For recording truck data, the truck length and speed are input, the sampling rate is automatically calculated and the triggering is automated. For trucks 1000 data points per channel are stored. The files created are read directly into LOTUS for display and analysis.

USES OF MDD

The MDD is used to monitor the pavement response under a single load or performance in repeated load tests. Under a single load the MDD measures the relative deflection between its position and the anchor. When the MDD is installed the no load output voltage is recorded. After repeated load, changes in the no-load reading measures the permanent deformation that has occurred. By placing the MDD's at layer interfaces, it is possible to monitor the deformation that has occurred in each layer of the structure.

To date, no repeated load tests have been performed using MDD in the USA, although some are planned for the summer of 1989. However, South African researchers have conducted numerous accelerated load tests over the past decade using their Heavy Vehicle Simulators (Freeme, 1982). The results of one of these investigations is shown in Figure 3 (DeBeer, 1988). This shows the performance of a lightly cemented granular base and thin surfacing under heavy loads. As shown, the induced rutting was measured to occur primarily in the cemented layer.

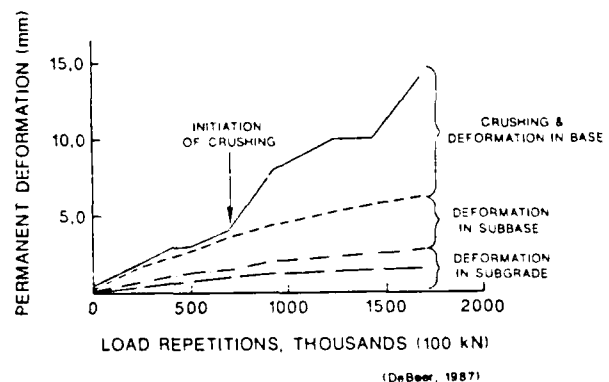


Figure 3. MDD results from accelerated road tests.

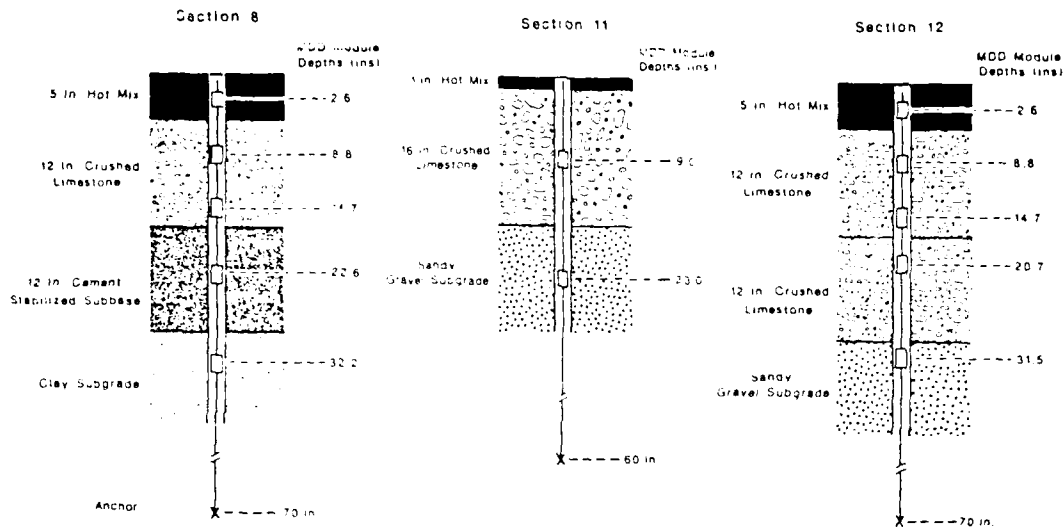


Figure 4. MDD Installation at the Texas A&M Research Annex.

In the remainder of this paper the observations of pavement response under Falling Weight Deflectometer (FWD) and Truck loadings are presented. The FWD observations are discussed in the next section.

FALLING WEIGHT DEFLECTOMETER TESTING

A Dynatest Falling Weight Deflectometer was used to test the three instrumented sections at the TTI Research Annex, Figure 4. The FWD surface geophones were fixed at 305mm (12-inch) spacing in all tests. With the current version of the MDD system the data acquisition is achieved via a connector cable as shown in Figure 2. This arrangement prevents the FWD loading plate from being directly lowered on top of the MDD installation. The FWD plate is therefore stationed as close as possible to the MDD hole, the distance from the MDD hole to the edge of the plate is usually set at 50mm to 100mm (2 to 4 inches). Typical MDD response under FWD loading is shown in Figure 5. This being for Section 12, note the decreasing deflection with depth.

To evaluate the repeatability of the Multi-Depth Deflectometers, the FWD load was dropped 14 times on Section 11. The maximum surface deflections (FWD) and maximum depth deflections (MDD) were recorded simultaneously and the summary statistics are shown in Table 1. Both the

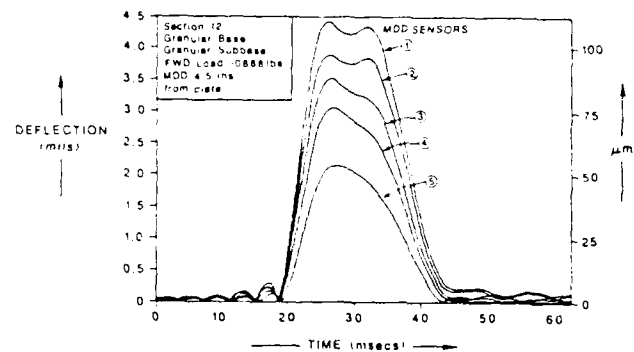


Figure 5. MDD response under FWD loading.

FWD Load (kN) (lbs)	FWD Deflections μm (mm)							MDD μm (mm)	
	W1	W2	W3	W4	W5	W6	W7	MDD1	MDD2
1.6	65	310	148	99	78	66	54	354	204
1.05	125.62	122.27	15.83	13.89	1.06	12.60	1.14	113.94	18.02
1.40	11.25	1.26	1.72	0.81	0.74	0.50	0.75	1.52	1.12
Standard Deviation	10.13	11.09	10.03	10.03	10.03	10.02	10.03	10.06	1.04
CV %	0.55	0.50	0.73	0.49	0.88	0.95	0.85	0.43	0.55

Table 1. Repeatability Measurement on Section 11, (n = 14)

FWD and MDD are highly repeatable.

In general, Non Destructive Testing of pavements is performed to characterize the in-situ moduli of each layer in the pavement structure. Several schemes are

available by which surface deflection data can be used to compute layer moduli. Validation of the results of the backcalculation process is often attempted by comparing the results with laboratory determined values. This process is difficult as it is very difficult to approximate the stress, environmental and material properties that exist in the field, particularly with unbound materials which have to be remolded. It is proposed that the MDD can be used to assist in validating the results of the modulus backcalculation process. By taking surface and depth deflections simultaneously under the FWD load two independent methods are available for back calculating layer moduli. The first using the FWD load and surface deflections, the second using FWD load and depth deflections.

To interpret the surface deflections, the backcalculation scheme proposed by Uzan was used (Uzan and Lytton, 1988). This consists of using a linear elastic program to generate a data base of theoretical deflection bowls for a range of modular ratios. Then using a pattern search technique, the measured bowls are matched with those in the data base (Uzan and Scullion, 1988).

To interpret the depth deflections a modification of the Uzan scheme was used (Scullion and Uzan, 1988). In this scheme the data base now consists of theoretical relative depth deflection profiles. The anchor movement is calculated for each modular ratio and automatically subtracted from the layer deflections to simulate the MDD measurements.

The FWD and MDD values collected on each of the three sections are shown in Tables 2, 3 and 4. Section 8 was modelled as 127mm (5-inch) asphalt over 305mm (12-inch) granular base and 305mm (12-inch) cement stabilized subbase, Section 12 was modelled as 127mm (5-inch) asphalt over 610mm (24-inch) granular base. Section 11 was modelled as 25mm (1-inch) asphalt over 406mm (16-inch) granular base. In all cases, a rigid layer was assumed to exist at 6.3m (250-inch). The modulus of the thin surfacing on Section 11 was fixed at 3450 MPa (500 Ksi), the modulus of all the other layers was calculated from either the surface or depth deflections. The results of the backcalculation analysis are shown in Table 5.

Table 5 provides a means of evaluating if layered linear elastic theory (and the backcalculation scheme used) do an adequate job of characterizing layer moduli. If there is reasonable agreement between surface and depth deflection moduli then it can be concluded that the pavement structure has been adequately modelled. For the three pavements tested, the following can be concluded.

- 1) Section 12 (Thick asphalt over thick granular base)

There is good correspondence between the layer moduli, particularly in the surface and base values. The high surface modulus 9000 MPa (1300 ksi) is realistic as the surface temperature at the time of test was 7°C (45°F). Subsequent, laboratory tests on the surface layer has yielded moduli in this range. It can be concluded that linear elastic theory produces adequate moduli values for this pavement.

- 2) Section 8 (Thick asphalt, granular base over cement stabilized subbase).

This is a difficult section to analyze. The cement stabilized layer is very stiff approaching lean concrete. As shown in Table 2, the MDD could give some surprising results. Note at the higher load level, there is little difference in deflection between MDD's 3, 4 and 5. This inverted deflection bowl is impossible to fit with linear elastic theory and hence the large errors were observed in matching measured and calculated deflections.

Nevertheless, at the low load level 49.2KN (11072 lbs), there is very good agreement between surface and depth moduli.

- 3) Section 11 (Thin Surfacing over thick granular base)

There is poor agreement between surface and depth deflection moduli. Using linear elastic theory appears to over predict the modulus of the pavement layers. The deflections and

Table 2. FWD and MDD Maximum Deflection Data for Section 8
at TTI Research Annex
(Edge of FWD Plate to Center of MDD hole = 114mm (4.5 inch))

FWD LOAD KN (LBS)	FWD SENSORS μm (MILS)							MDD μm (MILS)				
	1	2	3	4	5	6	7	1	2	3	4	5
49.2 (11072)	155 (6.09)	110 (4.34)	71 (2.78)	58 (2.30)	50 (1.96)	44 (1.73)	37 (1.45)	63 (2.48)	43 (1.68)	32 (1.25)	29 (1.16)	29 (1.14)
64.3 (14464)	238 (9.38)	154 (6.08)	101 (3.97)	84 (3.30)	72 (2.83)	61 (2.41)	50 (1.97)	77 (3.03)	51 (2.02)	33 (1.29)	31 (1.24)	28 (1.12)
816 (18352)	266 (10.48)	178 (6.99)	116 (4.58)	96 (3.77)	82 (3.25)	71 (2.74)	58 (2.29)	81 (3.21)	68 (2.07)	27 (1.07)	29 (1.15)	27 (1.06)

Table 3. FWD and MDD Maximum Deflection Data for Section 11 at
TTI Research Annex
(Edge of FWD Plate to Center of MDD Hole = 89mm (3.5 inch))

FWD LOAD (KN) LBS.	FWD SENSORS μm (MILS)							MDD μm (MILS)	
	1	2	3	4	5	6	7	1	2
75.3 (16943)	761 (29.96)	339 (13.36)	160 (6.31)	104 (4.11)	86 (3.38)	60 (2.36)	49 (1.93)	379 (14.91)	239 (9.44)
54.0 (12150)	574 (22.60)	257 (10.14)	123 (4.85)	83 (3.27)	67 (2.65)	48 (1.89)	37 (1.45)	303 (11.95)	184 (7.23)
48.7 (10966)	528 (20.82)	230 (9.05)	105 (4.15)	71 (2.79)	56 (2.20)	42 (1.65)	34 (1.33)	275 (10.83)	164 (6.46)
31.2 (7022)	350 (13.79)	134 (5.28)	64 (2.54)	41 (1.60)	32 (1.26)	25 (0.98)	21 (0.84)	182 (7.15)	105 (4.13)

Table 4. FWD and MDD Maximum Deflection Data for
Section 12 at TTI Research Annex
(Edge of FWD Plate to Center of MDD Hole = 114mm (4.5 inch))

FWD LOAD KN (LBS)	FWD SENSORS μm (MILS)							MDD μm (MILS)				
	1	2	3	4	5	6	7	1	2	3	4	5
48.4 (10888)	212 (8.36)	163 (6.41)	98 (3.85)	65 (2.58)	48 (1.91)	39 (1.53)	34 (1.33)	112 (4.41)	98 (3.88)	89 (3.52)	78 (3.06)	54 (2.14)
61.9 (13912)	228 (11.35)	217 (8.56)	132 (5.20)	91 (3.58)	56 (2.62)	55 (2.17)	44 (1.73)	155 (6.11)	139 (5.49)	127 (5.01)	111 (4.39)	80 (3.16)
78.7 (17704)	352 (12.88)	253 (9.96)	156 (6.14)	105 (4.13)	78 (3.08)	63 (2.49)	52 (2.05)	189 (7.46)	172 (6.78)	154 (6.08)	134 (5.29)	95 (3.75)

Section	Load, KN (LBS)	SURFACE DEFLECTION MODULI MPa (ksi)					DEPTH DEFLECTION MODULI MPa (ksi)				
		E _S	E _B	E _{SB}	E _{SG}	%Error	E _S	E _B	E _{SB}	E _{SG}	%Error
8	49.2 (11072)	10300* (1500)	446 (64.8)	14800 (2148)	100 (14.6)	1.96	10300* (1500)	563 (81.8)	13800 (2007)	110 (16.2)	7.1
8	64.3 (14464)	7760 (1126)	423 (61.5)	11200 (1623)	98 (14.3)	0.84	10300* (1500)	510 (74.6)	19300 (2802)	165 (24.0)	7.4
8	81.6 (18352)	10100 (1470)	444 (64.5)	13520 (1962)	106 (15.4)	0.55	10300* (1500)	760 (110)	34500* (5000)	169 (24.5)	10.4
11	75.3 (16943)	3450 (500)	452 (65.7)	- (-)	152 (22.0)	9.14	3450 (500)	361 (52.4)	- (-)	77 (11.2)	.01
11	54.0 (12150)	3450 (500)	437 (63.5)	- (-)	138 (20.1)	8.6	3450 (500)	270 (39.2)	- (-)	80 (11.6)	.05
11	48.7 (10966)	3450 (500)	421 (61.1)	- (-)	146 (21.2)	9.9	3450 (500)	254 (36.9)	- (-)	84 (12.2)	.03
11	31.2 (7022)	3450 (500)	400 (58.1)	- (-)	161 (23.4)	10.4	3450 (500)	222 (32.2)	- (-)	89 (12.9)	.03
12	48.4 (10888)	8900 (1291)	479 (69.5)	- (-)	143 (20.7)	4.9	9000 (1307)	482 (70.0)	- (-)	127 (18.4)	2.1
12	61.9 (13912)	8400 (1222)	456 (66.2)	- (-)	133 (19.3)	3.9	9700 (1405)	467 (67.9)	- (-)	99 (14.3)	1.8
12	78.7 (17704)	10300 (1497)	494 (717)	- (-)	144 (21.0)	4.0	9430 (1369)	464 (67.4)	- (-)	113 (16.4)	1.8

Table 5. Comparison of Moduli Independently Calculated using Surface and Depth Deflections.

1. E_S, E_B, E_{SB}, E_{SG} - Moduli of Surface, Base, Subbase, Subgrade
2. %Error - The error per sensor between measured and best fit theoretical bowl.
3. * - Hit moduli upper limit

strains induced in the base course and subgrade were measured to be 50 to 100% higher than those predicted using linear elastic theory. It is recommended that other theories be evaluated for modelling this pavement type.

By placing MDD's at various depths in a layer permits the calculation of the

average vertical compressive strain in that layer, simply by subtracting the maximum MDD values and dividing by the distance between them. Compressive strains in the granular base course were calculated for each of the three sections and the results are presented in Figure 6. It is noted that the strains in both Section 8 and 12 appear to increase linearly with load whereas the strains in

Section 11 are considerably higher and have a distinct curvilinear relationship. This appears to indicate that moving to a non-linear stress strain relationship for this pavement section is warranted.

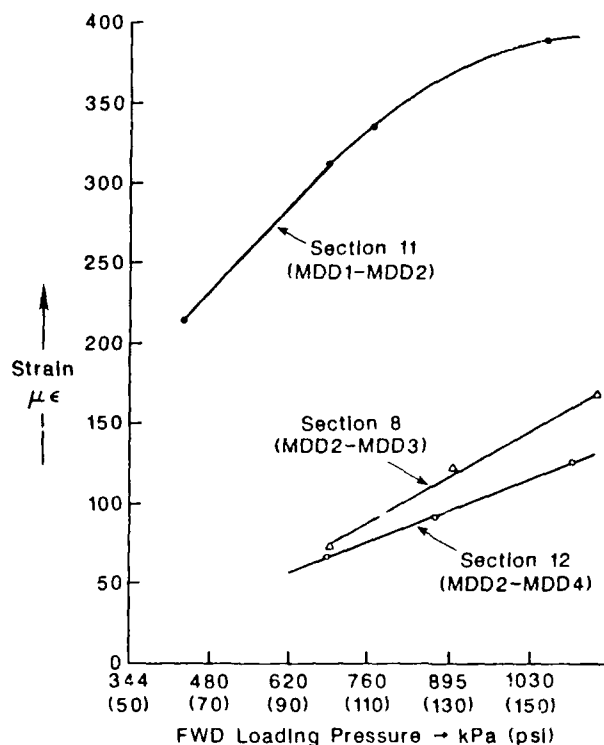


Figure 6. Vertical Compressive Strains calculated from Tables 2, 3, and 4.

RESPONSE UNDER TRUCK LOADS

Two sections at the Waterways Experiment Station's experimental test track were instrumented with MDD's in December, 1988. The layering information and MDD locations are shown in Table 6.

Section 12 has 127mm (5-inch) of asphaltic concrete directly on the subgrade whereas Section 10 has 102mm (4-inch) of surface over 102mm (4-inch) of crushed limestone base. The subgrade at both sites was lean clay.

Two fully loaded standard 3S2 vehicles (18 wheelers), one with all tires at a pressure of 276 kPa (40 psi), the other with pressures of 758 kPa (110 psi), were used to test the pavements. The loads on each wheel group shown are in Table 7, Wheel group 1 being the single tire steering axle all other wheel groups

Section	Thickness mm (ins)		MDD Locations mm (ins)			Anchor mm (ins)
	Surface	Base	1	2	3	
12	127 (5)	0 (0)	127 (5)	438 (17.25)	-	730 (28.7)
10	102 (4)	102 (4)	110 (4.3)	265 (10.4)	612 (24.1)	1850 (73)

Table 6. Layer Thicknesses and MDD Locations at WES

PRESSURE	WHEEL LOAD kN (lBS) ON EACH AXLE				
	1	2	3	4	5
Low	21.71 (4880)	38.41 (8635)	37.59 (8450)	36.76 (8265)	38.50 (8655)
High	21.88 (4920)	38.36 (8625)	36.61 (8230)	34.85 (7825)	37.43 (8415)

Table 7. Loads used to test WES Instrumented Sections

have dual tires.

A typical MDD output for the high tire pressure truck on Section 10 is shown in Figure 7. The MDD deflection responses for each of the truck's 5 axles are clearly visible. These curves represent the relative deflection responses at depths of 110, 265, and 612mm (4.3, 10.4, and 24.1-inch). From the information shown in Figure 7, it is relatively simple to compute the vertical compressive strains within the pavement layers.

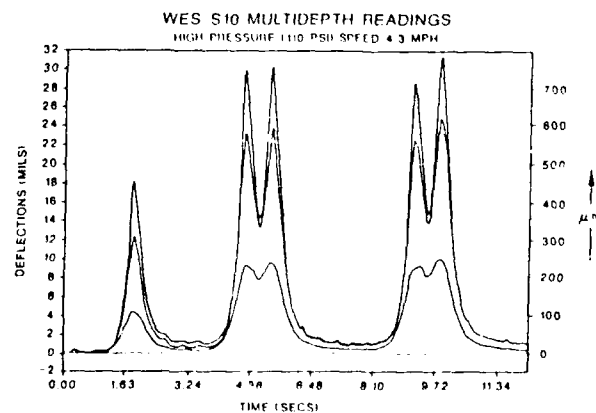


Figure 7. MDD response from Section 10 at WES.

Average base strains are calculated as the deflection measured by MDD 1 minus MDD 2 divided by the distance between the sensors, 155mm (6.1-inch). Similarly

strains in the subgrade are calculated by MDD 2 minus MDD 3 divided by the appropriate sensor spacing. Figure 8 shows the base and subgrade strains calculated from the deflection bowls shown in Figure 7. The maximum MDD deflections and strains are tabulated below in Table 8.

The summary data for all 12 runs (2 trucks x 3 speeds x 2 sections) is presented in Table 9. In this table only highest maximum deflections are reported (in Table 8 axle number 5 provided the highest maximum deflection). Note in Section 10 three MDD's were installed, therefore base and subgrade strains can be calculated. Section 12 had no base, it consists of 127mm (5 inches) of asphaltic concrete over the subgrade. The two MDDs were installed in the subgrade on Section 12, therefore only subgrade strains can be computed.

The subgrade strain results for section 12 are plotted in Figure 9. In all cases the high tire pressures increased the strain at the top of the

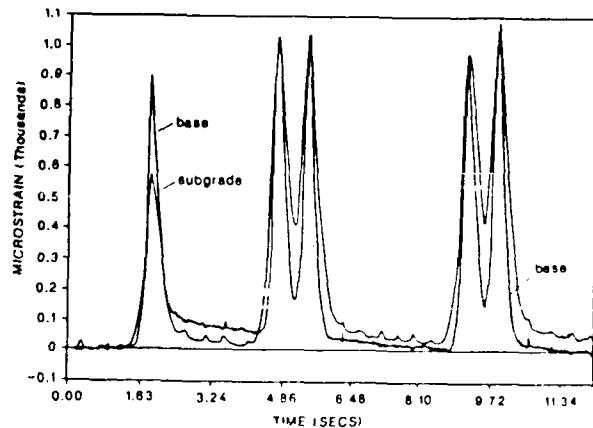


Figure 8. Corresponding strain calculated for Section 10 at WES.

Axle	Max. Multidrop Deflection μ m (mils)			Strain μ e	
	1	2	3	Base	Subgrade
1	450 (17.71)	313 (12.31)	112 (4.42)	885	565
2	746 (29.39)	589 (23.18)	219 (9.40)	1017	1002
3	759 (29.87)	604 (23.77)	245 (9.68)	999	1026
4	719 (28.29)	571 (22.49)	233 (9.18)	951	967
5	789 (31.08)	629 (24.76)	252 (9.91)	1035	1079

Table 8. Maximum Deflection and Strains, Section 10.

Section	Tire Pressure kPa (psi)	Speed Km/hr (mph)	Highest Max. Deflection μ m (mils)			Strains	
			MDD 1	MDD 2	MDD 3	Base	Subgrade
10	758 (110)	6.9 (4.3)	789 (31.08)	629 (24.76)	252 (9.91)	1035	1079
10	758 (110)	18.5 (11.5)	711 (28.00)	549 (21.63)	232 (9.13)	1045	909
10	758 (110)	38.1 (23.6)	630 (24.79)	491 (19.34)	210 (8.25)	888	806
10	276 (40)	7.1 (4.4)	742 (29.23)	581 (22.88)	242 (9.53)	1041	970
10	276 (40)	16.1 (10.0)	660 (25.98)	520 (20.49)	224 (8.83)	855	848
10	276 (40)	28.0 (17.4)	591 (23.26)	467 (18.38)	196 (7.81)	816	769
12	758 (110)	4.3 (2.7)	815 (32.09)	288 (11.33)	-	-	1693
12	758 (110)	19.8 (12.3)	689 (27.12)	256 (10.08)	-	-	1390
12	758 (110)	31.0 (19.2)	615 (24.21)	233 (9.17)	-	-	1228
12	276 (40)	7.4 (4.6)	724 (28.51)	262 (10.31)	-	-	1485
12	276 (40)	18.2 (11.3)	589 (23.20)	226 (8.90)	-	-	1167
12	276 (40)	30.0 (18.6)	543 (21.38)	213 (8.39)	-	-	1060

Table 9. Pavement Response to High and Low Pressures on Instrumented WES Sections.

subgrade by 10 to 15 percent. This vertical compressive strain in the subgrade is one of the parameters used by pavement designers to estimate rutting of the structure. Usually a fourth power relationship is employed relating strains and pavement life. Using such a relationship, a 10% increase in subgrade strain translates to over a 30% decrease in life.

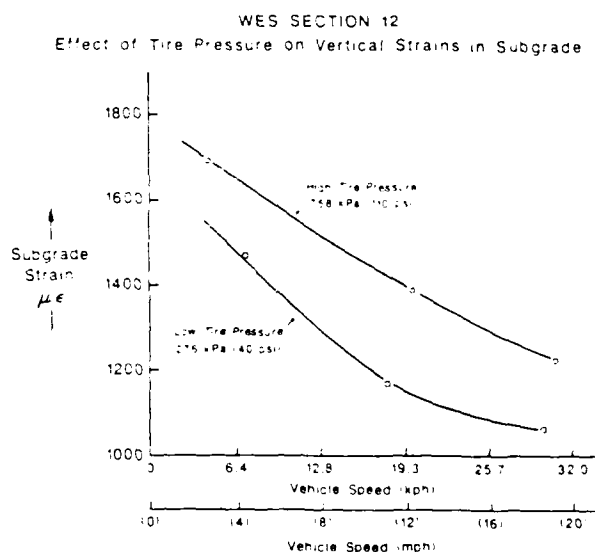


Figure 9. Effect of tire pressure on subgrade strains.

CONCLUSIONS AND RECOMMENDATION

The conclusions of this study are as follows:

- 1) The MDD appears to be an excellent tool for pavement research, it provides the capability of monitoring the response and performance of individual layers within the structure. The system is durable and gives repeatable responses. An instrumented site has been in operation at the Texas A&M Research Annex for over one year without any problems.
- 2) The MDD can be used to assist in validating modulus backcalculation procedures. The layer moduli obtained from interpreting surface deflections is frequently used to

estimate critical strains within the pavement layers. These strains can be measured with the MDD. The results presented in this paper concluded that the linear-elastic backcalculation scheme worked well with thick 125mm (5-inch) surfacing, but poorly on the section with thin 25mm (1-inch) surfacing and thick granular base. On the thin pavement, the linear elastic approach would have under estimated vertical compressive strains by 50 to 100%.

- 3) Under truck loading the MDD monitored that as tire pressures increased from 276 kPa to 758 kPa (40 to 110 psi), the strain at the top of the subgrade increased by 10 to 15%.

Efforts are underway in Texas to improve the MDD system. These include the following:

- 1) An experimental version of the MDD is being developed with an accelerometer (or geophone) mounted on the center core and anchor. This will permit measurement of the actual anchor movement, which can then be compared with the calculated movement.
- 2) The top cap is being redesigned so that the cables can be placed in a shallow saw cut. The connector cable will no longer be required. The MDD system will therefore be permanently installed flush with the surface. The FWD load plate can then be placed directly over the MDD hole.
- 3) An evaluation is being made of using DC rather than AC LVDT's. The DC units are simpler to use and will make the system less expensive as the signal conditioner box will no longer be required. However, one concern is the durability of the DC compared with the AC units.

It is also planned to evaluate if the MDD can be used in conjunction with new Weigh-in-Motion technology to develop a low cost pavement instrumentation system. In the near future, an MDD and Piezo-electric film strip will be installed beside one of the State's exist WIM Stations. Such a system would be able to

record for each axle, the axle load, and strains induced in each layer.

ACKNOWLEDGMENTS

The Texas Department of Highways and Public Transportation has sponsored the MDD studies in Texas. The support of Bob Briggs and Bob Guinn of the Pavement Management Section is acknowledged. The Waterway Experiment Station installation is part of the Central Tire Inflation pressure study which is sponsored by the National Forestry Service, the Federal Highways Administration and Corp of Engineers.

REFERENCES

1. Basson, J. E. B., Wijnberger, O. J., Skultety, J., "The Multidepth Deflectometer: A Multistage Sensor for the Measurement Deflection and Permanent Deformations at Various Depths in Road Pavements", Technical Report RP/3/81, Institute of Transportation and Road Research, South Africa, February 1981.
2. DeBeer, M., Horak, E., Visser, A. T., "The Multidepth Deflectometer System for Determining the Effective Elastic Moduli of Pavement Layers". First International Symposium on NDT and Backcalculation of Moduli ASTM Conference, Baltimore, Maryland, 1988.
3. Freeme, C. R., Maree, J. H., and Viljoen, A. W., "Mechanistic design of asphalt pavements and verifications using the Heavy Vehicle Simulator". Proceedings 5th International Conference on the Structural Design of Asphalt Pavements. Vol I, pp 156-173, Delft, Holland, 1982.
4. Scullion, T., Brigg, R. C., Lytton, R. L., "Using the Multidepth Deflectometer to Verify Modulus Backcalculation Procedures" paper to the First International Symposium on NDT of Pavements and Backcalculation of Moduli, ASTM Conference, Baltimore, Maryland, 1988.
5. Scullion, T., Uzan, J., Yazdani, J. I., Chan, P., "Field Evaluation of the Multidepth Deflectometers", Texas Transportation Institute Research Report 1123-2, College Station, Texas, September, 1988.
6. Uzan, J., Lytton, R. L., and Germann, F. P., "General Procedures for Backcalculating Layer Moduli", First Symposium on NDT of Pavements and Backcalculation of Moduli, ASTM, Baltimore, Maryland, July, 1988.
7. Uzan, J., Scullion, T., Michalek, C. H., Parades, M., and Lytton, R. L., "A Microcomputer Based Procedure for Backcalculating Layer Moduli from FWD Data", Texas Transportation Institute Research Report 1123-1, College Station, Texas, September, 1988.

**Session 6:
NDT in Cold Regions**

**NDT IN COLD REGIONS: A REVIEW OF THE
STATE-OF-THE-ART OF DEFLECTION TESTING**

N. F. Coetzee
R. G. Hicks

Dynatest Consulting, Inc.
Oregon State University

ABSTRACT

This paper provides an overview of the state-of-the-art of Non-Destructive Testing (NDT) of pavements, primarily from the structural response perspective. For the most part, in terms of typical equipment currently in use, this involves measurement of surface deflections under applied loads. The various measuring device categories, based on loading characteristics, are briefly discussed, i.e. static or slowly moving load, dynamic vibratory load, and dynamic impulse load. Perceived advantages and disadvantages of the loading characteristics are noted.

Typical currently available equipment in each category is briefly described, and data on the operating characteristics of each, as published by various researchers, is provided. The increasing use of Falling Weight Deflectometers (FWDs) is discussed, and the most recent data on availability, based on manufacturer's information, is provided. The use of NDT data in analyzing specific phenomena associated with pavements in cold regions, such as load restrictions and load related damage during spring thaw, is also discussed.

INTRODUCTION

Evaluation of pavement condition is desirable from both a network level, for pavement management system purposes, and

a project level for specific rehabilitation design purposes. Testing techniques for evaluation can generally consist of destructive measures, usually involving removal of material for laboratory testing purposes, or in-situ non-destructive testing (NDT) approaches. This paper provides an overview of the state-of-the-art of pavement NDT, primarily from the structural response perspective, with general indications of significant applications for cold regions. Other NDT techniques are available for consideration of layer thicknesses, shape and roughness, surface distress and surface texture (1). The most common NDT approach for pavement structural evaluation involves consideration of surface deflections under an applied load using various types of equipment, ranging from the Benkelman beam, originally used in 1956 (4), to the current equipment of choice viz. the Falling Weight Deflectometer (FWD). Other approaches, such as spectral analysis of surface waves (SASW) (5,6) and laser measurements of deflections under moving loads (7) are at various stages of development and are not in common usage at this point.

TYPES OF NDT DEFLECTION MEASUREMENTS

The commonly used NDT equipment for deflection testing can be categorized according to the nature of the load applied to the pavement surface. Three

characteristic loading modes currently exist: static or slowly moving load, steady state vibratory load and transient impulse load. Each is discussed briefly, in turn. Complete descriptions are available in References 1, 2, 3 and 4.

Static or slowly moving load.

Equipment for measuring deflection that falls into this category includes the plate loading test, the Benkelman or deflection beams, the curvature meter and the automated deflection beams such as the California Traveling Deflectometer, La Croix Deflectograph, the Transport and Road Research Laboratory (TRRL) Pavement Deflection Data Logging (PDDL) machine, and the CEBTP Curviameter. Use of this type of equipment involves a realistic load magnitude, since an actual vehicle applies the load or provides the reaction frame. The equipment itself varies in cost, sophistication and complexity, and production capability is related to this. For instance, the automated equipment can provide high measurement coverage, taking deflection measurements at 3.5 to 12m (11 to 40 ft.) spacings while moving at a speed of 2 to 18 kph (1.25 to 11 mph) (1, 4). The major disadvantages associated with this type of equipment are:

- (i) Load duration is typically not representative of traffic load duration. Flexible pavement material response is affected by load duration, so that the measured deflections may not be representative of those expected under dynamic traffic loads. This is illustrated by the fact that, for instance, Benkelman beam deflections depend on the technique used for measurement i.e. whether the rebound method, where the probe is placed between the loaded wheels which are then moved away, or the WASHO method, where the deflection is measured as the loaded wheels approach the probe, is used. The automated beams provide measurements similar to the WASHO method, which may be about half that measured using the rebound method (1).

- (ii) A fixed reference point is required, and this is provided by the beam supports. Problems arise if the support points fall within the deflection basin created by the wheel load (1, 4).

- (iii) Measurement of the deflection basin itself is difficult. Typically only center deflections are measured.

Steady state vibratory load.

Equipment falling in this category includes the commonly available commercially produced Dynaflect and Road Rater, as well as the custom built Waterways Experiment Station (WES) 16 kip Heavy Vibrator and Federal Highway Administration (FHWA) Cox Vibrator. All of these devices produce a sinusoidal vibration on the pavement surface using a dynamic force generator (1, 2, 3, 4). This sinusoidal force is superimposed on a static preload placed on the pavement surface, as shown in Fig. 1. The preload must be larger than one-half the peak-to-peak dynamic sinusoidal force in order to prevent the load plate from lifting off the pavement surface during the loading period. Frequency and dynamic force may be variable, with an approximately 40kN (9000 lb.) maximum force currently possible with commercially produced equipment, and a frequency range of 5 to 80 Hertz (Hz) (4). The WES Heavy Vibrator uses a 133kN (30000 lb.) peak-to-peak force and a 71kN (16000 lb.) static preload, which requires use of a fairly large vehicle. It has a 5 to 90 Hz frequency range. Advantages of this type of equipment include:

- (i) Deflection basins can be measured
- (ii) No fixed reference is needed since velocity transducers are used
- (ii) Speed of data measurement
- (iv) Relatively low cost.

Disadvantages include:

- (i) Load characteristics that may be unrealistic in terms of magnitude, duration and repetition. A moving wheel load typically applies a discrete load pulse to the pavement, followed by a rest period, unlike the repeated steady state forced vibration mode employed by this type of equipment.
- (ii) The static preload is of a similar order of magnitude as the peak-to-peak dynamic force and has a significant effect on the state of stress in the pavement. In stress sensitive materials this affects the deflection response and possibly the interpretation of the response.

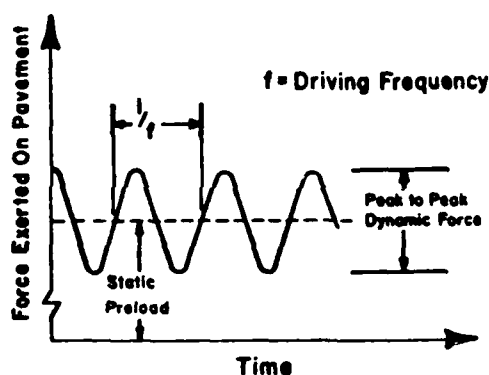


Fig. 1 Typical dynamic force output of steady state vibrators
(From Ref. 4)

Transient impulse load.

The equipment falling into this category are typically known as Falling Weight Deflectometers (FWD). A dynamic impulse load is applied to the pavement by dropping a mass from some specific height to the pavement, with the load transferred through a buffer system to the load plate, as shown in Fig. 2. An idealized load pulse is shown in Fig. 3. The load magnitude can be varied by varying mass and height for a given test, and the width of the load pulse is controlled by buffer characteristics to simulate a moving wheel load. This is

typically of the order of .025 to .035 seconds. Load ranges available are from 5kN to 245kN (1500 lb. to 55000 lb.) on different machines. Commercially available FWDs are marketed by Dynatest, Phoenix, and KUAB.

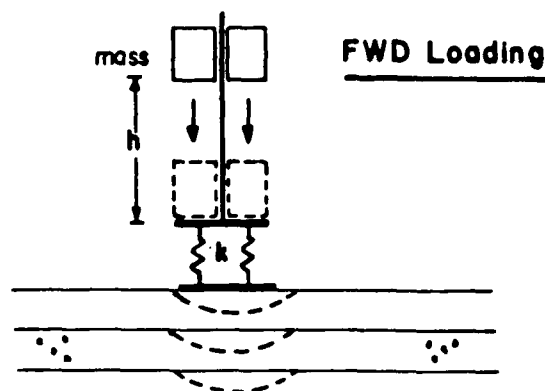


Fig. 2 Basic principle of Falling Weight Deflectometer (FWD of IDM)
(h = drop height)
(k = buffer constant)
(From Ref. 4)

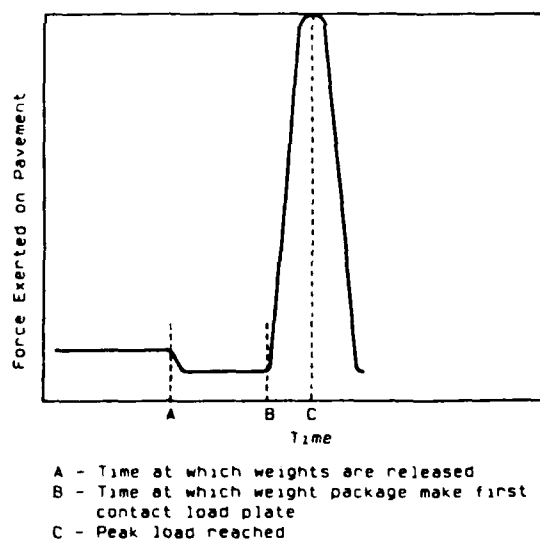


Fig. 3 Typical force output of Falling Weight Deflectometer.
(From Ref. 3)

The makers of Road Rater have recently introduced an FWD also, known as the JILS system. Deflection basins are measured with up to 7 sensors, and all data collection and equipment func-

tions are automated through the use of computers. Advantages of the impulse deflection devices include:

- (i) Deflection basins can be measured very accurately
- (ii) No fixed reference is necessary since, typically, velocity transducers are used
- (iii) Speed and ease of data acquisition
- (iv) Traffic loads expected on the pavement can be simulated in terms of magnitude, duration and repetition
- (v) No preload is required
- (vi) A wide range of loading is possible.

The major disadvantages of the FWDs are that they have a relatively high initial cost and are relatively complex systems. Maintenance and operational costs for FWD's may be significant, depending on the type of FWD being used.

TYPICAL NDT DEFLECTION EQUIPMENT, TRENDS AND DEVELOPMENTS

Characteristics of commercially available equipment have been summarized in various publications (1, 2, 3, 4), and Table 1 from one of these publications (3) is included here. An excerpt from a tabulated field evaluation, related to operational characteristics, from Ref. 4 is included as Table 2. The information in Tables 1 and 2 is slightly dated, but is supplemented with additional information in this section.

The major trend in deflection measurements appears to be the increasing popularity of the FWD equipment. For instance, as of 1987, only 11 states were using FWDs, while one state was considering the purchase of an FWD (4). Currently, at least 25 states and 1 territory own or are in the process of acquiring FWDs. Also, the Strategic Highway Research Program (SHRP) is using FWDs for deflection measurements in the Long Term Pavement Performance (LTPP) program. A total of about 70 FWDs are in use in the USA, and probably twice as

many in the world. One state owns 7 machines and has 4 on order. The reasons for this trend appear to be related to the productivity of the equipment, the ability to measure deflection basins similar to those produced by a moving wheel load, as well as the accuracy and reproducibility of the measurements. These features are ideally suited to applications in terms of mechanistic design procedures, which are generally the direction in which pavement analysis and design has been heading in the recent past. Developments in terms of this type of NDT measurement have been, until now, mainly related to specific improvements to the FWD equipment available. Table 3, based on information provided by the FWD manufacturers, provides information on currently available models. Technical specifications can be obtained from the manufacturers that will update the information in Table 1. Performance characteristics may vary widely between the types listed in Table 3, particularly in terms of deflection measurement accuracy and repeatability, as well as equipment reliability. To some extent these issues will be addressed by the independent calibration verification techniques being developed by SHRP.

Some of the newer developments for the equipment includes options such as increased number of deflection sensors, sensor locations allowing testing of longitudinal joints while being aligned with the traffic direction, fluid filled load pads to ensure even pressure distribution under the load plate and larger range sensors.

Table 1a Characteristics of commercially available nondestructive testing (NDT) devices (1 in = 25.4mm, 1 lb = 4.45N) (From Ref. 3)

Device Name	Principal of Operation	Load Actuator System	Min. Load	Max. Load	Static Weight on Plate	Type of Load Transmission	Method of Recording Data
Benkelman Beam (AASHTO)	Deflection Beam	Loaded Truck Axle	N/A	N/A	N/A	Truck Wheels	Manual
Deflection Beam (British)	Deflection Beam	Loaded Truck Axle	N/A	N/A	N/A	Truck Wheels	Manual
La Croix Deflectograph	Mechanical Deflection Beam	Moving Truck Loaded with Blocks or Water Weights	Empty Truck Weight	Loaded Truck Wheel Weight	N/A	Truck Wheels	Manual, Printer, or Automated
Dynaflect	Steady State Vibratory	Counter Rotating Masses	1,000	1,000	2,100	Two 18" dia Urethane-Coated Steel Wheels	Manual, Printer, or Automated
Model 400 B Road Rater			500	2,800	2,400	Two 6" by 7" Pads with 5.5" Center Gap ^{xxx}	
Model 2000 Road Rater	Steady State Vibratory	Hydraulic Actuated Masses	1,000	5,500	3,800	Circular Plate 18" dia ^{xx}	Manual, Printer, or Automated
Model 2008 Road Rater			1,000	8,000	5,800		
KUAB 50 Falling Weight Deflectometer	Impulse	Two Dropping Masses	1,500	12,000	?	Sectionalized Circular Plate 11.8" dia ^x	Manual, Printer, or Automated
KUAB 150 Falling Weight Deflectometer			1,500	35,000	?		
Dynatest Model 8000 Falling Weight Deflectometer	Impulse	Dropping Masses	1,500	24,000	?	Circular Plate 11.8" dia	Manual, Printer, or Automated

^x Solid Plates and Plates of Other Diameters are Available

^{xx} Plates of Other Diameters are Available

^{xxx} Circular Plates are Available

Table 1b Characteristics of commercially available nondestructive testing (NDT) devices (Continued) (1 in = 25.4mm) (From Ref. 3)

Device Name	Type of Carriage	Type of Prime Mover	Basic Cost	Contact Area	Vibratory Freq. & Range	Deflection Measuring System	Number of Deflection Sensors	Normal Spacing of Sensors	Load Measuring System
Benkelman Beam (AASHTO)	N/A	N/A	\$1,000	N/A	N/A	Dial Indicator	1	N/A	None
Deflection Beam (British)	N/A	N/A	\$1,500	N/A	N/A	Dial Indicator	1	N/A	None
La Croix Deflectograph	Truck	None	\$166,500 ^{xx}	N/A	N/A	Inductive Displacement Transducers	2 (one in each wheel path)	N/A	None
Dynaflect	Trailer	Tow Vehicle	\$22,185	~32 in ²	8 Hz	Velocity Transducers	5	Center & at 1' Intervals	None
Model 400 B Road Rater			\$30,580	36 in ²			4		
Model 2000 Road Rater	Trailer ^x	Tow Vehicle	\$40,800	254 in ²	5 Hz to 70 Hz	Velocity Transducers	4	Center & at 1' Intervals	Load Cell
Model 2008 Road Rater			\$64,000	254 in ²			4		
KUAB 50 Falling Weight Deflectometer	Trailer	Tow Vehicle	\$70,000	109 in ²	N/A	Seismic Deflection Transducers	5	Center & 0.6' to 8.0'	Load Cell
KUAB 150 Falling Weight Deflectometer			\$85,000	109 in ²			5		
Dynatest Model 8000 Falling Weight Deflectometer	Trailer	Tow Vehicle	\$88,500	109 in ²	N/A	Velocity Transducers	7	Center & 0.6' to 7.4'	Load Cell

^x Earlier versions of the Model 400 were mounted on vehicles.

^{xx} \$71,000 without truck but requires 1 to 3 man months to install on purchaser's vehicle

Table 2 Summary of field evaluation of selected equipment
(Operational Characteristics only - Abridged from Ref. 4)

	Benkelman Beam	Curviameter	Dynalect	Dynatest 8000 FWD	KUAB 150 FWD	Phoenix ML10000 FWD	Road Rater 2000
Operating Crew Size							
(a) Number of operators (including driver) used in field study	2	3-4	1	1	1-2	1-2	1
(b) Number of operators (including driver) used in routine work	2	2	1	1	1	1	1
Productivity (decimal minutes)							
(a) Average total time* (from arrival to departure, including set-up time)**	4.3 (1.4)	4.2 (4.2)	1.2 (1.2)	0.9 (0.3)	2.9 (0.48)	5.0 (0.55)	3.9 (0.43)
(b) Maximum total time	14.0	25.0	2.6	3.0	10.0	9.6	15.0
(c) Minimum total time	1.8	0.5	0.6	0.5	1.0	2.8	2.3
(d) Average test time (after set-up to departure)**	3.2 (1.1)	2.3 (2.3)	0.9 (0.9)	0.5 (0.17)	1.4 (0.23)	4.4 (0.49)	3.4 (0.38)
(e) Maximum test time	13.7	9.5	1.7	1.4	3.4	9.1	11.0
(f) Minimum test time	0.5	0.3	0.4	0.3	0.5	2.3	1.9

* In-service pavements only

** Times in parenthesis are average time divided by
number of deflection measurements performed.

Table 3 Current FWD equipment available
(Manufacturer's Information)

<u>Manufacturer</u>	<u>Models</u>	<u>Load Range</u>	
		<u>kN</u>	<u>(kips)</u>
Dynatest	8000	6 - 120	(1.5 - 27)
	8081	28 - 245	(6.5 - 55)
JILS	JILS 10	4 - 44	(1 - 10)
	JILS 20	8 - 107	(2 - 24)
KUAB	2M-14	12 - 62	(3 - 14)
	2M-23	12 - 102	(3 - 23)
	2M-33	12 - 147	(3 - 33)
	2M-44	12 - 196	(3 - 44)
Phoenix	ML 6	10 - 60	(2.2 - 13.5)
	ML 11	10 - 110	(2.2 - 24.7)
	ML 25	50 - 250	(11.2 - 56.2)

COMPARISON OF MEASURED DEFLECTIONS AND EQUIPMENT

The various types of equipment discussed in the preceding section have been compared and evaluated during various studies using different approaches

and criteria (2, 3, 4, 5, 6). Typically not all types of equipment are included in all studies. In particular, the automated beams are seldom used in the U.S.A. and hence have not been readily available for comparisons in the field, although a CEBTP Curviameter was in-

cluded in a recent study (4). However, the Benkelman beam has been included in all the listed studies, and this may provide an indication of deflection measurements that could be expected from the automated beams (1). Operational characteristics are such that the FWD appears to be the most efficient and versatile piece of deflection testing equipment available, as evidenced by the information presented in Table 2, which was measured during the most recent comparison study (4). It should be noted, of course, that the Benkelman beam will always have the advantage of simplicity and low initial cost over most other equipment. However, the general consensus is toward the use of equipment which can measure deflection basins, particularly if the information is to be used in analyses based on mechanistic design procedures (3, 4).

From a technical standpoint relating to the mechanistic approaches, the questions that arise generally relate to the reliability and accuracy of the deflections measured, as well as comparisons with actual deflections induced by moving wheel loads. Hoffman and Thompson (9), in comparing Benkelman beam, Road Rater (RR), Dynatest FWD and actual deflections under a moving wheel conclude that: "Overall, the FWD is the best NDT device to simulate pavement response under moving loads. The RR, because of harmonic loading without rest periods and static preload, induces pavement deflections lower than those achieved with the FWD and moving loads." They also concluded that RR and FWD deflections are significantly different; that they are correlated; that surface deflections are highly sensitive to RR load and frequency and that RR deflections should be converted to FWD values for structural evaluation purposes. They could not predict Benkelman beam deflections from RR measurements. An accelerometer embedded in the pavement was used to measure actual pavement deflections, and excellent agreement was found when compared with FWD measured deflections, as shown in Fig. 4. This study considered one piece of equipment from each characteristic load group, and the conclusions indicate that the static or slow moving load does not represent traffic loading very well, while the FWD does.

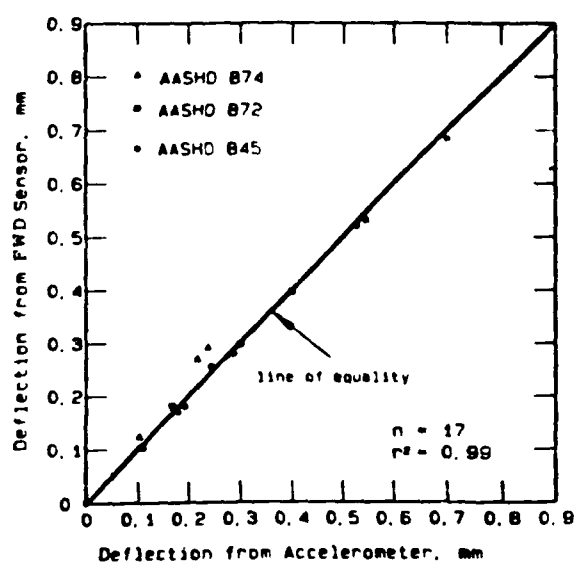


Fig. 4 FWD versus accelerometer deflections. (From Ref. 9)

Similar specific studies are reported by Ullidtz (10), and again, as shown in Fig. 5, the FWD very accurately simulates a moving wheel load. Fig. 5 also clearly illustrates the differences between Benkelman beam, FWD and actual deflections. Note that the moving wheel load is the same wheel for both the moving wheel (accelerometer) and the Benkelman beam deflections.

Fig. 5 illustrates one end of the spectrum of problems associated with using measured deflections to evaluate the effects of a moving wheel load on a pavement. It is apparent that the static or slow moving load substantially overestimates the moving wheel deflections. This is probably associated with non-linear and time-dependent pavement material response. These types of response can cause difficulties, in general, with extrapolation from one load level to another, as indicated by Smith and Lytton (3), who illustrate the point with deflections extrapolated from measurements by a light load vibratory device being very different from the actual deflections measured at higher load levels by the FWD. Obviously such an extrapolation would introduce gross errors into the design process for higher loads. Hudson et al. (4) allude to this problem, but indicate that the pavements tested during their study do not show

evidence of such non-linear behavior. However, other researchers have documented similar problems. Ullidtz (10), for instance, extrapolated measurements from a Heavy Vibrator (similar to the WES 16 kip) to the same load levels as used by an FWD and found significant differences. In fact, this problem is one of the reasons behind the development of the Heavy Weight Deflectometer (HWD) which has a load range of 28kN to 245kN (6500 lbf. to 55000 lbf.) and is intended for testing heavy load pavements. Obviously, the problem of non-linear material response can be dealt with by taking deflection measurements at differing load levels, preferably spanning the design load level. The multiple load level ability of the FWDs makes this a relatively simple procedure for the dynamic impulse load equipment.

Three basic approaches are commonly used viz. component analysis, deflection based or analytically based procedures (11). Various publications have covered these approaches in detail (11, 12, 13, 14, 15, 16). The analytically based procedures (16, 17, 18, 19, 20, 21, 22, 23, 24, 25, 26, 27, 28), usually involving back calculation of layer moduli from deflection basin data, appear to have the most promise for application in cold regions. Specific systems have been developed for these applications, such as the Alaska overlay design method, for instance, by Hicks et al. (24, 28). During most of the year, use of NDT deflection data is no different in cold regions than elsewhere. However, the critical consideration usually involves the spring-thaw period, when pavements may be in a severely weakened condition as the thaw front progresses downward.

USE OF NDT DEFLECTION DATA IN COLD REGIONS

Typical applications of deflection measurements are directed at evaluating pavement structural response for use in determination of structural adequacy as well as designing rehabilitation alternatives (1).

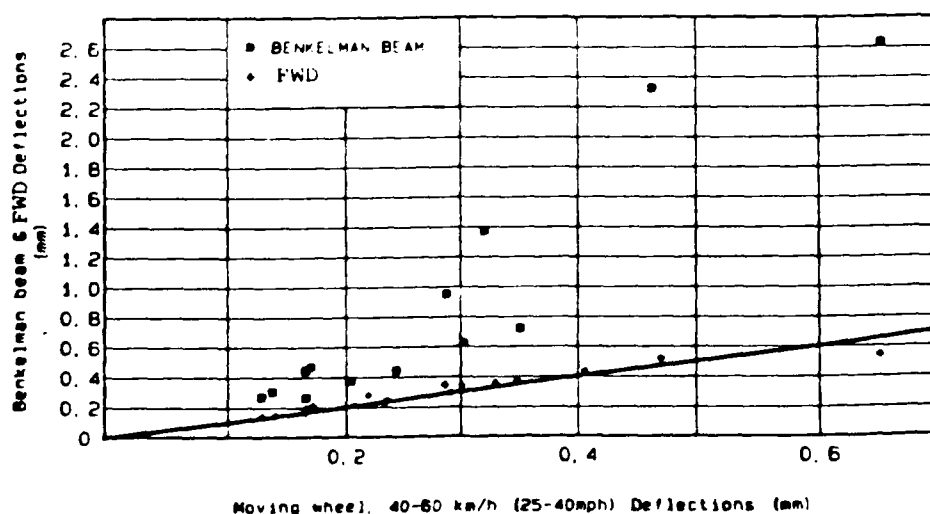


Fig. 5 Comparison of deflections (μm) measured under a moving wheel load, the FWD, and Benkelman beam tests. (From Ref. 10)

During this period, when the pavement is partially thawed, drainage of the upper layers is inhibited by the underlying frozen material, and deflections under load increase significantly. Damage associated with these higher deflections is also significantly higher than what would occur in the thawed pavement under the same load. To minimize these effects many authorities apply load restrictions during the critical thaw period. Mahoney et al. (18) have published, for instance, the approach developed for the State of Washington. Typically, deflections are monitored during the spring, and load restrictions applied when some predetermined deflection is observed. Fig. 6 provides an example of deflections measured during spring thaw in Alaska at various load levels, and Fig. 7 shows the estimated equivalent thaw depths associated with these deflections. Load related damage factors are being developed from this data, which will be published in the future. It is of interest to note that maximum damage does not necessarily coincide with maximum deflections.

CONCLUSIONS

An overview of NDT deflection testing equipment, trends and developments has been provided. Typical equipment and

operating characteristics are provided. Use of NDT deflection data has been briefly described, with indications of applications specific to cold regions. Specific conclusions include:

- 1) Various types of NDT equipment are available for measuring pavement surface deflections.
- 2) Not all NDT equipment can simulate the effect of moving wheel loads, and extrapolation to load levels different from those at which the deflection were measured may be incorrect. The impulse load equipment (FWD's) appear most suited to simulating typical wheel loads.
- 3) There appears to be a trend toward using FWDs for deflection measurements due to their productivity, accuracy, repeatability and realistic, variable load capabilities.
- 4) Use of NDT deflection data in cold regions is generally similar to that in other regions except during the critical spring thaw period. It may be possible to predict thaw depth from deflection basin evaluation. Load related damage can be evaluated, using mechanistic analysis techniques, and used for load restriction applications.

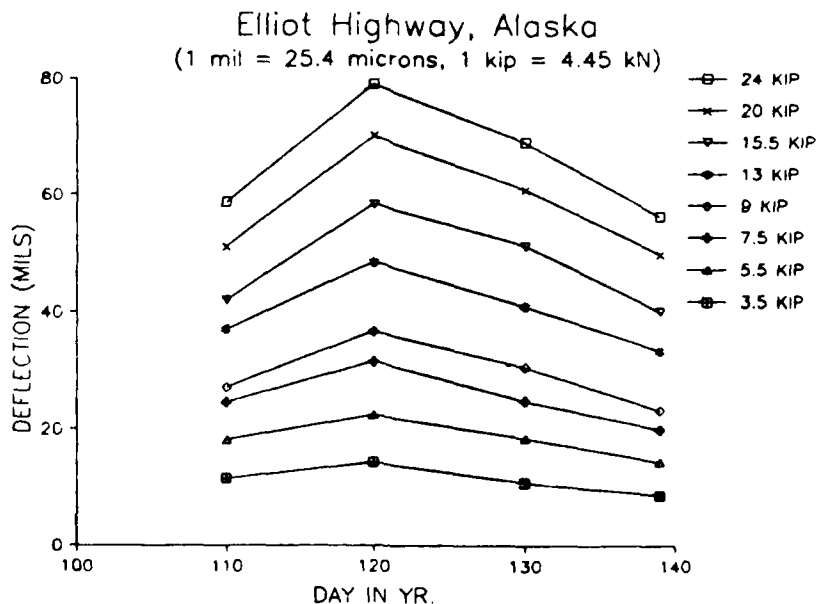


Fig. 6 Spring thaw normalized deflections

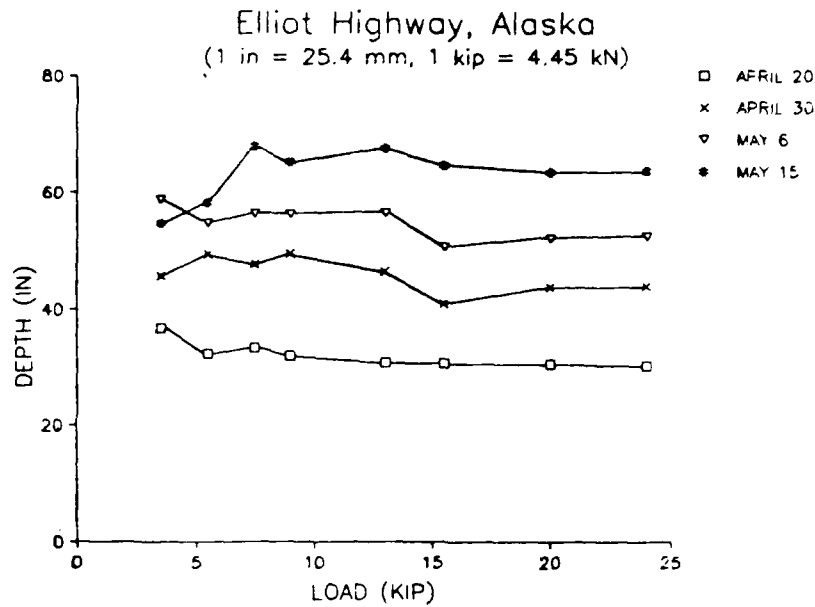


Fig. 7 Estimated equivalent thaw depth

REFERENCES

- (1) Epps J.A. and Monismith C.L. "Equipment for Obtaining Pavement Condition and Traffic Loading Data", NCHRP Synthesis of Highway Practice No. 126, Transportation Research Board, Washington D.C., 1986
- (2) Bush A.J. "Nondestructive Testing for Light Aircraft Pavements. Phase I. Evaluation of Nondestructive Testing Devices", USDOT, Federal Aviation Administration, Report No. FAA-RD-80-9, Washington D.C., 1980
- (3) Smith R.E. and Lytton R.L. "Synthesis Study of Nondestructive Testing Devices for Use in Overlay Thickness Design of Flexible Pavements", USDOT, Federal Highway Administration, Report No. FHWA/RD-83/097, Washington D.C., 1984
- (4) Hudson W.R., Elkins G.E., Eden W., and Reilley K.T. "Evaluation of Pavement Deflection Measuring Equipment", USDOT, Federal Highway Administration, Report No. FHWA-TS-87-208, Washington D.C., 1987
- (5) Heisey J.S., Stokoe K.H., Hudson W.R. and Meyer A.H. "Determination of In Situ Shear Wave Velocities from Spectral Analysis of Surface Waves", Center for Transportation Research, Research Report 256-2, The University of Texas at Austin, Austin TX, 1982
- (6) Nazarian S. and Stokoe K.H. "Evaluation of Moduli and Thicknesses of Pavement Systems by Spectral-Analysis-of-Surface-Waves Method", Center for Transportation Research, Research Report 256-4, The University of Texas at Austin, Austin TX, 1983
- (7) Elton D.J. and Harr M.E. "New Nondestructive Pavement Evaluation Method", ASCE, Journal of Transportation Engineering, Vol. 114 No. 1, Jan. 1988, New York, 1988

- (8) Strategic Highway Research Program "FOCUS", SHRP, Washington D.C., July 1988
- (9) Hoffman M.S. and Thompson M.R. "Comparative Study of Selected Nondestructive Testing Devices", Transportation Research Board, TRR 852, Washington D.C., 1982
- (10) Uliditz, P. "Pavement Analysis", Elsevier Science Publishing Co. Inc., New York, 1987
- (11) Finn F.N. and Monismith C.L. "Asphalt Overlay Design Procedures", NCHRP Synthesis of Highway Practice 116, Transportation Research Board, Washington D.C., 1984
- (12) Kingham R.I. "Development of the Asphalt Institute's Deflection Method for Designing Asphalt Concrete Overlays for Asphalt Pavements", The Asphalt Institute, Research Report 69-3, College Park MD, 1969
- (13) The Asphalt Institute "Asphalt Overlays for Highway and Street Rehabilitation", the Asphalt Institute, Manual Series No. 17 (MS-17) College Park MD, 1983 edition
- (14) Skog J.B., Mathews J.A., Mann G.W. and Roberts D.V. "Statewide Flexible Pavement Performance and Deflection Study", Caltrans Report No. FHWA-CA-TL-78-28, Sacramento CA, 1978
- (15) Caltrans "Asphalt Concrete Overlay Design Manual", Caltrans, Sacramento CA, 1979
- (16) Lytton R.L. and Smith R.E. "Use of Non-destructive Testing in the Design of Overlays for Flexible Pavements", Transportation Research Board, TRR 1007, Washington D.C., 1985
- (17) Marchiona A., Cesarini M., Fornaci M.G. and Melgarini, M. "Pavement Elastic Characteristics Measured by Means of Tests Conducted with the Falling Weight Deflectometer", Transportation Research Board, TRR 1007, Washington D.C., 1985
- (18) Mahoney J.P., Lary L.A., Sharma J., and Jackson N. "Investigation of Seasonal Load Restrictions in Washington State", Transportation Research Board, TRR 1043, Washington D.C., 1985
- (19) Hasain S. and George K.P. "In-situ Pavement Moduli from Dynaflect Deflections", Transportation Research Board, TRR 1043, Washington D.C., 1985
- (20) Mamlouk M.S. "Use of Dynamic Analysis in Predicting Field Multilayer Pavement Moduli", Transportation Research Board, TRR 1043, Washington D.C., 1985
- (21) Uliditz P. and Stubstad R.N. "Analytical-Empirical Pavement Evaluation Using the Falling Weight Deflectometer", Transportation Research Board, TRR 1022, Washington D.C., 1985
- (22) Mahoney J.P., Coetzee N.F., Stubstad R.N., and Lee S.W. "A Performance Comparison of Selected Backcalculation Computer Programs", presented at the ASTM First International Symposium on Nondestructive Testing of Pavements and Backcalculation of Moduli, Baltimore MD, 1988
- (23) Irwin L.H., Yang W.S. and Stubstad R.N. "The Importance of Deflection Reading Accuracy and Layer Thickness Accuracy in Back-Calculation of Pavement Layer Moduli", presented at the ASTM First International Symposium on Nondestructive Testing of Pavements and Backcalculation of Moduli, Baltimore MD, 1988
- (24) Yapp M., Hicks R.G., and Connor B. "Development of an Improved Overlay Design Procedure for the State of Alaska", Vol. II: Final Report, State of Alaska, Dept. of Transportation and Public Facilities, Fairbanks AK, 1987
- (25) Ali N. and Khosla N.P. "Determination of Layer Moduli

Using a Falling Weight Deflectometer", Transportation Research Board, TRR 1117, Washington D.C., 1987

- (26) Lee S.W. "Backcalculation of Pavement Moduli by Use of Pavement Surface Deflection", Ph.D. Dissertation, University of Washington, Seattle WA, 1988
- (27) Lee S.W., Mahoney J.P. and Jackson N.C., "A Verification of Backcalculation of Pavement Moduli", presented at the 1988 Annual Meeting of the Transportation Research Board, Washington D.C., 1988
- (28) Zhou H., Hicks R.G. and Bell C.A. "BOUSDEF: A Backcalculation Program for Determining Moduli of Pavement Structure", Transportation Research Institute, Oregon State University, Transportation Research Report 88-10, Corvallis OR, 1988

**APPLICABILITY OF SPECTRAL-ANALYSIS-OF-SURFACE-WAVES
METHOD IN DETERMINING MODULI OF PAVEMENTS**

SOHEIL NAZARIAN
The University of Texas at El Paso
El Paso, Texas 79968

ABSTRACT

In order to correctly predict the response of a pavement section, two important items should be considered. First, a realistic theoretical model is required. Second, and perhaps more importantly, material properties should be determined accurately. The most common material characterization methods are the deflection-based nondestructive testing methods. These testing methods can be implemented in the field quite rapidly; however, they suffer from several limitations which may result in erroneous material properties. For example, when bedrock or permafrost is present at shallow depths, when the pavement layers are thin, or when the subgrade consists of several layers, the deflection-based methods yield questionable modulus values. An alternative in situ testing technique, which does not suffer from the above limitations, is the Spectral-Analysis-of-Surface-Waves (SASW) method.

Over the last eight years, the SASW method has been used to determine the stiffness profile of numerous soil deposits and pavement systems. The SASW method is a nondestructive testing method which is theoretically sound and is based upon the theory of wave propagation in layered medium. The SASW method yields a modulus profile at low-strains. However, when combined with proper laboratory tests or empirical relationships, moduli at any strain level can be determined. Through analyses similar to those used in geotechnical earthquake engineering,

stresses and strains at any point in the pavement deposit can be determined.

In this paper, the analytical and experimental aspects of the SASW method are described, the strengths and weaknesses of the method are discussed, and several case studies are included to demonstrate some of the benefits of the method.

INTRODUCTION

Many major highways and airport runways are approaching the end of their serviceable lives. The cost involved in rehabilitation of these facilities is astronomical. Methodologies used to determine the need for or the type of improvements to be applied to a deteriorated pavement section are based upon empirical and experience-based procedures. Unfortunately, in many cases, the selected rehabilitation process is not effective and the pavement deteriorates prematurely. Fortunately, new mechanistic pavement design procedures are being developed to overcome this problem.

A well-developed mechanistic procedure should be capable of incorporating several important parameters in the design. A partial list of these parameters are:

1. traffic loading;
2. environmental factors, such as annual precipitation, and ambient temperature;
3. stiffness properties of the roadbed soil and paving materials; and,

4. characteristics of the paving materials and roadbed soil in terms of dynamic and/or nonlinear behavior.

The theoretical model utilized to determine the strength and deformation parameters (such as stress and strain distribution within pavement layers) should be based upon relatively few simplified assumptions and these assumptions should not deviate significantly from the actual field conditions. In order to calculate the distribution of stresses and strains within the pavement system, two of the parameters mentioned above (i.e., items 3 and 4) should be determined and defined quite accurately. A precise method for determining the properties of pavements is necessary, if meaningful maintenance inspections are to be performed regularly and/or overlays are to be designed effectively.

Nondestructive testing (NDT) techniques are typically utilized to determine the properties of paving layers and roadbed soil. The most common NDT techniques are the deflection-based techniques. Two devices that are utilized for this purpose are the Falling Weight Deflectometer and the Dynaflect. Both devices are well-known and need not be described herein. However, the main differences between the two devices are: 1) the method in which the energy is applied to the pavement surface (impulsive for FWD versus steady-state for Dynaflect) and, 2) the magnitude of the load.

The FWD and Dynaflect devices are excellent tools for testing pavements at the network level because deflection data can be collected quite rapidly in the field. However, in project level studies, the deflection-based methods should be utilized carefully. Several cases when the stiffnesses obtained from deflection-based NDT methods may be in error are:

1. when a layer is quite thin, such as many asphaltic-concrete layers,
2. when a relatively stiff layer is present near the surface (see Briggs and Nazarian, 1989),
3. when a layer such as the subgrade layer consists of several sublayers and,
4. when the actual layer thicknesses are not precisely known.

Another factor which should be considered carefully, is the so-called "dynamic effects" associated with the fact that the load imparted by the deflection-based devices are dynamic, whereas, during the data reduction the load is assumed to be static. This factor may result in large errors in the back-calculated moduli (Roesset and Shao, 1985; Davies and Mamlouk, 1985).

An alternative method for determining the stiffness profile of pavement systems is the Spectral-Analysis-of-Surface-Waves (SASW) method. The SASW method, which is also nondestructive, can be categorized as a seismic (wave propagation) testing technique because it is based upon the theory of elastic wave propagation in a layered medium. In this paper, the theoretical and experimental aspects of the SASW method are thoroughly described. The limitations as well as the advantages of the method are then presented. The recent improvements and future developments of the technique are also presented. Finally, several case studies are included to demonstrate situations where the SASW method can be employed very effectively to solve pavement related problems.

SPECTRAL-ANALYSIS-OF-SURFACE-WAVES METHOD

Background

For engineering purposes, many pavement systems can be, with reasonable accuracy, approximated by a layered half-space. With this approximation, a pavement profile is assumed to be homogeneous and to extend to infinity in two horizontal directions while being heterogeneous in the vertical direction. This heterogeneity is often modelled by a number of layers with constant properties within each layer. In addition, it is assumed that the material in each layer is elastic and isotropic.

When the surface of a half-space is disturbed by an impact, two types of waves propagate in the system — body waves and surface waves.

Body waves, which consist of shear waves (S-waves) and compression waves (P-waves), travel in the body of the medium and attenuate quite rapidly near the surface. For compression waves the directions of particle motion and wave propagation are the same; that is, P-waves exhibit a push-pull motion. Shear waves generate a shearing motion, which

causes particle motion to occur perpendicular to the direction of wave propagation. Compression waves travel faster than shear waves. The ratio of the velocity of propagation of the P-waves to S-waves is a function of Poisson's ratio, and this velocity ratio increases as Poisson's ratio increases.

Many types of surface waves have been identified and described. The major type is Rayleigh waves (R-waves). Surface waves propagate near the surface of the half-space. Rayleigh waves (R-waves) propagate with a velocity close to that of S-waves. As shown in Fig. 1, particle motion associated with R-waves is composed of both vertical and horizontal components, which, when combined, form a retrograde ellipse near the surface. However, with depth, the particle motion changes to pure vertical and finally, to a prograde ellipse as illustrated in Fig. 1. The amplitude of the motion of R-waves attenuates quite rapidly with depth. At a depth equal to about 1.5 times the wavelength, the vertical component of the amplitude is about ten percent of the original amplitude at the ground surface.

Miller and Pursey (1955) found that for a homogeneous, isotropic, elastic half-space, approximately 67 percent of the input energy propagates in the form of R-waves while S- and P-waves carry 33 percent. At the surface of an elastic

half-space, body waves attenuate inversely proportionally to the square of the distance from the source; whereas, the surface wave amplitude decreases in proportion to the reciprocal of the square root of distance from the source. As such, body wave energy is present in records captured by receivers located at the surface of a half-space. However, an adequate distance away from the source the body wave energy is very small relative to the surface wave energy and for all practical purposes the contribution of the body wave energy to the captured signal can be neglected.

In wave propagation techniques, such as the SASW method, the goal is to determine the variation in wave velocity with depth. Wave velocity is a direct indication of the stiffness of the material; higher wave velocity is associated with higher stiffness. Propagation velocities per se have limited use in engineering applications. In material characterization for pavement engineering, Young's moduli of different layers are needed. Shear wave velocity is usually measured for this purpose. Elastic theory is employed to determine Young's modulus from shear wave velocity. Shear modulus, G , is equal to:

$$G = \rho V_s^2 \quad (1)$$

where, V_s is shear wave velocity and ρ is

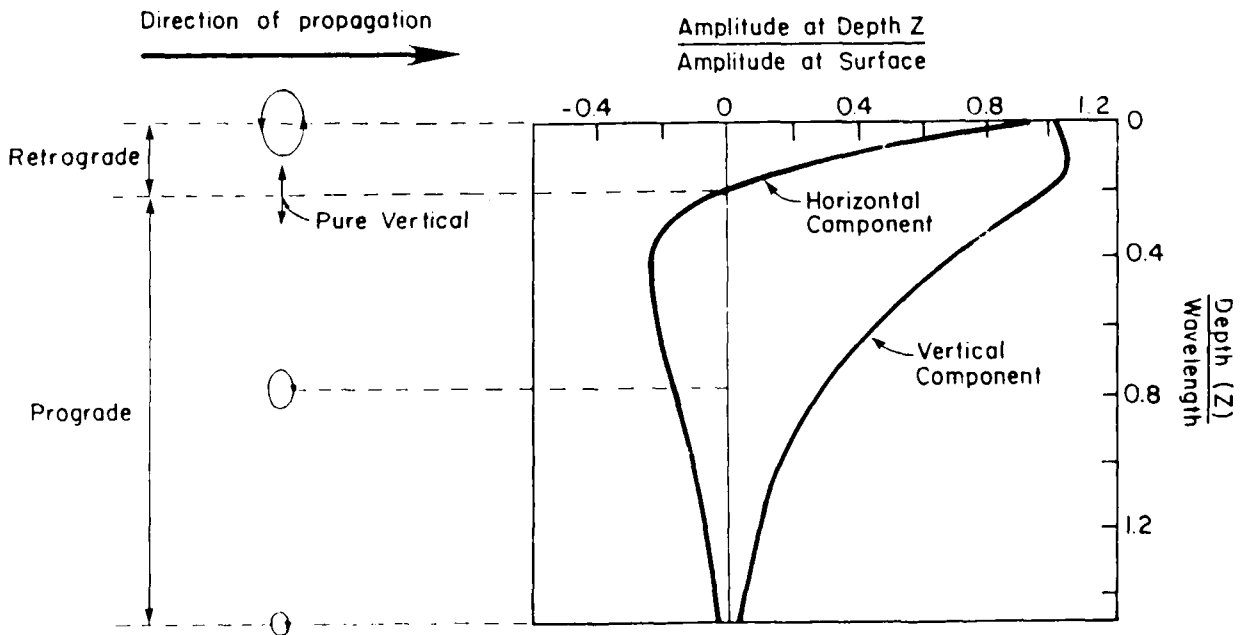


Figure 1 - Amplitude and Particle Motion Distribution with Depth for Rayleigh Waves (after Richart et al, 1970)

mass density. Young's modulus, E , and shear modulus, G , are related through Poisson's ratio, ν . This relationship is:

$$E = 2 G (1 + \nu). \quad (2)$$

Moduli determined from wave propagation techniques are small-strain moduli, also known as elastic moduli. A pavement section may experience higher strain amplitudes. Two basic approaches are used today to evaluate nonlinear moduli of pavement systems.

The first approach is to employ high intensity loads in an attempt to evaluate the nonlinear behavior of the pavement. Elastic theory is then used to backcalculate the modulus profile. The advantage of this approach is that an equivalent nonlinear modulus of the pavement may be determined. However, if these moduli are used to determine the stresses and strains in the pavement system, substantial errors may occur. As the modulus profile is approximated with only three or four equivalent moduli this approach may only be appropriate for calculating surface displacements under loads similar to those used to evaluate the equivalent moduli. The FWD device can be used to implement this approach.

The second approach is to determine elastic moduli in situ and to perform laboratory tests on representative samples to define variation in moduli with change in strain level and to some extent with stress state. By incorporating the laboratory and field results, the actual nonlinear behavior of the pavement system can be determined for any load level. Over thirty years of research in geotechnical earthquake engineering have shown that the second

approach is very appropriate and yields consistent and realistic results. The SASW testing method falls into this second category of testing.

The variation in Young's modulus with strain level for a clay is shown in Fig. 2. For convenience, moduli are normalized relative to the elastic modulus. If a normalized modulus-strain curve such as that shown in Fig. 2 is available for the material, then moduli at higher strains can be determined once elastic modulus has been measured in the field. Hardin and Drenvich (1972) and Seed et al (1986) have suggested empirical relationships for determining the modulus-strain relationship, if performing laboratory tests is not possible due to time or budgetary constraints. An example of one possible procedure to incorporate the load-induced nonlinear behavior of materials in mechanistic pavement design is presented in Nazarian et al (1987).

Theoretical Aspects

The SASW method is based upon the generation and detection of surface waves. As mentioned before, in a homogeneous, isotropic, elastic, half-space, the velocity of surface waves does not vary with frequency (wavelength). However, since the properties of pavement layers vary with depth, surface wave velocity will vary with wavelength. This frequency dependency of surface waves in a heterogeneous medium is termed dispersion, and surface waves are said to be dispersive waves. A plot of wave velocity versus wavelength is called a dispersion curve. The velocity of propagation of interest in SASW testing is called the surface wave phase velocity (sometimes called apparent surface wave velocity). Phase velocity is defined as the velocity with which a seismic disturbance of a single frequency is propagated in the medium.

An idealized profile of a pavement system is shown in Fig. 3. The model shows the typical (two to four) layers corresponding to the traditional layers used in pavement design (Fig. 3a). In the model used to simulate analytically the SASW test, each of these traditional layers can be divided into several sublayers as illustrated in Fig. 3b. These sublayers are used to determine the variation in modulus within each traditional pavement layer. In each sublayer, values of thickness (d), Poisson's ratio (ν) and mass density (ρ)

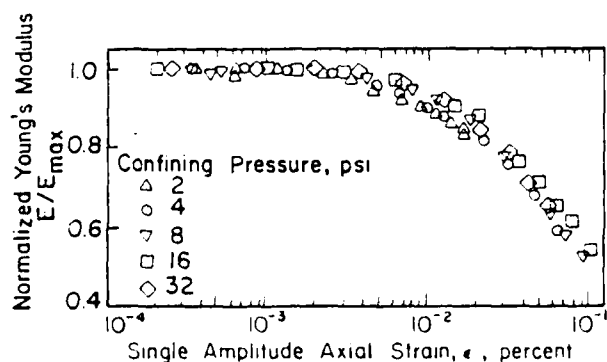


Figure 2 - Variation in Normalized Shear Modulus with Shearing Strain and Confining Pressure

are assigned. However, the most important material parameter is the stiffness of each layer which is introduced into the model as shear wave velocity.

Different methods used to determine the dispersion function are discussed in Nazarian (1984). The reader is referred to this publication for more information. The first theoretical solution for modelling the dispersive characteristics of surface waves in a form suitable for implementation in a computer algorithm was developed by Thomson (1950) and was revised and slightly corrected by Haskell (1953). The Haskell-Thomson technique builds up the surface wave dispersion function as the product of layer matrices. These matrices relate the displacement components as well as the stress components acting on one interface to those associated with the adjacent interface. The product of these layer matrices then relates the stress and displacement components of motion at the deepest interface to those at the free surface.

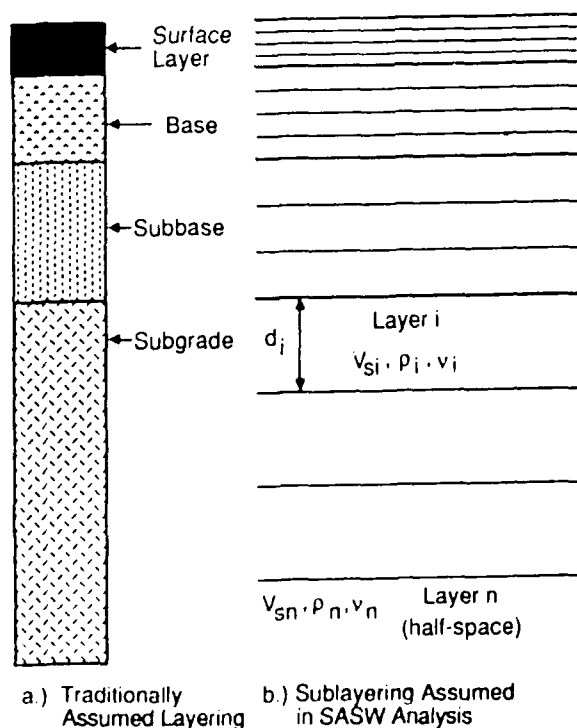


Figure 3 - Idealized Profile of a Pavement System

The Haskell-Thomson formulation can be effectively used to determine the dispersion characteristics of earth at low frequencies (less than 0.2 Hz) which correspond to wavelengths on the order of several kilometers. However, for pavement applications frequencies in the range of say 10 Hz to about 50 kHz should be excited and detected. At such high frequencies, some components involved in the calculation of phase velocities become extremely large, causing a loss of significant figures in the dispersion function which, in turn, make it impossible to obtain accurate values for phase velocity at a given frequency. In extreme cases, these values may exceed the definition of the infinity of the computer.

Dunkin (1965) reformulated the Haskell-Thomson formulation to allow the use of high frequencies in the solution of the dispersion function. Thrower (1965) independently reformulated the Haskell-Thomson solution to circumvent the problem of large values.

In soil sites the stiffness of different layers gradually increases with depth so that the normal modes of propagation of Rayleigh waves are

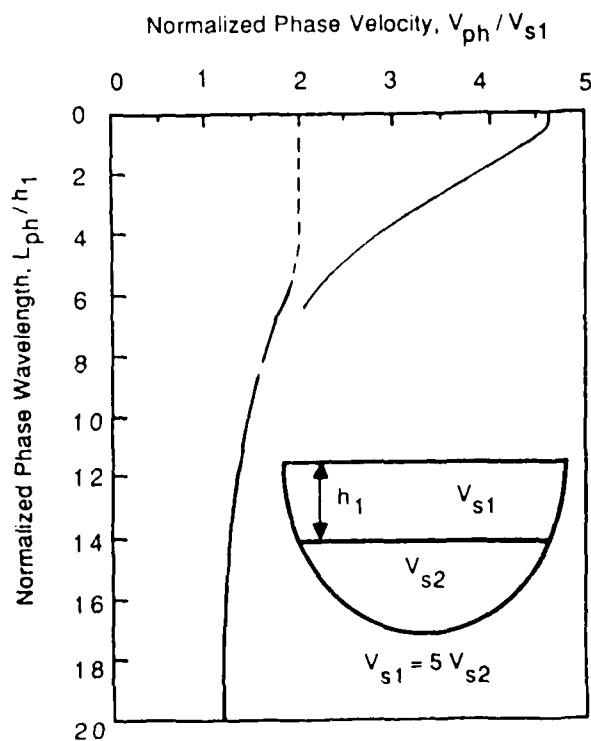


Figure 4 - Theoretical Dispersion Curve for a Stiff Layer Underlain by a half-space

anticipated. For a pavement, on the contrary, the stiffness of the near surface material is much higher than the underlying soil, and the normal mode of vibration should be expected in the subgrade. Thrower (1965) indicated that the assumption of a plate on a half-space can be used adequately to model a pavement system. For wavelengths with phase velocities greater than shear wave velocity of the subgrade material, modes similar to antisymmetrical modes of propagation in a plate approximate pavement systems appropriately.

To apply the Haskell-Thomson type solution to pavement engineering several simplifying but realistic assumptions must be made. These assumptions are:

1. the problem can be approximated as a plane strain problem;
2. stress waves propagating in the medium are solely surface waves;
3. each layer is horizontal and homogeneous; and,
4. each layer is assumed to extend horizontally to infinity.

Sanchez-Salinero et al (1987) demonstrated that in the range of stiffnesses of interest in pavement engineering, the effects of the first two assumptions are minor; but the savings in terms of computational time is significant. Sheu et al (1987) based upon an experimental investigation of jointed concrete slabs, showed that a proper test set-up can be used to minimize and essentially eliminate any boundary effects on the final test results. The findings of this research have not been implemented yet.

A typical dispersion curve from a two-layer pavement system is shown in Fig. 4. For short wavelengths, the phase velocity is about 90 percent of the shear wave velocity of the upper layer. This phase velocity is about equal to the Rayleigh wave velocity of a homogeneous half-space consisting of the upper material only. At long wavelengths, the phase velocity becomes asymptotic to the R-wave velocity of the bottom layer (the half-space.) The discontinuity in the curve represents a change in the mode of vibration as discussed in Nazarian (1984).

As mentioned before, besides the stiffness parameter (i.e., shear wave velocity), Poisson's ratio and mass density are entered into the model. It can be demonstrated (Nazarian, 1984) that the effect of these two parameters on the

dispersion characteristics of surface waves is minimal and is typically less than five percent.

Experimental Aspects

A complete investigation of a site with the SASW method consists of three phases: field testing, determination of dispersion curve, and determination of stiffness profile. Each phase is described in this section.

Field Testing. The main goal in performing the SASW test in the field is to obtain an experimental dispersion curve. Two spectral functions, the cross power spectrum and the coherence function, are utilized for this task. A schematic diagram of the SASW testing is shown in Fig. 5. To perform a test in the field, several steps should be taken. These steps, which are itemized for ease of reference, are:

1. An imaginary centerline for the receiver array is selected.
2. Two receivers are then placed on the ground surface an equal distance from the centerline.
3. A disturbance is applied to the ground surface to generate stress waves which propagate mostly as surface waves of various frequencies.
4. The signals from similar disturbances are averaged together.
5. The records are monitored, captured and saved for further reduction.
6. After testing is completed, the receivers are kept in their original positions, but the source is moved to the opposite side of the imaginary centerline and Steps 3 through 5 are repeated.
7. Steps 3 through 6 are repeated for other spacings.

Equipment. As mentioned in Steps 2, 3 and 5, two or more receivers, a source and a recorder are required for collecting data.

Typically, accelerometers are used to capture high-frequency (above 300 Hz) waves. Based on much experience, use of geophones (velocity transducers) to capture lower-frequency waves (less than 300 Hz) is highly recommended.

Sources used in the SASW test should be able to generate surface waves over a wide range of frequencies (from 10 Hz to more than 50 KHz). Ordinary hand-held or sledge hammers can be used effectively at

The recording device used successfully to collect field data is a spectral analyzer. A spectral analyzer has the capability of capturing data in the time domain, digitizing the data properly, operating a fast-Fourier transform (FFT) on the signal and, finally, performing spectral analysis.

Hiltunen concluded that the dispersion curve is independent of source-to-near-receiver distance if wavelengths larger than twice the receiver spacing are eliminated.

There are two other advantages associated with the CRMP geometry. By averaging data from forward and reverse profiles any phase shift caused by the recording device or the receivers can be eliminated. Also, if dipping layers are

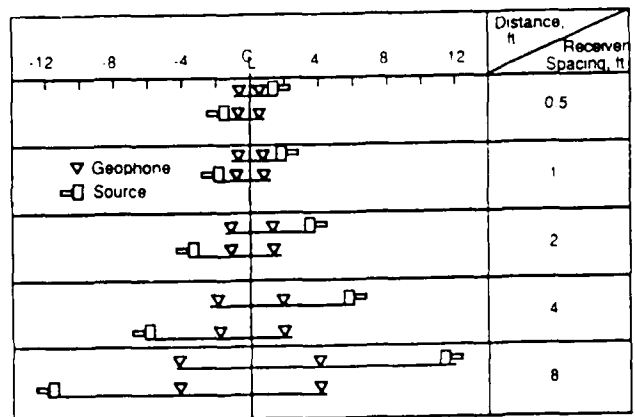


Figure 6 - Schematic of Experimental Arrangement for SASW Tests

present in the profile, averaging will minimize its affect on the experimental dispersion curve.

The quality of the collected data can be significantly enhanced by generating and averaging spectral functions several times. The frequency averaging minimizes the amplitude of incoherent background noise and improves the quality of the actual signal. Typically, five averages are adequate to ensure high-quality spectral functions.

Tests at receiver spacings of 0.5 ft through 8 or 16 ft are generally carried out at a pavement site. This testing set-up requires about 30 to 50 minutes. As such, the SASW tests are not nearly as economical as other nondestructive tests. However, when the SASW testing method is automated, the SASW and deflection based tests can be performed at comparable costs and testing times.

Construction of Experimental Dispersion Curve

As mentioned before, from field testing two sets of spectral functions are obtained from each spacing. These two functions are the phase of the cross power spectrum and the coherence function. In this section the process used to obtain a dispersion curve from these spectral functions is discussed.

The coherence function is used to visually inspect the quality of signals being recorded in the field. Upon averaging the signals, the coherence function will have a real value between zero and one in the range of frequencies being measured. A value of one indicates perfect correlation between the signals being picked up by the receivers (which is equivalent to a signal-to-noise ratio of infinity). Similarly, a value of zero for the coherence function at a frequency represents no relation between the signals being detected. With this approach, data collected in the field can be conveniently checked in the field, and the test can be modified and repeated if necessary. In addition, the range of frequencies that are contaminated can be identified and omitted during data reduction.

The phase information of the cross power spectrum is used to obtain the relative phase shift at each frequency. This phase shift results from the fact that waves sensed at the near receiver must travel an additional distance D (see Fig. 5) to be sensed at the far receiver. This phase shift can be translated into travel time.

Construction of dispersion curves has been discussed in detail in Nazarian and Stokoe (1985). In summary, the range of frequencies with a coherence value of more than 0.90 are selected from the record. For each frequency (f) in this range, the phase shift is picked from the phase information of the cross power spectrum. Knowing the phase (ϕ), the travel time (t) can be calculated by:

$$t = \phi/360f \quad (3)$$

and the phase velocity (V_{ph}) can be obtained by:

$$V_{ph} = D/t \quad (4)$$

where D is the distance between the receivers. The wavelength L_{ph} is related to velocity and frequency by:

$$L_{ph} = V_{ph}/f \quad (5)$$

Typical records from spectral analyses performed on signals measured on an Asphaltic Concrete Pavement (ACP) are shown in Fig. 7. Figure 7a is the coherence function and Fig. 7b is the phase information from the cross power spectrum. The dispersion curve constructed from this record is shown in Fig. 8 in the range of wavelengths of 0.5 to 2 ft (for clarity, only every 6th data point is plotted). The solid circles numbered 1 to 5 in Fig. 8 correspond to the points marked as 1 to 5 on the phase information of cross power spectrum in Fig. 7b. These points are positioned every 1000 Hz at frequencies from 1000 to 5000 Hz.

The dispersion curve between points 1 and 2 (frequencies from 1000 to 2000 Hz) covers a range of wavelengths from 1.13 to 1.65 ft. However, for a similar increment in frequency range between points 4 and 5 (frequencies from 4000 to 5000 Hz), a smaller portion of the dispersion curve corresponding to a range of wavelengths of 0.61 to 0.72 ft is obtained. As such, for a given record, the dispersion curve is better defined at the higher frequencies in the record, and for that reason the range of frequencies at different receiver spacings should be reduced to gain better resolution at lower frequencies.

Once the dispersion data (phase velocity versus wavelength) for all frequencies and all spacings are determined, an averaging process is used to reduce the number of dispersion data points from several thousands to several

hundreds. The criterion used to average data obtained at different spacings is as follows. At each frequency, the mean, standard deviation and coefficient of variation of velocities are calculated. If the coefficient of variation is less than 7.5 percent, the mean is accepted as the average. However, if the coefficient of variation does not satisfy this criterion, points that are outside 0.67 times one standard deviation (outliers) are omitted, and the process is repeated.

Determination of Stiffness Profile

In this step, the thickness and stiffness of different layers in the pavement profile are determined from the experimental phase velocity-wavelength relationship. This process is loosely called the inversion of the dispersion curve or in short "inversion". The inversion process is the most important step in performing the SASW tests and without it no meaningful stiffness profile can be determined.

In general terms, this problem can be formulized as:

$$g(d, m) = 0 \quad (6)$$

where d is a vector representing the observed data, m is a vector corresponding to the parameters that should be determining and g is a matrix corresponding to the relationship between m and d . For example, in the SASW tests, d corresponds to phase velocities at given wavelengths (as measured in the field); parameters m are the shear wave velocities and thicknesses of different layers and g is the Haskell-Thomson algorithm. Our goal is to determine

vector m (stiffness profile) given vector d (experimental dispersion curve). The most desirable and accurate approach to this problem would be an analytical solution. In mathematical terms this solution can be written as:

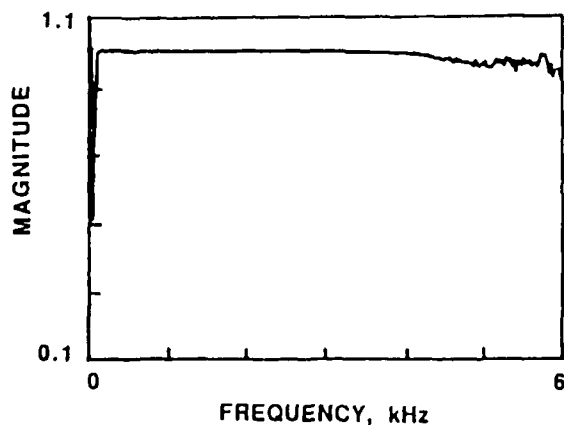
$$m = g^{-1}(d) \quad (7)$$

Note that to obtain the analytical solution one should be able to separate the model parameters from the data. In addition one should be able to obtain readily the inverse of the g matrix. Unfortunately, both of these criteria (separating m and d and obtaining inverse of g) are mathematically impossible for the Haskell-Thomson solution.

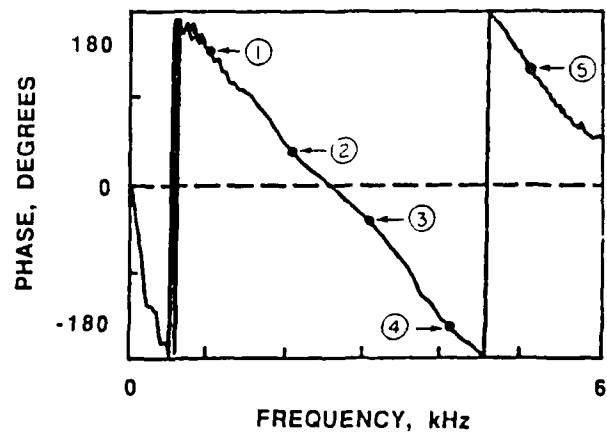
The alternative approach is to perform forward modeling. In the forward modeling (a.k.a. backcalculating or system identification) process, values are assigned to vector m . Based on this vector m and the model g , a vector t containing theoretical data comparable to d (observed data) is obtained. If the difference between d and t is less than a given tolerance, it is assumed that the vector m corresponds to the model representative of the measured system. If the difference between d and t is not within tolerance, the vector m is modified and a new t is calculated.

The major weaknesses of forward-modelling are: (1) many iterations are required; and (2) the number of iterations depends on the experience of the person performing forward-modelling.

Two means of improving the process, which have not yet been implemented, are by utilizing either optimization techniques (Reklaitis et al, 1983) or generalized inverse theory (Menke, 1984).



a) Coherence Function



b) Cross Power Spectrum

Figure 7 - Typical Spectral Function for SASW Tests

It would be beneficial to define these two processes.

In general terms, optimization theory is a group of mathematical calculations combined with numerical methods for finding the best candidate from a collection of alternatives without having to evaluate all possible alternatives (Reklaitis et al, 1983). In the optimization technique one minimizes (or alternatively maximizes) a series of functions. As applied to the SASW method, the objective is to minimize the function e where

$$e = |d - t| \quad (8)$$

In optimization techniques, the general solution is coded in a computer program and the specific function is included in the program through a subroutine.

In simple terms, when optimization techniques are applied to determine the stiffness profile from the field dispersion data, the algorithm developed will automatically go through iterations and will find the best match between the theoretical and experimental dispersion data or (as mentioned before) will minimize function e introduced in Eq. 8.

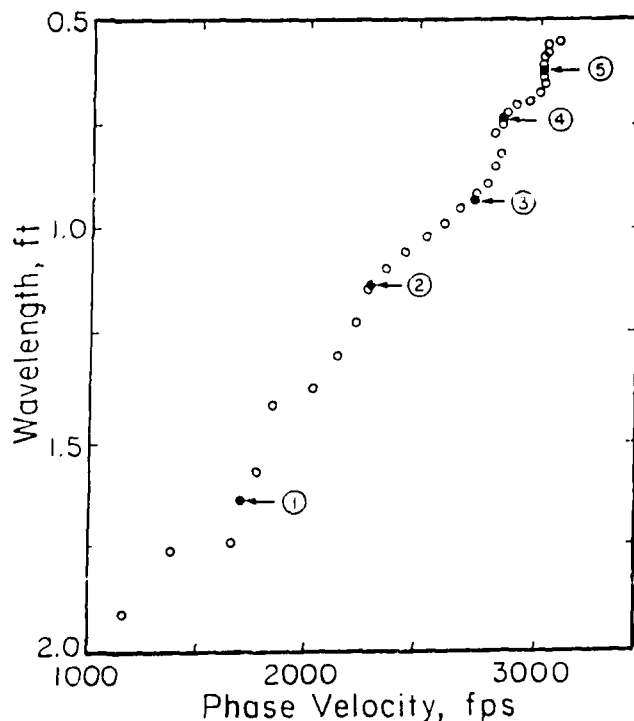


Figure 8 - Dispersion Curve Obtained from Phase of Cross Power Spectrum shown in Figure 7

The advantage of this technique is that the process will be much faster.

The last alternative is the use of general inverse theory to determine the model parameters, m , given observed data, d , and the model, g . A simplified way of describing the use of general inverse theory is that, based upon an assumed probability density function over the observed data and model parameters, a priori information on the model parameters, and the information on the model, one can obtain the model parameters readily. We distinguish between the optimization and utilization of inverse theory by indicating that the optimization is used to automate forward-modelling; whereas, utilization of inverse theory will yield the model parameters by containing observed data, model and probability functions.

Presently forward modelling techniques are utilized for carrying out the "inversion" process. A shear wave velocity profile is assumed and a theoretical dispersion curve is constructed. The experimental and theoretical curves are compared, and necessary changes are made in the assumed shear wave velocity profile until the experimental and theoretical dispersion curves match with a reasonable tolerance. A user-friendly, interactive program called INVERT (Nazarian, 1984) has been developed to perform this task. An engineer can be trained in a reasonable amount of time to perform inversion using this program. As discussed previously in this paper, the theoretical model developed for the inversion process is based on a Haskell-Thomson type matrix solution for elastic waves in a multilayered solid medium.

CASE STUDIES

In this section, several case studies are presented to demonstrate some of the clear advantages of the SASW method compared to other nondestructive testing techniques.

Case 1 - Determination of Layering

A series of tests was performed at nine randomly-selected flexible pavement sections with significantly different profiles to substantiate the accuracy with which layer thicknesses can be determined by the SASW method. The sites were located at the Pavement Testing Facility operated by the Texas Transportation Institute (TTI). Material

profiles of all sections are included in Table 1. The thickness of the asphaltic-concrete surface layer varied from 1 to 5 inches. The base and subbase materials were either crushed limestone or a mixture of crushed limestone with lime or portland cement. No information regarding the types or thicknesses of the layers was provided during the data collection or reduction phases. Only after the results were reported to the funding agency were the pavement profiles provided.

The results of this study are reported in full detail in Nazarian et al (1988). Layer thicknesses determined from the SASW tests are compared with those obtained from construction drawings in Table 1 and Fig. 9. In general, thicknesses determined by the SASW tests seem very reasonable. The accuracy of the layer boundaries determined could have been improved by assuming more layers. However, the practical value of more detailed profiles is questionable in the design process but may be important for construction control.

It is important to note that, when the stiffness of two adjacent layers are quite similar, it is not possible to distinguish between these two layers. For example, when the stiffness of say the AC and base layers are similar, it is not possible to identify the thickness of the AC layer. For design purposes, this matter is not a significant consequence.

Case 2 - Utility of Inversion Process

To test the utility of the inversion process, two series of tests at the same site were performed on the embankment of an overpass. The first series of tests was performed after the embankment was raised to its final elevation but before placement of the pavement. Crosshole seismic tests (Richart et al, 1970) were carried out at this time also. The second test series was performed after the granular base and pavement were placed. The nominal thicknesses of the asphalt and base layers were 2.5 and 15 in., respectively.

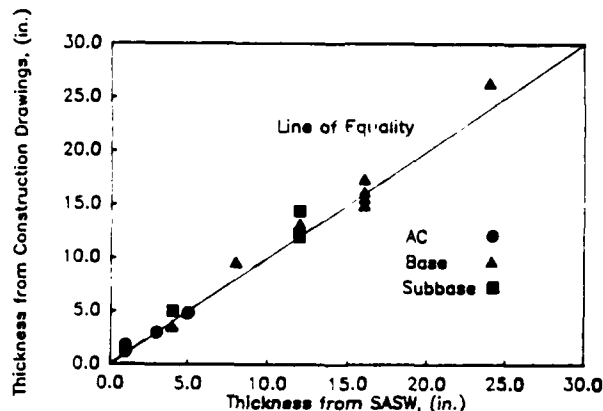


Figure 9 - Comparison of Thicknesses from SASW and Construction Drawings (Case 1)

Table 1 - Comparison of Thicknesses from SASW and Construction Drawings (Case 1)

Section	Thickness from Construction Drawings, in.			Thickness from SASW Profile, in.			Material Type	
	AC	Base	Subbase	AC	Base	Subbase	Base	Subbase
2	1	12	4	1.2	13.2	5.0	LS+C	LS
4	5	12	12	4.8	12.0	14.4	LS+C	LS
7	1	4	12	1.2+	3.6+	12.0	LS	LS+C
9	5	8*	--	4.8	9.6*	--	LS	LS
10	1	16*	--	1.8	15*	--	LS	LS
11	1	16*	--	1.8	17.4*	--	LS	LS
16	5	24*	--	4.8	26.4*	--	LS+C	LS+C
17	3	16*	--	3	16.2*	--	LS+L	LS+L
18	1	16*	--	1.2	15.6*	--	LS+L	LS+L

LS+C: Crushed Limestone mixed with 4% Cement LS: Crushed Limestone

LS+L: Crushed Limestone mixed with 2% Lime

* Subbase and Base constructed from same materials.

+ AC Layer and Base have similar modulus and would be interpreted as one layer if the material profile was never known.

As reflected in Fig. 10, Young's modulus profiles from the SASW and crosshole tests performed during the first series of tests agree quite well. The Young's modulus profile obtained from the second series of SASW tests is also included in Fig. 10. Generally, the two profiles obtained by the SASW method match quite well. However, in the range of depths of 1.5 to 2.5 ft, the difference in Young's moduli is about 34 percent. This is because the first few feet of the ground were compacted further due to placement of the base layer and pavement. At depths below 4.5 ft, the percentage deviation between moduli oscillate between high (48%) and low (4%) values. This occurs because of the coarse layering which was used to reduce the first SASW test series. Had finer layering been chosen, the results would have been in better agreement at depths of 5 and 6 ft.

Case 3 - Presence of Bedrock

This case study is included to demonstrate the applicability of the SASW method in determining the stiffness profile at a site where bedrock is near

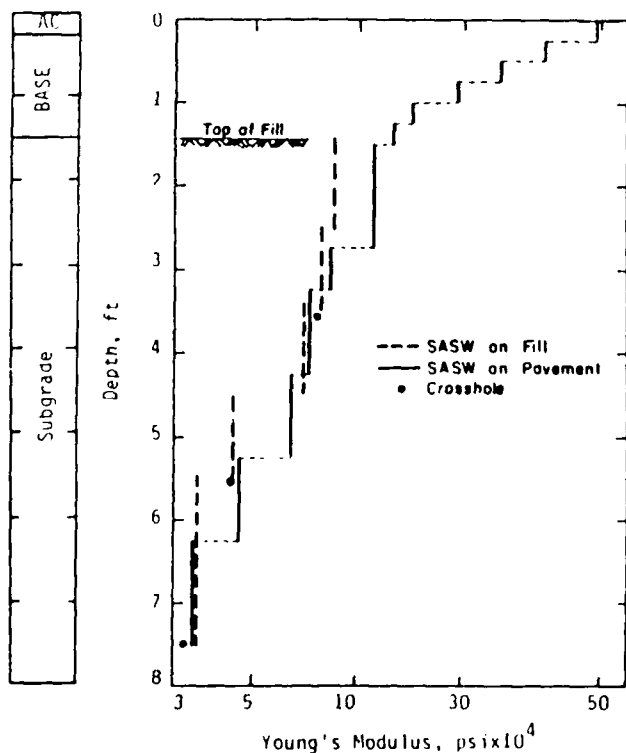


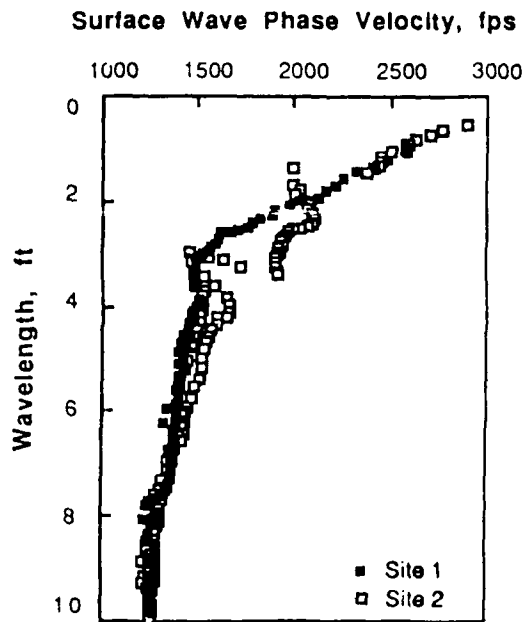
Figure 10 - Comparison of Young's Modulus Profiles from before and after Placement of Pavement Layers (Case 2)

the ground surface. Two sites, about 1000 ft apart, were selected near Austin, Texas. Both sites had identical pavement layers. The top layer was asphaltic-concrete with a nominal thickness of 1.5 in. The base material was a very dense granular base layer with a thickness of 15 in. The first site was located in a valley. The layer between the base and limestone was simply rock-fill material. Limestone was not encountered within the maximum depth of drilling (25 ft). The subgrade of the second site consisted of about 5 ft of rock-fill material over limestone. A series of SASW tests was performed at each site.

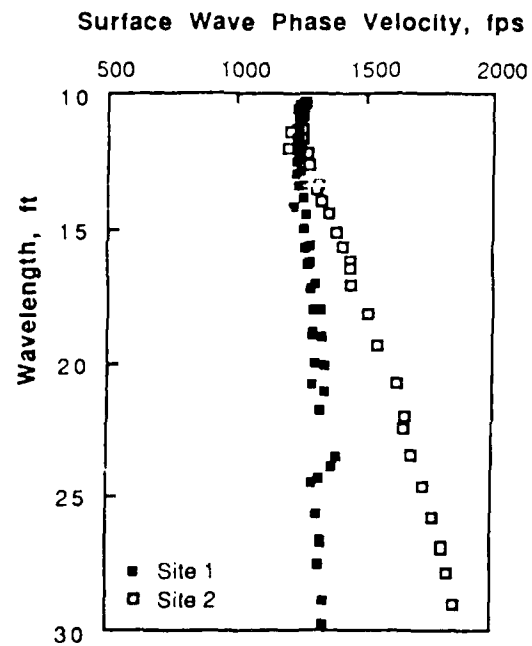
Dispersion curves obtained from the two sites are compared in Fig. 11. It can be seen that the two curves are similar up to a wavelength of about 2 ft. Between wavelengths of about 2 and 6 ft, the dispersion curve from Site 2 exhibits higher phase velocities. The most significant difference between the two curves occurs in the ranges of wavelengths of 15 to 30 ft, where phase velocities for Site 1 are more or less constant. Phase velocities for the second site increase significantly with wavelength. The presence of a very stiff layer was quite obvious using the SASW method even before the reduction of data (i.e., the inversion process). However, with deflection-based methods, the existence of bedrock is not obvious, and if the location of bedrock is not known, the stiffness profile obtained after backcalculating moduli will be in error.

The composite profile of one of the sites is shown in Fig. 12. Based upon comparison with the drilling logs, the thicknesses of different layers were predicted closely in both cases. A series of crosshole seismic tests was carried out at each site as well. Values of Young's modulus obtained by the two methods are typically within 25 percent as reflected in Fig. 12 which represents good agreement.

Modulus profiles from Sites 1 and 2 are compared in Fig. 13. Near the surface (i.e. for the AC and base layer) the stiffnesses are close. However, down to a depth of about 50 in. the subgrade at Site 2 is stiffer than that at Site 1. The subgrade materials of the two sites exhibit quite similar stiffnesses from a depth of 50 in. to about 80 in. where limestone is encountered at Site 2. The detailed and accurate modulus profiles obtained at these two sites demonstrates the value of the SASW method.



a. Range of Wavelengths of 0 to 10 ft



b. Range of Wavelength of 10 to 30 ft

Figure 11 - Comparison of Dispersion Curves from Sites 1 and 2 (Case 3)

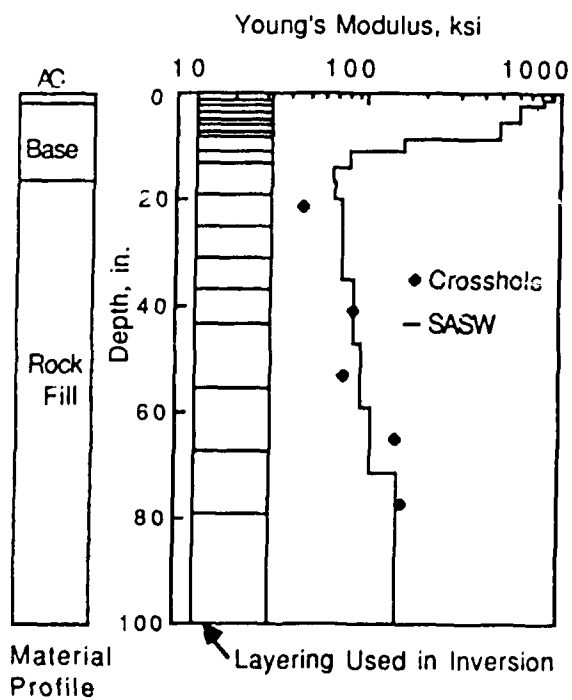


Figure 12 - Composite Profile at Site 1 (Case 3)

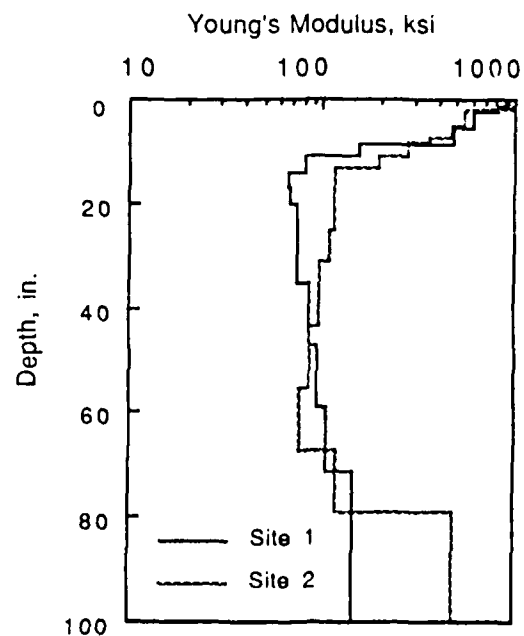


Figure 13 - Comparison of Stiffness Profiles from Site 1 and Site 2 (Case 3)

Case 4 - Diagnostic Tool

Two sites, 0.8 miles apart, were tested to determine why one section rutted while the other did not. Visually, the pavement at Site 1 was in excellent condition, and no cracking or depression could be located. On the other hand, Site 2 was selected at a point where cracks were visible, and the pavement was rutted approximately 1 in.

Based upon construction drawings, material profiles of the two sites were the same consisting of 1 in. of AC, underlain by about 10 in. of granular base on a clayey subgrade.

The average dispersion curves obtained at the two sites over a range of wavelengths of 0 to 3 ft are compared in Fig. 14. The two curves follow each other quite well in the range of wavelengths less than 0.5 ft and greater than 2.5 ft. However, in between these limits, phase velocities from Site 2 are less than those from Site 1. This indicates that for layers relatively

close to the surface, Site 1 exhibits greater stiffness than Site 2. This comparison demonstrates the role of dispersion curves as a valuable tool to detect changes in stiffness profile with time or location.

Young's moduli obtained from the two sites are compared in Fig. 15. The base materials are about 70 percent stiffer at Site 1 than Site 2, and the subgrade is about 15 percent stiffer at Site 1. One possible reason for the deterioration of the pavement at Site 2 is due to the softer base material. Subsequent coring of the two sites confirmed the existence of a softer base material (Nazarian et al, 1967).

CONCLUSIONS

The theoretical and experimental aspects of the SASW method were described herein. Compared to other nondestructive testing methods, the SASW method yields a more detailed modulus profile. This feature is quite desirable for project

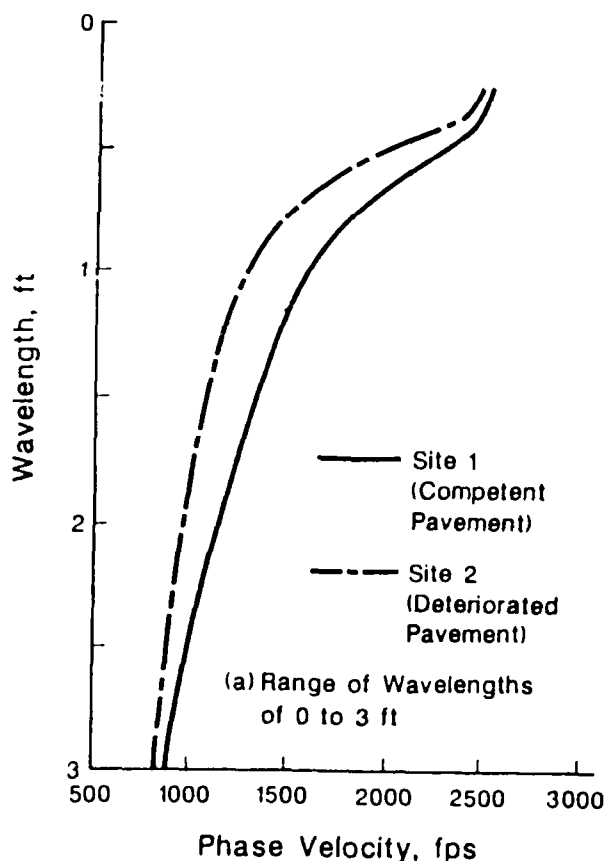


Figure 14 - Comparison of Dispersion Curves from Competent and Deteriorated Sites (Case 4)

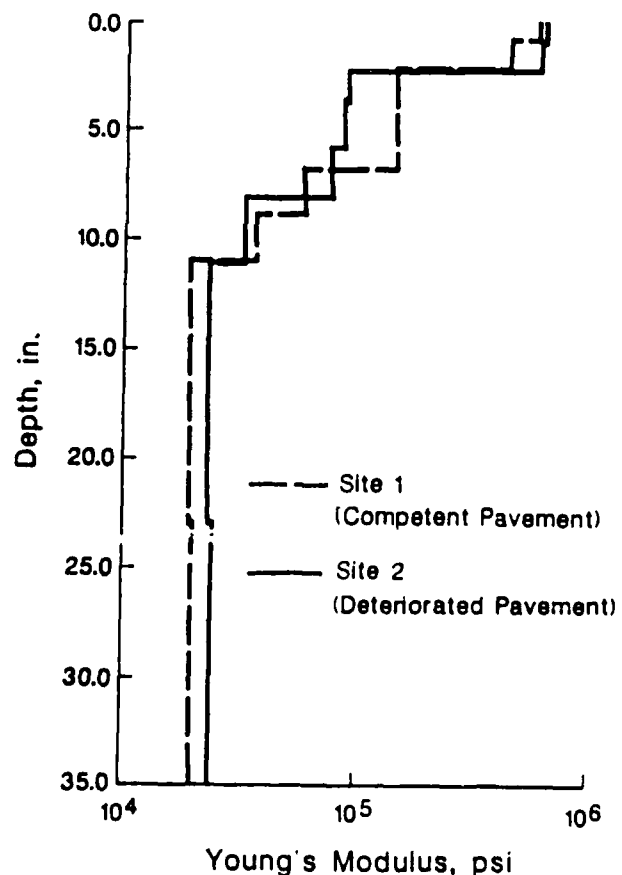


Figure 15 - Comparison of Young's Modulus Profiles from Competent and Deteriorated Sites Case (4)

level studies. In particular, the SASW method is sensitive to the properties of thin surface layers and layering within the subgrade; whereas other NDT methods typically result in erroneous modulus profiles.

Four case studies were presented to show some of positive aspects of the SASW method such as obtaining layer thicknesses, demonstrating the utility of the inversion process, determining the location of bedrock and correctly obtaining the modulus of the subgrade overlying the bedrock; and finally, as a diagnostic tool for determining the cause and extent of deterioration in a pavement system.

ACKNOWLEDGEMENTS

In the last eight years, the author has had the pleasure of interacting with several governmental organizations. Most of this work has been funded by the Texas State Department of Highways and Public Transportation. The financial support of other organizations such as the U.S. Air Force, U.S. Army Corps of Engineers, U.S. Bureau of Reclamation and U.S. Geological Survey is highly appreciated.

Above all, the author is in eternal debt to Dr. Ken Stokoe, a mentor and a friend for the last eight years.

REFERENCES

1. Briggs, R.C. and Nazarian, S. "Effects of Unknown Rigid Subgrade Layers on Backcalculated Pavement Moduli and Predictions of Pavement Performance," Transportation Research Record, Washington, D.C., 1989, (accepted for publication).
2. Davies, T.G. and Mamlouk, M.S., "Theoretical Response of Multilayer Pavement Systems to Dynamic Nondestructive Testing," Transportation Research Record 1022, Washington, D.C., 1985, pp.1-6.
3. Drenvich, V.P., Kim, S.I., Alexander, D.R., and Kohn, S., "Spectral Analysis of Surface Waves in Pavement Systems with Random Noise Excitation," Expanded Abstracts with Biographies, 55th Annual International Society of Exploration Geophysicists Meeting, Washington, D.C., October 6-10, 1985, pp. 143-145.
4. Dunkin, J.E. "Computation of Modal Solutions in Layered, Elastic Media at High Frequencies," Bulletin of Seismological Society of America, Vol. 55, No. 2, 1965, pp. 335-358.
5. Hardin, B.O., and Drenvich, V.P., "Shear Modulus and Damping in Soils: Measurement and Parameter Effects," Journal of the Soil Mechanics and Foundations Division, ASCE, Vol. 98, No. SM6, 1972, pp. 603-624.
6. Haskell, N.A., "The Dispersion of Surface Waves in Multilayered Media," Bulletin of the Seismological Society of America, Vol. 43, No. 1, 1953, pp. 17-34.
7. Hiltunen, L.R., "Experimental Evaluation of Variables Affecting the Testing of Pavement by the Spectral-Analysis-of-Surface-Waves Method," Ph.D. Dissertation, The University of Michigan, Ann Arbor, MI, 1988, 303 p.
8. Menke, W., Geophysical Data Analysis: Discrete Inverse Theory, Academic Press, Orlando, FL, 1984, 256 p.
9. Miller, G.F., and Pursey H., "On the Partition of Energy between Elastic Waves in a Semi-Infinite Solid," Proceeding, International Conference on Microzonation for Safer Construction: Research and Application, Vol. II, Seattle, WA, 1955, pp. 545-558.
10. Nazarian, S., "In Situ Determination of Elastic Moduli of Soil Deposits and Pavement Systems by Spectral-Analysis-Surface-Waves Method," Ph.D., Dissertation, The University of Texas at Austin, Austin, TX 1984, 453 pp.
11. Nazarian, S., Stokoe, K.H., II, "In Situ Determination of Elastic Moduli of Pavement Systems by Spectral-Analysis-of-Surface-Waves Method (Practical Aspects)," Research Report 368-1F, Center for Transportation Research, The University of Texas at Austin, 1985, 161 pp.
12. Nazarian, S., Stokoe, K.H., II, and Briggs, R.C., "Nondestructive Delineating Changes in Modulus Profiles of Secondary Roads," Transportation Research Record, Washington, D.C., 1987, (accepted for publication).
13. Nazarian, S., Stokoe, K.H., II, Briggs, R.C., and Rogers R.B., "Determination of Pavement Layer Thicknesses and Moduli by SASW Method", Transportation Research Record, Washington, D.C., 1988, (accepted for publication).
14. Reklaitis, G.V., Ravindran A., and Ragsdell, K.M., Engineering Optimization Methods and

- Applications, Wiley and Son, New York, 1983, 684 p.
15. Richart, F.E., Hall, J.R. and Woods, R.D., Vibrations of Soils and Foundations, Prentice Hall, Inc., Englewood Cliffs, NJ, 1970, 414 p.
 16. Roesset, J.M. and Shao, K.Y., "Dynamic Interpretation of Dynaflect and Falling Weight Deflectometer Tests," Transportation Research Record 1022, Washington, D.C., 1985, pp. 7-16.
 17. Sanchez-Salinero, I., Roesset, J.M., Shao, K-Y, Stokoe, K.H., II, and Rix, G.J., "Analytical Evaluation of Variables Affecting Surface Wave Testing of Pavements," Transportation Research Record, Washington, D.C., 1987, (accepted for publication).
 18. Seed, H.B., Wong, R.T., Idriss, I.M. and Tokimatsu, K., "Moduli and Damping Factors for Dynamic Analyses of Cohesionless Soils," Journal of Geotechnical Engineering, ASCE, Vol. 112, No. 11, 1986, pp. 1016-1032.
 19. Sheu, J.C., Stokoe, K.H., II, and Roesset, J.M., "Effect of Reflected Waves on SASW Testing of Pavements," Transportation Research Record, Washington, D.C., 1987, (accepted for publication).
 20. Thomson, W.T., "Transmission of Elastic Waves Through a Stratified Solid," Journal of Applied Physics, Vol. 21, 1950, pp. 89-93.
 21. Thrower, E.N., "The Computation of the Dispersion of Elastic Waves in Layered Media," Journal of Sound and Vibration, Academic Press, London, England, Vol. 2, No. 3, 1965, p. 210-226.

ALASKA'S EXPERIENCES WITH NON-DESTRUCTIVE TESTING

Billy Connor, P.E., ADOT&PF Statewide Research Manager

ABSTRACT

Alaska has been using deflection testing since the mid 1960's to estimate pavement strength and predict pavement performance. The first use of these data was primarily for establishment of load restrictions. In 1981 deflection data became the basis for overlay design. The Alaska Department of Transportation purchased a RoadRater in 1981. However, the low load and cyclic loading proved not to be useful, especially during spring thaw. As a result, a falling weight deflectometer was purchased in 1983. Since that time, deflection data has been used to analyze pavement structures for design as well as for load restrictions.

Use of nondestructive testing in cold regions presented unique problems which require specialized techniques. These include the need to estimate accurately thaw depths and seasonal effects. Alaska is implementing a mechanistic overlay design procedure which requires that these effects be taken into account. Numerous techniques have been tried with varying levels of success. However, no technique has proven to be completely successful. For example, backcalculation procedures which have proven successful in temperate climate have severe limitations when used during spring thaw or when frozen soils are near the surface. This paper discusses Alaska's experience including what has and what has not been successful.

INTRODUCTION

Non-destructive testing (NDT) in Alaska has evolved from the use of the Benkelman beam to the current use of the falling weight deflectometer. As technology improved, the confidence in deflection based procedures increased. Deflection data is used to establish load restrictions, predict pavement performance, design overlays and research. NDT has provided an invaluable tool to measure in-situ soils properties and structural response and the ability to estimate soil layer strengths. As a result, our understanding of pavement response and performance has improved dramatically over the last 20 years. This paper discusses Alaska's experiences, both positive and negative, in hopes that others will benefit.

LOAD RESTRICTIONS

The use of non-destructive testing began in Alaska in the 1960's with the implementation of the Benkelman Beam to establish load restrictions during spring thaw. These early procedures required load restrictions when the deflection exceeded the 0.050 inches. Even then, the use of the Benkelman Beam was limited primarily to the urban areas.

A procedure was developed in 1980 for establishing load restrictions based upon the premise that the springtime damage would be limited to that which would normally occur during the summer months.(1) Through the use of the Canadian Good Roads Association life prediction curves shown in Figure 1, the curves shown in Figure 2 were developed. The curves were based upon equation 1.

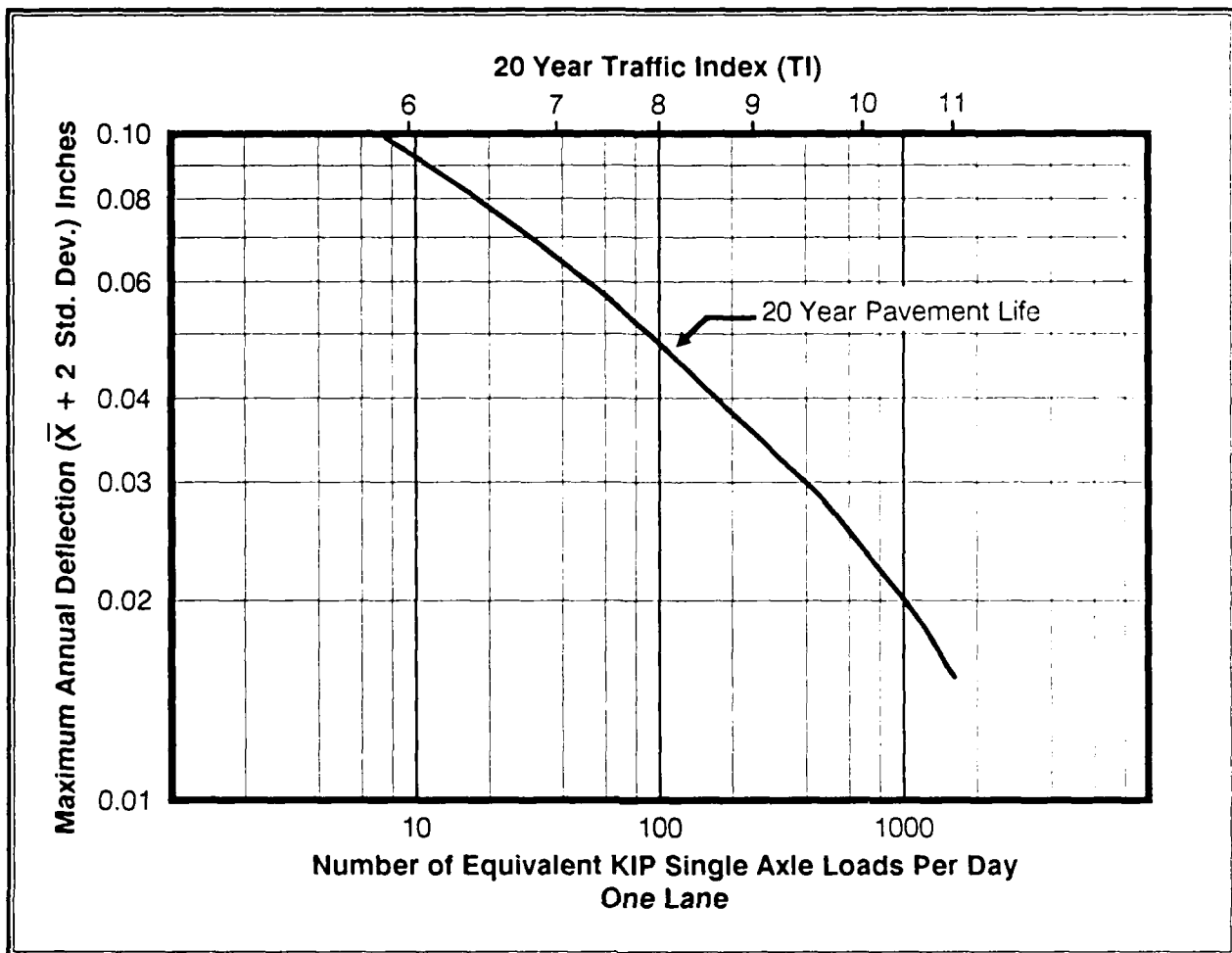


Fig. 1. CGRA life prediction cruves.

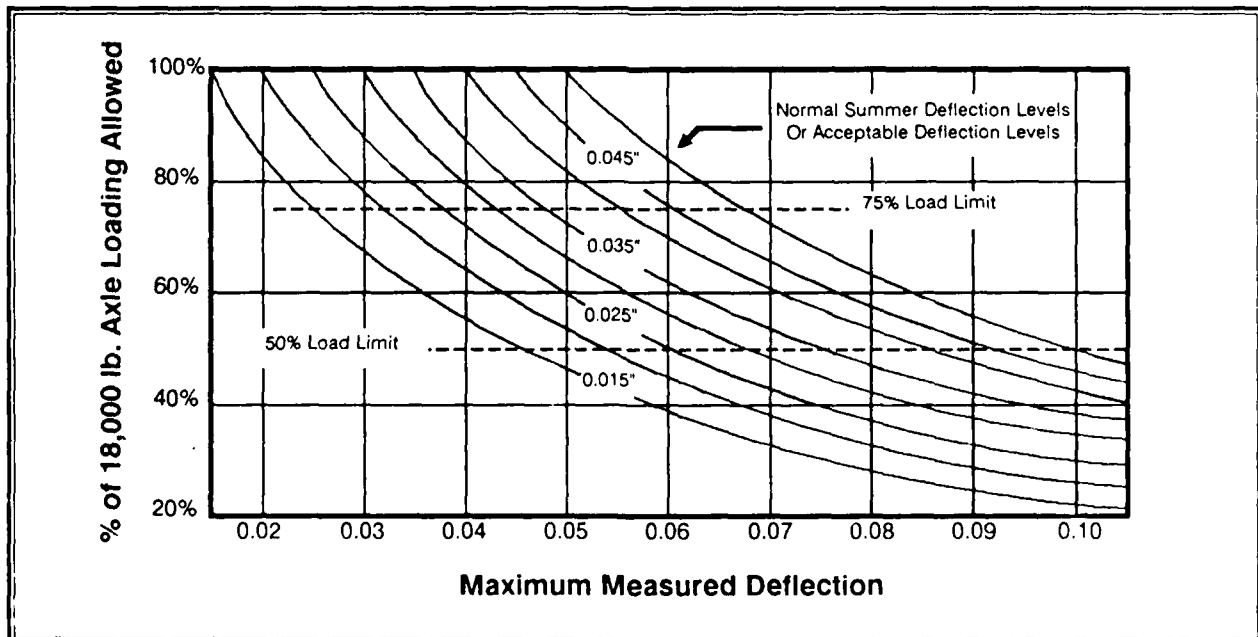


Fig 2. Determination of required load restrictions.

$$\frac{N_{f(\text{spring})}}{N_{f(\text{summer})}} = \left(\frac{W_2 + 1}{W_1 + 1} \right)^{4.79} \quad \text{eq . 1}$$

where:

$N_{f(\text{spring})}$ = the number of cycles to failure failure based on the spring deflection

$N_{f(\text{summer})}$ = the number of cycles to failure based on the summer deflection

W_2 = the spring single axle loading

W_1 = the legal single axle load (18 kips)

These curves provided a simple method of determining the required load limits required for any set of deflection measurements. In actual practice only two values of load limits are used, 75% and 50%.

PAVEMENT DESIGN

In the late 1960's and the early 1970's, state policy concentrated on getting a paved surface on all of Alaska's primary network. As a result, the structural section usually consisted of 3 to 4 feet of borrow, 6 inches of subbase (1 inch minus), 6 inches of base course (3/4 inch minus) and 2 inches of hot asphalt pavement. By 1977, rapid deterioration of some paved sections precipitated the need for improved design procedures. The Statewide Materials Laboratory began a four year research program to determine why some roadway sections failed while others had good performance.(2) As part of this study, 120 one-mile roadway sections were monitored using the Benkelman Beam. From this work, relationships were found between fines content, deflection, and performance. A design procedure based on this study was developed in 1981 which limited the fines content with depth. This design procedure predicts the Benkelman Beam deflection at the top of the base course. The predicted deflection is then used with the Asphalt Institute overlay design curves to determine the pavement thickness. This design procedure is still in use.

As part of the 1981 Pavement Design Guide, an overlay design procedure was developed which required the use of deflection testing during the spring thaw period using the

Canadian Good Roads Association (CGRA) rebound method and the Asphalt Institute overlay design curves. This procedure has several problems. First, it does not consider the current condition of the pavement. The deflection may show no overlay is required while the surface shows fatigue cracking. Second, it does not consider the thickness of the existing pavement which has an effect on the pavement performance after the overlay. Thirdly, the procedure does not consider the relationship between the pavement modulus and the fatigue life. As a result, this procedure is being replaced with a fully mechanistic design procedure.

SAMPLING INTERVAL

In an effort to determine the appropriate sampling interval, McHattie and Connor reviewed the deflection data collected on the 120 roadway sections. Through the use of the Student's T table for a confidence level of 90% that no more than 0.01 inch error in the true mean deflection would occur, the sampling interval in Table 1 was developed. Table 1 represents the number of measurements required to characterize the smallest design section. The minimum number of deflection measurements required per section is not dependent upon the the section length. For example, if the smallest design segment is 0.10 mile, and the average deflection is anticipated to be 30 mils, and the standard deviation is anticipated to be 12 mils, then there must be 4 measurements per 0.10 mile or 40 measurements per mile. However, this approach is rarely used in the design of a deflection measurement program.

Table 1: Deflection Sampling Frequency

Average Deflection (mils)	Standard Deviation (mils)	Minimum Number of Measurements
5	6	2
5-40	12	4
> 40	20	7

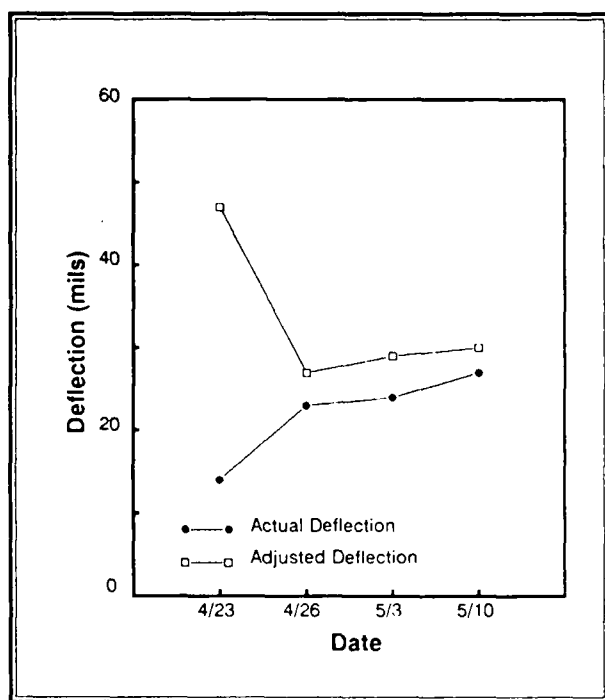


Fig. 3. Comparison of actual and adjusted deflections.

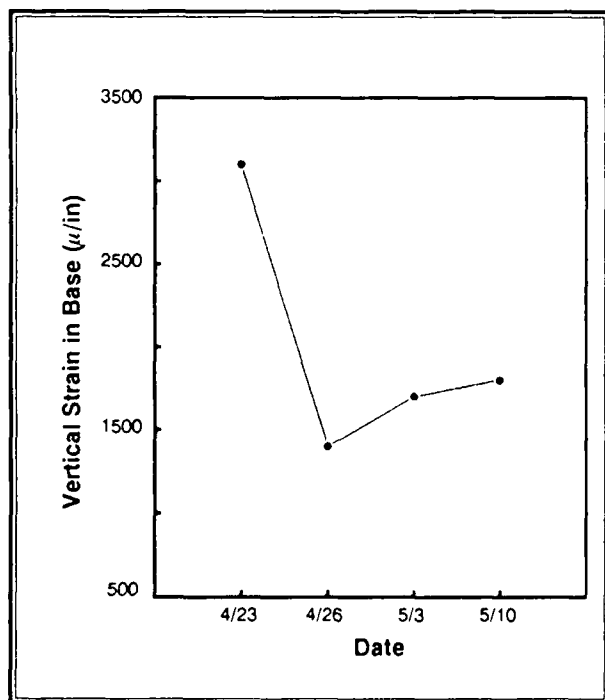


Fig. 4. Vertical strain in base.

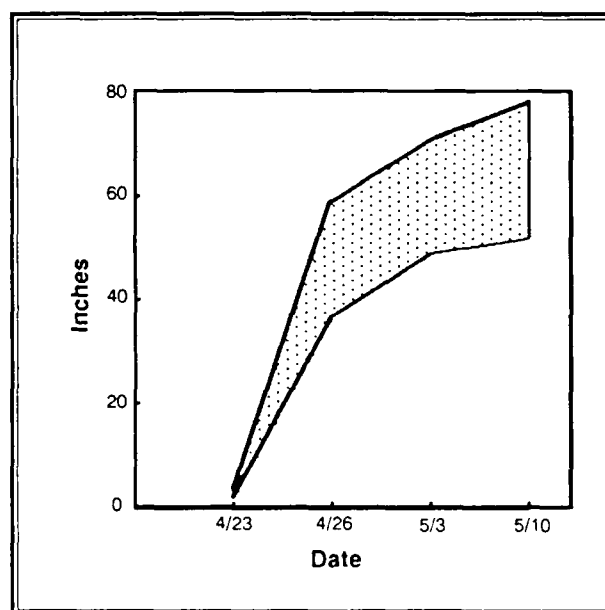


Fig. 5. Predicted thaw depth using FROST.

CURRENT PRACTICE

The use of the FWD is well established within the DOT&PF. Deflection data is required for all rehabilitation projects. However, the use of the deflection varies with the designer. Most designers still use the Asphalt Institute design curves and the center deflection to determine the required overlay thickness. However, the trend is to move toward the fully mechanistic approach especially in the high traffic areas.

Statewide Research with the aid of Oregon State University (OSU) has developed a fully mechanistic overlay design procedure which is currently in the process of being implemented (6). At the heart of the procedure are two computer programs developed at OSU, BOUSDEF and MECHOD. BOUSDEF is a backcalculation routine which is based upon the equivalent layer approach. This program has the primary advantage of speed. Typical backcalculations take about 15 seconds on an IBM AT computer. The backcalculation procedures run on the same computer take about 25 minutes or more. The program has also proven to be more reliable for backcalculation of moduli during spring thaw. The moduli predicted by BOUSDEF have also compared well with the linear elastic approaches.

The MECHOD computer program simply automates the mechanistic design approach. The

LIFE PREDICTION

As part the development of a life cycle costing model, an equation was developed which correlated fatigue cracking, the Benkelman Beam deflection and the number of equivalent axle loadings (EAL) shown in equation 2 (3)

$$\log(\text{FC}) = -19.05 + 5.67 \log(\text{BB}) + 2.09 \log(\text{N}) \quad \text{eq. 2}$$

where:

FC = % fatigue cracking

BB = Benkelman Beam deflection

N = Number of 18 kip equivalent axle loadings

This equation has proven very useful in estimating remaining life of pavements.

ROAD RATER

The State of Alaska bought a Road Rater Model 2000 in 1981 in an effort to replace the Benkelman Beam. However, it soon became apparent that the Road Rater would not be useful in Alaska. The first efforts to use the Road Rater consisted of developing a correlation between the Benkelman Beam and the Road Rater as shown in equation 3.(4)

$$\text{RR} = (0.11)\text{BB} + 0.5 \quad \text{eq. 3}$$

$$R^2 = 0.60$$

where:

RR = the Road Rater center deflection

BB = the Benkelman Beam deflection

Repeatability tests were then performed to determine the repeatability of the test. It was found that when the granular layers were soft, standing waves were set up which caused the center deflection to be lower than the distant deflections. The primary reason was found to be that the vibratory load liquified the soil layers causing unpredictable results. As a result, the deflections measured became a function of the load and the frequency. The use of the Road Rater was abandoned.

FALLING WEIGHT DEFLECTOMETER

Alaska purchased its first falling weight deflectometer (FWD) in 1983. Again, a correlation was developed between the Benkelman Beam and the FWD as shown in equation 4.(4)

$$\text{FWD} = (0.97)(\text{BB}) + 0.00523 \quad \text{eq. 4}$$

$$R^2 = 0.88$$

where:

FWD = the center deflection of the falling weight deflectometer

BB = the Benkelman Beam deflections

As can be seen, the FWD correlates quite well with the Benkelman Beam. The FWD also offers the advantage of defining the deflection basin which has been recognized as necessary data to determine the soil reaction to loading. This additional data spawned several research studies which more accurately define the pavement structure and its response.

Stubstad and Connor recognized that the maximum center deflection may not correspond with the period of maximum damage potential.(5) Several deflections were analyzed using ISSEM4 and Chev N-layer computer programs to determine when the maximum damage potential would occur during spring thaw. A typical analysis is shown in Figure 3. The maximum fatigue damage potential in this example was found to occur when the thaw depth was about 1 foot. This trend can be observed in all pavements which have frost susceptible base courses. In order to take advantage of the existing load restriction procedures, the computer program FROST was developed which presented an equivalent center deflection which would cause the same damage as a completely thawed embankment. This was accomplished by comparing the horizontal tensile strains in the bottom of the asphalt layer and the shear stress in the base course as shown in Figure 4. A by-product of this analysis was an estimation of the thaw depth which can be used as a first estimate of thaw depth in the backcalculation of moduli, as shown in Figure 5. However as the thaw depth increases the uncertainty of the prediction also increases.

Load Data:								File in Use	
Load Force (lbs): 9000 Load Radius (in.): 5.90								TEST	
Layer Properties:									
Number of Layers: 4				Season(s) for Analysis					
Layer Thickness		Spring (Y)		Summer (Y)		Fall (Y)		Winter (Y)	
No.	(inch.)	Modulus	Pois	Modulus	Pois	Modulus	Pois	Modulus	Pois
1.	2.0	1000000	0.35	500000	0.35	500000	0.35	3000000	0.30
2.	12.0	10000	0.40	50000	0.40	40000	0.40	250000	0.35
3.	36.0	250000	0.45	25000	0.45	20000	0.45	250000	0.35
4.	0.0	250000	0.45	10000	0.45	8000	0.45	250000	0.35
5.	0.0	0	0.00	0	0.00	0	0.00	0	0.00
Traffic Data:									
Hist. Repetitions:		50000		275000		200000		150000	
Future Repetitions:		60000		300000		250000		150000	
Reliability Level (%): 80				Standard Deviation: 0.45					
Mixture Properties:									
Bulk Specific Gravity:		2.500							
% of Asphalt (by weight): 6.00				% of Air Voids: 4.00					
Press [Esc] to Save and Exit									

Fig. 6. Input screen for MECHOD.

input screen shown in Figure 6, requires only moduli and traffic data as input. As shown, the programs allows the year to be broken into 4 seasons to account for the variability of materials strength through the year. The traffic must also be distributed through the four seasons. Since the concept of remaining life is incorporated into the procedure, the past traffic is also required. The flow of the program is as follows:

1. Determine the horizontal strain in the bottom of the pavement layer and the vertical strain at the top of the subgrade for each season using ELSYM5.
2. Estimate the number of cycles to failure both in fatigue and permanent deformation.
3. Check the number of cycles to failure against the total traffic, past and future, to determine if the predicted life is less that the anticipated traffic loadings.
4. If yes, then quit. If no, add 1/2 inch of pavement.
5. Go to step 1.

The procedure proposed for Alaska is similar to commonly used mechanistic design techniques. However, MECHOD greatly simplifies the process. The output provides a dis-

tribution of damage through the seasons allowing the designer to determine when the damage is occurring.

*Thickness and modulus used in the forward calculation of the deflection basin.

The moduli required for the procedure will come primarily from backcalculated moduli using the FWD and BOUSDEF. The department will allow the use of other backcalculation procedures such as ELMOD3 or ELSDEF.

BACKCALCULATION

One of the most difficult parts of any mechanistic design procedure is the determination of soil moduli. All of the backcalculation procedures require accurate determination of soil layer thicknesses. This is generally not difficult; however, in northern climates the thickness of the thawed layer is not as simple. It is far too costly to drill at each location to determine the thaw depth. Other geophysical methods such as seismic techniques or ground penetrating radar are currently not sufficiently developed. Therefore, some means of determination of the depth of thaw is required. Consider the problem shown in Figure

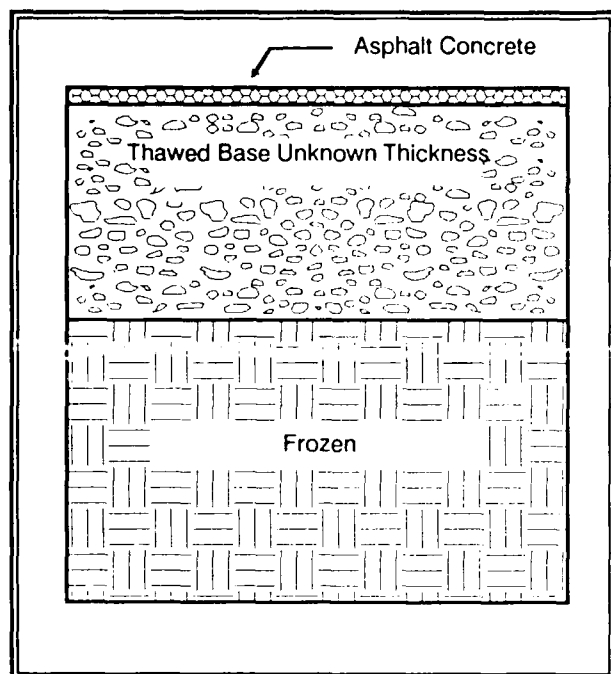


Fig. 7. Typical spring soil profile.

7. The asphalt layer thickness and modulus can be readily estimated. The modulus of the frozen layer can be estimated to be about 250 ksi. However, the thickness and modulus of the thawed layer is usually not known. Unfortunately, there is no known closed form solution to this problem. (Since 90% of the pavement damage may occur during the spring thaw, a solution to this problem is imperative.)

In order to demonstrate one possible solution procedure, the deflection basin for Figure 8 was computed using ELSYM5. BOUSDEF was then used to estimate the modulus of the thawed base course as a function of thickness as summarized in Table 2. Table 2 also shows the effect

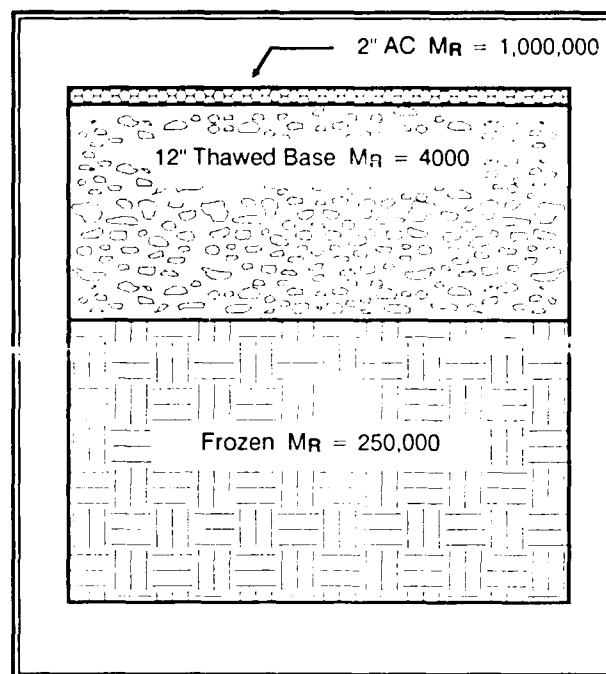


Fig. 8. Example problem for back calculation.

of the error in thickness and modulus on the predicted horizontal strain at the bottom of the pavement layer and the estimated pavement fatigue life using the Asphalt Institute equation. These errors are significant and demonstrate the need for good thickness estimation.

SUMMARY

Non-destructive testing using the falling weight deflectometer has become an integral part of the Alaska Department of Transportation and Public Facilities. Deflection data is used to establish load restrictions, design overlays, estimate

Table 2: Summary of the Test Case

Estimated Thickness	Modulus	Microstrain	Fatigue Life	% Error in Fatigue Life
10	4,287	612	37,544	11
12	5,094	607	38,572	14
14	5,910	597	40,739	21
16	6,732	583	44,048	30
18	7,223	577	45,574	35
18*	6,000	632	33,744	--
20	8,543	547	54,744	61

remaining life, and research. Over the last 20 years, considerable improvements have been made in the application and understanding of the data collected by NDT devices. New techniques in backcalculation of moduli have allowed the determination of soil response based upon in-situ measurements have enhanced the knowledge of seasonal variation of soil strength and pavement damage. In-situ measurements also allow design procedures to be readily checked after the embankment has been built.

However, there are still several problems. Current backcalculation procedures are still very much an art. The users of the available computer programs must be keenly aware of the expected range of moduli. Because there is no unique solution in the determination of moduli, the seed moduli and range of moduli required by most backcalculation programs will affect the final solution. Therefore, the user must have a reasonable idea of what the moduli are.

In northern climates the thaw depth in the spring adds another variable in the equation. The estimation of the thawed layer thickness, as has been shown, can have dramatic effects on the predicted moduli and the estimated pavement life. Techniques must therefore be developed to estimate this thickness.

In conclusion, non-destructive testing has proven to be a most valuable tool in predicting pavement performance through in-situ testing. New methods such as seismic and ground looking radar offer the ability to improve our current capabilities especially in the determination of layer thicknesses. There has been considerable progress in the past 20 years; however, much is to be learned.

REFERENCES

(1) Connor, B., Rational Seasonal Load Restriction and Overload Permits, Alaska Department of Transportation and Public Facilities Statewide Research Report FHWA-AK-RD-80-02, 52 pp., 1980.

(2) McHattie, R., B. Connor, and Dave Esch, Pavement Structure Evaluation of Alaskan Highways, Alaska Department of Transportation and Public Facilities Statewide Research Report FHWA-AK-RD-80-01, 208 pp., 1980

(3) Kulkarni, R., C. Saraf, F. Finn, J. Hilliard, and C. Van Til, Life Cycle Costing of Paved Alaskan Highways, Volume I, Alaska Department of Transportation and Public Facilities Statewide Research Report AK-RD-83-05, 99 pp., 1982.

(4) McHattie, R.L., Deflection Testing and Its Application to Pavement Rehabilitation in Alaska, Alaska Department of Transportation and Public Facilities Statewide Research Report FHWA-AK-RD-85-15, 102 pp., 1985.

(5) Stubstad, R.N., and B. Connor, Prediction of Damage Potential on Alaskan Highways During Spring Thaw Using the Falling Weight Deflectometer, Alaska Department of Transportation and Public Facilities Statewide Research Report AK-RD-83-11, 20 pp., 1982.

(6) Yapp, M., R.G. Hicks, and B. Connor, Development of an Improved Overlay Design Procedure for the State of Alaska, Volume II, Final Report, Alaska Department of Transportation and Public Facilities Statewide Research Report FHWA-AK-RD-88-06A, 1987 (in Publication Process).

EXPERIENCE WITH NONDESTRUCTIVE TESTING OF TWO
INSTRUMENTED AIRFIELD PAVEMENTS IN MANITOBA, CANADA.

GANI V. GANAPATHY

PUBLIC WORKS CANADA,
WINNIPEG, MANITOBA, CANADA.

ABSTRACT

Two instrumented airfield taxiways, one flexible and the other rigid, were tested non-destructively using the Dynatest 8000 Falling Weight Deflectometer (FWD). The FWD drops were made at locations with and without the instruments. The instrumentation consisted of flat plate piezo-electric load cells in the flexible pavement whereas, the rigid pavement was instrumented with hermetically sealed resistance type strain gauges used typically in exposed concrete structures. The gauges for the flexible pavement were placed to obtain the critical strains (and hence by extension the stresses) at the bottom of the asphalt, top of the subgrade, at some locations in the granular layer and in the subgrade 1.0 m below the pavement structure. This pavement was also instrumented with piezometers at various depths to obtain an idea of the influence of pore water pressure on the stresses and strains in the pavement. The instrumentation for the rigid pavement consisted of embedding the strain gauges at different depths of the slab. No instruments were placed in the granular base or in the subgrade. In addition to FWD testing, the pavements were tested by repetitive

static plate load tests. Finally the strains were measured under the gear loads of B-737 aircraft. In the case of the rigid pavement, additional data was collected under Hercules aircraft of the Canadian Ministry of National Defence who happened to be using the strip during one of their manoeuvres at the time of testing. The paper presents the details of the pavement structure, subgrade conditions and material properties as obtained during the construction. Instrumentation and testing programme are described. The analyses consisted of backcalculating the moduli from the FWD deflection basin and calculating the strains and stresses at the location of the instruments. These are compared with the values measured directly from the instruments. The results are also compared with those obtained from static plate load tests and from the passing aircraft load. The advantages and disadvantages of FWD testing and backcalculation of the moduli are discussed. The validity of the FWD loads to represent aircraft gear load is discussed. It is suggested that FWD alone may not be the ideal method to evaluate airfield pavements.

Introduction

Deflection testing has been long recognized as a means of assessing the structural capacity of pavements. The concept and equipment were first introduced by Benkelman and was later used in the AASHO Road Tests in the early sixties. In the last fifteen years there has been a tremendous improvement in the deflection measuring equipment with sensitive accelerometers and automatic data loggers and data processors. These machines are sophisticated, accurate, have a high degree of repeatability and can simulate the actual traffic loads. They can collect a vast amount of data in a short time. Unlike the Benkelman Beam, the Shell vibrator or the plate load tests, which could measure deflections at only one point, these modern deflection measuring equipment can measure deflections at different points and thus define the entire deflection basin. An excellent review of these machines, their capabilities and limitations can be found in the literature [1-4].

While we possess the capability of measuring the pavement response to a given loading condition fairly accurately, the interpretation of the measurements has remained a thorny problem. This was evident in the papers presented at the Third International Conference on the Design of Concrete Pavements at Purdue University in 1985 [5,6], at the Sixth International Conference on Structural Design of Asphalt Pavements in Ann Arbor in 1987 and again at the ASTM symposium in Baltimore in 1988.

The single most important result to be derived from deflection testing is a measure of stiffness of the pavement layers. This measure of stiffness has been variously called "elasticity modulus", "deformation modulus", "resilient modulus" or "stiffness modulus".

In this paper this is simply referred to as modulus. The most common analysis of the deflection data consists of an iterative process of matching the observed deflection basin to a theoretically calculated basin using the layered elastic theory. The iteration is, generally, started by assuming certain seed values of moduli for the component layers. Generally, a variance of three to five percent between the theoretical and observed deflection basins is considered to be an acceptable match. Various computer algorithms for the solution of the layered elastic theory are available.

The problem with this approach is that the solution obtained in this manner is not unique. As is well known from the theory of Burmister [7] and subsequent extensions by Acum and Fox [8] and Jones [9], it is the modular ratio of the component layers that determines the surface deflections. Therefore, a large number of combinations of moduli can lead to the same deflection basin. Thus it is necessary to temper the results of backcalculation analyses with engineering judgement and other independent means of measuring the moduli of the pavement materials. Such independent measurement has been, traditionally, laboratory triaxial tests under repeated loading conditions. Recent attempts by Briaud et al [10,11] and a study being conducted by the author may provide alternate means of measuring the moduli.

The measurement or derivation of a modulus value per se is not the ultimate objective of pavement design or evaluation process. Pavement design and evaluation are based on certain critical stresses or strains within the pavement structure. Thus, there is a need to understand whether backcalculated moduli can be used with confidence to compute these



FIG.- 1. Geographical location of the sites

TABLE -1. Climatic Data on the Test Sites

	THOMPSON	BRANDON
TEMPERATURES: (°C)		
MAXIMUM	31.4	35.0
MINIMUM	-46.5	-38.1
MEAN	-4.0	1.5
PRECIPITATION: (cm)		
RAINFALL	35.7	33.9
SNOWFALL	252.0	116.9
FREEZING INDEX (DAYS C)	2963	2017
THAWING INDEX (DAYS C)	1641	2619

NOTE: DATA IS 35 YEAR AVERAGE

stresses and strains. This can be done only by actually measuring the displacement and strains within the pavement structure and comparing these with those derived by backcalculation.

This paper describes such an attempt where two airfield taxiways, one flexible and the other rigid, have been instrumented with displacement gages or strain gages and tested under different loading conditions. The loading devices used were the Dynatest 8000 falling weight deflectometer (FWD), static plate load and actual aircraft loads.

Test Sites

The pavements are two short taxiways approximately 200 to 250 m long in the regional airports of Thompson and Brandon, both in the province of Manitoba, Canada. Fig. 1 shows the geographic location of these two sites. Table 1 shows some pertinent environmental conditions at the two sites. Fig. 2 shows the typical geotechnical and subgrade conditions. The airports are served by B-737 jet aircraft and are also being used by several other smaller types of aircraft mainly for charter and flight training services. These two airports were chosen for this study because, the two taxiways in question were totally reconstructed from subgrade up. This made it easy to install the instruments without great problems. Also it was possible to have a fairly good idea of the properties of the materials that went into their construction. Figs. 3 and 4 show the locations of the test sites at Thompson and Brandon airports respectively. Taxi A at Thompson is a flexible pavement while Taxi B at Brandon is a rigid pavement. Figs. 5 and 6 show the typical cross sections as well as the locations of the instruments. Tables 2 and 3 show the elevations of the instruments at the different locations at the two sites.

Instrumentation

a) Thompson

Because the pavement at Thompson is of the flexible type, the primary instrumentation consisted of 230 mm diameter flat plate diaphragm type piezoelectric load cells (Figs. 7 and 8). The cells were supplied by RST Instruments Ltd. of Vancouver, B.C. Canada. Table A-1 in Appendix A shows the specification of these cells. The cells were laid flat on a firm bedding of sand. The transducers were integral parts of the load cells and were connected to the cells by a 600 mm long stainless steel tube. The cells were delivered with 12 m long color coded lead cables sheathed in insulated, grounded and grease filled outer metallic jacket. Each unit came with a zero voltage calibrated in the factory. The zero voltage and the calibrations were checked on receipt at the site. At each subsequent stage of handling and installation of the gages the zero readings were checked with a hand-held voltmeter. The working condition of the gages after they were buried in the ground was checked occasionally by running the construction equipment at their locations and noting the responses of the cells. The instruments were replicated in sufficient numbers to allow for any possible malfunctioning of the gages during the test period.

A brief description of the load cells that were placed at the bottom of the asphalt layer is appropriate here. These gages were supplied with a second 10 m long hermetically sealed stainless steel tube filled with oil and flushed of all air. These are the repressurizing tubes. As the hot asphalt cooled and hardened, the initial contact between the cell face and the mat would be lost. The contact was reestablished by crimping the repressurizing tubes from the end

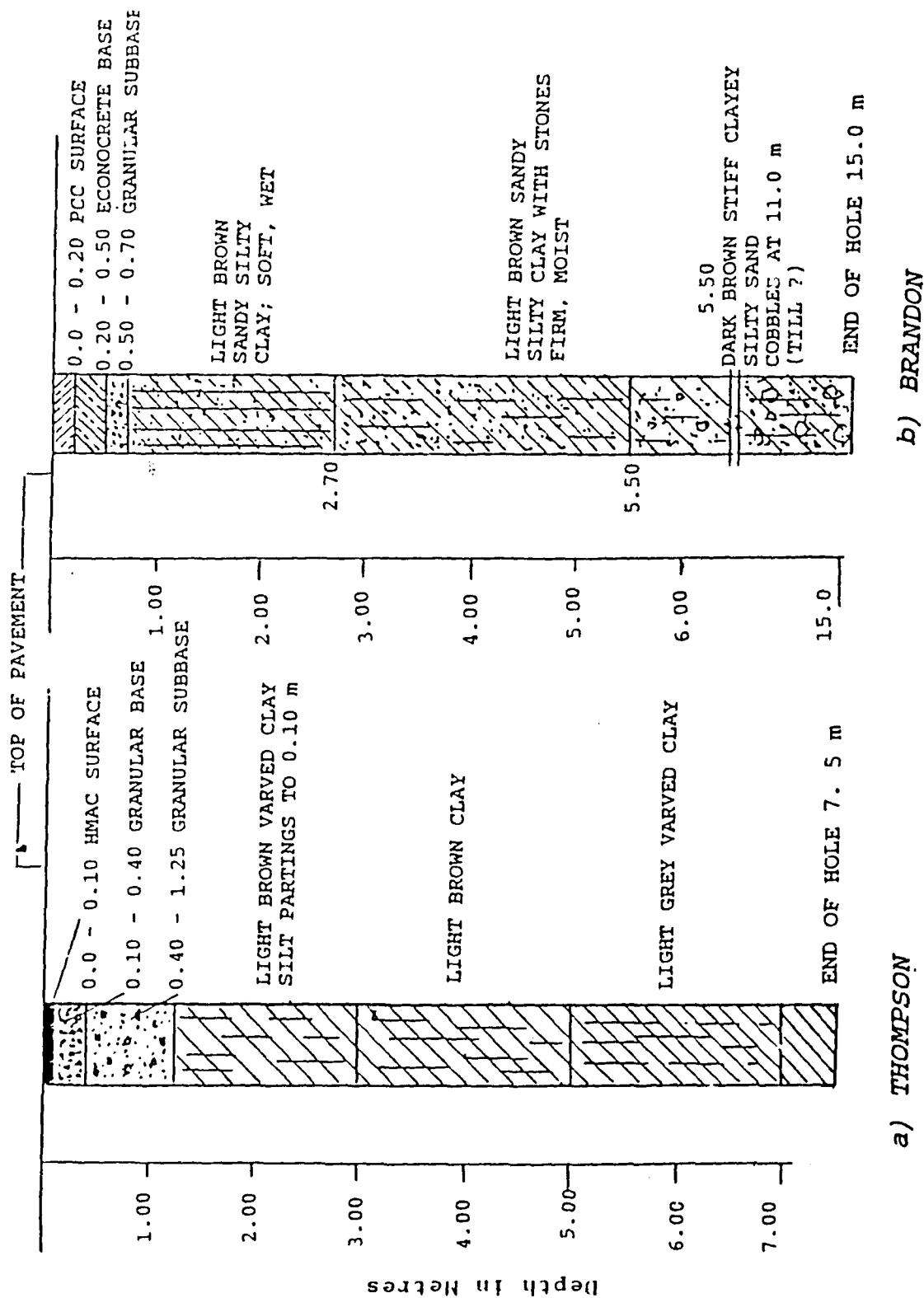


FIG.- 2. TYPICAL SUBGRADE CONDITIONS AT THE TEST SITES

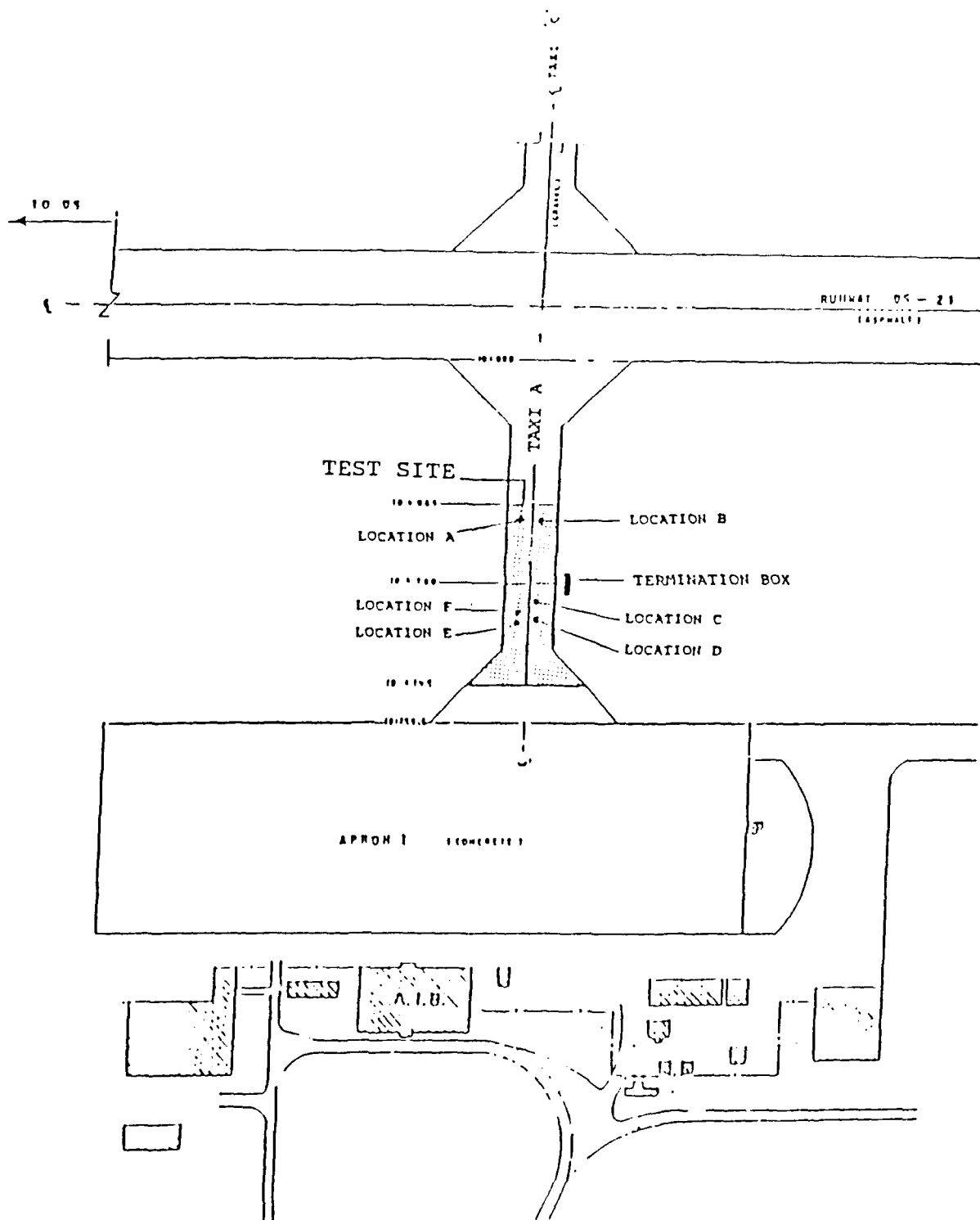


FIG.- 3. Test site at Thompson

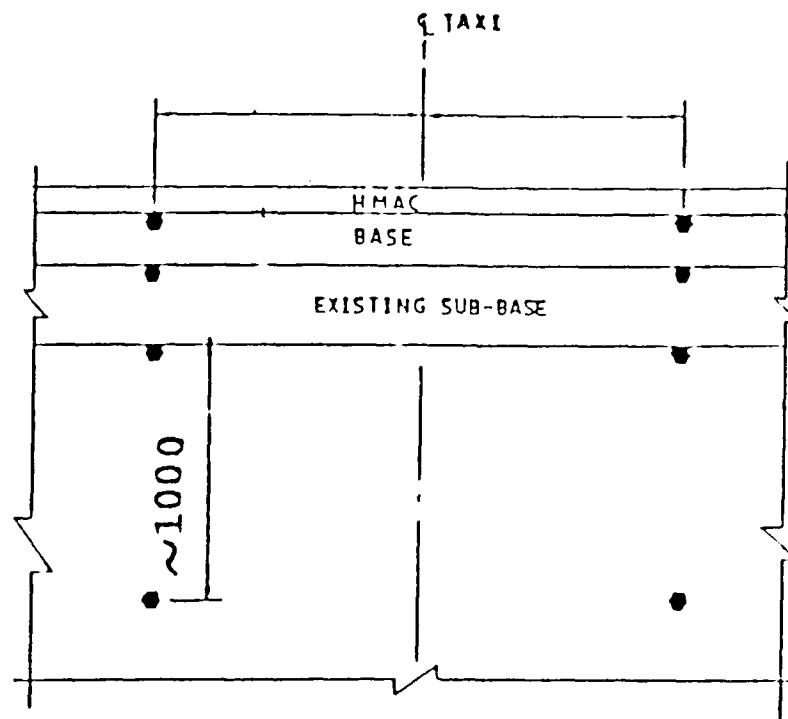


FIG.- 5. Arrangement of load cells in the pavement at Thompson

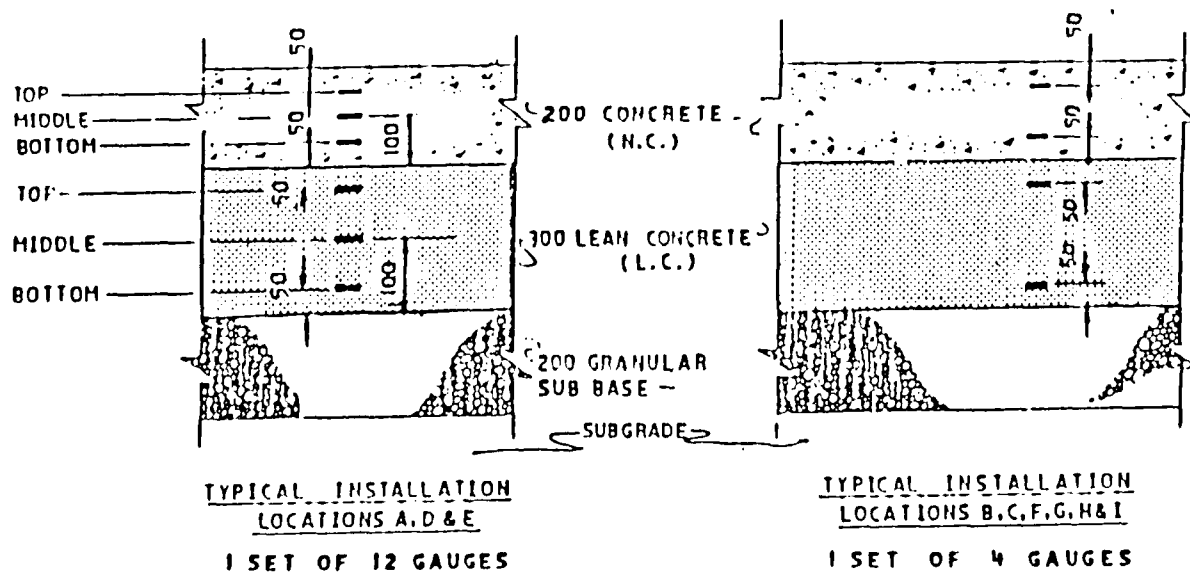


FIG.- 6. Arrangement of strain gages in the pavement at Brandon

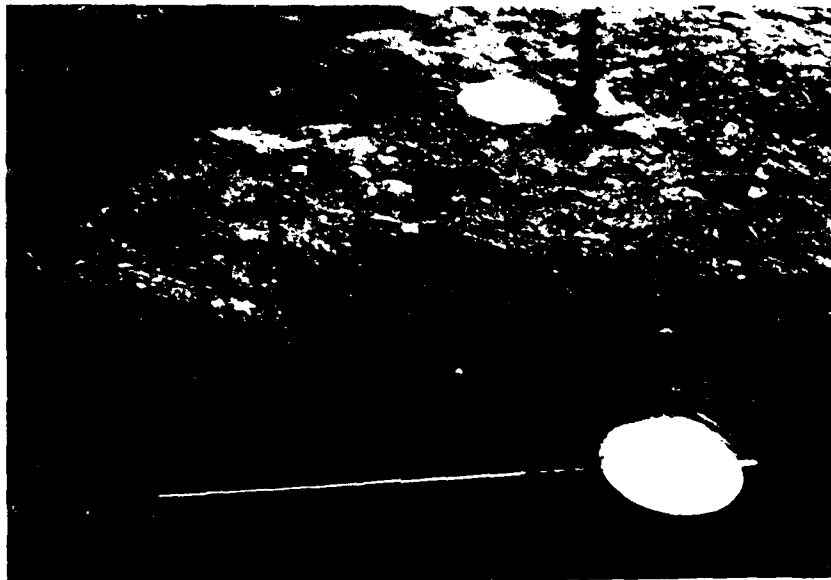


FIG. - 7. - Flat plate diaphragm load cells
for unbound materials

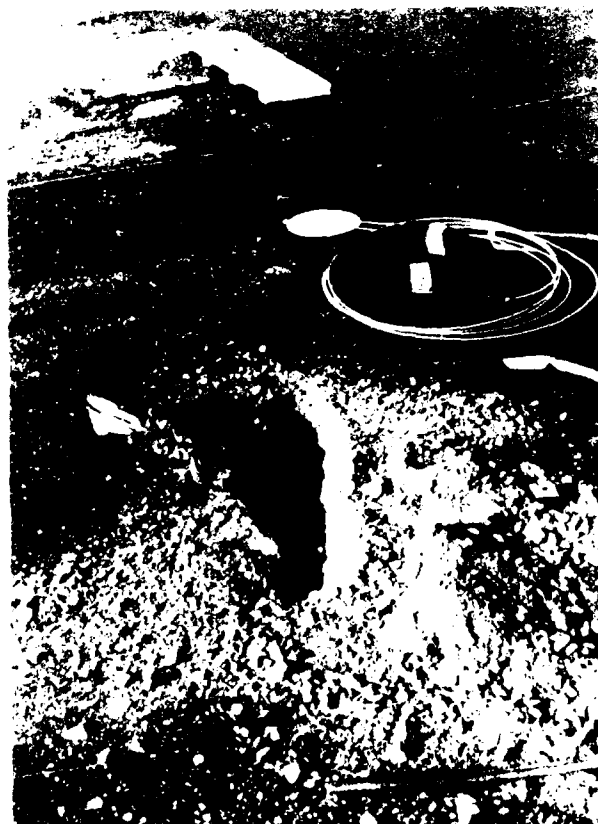


FIG. - 8. - Flat plate diaphragm load cells
under asphaltic concrete

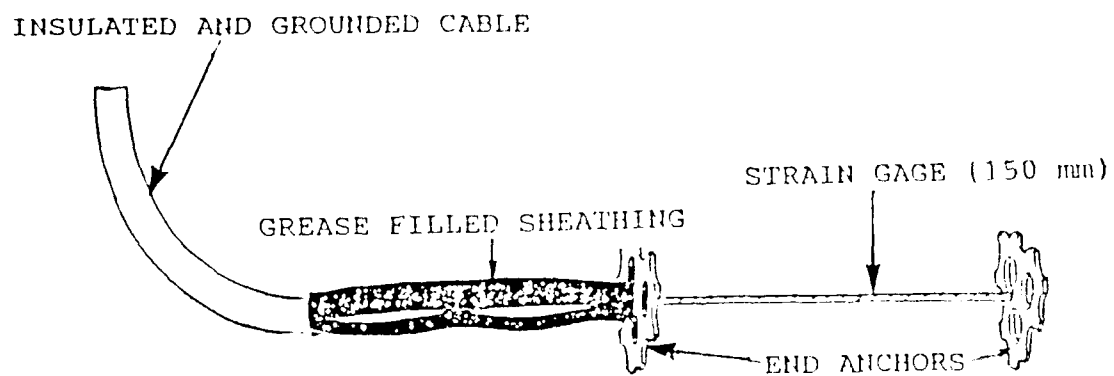


FIG.- 9. - *Resistance strain gages with two end anchor plates*

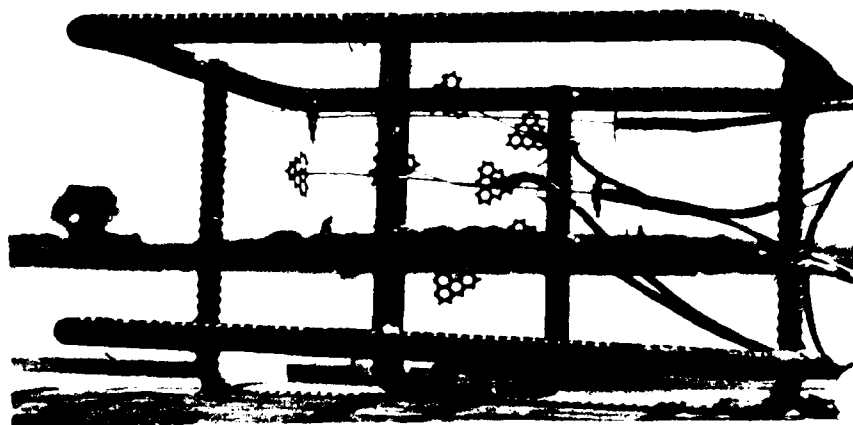


FIG.- 10. - *Strain gage assembly being prepared in a steel cage*

TABLE - 2. Thompson: Taxi - A: Locations and Elevations of Load Cells

STATION	CHAINAGE	OFFSET	LEVEL	ELEV.	CELL #	DESIGNATION
A	10+080.4	2.50 R.	B.O. HMAC	214.889	389	CL-A-AC
			B.O. BASE	214.508	316	CL-A-B
			SUBBASE	213.921	320	CL-A-SB
			CLAY	213.250	311	CL-A-SG
B	10+080.4	1.80 L.	B.O. HMAC	214.898	390	CL-B-AC
			B.O. BASE	214.591	317	CL-B-B
			SUBBASE	213.918	345	CL-B-SB
			CLAY	213.163	319	CL-B-SG
C	10+106.3	1.65 L.	B.O. HMAC	214.611	399	TL-C-AC
			B.O. BASE	214.203	318	TL-C-B
			SUBBASE	213.421	312	TL-C-SB
			CLAY	212.895	314	TL-C-SG
D	10+107.4	0.93 L.	T.O. COLUMN	214.603	310	TL-D-AC
				214.239	324	TL-D-SB
			T.O. SUBGRADE	213.199	313	TL-D-SG
E	10+109.6	2.50 L.	B.O. HMAC	214.538	307	TL-E-AC
			B.O. BASE	214.039	321	TL-E-B
			SUBBASE	213.424	315	TL-E-SB
			CLAY	212.940	323	TL-E-SG
F	10+111.4	2.50 L.	T.O. COLUMN	214.562	391	TL-F-AC
				214.170	322	TL-F-SB
			T.O. SUBGRADE	213.210	309	TL-F-SG

TABLE - 3. Brandon: Taxi - B: Locations and Elevations of Strain Gages

STRAIN GAUGE SCHEDULE							
NO.	LOCATION	NO.	LOCATION	NO.	LOCATION	NO.	LOCATION
1	A - LC - BP	16	B - MC - TT	31	D - MC - TP	46	F - LC - TT
2	A - LC - BT	17	C - LC - BT	32	D - MC - TT	47	F - MC - BT
3	A - LC - MP	18	C - LC - TT	33	E - LC - BP	48	F - MC - TT
4	A - LC - MT	19	C - MC - BT	34	E - LC - BT	49	G - LC - BT
5	A - LC - TP	20	C - MC - TT	35	E - LC - MP	50	G - LC - TT
6	A - LC - TT	21	D - LC - BP	36	E - LC - MT	51	G - MC - BT
7	A - MC - BP	22	D - LC - BT	37	E - LC - TP	52	G - MC - TT
8	A - MC - BT	23	D - LC - MP	38	E - LC - TT	53	H - LC - BT
9	A - MC - MP	24	D - LC - MT	39	E - MC - BP	54	H - LC - TT
10	A - MC - MT	25	D - LC - TP	40	E - MC - BT	55	H - MC - BT
11	A - MC - TP	26	D - LC - TT	41	E - MC - MP	56	H - MC - TT
12	A - MC - TT	27	D - MC - BP	42	E - MC - MT	57	I - LC - BT
13	B - LC - BT	28	D - MC - BT	43	E - MC - TP	58	I - LC - TT
14	B - LC - TT	29	D - MC - MP	44	E - MC - TT	59	I - MC - BT
15	B - MC - BT	30	D - MC - MT	45	F - LC - BT	60	I - MC - TT

LEGEND: EX. A-MC-TP MEANS GAGE LOCATION "A"
NORMAL CONCRETE, TOP ROW PARALLEL TO
TRAFFIC

till the load cell responds. These cells were rezeroed at this voltage.

At each instrument location four load cells were installed as noted below:

- 1) at the interface of the asphaltic concrete and granular base.

- 2) at the interface of the granular base and granular subbase.

- 3) at the interface of subbase and the subgrade.

- 4) at some depth in the subgrade, generally between 600 and 1000 mm.

Table 2 shows the elevations of the cells at the different locations.

In addition, Casagrande type piezometers with piezoelectric sensors were also installed near the locations of the load cells. The purpose of these piezometers was to measure any possible pore pressure build-up in the pavement layers as well as in the subgrade either due to loading, or due to fluctuations in ground water level. The piezometers were installed in the middle of the base layer, in the middle of the subbase layer and at 2.5 m, 5.0 m and at 10 m depths below the pavement surface. As it turned out no recordable change in pore pressure was noticed in any of the piezometers either under loaded or under unloaded conditions. It was concluded that pore pressures do not play any role in the response of the pavement at this site.

b) Brandon

Taxi B at Brandon is a rigid portland cement concrete (pcc) pavement with a lean concrete base placed on compacted crushed granular base. Because of the different type of pavement involved, the instrumentation was also of different type.

The gages were AILTECH fixed wire embeddable, integral lead strain gages manufactured by Eaton

Corporation and distributed by Intertechnology Ltd. in Toronto, Canada. The strain elements are hermetically sealed in weather-proof jackets and attached at the ends to two anchor plates (Fig.9). They were delivered with 33 m of color coded cables protected in insulated, grease filled and grounded sheath. The gages were 150 mm long with a nominal resistance of 350 ohms, capable of linear resistance-voltage relationship between -40°C and $+80^{\circ}\text{C}$, and were temperature compensated. Table A-2 in Appendix A gives the specifications for these gages. Each gage was delivered with a factory calibration chart which was checked before acceptance on site. As in Thompson, the integrity of the gages and the lead wires was constantly checked after each stage of handling and installation.

Gages were installed in the centre of the slab, in pairs across the joints and at different levels in the normal pcc as well as in the lean concrete base. In the case of centre slab locations three layers of gages in pcc and three layers in the lean concrete were placed. Each layer had gages in two mutually perpendicular directions, parallel and transverse to traffic flow, to measure the strains due to the bidirectional bending of the slab. At joint locations, because of essentially unidirectional bending, only transverse gages were placed. Also, there were only two layers of gages in the pcc as well as in the lean concrete layer. Fig. 10 shows the strain gage assembly prior to being buried in the concrete.

The assembly was anchored in place by long reinforcing steel bars driven into the base. It was encased in the fresh concrete about five to ten minutes before the paver reached the location (Fig. 11). This ensured that the encapsulating concrete was still wet and plastic and that when the paver passed the location the



FIG.- 11. - *Concrete encapsulation of strain gages just prior to burial in concrete*

gages were buried in a homogeneous medium. Care was taken during the placing of concrete so that the gages were not dislocated or damaged. As mentioned earlier, the integrity of the gages was checked at each stage; during paving, after paving and after 1, 3, 7 and 14 days of curing.

Data logging equipment

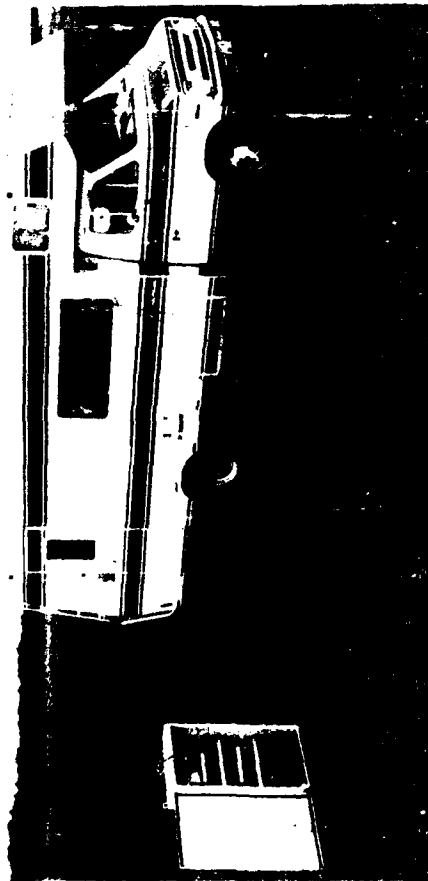
Contrary to our expectations, considerable difficulty was experienced in the acquisition of the data logging equipment. The difficulty appeared to be in obtaining the required scanning rate, the number of gages to be read at one time and the desired accuracy of the readings. Finally, a data acquisition unit was designed and assembled in-house which would read 16 gages at 50 readings per second per gage to an accuracy of one microvolt under an excitation voltage of 5 V and with a full Wheatstone bridge. The entire operation can be controlled by a microcomputer carried in an equipment van (Fig. 12).

Test Procedures

The basic test procedures were common to both sites. Some additional tests were carried out at Brandon to measure the load transfer efficiency of the joints and isotropy in the rigid pcc pavements. Essentially, the tests can be categorized as :

- a) static load tests using a rigid 600 mm diameter steel plate and sufficiently heavy reaction.
- b) dynamic or impulse loading using the Dynatest model 8000 FWD.
- c) actual aircraft load which was the B-737-200 series aircraft operating in and out of the two airports on a commercial scheduled basis.

In Brandon, further opportunity presented itself when Hercules C-130 military aircraft used the airstrip for brief periods of time. In addition to tests at the gage locations, loads were dropped at several points around the gage locations at pre-determined distances and the response of the gages was measured. These are



a) van housing the datalogger and microcomputer



b) view of the instrument console

FIG.- 12. - Readout unit

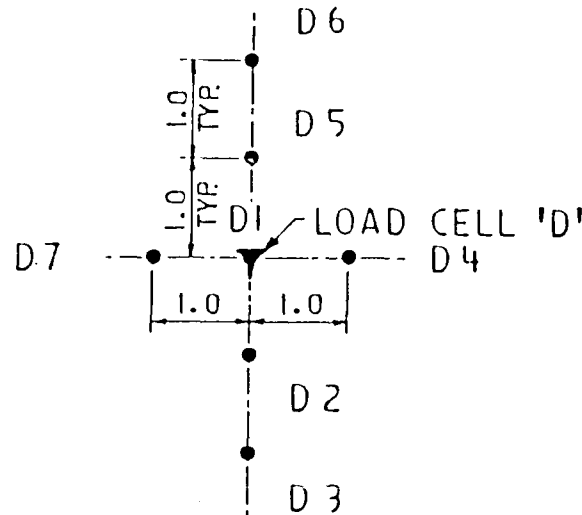


FIG. 13. THOMPSON TAXI A: LAYOUT OF SATELLITE TESTS

referred to as satellite tests (Fig.13). The purpose of the satellite tests was to determine the wander effect of the aircraft as well as to determine the zone of influence of a given load.

While a wide variety of tests was done at both the airports, not all the results are relevant to the present paper. Therefore, only a limited amount of data is presented here with a view to compare the calculated moduli values, stresses and strains in the pavements under the three different loading conditions mentioned above.

Method of Analysis

a) Thompson

For the flexible pavement at Thompson, the direct output from the tests are the deflection basin from the FWD tests and the maximum deflection under the load during the plate load tests. In addition,

the responses of the load cells were measured under the FWD tests, the static plate load tests and under the passing aircraft.

The FWD data was analysed by the layered elastic theory using the ELMOD and ISSEM 4 computer programs developed by the Dynatest Inc. These programs lead to values of layer moduli as well as stresses in the layers. The calculated values of stresses are compared with the values measured by the load cells. The plate load test data was analysed using the Tables and charts published by Peattie [12] using the modular ratios derived from the ELMOD analysis. The aircraft loads were analysed in a similar manner.

All computations for the FWD and plate load tests were done for normalised contact pressures of 500, 750, 1200 and 1500 kPa. For the aircraft loads the results were normalised for the rated tire pressure of 1240 kPa. The results

of these computations are shown in Table 4 through 6.

b) Brandon

The analysis of the rigid pavement at Brandon was somewhat complicated by the fact that the pavement was a composite construction consisting of normal pcc and a lean concrete base.

The FWD results were analysed using the ISSEM 4 program modelling the pavement as a three layer system. The top pcc formed the first layer, the lean concrete the second and the base-subgrade combination as a composite third layer. This analysis led to unreasonable values for the moduli for each layer as well as to stresses at the interface of each layer. The stresses and strains due to all loading conditions (the static plate load, the aircraft gear loads and the FWD) were computed using the nomographic method [13] for Westergaard's solution to this problem. The modulus of subgrade reaction for this site was obtained from the records of load tests carried out by the Canadian Ministry of Transport (MOT). The elasticity moduli for the normal pcc and for the lean concrete were obtained from compressive strength tests and using the guidelines given by the Canadian Standards Association (CSA-CAN3-A23.1) and the American Concrete Institute (ACI-318-81). The computed stresses are compared with the measured stresses. The results are shown in Table 7 through 10.

Results and Discussion

a) Thompson

Tables 4 to 6 summarise the results of tests in July 1986 and in September 1987. Figs. 14 shows the same results in the graphical form. In interpreting these results, one has to first establish the validity and the credibility of the observed values. There are no direct ways to do this. However, as mentioned ear-

lier, considerable care was taken in the installation of these gages and in ensuring that they were working properly throughout the various stages of construction of the taxiways. The measurements over the past three years show a consistent trend. Except for the test series with the Dynatest 8081 Heavy Weight Deflectometer (HWD) in 1987, the stress distribution shows the classical pattern. The 1987 test series is discussed later. The differences between the summer tests (July 1986) and the fall tests (Sept. 1987) are unmistakable. Thus it is submitted that the gage readings are credible. The differences between the observed stresses and those calculated using classical theories or the backcalculated moduli values are real and need to be explained.

While the pattern of gage readings is what one would expect from classical layered theories for pavement structures, there are differences which are disturbing. Fig. 14 compares the actual stresses measured under aircraft loads to those measured during plate load tests as well as the FWD tests. It would appear that the FWD tests would simulate the stresses due to the aircraft in the lower layers (granular bases and the subgrade) reasonably well. It should be mentioned here, however, that the aircraft seldom passed directly over the gage locations whereas, the other tests were done precisely at the gage points. Despite this limitation, the correlation between the stresses in the lower layers is acceptable. It can be concluded that the wander effect of the aircraft does not materially affect the stresses in the lower layers. On the other hand, both the plate load and the FWD tests tend to underestimate the stresses in the surface layer. Therefore, if one would use the asphalt strain criterion for the design and evaluation of a pavement, one would be erring on the unsafe side. It should be mentioned here that the plate load tests tend to underestimate the

TABLE 4: THOMPSON: TAX' A: SUMMARY OF MODULI FROM ELMOD ANALYSIS.

LOCATION B:

DATE: JULY 1986.

CONTACT PRESSURE (kPa)	GAGE No.	ELEVATION	STATION--> LAYER	MODULI IN MPa----->					MEAN OF 5 LOCATIONS	STANDARD DEVIATION	COEFF. OF VARIATION
				1	2	4	6	7			
500	1	214.398	AC	807	1661	2096	1697	1737	1600	426	26.6%
	2	214.591	BASE	248	255	230	281	275	258	18	7.2%
	3	213.918	SUBBASE	149	153	138	169	165	155	11	7.2%
	4	213.163	SUBGRADE	98	108	115	117	101	108	7	6.9%
1000	1	214.398	AC	961	1906	1478	1914	2001	1652	391	23.6%
	2	214.591	BASE	259	264	252	294	278	269	15	5.6%
	3	213.918	SUBBASE	156	159	151	177	167	162	9	5.6%
	4	213.163	SUBGRADE	98	103	110	118	101	106	7	6.8%
1500	1	214.398	AC	1071	1317	1129	2370	2648	1707	666	39.0%
	2	214.591	BASE	259	297	270	307	281	283	17	6.2%
	3	213.918	SUBBASE	156	178	162	185	169	170	10	6.2%
	4	213.163	SUBGRADE	109	108	122	118	103	112	7	6.2%

TABLE 4A: THOMPSON TAXI A: SUMMARY OF MODULI FROM ELMOD ANALYSIS
LOCATION B:

DATE: SEPT 1987.

CONTACT PRESSURE (kPa)	GAGE # No.	LAYER ELEVATION	MODULI IN MPa							MEAN OF 7 LOCATIONS MPa	STANDARD DEVIATION	COEFF. OF VARIATION
			1	2	3	4	5	6	7			
500	1	214.898 AC	11133	11495	10797	15387	11432	15922	15013	13026	2116	16.1%
	2	214.591 BASE	232	295	235	231	292	262	237	253	24	9.6%
	3	213.918 SUBBASE	140	171	141	139	175	157	142	152	14	9.5%
	4	213.163 SUBGRADE	133	116	138	138	121	139	118	129	10	7.4%
750	1	214.898 AC	12542	16850	12332	11489	14408	20160	14182	14566	2809	19.3%
	2	214.591 BASE	252	276	271	273	292	285	257	272	13	4.5%
	3	213.918 SUBBASE	151	166	163	164	175	171	154	163	8	4.5%
	4	213.163 SUBGRADE	126	121	123	125	122	133	114	123	5	4.3%
1200	1	214.898 AC	10712	14508	12461	13022	15562	21935	16450	14979	2354	22.1%
	2	214.591 BASE	271	284	272	292	278	284	249	276	13	4.7%
	3	213.918 SUBBASE	163	170	163	175	167	171	149	163	8	4.7%
	4	213.163 SUBGRADE	125	119	130	130	130	135	114	126	7	5.4%
1500	1	214.898 AC	11532	18218	10642	14314	15344	24671	16488	15887	4346	27.4%
	2	214.591 BASE	272	277	291	290	306	283	250	281	16	5.8%
	3	213.918 SUBBASE	164	166	175	174	184	170	150	169	10	5.8%
	4	213.163 SUBGRADE	125	127	137	130	139	139	113	130	9	6.7%

TABLE 5 THOMPSON TAXI A: SUMMARY OF ELASTIC LAYER ANALYSES AFTER PEATTIE

USING MODULI VALUES FROM ELMOD ANALYSIS

LOCATION 8

DATE: JULY 1986

No.	ELEVATION	LAYER	STATION-->	1	MEAN OF 5 LOCATIONS	LAYER THICKNESS	CONTACT PRESSURE (kPa)						
							STRESS			PLATE LOAD-->			
							(mm)	FACTORS	152.5	300.96	600	760	1240
1	214.398	AC		346	1653	102		0.560	85	169	336	426	694
2	214.591	BASE		255	271	307		0.246	38	74	146	187	305
3	213.918	SUBBASE		154	163	673		0.110	17	33	66	84	136
4	213.163	SUBGRADE		102	102	INFINITE							

DATE: SEPT. 1987

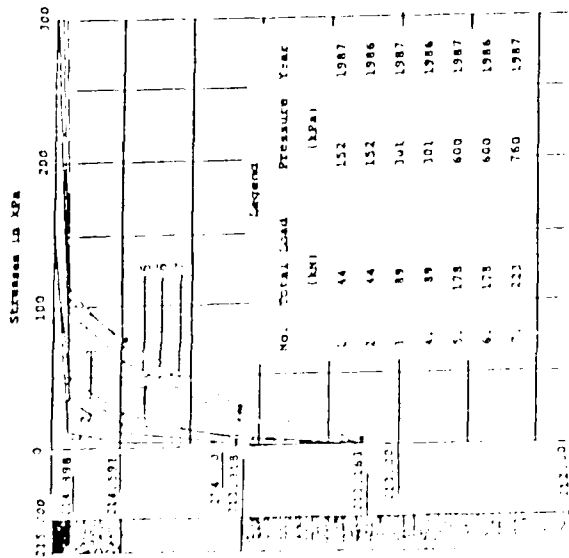
No.	ELEVATION	LAYER	STA 198-->	1	MEAN OF 7 LOCATIONS	LAYER THICKNESS	STRESS	CONTACT PRESSURE (kPa)									
								PLATE LOAD-->									
								(---MODULI IN MPa---)	(mm)	FACTORS	152.5	300.96	600	760	1240	500	750
1	214.398	AC		11480	14614	102	0.436	66	131	262	331	411	541	700	845	654	
2	214.591	BASE		257	271	307	0.188	29	57	113	143	183	233	34	141	235	282
3	213.918	SUBBASE		155	163	673	0.019	3	6	11	14	24	24	10	14	24	29
4	213.163	SUBGRADE		127	127	INFINITE											

TABLE 6: THOMPSON, TAXI-A: SUMMARY OF STRESSES AT LOCATION B

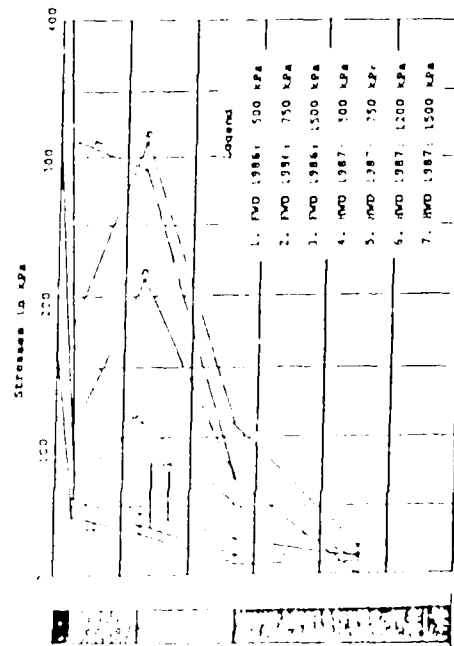
TYPE OF TEST	<-----PLATE LOAD----->										<-----F W D----->										<-----AIRCRAFT----->										
	(5 T) (10 T) .20 T) (25 T)																														
STRESS LEVEL (kPa)	152.48	300.96	600	760							500	750	1200	1500																	
GAGE #	ELEVATION	JULY, 1986: TEMP.: 20 C - 24 C :										STRESSES IN kPa:																			
390	14.898	34	49	112	M						44	56	M	73																	
317	14.591	12	26	74	S						30	36	S	45																	
345	13.918	2	5	25	E						8	14	E	26																	
319	13.163	1	1	2	D						9	15	D	9																	

GAGE #	ELEVATION	SEPT., 1987: TEMP.: 5 C - 12 C :										STRESSES IN kPa:																			
390	14.898	14	46	96	104						70	110	180	310																	
317	14.591	6	20	63	83						110	210	310	290																	
345	13.918	2	7	21	26						50	70	110	70																	
319	13.163	2	1	0	2						10	0	20	0																	

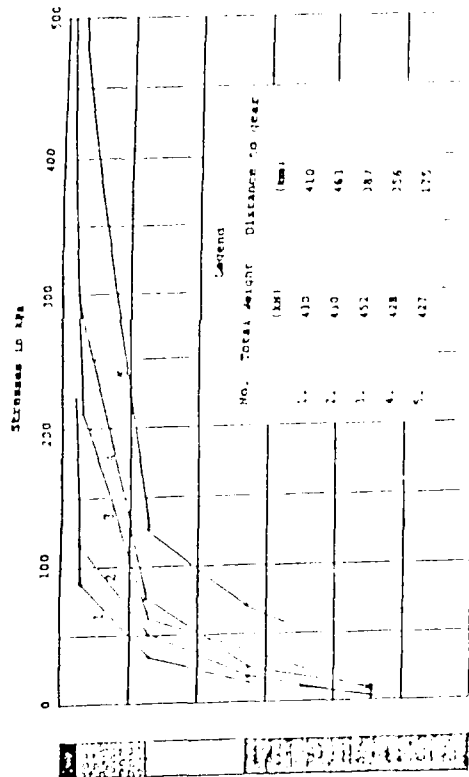
(** = MISSED READINGS)



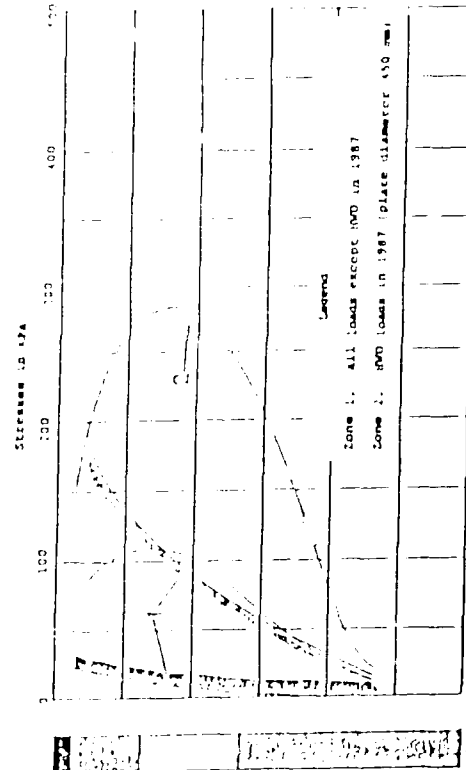
a) static plate loads (plate diameter 500 mm)



b) FWD and HWD tests



c) static plate loads



d) envelope of stress distribution under all loads

FIG. 14. THOMPSON TAXI A: STRESS DISTRIBUTION UNDER DIFFERENT LOADS

TABLE 7: BRANDON, TAXI-B: SUMMARY OF STRESSES AT LOCATIONS D AND E

TYPE OF TEST	<-----PLATE LOAD----->					<--FWD-->		<-----AIRCRAFT----->			
(kN)	99.2	197.3	296.0	392.4	477.6	B 737 C	130 C	130 C	130 C	130 C	130 C
STRESS LEVEL (kPa)	624	1241	1861	2465	3003	1340	1240	660	660	660	660
GAGE #	ELEVATION					TEMP: 6 C - 10 C					
SEPT. 1985 AND APRIL 1986											
	1	2	3	4							
D 31	N TP	67	335	468	535	870	99	164			
D 29	N MP	67	67	201	201	201	31	83			
D 27	N BP	-67	134	-201	-268	-335	20	10			
D 25	L TP	-186	-233	-326	-419	-513	-24	-50			
D 23	L MP	-280	-373	-513	-653	-792	-33	141			
D 21	L BP	-466	-559	-839	-1165	-1305	-145	-132	-276		
D 32	N TT	67	134	201	201	134	18			515	52
D 30	N MT	67	-67	-134	-67	870	29				
D 28	N BT	-268	-268	-335	-602	-602	17			198	***
D 26	L TT	-233	-280	-373	-559	-653	9				
D 24	L MT	-280	-326	-513	-653	-699	-28			-374	
D 22	L BT	-373	-606	-839	-1072	-839	-81			-610	***

TYPE OF TEST	<-----PLATE LOAD----->					<--FWD-->		<-----AIRCRAFT----->			
(kN)	103	200	299	397	452	C 130 B	737 C	130 B	737		
STRESS LEVEL (kPa)	648	1258	1880	2496	2842	1340	660	1240	660	1240	-->
GAGE #	ELEVATION					TEMP: 6 C - 10 C					
SEPT. 1985 AND APRIL 1986											
	5	6	7	8							
E 43	N TP	67	335	268	535	937	108				
E 41	N MP	134	268	335	335	803	46			433	249
E 39	N BP	-134	-67	-67	-201	67	13			349	
E 37	L TP	-280	-326	-419	-513	-280	9				85
E 35	L MP	-186	-420	-513	-606	-466	-28			-92	-100
E 33	L BP	-326	-513	-559	-699	-886	-114			-274	-361
E 44	N TT	134	335	535	736	736	63			114	250
E 42	N MT	47	201	233	233	466	35			73	
E 40	N BT	-67	67	134	468	468	38				-54
E 38	L TT	-186	-186	-233	-186	-93	-11			-121	
E 36	L MT	-233	-326	-186	-93	-186	-45				-542
E 34	L BT	-326	-420	-280	-699	-347	-91			-237	-955

*** MISSED READINGS

TABLE.8 : BRANDON: TAXI-B: MEASURED AND THEORETICAL STRESSES UNDER PLATE LOADS

LOCATION LOAD (kN)	p (kPa)	West Theor M(kN-m)	Meas	Packards Stresses (kPa)		Measured Stresses (kPa)		Stress Ratio	
				top	bottom	top	bottom	top	bottom
D par	99	622.5	0.550	0.027	610	-404	67	-466	9.1 0.9
	197	1238.7	1.095	0.024	1214	-803	335	-559	3.6 1.4
	296	1861.1	1.645	0.039	1825	-1207	468	-839	3.9 1.4
	392	2464.7	2.178	0.040	2417	-1598	535	-1165	4.5 1.4
	478	3005.5	2.656	0.038	2947	-1949	870	-1305	3.4 1.5
D trans	99	622.5	0.550	0.021	610	-404	67	-373	9.1 1.1
	197	1238.7	1.095	0.040	1214	-803	134	-606	9.1 1.3
	296	1861.1	1.645	0.047	1825	-1207	201	-839	9.1 1.4
	392	2464.7	2.178	0.060	2417	-1598	201	-1072	12.0 1.5
	478	3005.5	2.656	0.044	2947	-1949	134	-839	22.0 2.3
E par	103	647.6	0.572	0.026	635	-420	67	-326	9.5 1.3
	200	1257.5	1.111	0.034	1233	-816	335	-513	3.7 1.6
	293	1842.3	1.628	0.040	1806	-1195	268	-559	6.7 2.1
	397	2496.2	2.206	0.046	2447	-1619	535	-699	4.6 2.3
	452	2842.0	2.512	0.039	2787	-1843	937	-886	3.0 2.1
E trans	103	647.6	0.572	0.036	635	-420	134	-326	4.7 1.3
	200	1257.5	1.111	0.074	1233	-816	335	-420	3.7 1.9
	299	1880.0	1.662	0.107	1843	-1219	535	-280	3.4 4.4
	397	2496.2	2.206	0.186	2447	-1619	736	-699	3.3 2.3
	452	2842.0	2.512	-----	2787	-1843	736	-347	3.8 5.3

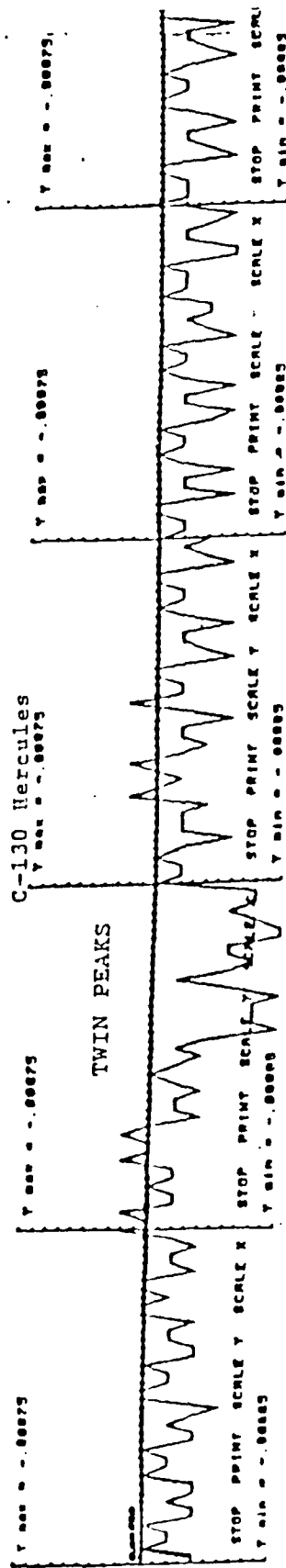
TABLE.9 : BRANDON: TAXI-B: MEASURED AND THEORETICAL STRESSES UNDER FWD LOADS

LOCATION LOAD (kN)		Westergaard stresses (kPa)		Packards stresses (kPa)		Measured stresses (kPa)	
		top	bottom	top	bottom	top	bottom
D	92	421	-631	722	-477	60	-50
E	97	443	-665	761	-503	80	-60
F	96	486	-729	834	-551	350	-80
G	93	471	-706	808	-534	240	-225
I	90	456	-584	782	-516	120	-70

TABLE.10 : BRANDON: TAXI-B: MEASURED AND THEORETICAL STRESSES UNDER AIRCRAFT LOADS

(LOCATION D AND E)

AIRCRAFT		<- Westergaard stresses--->				<--Packard-stresses-->				<-----aircraft----->	
		(kPa)		(kPa)		(kPa)		(kPa)		(range of stresses)	
		0 cm	30 cm	60 cm	0 cm	30 cm	60 cm	0 cm	30 cm	60 cm	(from Table 7)
		offset	offset	offset	offset	offset	offset	offset	offset	offset	
B-737-200	top	891.1	467.0	282.7	905	357	216	91	433		
	bottom	-589.4	-308.9	-187.0	-598	-236	-143	-132	-361		
C-130	top	1414.2	700.6	434.6	1207	570	340	52	250		
	bottom	-935.4	-463.4	-287.5	-798	-377	-225	-255	-610		



SINGLE PEAK B-737-200

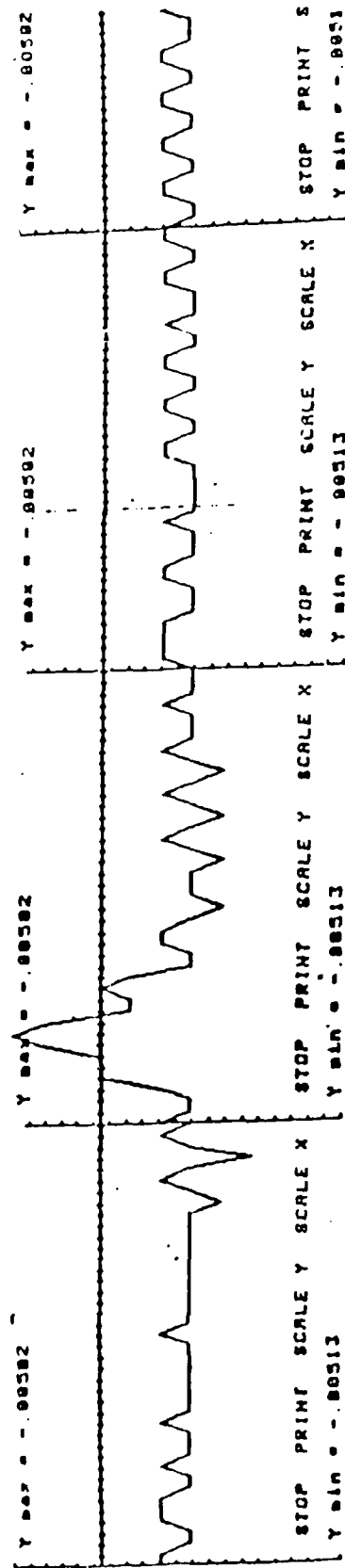


FIG. 16. BRANDON TAXI B: STRAIN GAGE RESPONSES UNDER B-737 AND C-130 AIRCRAFT

While the stresses measured in the field by plate load and the FWD tests show reasonable correlation, at least for the lower layers, the same cannot be said for the stresses computed using the backcalculated moduli. Table 5 shows the results of theoretical calculations using layered elastic theories. First the stresses were calculated using Peattie's charts [12]. In order to calculate the different stiffness ratios and other parameters needed in Peattie's calculations the moduli values were obtained from the ELMOD analysis of the FWD deflections. ELMOD is the software program developed by Dynatest Inc. to analyse the field FWD data. Secondly the moduli and the stresses were also calculated using the ISSEM 4 layered elastic program also developed by Dynatest Inc.. The ISSEM 4 uses ELSYM 5 as a subroutine in calculating stresses and strains. Table 6 presents the measured stresses. As can be seen from Tables 5 and 6 the correlation between observed and measured stresses is not as satisfactory as with actually measured values under different loading conditions. This can lead to only one conclusion. While the test methods are reliable, the interpretation and the computation of moduli or stresses need more work and refinement.

b) Brandon

Taxi B at Brandon is a composite rigid pavement with a 200 mm surface course of normal portland cement concrete (p.c.c) and 300 mm lean concrete base. During construction particular attention was paid to achieve a good bond between the two layers. One study [15] showed that the degree of composite action between the two layers could be as high as 90 % for up to twice the service load. The analysis

of this pavement is somewhat more complicated than the layered elastic flexible system at Thompson on two grounds:

- a) One is never sure of the degree of bond
- b) There is, as yet, no reliable method of analysis for such pavements.

In this study two approaches were used. The first was to use the classical Westergaard solution to the problem using a transformed section. The second method was to use the charts and tables published by Packard [16] for such structures. The author is grateful to Packard for extending his tables to include the cross section at Brandon [17].

Table 7 is the summary of stresses observed during the static plate load, the FWD tests and under the aircraft gear loads. It will be noticed that the gage readings under aircraft loads are incomplete. This was due to the difficulties experienced with the dataloggers as explained previously. Only the results for the centre slab locations (D and E) are presented here. It can be seen that, in general, the tests do not correlate very well with those produced by the aircraft unlike in the case of Thompson.

In Brandon only the model 8000 FWD was used. It could be that this machine was too light to simulate actual aircraft loads on a rigid pavement. Arguments for and against such perceptions can be found in the literature [5,6]. However, of the two test methods, the FWD does seem to simulate the B-737-200 aircraft better than the static plate load test. Other observations from Table 7 include:

- a) Under all three types of loading (static, FWD and the aircraft) the bottom lean concrete appears to respond more isotropically than the top normal concrete. No explanation is offered for this behaviour. However, it is suggested that the methods of analysis for such structures should consider this factor.
- b) As to be expected, static

stresses even in the lower layers. Before proceeding to compare the computed stresses to the measured stresses, the trend shown by the 1987 HWD test series needs to be explained. During the analysis of the 1985 and 1986 FWD test results, it was suggested that the FWD could not apply loads heavy enough to produce meaningful results for a pavement with a construction as substantial as that under Taxi A in Thompson. While it is clear from Fig. 14 that this is not quite true, it was decided to use the heavier version of the Dynatest FWD, the HWD, for the 1987 test series. While the stresses in the subbase and the subgrade were not significantly affected by the heavier machine the trend in the base and in the asphalt layers was quite different from the ones observed in the previous years. Except for curve 7 in Fig. 14 (b), which is considered to be an anomaly and not the true reading, the trend showed that the asphalt stresses were much smaller than the stresses in the base. The HWD used a 450 mm diameter plate rather than the standard 300 mm plate for the FWD. This was twice the diameter of the load cell at the bottom of the asphalt layer. It is well known that the contact pressure under a rigid base would not be uniform, rather has the shape of an inverted saddle with high edge stresses and relatively low stresses in the middle as shown in Fig. 15 [14]. Thus the asphalt gage at the shallow depth of only 100 mm below the surface is subjected to a lower direct vertical pressure in addition to high confining pressure from high edge stresses resulting in a lower stress at that point. At the location of the second gage in the base, this effect of the contact pressure is not felt. It should be noticed that the same trend is not noticed under the static plate load tests which used even larger plate with 600 mm diameter. It is suggested that with larger plates, the effect of confining edge stresses is far removed from the

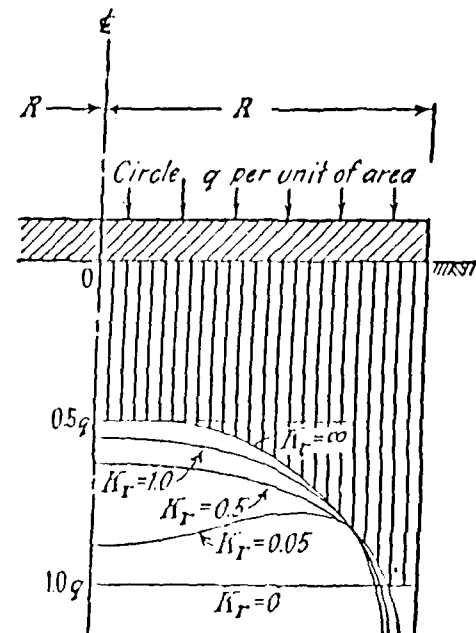


Fig. 15. Contact Pressure Under Circular Footings of Different Rigidities. (after Terzaghi [14]).

K_r = Rigidity Factor
 q = uniform pressure
 = Load/Area

load cells. Also, the gages were read when the deflections under the static load have come to a steady state. Thus the asphalt would creep and comply with the plate resulting in a more uniform stress distribution. Hence the same effect is not felt during the static plate load tests. Unfortunately, this hypothesis could not be verified by repeating the tests in 1987. If this hypothesis were to be true, then it leads one to the conclusion that one should be careful in interpreting the results from FWD tests. Also in planning instrumentation in the pavement layers, one should consider the relationship between the plate size and the thickness of the surface layer. Otherwise the results could be interpreted wrongly.

STRESS RATIO = THEORETICAL/OBSERVED STRESSES

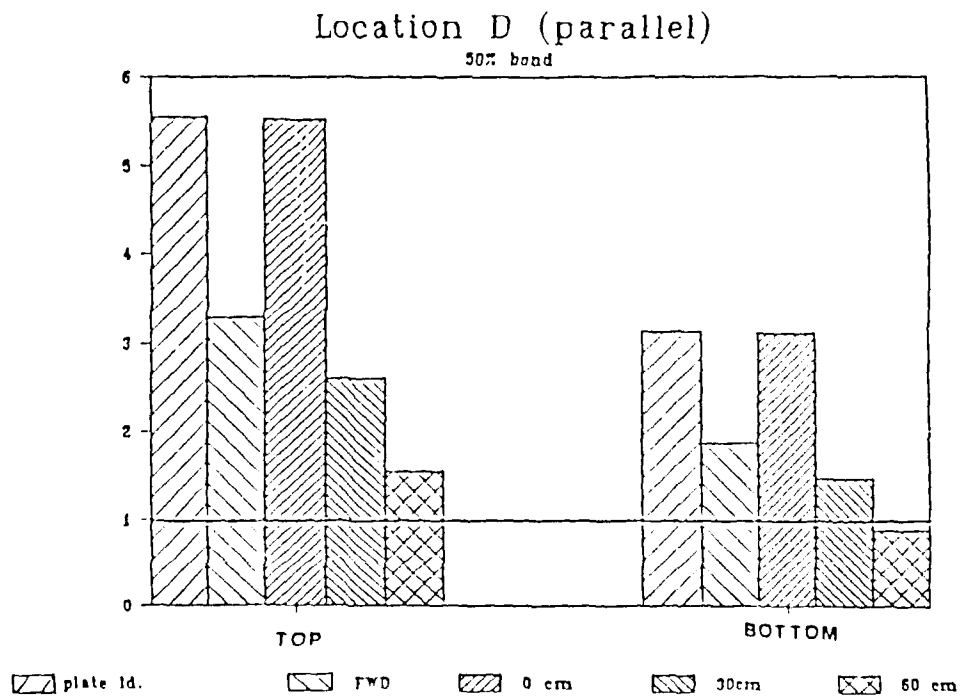
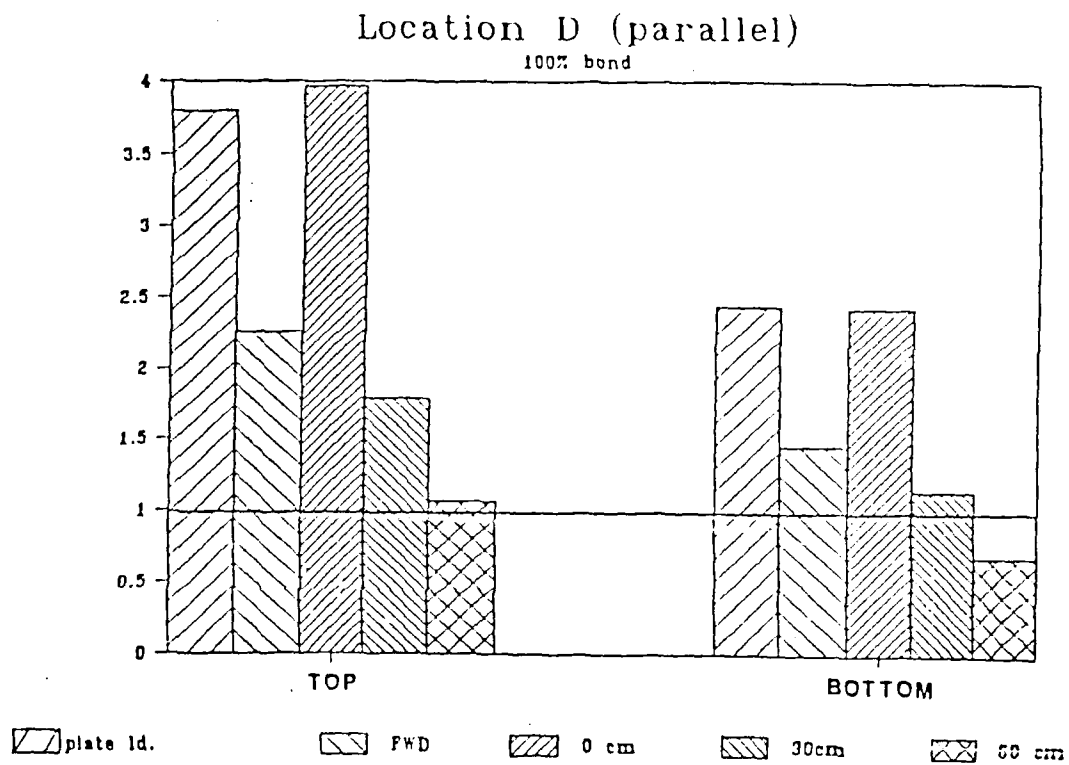


FIG. 17. BRANDON TAXI B: THEORETICAL AND OBSERVED STRESSES

loads produce much higher stresses than impulse loads. While this is clear from the results of the plate load tests it was also verified (though by pure chance) for aircraft loads as is seen for aircraft 4 in Table 7. This aircraft, for some unknown reason, happened to stop precisely at the gage location giving rise to the very high stresses. The other high reading, under aircraft 7, at the bottom of the lean concrete is considered to be a test error rather than a true reading.

c) The stresses produced by FWD loading is closer to those produced by the B-737-200 aircraft than the ones observed under the Hercules C-130 aircraft. The reason for this is suspected to be the difference in the gear arrangement for these two aircraft. B-737 has a dual wheel while the Hercules has a single tandem arrangement. Fig. 16 reproduces part of the strip chart output from the HP-87 field computer used to collect the field data. One can see the dual peaks of the Hercules gear as against the single pronounced peak for the B-737. It is suggested that the recorded response under the Hercules is the superposition of two wheel loads in quick succession while the B-737 wheels load the gages simultaneously in the form of an equivalent single wheel load. No verification is offered for this hypothesis at this time. If this were true, then one has to question seriously whether the single plate loading by the FWD can truly simulate the tandem and dual tandem gear configurations of some of the heavier aircraft and multiple axle loads of some of the trucks using our provincial and State Highways.

Tables 8 through 10 compare the stresses derived from the analytical methods, referred to earlier, with the observed stresses. Fig. 17 shows the same results in terms of the ratios of theoretical to observed stresses. In addition to these methods it was attempted to compute these stresses using the

ELMOD and the ISSEM 4 software without much success. It should be recognized that these programs are meant for flexible pavements. Dynatest's ELCON program is not available to the author. Another program RPEDD 1, developed by the Texas Transportation Institute, was not available to the author at the time of this writing. These two latter programs are said to be specifically meant for the analysis of rigid pavements.

As can be seen from Tables 8 through 10 and from Fig. 17 the correlation between computed stresses and observed stresses is even less satisfactory than the actual measured values would indicate. It would therefore appear that there are some legitimate concerns in using the backcalculated moduli to compute the stresses in rigid composite pavements. It would also appear that the established theories for rigid composite pavements do not predict the stresses satisfactorily.

Summary and Conclusions

This paper documented the experience with nondestructive testing of two instrumented airfields in Canada. The testing equipment were the Dynatest 8000 FWD and 8081 HWD. One of the pavements was a flexible type and the other a composite rigid pavement. The design aircraft for both these pavements is the Boeing B-737-200. The pavements were instrumented with load cells and resistance type wire strain gages. They were tested non-destructively with static plate loads, the FWD or HWD and under commercial scheduled B-737 aircraft traffic. The rigid pavement was also tested with Hercules C-130 aircraft.

The observed stresses under different loading conditions were compared with those produced by the design aircraft. In addition, stresses were calculated using the moduli derived from backcalculation. These were also compared to the observed stresses.

From the results presented in

this paper the following conclusions are drawn:

1) The FWD tests simulated the B-737 aircraft reasonably well insofar as the actual stresses in the pavement are considered.

2) The correlation between the measured stresses under FWD loads and actual aircraft loads was better in the case of flexible pavements than for the rigid composite pavement tested in this study.

3) In flexible pavements the FWD tests produced stresses, in the lower layers, similar to those produced by the design aircraft.

4) Both plate load tests and the FWD tests underestimated the stresses in the asphaltic concrete surface layers. This could lead one to err on the unsafe side if one is using these tests to evaluate the pavements based on asphalt strain criterion.

5) Whether one used the standard version of the FWD or the heavier HWL, the pavement response seemed to be comparable in the lower layers. However, the use of larger plates might produce confining stresses in the upper layers to alter the stress distribution. Thus in choosing to instrument pavements, one should consider the relationship of the plate diameter to the thickness of the surface layers.

6) While the measured stresses from the FWD tests and the plate load tests correlated reasonably with the observed stresses under the design aircraft, the same cannot be said about stresses computed with the backcalculated moduli values using different layer elastic algorithms. Therefore, it is submitted that while nondestructive testing equipment are reliable tools for pavement evaluation and design, further work is necessary to refine the backcalculation methods to produce reliable stress predictions.

7) In the case of the rigid composite pavement the stresses measured in the upper layer under FWD testing correlated well with the stresses measured under actual aircraft loads. However, consi-

derable variation was observed in the lean concrete base. Similar observations were made by van Dijk et al [18].

8) In the case of the rigid composite pavement, the lower lean concrete layer showed more isotropic behaviour while the upper normal concrete layer did not. Therefore, analysis methods for such structures should consider this factor.

9) The FWD loads appeared to simulate the dual gear configuration of the B-737-200 aircraft reasonably well. However, this was not the case with the tandem gear load of the Hercules C-130 aircraft. This raises a question whether the FWD loading would truly simulate the tandem and dual tandem gear configuration of some heavier aircraft and multiple axle trucks.

10) The currently available methods for analysis of composite rigid pavements appear to grossly overestimate the stresses produced in the pavement.

ACKNOWLEDGEMENTS

This paper is published with the permission of the senior management of Transport Canada and of Public Works Canada. The author wishes to thank them and acknowledge their support and encouragement in the form of material and personnel resources throughout this study.

WAIVER

The opinions expressed in this paper are personal views of the author and should not be construed as official policy or position of Transport Canada or of Public Works Canada.

REFERENCES

- [1] Clayton, Sparks and Associates, "Pavement Deflection Testing Vehicle - A Feasibility Study," Report to Transport Canada, 1980.
- [2] Hoffmann, M.S. and Thompson, M.R., "Comparative Study of Selected Nondestructive Testing Devices," Transportation Research Record No. 852, pp. 32, Transportation Research Board, National Academy of Sciences, Washington, D.C., 1983.
- [3] Kennedy, C.K., "Equipment for Assessing the Structural Strength of Road Pavements," Proceedings, International Symposium on Bearing Capacity of Roads and Airfields, vol. 1, pp. 421-434, Norwegian Institute of Technology, Trondheim, Norway, 1982.
- [4] Elkins, G.R., Uddin, W. and Hudson, W.R., "Side-By-Side Field Evaluation of Deflection Testing Devices" Report prepared for the Centre for Transportation, University of Texas, Austin, Texas, Sept. 1987.
- [5] Bush, III, A.J., Alexander, D.R. and Hall, Jr., J.W., "Non-destructive Airfield Rigid Pavement Evaluation," Proceedings, Third International Conference on Concrete Pavement Design and Rehabilitation, Purdue University, West Lafayette, 1985.
- [6] Uddin, W., Smith, P. and Treybig, H.J., Discussion of Ref. [5].
- [7] Burmister, D.M., "The General Theory of Stresses and Displacements in Layered Soil Systems" Journal of Applied Physics, vol. 16, 1945.
- [8] Acum, W.E., and Fox, L., "Computation of Load Stresses in a Three Layered System," Geotechnique, vol. 2, pp. 293 - 300, 1951.
- [9] Jones, A., "Tables of Stresses in Three Layered Systems" Highway Research Board Bulletin 342, 1962.
- [10] Briaud, J.-L., "The Pressuremeter: Application to Pavement Design," Ph.D. Dissertation, Department of Civil Engineering, University of Ottawa, Ottawa, Canada, 1979.
- [11] Briaud, J.-L., Cosentino, P.J. and Terry, T.A., "Pressuremeter Moduli for Airport Pavement Design and Evaluation" Report No. DOT/FAA/PM-87/10 prepared by the Department of Civil Engineering, Texas Transportation Institute, Texas A&M University, 1987.
- [12] Peattie, K.R., "Stress and Strain Factors for Three Layer Elastic systems" Highway Research Board Bulletin 342, 1962.
- [13] Pickett, G. and Ray, G.K., "Influence Charts for Concrete Pavements," Transactions, ASCE, vol. 116, pp. 49-73, 1951.
- [14] Terzaghi, K. "Theoretical Soil Mechanics", Wiley, New York, 1942.
- [15] Lukoshenko, J. "Composite Action of a Normal Concrete Econcrete Pavement Based on Field Measurements" Unpublished B.Sc. Thesis, University of Manitoba, April, 1988.
- [16] Packard, R., "Structural Design of Concrete Pavements with Lean Concrete Bases," Proceedings, Second International Conference on the Design and Rehabilitation of Concrete Pavements, Purdue University, West Lafayette, Indiana, 1981.
- [17] Packard, R., Personal Communication, 1983.

[18] van Dijk, F.J.V., Weder, C.J., and Rol, A.H., "Evaluation of the Bearing Capacity of the Runways and Taxiways at Amsterdam Airport Schipol," Proceedings, International Symposium on Bearing Capacity of Roads and Airfields, Norwegian Technical University, Trondheim, Norway, 1982, pp. 1081-1091.

APPENDIX A

TABLE A-1

SPECIFICATIONS FOR AILTECH CONCRETE EMBEDDED STRAIN GAGES.

Resistance 350 ohmm + 3%

Gage factor 2 + 3%

Rated Strain level 20,000 micro-inch per inch

Operable temp.: - 50 to +82 ° C

Compensated Temperature Range: -25 to + 74 ° C

Terminal Slope : 0 + 80 micro-inches over -25 to + 74 ° C

Gage Factor change: inversely with temperature @ 1% per 55 ° C

Gage Length 152 mm

TABLE A-2

SPECIFICATIONS FOR FLAT PLATE PIEZOELECTRIC LOAD CELLS.

DIAMETER 230 mm

Excitation Voltage: 10 v max.

Response Voltage: 70 mv

Nonlinear Hysteresis: max 0.2 %

Pressure Range: 0 - 1.0 MPa

Accuracy within + 7 kPa

Operating Temp.: -40 ° to + 40 ° C

Suitable for direct burial in soil

**Session 7:
Load Deformation
Measurements**

APPLICATIONS OF FIELD INSTRUMENTATION AND PERFORMANCE MONITORING OF RIGID PAVEMENTS

Raymond S. Rollings, U.S. Army Engineer Waterways Experiment Station
David W. Pittman, U.S. Army Engineer Waterways Experiment Station

Abstract

This paper reviews some of the past instrumentation and performance measuring used by the Corps of Engineers to develop their rigid pavement design procedures and will consider two areas where future studies could improve our understanding of rigid pavement performance. Results of instrumented model tests and full-scale traffic tests gave confidence in the Westergaard edge loaded analytical model to calculate design stresses. This model has been the backbone of the design concept for over 40 years now and continues to serve the Corps of Engineers well. Also performance measurements of joints developed the concept of joint load transfer that allowed more economical design of pavements and also defined standards of joint design. There are still challenges facing the Corps of Engineers where instrumentation and performance measurements in the field can help develop better design standards. The actual effects of temperature and moisture gradients on rigid pavement performance remain poorly understood even through we have been aware since the 1930's that they develop stresses in the pavement. Also our understanding of bonding in rigid pavement overlays remains poor and could be improved by field measurements.

Introduction

Pavement design developed from a blend of theory, laboratory testing, field tests, and performance monitoring. This testing and performance monitoring was critical because it allowed the theoretical concepts to be checked and modified to reflect actual conditions. Without this blend of theory, testing, and performance monitoring, modern pavement design would not have developed to its present level.

This paper will review four specific aspects of the Corps of Engineers rigid pavement design procedure to illustrate the importance of developing a complete blend of theory, testing, and performance data. Where adequate theory was developed, appropriate testing was conducted, and sufficient field performance data was collected, the Corps of Engineers rigid pavement design procedure is a powerful and useful tool. Where any one of these parameters is not fully developed, the design procedure is weaker and more limited. The four specific aspects of the design procedure that will be considered in this paper are load-induced stresses, load transfer, temperature induced stresses, and bonding for rigid overlays.

Analytical Model

The Corps of Engineers was charged with developing airfield pavement design procedures during World War II and has been heavily involved in this field ever since. When the Corps of Engineers first got involved the only appropriate analytical model available for rigid pavements was the Westergaard interior load model (Westergaard 1936a); however, its validity was uncertain. Consequently, one of the first tasks was to establish the validity of the Westergaard model.

A series of full scale accelerated traffic tests were conducted at Lockbourne, Ohio during and shortly after World War II to develop basic performance data for rigid pavement design. Figure 1 shows a sample of strain measurements gathered from one test. These measurements showed that the Westergaard interior load analytical model overestimated the stress and strain actually experienced by the pavement. The analytical model calculated strains follow the shape and form of the measurements and gave conservative results. However, observation of the test slab performance showed that the edge of the trafficked slab was where the critical stresses occurred and cracking started. Consequently, the interior load analytical model was of limited usefulness.

In 1948 Dr. Westergaard published his edge load analytical model (Westergaard 1948), and solutions for this model were greatly simplified when Pickett and Fay published their influence charts (Pickett and Fay 1950). The validity of this analytical model was checked by small scale model tests (Gellinger and Carlton 1950) and full scale accelerated traffic tests (Sale and Hutchinson 1959). Figure 2 shows a sample of strain measurements from the small scale model, and the analytical model once again gives generally conservative results and the calculated results do follow the appropriate shape.

The early testing at Lockbourne found that keys, dowels, and short spacing on contraction joints improved pavement performance. This developed the concept of load transfer recognizing that an adjacent slab can help carry the load on a slab edge if the joint is

properly designed. Figures 3 and 4 show sample results of strain measurements and theoretical calculations. The shape of the calculated strains for the multiple wheel gear and the measured strains are once again similar, and the analytical model gives conservative results. When the measured load transfer is included in the theoretical calculations the disparity between calculated and measured strains is reduced, but the analytical model results are still conservative.

The measured strains were from a load cart moving at about 4.8 mph. If, as in Figure 5, a dynamic elastic modulus is used for the theoretical calculations rather than a static modulus, the agreement between measured and theoretical strain magnitudes is improved, but the model is still conservative. The actual pavement problem is a dynamic problem rather than a static one for all but stopped or parked aircraft. Early tests with an instrumented aircraft (Ohio River Division Laboratory 1943) found that static loads were the most severe loads, and this was later confirmed by much more comprehensive testing (Ledbetter 1976). Even though the pavement problem is a dynamic problem it is analyzed as a static problem. This approach is a conservative simplification, and appropriate dynamic measures for parameters such as the concrete flexural strength or the modulus of subgrade reaction have not been developed. Based on observation of in-service pavements, runway interiors where aircraft seldom stop are made thinner in recognition of the actual dynamics of the problem.

The Westergaard edge load analytical model is the heart of the Corps of Engineers rigid pavement design procedure. The instrumented models and test sections and the performance data collected from the accelerated traffic tests and from in-service pavements shows that the model can be used with static material and load properties to give conservative results. It is effective for calculating the relative interactions of load size and configurations, pavement thickness, concrete modulus of elasticity and Poisson's ratio, and modulus of subgrade reaction. Today, it is common for the author of a new powerful finite element

rigid pavement model to first establish its validity by showing that it gives the same results as the Westergaard model. Recognizing the conservative nature of the Westergaard model as evidenced by results such as Figures 1 through 5 and remembering the dynamics of the situation, it makes one wonder if some theoretical modelers might have lost sight of the question.

Load Transfer

The model and full scale traffic tests demonstrated that load transfer across joints did exist, and if this was recognized in design, thinner, more economical designs would result. Based on laboratory and field measurements, 25 percent load transfer was selected as the standard design assumption. Table 1 shows the combined results from Corps of Engineers measurements of load transfer. The mean keyed joint load transfer barely exceeds the design assumption, and as might be expected, the keyed joint field performance has never been

as good as the doweled construction joint (Barenberg and Smith 1979, Grau 1979). For this reason the Corps of Engineers limits the use of keyed joints on thin pavements or under channelized heavy cargo or bomber aircraft traffic or on soft subgrades.

The load transfer data is sufficient to determine appropriate design values for the most common joint types used by the Corps of Engineers (keyed and doweled construction and aggregate interlock contraction joints) and to develop appropriate limitations on their use. However, for new construction procedures such as roller compacted concrete, insufficient data have been collected from different sites to allow selection of a design load transfer value. At the current time, roller compacted concrete pavements are designed for no load transfer (Rollings 1988a) although if sufficient data are collected the results in Table 1 suggest that a 10 or 15 percent load transfer value for design could be appropriate.

Table 1. Representative Corps of Engineers Load Transfer Measurements for Full Scale Tests Section and In-Service Pavements

<u>Type of Joint</u>	<u>Number of Data Points</u>	<u>Load Transfer</u>		<u>Coefficient of Variation, %</u>
		<u>Range</u>	<u>Mean</u>	
Plain Concrete				
Doweled Construction Joint	195	0.0-50.0	30.6	38.0
Doweled Expansion Joint	15	15.4-42.6	30.5	24.4
Contraction Joint with Aggregate Interlock	46	15.6-50.0	37.2	19.2
Tied Contraction	6	23.9-34.8	29.2	13.4
Doweled Contraction	4	28.2-42.8	35.1	17.3
Keyed Joint	61	5.6-49.0	25.4	41.4
Tied Key Joint	2	25.6-26.1	25.8	--
Lockbourne "Free" (butt) Joint	8	5.8-24.5	15.5	40.9
Roller-Compacted Concrete Pavement				
Transverse Cracks*	16 ^a	--	18.6	36.0
Longitudinal Cold* Joints	8	--	12.3	45.5

* All measurements are from one project.

Temperature Stresses

When a temperature gradient exists in the pavement, the differential volume changes in the top and bottom of the slab develop stresses in the concrete. The existence of this gradient is well established by field measurements. Methods of calculating these stresses were developed as far back as the 1920's (Westergaard 1926b), and a variety of methods exist for calculating temperature induced stresses today.

Even though the theoretical magnitude of the stresses may be calculated, it is not clear what should be done with them. Should these stresses be simply added and subtracted to load induced stresses? How should the theoretical stresses be adjusted for creep? Although we can calculate the stresses and can measure temperature gradients and strains in the field, there is no data on how these stresses actually affect the pavement performance.

Figure 6 illustrates one possible effect of temperature induced stress. In laboratory concrete beam fatigue testing, some load is maintained on the beam at all times to avoid rebound. As shown in Figure 6 the ratio of the minimum "at rest" load to the maximum, fully applied load has a major impact on the concrete fatigue relationship. In the field the pavement temperature gradient may maintain some minimal "at rest" stress in the pavement. As the pavement temperature varied at different times of day and during different seasons at the AASHO Road Test, the calculated ratio of the temperature stress to the sum of the temperature and load stresses varied from 0.16 to 0.60 (Rollings 1988b). This would imply that there is no single unique fatigue relation for concrete pavements.

Corps of Engineers maximum joint spacing and slab size for rigid pavements are determined based on the thickness of the slab. No formal analysis of temperature or other effects are made, and conventional pavements built with these criteria have not had curling problems in the field.

When steel fiber reinforced concrete pavements were introduced, their high strength allowed slab lengths to be increased to 50 or more ft compared with conventional 15 to 25 feet joint spacing. As shown in Figure 7 the amount of

differential shrinkage needed to cause curl is a function of slab thickness and joint spacing. The steel fiber reinforced pavements in Figure 7 required only a fraction of the shrinkage needed by the conventional concrete slabs to develop curling problem. An inspection of these slabs in the field found that slab curling with resulting corner breaks was a universal problem (Rollings 1986). Even though normal Corps of Engineers' joint spacing criteria avoids curling problems without having to make temperature or other complex calculations, they cannot be extrapolated to new problems such as the large, thin fiber reinforced slabs. Without the combination of theory, testing, and field performance we cannot now determine appropriate joint spacing criteria and simply require that they are the same joint spacing as conventional pavements.

Rigid Overlay Bonding

There are three recognized levels of bond between a rigid overlay and a base slab. Full bonding ensures monolithic action between the overlay and base by requiring careful surface preparation and bonding grout; partial bond simply requires minimal surface cleaning before placing the overlay; and unbonded overlays use a bond breaking layer such as asphalt concrete to ensure there is no bond between the overlay and base. These terms for bonding are based on construction procedure and not on any actual levels of bond.

The Corps of Engineers design method for rigid overlays is entirely empirical and is based on accelerated traffic tests conducted in the 1950's (Rollings 1988b, Mellinger 1963). When this design procedure was being developed in the 1950's, there were not theoretical models available capable of analyzing the layered structure of a concrete overlay on a concrete base pavement. Consequently, the engineers were forced to use empirical relations developed from the performance data of limited accelerated traffic testing. This was a practical solution to the problem, and this empirical design method continues in use and has been adopted by many organizations.

Today we have analytical models capable of analyzing the overlay

problem, and the accelerated traffic tests provide some performance data. However, no tests have been conducted to determine the nature of the bond between the overlay and base pavements. Consequently, it is difficult to determine what form of friction or adhesion should be used to model this interface in the new more powerful analytical models. A number of assumptions can be made on how to model this interface, but now detailed test data such as the model or full scale traffic test section strain tests for the Westergaard model are needed to determine how well or poorly these assumptions model the real pavement performance.

Conclusion

Table 2 summarizes the status of four elements of the Corps of Engineers rigid pavement design procedure. For calculating design stresses, the Westergaard edge loaded model provides a theoretical base that has been checked with detailed test data, and correlated to field performance. It has served the Corps of Engineers well for over forty years and remains the standard against which new methods are checked. The concept of load transfer can be incorporated within the theoretical model and has been checked with field measurement

and performance. This concept allows design of more economical pavements.

A variety of theoretical models can be used to calculate temperature effects and stresses, and there have also been some test measurements of these effects. However, this work has never been tied to actual field performance so it has little impact on design practice. Instead experience and empirical guidance are used to keep avoid problems. The bonding between overlays can now be modeled analytically, and there is some performance data upon which the old empirical design relationships were developed. However, the lack of good test information concerning the nature and effect of the overlay interface makes it difficult to upgrade current overlay design practice with the new improved analytical models.

Those design elements in Table 2 that include an analytical basis that has been verified by testing and correlated to field performance are included in design practice and have major impact on design. If any one of these three aspects are missing, then the design element is included only crudely in the design process. Consequently, any pavement development work should ensure that all three parameters of theory, test verification, and correlation to actual performance are included.

Table 2. Summary of Needs for Corps of Engineers Rigid Pavement Design Procedure

<u>Design Element</u>	<u>Theoretical Model</u>	<u>Verified by Field or Model Tests</u>	<u>Correlated to Field Performance</u>
Stress Calculations	Yes	Yes	Yes
Load Transfer	Yes	Yes	Yes
Temperature Effects	Yes	Yes	No
Overlay Bonding	Yes	No	Yes

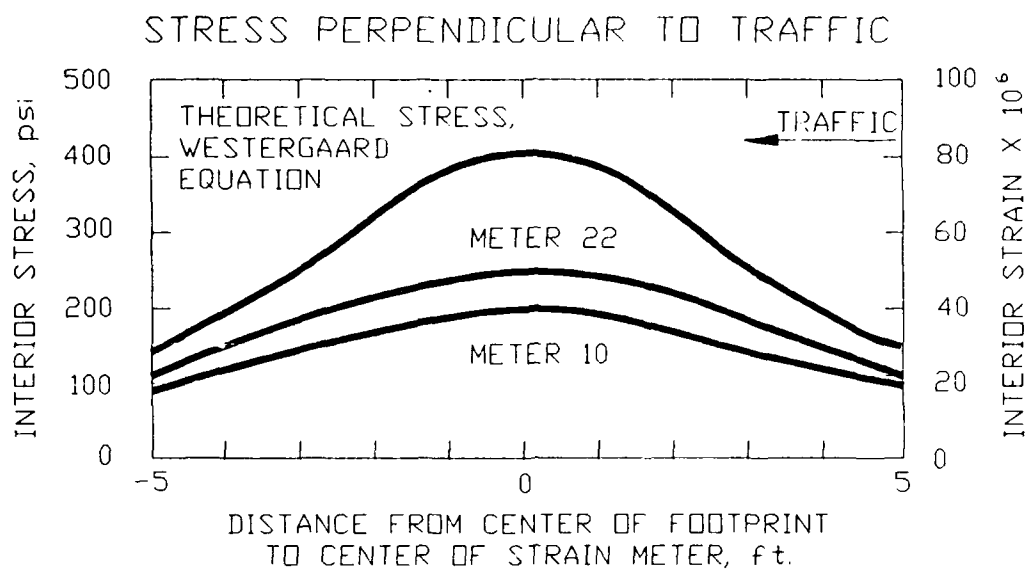


Figure 1. Sample Measured and Calculated Strains from Lockbourne Test No. 1 (Ohio River Division Laboratory 1946)

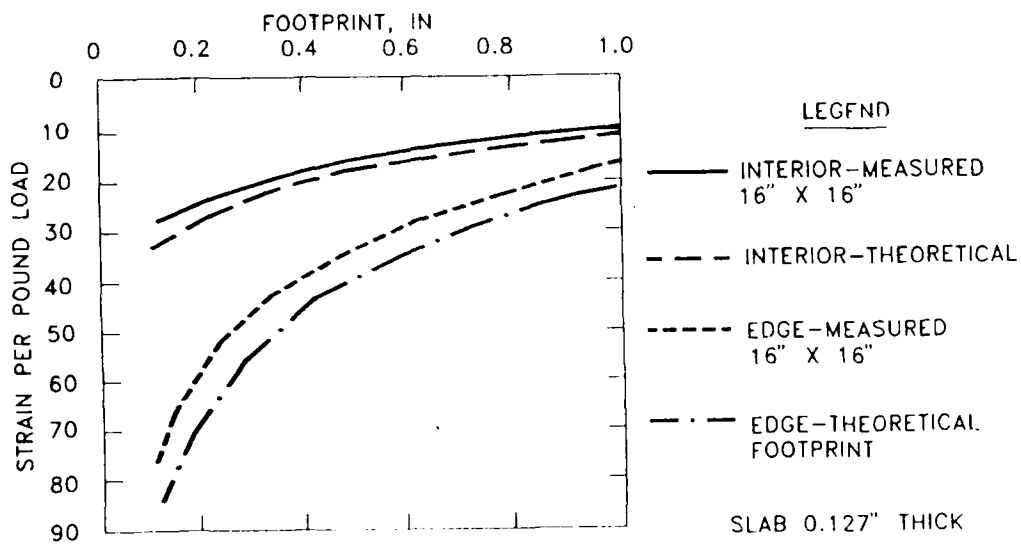


Figure 2. Sample Results from the Corps of Engineers Pavement Model (Ohio River Division Laboratory 1964)

LOCKBOURNE NO.2 MODIFICATION MULTIPLE WHEEL STUDY

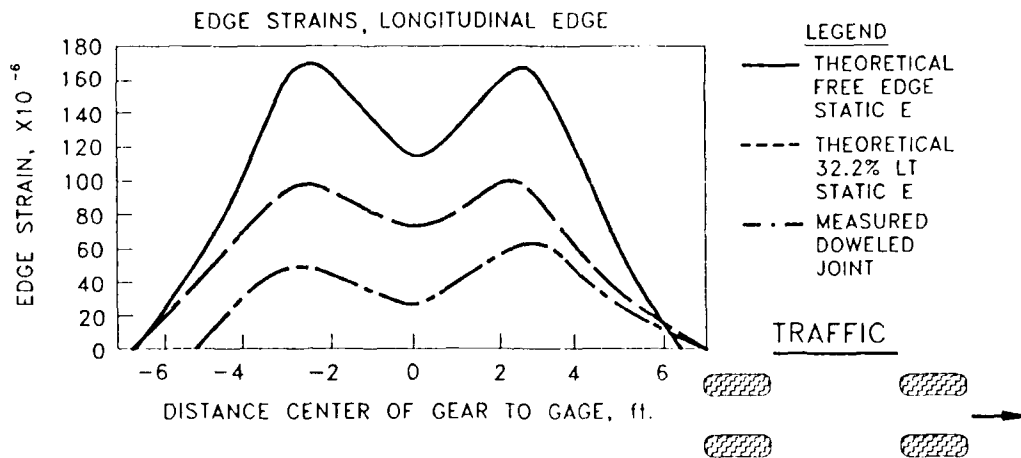


Figure 3. Sample Calculated and Measured Strains at a Doweled Joint (Modified from Ohio River Division Laboratory 1950)

LOCKBOURNE NO.2 MODIFICATION MULTIPLE WHEEL STUDY

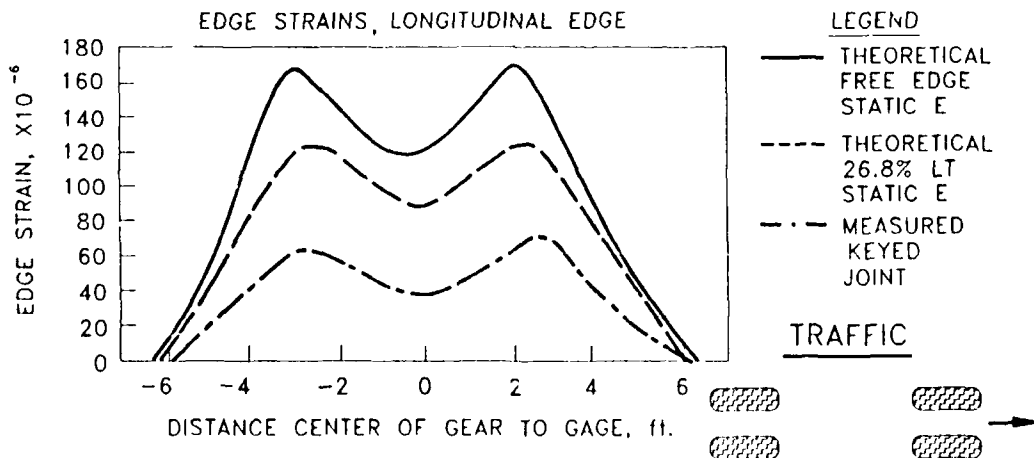


Figure 4. Sample Calculated and Measured Strains at a Keyed Joint (Modified from Ohio River Division Laboratory 1950)

LOCKBOURNE NO.2 MODIFICATION MULTIPLE WHEEL STUDY

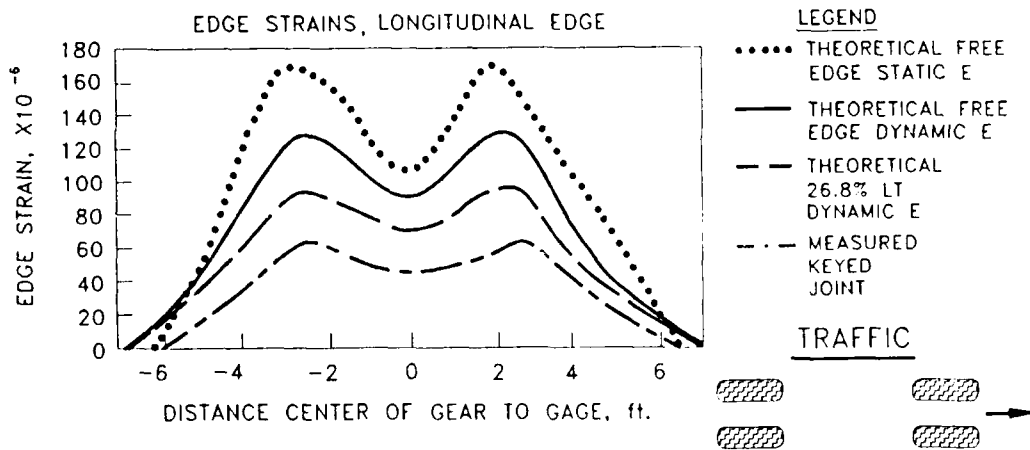


Figure 5. Comparison of Measured Strains and Calculated with Static and Dynamic Properties for a Keyed Joint (Modified from Ohio River Division Laboratory 1950)

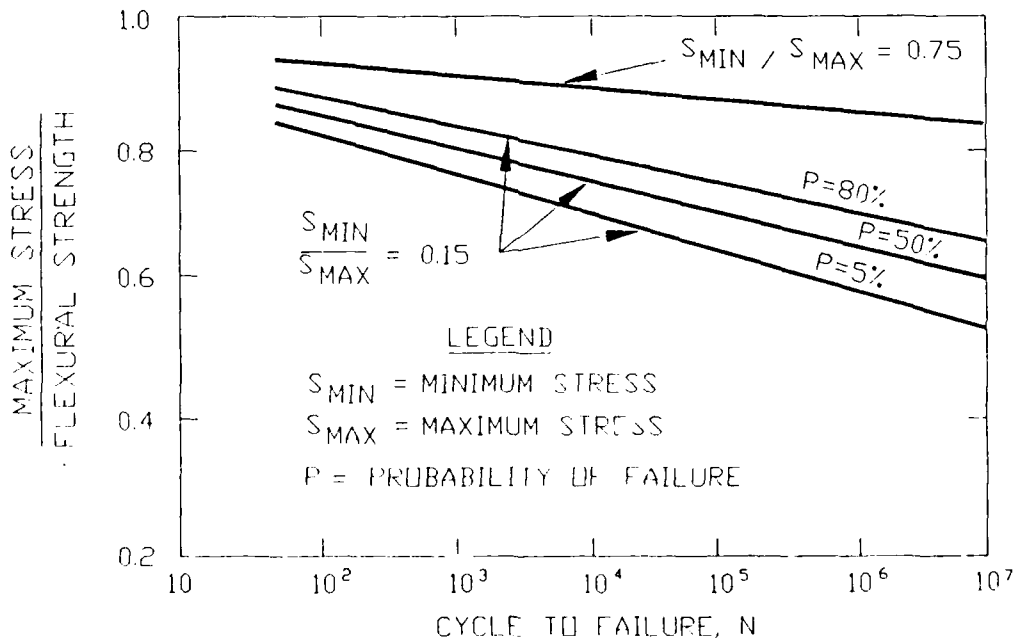


Figure 6. Effect of Minimum to Maximum Test Stress Ratio on Fatigue Relations (American Concrete Institute 1986)

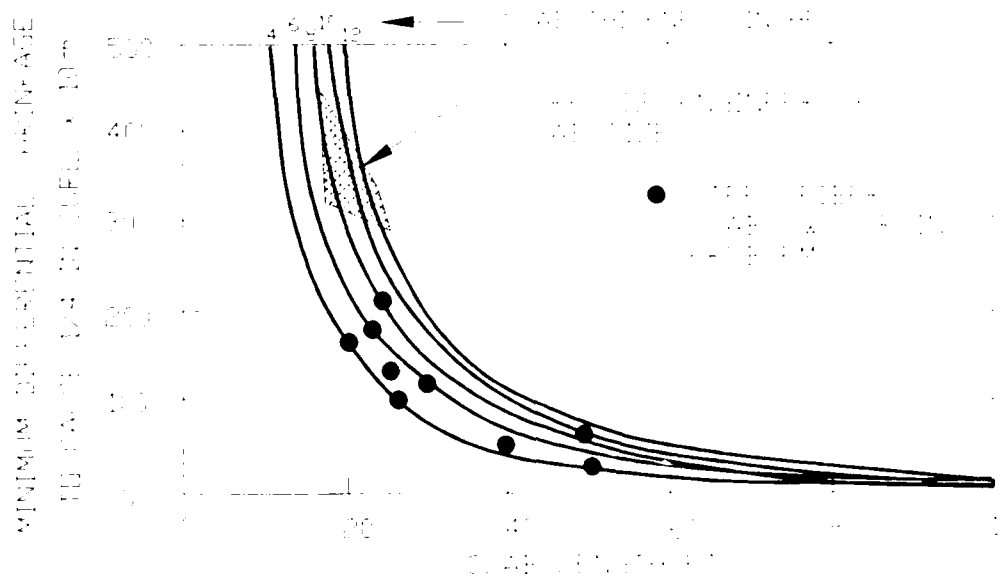


Figure 7. Effect of Slab Length and Thickness on Amount of Differential Shrinkage needed to cause curling (Modified from Rollings 1986)

Acknowledgements

The views expressed in this paper are those of the authors alone. The support of the US Army Engineer Waterways Experiment Station in preparing this paper is gratefully acknowledged. Review and comments on this paper by Dr. Paul Hadala, Mr. Harry Ulery, and Dr. Walter Barker are gratefully acknowledged. This paper is published with the permission of the Chief of Engineers.

References

- American Concrete Institute. 1986. "Considerations for Design of Concrete Structures Subjected to Fatigue Loading," ACI 215R-74 (Revised 1986) Detroit, MI.
- Barenberg, E. J., and Smith, R. E. 1979. "Longitudinal Joint Systems in Slip-Formed Rigid Pavements, Vol I - Literature Survey and Field Inspection," Report No. FAA-RD-79-4-I, Department of Transportation, Federal Aviation Administration, Washington, DC.
- Grau, R. W. 1979. "Evaluation of Drilled and Grouted-in-Place Dowels for Load Transfer of Portland Cement Concrete, Tyndall Air Force Base, Florida," Technical Report GL-79-11, U.S. Army Engineer Waterways Experiment Station, Vicksburg, MS.
- Ledbetter, R. H. 1976. "Pavement Response to Aircraft Dynamic Loads; Compendium," Technical Report S-75-11, Vol III, U.S. Army Engineer Waterways Experiment Station, Vicksburg, MS.
- Mellinger, F. 1963. "Structural Design of Concrete Overlays," Title No. 60-15, Journal, Vol 60, No. 2, American Concrete Institute, Detroit, MI.
- Mellinger, F. M. and Carlton, P. F. 1955. "Application of Models to Design Studies of Concrete Airfield Pavements," Proceedings, Highway Research Board, Vol 34.
- Ohio River Division Laboratory. 1950. "Lockbourne No. 2 Modification Multiple Wheel Study," U.S. Army Corps of Engineers, Mariemont, OH.

Ohio River Division Laboratory. 1946. "Lockbourne No. 1 Test Track, Final Report," U.S. Army Corps of Engineers, Mariemont, OH.

_____. 1943. "Final Report on the Dynamic Loadings on Concrete Test Slabs-Wright Field Slab Tests," U.S. Army Corps of Engineers, Mariemont, OH.

_____. 1964. "Small Scale Model Study to Determine Minimum Horizontal Dimensions for "Infinite" Slab Behavior," Technical Report No. 4-32 U.S. Army Corps of Engineers, Cincinnati, OH.

Pickett, G. and Kay, G. K. 1951. "Influence Charts for Concrete Pavements," Transactions. American Society of Civil Engineers, Vol 116.

Rollings, R. S. 1988a. "Design and Construction of Roller Compacted Concrete Pavements," 14th Australian Road Research Board Conference, Canberra, Australia.

_____. 1988b. "Design of Overlays for Rigid Airport Pavements," DOT/FAA/PM-87/19, Federal Aviation Administration, Washington, DC.

Rollings, R. S. 1986. "Field Performance of Fiber Reinforced Concrete Airfield Pavements," DOT/FAA/PM-86/26, Federal Aviation Administration, Washington, DC.

_____. 1981. "Corps of Engineers Design Procedures for Rigid Airfield Pavements," 2nd International Conference on Concrete Pavement Design, Purdue University, West Lafayette, IN.

Sale, J., and Hutchinson, R. 1959. "Development of Rigid Pavement Design Criteria for Military Airfields," Journal of the Air Transport Division, Vol 85, AT3, American Society of Civil Engineers, NY.

Westergaard, H. M. 1948. New Formulas for Stresses in Concrete Pavements of Airfields. Transactions, American Society of Civil Engineers, Vol 113.

_____. 1926a. Stresses in Concrete Pavements Computed by Theoretical Analyses. Public Roads, Vol 7, No. 2, pp 25-35.

_____. 1926b. "Analysis of Stresses in Concrete Pavements due to Variations of Temperature," Proceedings, Highway Research Board.

IN-SITU STRAIN MEASUREMENTS IN HOT-MIX ASPHALT PAVEMENTS

David A. Anderson, The Pennsylvania State University
Peter E. Sebaaly, The Pennsylvania State University

ABSTRACT

More reliable and long-lived techniques are needed for measuring strains in the hot-mix asphalt layers of hot-mix asphalt pavements. This paper presents the results of measurements obtained from three different types of strain gauges. Good correlation was observed between the measurements from two of the gauge types and the calculated strains. Longevity of the gauges under accelerated loading was poor but corrective actions are offered.

INTRODUCTION

The need for accurate and reliable measurements of the response of pavement systems to traffic loading has become more important with the development of more sophisticated analytical models, the trend towards mechanistic design methods, and the use of accelerated loading facilities. This paper documents measurements obtained with three types of strain gauges at the Federal Highway (FHWA) Accelerated Loading Facility (ALF) in McLean, Virginia (1).

BACKGROUND

Lane 1 was constructed in the summer of 1986 with 125 mm of hot-mix asphalt and 150 mm of dense-graded crushed aggregate subbase placed on a compacted subgrade with a CBR of 5. Lane 2 was of similar

construction, except that 180 mm of hot-mix asphalt and 305 mm of crushed aggregate subbase were used (1).

The instrumentation installed at the time of construction included two types of strain gauges, selected from the group 1.1 and 2.3 gauges that were used in the OECD trials in Nardo, Italy (2). The group 1.1 gauges are often referred to as "H" gauges and are shown schematically in figure 1. These gauges may be fabricated in a number of configurations.

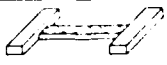
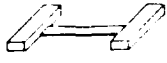
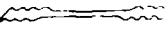


GROUP	SCHEMATIC CONSTRUCTION	ASSEMBLY
1.1		FIXATION OF ANCHOR BARS IN THE LABORATORY
1.2		GAUGE GLUED TO SUPPORT AND FIXATION OF ANCHOR BARS IN THE LABORATORY
1.3		
1.4		GLUED ON A BLOCK OF SHEET ASPHALT
2.3		GLUED ON CORE TAKEN FROM THE PAVEMENT

Figure 1. Classification of Nardo Gauges

In this study premounted strain gauges, manufactured by Kowya especially for this application (Part No. KFC 30-C-11), were fastened to two 9.5 mm by 9.5 mm by 100 mm brass anchor bars. The group 2.3 gauges, developed and manufactured by Christison (3) of the Alberta Research Council (ARC), consist of two strain gauges mounted on plastic film and embedded in a 20 mm thick by 165 mm by 165 mm wide block of asphalt mastic.

Neither the H gauge or the Christison gauge can be used in retrofitting situations. Therefore, subsequent to the construction, one of the sections was retrofitted with group 3.1 gauges, figure 1. With this scheme, a core is first removed from a remote section of the test area and fitted with strain gauges in the desired configuration. The core is then cemented with epoxy into a core hole drilled at the test location. Essential to the success of this scheme is the use of two differently sized core barrels such that the replacement core fits into the core hole with a minimum clearance (4). It is also necessary that the stiffness of the epoxy match the stiffness of the hot-mix asphalt so that the epoxy disturbs the strain field around the core as little as possible.

GENERAL APPROACH

Three main factors are of concern with respect to the performance of strain gauges installed in hot-mix asphalt pavements: (a) the accuracy of the measured strain, (b) the repeatability of results, and (c) the long-term serviceability of the gauge.

The data acquisition system at the ALF site is based on an IBM PC/AT personal computer and several Data Translation D2801A A/D boards (1). A custom data acquisition program is used to collect data from the strain gauges and other transducers. The system also assembles the collected data in ASCII or ASYSTTM files for further analyses.

The accuracy of the measured strains was verified by comparing them to strains obtained from theoretical calculations. The in-situ mechanical properties necessary for these calculations were estimated from back-calculations based on Falling Weight Deflectometer (FWD)

measurements conducted throughout the test period (5).

The repeatability of the strain measurements was assessed in terms of within-and between-gauge variability. In this study, when response measurements were acquired, each combination of load level and lateral wheel placement was repeated three times. Therefore, the mean and standard deviation of the measurements were calculated for the three types of gauges, different load levels, and wheel placement. (Note: The lateral position of the ALF loading dolly can be operator selected while the machine is in operation.)

The long-term serviceability of the gauges was investigated by monitoring both the long-term accuracy and the long-term repeatability of the gauges. This was done at various levels of load application, or equivalent single axle load repetitions (ESAL), throughout the test period. Because different load levels were used for different test sections, the loading history was converted to AASHTO 80-kN ESAL's.

EVALUATION OF H GAUGES

Six H-gauges were installed in lane 2 section 3 at the bottom of the hot-mix binder course as shown in figure 2.

H Gauge Variability. Based on the symmetry of the layout shown in figure 2, strain gauges 1, 2, 3, and 4 should yield identical strains when the centerline of the dual wheels (84-kN) pass over the pavement centerline. The peak strain measured from the four strain gauges are plotted in figure 3 as a function of the number of 80-kN ESAL repetitions.

The data in figure 3 indicate a large variability between the measurements for the four gauges. During the post mortem evaluations of these test sections, large blocks of the pavement, approximately 1 m by 1 m, were removed and it was noticed that the anchor bars were loose. Some of the anchor bars had loosened during trafficking, such that considerable bending would have to occur in the pavement before the gauges could experience any strain. This looseness decreased the apparent sensitivity of the loose gauges such that

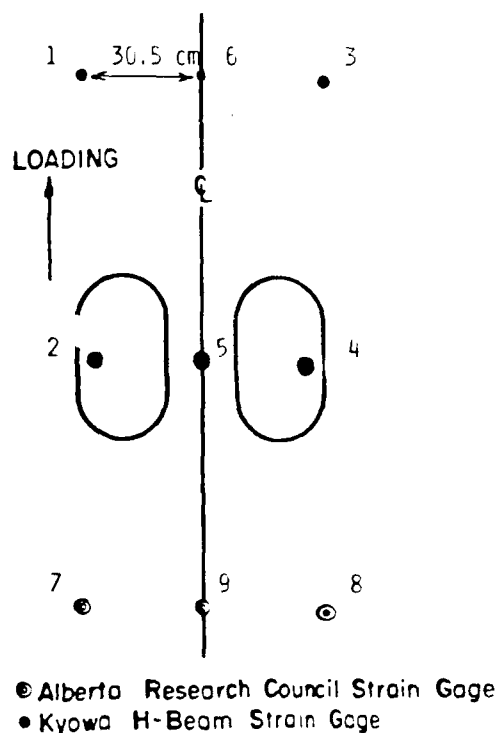


Figure 2. Location of Alberta and H-Beam Strain Gauges.

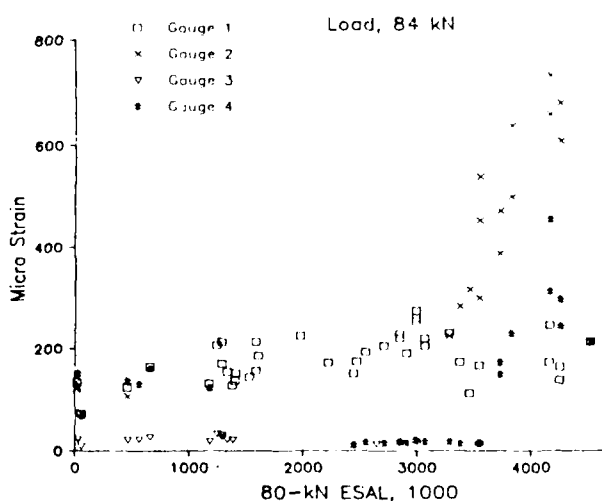


Figure 3. Strain Data from four H-Gauges.

the measured strains much were less than the actual strains.

The sets of measurements from gauges 1, 2, 3, and 4 were compared and those data points that were in obvious error

(strains too small - loose gauges) were discarded, giving the data shown in figure 4. Only with multiple strain gauges was it possible to identify those gauges with anomalous results. As indicated in figure 4, the magnitude of the strains increased with increasing numbers of accumulated ESAL. Calculated strains are also shown in figures 4. The differences between the measured and theoretical strains were very small prior to 3.5 million accumulated ESAL. The large difference between theoretical and measured strains after 3.5 million repetition is due to the extensive fatigue of the asphalt layer.

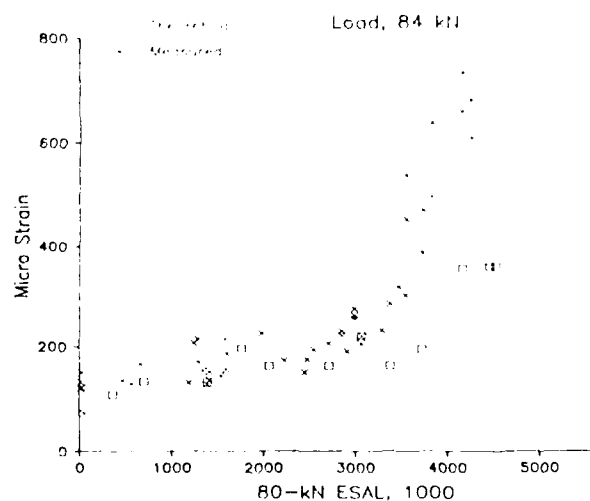


Figure 4. Strain Data from Four H-Gauges

H Gauge Repeatability. The repeatability of the measurements from the H gauges was studied at an early stage of the experiment when most of the gauges were still tightly anchored in the binder layer. To demonstrate the within- and between-gauge variability, the measured strain values for five load levels and three passes of the test wheels are given in table 1. The average standard deviation within the three repeated measurements is approximately $4\text{-}\mu$ strain, which compares favorably with the magnitude of the actual readings. Repeatability between gauges can also be observed in table 1 by comparing the readings of the gauges placed to the right and left of the centerline and by comparing gauges at different stations. The repeatability of the gauges was considered good at the early stage of loading. However, the repeatability between different gauges was

Table 1. Kyowa gauge measurements during testing of section 2-3 with test wheels centered on the pavement centerline.

Dual Wheel Load	Station	Microstrain		
		0.304 m Left of Centerline	Centerline	0.304 m Right of Centerline
42 kN	112	54.2	50.4	55.4
		53.2	70.2	56.4
		<u>58.9</u>	<u>57.3</u>	<u>57.6</u>
	Average	55.4	59.3	56.5
	110	NA	52.3	39.7
		NA	53.5	55.7
		<u>NA</u>	<u>48.8</u>	<u>NA</u>
	Average	NA	51.5	47.7
52kN	112	72.4	81.9	74.0
		76.9	81.9	74.3
		<u>76.2</u>	<u>92.9</u>	<u>75.9</u>
	Average	75.2	85.6	74.7
	110	NA	95.1	81.9
		NA	93.9	63.9
		<u>NA</u>	<u>97.3</u>	<u>84.4</u>
	Average	NA	95.4	76.7
63 kN	112	107.4	127.6	99.8
		101.4	118.4	98.9
		<u>95.4</u>	<u>113.4</u>	<u>94.8</u>
	Average	101.4	119.8	97.8
	110	NA	117.8	103.9
		NA	116.8	92.0
		<u>NA</u>	<u>119.4</u>	<u>94.5</u>
	Average	NA	118.0	96.8
73 kN	112	124.1	129.8	113.7
		126.0	150.9	115.0
		<u>126.6</u>	<u>139.5</u>	<u>113.1</u>
	Average	125.6	140.1	113.9
	110	NA	130.4	81.9
		NA	132.0	98.6
		<u>NA</u>	<u>132.3</u>	<u>77.5</u>
	Average	NA	131.6	86.0
84 kN	112	142.3	168.5	122.2
		142.0	162.2	120.9
		<u>143.0</u>	<u>164.7</u>	<u>123.1</u>
	Average	142.4	165.1	122.0
	110	NA	166.6	118.1
		NA	166.6	117.2
		<u>NA</u>	<u>163.5</u>	<u>120.0</u>
	Average	NA	165.6	118.4

often poor after considerable loading, as shown in figure 3.

Serviceability. The long term serviceability of the H gauges can be observed from the data shown in figure 4. In general the rate of failure of the H gauges was as high as 50 percent. The long term repeatability of the surviving gauges was also investigated and is shown in table 2. Except for the test period near the terminal life of the section the data show good within-gauge repeatability. Since most of the gauges failed at various

tically deform the hot-mix asphalt. A 0.01 in thick aluminum strip will generate approximately the same force. Therefore, the stiffness of the H-gauge is extremely important. The Kowya H-gauge and most aluminum H-gauges are unacceptably stiff.

Alberta Gauges

Accuracy of Measured Strains. Three Alberta gauges were installed in lane 2 section 3, at the locations shown in figure 2. Strain gauge 7 failed very

Table 2. Kyowa gauge measurements during testing of section 2-3 using ALF dual wheel load of 84 kN

Day of Test	Microstrain	Average	Standard Deviation
12	31.5 29.3 30.2	30.3	1.10
50	105.8 104.2 105.2 105.8 106.4	105.5	0.8
122	132.3 132.9 129.1 129.8 132.3	131.3	1.7
140	658.9 671.5 634.3 622.3 628.0	643.0	21.2

loading stages, the between-gauge repeatability could not be investigated.

Looseness of H-Gauges. The author's were concerned about the looseness of the H-gauges and sought an answer for the cause of the looseness. Assuming the stiffness of the plastic strip is 4×10^7 lb/in², and that the underside of the pavement undergoes a strain of 800 microstrain, the force on the anchor bars will be 35 - 40 lb. The author's feel that this is sufficient force to plas-

early during the loading period. The data for gauges 5 and 6 show a very large difference between the theoretical strains and the measured values throughout the entire test period and the theoretical strains are very large compared to the measured values.

Repeatability of the results. Very few data points were obtained from the Alberta gauges as a result of difficulties encountered in the balancing of the gauges during testing. Most of the collected

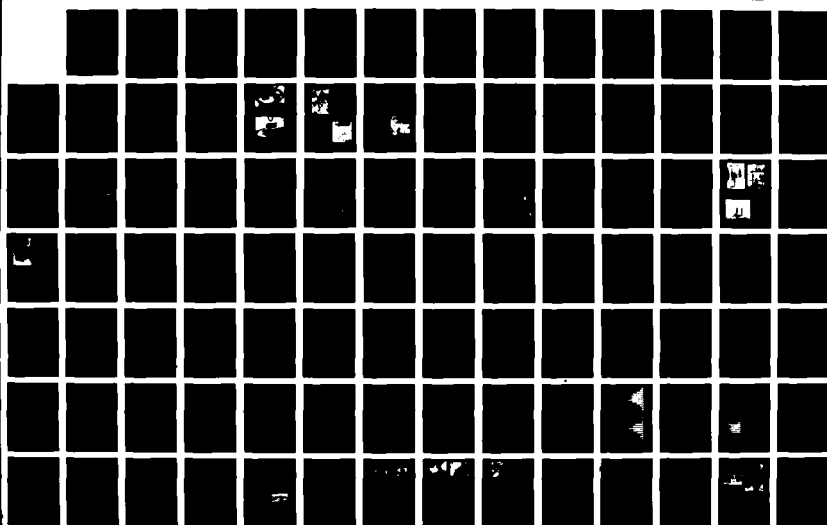
NO. 424-301

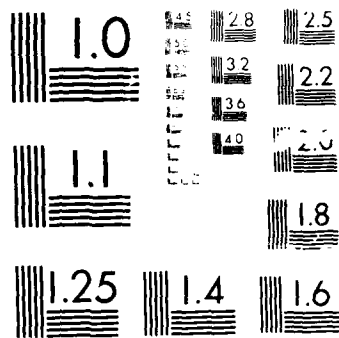
STATE OF THE ART OF PAVEMENT RESEARCH
SYSTEMS FOR ROADS AND AIR. (U) COLD REGIONS RESEARCH AND
ENGINEERING LAB HANOVER NH V JANOO ET AL. SEP 89
CRREL-SR-89-23

UNCLASSIFIED

F/B 13/2

ML





data were unrealistic, and therefore a meaningful conclusion regarding repeatability could not be made.

Serviceability. The failure rate of the Alberta gauges was unacceptably large. Among the three gauges installed in lane 2 section 3, none produced any realistic data. This is not meant to be critical of these gauges; they have been used successfully by others in field applications (3).

The cables leading from these gauges and from the H gauges were anchored on the compacted subbase with 10 penny nails bent in the form of a U at the head end and driven into the subbase. Although this technique has worked successfully before, in this application the nails sometimes wore through the cable insulation and shorted the lead wires. This, and the large strains caused by the large wheel loads (as large as 84 kN per dual tires) probably was, in large part, responsible for the premature failure of both the H gauges and the Alberta gauges.

Instrumented Cores

Four instrumented cores were used to retrofit lane 2 section 1. The locations of the cores are shown in figure 5.

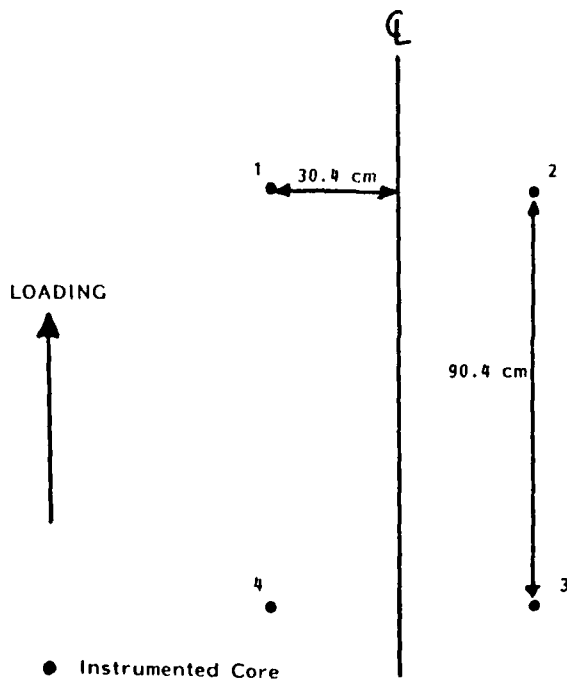


Figure 5. Location of Instrumented Cores.

Accuracy of Measured Strains. When the centerline of the dual tires passes over the centerline of the pavement, the gauges on all four cores shown in figure 5 should measure identical strains. The measurements from these cores are plotted in figure 6 as a function of the number of applied 80-kN ESAL repetitions. The loading period of test 2-1 spanned the period from April to December of 1988. As a consequence, the average pavement temperature was a major variable in the response of the test section. This is reflected in figure 6 where the strains increase and then decrease with increased load application.

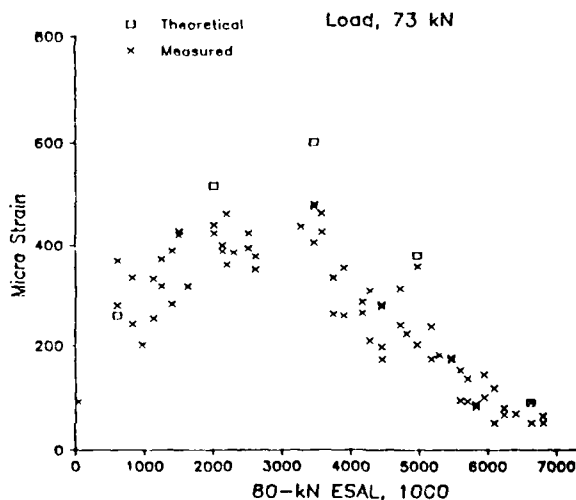


Figure 6. Strain Data from Four Instrumented Cores.

Repeatability of the results. The repeatability of the strain measurements was investigated at various stages throughout the test period. The readings from core 1 were evaluated in terms of the mean and standard deviation, table 3. The data indicate good measurement repeatability throughout the test period except at 144 days into the loading period where a standard deviation of 15.95 was encountered.

Serviceability. The long-term serviceability of the instrumented cores was unacceptable. The test period lasted for 210 days. Of the four cores, two cores failed after 68 days and one core failed after 98 days of testing. Only one

core produced valid data the entire loading period. However, the long-term repeatability of the surviving core gauge was good, based on the data in table 3.

in figure 7. Also shown in the figure are strains calculated from static and dynamic analyses. The static strains were calculated with the BISAR computer program

Table 3. Instrumented core measurements during testing of section 2-1 using dual wheel load of 73 kN.

Day of Test	Average Pavement Temperature	Microstrain	Average	Standard Deviation
1	55.6	90.8 86.2 92.6	89.9	3.3
34	59.9	291 286 278	285	6.3
74	76.5	440 440 430	437	6.1
110	73.5	406 405 395	402	5.8
144	65.3	201 200 228	210	16.0
175	48.9	51.6 53.4 62.0	55.7	5.5

LOAD-UP STUDY

A load-up study, in which the dual wheel loads were increased from 42 kN to 84 kN was conducted on January 29, 1987, the first day of loading on section 2-3. Strains were measured with the dual tires in three lateral positions: with the centerline of the duals passing over the pavement centerline and passing 0.3 m to the left and 0.3 m to the right of the centerline.

Strain gauge data for the centerline gauges, measured during the load-up study with this dual tires centered over the centerline gauges, are shown graphically

and the dynamic strains were calculated with the DYNAMIC1 Computer Program (5).

There is relatively good agreement between the measured and calculated strains, especially for the smaller load levels. At the high load levels, both the dynamic and static calculated strains were lower than the measured strains. This difference may be explained by the non-linear behavior of the subbase and subgrade material under heavy loads. Within the range of expected highway traffic loading, 80 to 106 kN axle loads, the H gauge and calculated dynamic or static strains are very similar.

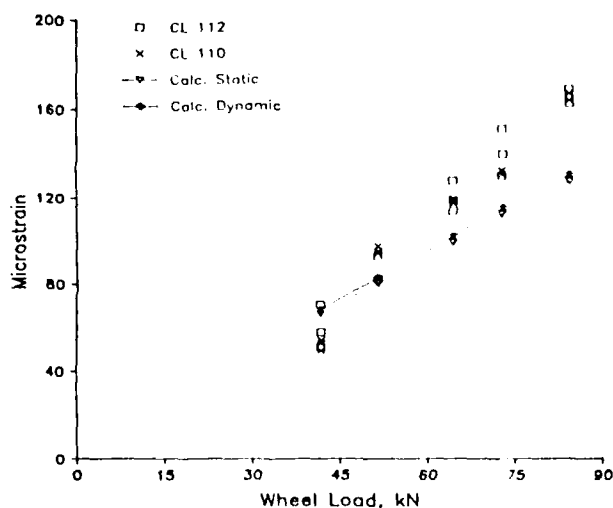


Figure 7. Comparison of Calculated Static and Dynamic Strains with Measured Strains.

FINDINGS

Based on the authors' experience at the FHWA Accelerated Loading Facility the following findings are warranted:

1. The H-gauges that are constructed with the Kowya gauges mounted on the plastic strips are too stiff and will loosen on the pavement.
2. Multiple gauges are needed to obtain accurate estimates of strain.
3. The lateral and longitudinal position of the test wheel must be known to plus or minus one inch in order to match calculated and measured strains.
4. The time history of the strain, rather than the peak strain, is needed to make reasonable judgments with respect to the validity of the data.
5. The repeatability of the instrumented core and H-gauges is good.
6. The instrumented core gauges are acceptable for retrofitting purposes.
7. Installation procedures are critical to the success of in-situ strain measurements.

ACKNOWLEDGEMENTS

This work was in part sponsored by the FHWA. The opinions expressed in this paper are those of the author's and may not agree with those of others. The cooperation of Ray Bonaquist and Charles Chiurilla of the FHWA and Dick Penuska of Engineering Incorporated Services Company is gratefully acknowledged.

REFERENCES

1. D. A. Anderson, W. P. Kilareski, and Z. Siddiqui, Pavement Construction and Instrumentation for The Accelerated Loading Facility, Interim Report, Report No. PTI 8619, Pennsylvania Transportation Institute, Pennsylvania State University, University Park, PA, 1986.
2. Organisation for Economic Co-Operation and Development, Full-Scale Pavement Tests, Paris, 1985.
3. J. T. Christison, K. O. Anderson, and B. P. Shields, "In-Situ Measurements of Strains and Deflections in a Full-Depth Asphaltic Concrete Pavement," Proceedings of the Association of Pavement Technologists, Vol. 47, 1978, pp. 398-433.
4. M. Huhtala, Personal communication, 1987.
5. David A. Anderson, et. al., Pavement Testing Facility - Pavement Performance of the Initial Two Test Sections, Report No. PTI 8719, Pennsylvania Transportation Institute, Pennsylvania State University, University Park, PA, 1988.

IOWA DEPARTMENT OF TRANSPORTATION
WEIGH-IN-MOTION

Bill McCall, Director

Office of Transportation Research
Iowa Department of Transportation

The contents of this paper reflect the views of the author, who is responsible for the facts and the accuracy of the data presented herein. The contents do not necessarily reflect the official views or policies of the Iowa Department of Transportation. This does not constitute a standard, specification or regulation.

This paper contains discussion on weigh-in-motion systems. The definition of weigh-in-motion is followed by generic descriptions of the uses of weigh-in-motion technology, system accuracy, factors that affect system accuracy, national standards, and the Iowa and Minnesota experience with low-cost automatic weight and classification based on piezo cable technology.

The definition of weigh-in-motion is "weighing a highway vehicle by attempting to approximate the gross weight or the portion of the weight carried by a wheel, an axle, or a group of axles by measuring, during a short period of time, the vehicle component of dynamic force that is applied to a smooth, level road surface by the tires of the moving vehicle" (1). The weight of the vehicle does not change when it moves over the road, but the dynamic force applied to the roadway surface by a rolling tire on the vehicle varies dramatically when the tire/wheel mass accelerates vertically.

There are three basic types of weigh-in-motion systems. These are slow speed weigh-in-motion, medium speed weigh-in-motion, and high speed weigh-in-motion. Slow speed weigh-in-motion estimates the static weight of vehicles moving up to 10 mph, medium speed weigh-in-motion up to 40 mph, and high speed weigh-in-motion at posted speeds.

Weigh-in-motion systems can be used for either law enforcement or highway planning and design. In law enforcement applications, medium speed weigh-in-motion systems are used to sort legal trucks from those that are not. Those meeting regulations can be allowed to pass without weighing at a static scale. The Arizona Department of Transportation is currently attempting to develop a slow speed weigh-in-motion installation that is capable of accuracies required to issue weight citations. This paper will focus primarily on the application of high speed weigh-in-motion systems to obtain highway planning and design data. In the past, heavy vehicle loading data has been gathered by many state departments of transportation using the permanent enforcement scales and portable scales. Data was collected manually over relatively short periods of time usually in the summer months and on weekdays by part-time staff. The manually gathered data has some serious weaknesses. Usually, the data is collected at a rather limited number of sites and is biased because trucks make a conscious effort to bypass data collection stations. In addition, there is a cost to the trucking industry because of delays incurred at weighing locations and of course the associated cost to departments of transportation to staff those stations.

A report titled Overweight Trucks--The Violation Adjudication Process, Federal Highway Administration, dated July 1985 pointed out that "Recent studies suggest that 25-35 percent of large loaded trucks are overweight. At some locations, the figure may range as high as 100 percent." This observation is based on data from weigh-in-motion systems. Further, the authors of National Cooperative Highway Research Program (NCHRP) Synthesis 131, "Effects of Permit and Illegal Overloads on Pavements," 1987, estimate that 10 to 20 percent of all trucks over 10,000 pounds are operating overweight (6). The authors state that this observation is consistent with findings of several weigh-in-motion studies. Manually collected data reported in the Iowa Department of Transportation's 1987 Truck Weight Report states "over 11 percent of all trucks weighed were found to be exceeding Iowa weight limits." Weigh-in-motion systems gather much more representative data reflecting actual traffic stream loading than do processes using manual intervention. Weigh-in-motion systems can operate unattended 365 days a year; 24 hours a day or be programmed to collect data over any period.

There are five general weigh-in-motion technologies currently offered. These are bending plate, load cell, capacitive, bridge, and piezo.

Bending plate technology typically employs a high strength steel plate with strain gages mounted on it. Plates measure typically 4 or 6 feet wide by 2 feet long. Two or three are mounted across a traffic lane normally covering both wheel tracks. A light-weight frame supports the plates in about a 2 inch deep pit. The rather shallow pit depth is a factor which helps keep installation costs down. Bending of the plate under load as the vehicle crosses it is measured by the strain gages located in the underside of the plate. For environmental protection the entire plate is encapsulated in a protective covering.

Load cell technology is usually found in a deep pit system with two rectangular

weighing platforms measuring about 5 feet by 2 feet, resting on a common concrete foundation. One platform is located in each wheelpath. Loads applied to the platform produce vertical movement in the centrally located oil filled piston which acts as a load cell.

Capacitive technology usually found in portable systems employs sheets of steel separated by a dielectric. The assembly acts as a capacitor. Compression of the capacitive mat under load produces an increase in capacitance which is interpreted as a weight by the attached microprocessor base data collection system. The capacitance mat is typically nailed down to the road surface making a temporary installation.

The bridge weighing system utilizes strain transducers bolted to the underside of support beams of a highway bridge. Switches are placed in the road in front of the bridge for measuring vehicle speeds. This approach approximates the weight of the truck by measuring the structural response, i.e., bending moment and calculating the dynamic weight causing the moment.

Piezo electric weigh-in-motion systems utilize a physical phenomenon called "piezo electricity." When a force is applied to certain parallel faces of sole crystalline materials, electrical charges of opposite polarity appear at the parallel faces. The magnitude of the piezo effect is dynamic, in that the charge is generated only when the force is changed. Therefore, the static weight of axles can be correlated to the magnitude of the output from the piezo electric cable. Piezo electric systems can be mounted at the surface of the pavement making the system permanent.

The technologies described above typically utilize state-of-the-art microprocessors. The signal that is generated by the dynamic force applied to the transducer mounted on the roadway is translated into weight predictions by algorithms developed by the equipment vendors.

Appendix 1 contains a list of weigh-in-motion equipment suppliers along with the type of systems provided. In addition to axle weights, weigh-in-motion systems typically provide the time of vehicle passage, the number of vehicles that have passed during a preselected period, vehicle speed, number of axles, axle spacings, vehicle type based on axle spacings, axle combination weights, and gross vehicle weight.

Figure 1 illustrates the output from the low-cost automatic weight and classification system based on piezo electric technology that was evaluated in the states of Iowa and Minnesota (2-3). The header states that the data was gathered on January 31, 1989 by the GK Instruments' automatic weight and classification system. The speed is in miles per hour, the weight in ten pound units, and the axle spacings in tenths of feet. The transducers are 16 feet apart, and the self-calibration factor is 1.24.

Therefore, in Figure 1 vehicle number 7324 was traveling 64 mph, had five axles, and was a class 99 vehicle which is a five-axle semi-truck. Gross weight was 27,090 pounds. The line labeled WT shows that the lead axle weighed 7,310 pounds, the first drive axle 6,680 pounds, the second drive axle 4,150 pounds, and the trailer tandem axles 4,630 pounds and 4,320 pounds. In the WB wheelbase line, the distance between the steering axle and the first drive axle is 12.5 feet. The distance is 4.4 feet between the drive axles, 32 feet between the last drive axle and the first trailer tandem, and 4.1 feet between trailer tandems. The last line shows sum of tandem axles at 10,830 and 8,950 pounds.

```

31 JAN 1989  GK AMACB  MPH - 10 lbs - .ft X - 160 F1 = 1.24 F2 = 1.00
LANE  TIME      COUNT    SPEED    AXLE    F/CL    GROSS/WT
01    09 22 34    7323      0061     02     02     0298
WT    0193 0105
WB    7084
T/T

01    09 22 39    7324      0064     05     99     2709
WT    0731 0668 0415 0463 0432
WB    0125 0044 0320 0041
T/T    1083 8950

```

Figure 1

Accuracy of weigh-in-motion systems can be defined in terms of percent difference and the variability of the percent difference. Percent difference is the ratio of the difference between the weigh-in-motion and the static weight to the static weight expressed as a percentage.

$$PD = \frac{\text{Static} - \text{WIM} \times 100}{\text{Static}}$$

The average of the percent difference is the systematic difference. The standard deviation of the percent difference, which measures the spread or variation of individual measurement, is the random difference. The term difference is used in preference to error since analysis suggests much of the difference between static and dynamic weight is a result of actual dynamic variations between static weights and dynamic forces that occur as the vehicle travels the roadway. As mentioned earlier in the paper, the dynamic force applied to the roadway surface by a rolling tire on the vehicle varies dramatically when the tire/wheel mass accelerates vertically. This

acceleration can be induced by a number of vehicle and highway factors. Vehicle factors include vehicle shape, size, weight, mass, mass moments of inertia, suspension system, tires, aerodynamic characteristics, speed, and payload shifting. Roadway factors include longitudinal profile, grade, curvature, and cross-slope. All factors cause the moving vehicle to exert a dynamic load on the pavement. Previous research (4) has pointed out that heavy vehicles have a natural frequency of oscillation between one-half and four hertz. In addition, wheels oscillate at a frequency of between eight and twelve hertz when displaced suddenly but the oscillations are quickly dampened. Further variations in dynamic wheel force can be caused by tires that are not truly round or balanced.

Roadway factors can have a significant affect on the difference between static weight and estimates made by weigh-in-motion equipment. In a study of the dynamic force applied to the roadway surface by a rolling truck tire (4), it was observed that placing a sheet of 3/8 inch plywood to create a "bump" affect in the roadway can cause forces to be over 40 percent greater than the static load. The difference between the force and the static load is, in part, dependent upon vehicle characteristics and the static weight of the vehicle.

The most recent research conducted dealing with weigh-in-motion accuracy and pavement roughness (5) concluded that sections of smooth pavement can be shorter for the approach to weigh-in-motion scales than are generally being used at the present time. The researchers developed an empirical relationship to predict axle and gross weighing error as a function of pavement roughness. The research provides a method to determine the predicted error based on pavement roughness and provides an analytical approach necessary to reduce the predicted error to an acceptable level. A smoothed site approach can then be calculated.

The National Cooperative Highway Research Program 3-39, "Evaluation and Calibration Procedures for Weigh-in-

Motion Systems" has as objectives, to develop procedures covering all weigh-in-motion system applications for acceptance testing, on-site calibration, and periodic verification of system performance. Acceptance testing is defined as a national type testing intended to provide a rigorous and definitive assessment of whether a new weigh-in-motion system or a significantly different model of an existing weigh-in-motion system meets the performance specifications that had been defined for it. It is anticipated that national type testing will be normally carried out by a participating laboratory or some other suitably equipped and certified facility.

On-site calibration is defined as testing that will verify that the observed level of performance on the actual highway site is statistically consistent with the national type testing results. If the results are not consistent with the national type testing results, the procedure will indicate whether the difference in results is due to the weigh-in-motion equipment, the condition of the approach pavement, the condition of the trucks used in the test, and the installation procedure.

Periodic performance testing will provide periodic verification of the system's performance under actual site conditions.

ASTM is in the process of developing a "Specification for Highway Weigh-in-Motion (WIM) Systems With User Requirements and Test Method." The objective of the specification is to provide standards and performance requirements for automatic weigh and classification systems. The specification will include highway conditions to be provided by users in order for the weigh-in-motion equipment to meet performance standards. In addition, a test method for weigh-in-motion systems is included. The draft specification is currently in the process of being finalized.

The Heavy Vehicle Electronic License Plate Program is a multi-state project that will culminate in a demonstration

project using automatic weigh-in-motion, automatic vehicle identification, automatic vehicle classification, and supporting computer systems to facilitate heavy truck movements along the West Coast states stretching from Washington to Texas.

The program required weigh-in-motion systems to be evaluated and a specification for procurement to be developed. The Weigh-in-Motion Performance Specification Subcommittee of the Heavy Vehicle Electronic License Plate Program contracted with the Texas Transportation Institute to conduct the evaluation and prepare the performance specification. System tests were conducted in the states of Texas, Illinois, Idaho and Oregon on the Streeter Richardson's portable, PAT's permanent, Streeter Richardson's permanent, Golden River's portable, CMI Dynamics' permanent, and Bridge Weighing Systems' portable systems. The report is expected to be released by June 1989.

National Cooperative Highway Research Program G3-36 "Development of a Low-Cost Bridge Weigh-in-Motion System" has as objectives, to develop a low-cost bridge weigh-in-motion system capable of providing the traffic data used in design and maintenance of highways and bridges. The system shall be able to record gross vehicle weights and classify vehicles at a minimum, and also be able to report individual axle weights within the limits of the specific bridge and site characteristics. The system shall use state-of-the-art technology and have a target purchase price of from \$5,000 to \$10,000 per unit, have a low life cycle cost, and be capable of interfacing with automatic vehicle identification equipment and be deployed on both bridges and large culverts. This project is currently underway and is scheduled to be completed by August 1989.

The piezo electric phenomenon may be the most talked about technology to be used for weigh-in-motion. There are several variations of sensor designs. The most common, at this time, may be piezo cable.

The Iowa and Minnesota Departments of Transportation have evaluated a low-cost automatic weigh and classification system using piezo electric technology. The transducer consists of a 3 millimeter diameter piezo cable, 3 meters long, mounted in a 1 inch aluminum channel and capsulated in urethane rubber. The finished assembly is 3 meters long and has a RG58 feeder cable. The processing electronics are housed in an 8 inch x 5 inch x 8 inch box. This system is programmable and includes such factors as an initial calibration factor, a self-calibration lead axle target weight, and other parameters for setting up the system such as site identification, time and date, and transducer spacing. The system is capable of predicting tire footprint width and length data.

This data can be used to distinguish between single and dual wheel axles and possibly predict contact tire pressure. The system is also self-calibrating and temperature compensated. All output is ASCII and RS232-C compatible. The external data transmission rate can either be 300 or 1200 baud.

The self-calibration feature is designed to maintain accuracy between initial calibration and periodic system performance verification. Self-calibration is based on the system comparing the mean of a sample of five-axle semi steering axles' weigh-in-motion weight to an initial steering axle weight programmed into the system based on site specific data. Initial system calibration is accomplished using a statistically significant sample of vehicles taken from the actual traffic stream.

The site location and installation of the system is extremely important. Site characteristics have a great deal of influence on the difference obtained between static weighings and weight predictions made by weigh-in-motion equipment. Site evaluation factors are pavement rigidity, pavement profile, surface condition, lane width, availability of services, and highway maintenance schedules. In Iowa, the system is installed in portland cement concrete and in Minnesota in asphaltic cement concrete.

The piezo cable transducer detects not only the force from the tires but also forces created by pavement bending. The very flexible nature of asphaltic cement concrete was observed in the waveform output of the piezo cable charge amplifiers. At times the bending caused as much as 80 percent of the waveform to be below the steady state nonactuated condition.

A Dynatest model 8000 falling weight deflectometer was used to measure the flexible character of the ACC pavement observed in the output waveform. The load from the falling weight deflectometer was 9,884 lbs. on the 5.91 inch radius load plate. Pavement temperature was 40°F. The deflection at the center of the applied load was 7.8 mills. This deflection basin indicated that the test section was quite flexible and not typical for an asphaltic cement concrete pavement.

In portland cement concrete, bending caused the waveform to fall beneath the steady state level from about 5 to 10 percent. A Model 400 Roadrater was used to measure the flexible character of the PCC pavement observed in the output waveform. A 2,000 lb. load at 30 hertz was applied. Pavement temperature was 36°F. Deflection at the center of the applied load was 0.8 mills. The deflection basin showed the portland cement concrete section to be typical of a pavement in good condition with good subgrade support. The significant bending of the ACC pavement and the resulting recovery seemed to cause several problems. The algorithm developed for this system recognized not only the waveform from the piezo cable as an axle but also the recovery of the pavement. Experience suggests that the algorithm used to estimate static weight needs to be reconsidered to take into account pavement bending. Also, perhaps other schemes of signal processing could be used that would eliminate the unwanted signal.

Pavement profile has a significant influence on vehicle dynamics and resulting accuracy. The smoother the site profile and surface condition, the

less the difference between the weigh-in-motion output and static weight. The profile at the portland cement concrete site located in Iowa is 1.4 inches in each wheelpath in 500 feet preceding the transducer installation as measured with a 25 foot profilometer.

The low-cost automatic weigh and classification system can be installed using four people, a pavement saw, a small trencher, and the necessary epoxy and tools. Whether conditions must be dry, with pavement temperatures preferably in the 50°F to 80°F range. of course, the necessary traffic control must be established before beginning the installation. Transducer locations are marked with a waterproof material. Slot cutting and shaping must be done very carefully to ensure that the transducers remain flush with the surface of the pavement. The transducers could perhaps be placed slightly below the surface and topped with urethane rubber.

Again, system accuracy is defined in terms of percent difference and the variability of the percent difference.

$$PD = \frac{\text{Static} - \text{WIM}}{\text{Static}} \times 100$$

The mean of the percent difference is the systematic difference. The standard deviation of the percent difference is the random difference.

Given the Iowa site condition, a profile of 1.4 inches in 500 feet in both wheelpaths leading the transducer assembly as measured with a 25 foot profilometer, the low-cost automatic weight and classification system seems to be capable of predicting axle weights and axle group weights with an absolute random difference of less than 1,200 lbs. for axles weighing less than 10,000. The systematic difference is less than 250 lbs. The random difference is less than 12 percent for axles and axle groups weighing greater than 10,000 lbs. The systematic difference is less than 2 percent. A total of 1,951 randomly selected axle and axle groups were compared. Again, based on the Iowa case results, this system is capable of predicting gross vehicle weight with a

random difference of less than 10 percent. The systematic difference is less than 1 percent. 668 randomly selected trucks were compared during the evaluation.

The data taken at the asphaltic cement concrete pavement site resulted in larger differences between weigh-in-motion estimates and static weight. The random difference for axles and axle groups weighing less than 10,000 lbs. is 1,420 lbs. The systematic difference is less than 130 lbs. For axles weighing more than 10,000 lbs. the random difference is less than 17 percent. The systematic difference is less than 1 percent. 672 randomly selected axle and axle groups were compared. The random difference is approximately 15 percent for gross weight. The systematic difference is less than 2 percent. 161 randomly selected trucks were compared during the evaluation.

Compensated vehicle classification accuracy is a measure of how well the system identifies a number of vehicles treated only as a group. For several classification categories, compensated accuracy is equal to one minus the summation of the absolute difference in manual and automatic weigh and classification class total for all classifications observed divided by the overall manual total. It is a measure of how similar the manual classification totals are to the system totals. This measure of accuracy allows compensation or cancelling to occur between classes since the vehicles lost from one particular class may be compensated or by those gained from another.

The compensated accuracies are greater than 95 percent in both portland cement concrete and asphaltic cement concrete. 5,843 vehicles were classified. The overall count accuracy is greater than 99 percent at both sites. 4,812 vehicles were counted. Time based video recording was used to support manual classification.

Data taken from both the asphaltic cement concrete and portland cement concrete sites indicate the system is

capable of measuring axle spacing within plus or minus 1.5 inches, speed within plus or minus 1/2 mph, and tire length and width with a random error of between 1 and 2 inches. The population was 326 for axle spacing, 49 for vehicle speed, and 240 for tire width and length. Random vehicles were used to determine axle spacing and tire width and length accuracy.

APPENDIX 1

Weigh-in-Motion Equipment Suppliers

This listing is a combination of information from the Heavy Vehicle Electronic License Plate Program, Strategic Highway Research Program, and current vendor data.

Bridge Weighing Systems, Inc.

Contact: Richard Snyder
University Circle Research
Center 1
1100 Cedar
Cleveland, OH 44106
(216) 229-8400

Type: Portable, semi-portable and
permanent bridge WIM
systems

CMI - Dynamics, Inc.

Contact: Jeff Davies
820 Lafayette Road
Building #1, Suite 203
Hampton, NH 03842
(603) 926-1200

Type: Low, medium and high speed
permanent load cell WIM
systems High speed,
permanent piezo electric
WIM system

Culway

Contact: Snowy Mountains
Engineering Corporation
P.O. Box 356
Cooma NSW 2630
AUSTRALIA
Telephone: International 61-
64-520222
Telex: SMEC AA61153
Fax: International 61-64-
520400

Type: High speed, portable, strain
gauge on culvert WIM
system

Data Dynamics

Contact: John Fung
#B-5660 McAdam Road
Mississauga, Ontario
Canada, L4Z1T2
Telephone: (416) 890-0797
Fax: (416) 890-6117

Type: Low, medium and high
speed, permanent, strain
gauge WIM systems medium
and high speed, permanent,
piezo electric WIM systems

Data Instrument AS

Contact: Data Instrument AS
Nye Sandviksvel 56A
P.O. Box 1561
N - 5035 Bergen Norway
Telephone: International 47
5 31 14 15
Telex: 40941
Fax: International 47 5 32 33
96

Type: High-speed, permanent,
piezo electric WIM system

EMX Incorporated

Contact: Joe Rozgonyi
3570 Warrensville Center
Road
Shaker Heights, Ohio 44122
Telephone: (216) 991-4333
Fax: (216) 464-2980

Type: High speed, portable,
capacitance pads for WIM
vendors

GK Instruments, Ltd.

Contact: Geoff Kent
Simpson Road
Fenny Stratford
Milton Keynes, MK1 1HN
England
Telephone: International 44
908 75742
Fax: International 44 908
640783

15212 Race Track Road
Tampa, Florida 33626
Telephone: (813) 855-6556
Fax: (813) 855-3272

Type: High-speed, permanent,
piezo electric WIM system

Low, medium and high
speed, permanent, bending
plate WIM systems High
speed, portable, capacitance
pad WIM system

Streeter - Richardson

Golden River Corporation

Contact: Walter O'Connell
7672 Standish Place
Rockville, MD 20855
Telephone: (301) 340-6800
Fax: (202) 294-0473

Type: High speed, portable,
capacitance pad WIM system

Contact: Susan Smith
155 Wicks Street
Grayslake, IL 60030
(312) 223-4801
(800) 323-9441

Type: Slow, medium and high
speed, permanent, bending
plate WIM systems Medium
speed, portable, capacitance
pad WIM system

International Road Dynamics, Inc.

Contact: Terry Bergan
#A5-116 103rd Street
Saskatoon, Saskatchewan,
CANADA S7N 1Y7
Telephone: (306) 955-3626
Fax: (306) 373-5781

Type: High speed, permanent,
piezo electric WIM system
Low and high speed,
permanent, load cell WIM
systems

Toledo Scale

Contact: Systems Divisions
60 Collegeview Road
Westerville, OH 43081
(614) 898-5110
(800) 523-5123

Type: Low and medium speed load
cell WIM systems

PAT Equipment Corporation

Contact: Joe Madek
237 Cedar Hill Street
Marlboro, MA 0175201
Telephone: (508) 481-1411
Fax: (508) 481-3395

Siegfried Gasser
7575 Ettlingen
Hertzstrasse 32-34
Krlsruhe
West Germany
Telephone: International (0
72 43) 709-0
Telex: 782 862 pat d
Fax: International (0 72 43)
709-191

Type: Low speed, portable,
bending plate WIM system

Trevor Deakin Consultants, LTD

Contact: Ascot Court, White Horse
Technology Park
Trowbridge, Wilts BA14
OXA
Telephone: Trowbridge
(0225) 760099
Telex: 449441 Gage G
Fax: (0225) 762751
Cables: Technique, Rode,
Bath

Type: High speed, permanent,
piezo electric WIM system
High speed, permanent, load
cell WIM system low speed
transportable load cell WIM
system

Truveio

Contact: James E. Kelly, P.E.
AVIAR, Inc.
P.O. Box 162184
Austin, TX 78716
Telephone: (512) 327-9439
Fax: (512) 327-0822

Type: Variable speed, permanent
and portable capacitance
pad WIM systems

BIBLIOGRAPHY

National Cooperative Highway Research
Program 3-39 "Evaluation and
Calibration Procedures for Weigh-in-
Motion Systems."

ASTM, "Specification for Highway
Weigh-in-Motion (WIM) System With User
Requirements and Test Method,"
Subcommittee E17.41.

Heavy Vehicle Electronic License Plate
Program, Louis A. Schmitt, Deputy
Director, Transportation Planning
Division, Arizona Department of
Transportation.

W. D. Cunagin, "Development of Weigh-
in-Motion Performance Specification,
Heavy Vehicle Electronic License Plate
Program, draft in process.

REFERENCES

1. Lee, Clyde - "Concepts of Weigh-in-Motion Systems," National Weigh-in-Motion Conference, Denver, Colorado, (July 1983).
2. Davies, Peter - "Automated Traffic/Truck Weight Monitoring Equipment Weigh-in-Motion," Federal Highway Administration Report, Number FHWA-DP-88-006 (May 1988).
3. Davies, Peter and McCall, Bill - "A Low-Cost Automatic Weigh and Classification System Based on Piezo Electricity," Proceedings of the Australian Road Research Board, Part 6, Canberra, Australia (August 1988)
4. Cunagin, W. D. - "Use of Weigh-in-Motion Systems for Data Collection and Enforcement," National Cooperative Highway Research Program, Report Number 124.
5. SPARTA, Inc. - "Calibration of Weigh-in-Motion (WIM) Systems, Volume I: Summary and Recommendations, Volume II: Final Report," Federal Highway Administration Report, Number FHWA-RD-88-128 and 129 (August 1988).
6. Terrell, Ronald and Bell, Chris - "Effects of Permit and Illegal Overloads on Pavements," National Cooperative Highway Research Program, Report Number 131.
7. Federal Highway Administration, "Overweight Vehicles--PERMITS AND PENALTIES, An Inventors of State Practices for Fiscal Year 1987," Report 9 (January 1989).

SHRP PROTOTYPE PROCEDURES FOR CALIBRATING
FALLING WEIGHT DEFLECTOMETERS

Cheryl Allen Richter
Lynne H. Irwin

Strategic Highway Research Program
Cornell University (Strategic Highway
Research Program January 1988 to
January 1989)

ABSTRACT

In the fall of 1988, SHRP developed and implemented prototype calibration procedures for both load and deflection measurement devices on falling weight deflectometers (FWDs). The Indiana Department of Highways (IDOH) and Purdue University assisted this endeavor by constructing a prototype calibration station at the IDOH Research Facility in West Lafayette, Indiana. This facility was then used to calibrate the four SHRP FWDs and the IDOH FWD. The methods and equipment used are suitable for any FWD which uses a geophone for deflection measurement. Modification of the hardware used in the calibration process would be required to accommodate LVDTs.

The calibration process consists of three stages: (1) absolute calibration of the load cell; (2) absolute calibration of the geophones; and (3) relative calibration of the geophones. A specially designed load cell and a commercial LVDT are used for the absolute calibration of the load cell and geophones, respectively. In the relative calibration process, measurements made with all of the geophones stacked in a special frame (so that all are subjected to the same pavement deflection) are compared, to ensure that the FWD is measuring consistently from one geophone to the next.

Like any prototype, the initial SHRP FWD calibration effort raised several questions, and brought to light some problems. However, the authors believe it provides an excellent basis for future work in the area of FWD calibration.

INTRODUCTION

The collection of pavement deflection data with falling weight deflectometers is one aspect of the pavement monitoring effort being carried out for the Long Term Pavement Performance (LTPP) studies of the Strategic Highway Research Program. The magnitude and importance of this effort make it imperative that the data collection devices be as accurate and consistent as possible. In order to ensure the required accuracy in the SHRP falling weight deflectometers (FWDs), the development and implementation of calibration procedures for the FWDs was undertaken in the fall of 1988. SHRP was assisted in this effort by the Indiana Department of Highways Division of Research and Purdue University.

This paper describes the prototype equipment and methods used in the initial SHRP FWD calibration efforts at the Indiana Department of Highways Division of Research Facility in West Lafayette, Indiana.

The calibration measurements were made under dynamic conditions which resembled actual field test conditions to the greatest extent possible. The procedures and equipment used are suitable for use with any FWD which uses a geophone as the deflection measurement device. Calibration of FWDs which use a linear variable differential transducer (LVDT) as the deflection measuring device would require slightly different equipment and procedures.

THE CALIBRATION PROCESS

The basic calibration of the Dynatest FWD measurement systems is done by the manufacturer, and in fact cannot be done by anyone else. However, we do have the ability to refine that calibration, through the use of relative gain factors in the data collection software.

As delivered, the geophones on the SHRP FWDs were calibrated by the manufacturer to a specified accuracy of two percent of the measured reading, and have a repeatability of plus or minus two microns. The relative gain factors, which are simply multipliers for the output from the FWD system processor units, are initially set to 1.00, but can be adjusted within the range 0.98 to 1.02. The manufacturer indicates that the need for adjustments outside this range is indicative of a damaged sensor.

The calibration process used by SHRP consists of three stages: (1) absolute calibration of the FWD load cell; (2) absolute calibration of the geophones; and (3) relative calibration of the geophones. The final result of the process is a set of calibration factors which, in effect, fine tune the calibration of the FWD measurement systems. In the absolute calibration of the FWD load cell, an independent reference system is set up so that both load cells measure the same applied force under conditions which approximate actual field test conditions as closely as possible. The absolute calibration of the geophones is a similar process. The net effect of these processes is to reduce the systematic error of the measurements (i.e., move the individual sensor readings closer to the true deflection). The basic assumption is that the mean of a number of measurements

made with the independent reference system is a reasonable estimate of 'truth'. The ratio of the mean reference measurement to the mean FWD measurement is used as the new relative gain (i.e., a multiplier to correct the FWD reading to match that of the reference measurement system).

Because there are random errors associated with the reference measurements, and because the number of drops used to establish the mean reading for each sensor is relatively small (ten per drop height), each geophone will be calibrated to a slightly different (random) estimate of the true mean deflection. Hence the geophone reading distribution for the different geophones will still be scattered about the true deflection, but the range will be reduced, and it will be unbiased. Note that the mean geophone reading for each sensor is now equal to the mean reference reading for that geophone.

In the relative calibration process, the gain factors are adjusted further, so that all of the geophones for the FWD are calibrated to the same estimate of the true deflection. This process is based on the fact that the overall mean deflection as measured simultaneously by seven geophones which are all in absolute calibration is a better estimate of the true deflection than an estimate based on only one geophone. The final adjustment factor is found by taking the ratio of the overall mean deflection reading to the mean for each individual sensor. The new relative gain is found by multiplying the result by the current relative gain (i.e., that which was entered as a result of absolute calibration). When this process is completed, it is expected that the means of a series of deflection measurements will be the same for all geophones. The only remaining error will be the replication or measurement error.

LOAD CELL CALIBRATION

Calibrating an FWD load cell under dynamic 'field' conditions presented some interesting challenges. Some of these challenges were recognized at the outset, and others were discovered as the SHRP calibration work progressed. The most obvious problem was the design of an appropriate reference load measurement

system. The configuration of the SHRP falling weight deflectometers (and all others manufactured by Dynatest) is such that the upper surface of the reference load measuring system cannot be more than 9 cm (3.5 inches) higher than the surface of the surrounding pavement. This low profile could be achieved by fitting a load cell of greater height into the pavement, but such an approach makes the calibration equipment less portable than it would otherwise be, and the presence of a pavement depression to hold the load cell may present maintenance and/or safety hazards when not in use, particularly if the calibration work cannot be done indoors. Consequently, a reference load cell with total height less than 9 cm was selected as the preferred alternative.

An additional constraint on the load measurement system is that its design must be such that the possibility of eccentric loadings, which could result in failure of both the reference load cell and the FWD load cell, be minimized. This problem was avoided by making the diameter of the reference load cell the same as that of the FWD load plate (i.e., 30 cm), so that proper alignment of the two systems could be easily checked.

The appropriate reference load cell geometry could have been achieved by using three commercially available load cells sandwiched between two metal plates of the appropriate diameter. However, cost considerations resulted in the selection of a custom made load cell designed to meet the particular constraints of this problem. The reference load cell used in this prototype effort consisted of an aluminum case, 30 cm (11.8 inches) in diameter, and 8.3 cm (3.25 inches) high, with four measuring links equally spaced on a 19 cm (7.5 inch) circle (some modifications to this design will be made for future SHRP calibration work). A ribbed rubber sheet, identical to that on the bottom of the FWD loading plate, was glued to the bottom of the reference load cell to ensure uniform pressure on the pavement surface.

In the initial calibration trials with this reference load cell, it was found that the reference load cell had a tendency to 'walk' out from under the FWD loading plate as the testing progressed, particularly if the pavement on which the

testing was being conducted was not level. Consequently, it was decided to bolt the reference load cell to the FWD loading plate, by first removing the plastic plate on the bottom of the FWD load plate assembly, and then bolting the reference load cell in its place. This arrangement, which is illustrated in figures 1 and 2, has proven to be highly satisfactory.

For each of the five FWDs, load cell calibration data was collected at four load levels (ranging from 40 to 125 kN), with ten tests at each level. In addition, multiple sets of data were obtained for some or all load levels for each of the five FWDs so that the repeatability of the process could be evaluated.

The repeatability of this process for individual load levels is very good (difference in gain adjustment factors for two different data sets at the same load level for the same FWD typically 0.002 or less). However, load level does have an impact on the results, with the factors for the higher load magnitudes consistently less than those for the lower drop heights.

The new relative gain factors (calibration factors) were computed by using a linear regression forced through zero on data from all four drop heights (a total of forty x-y pairs). The fit obtained in these regressions was very good, with the coefficient of determination (R squared) typically 0.999, and the standard error of the regression coefficient always less than 0.002 and frequently less than 0.001. The data available to evaluate the repeatability of this approach is more limited than that for individual drop heights, but it too appears to be highly repeatable.

ABSOLUTE CALIBRATION OF GEOPHONES

The principal problem in the absolute calibration of the deflection measurement system of an FWD is the establishment of a reference measurement system which can accurately measure pavement deflections simultaneously with the FWD measurement system, under conditions which



Figure 1: The plastic plate (left) which is ordinarily on the bottom of the FWD loading plate, and the SHRP reference load cell (right). Note that both are equipped with matching ribbed rubber sheets.

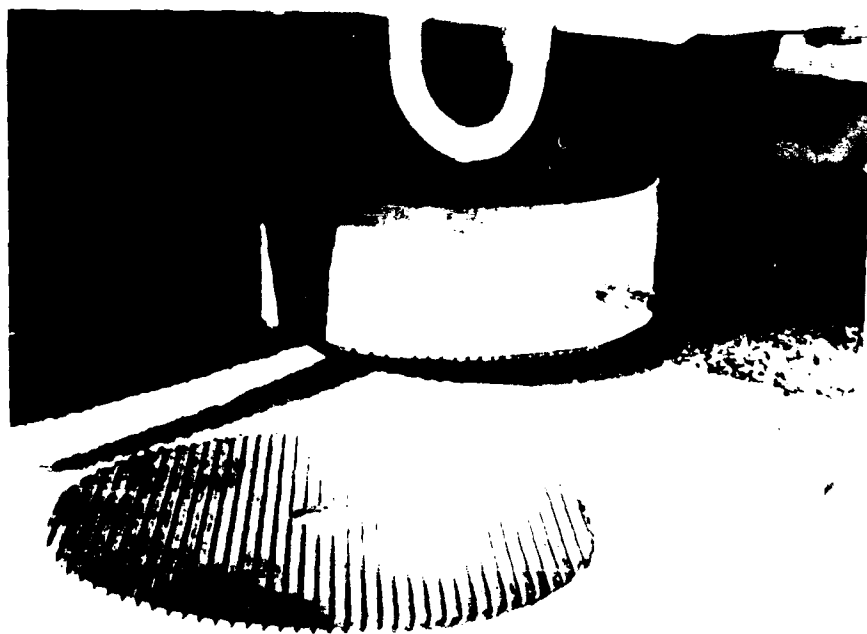


Figure 2: The SHRP reference load cell attached to the bottom of an FWD loading plate. A spare ribbed rubber sheet is in the foreground.



Figure 3: The LVDT and geophone holders, with all instrumentation in place for calibration testing.

approximate field test conditions as closely as possible. A number of different measurement devices could have been used for this process. SHRP chose to use a commercially available linear variable differential transducer (LVDT) as the reference deflection measurement device because it can be accurately and independently calibrated with a micrometer.

The trick in using an LVDT for this purpose is in suspending it in such a fashion that it is subjected to the same deflection as that the FWD geophone under test is undergoing, without being subjected to any additional motion during the period of the test. To accomplish this, the LVDT and the geophone were mounted in special holders so that the magnetized tip of the LVDT core was always in contact with the top of the holder for the geophone, and hence was always subjected to the same movement as the geophone. Both of these holders were provided by the two manufacturer as a

part of their absolute calibration verification device. The geophone holder is such that the actual mounting of the geophone is nearly identical to that used in routine FWD testing). The LVDT holder was mounted on the end of a section of wide-flange beam, and the geophone holder was designed to rest on the pavement. An additional feature of the LVDT holder is a provision for the placement of a second geophone on its top, so that one can verify that the LVDT housing does not move during the period of the test. The two holders are illustrated in figure 3.

One problem encountered in the course of the SHRP calibration work was that the geophone holder had a tendency to 'scoot' (i.e., move horizontally from the initial position) after repeated tests, resulting in invalid deflection measurements, because the LVDT core was no longer vertical. The temporary fix for this problem was to check the positioning of the LVDT frequently. An improved design will be used for any future SHRP calibration work.

In order to ensure that the LVDT remained motionless during the time of the testing, the beam on which the LVDT holder was mounted was attached to an outside wall of the Indiana Department of Highways Research Building. The beam, with the LVDT and geophone holders, is shown in figure 4. The inertial mass of

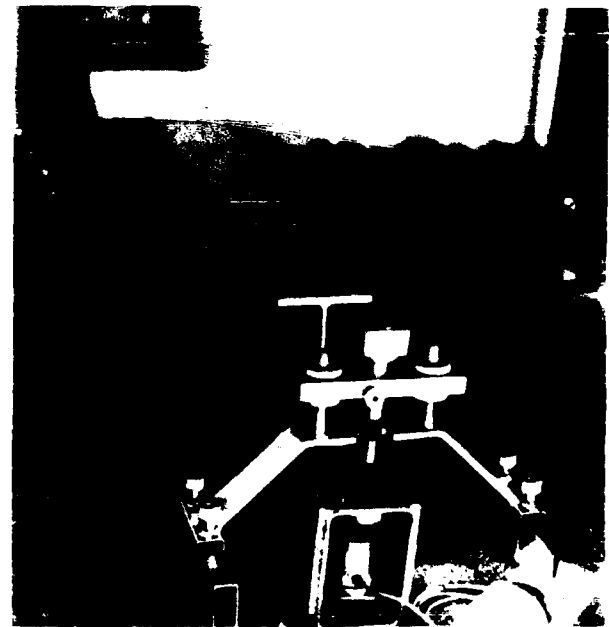


Figure 4: The geophone calibration beam, with the LVDT and geophone holders.

the building is sufficiently great that it is not affected by the FWD load until after the peak deflection reading has registered, and it is not highly susceptible to motion due to wind or other factors.

The beam from which the LVDT holder was suspended was approximately eight feet long. The length of the beam was selected by examining the results of deflection tests conducted at a series of points, from the wall of the building out, to determine where irregularities due to construction debris, etc. ceased to significantly affect the deflection readings.

Geophone calibration data was collected at two deflection levels, for all of the geophones of all five FWDs, with the lower of the two levels around 100 microns, and the higher at about 400 microns. Ten sets of deflection data were collected for each deflection level in each trial. In addition, data was collected at deflection levels of (approximately) 175 and 250 microns for one of the geophones, and multiple sets of data were collected at the highest deflection level for that same geophone.

As with the load cell calibration, the results of the geophone calibration are highly repeatable for individual deflection levels, but are dependent deflection magnitude. For the data obtained, the variation in calibration factors from one data set to another (for the same geophone at a given deflection level) is typically 0.001, though in one instance it is as high as 0.012 (no obvious explanation for this anomaly has been identified).

Relative gain factors were computed by using a linear regression forced through zero on the combined data for two load levels (a total of 20 x-y pairs). The fit obtained in these regressions was very good, with the coefficient of determination (R squared) typically 0.998 or better, and the standard error of the regression coefficient 0.002 or less.

One aspect of the SHRP calibration results which differed from expectations was that the absolute calibration factors derived from the geophones had an overall mean of 0.99. It would be expected that they would be randomly distributed about a mean of 1.00. One possible explanation for this is that there are systematic differences between the calibration methods used by the FWD

manufacturer in Denmark and those used in SHRP. Also, possibly due to differences in the geologic materials in Panama, and in Denmark, the geophones could have been subjected to a slightly different range of frequencies in the ground vibration.

RELATIVE CALIBRATION

Of the three stages in the SHRP FWD calibration process, the relative calibration is the simplest. In this process, the sensor geophones are placed in a special frame (as shown in figure 5), so that all can be subjected to, and thus measure, the same pavement deflection simultaneously. The relative calibration stand used for this process is a standard piece of equipment supplied by the FWD manufacturer with every FWD (although the relative calibration frames supplied with the SHRP FWDs can hold all seven geophones simultaneously, earlier models can accommodate only four sensors. The four sensor stand is adequate for the process, but must be used with greater care to ensure that the results will be reliable and repeatable).



Figure 5: The relative calibration stand, with sensors in place for relative calibration. Bob Briggs (Texas Dept. of Highways and Public Transportation) is pointing to the marked test point.

However, the procedure used by SHRP differs somewhat from the procedure recommended by the manufacturer [1].

In the SHRP relative calibration procedure, the seven geophones are placed in the relative calibration stand. The position of the stand and the FWD drop height are then adjusted so that the deflections registered by the geophones are on the order of 400 microns or more. When an appropriate test point and drop height have been identified, the test point is marked (by a small divot, or a washer glued to the pavement), so that it can be precisely relocated. Ten deflection tests are made, with the relative calibration stand held vertically, so that its bottom is in firm contact with the marked test point. Then the sensors are rotated in the stand, and the testing is repeated, until all of the sensors have occupied every position in the stand. This will require a total of seven sets of ten deflection tests.

A statistical analysis of variance was performed, to partition the variation in the deflection readings into three sources: (1) position in the stand; (2) sensor number; and (3) random error. If the test is conducted properly, position in the stand will not be statistically significant. If sensor number is found to be significant, adjustments to the relative gain factors are needed. The adjustment factor for the relative gain is computed by dividing the overall mean of all of the deflection readings obtained by the mean for each individual sensor. The resulting ratios should be in the range 0.98 to 1.02. Ratios outside of that range are indicative of problems (i.e., a damaged sensor, or errors in the calibration testing).

In the calibration work conducted in Indiana, the relative calibration process was repeated from three to twelve times for each of five FWDs (the four SHRP units and the Indiana Department of Highways FWD). In all, twenty-nine sets of relative calibration data were obtained, and analyses of variance were completed for twenty of them. In the instance where twelve sets of data were acquired for one FWD, the sets consisted of three repeat tests at each of four load/deflection magnitudes.

The ratios computed from the relative calibration test results were highly repeatable. Typically, the variation

from one set of data to the next for a single FWD was 0.001 or less. In addition, load/deflection magnitude does not appear to affect the relative calibration ratios.

Nineteen of the twenty analyses of variance indicated that the position in the sensor stand was not a statistically significant source of variation at a confidence level of 0.05. In the testing for the twentieth set of data, the relative calibration stand was not held vertically. The authors believe this deviation from the correct procedure explains the difference in the results. It is worth noting that this deviation had no noticeable effect on the calibration ratios computed from the relative calibration data.

SUMMARY

The final results of the SHRP calibration effort conducted with the assistance of the Indiana Department of Highways Research Division and Purdue University indicated that the measurement systems of the four SHRP FWDs and the IDOH FWD were all within one percent of the reference measurement systems used. It should be noted that these results are applicable to the conditions at one particular place, at one particular time. The effect of different pavement and temperature conditions on the calibration of falling weight deflectometers needs further exploration.

Further work is needed to explore the long term repeatability of the calibration process, and to refine the hardware and procedures used. Ultimately it is hoped that this work will lead to the establishment of FWD calibration facilities in each of the four SHRP regions, as a minimum.

The procedures and equipment discussed herein were developed and/or selected to meet the needs of the Strategic Highway Research Program. They are presented here for the benefit of those who may wish to undertake similar efforts, but in no way constitute a standard or specification.

ACKNOWLEDGMENTS

The success of the efforts discussed herein was due in no small part to the work of a number of individuals at the Indiana Department of Highways Division of Research and Purdue University. The authors, and the Strategic Highway Research Program, are particularly indebted to Rebecca McDaniel (IDOH), for her willingness to act as a liaison between SHRP, IDOH, and Purdue, as well as help out wherever and whenever needed, to Carl Berryman and Robert McConnel of IDOH for their efforts in developing and exercising the data acquisition system for the independent reference systems, and to Thomas White of Purdue for his general support and assistance. SHRP's pilot FWD calibration project was a truly cooperative project.

REFERENCES

- [1] DYNATEST 8000 FWD TEST SYSTEM
OWNER'S MANUAL, PART 1, OPERATING
INSTRUCTIONS, Dynatest Consulting, Inc.,
Ojai, CA, Undated (issued May 1988), pp.
9.1 - 9.3.

IOWA DEPARTMENT OF TRANSPORTATION
PAVEMENT INSTRUMENTATION

Roman Dankbar

Office of
Transportation Research

OVERVIEW

The project was initiated to achieve two primary objectives and several secondary objectives. The primary objectives include the demonstration of pavement instrumentation installation techniques and the verification of design procedures in an effort to improve rigid pavement performance in Iowa. Secondary objectives of the study include the evaluation of the behavior of the pavement in relationship to the loads under various temperature and moisture conditions in the subgrade. This type of result is aimed at improving the design of the subgrade, pavement slab, drainage systems and the administration of the highway weight embargo legislation.

A forty foot long section of twenty four foot ten inch wide by eleven inch thick, doweled joint reinforced pavement, part of I-80 in Pottawattamie County, Iowa, was instrumented with some 120 instruments. They included weldable strain gages on selected dowel bars at three consecutive joints, and concrete strain gages at selected locations across the slab at two midslab and two exterior corner locations. The strain gages were installed prior to the placement of the new eleven inch thick pavement. The site also includes some sixteen deflection gages at locations near the joints and midslab in the wheel path areas.

Metal pipes were placed under each of three consecutive joints and in the two midslab locations, in the base material. Temperature sensors were placed near the surface of the pavement, at top of the variable thickness base material, and 6 inches into the subgrade. An additional single unit was placed outside the slab to measure ambient air temperature. Over 90% of the instruments were found to provide a completed electrical circuit when measured after construction of the pavement.

CLASSIFIER UNITS - PIEZO SENSORS

The system is set up to be triggered by a weigh-in-motion piezo-electric arrangement in each of the travel lanes. The collection of strain, deflection, and temperature data is accomplished by a micro computer controlled data acquisition system at the site and transmitted via telephone to a central site for analysis. The weigh-in-motion site will provide information on axle and gross weights, axle spacing, vehicle classification, speed and lateral location within each lane. Monthly moisture and density measurements of the subbase and subgrade are currently being performed through the metal pipes installed concurrently with the instrumentation system.

SITE CHARACTERISTICS

Factors considered in selecting site:

1. The pavement was being replaced as part of the reconstruction project. This provides an opportunity for good documentation of the base and pavement characteristics of the reconstruction.
2. The bridge could be used as a weigh-in-motion site for calibrating the sensors in the pavement to known loads. It also could be used for identification of the lateral location and speed of the vehicles entering the test site and crossing the traffic loops. Lane changing by the vehicles is reduced on the bridge.
3. This route provided the heavy truck traffic and a mix of truck configurations to adequately test the pavement strain theories.
4. The section is near the low point of a 1,400 ft. sag vertical curve providing a relatively flat grade across the test site. The effects of grade are minimized in the test.
5. The new pavement created a very good chance for smooth pavement profile at the beginning of the test.
6. A static weight station is located east of the site approximately 15 miles on both the east and west bound lane and can be used to check the correlation of weights and strains. A continuous traffic recorder is located in the new pavement approximately one mile east of the site in the west bound lanes that can provide ADT counts for pavement wear calculations.

DATA HANDLING

Equipment Selection

Original plan called for field units to have ability to scan up to 120 separate gages at the rate of 1000 times/sec.

Major suppliers were contacted and discussions were held with two companies.

Due to cost involved, a compromise was reached to limit the number of sensors to less than 2/3 of the total at any one time and accept a scan rate of 300-400 times/sec./gage.

The hardware includes two microprocessors with keyboards and monitors (field and office units), a data collection unit with two extenders, printer, plotter and modems.

Hewlett Packard equipment was selected for the project.

- Model 310 series work station for Ames Central Office.
- Model 320 series engineering work station for the field.
- Central Office microcomputer has a color graphic monitor, one megabyte of RAM and a 20 megabyte hard disk with the floppy disk.
- An 8-pen plotter and printer are connected to this unit and housed in a mobile cabinet for flexibility of use allowing movement to various offices.
- A 3600 baud modem is used for communication with field unit.

The field unit is equipped with a monochrome monitor, three megabytes of RAM, and 40 megabyte hard disk. It is also connected to the Central Office via 3600 baud modem. Each of the units comes with the Basic 4.0 operating system.

The heart of the data collection system is HP3852A Data Acquisition and Control Unit with 2 extender units (3853A).

Accessories include two 24-channel multiplexers, two 13-bit

high speed voltmeters, a 5-channel counter totalizer, data acquisition software routines, a DC power supply and enough connection devices to monitor forty 120 ohm strain gages and eighty 350 ohm strain gages simultaneously.

EQUIPMENT INSTALLATION

The equipment was assembled by the research staff in Ames before anything was taken to the field to ensure that all parts were compatible. This proved to be a wise move since several parts had to be exchanged due to incompatibility including the plotter which was incompatible with the microprocessor.

Assembly in Ames allowed the research team to do internal testing and gain an understanding of the functions of the various parts of the equipment and develop the necessary programs for the operation of the data collection equipment.

The software had to be developed by use of a private consultant experienced in the use of this particular kind of equipment.

Who will provide this type of service should be determined when purchasing the equipment.

SITE PREPARATION

Coordination is the major consideration in this phase of the project.

The 150 mile distance from the central office added to the difficulty in getting the project built and accomplishing the needed instrument calibration for data collection.

Coordinating with the paving contractor is of major importance.

Coordination with local maintenance forces also essential - Garage and Equipment.

Close coordination with Iowa State University (ISU) staff in gage and site preparation was also highly essential.

GAGE INSTALLATION

Gages and associated equipment were prepared in laboratory. Experienced personnel are required to ensure proper installation.

It is important that adequate staff be provided especially where installation takes place in front of paver.

An installation plan should include layout sheets and a walk through made in the lab.

Ensure that the right equipment and materials are available to avoid panic at paving time.

To prevent the possibility of concrete roll pressures in front of the paver from overturning the bar cages, some hand placement was done by the researchers.

In August 1987, continuity testing of the instruments was carried out in the field.

At that time, 92% of the gages were responding. This, we felt, was very good since other study results showed a 50% failure rate not uncommon. However, circuit tests taken in October 1988 indicated an alarming number of concrete strain gages have failed.

We are fortunate at the Iowa DOT to have an electrician who is knowledgeable on computer operation, and specifically, computerized data collection hardware.

RESEARCH RESULTS

The results to date illustrate that pavement instrumentation can be accomplished with careful planning and proper coordination of the parties involved.

The project has the potential to measure deflection, concrete and dowel bar strain at successive joints and relate this to the loads and the moisture/density changes in the pavement subbase and subgrade.

The project has proceeded at a pace less than expected. Software development and the change in WIM has caused delays to the project.

The test for this project is yet to come--data collection.

Once the instruments are calibrated and data collection begins, it will continue for 2 years.

COSTS

Initial funding for the project:

FHWA	\$75,000
------	----------

IHRB	\$81,000
------	----------

Budgeted services DOT	\$12,400
--------------------------	----------

Additional funding from FHWA	\$38,000
---------------------------------	----------

Installation costs were higher than expected. ISU costs were \$7,500 higher than estimated.

WIM and vehicle classification costs increased from \$4,500 to \$30,500.

Power and telephone supply to site was \$6,000 over estimated cost.

Monthly service charges were not included in the estimate. These charges will be about \$3,000 over the life of the project.

INTERIM REPORT

A copy can be obtained by sending request to the Iowa Department of Transportation, Office of Transportation Research, 800 Lincoln Way, Ames, IA 50010.

Session 8:
Correlation Between
Field and Lab Results

A DIRECT COMPARISON OF NONDESTRUCTIVE, LABORATORY, AND *IN SITU* TESTING

Mark Anderson, Ph.D., P.E. and David A. Timian
Gulf Coast Division, Applied Research Associates, Inc.

ABSTRACT

A direct comparison of various state-of-the-art evaluation techniques has been completed on a full-scale pavement test facility at Tyndall Air Force Base, Florida. The outstanding feature of the collected data is the use of independent testing techniques to obtain comparison data. These techniques included non-destructive field testing with a Falling Weight Deflectometer, *in situ* field testing with a seismic cone penetrometer, and various laboratory tests.

Nondestructive testing was conducted after construction to determine backcalculated moduli values. In addition, an independent measure of the pavement structural capability was achieved by the use of a seismic cone penetrometer. The seismic cone penetrometer allows a measure of failure properties during penetration, as well as "downhole" wave propagation tests. The downhole tests included both compressional and shear wave velocity tests. Standard laboratory materials characterization tests were completed on the pavement system components, as well as more advanced laboratory tests. Moduli and strength values from the nondestructive, *in situ*, and laboratory testing are compared and discussed.

KEYWORDS: Falling Weight Deflectometer, seismic cone penetrometer, *in situ* testing, wave propagation, backcalculation, layer moduli, shear strength.

BACKGROUND

A full-scale pavement test facility has been constructed at Tyndall Air Force Base, Florida. The test facility (Test Site 9700) is located about 12 miles southeast of the Headquarters, Air Force Engineering and Services Center (HQ/AFESC) and contains 12 pavement test sections constructed for an ongoing study of the effects of high pressure aircraft tires on Air Force runways. The test section described herein (Section 9) consists of an existing full-depth Portland cement concrete (PCC) pavement which was overlain with asphaltic concrete (AC). Additional testing was completed on this section to support an ongoing study examining structural response models used for the backcalculation of moduli values from Falling Weight Deflectometer (FWD) tests. The test section will be referred to herein simply as Site 9700.

EQUIPMENT

ARA Seismic Cone Penetrometer

Applied Research Associates, Inc. (ARA) has developed a state-of-the-art seismic cone penetration system. Quasi-static cone penetration testing has been used in Europe for almost a half century to provide continuous descriptions (profiles) of subsurface conditions. This method has only recently gained acceptance in the United States for geotechnical

explorations. The quasistatic penetration test measures the resistance to penetration of a conical tip and along a friction sleeve located immediately behind the tip. Penetration results can be empirically and/or theoretically related to material properties. Recent advances in hardware and software have improved the amount and quality of data retrieved from a cone penetration test. The ARA seismic cone penetration system (Shinn, et al 1988) integrates all the recent advances in cone penetration technology into a single unit. These technologies include: a microcomputer based data acquisition system, field repairable electric cone penetrometers, a large magnitude seismic wave generation system, and field data analysis and plotting systems.

A schematic view of the ARA electric cone penetrometer is shown in Figure 1. The cone and sleeve dimensions are standard (ASTM D 3441). The cone has a 60 degree point angle, a base diameter of 35.7 mm (1.406 in), and a projected area of 10 cm² (1.55 in²). The friction sleeve has outside diameter of 35.7 mm (1.406 in) and surface area of 150 cm² (23.2 in²). The electric cone penetrometer includes two load cells which monitor tip load and the summation of the tip and sleeve loads. Cone penetration data are acquired and recorded digitally, using a microcomputer based data acquisition system. Real time analysis is utilized for the conversion of load cells outputs to the recorded digital values of tip stress and sleeve stress. The typical acquisition rate is one digital record per second, resulting in a resolution of one test per 20 mm (0.8 in) when penetrating at the standard rate of 20 mm/s (4 ft/min).

The ARA seismic wave generation system is illustrated in Figure 2. The ARA electric cone penetration system includes a triaxial geophone configuration, mounted just behind the cone expansion sleeve, which is used to monitor the arrival of waves generated at the surface. The vertically oriented geophone is used to monitor the arrivals of compressional (P) waves. The two horizontally mounted geophones are used to monitor the arrivals of shear (S) waves. The ARA wave generation system shown in Figure 2 provides large magnitude seismic waves which can improve signal-to-noise ratios, allowing seismic profiling at great depths and through weak materials. The compressional waves are generated by a 1.33 kN (0.3 kip)

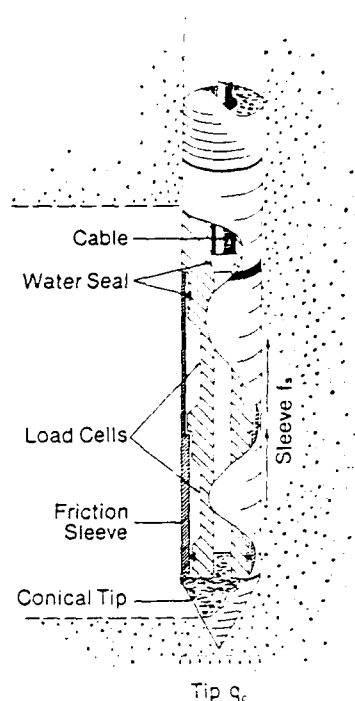


FIGURE 1. Schematic of the ARA Electric Cone Penetrometer

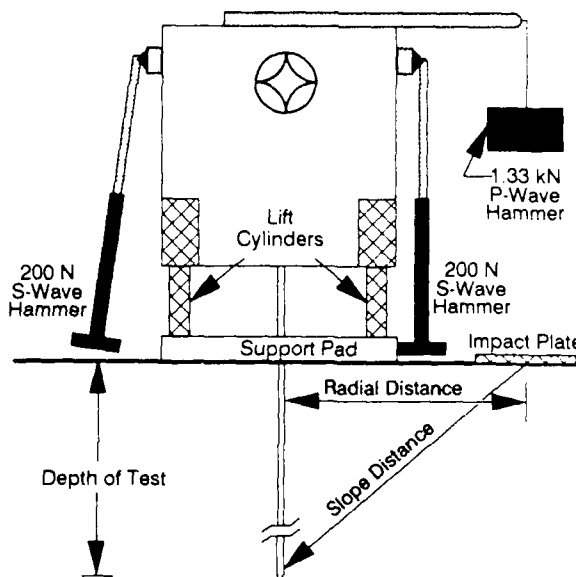


FIGURE 2. Schematic of the ARA Wave Generation System

drop weight system. Energy transfer to the system can be varied by adjusting the drop height of the weight. The shear waves are generated by a pair of 0.2 kN (40 lb) swing hammers, oriented to provide shear waves of reversed polarity for easy

interpretation. The hammers, which can be swung manually or in an automated mode, impact the front support pad of the cone penetration vehicle to provide shear waves of relatively high energy compared to traditional (sledge) hammers. The high shear wave energy imparted by the 0.2 kN (40 lb) hammers is especially important when testing pavement systems, because surface roughness may reduce the coupling between the support pad and the pavement system. The ARA seismic wave generation system has been used successfully for seismic tests at depths of 46 m (150 ft).

The ARA seismic cone penetration system combines the advanced capabilities of electric cone and seismic testing in a heavy-duty testing vehicle. The truck is weighted in a balanced configuration with an additional 58 kN (13 kip) of steel and a 22 kN (5 kip) water tank to provide an overall vertical load (push) capability of 200 kN (45 kip). This configuration provides the push capability which has allowed ARA to penetrate very strong cemented soils, as well as asphaltic concrete pavements, without the need for drilling or coring.

AFESC/RDCP Falling Weight Deflectometer

The Airbase Operating Surfaces Branch of the Air Force Engineering and Services Center (AFESC/RDCP) maintains a Dynatest 8000 Falling Weight Deflectometer (FWD) System for use in pavements research. An illustration of the AFESC/RDCP FWD is shown in Figure 3.

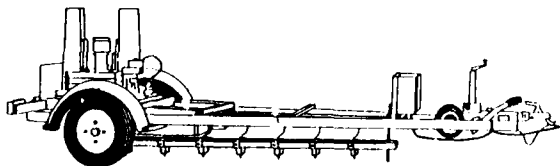


FIGURE 3. The AFESC/RDCP FWD System (Dynatest FWD System 8000)

The FWD is an impulsive deflection device whose basis is to lift a weight to a height above the pavement and drop it on a buffer system which transfers the impulse to a load plate. Subsequent measurements include the impulse force transmitted to the load plate and the peak deflections at various radial distances from the impact point. An idealized impulsive deflection test is illustrated in Figure 4. The

buffer system, idealized as linear springs in Figure 4, helps spread the duration of the loading function to about 31 msec. The AFESC/RDCP FWD is set up in the standard Air Force configuration (Brown 1988), with equal sensor spacings of 25 mm (1 ft), and a maximum impulse force of about 111 kN (25 kip).

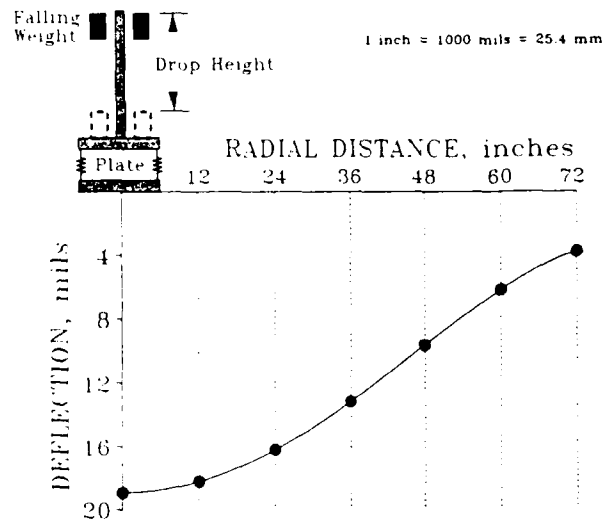


FIGURE 4. Idealized Impulsive Deflection Test with Typical "Basin"

The envelope of measured peak deflections, shown as a solid line in Figure 4, is typically referred to as a deflection "basin". Real deflection basins change with time (Anderson and Drnevich 1989) and are not truly represented by the idealized basin shown in Figure 4. However, assuming that the peak deflections form a basin is a mathematical convenience which greatly simplifies the analysis of impulsive load-deflection data. For the purposes of this paper, the term basin will refer to the envelope of peak deflections.

AFESC/RDCP Engineering Laboratory

The AFESC/RDCP maintains state-of-the-art engineering research laboratories for organizing, developing, and testing new ideas for the innovative solution of pavements problems. The AFESC/RDCP facilities include an asphalt laboratory, a concrete laboratory, and a soils laboratory. The laboratories are currently equipped and staffed to perform most standard pavements and geotechnical tests, as well as many advanced and experimental tests.

RESULTS OF LABORATORY TESTING

Asphaltic Concrete Testing

The asphaltic concrete overlay was constructed in two lifts, each of which had a thickness of 76 mm (3 in). Core samples of asphaltic concrete were obtained and separated by lift. Laboratory testing included: (1) asphalt content by extraction (ASTM D 2172), (2) bulk density (ASTM D 2726), (3) theoretical maximum (Rice) density (ASTM D 2041), (4) Marshall stability and flow (ASTM D 1559), (5) and resilient modulus tests (ASTM D 4123). Table 1 summarizes average values for all of the tests mentioned above except the resilient modulus tests, which are displayed graphically in Figure 5.

TABLE 1. Asphaltic Concrete Test Results

Laboratory Test	Upper Lift	Lower Lift
Asphalt Content	6.31%	6.47%
Bulk Density	24.0 kN/m ³ (153 pcf)	23.4 kN/m ³ (149 pcf)
Theoretical Maximum Density	25.0 kN/m ³ (159 pcf)	24.8 kN/m ³ (158 pcf)
Stability	12.7 kN (2850 lb)	13.8 kN (3100 lb)
Flow	3.3 mm (0.13 in)	2.8 mm (0.11 in)

The resilient modulus data presented in Figure 5 represents both test results and calculated values. Tests were performed at load frequencies of 5 and 10 Hz, with repeated loads applied at 1 sec intervals. The FWD has a predominate load frequency of about 16 Hz (Anderson 1988a). For comparison with backcalculated moduli values based on FWD tests, a set of 16 Hz data was calculated based on the assumption that a standard curve family could be fit to the data. A curve family of the form presented by Kingham and Kallas (1972) was assumed, and the 16 Hz values corresponding to the laboratory test temperatures were computed. A value of resilient modulus at the time of the field testing was estimated from Figure 5 based on the estimated mean pavement temperature. Mean pavement temperature was estimated by the Kentucky method (Southgate and

Deen 1969), using the measured pavement surface temperature and the 5-day mean air temperature, and was 76 degrees Fahrenheit. From Figure 5, the estimated value of resilient modulus (for a loading frequency of 16 Hz) was about 500 ksi.

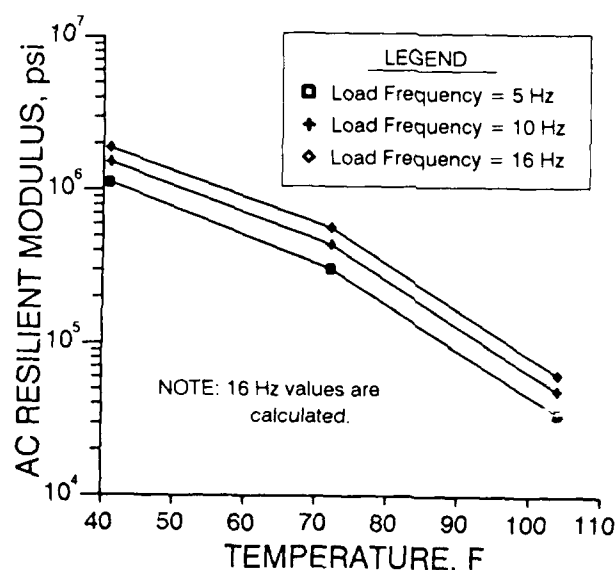


FIGURE 5. AC Resilient Modulus Results

Portland Cement Concrete Testing

Core samples from the existing 0.3 m (12 in) thick full-depth PCC pavement were obtained and tested for unit weight and modulus. The average unit weight was 17.9 kN/m³ (142 pcf). The PCC modulus was determined by the use of a James V-Meter. The V-Meter has been shown to be a good indicator of backcalculated PCC moduli (Anderson 1988a). Core samples of 51 mm (2 in) diameter were used to insure that the velocity measured was not dependent on Poisson's ratio (pure rod waves). The average PCC modulus was 41 GPa (6.0 million psi).

Subgrade Testing

Samples of the subgrade (sand) material were obtained and tested. Tests performed on the subgrade sand included: (1) moisture content test (ASTM D 2216), (2) moisture-density test (ASTM D 698), (3) particle size analysis (ASTM D 422), (4) Atterberg limits (ASTM D 4318), and (5) direct shear tests (ASTM D 3080). The subgrade material recovered was in a relatively dry state. Although there was

significant scatter in natural moisture content values, the minimum field moisture content was 3.5%. The moisture-density curve is shown in Figure 6. From Figure 6, the optimum moisture content is about 4% and the maximum dry density is about 15.4 kN/m^3 (98 pcf). The particle size distribution is shown in Figure 7.

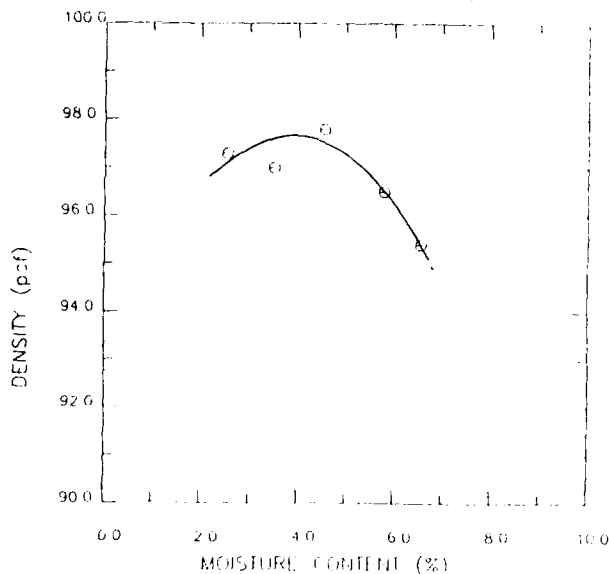


FIGURE 6. Moisture-Density Curve

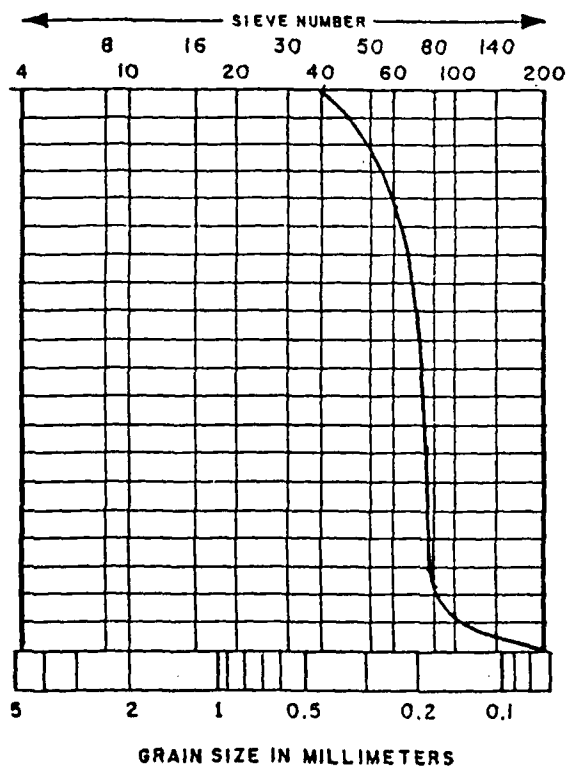


FIGURE 7. Particle Size Distribution

The curve shown in Figure 7 indicates a poorly graded sand. The Atterberg limits indicated a non-plastic material. Based on these results, the subgrade material was classified by the Unified Classification System as soil type SP, poorly graded sand. Four direct shear tests were conducted, representing two different moisture contents and two different dry densities. The range of each of these variables was chosen to represent the practical limit to be expected in the field. The moisture contents chosen were 3.5% and 26%, representing the low value measured in the field and the estimated saturation moisture content, respectively. The dry density values were chosen as 90 and 98 pcf, representing the maximum density from the moisture-density test and the minimum expected for a low relative density. There was little variation in friction angle with either of these variables, with the measured range from about 37 degrees to about 40 degrees. Graphical summaries of the direct shear tests are included in a following section.

RESULTS OF CONE PENETRATION TESTING

Cone Penetration Analytical Model

The shear strength of a soil can be estimated using seismic cone penetration data, an analytical model of the cone penetration process, and empirical relationships developed for sands. Vesic (1972) developed the original analytical model and Rohani and Baladi (1981) revised the model to include the shear modulus. Figure 8 illustrates the analytical model.

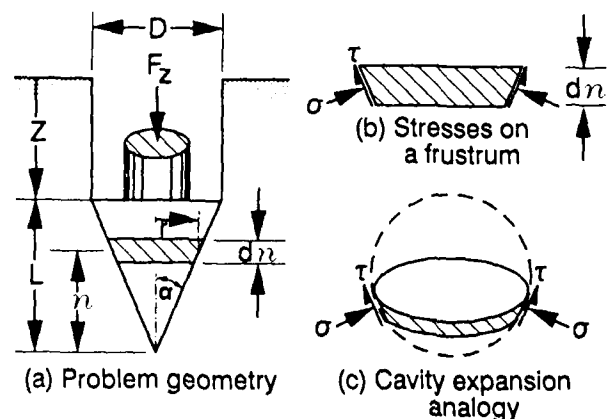


FIGURE 8. Cone Penetration Model (after Rohani and Baladi 1981)

The model illustrated in Figure 8 is based upon spherical cavity expansion in an elastic-plastic media. The penetration of the cone tip into soil very closely imitates this process. Stresses normal to the cone are assumed to be equivalent to the internal cavity pressure and are calculated as (Vesic 1972):

$$\sigma = 3(q + C \cot \phi) \left[\frac{1 + \sin \phi}{3 - \sin \phi} \right] \left[\frac{G'}{C + q \tan \phi} \right] \left[\frac{4 + \sin \phi}{3(1 + \sin \phi)} \right] - C \cot \phi \quad (1)$$

where σ = internal cavity pressure
 C = cohesive intercept
 ϕ = angle of internal friction
 G' = effective shear modulus
 q = geostatic stress = γd
 γ = soil density
 d = depth of interest

Shear stresses, τ , along the cone are calculated as:

$$\tau = C + \tan \phi \quad (2)$$

The total force on the tip, F_z , is:

$$F_z = \int_0^L (\sigma \tan \alpha + \tau) 2\pi r \, d\eta \quad (3)$$

where α = cone apex angle
 r = cone radius
 $d\eta$ = increment of depth

By definition, the tip stress, q_c , is

$$q_c = 4F_z / \pi D^2 \quad (4)$$

Definitions of α , r , $d\eta$, z , L , and D are illustrated in Figure 8. Combining Equations 1, 2, 3 and 4, the tip stress can be calculated as:

$$q_c = -C \cot \phi + \left[\frac{2 \tan \alpha (1 + \sin \phi) G'^m}{(D\gamma/2)^2 \tan^3 \phi} \right] \left[\frac{3(\tan \alpha + \tan \phi)}{(3 - \sin \phi)} \right] \left[\frac{\Omega}{(2-m)(3-m)} \right] \quad (5)$$

where $\Omega = (C + \gamma(z+L) \tan \phi)^{3-m} - \{ [C + \gamma(z+L) \tan \phi + (2-m)\gamma L \tan \phi] (\gamma z \tan \phi)^{2-m} \}$

and $m = (4 \sin \phi) / [3(1 + \sin \phi)]$

For most granular materials, the terms involving cohesion may be dropped from Equation 5, so that a continuous profile of friction angle, ϕ , may be computed by iterating between Equations 4 and 5 if the shear modulus and density are known.

Cone Penetration Resistance Results

Figure 9 illustrates the results of the penetration test at Site 9700. The figure includes profiles with depth of tip stress, sleeve stress, and friction ratio. The friction ratio is defined as the sleeve stress divided by the tip stress, usually expressed as a percentage.

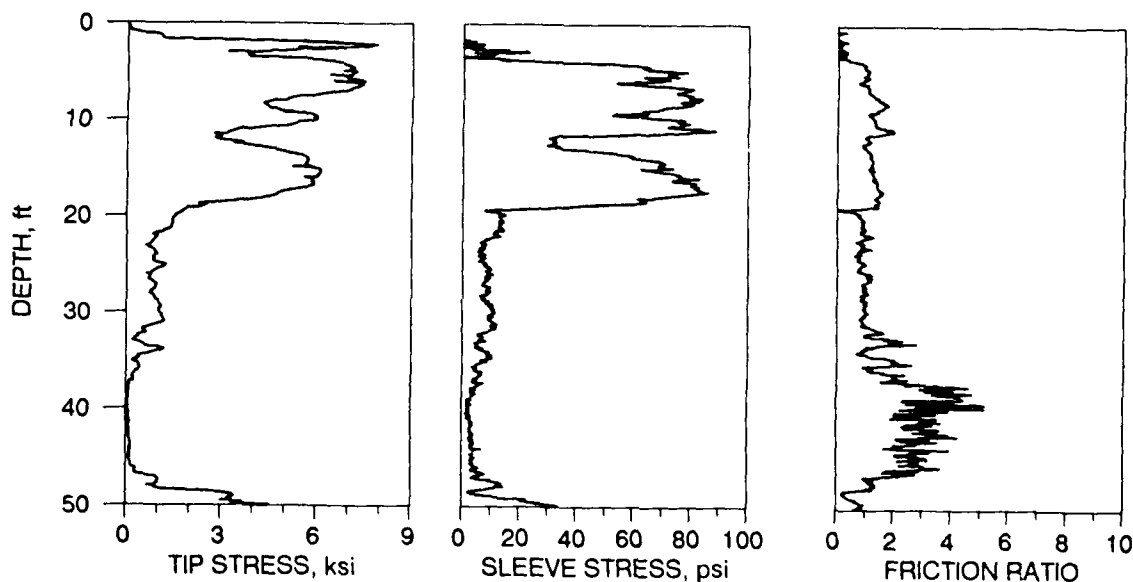


FIGURE 9. Penetration Profile Results for ARA Seismic Cone Penetrometer, Site 9700

The penetration profiles shown in Figure 9 indicate significant changes in subgrade properties at depths of about 5.2 m (17 ft) and 14 m (46 ft). Three major layers can be readily identified: (1) a stiff upper layer with tip resistances ranging from 21 MPa (3.0 ksi) to 52 MPa (7.5 ksi), (2) a very weak layer with tip resistances less than 7 MPa (1 ksi), and (3) a stiff lower layer which for modeling purposes can be assumed to be bedrock. These major layers can be further subdivided based on tip stress or on the basis of friction ratio. For example, a material change appears to occur at a depth of about 11 m (35 ft), based on the change in friction ratio from about 1% to about 3%. Friction ratio has been directly correlated with material type by Olsen and Farr (1986). Based on the friction ratio correlations and knowledge of the local geologic history, Site 9700 was characterized for modeling purposes as a sand over a clayey silt over bedrock.

Seismic Testing Results

Seismic data were obtained at various increments of depth using the ARA wave generation system previously shown in Figure 2. Data acquisition is triggered by the contact of the hammer with the impact plate. Data are acquired from all three geophones to determine wave arrival times. The geophone outputs are amplified and filtered to improve the signal-to-noise ratio. The data is viewed on the microcomputer screen to insure that an acceptable signal is received before saving the data for subsequent plotting. A series of seismic tests at different depths allows the determination of wave velocities as a function of depth.

Figure 10 shows typical waveform measurements from Site 9700. The traces in Figure 10 represent 3 different tests. One test was used to measure the compressional wave arrival. Two separate tests are used to determine the shear wave arrival. Since the tests have reversed polarity, the determination of the shear wave arrival is relatively easy by simply overlaying the two traces (as shown in Figure 10). The compressional wave arrivals are often difficult to determine and successful interpretation of compressional wave data often requires considerable experience and engineering judgment.

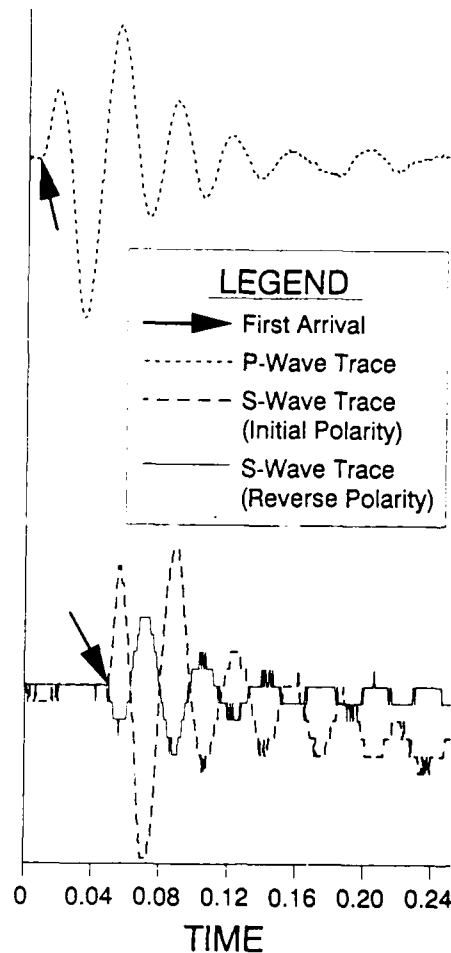


FIGURE 10. Typical Wave Traces for Arrival Time Measurements

Analysis of seismic "downhole" data utilizes the slope distance, or path length, which is known from the test geometry (see Figure 2) and the arrival times measured during penetration testing. For typical testing, analysis of the seismic data is simplified by the assumption that the wave velocity in a layer may be calculated as the change in total path length divided by the difference in arrival time. This is reasonably valid for deep layers, but can lead to significant errors in the case of a pavement surface which has relatively high wave velocity. For the testing reported herein, the actual path length was computed for each layer and previous results of wave velocity were used to determine the actual travel time in each layer, so that the actual travel time in the new layer was readily determined as the measured arrival time minus the summation

of the calculated travel times in all previous layers. Figure 11 summarizes graphically the wave velocity profiles from Site 9700.

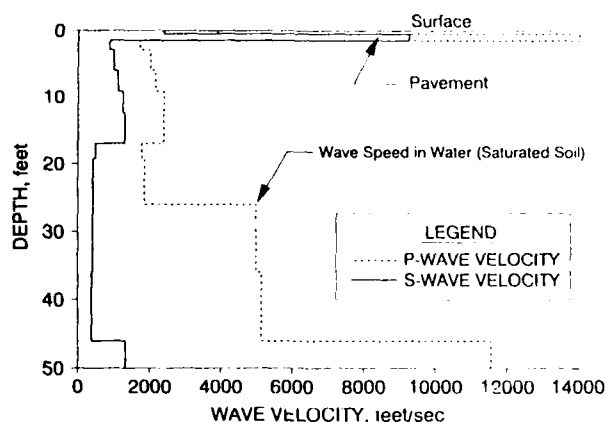


FIGURE 11. Velocity Profiles, Site 9700

The wave velocity data was used to calculate a profile of Young's modulus versus depth, which is presented in Figure 12. Of particular interest is the increase in compressional wave velocity to the speed of waves in water at a depth of 8 m (26 ft), indicating the location of the zone of saturation. Similarly, the differences in Young's modulus predicted by the two methods seem to indicate a zone of partial saturation between depths of 5 m (17 ft) and 8 m (26 ft).

Friction Angle Determination

A profile of friction angle versus depth was determined using Equations 4 and

5, shear moduli determined from the shear wave velocity profile (Figure 11), the tip resistance profile (Figure 9), and assumed values of total unit weight and cohesion. The unit weight was assumed to be 15.7 kN/m^3 (100 pcf) above the zone of saturation and 19.6 kN/m^3 (125 pcf) in the saturation zone. The subgrade material was assumed to be cohesionless. Figure 13 compares values of friction angle from cone penetration with laboratory direct shear tests. While the laboratory friction angle varied only from about 37 to about 40 degrees, the profile had significant variations. High friction values could possibly be due to a cementing action which can occur as shell fragments degrade. The low friction angles measured in the lower layer are also significant, since the material was assumed cohesionless (indicating an extremely weak layer).

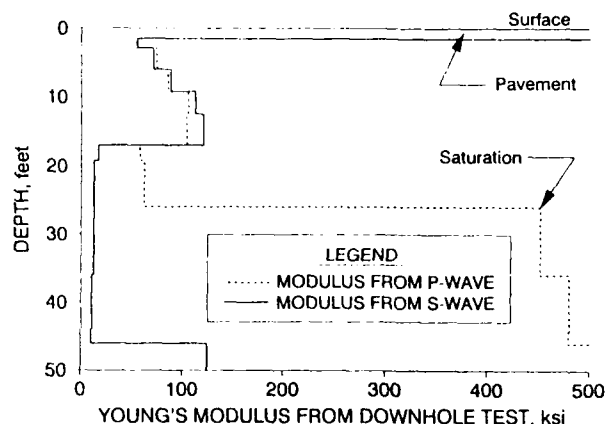


FIGURE 12. Modulus Profiles, Site 9700

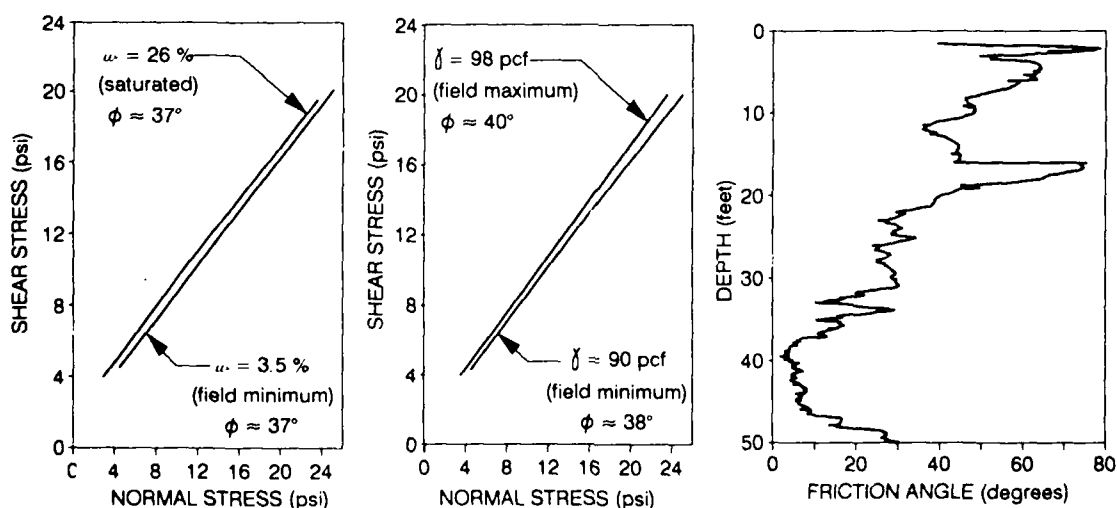


FIGURE 13. Laboratory Direct Shear Tests Compared with *In Situ* Friction Angle Values

RESULTS FROM NONDESTRUCTIVE TESTING

Nondestructive testing with the AFESC/RDCP Falling Weight Deflectometer was completed immediately prior to testing with the ARA seismic cone penetrometer. Raw data collected by the FWD is summarized in Table 2. Two drops at each of the four height settings were completed. It is common to ignore the first drop at any given drop height. All of the drops are included herein for completeness, but only the final drop at the highest load setting was used in the backcalculation.

Load (lb)	Sensor Deflection, mils						
	D ₁	D ₂	D ₃	D ₄	D ₅	D ₆	D ₇
9477	2.56	1.65	1.61	1.38	1.22	0.98	0.83
9441	2.72	1.77	1.81	1.54	1.38	1.14	0.98
11979	3.35	2.09	2.09	1.77	1.57	1.30	1.10
11979	3.46	2.20	2.17	1.89	1.69	1.42	1.22
18846	5.39	3.43	3.39	2.91	2.56	2.13	1.77
18810	5.31	3.43	3.27	2.91	2.52	2.13	1.85
27106	7.20	4.57	4.37	3.86	3.39	2.83	2.36
27106	7.17	4.53	4.21	3.70	3.27	2.76	2.36

Moduli were backcalculated in the following ways: (1) a default three-layer case was backcalculated using the program COMDEF (Anderson 1988b), (2) a default three-layer case was backcalculated using the program BISDEF (Bush and Alexander 1985), and (3) a four-layer case was backcalculated with BISDEF with the upper three layers variable and the lower layer fixed at the modulus determined from the shear wave data. In each of the default configurations, the common assumption of depth to bedrock equal to 6 m (20 ft) was used. In the four layer case, ground truth data were included from the cone penetration tests. The known thicknesses of the major layers were included, and the actual depth to bedrock of 14 m (46 ft) was used. Figures 14, 15, and 16 summarize the results of the backcalculations for the AC, PCC, and upper subgrade layers, respectively, as well as comparisons with other tests. Comparison data included the laboratory AC resilient modulus, the laboratory value of PCC modulus from the V-Meter test, and subgrade moduli values from the shear wave velocity profile. While all of the backcalculated moduli values would appear

reasonable under casual inspection, only the case which used ground truth data truly matched the comparison moduli values. Of particular interest was the subgrade modulus. In the default cases, COMDEF and BISDEF gave almost identical values for subgrade modulus. However, only for the four-layer case which used ground truth data did the subgrade modulus fall within the ranges of the field values.

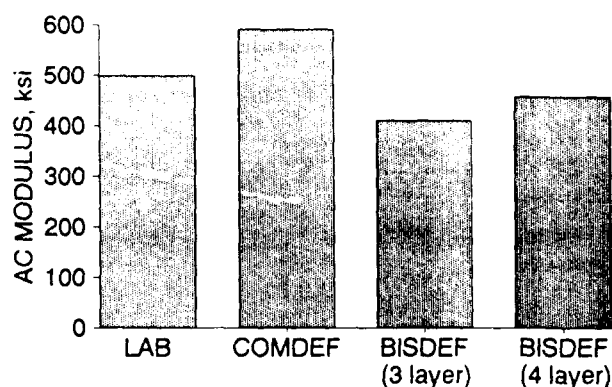


FIGURE 14. Backcalculated AC Moduli

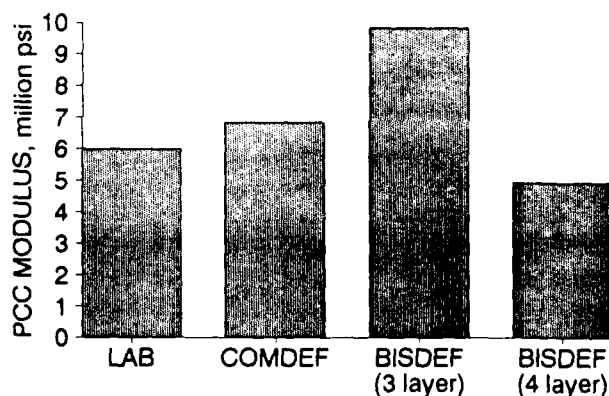


FIGURE 15. Backcalculated PCC Moduli

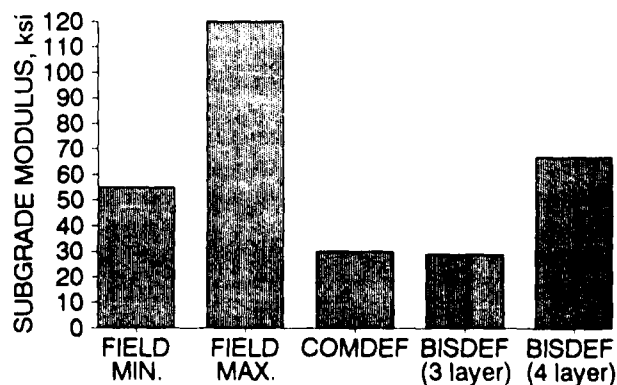


FIGURE 16. Backcalculated Subgrade Moduli

SUMMARY AND CONCLUSIONS

A direct comparison of data from several evaluation methods has been presented. This data set will be helpful in future modeling of pavement responses.

Microcomputer based data acquisition systems have improved the quality and quantity of data from field testing.

Ground truth data from seismic cone penetration tests greatly improved the backcalculation of layer moduli from the FWD testing. *In situ* penetration and non-destructive testing can be a useful combination for evaluation of pavement systems. The FWD provides rapid testing for routine evaluations and the penetration tests provide data for the calibration of structural response models.

In this study, differences in the shear and compressional wave velocity profiles made it easy to locate a zone of saturation.

Based on variations in properties from *in situ* tests and comparisons with laboratory data, it is concluded that traditional discrete sampling and laboratory testing does not provide a true representation of real pavement systems.

ACKNOWLEDGMENTS AND DISCLAIMER

The research described in this paper was completed at Tyndall Air Force Base, Florida and was funded by the Airbase Operating Surfaces Branch of the Air Force Engineering and Services Center (AFESC/RDCP) under Scientific and Engineering Technical Assistance (SETA) Contract Number F08635-88-C-0067, Subtasks 1.01 and 1.04. Project Officers for the subtasks were Mr. Charles E. Bailey and Mr James G. Murfee, respectively.

The contents of this paper reflect the views of the authors who are responsible for the facts and the accuracy of the data presented herein. The contents do not necessarily reflect the official views of the U. S. Air Force. This paper does not constitute a standard, specification, or regulation.

REFERENCES

Anderson, M., 1988a, *Backcalculation of Composite Pavement Layer Moduli*, Ph.D. Dissertation, University of Kentucky, Lexington, Kentucky.

Anderson, M., 1988b, "A Database Method for Backcalculation of Composite Pavement Layer Moduli," *STP-1026*, ASTM, Philadelphia, Pennsylvania.

Anderson, M. and Drnevich, V. P., 1989, "A True Dynamic Method for Nondestructive Testing of Rigid Pavements with Overlays," *Proceedings, Fourth International Conference on Concrete Pavement Design and Rehabilitation*, Purdue University, West Lafayette, Indiana.

Brown, R., 1987, "Airfield Pavement Evaluation, Rickenbacker Air National Guard Base, Ohio," Air Force Engineering and Services Center, Tyndall AFB, Florida.

Bush, A. J., III and Alexander, D. R., 1985, "Pavement Evaluation Using Deflection Basin Measurements and Layered Theory," *TRR 1022*, Transportation Research Board, Washington, DC.

Kingham, R. I. and Kallas, B. F., 1972, "Laboratory Fatigue and its Relationship to Pavement Performance," *RR-72-3*, The Asphalt Institute, College Park, Maryland.

Olsen, R. S., and Farr, J. V., 1986, "Site Characterization Using the Cone Penetrometer Test," *Use of In Situ Tests in Geotechnical Engineering*, Geotechnical Publication Number 6, Proceedings of In Situ '86 Conference, Blacksburg, Virginia.

Rohani, B., and Baladi, G. Y., 1981, "Correlation of Mobility Cone Index with Fundamental Engineering Properties of Soil," *SL-81-4*, USAE Waterways Experiment Station, Vicksburg, Mississippi.

Shinn, J. D., Timian, D. A., Smith, E. B., Morlock, C. R., Timian, S. M., McIntosh, D. E., 1988, "Geotechnical Investigation of the Ground Based Free Electron Laser Facility," *ARA-NED-88-10*, Applied Research Associates, New England Division, South Royalton, Vermont.

Southgate, H. F. and Deen, R. C., 1969, "Temperature Distribution Within Asphalt Pavements and Its Relationship to Pavement Deflection," *HRR 291*, Highway Research Board, Washington, DC.

Vesic, A. S., 1972, "Expansion of Cavities in Infinite Soil Mass," *Journal of the Soil Mechanics and Foundation Division*, ASCE, Volume 98, SM3, Paper 8790.

RESILIENT MODULUS DETERMINATION FOR FROST CONDITIONS

Edwin J. Chamberlain
David M. Cole
Glenn F. Durell

U.S. Army Cold Regions Research
and Engineering Laboratory
Hanover, New Hampshire 03755-1290

ABSTRACT

Resilient moduli for pavements subject to freezing and thawing can be obtained from laboratory repeated load triaxial tests. We have found that for the frozen condition, the resilient modulus is very sensitive to temperature or unfrozen water content. For the thawed condition, the modulus is primarily dependent upon the water content or moisture stress.

The modulus is also dependent upon the applied stresses, particularly for the newly thawed condition and the recovery period that follows. We empirically relate the moduli to the environmental and stress conditions using a multiple linear regression analysis. Resilient moduli obtained with this procedure typically vary over 3 or 4 orders of magnitude for a complete freeze-thaw cycle. It is difficult to obtain meaningful data for the thawed condition where the pore pressure is greater than or equal to zero.

The empirical equations are used in elastic layered models to calculate pavement deflections. Comparison with field pavement deflection measurements shows that the technique is valid. Good results are obtained, except for the period during the spring thaw when the soil is saturated and the resilient modulus is ill-defined. The appropri-

ate values for the resilient moduli for this condition are currently obtained by forcing the calculated and measured deflections to agree. This procedure is necessary until we have enough experience for making predictions of the appropriate resilient modulus value for the saturated condition.

INTRODUCTION

Modern pavement design methods require the use of some form of layered elastic analysis for predicting pavement response to wheel loading. These mechanistic methods commonly employ resilient moduli to characterize the stress/deformation properties of the different layers in the pavement system. In seasonal frost regions, the resilient moduli of the soil layers making up the pavement system vary greatly with season of the year. During the winter months, the resilient modulus of a fine-grained subgrade soil may be as great as 10-GPa, whereas during the spring thaw period, the resilient modulus may fall to near zero. Prediction of pavement response for these widely varying conditions requires a complete laboratory characterization of the resilient modulus throughout the freeze, thaw and recovery periods. This report presents the laboratory methods used at

CRREL to characterize the seasonal change in resilient modulus. A method for relating the resilient moduli to soil, stress and temperature parameters and the procedure for calculating and validating pavement response are also detailed.

BACKGROUND

The resilient moduli are determined in the laboratory using the repeated load triaxial (RLT) test. The test cells were specially designed to accommodate freezing temperatures and the measurement of very high and very low resilient moduli. We relate the resilient moduli to moisture and density, applied stress and temperature conditions with empirical equations using multiple linear regression techniques. We use these equations in concert with either predictions or observations of field conditions to calculate pavement responses using layered elastic methods. To validate these procedures, we compare the calculated pavement deflection basins with field observations made with a falling weight deflectometer. Results for several different soils were reported by Cole et al. (1986).

REPEATED LOAD TRIAXIAL TEST

Test Equipment

Special triaxial cells were constructed to accommodate frozen and thawed specimens and the instrumentation used to monitor the load and deformation (Cole et al. 1985). Cells for fine-grained samples of 50-mm diameter by 127-mm length and coarse-grained samples of 150-mm diameter by 381-mm length are shown in Figure 1. Both cells feature a base pedestal that can be removed with the specimen intact in its rubber membrane and load cap. This facilitates the testing sequence, which calls for several tests on a given specimen for different temperature and moisture stress conditions. With this

arrangement, a specimen need not be removed from its base while the temperature or the moisture stress is being adjusted. Additional pedestals allow up to six specimens to be tested in a rotating sequence with minimal sample disturbance.

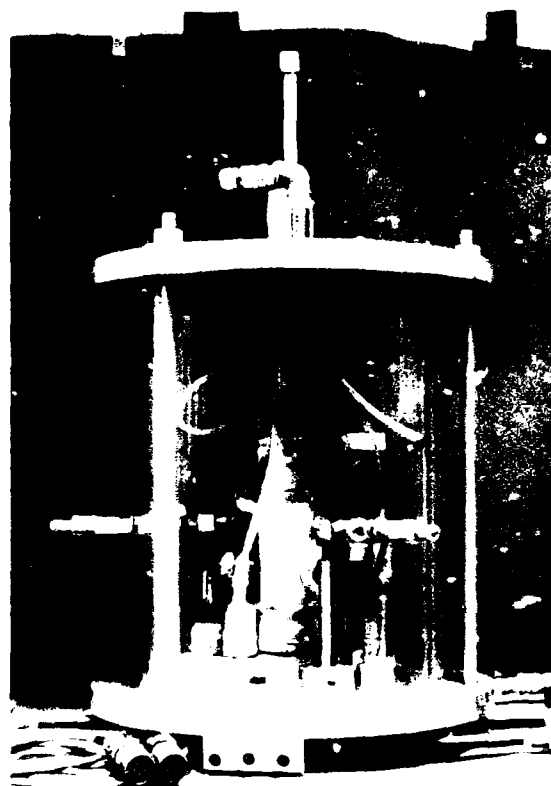
The repeated load is applied with a closed-loop electro-hydraulic testing machine to the loading piston of the triaxial cell. A miniature load cell, mounted inside the triaxial cell on the load piston provides both a measurement of the vertical load on the test specimen and the feedback signal to the testing machine. The load piston passes through two linear ball bushings to maintain alignment and minimize friction. An O-ring seal is used to prevent the escape of air during pressurizing of the cell.

The axial deformation measuring system employs four linear variable displacement transducers (LVDT's). The LVDT cores are mounted on two spring-mounted circumferential clamps positioned at the upper and lower quarter points along the length of the sample. To minimize the amount of transducer weight supported by the sample, the transducer barrels are mounted on double-hinged arms supported by vertical standards fastened to the cell base. This arrangement is especially critical for the very soft condition of some specimens immediately after thawing. Special signal conditioning and electronic circuiting allows the determination of the average differential movement between the clamps during loading. The LVDT transducer setup is shown in Figure 2.

The radial deformation measuring system employs three non-contacting displacement transducers (NCDTs) equally spaced around the specimen at mid-height. These devices are mounted on standards that bolt to the cell floor. This arrangement further minimizes the transducer weight supported by the test sample. The NCDTs produce a DC voltage output in linear proportion to the gap between the sensor face and an aluminum foil target mounted on the specimen



a. 152-mm-diameter specimen in the large cell.



b. 50-mm-diameter specimen in the small cell.

Figure 1. Fully assembled repeated load triaxial test cells.

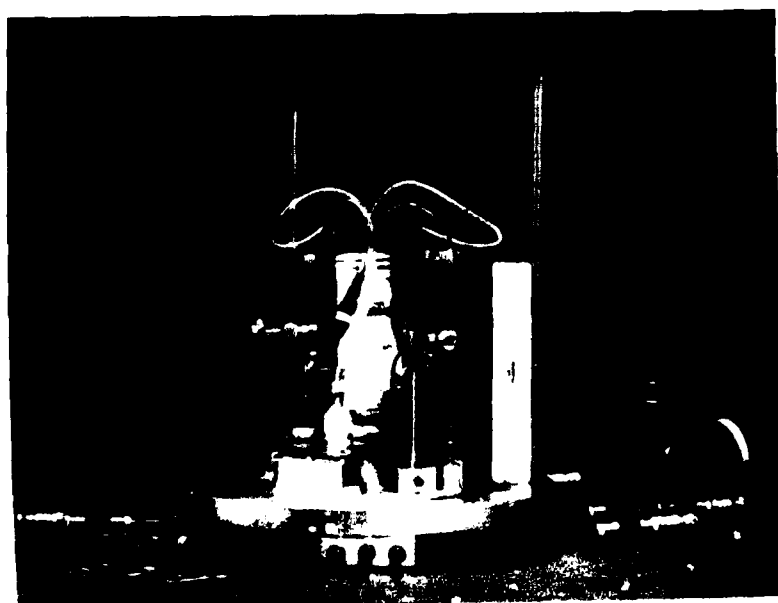


Figure 2. Installation of the LVDT transducers.

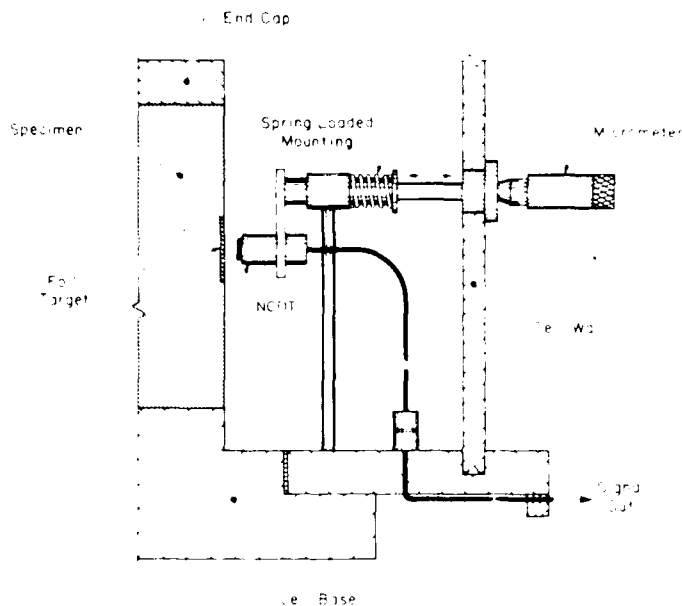


Figure 3. Detail of the NCDT transducer mounting.

surface. The signals of the NCDTs are averaged to determine the radial deformation during axial loading of the specimen. The gap between the NCDTs and the target can be adjusted without disassembling the test cell using micrometer heads mounted in the cell wall. Figure 3 shows a detail of the NCDT mounting.

Both sizes of RLT test cells have features that allow moisture to be adjusted in the test specimens and the measurement of moisture tension to be made. The base pedestal (Fig. 4) in the small cell contains both of these provisions. The porous drainage disk allows drainage under gravity and the ap-

plication of a vacuum to the sample to reduce the moisture content. The porous ceramic stone protruding from the base allows the moisture tensions to be measured to about -75 kPa. The larger RLT test cell has the same drainage provision built into the base pedestal. However, the porous ceramic cup material is too fragile to place in the base of this cell. To avoid breakage with the coarse granular materials, the porous ceramic cup is mounted on flexible tubing and placed through a hole in the top load cap.

The temperature for the RLT tests is controlled in an environmental chamber positioned between the cross heads of

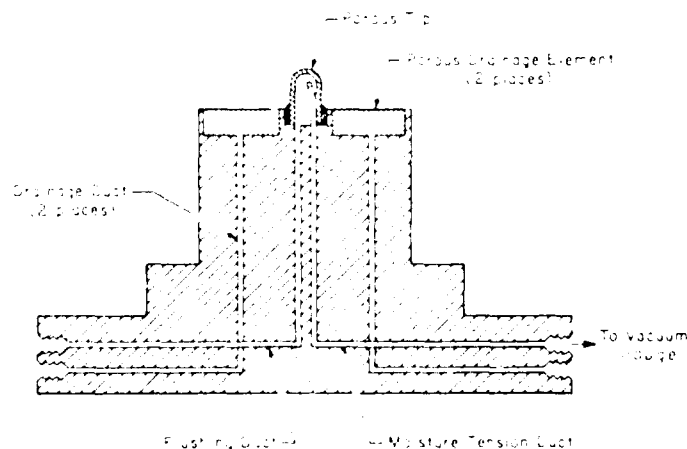


Figure 4. Cross section of the small triaxial cell base. Vacuum gauge continuously monitors moisture tension level. System may be flushed to expel gas bubbles.



Figure 5. Triaxial cell mounted in environmental chamber in test machine.

the test machine (Fig. 5). Controlled temperature air is circulated throughout the chamber to the required test temperature. Two additional features enhance the quality of the temperature control. A heat exchange plate, placed between the lower test machine platen and the base of the test cell, is used to absorb the heat flowing up through the platen into a circulating bath maintained at the test temperature. Small electric fans located inside the test cell are used to circulate the air to further ensure uniform specimen temperature.

The test machine is controlled using an electronic pulse generator. The signal is sent to a servo-valve which controls the flow of hydraulic fluid to an actuator piston located in the upper cross-head of the test machine. The actuator piston moves in response to the electric signal, moves the FLT cell piston, and thus the load through the

load cell to the test specimen. The load cell signal is compared electronically with the generated pulse and adjustments are automatically made to the servo-valve to maintain the desired load pulse.

The outputs of the load cell and the LVDT and NCDT displacement transducers are recorded on a high-speed pressurized-ink strip-chart recorder. This recording system allows us to view the deformation (Fig. 6) as it occurs and to make decisions about when a steady state response or excessive residual deformation has occurred. We have also tried digital and micro-computer based recording systems, but have not developed an efficient method of processing the very large amount of information gathered. Currently, we use only the steady-state resilient strain and the accompanying residual strain values. We determine these values directly from the strip-chart.

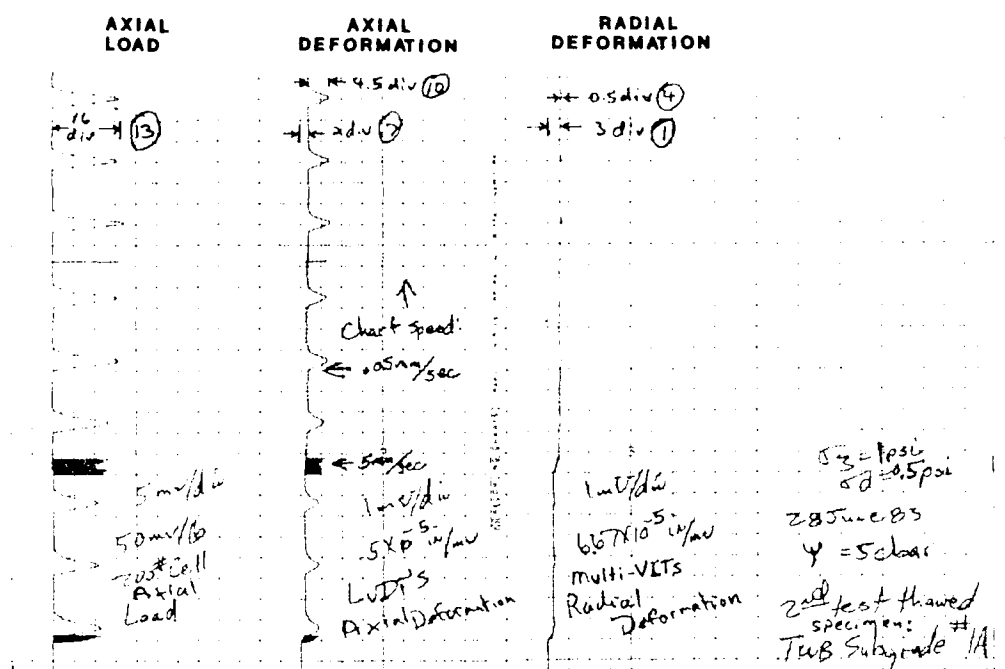


Figure 6. Typical strip chart showing load and axial and radial deformation traces.

Sample Preparation

Test specimens prepared from undisturbed frozen cores from pavement sections or from laboratory freezing tests are preferred. This requirement is especially critical for fine-grained materials where ice segregation and frost heave are significant. Generally, only the 50-mm-diameter silt and clay samples can be obtained this way. The diameter is machined to dimension on a metal-working lathe in a coldroom to a 2-mm tolerance. The ends are milled smooth and parallel to within approximately ± 0.1 mm. Latex rubber membranes and temporary end caps are placed on the prepared samples to protect from sublimation during storage.

The coarser grained larger diameter samples are compacted to field density in a special steel mold to the required length and diameter. These samples are soaked with water for 24 hours and frozen with water freely available at the base. The preferred rate of freezing is 25 mm/day. Rubber membranes and stacked plexiglass rings provide lateral con-

finement (but do not restrict vertical frost heave) during freezing. The ends are made flat and parallel with a special end capping procedure.

Test Procedures

a. Sample mounting and conditioning

The test samples are mounted on the specimen pedestals while frozen. A special flat pedestal, without the drainage disk and the porous cup, but with a temperature sensor, is used for the 50-mm frozen samples. The aluminum foil targets are placed between the two rubber membranes used to protect the test specimen. They can be seen in Figures 1 and 2. The clamps holding the LVDT cores are mounted on the specimen and the barrels put in place (Figure 2). The Multi-VIT transducers are positioned and the sensor leads connected to bulk head connectors in the base of the test cell. The cell is then carefully closed and the piston lowered to allow the load cell button to contact a recess in the specimen cap. All of this

assembly is done in a coldroom to ensure that the sample does not thaw during assembly. Fully assembled RLT test cells are shown for both sample sizes in Figure 1. The entire test assembly is then placed in a coldroom at the lowest specified test temperature for 24 hours. At least one hour before testing begins, the assembly is transferred to the environmental chamber in the test machine and the sensor leads are connected to the recording instruments. The mechanically refrigerated test chamber maintains the temperature to within $\pm 0.1^\circ\text{C}$ of the set value. Testing proceeds to warmer temperatures, allowing 24 hours for equilibrium each time. After a 50-mm-diameter specimen has been tested for all specified temperatures in the frozen state, it is removed from the special temperature pedestal, a hole is bored to accommodate the porous cup, and it is mounted on the standard base.

The samples are thawed at room temperature on their pedestals with a small weight placed on the top cap and a slight vacuum (-1 to -2 kPa) placed on the drainage line. This procedure ensures that the sample does not neck due to three-dimensional thaw consolidation. The base pedestal is next mounted in the base cell plate, the displacement transducers are positioned and the cell closed. Connections are then made for the displacement transducers and the cell pressure and drainage lines.

b. Applied load waveform

The test procedure allows for the application of a repeated load pulse that simulates the loading conditions associated with a field loading device. The waveforms for repeated load plate bearing (RPB) and falling weight deflectometer (FWD) field-test-loading devices that we have used are shown in Figure 7. We have found no difference in response to these two waveforms. Currently, although we are using only the FWD in the field, we specify the RPB load pulse for the repeated load triaxial tests because it is easier to record this pulse on the strip chart recorder. This pulse is on approximately 1 second and off 2 seconds.

c. Testing sequence

Once mounted and instrumented, the specimen is tested in the closed-loop, electro-hydraulic testing machine according to the test sequence given in the table on the next page.

The test starts with a frozen sample under a confining pressure of 69 kPa and the lowest temperature required. Generally, we use -10°C as the lowest temperature. Site conditions may dictate a lower (or higher) starting temperature. We then apply 200 cycles of the lowest cyclic axial stress (69 kPa) and observe the resilient axial deformation. If steady-state response is achieved prior to 200 cycles, the load-

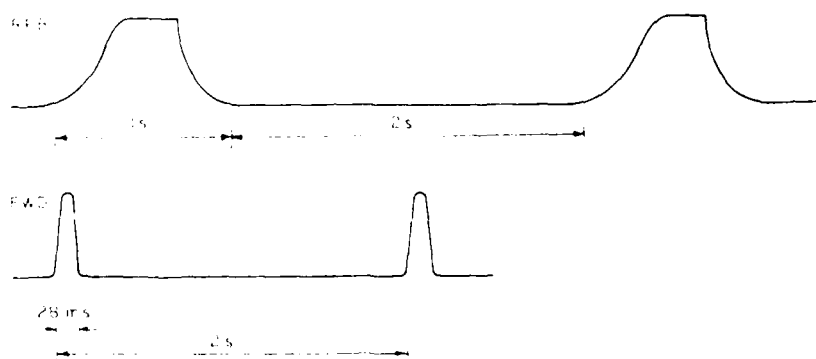


Figure 7. Waveforms of the repeated plate bearing (RPB) apparatus and falling weight deflectometer (FWD).

Test plan for repeated load triaxial tests.

State	Moisture stress, ψ (kPa)	Confining stress, σ_3 (kPa)	Temperature T (°C)	Cyclic deviator stress, σ_d (kPa)	Stress ratio (σ_1/σ_2)
FRCZEN	NA	69.0	-10 to -2	34.5 to 827.0	1.5 to 13
THAWED	0 to -75	6.9	22	3.5 to 13.8	1.5 to 3
	0 to -75	13.8	22	6.9 to 27.6	1.5 to 3
	0 to -75	27.6	22	13.8 to 55.2	1.5 to 3
	0 to -75	69.0	22	34.5 to 138.0	1.5 to 3

ing is stopped and the next level of axial stress is applied. Generally, we use a maximum axial deviator stress of 827 kPa. This procedure is repeated until the highest deviator stress level is reached. The test specimen is then removed from its pedestal and placed in the cold room to condition for 24 hours at the next highest temperature. Usually, a batch of samples are tested at the same temperature to save time. We repeat this axial stress sequence for all temperature levels up to about -2 °C. At temperatures closer to the melting point, large deformations associated with progressive melting of ice cause problems with the alignment and stability of the deformation sensors.

The frozen test sample is removed from the RLT cell on its test pedestal and allowed to thaw with a small dead load applied to its cap and a small vacuum applied to its base as previously described. Once the specimen has completely thawed and come to equilibrium with the applied stresses, we re-assemble the test cell and proceed to conduct the RLT test according to the sequence shown in the test plan table. We start with a moisture tension value of just below 0 kPa and a confining pressure of 6.9 kPa and proceed to apply repeated axial stresses at stress ratio levels of 1.5, 2, 2.5 and 3. If the residual strain exceeds 4 %, we terminate this stress ratio sequence, go to the next confining pressure level and repeat the stress ratio sequence. We continue this procedure until all confining stress levels up to 69 kPa have been used. If the total residual strain exceeds 20 % or the test speci-

men is otherwise badly deformed, we remove the test specimen and start with a new sample. Once the highest confining pressure (69 kPa) and highest stress ratio series is completed, the test specimen is removed from the RLT test cell on its pedestal. We then apply a vacuum to its base and allow the moisture to come to equilibrium to the next specified moisture tension level. This process usually requires several hours or in some cases a day or more. To make efficient use of time and the test equipment, we test other samples at different stress levels or at the same stress levels for replication. Usually, there are several thawed test specimens conditioning for moisture tension at the same time. The test sequence is continued until all moisture tension levels have been included. If we know the moisture tension levels that occur in the field, then we use the field levels to bound the laboratory test values. Otherwise, we generally use four moisture tension ψ values of about 0, 25, 50 and 75 kPa in the test sequence on fine-grained material. Values of ψ for coarser-grained materials are scaled down as required.

d. Test specimen analysis

After testing is completed, we determine the water content and density of the test sample. We then back calculate the moisture and density for each moisture tension level using observations made during the test series. The original weights and measures also allow the calculation of the initial moisture and density conditions.

e. Data reduction

For each set of applied deviator and confining stress conditions we calculate a resilient modulus and a resilient Poisson's ratio. The resilient modulus is determined by dividing the applied deviator stress by the recoverable steady-state axial strain. The resilient Poisson's ratio is calculated by dividing the recoverable radial strain by the recoverable axial strain. We tabulate the calculated resilient moduli and resilient Poisson's ratios along with the applied stress, temperature, moisture stress, moisture content and density values and enter them in a computer file.

DATA ANALYSIS

Resilient Modulus

We perform multiple linear regression analyses on the test data to obtain working relationships between the resilient modulus and sample and stress conditions. We have found that the frozen resilient modulus is stress independent for the range of stress of interest, whereas the thawed resilient modulus is very stress dependent. We have thus developed two separate expressions for modeling the resilient moduli.

a. Frozen condition.

The frozen resilient modulus can be expressed either directly in terms of temperature or in terms of unfrozen water content. Generally, a second order expression using temperature T in $^{\circ}\text{C}$ is sufficient to express the resilient modulus M_r , e.g.:

$$M_r = e(a + bT + cT^2)$$

where a , b and c are regression coefficients. However, we also developed a simpler expression based on unfrozen water content, which is a function of soil type and temperature. The unfrozen

water content w_u in % by weight is related to temperature with the following

$$w_u = \alpha \left[\frac{-T}{T_0} \right]^{\beta}$$

function:

where T_0 is a reference temperature of 1°C and α and β are constants determined from a linear regression analysis on the unfrozen water content vs temperature data obtained from a laboratory test. This allows the use of the following relationship:

$$M_r = A(w_u/w_t)^B$$

where w_t is the total water content and A and B are the regression coefficients.

b. Thawed or recovered condition.

We model the thawed and recovering stress-dependent resilient moduli using the nonlinear equation form given in eq 3:

$$M_r = K_1[f(\sigma)]^{K_2}$$

where $f(\sigma)$ is the stress function, K_1 is a constant dependent upon moisture tension and sometimes dry density and K_2 is a soil-dependent parameter statistically independent of the moisture tension or density. To normalize the moisture tension function for the regression analysis, we use the function $f(\psi)$:

$$f(\psi) = \frac{(101.36 - \psi)}{\psi_0}$$

The value 101.36 represents atmospheric pressure in kPa, ψ is moisture tension in kPa (expressed as a positive number). The dry density function is simply the ratio of the dry density of the

$$f(\gamma_d) = \frac{\gamma_d}{\gamma_0}$$

soil γ_d to unit density γ_0 :

$$K_1 = C_0 [f(\psi)]^{C_1} = [f(\gamma_d)]^{C_2}$$

where C_0 , C_1 and C_2 are determined from the regression analysis.

For the stress function, we try either the first stress invariant J_1 :

$$f_1(\sigma) = J_1 = \sigma_1 + 2\sigma_d$$

or the ratio of the second stress invariant J_2 to the octahedral shear stress τ_{oct} . The latter stress function is calculated from the confining stress σ_3 and the deviator stress σ_d using the following formula:

$$f_2(\sigma) = \frac{J_2}{\tau_{oct}} = \frac{9\sigma_3^2 + 6\sigma_3\sigma_d}{\sqrt{2}\sigma_d}$$

The use of J_1 is traditional in such analysis. The use of J_2/τ_{oct} , while somewhat unorthodox, has proven valuable since it reflects the tendency of the resilient modulus to increase with confining stress and to decrease with

principal stress ratio. Analysis made with this parameter results in a single curve in the resilient modulus versus stress function plane (Fig. 8). Analyses made with J_1 usually result in a series of curves (Fig. 8) in the resilient modulus vs stress function plane, each curve representing a different stress ratio for granular soils.

The calculated functions are placed in a data file to prepare for the linear regression analysis. The equations are linearized by taking the log of both sides. We currently conduct this analysis on PC type microcomputers. We set a confidence level of 95% and observe the coefficient of determination (correlation coefficient squared), the standard error and the regression coefficients. We choose the form of the equations that has the best fit for use in calculating pavement system response to loading. Figure 9 shows how the resilient modulus for the frozen condition varies with temperature for several different soil types. Figure 10

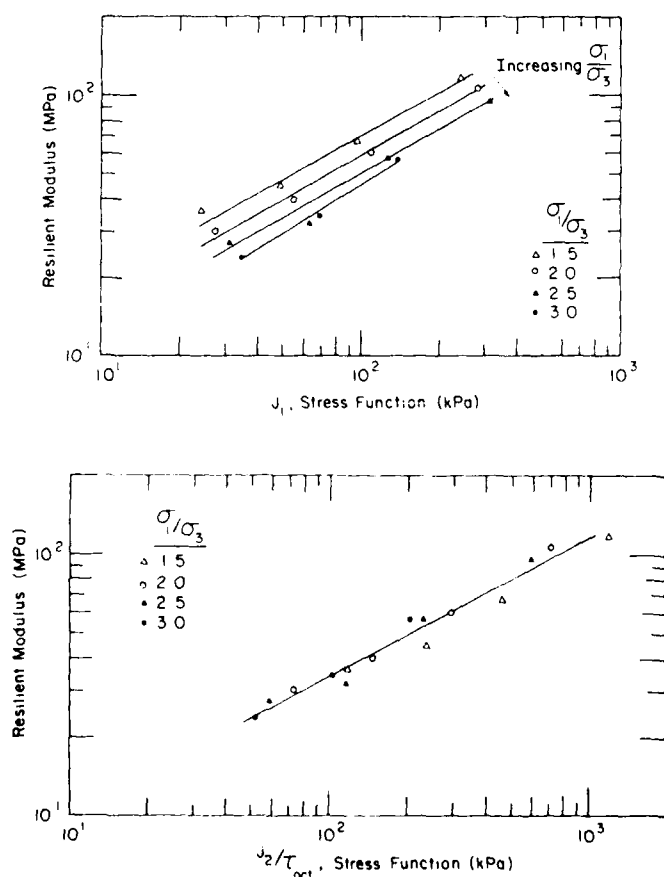


Figure 8. Example of the resilient modulus vs the two stress functions.

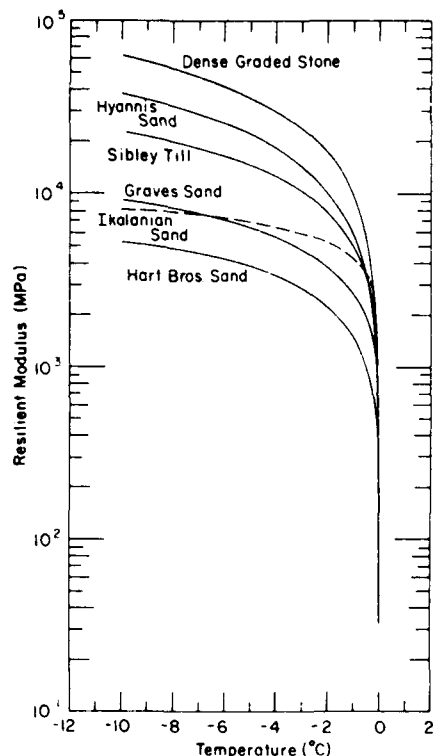


Figure 9. Resilient modulus vs temperature for several test soils.

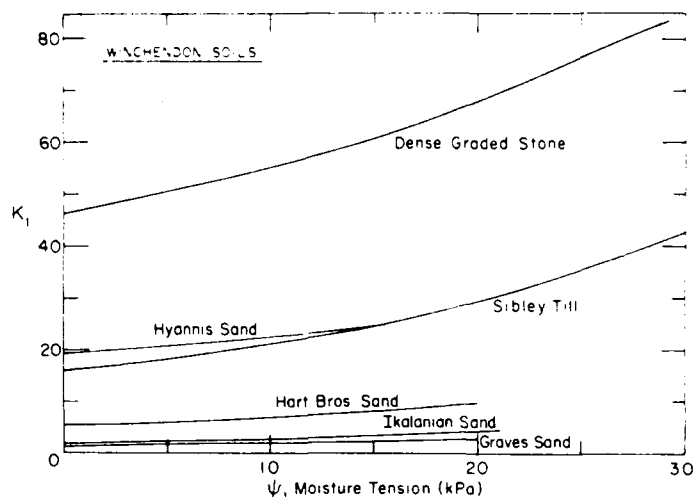


Figure 10. Example of the K_1 vs moisture tension for several test soils for the J_2/τ_{oct} stress function.

shows an example of the moisture tension dependency and Figure 8 the stress dependency of the resilient modulus for a thawed soil.

Resilient Poisson's Ratio

The measurement system described earlier allowed us to calculate Poisson's ratio directly. We performed regression analyses similar to those done for the resilient modulus in an effort to relate resilient Poisson's ratio to the pertinent variables. However, we did not find any significant relationships. Correlation coefficients have not exceeded 0.4 (versus 0.8 to 0.98 for the resilient modulus relationships) and in many cases were very near zero. Consequently, no stress- or moisture-tension-dependent model for Poisson's ratio has emerged from our analyses. We, therefore, use average values for each soil and frozen or thawed state.

PAVEMENT RESPONSE CALCULATIONS

The pavement response to loading is determined from an elastic layered computer model. For the nonlinear case of thawed soils, we have used the code NELAPAV (Irwin and Speck, 1986). The soil temperature, moisture stress and dry density data can be obtained from field measurements or from model calculations. The example illustrated here used the output of the FROST1 (Guymon et al., in press) frost-heave thaw-consolidation model developed at CRREL. Details of these calculations are in a report by Chamberlain et al. (in prep). The analysis requires temperature, moisture stress and dry density data for each unique layer in the pavement system. Layers are defined both by changes in material type and changes in temperature and moisture stress within each layer. Limits are assigned to how large the moisture tension or temperature differences can be within a layer

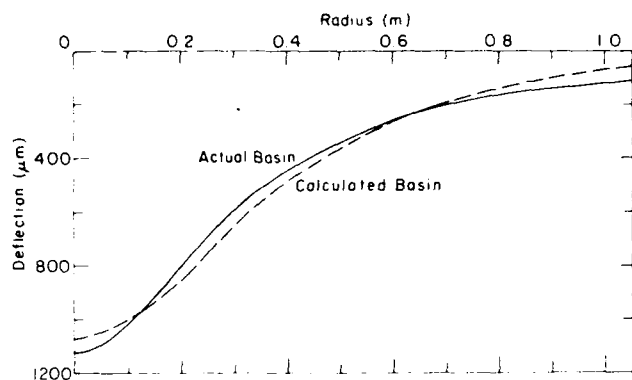


Figure 11. Example of a comparison of calculated and measured deflection basins.

before it is divided into sub-layers. The transition between frozen and thawed material always defines a sub-layer boundary. We developed a computer code called TRANSFORM (Chamberlain et al., in prep.) to make these calculations rapidly from the output files of FROST1. The TRANSFORM program also requires that the input control parameters for NELAPAV be included. The resulting files allow deflections, stresses and strains to be calculated using NELAPAV for particular soil and stress conditions. Figure 11 shows a pavement deflection basin calculated with this procedure. A deflection basin measured with the falling weight de-

flectometer for the same test and material conditions is also shown for comparison purposes. The good correlation between the observed and calculated values supports the validity of the laboratory test and analysis procedures.

DISCUSSION

The importance of using the procedures outlined in this report to determine the resilient moduli of soils in pavements subjected to freezing and thawing is illustrated in Figure 12. This figure shows that the magnitude of pavement deflection is highly dependent

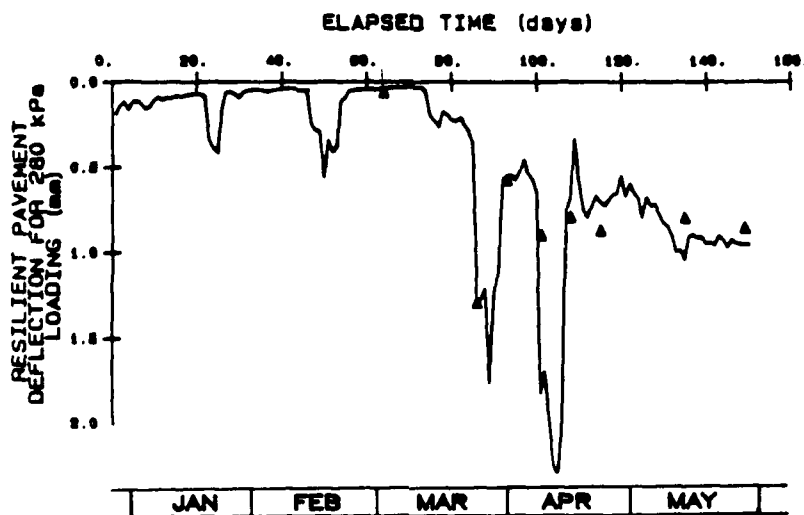


Figure 12. Example of resilient pavement deflection for a 280 kPa repeated load. Solid line is the calculated deflection and points are values measured with the FWD.

on the time of the year in seasonal frost regions. The solid line was determined using the laboratory procedures and the triangular points represent plate deflection data taken with the FWD for an applied stress of 280 kPa. During the winter period the pavement section is very stiff and the deflections are very much smaller than during the summer months. There are a couple of periods accountable to brief January and February thaws where the deflection increases sharply. However, these perturbations are dwarfed by the extremely large deflections that occur during the spring thaw period.

There is very good agreement between the laboratory and field data. This agreement is generally uncompromised by adjusting or "calibrating factors." There is one case, however, where adjustments must be made. That is for the case where the soil moisture develops positive pore pressures during thawing because the soil becomes saturated with water. It is technically very difficult to make laboratory measurements of the resilient modulus of saturated soils because they become very weak and difficult to handle and instrument. We place the slight vacuum on the soil moisture during thawing in order to avoid this condition.

Apart from the difficulty of testing saturated soil, there is considerable uncertainty about how the results would relate to field conditions. In thawing pavements the exact degree of saturation and the confinement of the soil moisture during loading are indeterminate. Saturation is seldom complete because of entrapped air in the melt water. This water is trapped between the pavement layer, the frozen soil layer and finer grained soils at the edge of the pavement. The system responds to loading something like a saturated sponge with some lateral confinement. This condition precludes any clear link between laboratory and field conditions for the "nearly" saturated case. To circumvent this difficulty, we reduce the resilient modulus of all saturated

layers by a constant factor to force the calculated deflections to agree with the observations. The same modifying factor is used for all saturated cases once the appropriate value is determined. Presently we need to continue this practice until we gain enough experience to select the proper correction factor or until we are able to make the appropriate laboratory measurements.

CONCLUSIONS

The laboratory testing methods and data analysis procedures detailed in this report allow the determination of the resilient response of soil and granular materials used in pavement systems throughout a freeze, thaw and recovery cycle. The resilient modulus in the frozen state is strongly related to temperature or unfrozen water content. The applied stresses become important factors once ice melting is significant. Soil moisture tension is the appropriate factor for monitoring the thawed and recovery phases. Most soils that we have tested exhibit large increases in resilient moduli after freezing and very large decreases after thawing. Recovery to normal period resilient moduli gradually occurs as moisture drains from the pavement system and moisture tensions increase. These seasonally varying resilient moduli can be determined using special repeated load triaxial test procedures and the resulting moduli can be related to temperature, moisture tension and dry density using multiple linear regression techniques. An elastic layered model can then be used to calculate pavement deflection, as well as stresses and strains within the pavement system.

The resilient Poisson's ratio can also be determined with the RLT test. However, it appears to be solely dependent on the frozen or thawed state and independent of soil moisture tension or stress conditions.

REFERENCES

- Chamberlain, E., T. Johnson, R. Berg and D. Cole (in prep.) Prediction of pavement behavior under loading during freezing and thawing. USA CRREL Report.
- Cole, D., G. Durell, and E. Chamberlain (1985) Repeated load triaxial testing of frozen and thawed soils. Geotechnical Testing Journal, volume 8, number 4, p. 166-170.
- Cole, D., D. Bentley, G. Durell and T. Johnson (1986) Resilient modulus of freeze-thaw affected granular soils for pavement design and evaluation. USA CRREL Report 86-4, 78 p.
- Guymon, G., R. Berg, T. Johnson and T. Hromadka (in prep.) Mathematical model of frost heave and thaw settlement in pavements. USA CRREL Report.
- Irwin, L. and D. Speck (1986) NELAPAV Users' Guide. Cornell University. Local Roads Rept. No. 86-1, 23 p.

BACKCALCULATION OF LAYER MODULI AND RUNWAY OVERLAY DESIGN:
U.S. COAST GUARD AIR STATION, KODIAK, ALASKA

Ted S. Vinson	Dept. of Civil Engineering, Oregon State University
Haiping Zhou	Dept. of Civil Engineering, Oregon State University
Ray Alexander	R and M Consultants, Inc., Anchorage, Alaska
R. Gary Hicks	Dept. of Civil Engineering, Oregon State University

The largest Coast Guard Air Station in the U.S. is at Kodiak Airport, Alaska. The mission of the Air Station is to patrol the outer continental shelf fishing grounds and support search and rescue operations. Runway 18/36 at Kodiak Airport is utilized primarily for the Coast Guard operations.

A visual condition survey of Runway 18/36 was conducted in March 1988. During the survey it was noted that the pavement surface is ravelling and poorly bonded in many areas and represents a serious maintenance and, possibly, a serious safety problem. Further, drainage is poor and often nonexistent over many sections of the runway. A cost effective solution to these problems will be to remove the old asphalt concrete (AC) pavement and overlay the underlying portland cement concrete (PCC) pavement.

To assess the condition of the existing PCC, a falling weight deflectometer (FWD) survey was conducted in October 1988. Moduli for the existing AC, PCC, and subgrade were backcalculated using two programs, ELMOD and BOUSDEF. A comparison was made between backcalculated moduli and laboratory moduli of AC and PCC samples obtained in a limited field coring program.

Backcalculated PCC moduli from ELMOD were used to design the overlay thickness. The required AC overlay thickness appears to be more sensitive to the fatigue failure criteria used for the PCC (in the mechanistic design approach) than the method (i.e., program) used to back-

calculate the PCC moduli from the FWD survey results.

INTRODUCTION

The U.S. Coast Guard utilizes Kodiak Airport to support the largest operating base in Alaska and the largest Coast Guard Air Station in the United States. The mission of the air station is to patrol the outer continental shelf fishing grounds and support Search and Rescue (SAR) Operations.

Air Station Kodiak is located approximately four miles southwest of the city of Kodiak on 615 acres initially developed by the U.S. Navy during World War II and now owned by the Coast Guard (re. Figure 1). The airport runways and terminal area were leased to the State of Alaska in 1972. The Coast Guard maintains their own operational area adjacent to the airport which includes Taxiway A and Parking Aprons 1, 2, and 3.

Runway 18/36 is 150 ft wide and 5,011 ft long. It is an asphaltic concrete secondary runway which intersects with runways 7/25 and 10/28. Runway 18/36 is vital for Coast Guard operations. C-130 aircraft utilize this runway for SAR operations when response time is critical. H-3 helicopters use runway 18/36 almost exclusively for SAR launches and other missions. This runway is used for training by all of the Coast Guard aircraft. This use reduces the amount of traffic on Runway 7/25, the primary run-

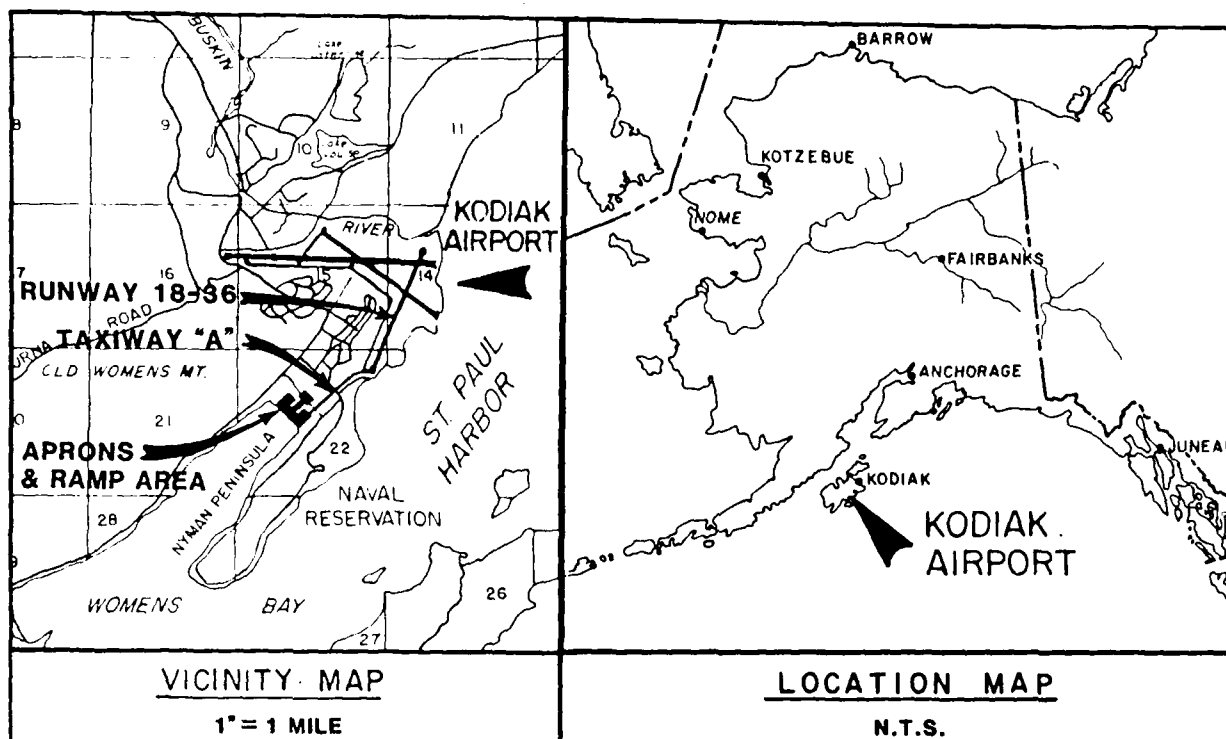


Figure 1. Vicinity and Location Maps, Coast Guard Air Station, Kodiak, Alaska

way, making 7/25 more accessible to other aircraft. Runway 18/36 is also preferable as a cross wind runway when high winds are from the north or south.

At the present time the pavement surface of Runway 18/36 is ravelling and poorly bonded in many areas. Drainage is also exceptionally poor in many areas. In recognition of this situation, the Coast Guard retained R and M Consultants, Inc., of Anchorage, Alaska, to design an overlay for the runway. A component of this work was the use of a Dynatest Falling Weight Deflectometer to determine in situ moduli for the existing pavement structure materials, and the subsequent use of these moduli in a mechanistic approach to asphalt overlay thickness design. The results from this component of the work are reported herein.

PAVEMENT CONDITION SURVEY

Pavement Structural Section for Runway 18/36

Runway 18/36 is an old pavement structure consisting of approximately 4 in. of asphalt concrete (AC) over approximately 6 in. of portland cement concrete

(PCC). The actual thickness of the AC varies from 3 to 7 in. and the PCC from 4 to 8 in. The construction history for the runway is not known at this time. The PCC is underlain by a silty-sandy gravel. This is most likely a fill material. Based on gradations for samples taken by the Alaska Department of Transportation (ADOT) in a 1982 field exploration program, the gravel fraction ranges from 28 to 64%, sand from 18 to 48%, and silt (and clay) from 10 to 24%. The average values of the fractions, based on nine gradation tests, are 50% gravel, 33% sand, and 17% silt (and clay). The majority of the samples taken had a frost susceptibility classification of F2. Under the same field exploration program, asphalt contents were determined for 23 cores. The asphalt contents ranged from 4.9 to 7.5%, with an average value of 5.9%.

Qualitative Survey

A preliminary pavement condition survey was conducted on March 17, 1988. The pavement structure evaluation was based on visual observation of the pavement surface and, as such, was entirely qualitative. The observations were

hampered by inclement weather including high winds and rain. The rain provided an opportunity to observe drainage from the paved areas.

The present pavement condition of Runway 18/36 represents a serious maintenance and, possibly, a serious safety problem. The pavement is in an advanced state of deterioration, particularly over the south half of the runway. The deterioration may be the result of (1) the pavement age and oxidation of the asphalt, (2) the pavement age and an accumulation of the effects of freeze-thaw cycling, (3) stripping of the asphalt cement from the aggregate, (4) weathering and breakdown of the aggregate in the mix, and (5) lack of compaction during original construction and/or other construction control problems.

Drainage from the pavement is very poor, if it exists at all. This is not just a consequence of problems with the cross-slope of the runway; it is also a result of areas of severe deterioration and loss of the pavement that have resulted in birdbaths ranging in size from one yd² to several tens of yd². The large birdbaths may also be associated with fill settlement.

Asphalt (AC) and Portland Cement Concrete (PCC) Coring Program

Thirty AC cores were obtained along Runway 18/36 on June 9, 1988. In addition to these, 41 cores were obtained by ADOT in 1982 as part of a program to evaluate the pavement, base, and subgrade conditions on the runway. A summary of core thicknesses from these programs is given in Figure 2. During the June 1988 coring program the bonding of the AC to the PCC was noted and the degree of surface ravelling was assessed. The results from this effort are presented in Figures 3 and 4.

Ravelling is the progressive separation of the aggregate particles in a pavement from the surface downward or from the edges inward. This erosion results in a rough, pock-marked pavement surface which can greatly reduce traction and drainage, both detrimental to use and safety of the pavement. Ravelling is caused by conditions such as lack of compaction during construction, construction during wet or cold weather, dirty or disintegrating aggregate, a lean asphalt

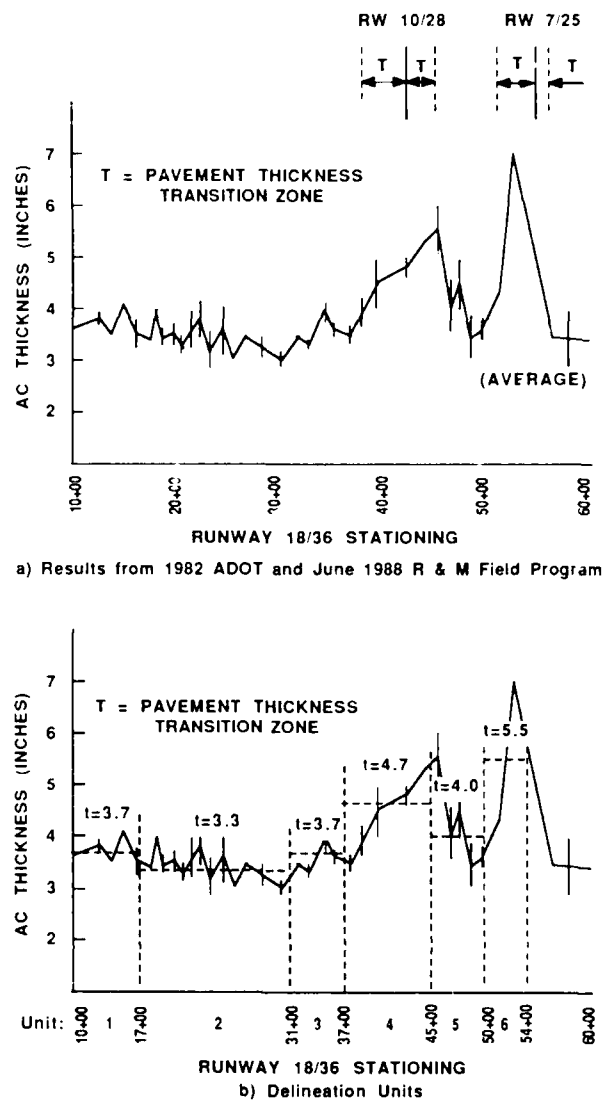


Figure 2. Summary of AC Core Thickness

mix, or overheating of the asphalt hot-mix.

Based on Figure 3, approximately 30% of the runway surface area (excluding the intersections with 10/28 and 7/25) is very ravelled and 55% is moderately to slightly ravelled. Note that most of the very ravelled surfaces occur at both ends of the runway.

An examination of several cores from the June 1988 program indicated that the top lift of AC pavement has a low density. This low density surface lift is probably due to under-compaction or construction during wet and cold conditions.

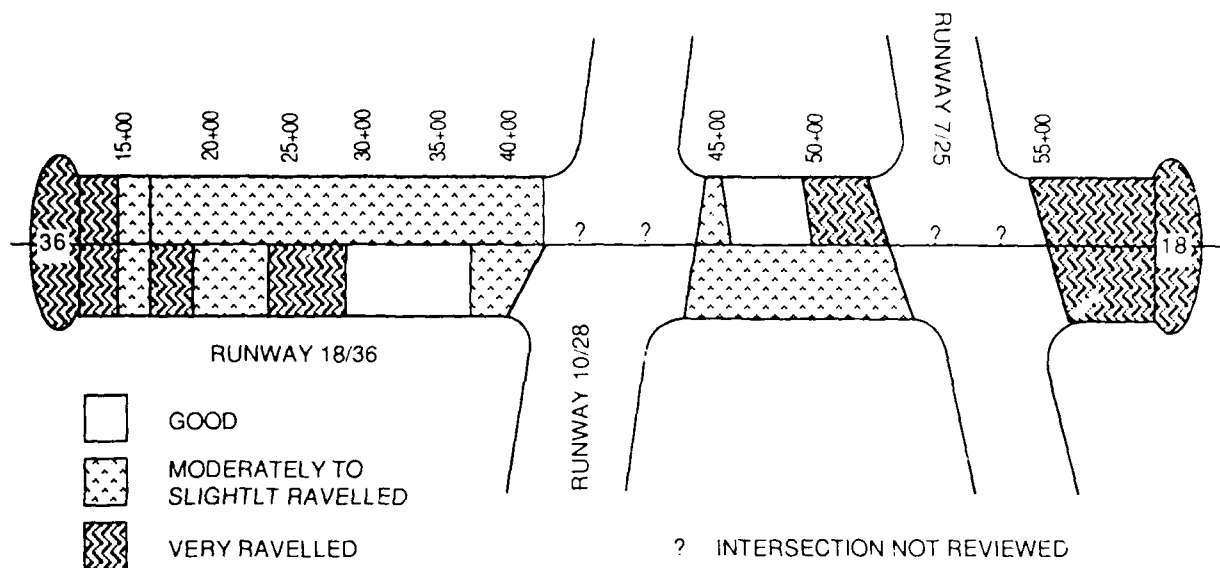


Figure 3. Ravelling Condition Survey for Runway 18/36

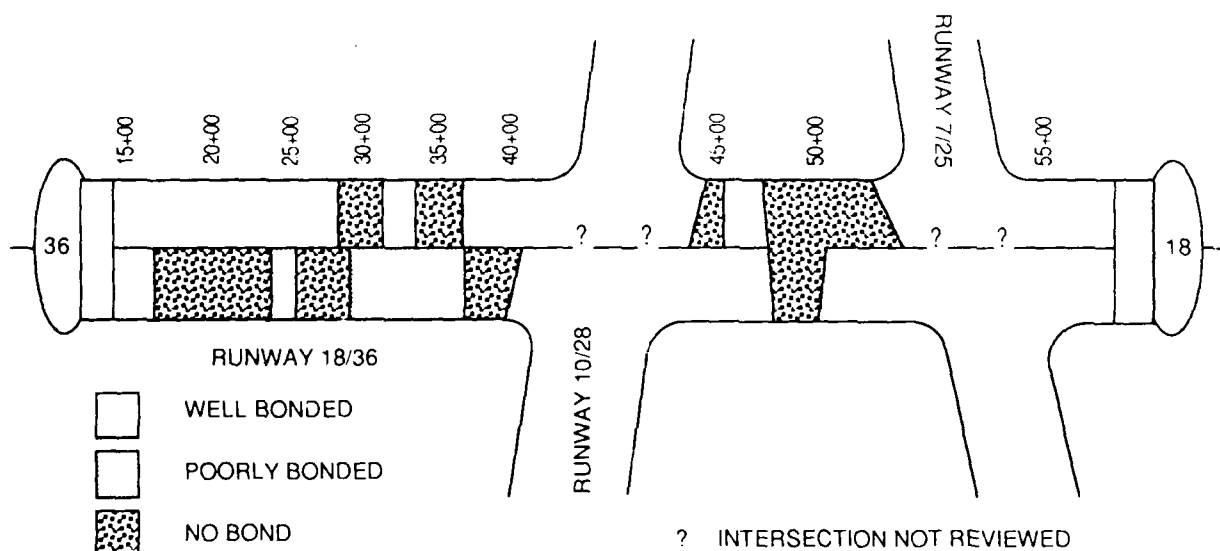


Figure 4. AC to PCC Bonding Condition Survey for Runway 18/36

The lateral extent of the low density surface closely matches the ravelled areas mapped on Figure 3. Further, the asphalt cement in the top lift appeared to be oxidized, possibly due to weathering or overheating during original production.

The AC pavement was placed directly on top of the PCC (original surface) along the entire runway except for the short section (approximately 500 ft) north of the intersection with 7/25. This short north section includes a crushed aggregate base between the AC

pavement and PCC. The condition of the bond between the AC and the PCC was evaluated by inspection of the pavement cores and holes.

Based on Figure 4, it may be noted that approximately 30% of the runway surface area (excluding the intersections with 10/28 and 7/25, and runway 18/36 north of 7/25) may not be bonded, 20% may be only poorly bonded, and about 50% may be well bonded to the underlying PCC. These percentages are purely estimates, based on a visual inspection of a limited number of cores.

FALLING WEIGHT DEFLECTOMETER (FWD) DEFLECTION SURVEY

During the period October 26-28, 1988, a FWD survey was conducted on Runway 18/36. Specifically, pavement conditions were evaluated at 146 locations on Runway 18/36. Forty-six locations were evaluated at 100-ft spacing on centerline, 50 locations were evaluated at 100-ft spacing 7 ft left of centerline, and 50 locations were evaluated at core sample locations 25 ft right and left of centerline. Overall, comprehensive coverage of the runway was achieved.

The deflection survey was conducted with a Dynatest Model 8000 FWD. The deflection gages were spaced at 0, 12, 18, 32, 47, 63, and 78 in. from the center of the falling weight. Load levels of approximately 14,000, 20,000, and 24,000 lbs were used in the survey and the 24,000-lb level was repeated.

ANALYSIS OF DEFLECTION DATA

The deflection data obtained in the survey were analyzed using the following steps: (1) delineation of pavement analysis units, and (2) backcalculation of pavement structure layer moduli.

Delineation of Pavement Analysis Units

Runway 18/36 has a length of approximately 5,000 ft. It is necessary to delineate the pavement into several analysis units so that variation of pavement response and structure properties for each analysis unit may be individually considered.

Two possibilities exist to delineate the pavement analysis unit. First, the pavement condition survey could be used, focusing on a qualitative assessment of the combined significance of surface ravelling and AC-PCC bonding to the FWD deflection survey results. Second, pavement sections could be delineated based on the average thickness of the AC surface layer. Rwebangira et al. (1987) established that values of moduli backcalculated from FWD deflection surveys are sensitive to layer thickness and depth to the stiff layer. Therefore, the latter approach was adopted.

Considering the results presented in Figure 2, it appears most appropriate to delineate six units for Runway 18/36.

The stationing and AC thicknesses for the pavement analysis units are presented in Table 1. The PCC was assumed to have a uniform thickness of 6.1 in. based on a limited field coring program conducted in October 1988.

Table 1. Delineation of Pavement Analysis Units

Delineation Unit	Station Number	AC (Surface) Thickness (in.)
1	10+00 - 17+00	3.7
2	17+00 - 31+00	3.3
3	31+00 - 37+00	3.7
4	37+00 - 45+00	4.7
5	45+00 - 50+00	4.0
6	50+00 - 54+00	5.5

Note: PCC thickness (base layer) is 6.1 in. for the entire length of the runway.

Backcalculation of Pavement Structure Layer Moduli

Two backcalculation programs, ELMOD and BOUSDEF, were used to determine the moduli values for the AC, PCC, and subgrade.

ELMOD Program. ELMOD, or Evaluation of Layer Moduli and Overlay Design is a proprietary program of Dynatest Consulting, Inc., Ojai, California. In this program the method of equivalent thickness is used together with Boussinesq's theory to calculate the layer moduli of a pavement structure using load deflection data generated by an FWD (Ullidtz and Stubstad, 1986). A maximum of four layers can be used and the program will allow consideration of non-linear subgrade response.

Table 2 summarizes the backcalculation results for the six delineation units using the ELMOD program. For the ELMOD backcalculation the modulus of the AC layer was estimated to be 800 ksi for

Table 2. Summary of Backcalculation Results from ELMOD

Delineation Unit	AC (Surface) Modulus (ksi)	PCC (Base) Modulus (ksi)	Subgrade Modulus (ksi)
1	800	3010 (970)*	22 (6)
2	800	2240 (1520)	22 (6)
3	800	3540 (1290)	22 (2)
4	800	3240 (900)	33 (6)
5	800	2460 (620)	26 (4)
6	800	2750 (580)	30 (2)

*Standard Deviation

the survey temperature of 45°F. A reduction of the modulus for the AC would give an increase in the modulus for the PCC.

BOUSDEF Program. BOUSDEF is a backcalculation program developed at Oregon State University (Zhou, et al., 1988). The program determines modulus values for each pavement layer from deflection basin data using the method of equivalent thicknesses and Boussinesq's theory. The program is capable of handling n-layers; it treats all layers as linear elastic materials. While the theoretical basis is similar to ELMOD, the program logic is the same as the logic for BISDEF (Bush, 1980).

Table 3 summarizes the backcalculation results from the BOUSDEF program for the pavement sections. The subgrade modulus was estimated using the AASHTO Guide equation (AASHTO, 1986) which has the form

$$E_{sg} = PS_f / (\gamma d_r) \quad (1)$$

in which

E_{sg} = in situ modulus of elasticity of the subgrade, psi;

Table 3. Summary of Backcalculation Results from BOUSDEF

Delineation Unit	AC (Surface) Modulus (ksi)	PCC (Base) Modulus (ksi)	Subgrade Modulus (ksi)
1	560 (170)*	1700 (630)	27 (7)
2	260 (140)	1390 (330)	30 (7)
3	320 (200)	2220 (770)	32 (2)
4	590 (60)	2620 (900)	38 (4)
5	560 (70)	1740 (500)	32 (3)
6	510 (140)	3470 (820)	36 (3)

*Standard Deviation

- P = dynamic load of the NDT device, lbs;
- d_r = measured NDT deflection at a radial distance of r from the NDT plate load center, mils;
- γ = radial distance from plate load center to point of d_r measurement, inches; and
- S_f = the subgrade modulus prediction factor (for subgrade with $\mu = 0.35$, $S_f = 0.293$).

Comparison of Backcalculated Resilient Modulus

Figure 5 presents comparisons of backcalculated resilient moduli using ELMOD and BOUSDEF. For both AC and PCC layers, BOUSDEF gave lower moduli than ELMOD in most cases, while for the subgrade, resilient moduli obtained from ELMOD are lower than those calculated using the AASHTO equation.

Both deflection survey data and the pavement condition survey (re. Figures 3 and 4) indicate that there should be significant variations in AC moduli along the runway. Severe ravelling and low density asphalt concrete could be found in many sections of the runway. These

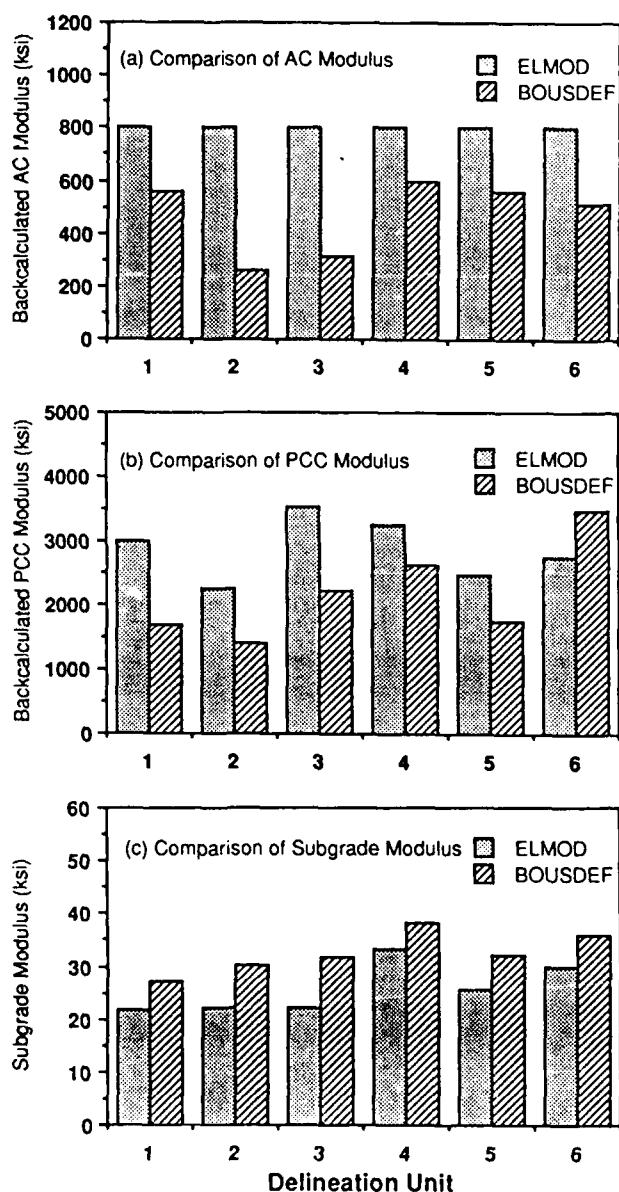


Figure 5. AC, PCC, and Subgrade Moduli Backcalculated with ELMOD and BOUSDEF

variations are not reflected in the ELMOD results. In this regard, the results from BOUSDEF appear to better reflect the actual surface condition of the runway.

Table 4 presents resilient moduli of AC and PCC field cores extracted at the time of the deflection survey. The resilient moduli were determined in the laboratory following ASTM D-4123. The laboratory AC moduli are greater than the moduli backcalculated with BOUSDEF and are close to those assumed for the ELMOD

backcalculation. The laboratory PCC moduli are approximately twice those backcalculated with both ELMOD and BOUSDEF. The laboratory moduli should be greater than the moduli backcalculated in the field owing to the fact that intact cores are tested in the laboratory whereas moduli backcalculated in the field reflect cracks in the slab, proximity to a joint, and joint transfer (all of which would tend to reduce the modulus).

The results from the PCC layer from BOUSDEF appear to be low, while the results from ELMOD appear to be more reasonable.

OVERLAY DESIGN RECOMMENDATIONS

Based on the March 1988 pavement inspection and evaluation, as well as the June 1988 coring project, the asphalt pavement structure of Runway 18/36 should be completely removed to expose the underlying PCC prior to construction of a new AC overlay. The present pavement condition presents a serious maintenance and, possibly, a serious safety problem. Both the surface of the AC and the bond with the PCC are in advanced stages of deterioration. Drainage, which was minimal by original design (due to limited cross slope), is greatly restricted by the ravelled surface over most of the pavement area.

The estimates of removed pavement quantities will be affected by the apparent deterioration of the top of the PCC. As previously discussed, approximately 50% of the existing AC overlay appears to be well bonded to the PCC. However, the cores also indicated the top of the PCC may be weathered and ravelling at several locations. During AC pavement removal, some quantity of PCC may also be picked up with the AC for disposal.

Figure 6 illustrates the proposed overlay design. The parameters used for the overlay design are listed in Table 5. The design aircraft load of 37,000 lbs represents a tire in the main gear assembly of a Hercules C-130 (HC-130).

Load Repetitions to Failure (N_f)

The load applications to failure were determined based upon the ratio of the maximum tensile stress to the static flexural strength (referred to as the

Table 4. Laboratory Resilient Moduli of AC and PCC Cores

Delineation Unit	Station (on C _L)	AC Modulus @ 70°F* (ksi)	AC Modulus @ 45°F** (ksi)	PCC Modulus (ksi)
1	15+50	290	870	5,800
2	21+50	240	720	5,180
2	29+50	230	690	4,860
3	36+60	170	510	3,090
4	44+95	120	360	3,120

*Test Condition

**Adjusted (based on AASHTO Guide Equation)

Table 5. Overlay Design Parameters

Design Parameter	Specification
Asphalt	AC-5
Asphalt content	6%
Penetration @ 77°F	140 (min)
Air voids	4%
P ₂₀₀	5%
Temperature	55°F
Vehicle speed	30 mph
Resilient modulus	850 ksi

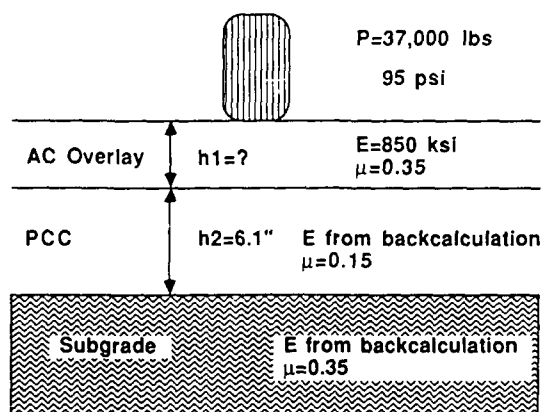


Figure 6. Schematic Representation of Overlay Design

stress ratio) in the PCC layer. (The static flexural strength is equal to the modulus of rupture.) Several relationships have been presented in the literature for the stress ratio versus load applications to failure, as shown in Figure 7. Obviously, there are substantial differences in the relationships presented.

PCA Method (Yoder and Witczak, 1966). The PCA criteria were developed by the Portland Cement Association. It

represents a lower bound of laboratory beam fatigue test results. The concrete layer is assumed to be capable of sustaining an infinite number of load applications if the stress ratio is less than 0.50.

Vesic's Method (Vesic and Domaschuk, 1966). Vesic analyzed the AASHTO road test data using Westergaard plate theory to determine stresses and established the following relationship:

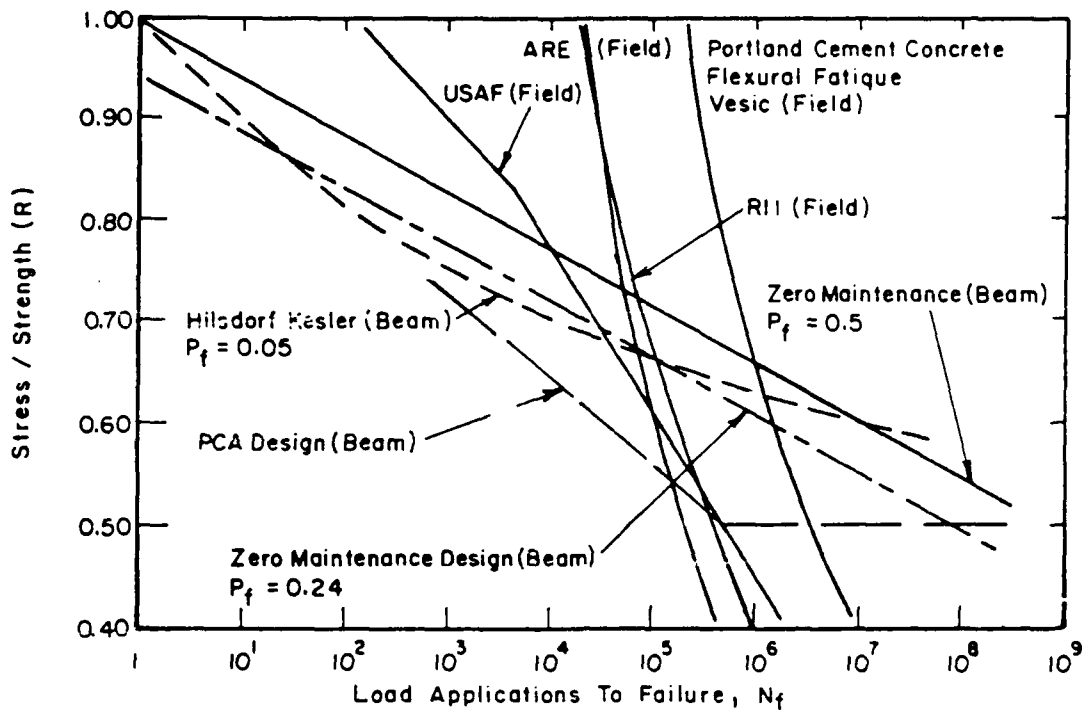


Figure 7. Summary of PCC Fatigue Models for Laboratory Beams and Accelerated Full-Scale Tests (after Majidzadeh, et al., 1985).

$$N_f = 225,000 \left(\frac{MR}{\sigma} \right)^4 \quad (2)$$

in which:

σ = the tensile concrete stress (psi).

Modulus of Rupture (MR)

The modulus of rupture for the existing PCC layer was estimated from average modulus values backcalculated from the deflection data. The PCC moduli backcalculated from ELMOD appear to be more reasonable than the PCC moduli backcalculated from BOUSDEF and were therefore used for the overlay design. The following relationships from Troxell, et al. (1968) were used to determine the modulus of rupture (MR) of the PCC:

$$MR = K \sqrt{f_c} \quad (3)$$

in which:

K = coefficient, ranges from 8 to 10,

and

$$\sqrt{f_c} = \frac{E}{33(\rho)^{1.5}} \quad (4)$$

in which:

E = modulus of PCC (psi), from backcalculation
 ρ = density of PCC (pcf)

For this design, the density (ρ) of the PCC was assumed to be 140 pcf and K was 10, so that

$$MR = \frac{E}{5470} \quad (5)$$

Overlay Thickness Determination

The tensile stress induced in the PCC by the design aircraft loading was calculated using the ELSYM5 program (Hicks, 1982). Table 6 summarizes the calculation results. As may be noted, the load repetitions to failure for a given thickness of overlay are significantly different for the two methods considered.

The Kodiak Airport master plan has forecast that Kodiak Airport can expect 107,000 operations per year by the year 2005. Assuming a conservative 1/4 of these operations would occur on Runway

Table 6. Summary of Overlay Thickness Design Calculations

Delineation Unit	Modulus of Rupture (MR) (psi)	AC Overlay (in.)	σ (psi)	$\frac{\sigma}{MR}$	Load Repetitions to Failure	
					PCA ($\times 10^3$)	Vesic ($\times 10^6$)
1	550	4	360	.65	8	1.3
		5	320	.58	57	2.0
		6	290	.53	240	2.9
		7	270	.48	∞	4.1
2	410	5	280	.68	3.5	1.0
		6	250	.61	24	1.6
		7	230	.56	100	2.3
		8	210	.51	400	3.3
3	650	3	420	.65	6	1.2
		4	380	.59	42	1.9
		5	340	.53	240	2.8
		6	310	.48	∞	4.2
4	590	3	360	.61	24	1.6
		4	330	.55	130	2.4
		5	300	.50	∞	3.6
5	450	4	310	.69	2.5	1.0
		5	280	.62	18	1.5
		6	250	.56	100	2.2
		7	230	.52	300	3.2
		8	210	.47	∞	4.6
6	500	4	310	.62	18	1.6
		5	280	.56	100	2.3
		6	260	.52	400	3.4
		7	230	.46	∞	4.8

18/36, one would expect something on the order of 27,000 operations per year. Alexander (1988) estimates that approximately 7,300 of these operations will be HC-130 aircraft, HH3F's, and HH52A helicopters since this is the preferred runway for Coast Guard operations. If a design life of 20 years is assumed, then a maximum of 140,000 HC-130 load applications are to be expected. Considering this number of load applications, the AC overlay thickness required by the PCA criteria is from 6 to 7 in. while using Vesic's criteria, a 4 in. overlay is satisfactory for the entire runway length. The required AC overlay thickness appears to be more sensitive to the fatigue failure criteria used for the PCC than the method (i.e., program) used to backcalculate the PCC moduli.

Two additional factors must be considered when evaluating the potential of a fatigue failure in the PCC. First, a forecast of the number of aircraft operations at Kodiak Airport does not translate directly to the number of stress repetitions at a point in the pavement structure. This results from the fact that aircraft do not traverse the same point on the pavement with each pass of the aircraft. Brown and Thompson (1973) established a 70 in. wander width for aircraft on a primary taxiway and a wander width of 140 in. on a runway interior

or parking apron. Second, the prediction of remaining life (expressed in load repetitions) in a pavement must begin with an estimate of the past accumulated damage (expressed in terms of load repetitions). That is,

$$\begin{array}{rcc} \text{Remaining} & & \text{Load} & & \text{Past} \\ \text{Fatigue} & = & \text{Repetitions} & - & \text{Accumulated} \\ \text{Life} & & \text{to} & & \text{Damage} \\ & & \text{Failure} & & \end{array}$$

In the analysis presented the past accumulated damage is considered to be negligible.

Table 7 presents a sensitivity analysis on the effect of the PCC modulus on load repetitions to failure. A 4 in. overlay thickness with the properties given in Table 5 was selected for the sensitivity analysis. Considering Vesic's criteria, a 4 in. overlay thickness would be acceptable if the PCC modulus was slightly greater than 1,000 ksi. Considering the PCA criteria, the PCC modulus must be 4,000 ksi to prevent fatigue distress in the PCC.

Examination of AC Overlay

In general, tensile strains are not likely to occur in an AC overlay on PCC. This was verified for a 4-in. overlay thickness using the ELSYM5 program. Reflection cracking is probably unavoid-

Table 7. Effect of PCC Modulus on Allowable Repetitions

PCC Modulus (ksi)	Modulus of Rupture MR (psi)	σ^* (psi)	$\frac{\sigma}{MR}$	Load Repetitions to Failure	
				PCA ($\times 10^3$)	Vesic ($\times 10^6$)
1,000	180	210	1.17	N/A	.1
2,000	370	290	0.78	N/A	.5
3,000	550	360	0.65	8	1.3
4,000	730	400	0.55	130	2.4
5,000	940	450	0.48	∞	4.5
6,000	1100	480	0.44	∞	6.1

*AC overlay = 4 inches, PCC = 6.1 inches, and subgrade modulus = 22.3 ksi

able, but the rate and extent of reflection cracking cannot be predicted. Further, an economic solution to the reflection cracking problem apparently does not exist, despite extensive work using techniques such as stress and strain relief interlayers, geotextiles, or reinforcing in the overlay. Rutting of an AC overlay is influenced primarily by the properties of the AC mix and the quality of construction. To prevent rutting a crushed aggregate must be used in the mix and the mix must be compacted to a high density during construction.

SUMMARY AND CONCLUSIONS

An FWD deflection survey was conducted on Runway 18/36 at the Coast Guard Air Station at Kodiak Airport, Alaska. Moduli for the existing AC, PCC, and subgrade were backcalculated using two programs, ELMOD and BOUSDEF. The AC moduli backcalculated with BOUSDEF appear to more accurately reflect the condition of the surface layer whereas the PCC moduli backcalculated with ELMOD appear to more accurately reflect the condition of the PCC. An AC overlay design based on the PCC moduli from ELMOD suggests that the required AC overlay thickness is more sensitive to the fatigue failure criteria used for the PCC than the method (i.e., program) used to backcalculate the PCC moduli from the FWD survey results.

ACKNOWLEDGEMENTS

Nick Coetze, Dynatest, Inc., performed the ELMOD calculations and provided valuable guidance in the mechanistic approach presented herein. Billy Connor and Rick Briggs, ADOT&PF arranged for the use of the Dynatest Model 8000 FWD in the deflection survey. Jim Rooney provided valuable review of the paper. Ms. Peggy Offutt skillfully typed and arranged all figures and tables in the "camera ready copy".

REFERENCES

AASHTO, *AASHTO Guide for Design of Pavement Structures 1986*, 1986.

- Alexander, R., "U.S. Coast Guard Support Center, Kodiak, Alaska, Runway 18/36 Repaving Design Development Submittal," Report submitted to U.S. Department of Transportation, U.S. Coast Guard, Seattle, WA, April 1988.
- Brown, D.N. and O.O. Thompson, "Lateral Distribution of Aircraft Traffic," Miscellaneous Paper S-73-56, U.S. Army WES, Vicksburg, MS, 1973.
- Bush, A.J., "Nondestructive Testing of Light Aircraft Pavements, Phase II, Development of the Nondestructive Evaluation Methodology," Final Report No. FAA-RD-80-9-II, Federal Aviation Authority, November 1980.
- Dynatest Consulting, Inc., *ELMOD - Evaluation of Layer Moduli and Overlay Design*, Undated.
- Hicks, R.G., "Use of Layered Theory in the Design and Evaluation of Pavement Systems," Report No. FHWA-AK-RD-83-8, July 1982.
- Majidzadeh, K., G.J. Ilves, and H. Sklyut, "RISC - A Mechanistic Method of Rigid Pavement Design," *Proceedings, Third International Conference on Concrete Pavement Design*, Purdue University, 1985.
- Rwebangira, T., R.G. Hicks, and M. Truebe, "Sensitivity Analysis of Selected Backcalculation Procedures," *Transportation Research Record 1117*, Transportation Research Board, Washington, DC, 1987.
- Troxell, G.E., H.E. Davis, and J.W. Kelly, *Composition and Properties of Concrete*, McGraw-Hill Book Co., 2nd Edition, 1968.
- Ullidtz, P. and R.N. Stubstad, "Analytical-Empirical Pavement Evaluation Using the Falling Weight Deflectometer," *Transportation Research Record 1022*, Transportation Research Board, Washington, DC, 1986.
- Vesic, A.S. and L. Domaschuk, "Theoretical Analysis of Structural Behavior of Road Test Flexible Pavements," *Highway Research Board, NCHRP Report 10*, 1966.
- Yoder, E.J. and M.W. Witczak, *Principles of Pavement Design*, Second Edition, John Wiley and Sons, Inc., 1975.
- Zhou, H., R.G. Hicks, and C.A. Bell, "BOUSDEF: A Backcalculation Program for Determining Moduli of a Pavement Structure," *Transportation Research Institute Report No. 88-10*, Oregon State University, January 1988.

VARIABILITY OF PAVEMENT LAYER MODULI FROM NDT MEASUREMENTS

by

G. R. Rada, Senior Pavement Engineer, Pavement Consultancy Services/LAW
W. Uddin, Senior Pavement Engineer, Texas Research and Development Foundation
M. W. Witczak, Professor, Civil Engineering Department, University of Maryland

ABSTRACT

At present, the most accurate and practical assessment of pavement structural capacity is achieved through the measurement and subsequent analysis of deflection basins resulting from a dynamically applied load. For mechanistic evaluation of pavements, the deflection data collected is generally analyzed to backcalculate the effective modulus of each pavement layer. When numerous deflection basins are analyzed, however, variable layer moduli are generally predicted. This variability and its magnitude are due to a number of pavement characteristics such as non-uniform layer thicknesses, varying material and subgrade soil properties, etc. There are also a number of factors that may lead to inaccurate moduli calculations or to the selection of non-representative modulus values for use in the evaluation process; e.g., presence of rigid layer, material non-linearity, environmental effects, etc. In this paper, a summary of the major factors affecting the backcalculation of effective layer moduli from deflection measurements is presented. These factors are grouped into four major categories: pavement-subgrade system, environmental conditions, deflection testing, and analysis techniques. Examples illustrating the influence of many of these factors are also presented. Additionally, procedures presently in use for taking these factors into account are discussed.

INTRODUCTION

Since its introduction several decades ago, nondestructive testing (NDT) has been an integral part of the structural evaluation of pavements. In the earliest years, this evaluation was based upon the analysis of a single deflection measurement resulting from a static or slow-moving load. However, as experience with deflection testing grew and technical advances were made, predictive capabilities greatly improved. Currently, the most accurate and practical assessment of pavement structural capacity is achieved through the measurement and subsequent analysis of deflections at various radial distances (i.e., deflection basin) resulting from a dynamically applied load.

Numerous methods for evaluating the structural capacity of pavements from

deflection basin data are presently available. All of these methods are based on the supposition that a unique set of layer elastic moduli exists such that the theoretically predicted deflection basin is equivalent to the measured deflection basin. In addition, most of these methods rely on layered elastic theory concepts and use a computerized iterative solution, a graphical solution or nomographs to backcalculate the elastic modulus of each pavement layer.

In many ways, deflection based pavement structural evaluations can be viewed as an inverted design process. When designing a pavement, the layer thicknesses and material properties are used to compute the pavement response (stresses, strains and displacements) for a specified set of loading conditions. In the pavement evaluation process, on the other hand, the resp-

onse of the pavement is measured and the effective in-situ moduli are backcalculated.

Unlike the design process, NDT based pavement evaluation studies seldom, if ever, yield a unique set of moduli. Instead, when numerous deflection basins are analyzed, variable layer moduli are generally calculated. This variability and its magnitude are due to a number of factors such as non-uniform layer thicknesses, varying paving material and subgrade soil properties, etc. An example of this variability is given in Figures 1, which shows the distribution of granular base moduli derived from the analysis of 90 deflection basin tests performed, using a falling weight deflectometer (FWD), at the FHWA's Accelerated Load Facility (ALF) in Virginia (13). As can be observed, modulus values range from 4 to 72 ksi, with a mean of 36 ksi.

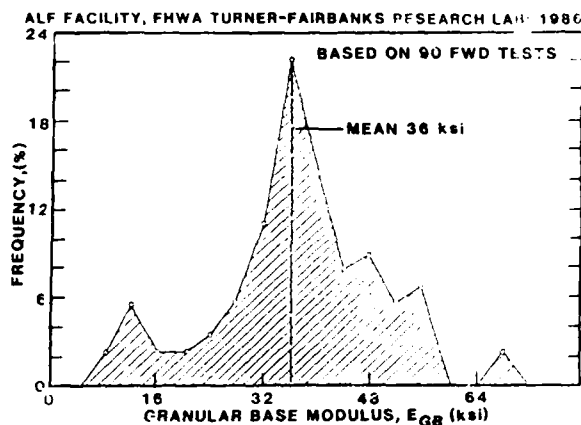


FIG 1 EXAMPLE OF LAYER MODULUS VARIABILITY

There are also a number of factors that, unless accounted for, may result in inaccurate moduli calculations or in the selection of non-representative values for use in the evaluation process; e.g., environmental effects, pavement discontinuities, material non-linearity, depth to rigid layer, etc. Figure 2, for example, illustrates the influence of material non-linearity and environmental factors upon the subgrade moduli calculated for two adjacent pavement test sections (13). As shown, all modulus values are lower (below line of equality) when non-linearity effects are incorporated into the analysis. Also, instead of a unique value, the average (non-linear) subgrade modulus (directly under the load center) varies from 3 to 9 ksi for Section No 1 and from 8 to 35

ksi for Section No 2 due to the varying environmental conditions in different seasons.

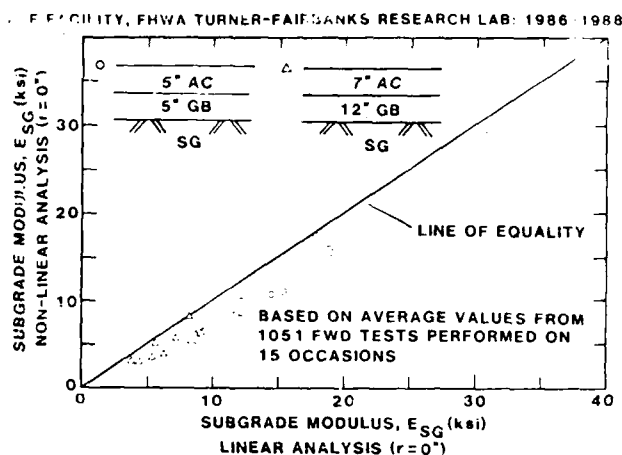


FIG 2 INFLUENCE OF MATERIAL NON-LINEARITY AND ENVIRONMENT UPON SUBGRADE MODULUS

In this paper, a summary of the major factors affecting the calculation of layer moduli and its variability is presented. For discussion purposes, these factors have been grouped into four major categories: pavement-subgrade system, environmental conditions, deflection testing and analysis (backcalculation) techniques. Examples illustrating the influence of many of these factors are provided. Additionally, procedures presently used for taking these factors into account are briefly discussed.

PAVEMENT-SUBGRADE SYSTEM

The influence of the pavement-subgrade system upon measured deflections is best illustrated by reference to Figure 3, which shows a pavement structure being deflected under a dynamic NDT load. As the test is conducted, the load applied to the surface is distributed through the depth of the pavement-subgrade system. The distribution of stresses, represented by the "Zone of Stress", is obviously dependent upon the stiffness of each layer. As the stiffness of the material increases, the stress is spread over a larger area (1).

Layer stiffnesses, in turn, are affected by layer thickness and modulus variations in both the vertical and longitudinal direction (12). Accordingly, these variations can be grouped into two broad categories: random variations and stratified variations.

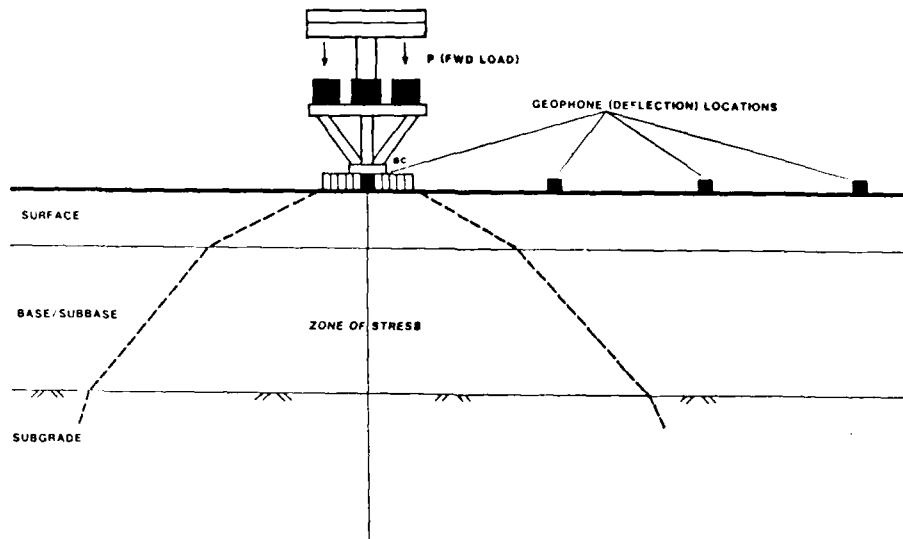


FIG 1 SCHEMATIC OF STRESS ZONE WITHIN PAVEMENT STRUCTURE UNDER THE FWD LOAD
(from AASHTO guide(1))

Random variations are due to the heterogeneous nature of the pavement materials and non-uniform layer thicknesses. This type of variation is normal (present in all pavements) but its magnitude depends, to a great extent, on such factors as construction quality. An example of this type of variation is illustrated in Figure 4, which shows normalized deflections (under center of load) over a 7 mile stretch of Interstate I-95 in the State of Delaware (16). With the exception of a few localized data points, deflection variations are relatively uniform throughout the length of the project.

Typically, random variations are incorporated into the pavement evaluation process through the selection of design values (deflections or predicted layer moduli) based on the statistical variability and desired confidence (reliability) level; e.g., use of 50th percentile deflection values (basin) for analysis of low volume roads, use of 85th percentile predicted layer moduli for evaluation of major roads, etc.

Stratified variations, on the other hand, are due to significant changes in layer thicknesses or material properties.

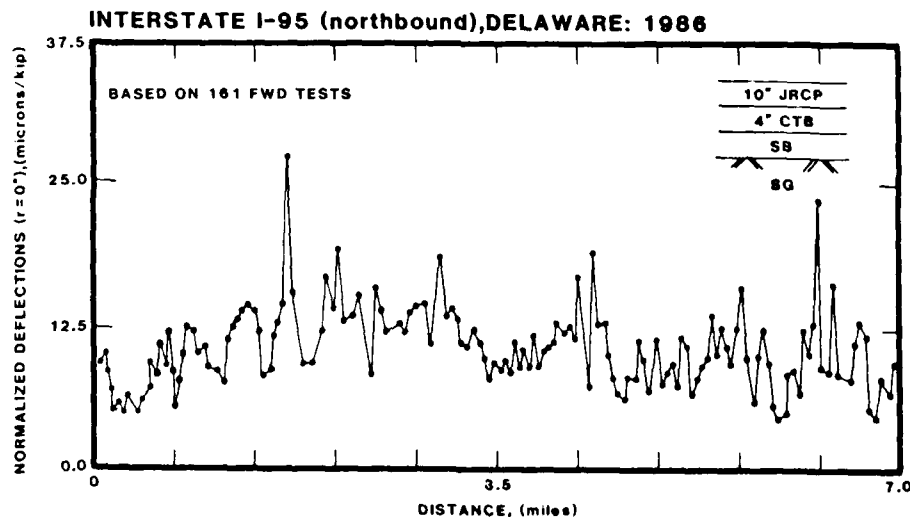


FIG 4 EXAMPLE OF RANDOM VARIATIONS DUE TO NON-UNIFORM THICKNESSES AND MODULI CHANGES

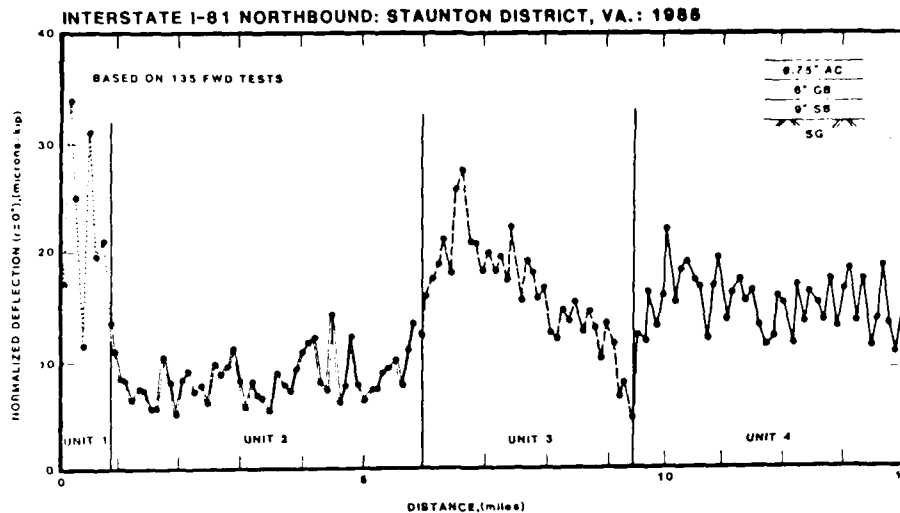


FIG 5 EXAMPLE OF STRATIFIED VARIATIONS DUE TO SHALLOW BEDROCK (cuts/fills)

Examples of stratified variation are shown in Figures 5 and 6. In Figure 5, a plot of normalized deflections (under center of load) over a 15 mile stretch of Interstate I-81 in the State of Virginia is presented (15). As shown, four distinct units (each with its own random variations) are apparent along this stretch of interstate. The stratified variations shown are due to the presence of bedrock at shallow depths (i.e., cuts and fills).

heavy traffic, have led to the development of edge punchouts.

Unlike random variations, stratified variations should not be directly incorporated into the layer moduli analysis. Instead, the measured deflections should be used to delineate unique (homogeneous) pavement sections along the length of the project prior to the backcalculation of layer moduli. An example of deflection based unit delineation has already been presented in Figure 5.

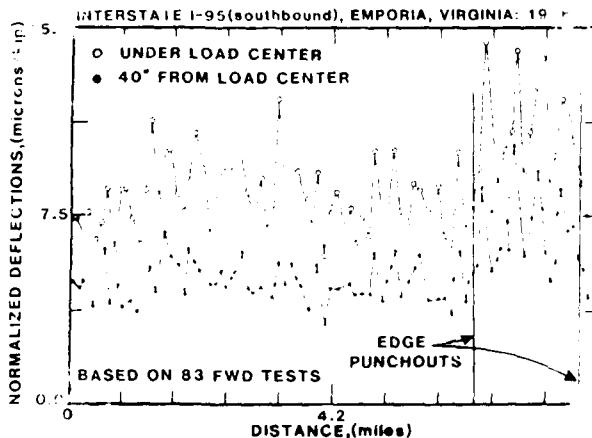


FIG 6 EXAMPLE OF STRATIFIED VARIATIONS DUE TO POOR DRAINAGE

Figure 6 also shows a plot of normalized deflections (under center of load and 40 inches away from center) for more than 8 miles of Interstate I-95 in the State of Virginia (14). As can be observed, significantly higher deflections occur between project mileposts 6.5 and 8.4 due to weaker subgrade conditions caused by poor drainage in the area which, along with

Another set of pavement related factors affecting deflection measurements and hence backcalculated layer moduli are pavement discontinuities (12,20). The presence of pavement discontinuities such as cracks and/or joints, and subsurface conditions such as voids beneath rigid pavements will lead to higher deflection readings and hence lower moduli for all other factors being the same. The magnitude of the deflection increase is, however, dependent on the degree and severity of cracking and/or the joint opening.

The influence of pavement discontinuities upon the pavement response is best illustrated by reference to Figure 7, which shows normalized deflection plots for two very similar pavement structures at Suffolk Municipal Airport in Virginia (17). The only difference between them is that one has been intentionally cracked to minimize reflective cracking in the AC overlay. As shown, deflection readings

under the load center are considerably higher for the cracked PCC while the far-away readings, which are primarily related to the subgrade strength, are almost the same. Consequently, the deflections measured under the load center indicate that the effective modulus of the cracked PCC is considerably lower. This is confirmed by reference to Table 1, which summarizes the backcalculated layer moduli.

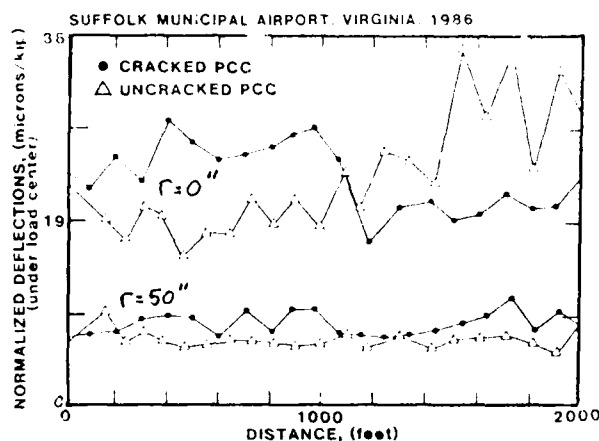


FIG 7 INFLUENCE OF CRACKING UPON MEASURED DEFLECTIONS

TABLE 1
PCC LAYER MODULI - CRACKED vs. UNCRACKED

	NUMBER OF HOT TEST POINTS	STATISTIC OF INTEREST	MODULUS (ksi)	
			PCC	SUBGRADE
CRACKED PCC	100	MEAN	1920	14.2
		STD. DEV.	1100	2.2
UNCRACKED PCC	202	MEAN	3780	14.7
		STD. DEV.	1610	2.7

However, while pavement discontinuities significantly affect the deflections and backcalculated effective moduli, measurement bias should not be built into the deflection testing. If deflection tests over cracked areas are avoided, for example, the effective layer moduli will not be representative of the overall pavement condition. Likewise, if deflection readings are taken in cracked areas only, unrealistically low effective moduli will result.

In addition to layer stiffness variations and pavement discontinuities, deflection measurements are also affected by the presence of a rigid (rock) layer at some finite depth (22,23). For all other factors the same, the measured deflections decrease as the depth to the rigid layer

decreases. This influence has already been illustrated in Figure 5, which showed significant variations in normalized deflections due to variable subgrade depths (i.e., cuts and fills) to bedrock.

Ignoring rigid bottom considerations in the analysis can lead to substantial errors in the calculated layer moduli, particularly the subgrade. The subgrade modulus can be significantly over-predicted, for example, if a semi-infinite soil layer is assumed, when bedrock exists at shallow depths. Unfortunately, no universally accepted procedure for incorporating rigid bottom effects is presently available. Existing procedures range from the use of an arbitrary depth of subgrade to the rigid layer (say 20 feet) to the correction of subgrade moduli based on the ratio of actual (finite depth) to equivalent (semi-infinite depth) outer deflections.

Non-linear behaviour of pavement materials and subgrade soils is another important pavement-subgrade system consideration in the backcalculation of effective in situ moduli from measured deflections (8,22). To date, numerous researchers have shown that the dynamic response of many paving materials is dependent on the state stress. Typically, unbound granular base/subbase materials stiffen (modulus increases) while cohesive subgrade soils soften (modulus decreases) as the stress state increases. More importantly, ignoring non-linearity in the analysis can lead to significant errors in the predicted moduli. An example of this has already been given in Figure 2, which showed the difference in subgrade moduli predicted using linear versus non-linear analysis techniques. As indicated, ignoring material non-linearity in the analysis results in higher predicted subgrade moduli directly under the load center.

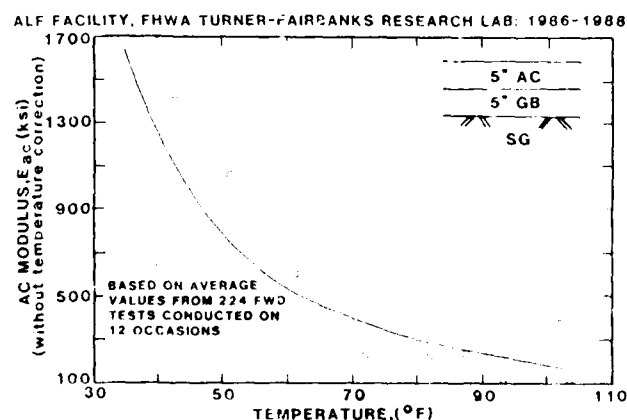
Several attempts have been made to date to incorporate material non-linearity into the backcalculation of layer moduli from deflection data. A few finite-element models, for example, are presently available that directly incorporate non-linearity. Most procedures, however, are based upon the use of layered elastic theory concepts and, consequently, incorporate non-linearity into the analysis by indirect means; e.g., use of outer deflection readings (or surface moduli) to es-

establish subgrade modulus versus stress (or radial distance) relations, and application of strain sensitive models for equivalent linear analysis.

ENVIRONMENTAL CONDITIONS

Without question, one of the most significant factors affecting the response of pavements to dynamically applied loads is the environment. Temperature affects deflection measurements and hence the effective layer moduli of both flexible (AC) and rigid (PCC) pavements. The stiffness of asphalt mixtures is very sensitive to seasonal temperature changes as well as daily temperature gradients throughout the depth of the asphaltic layer. As the temperature changes, the magnitude of the deflection under a given load also changes. For all other factors the same, surface deflections measured on a hot summer day will be larger than the deflection measured during a cooler period. In addition, the influence of temperature becomes more pronounced as the thickness of the asphalt layer(s) increases.

The effect of temperature upon asphaltic mixtures is best illustrated by reference to Figure 8. As shown, a significant decrease (from 1,700 to 100 ksi) in the average AC layer modulus occurs as the temperature increases (from 42 to 100 °F). The modulus-temperature relation shown in this figure was developed based on 224 deflection basin tests performed at the FHWA's ALF facility on 12 different occasions over an 18 month period (13).



Like flexible pavements, rigid pavement behavior is also affected by temperature. First, seasonal variations in tempe-

perature cause pavements to contract or expand. This in turn will influence the deflection response of a rigid pavement at joints and/or cracks because the opening will vary with the time of the year in which the pavement is tested. For all other factors the same, the contraction of the PCC layer during cooling periods results in higher deflection readings due to the widening of joint and/or crack openings. On the other hand, the expansion of the PCC and narrowing of joints and/or crack openings during warming periods results in lower deflection readings.

The deflection of rigid pavements is also influenced by daily temperature variations, which cause vertical temperature differentials throughout the slab and, in turn, cause the slab to curl in either a concave or convex form. This effect is particularly pronounced on edge and corner deflections. During early morning hours when the top of the slab is cooler than the bottom, higher deflections may be recorded near the pavement edge. As the pavement becomes warmer during the daytime, a reverse effect occurs and mid-slab deflections may become larger.

In addition to temperature, the response of both flexible and rigid pavements is also affected by moisture. In general, increasing the moisture content of any material layer within the pavement will tend to weaken the layer (i.e., lower the stiffness) and therefore cause an increase in the deflection response of the pavement. However, unlike temperature, moisture changes do not markedly change in a short time interval but are rather gradual throughout an annual cycle.

The combined effect of temperature and moisture upon the deflection response of pavements is best illustrated by reference to Figures 9 and 10. These two figures show the changes in measured deflections and predicted subgrade moduli, respectively, over an 18 month period for an AC pavement test section at the FHWA's ALF facility in Virginia (13). Although not shown in these figures, the combined moisture and temperature effect is particularly significant for pavements found in areas of frost or high swelling soils. The influence of ground freezing followed by frost thawing will, for example, lead to extreme differences in pavement deflection responses.

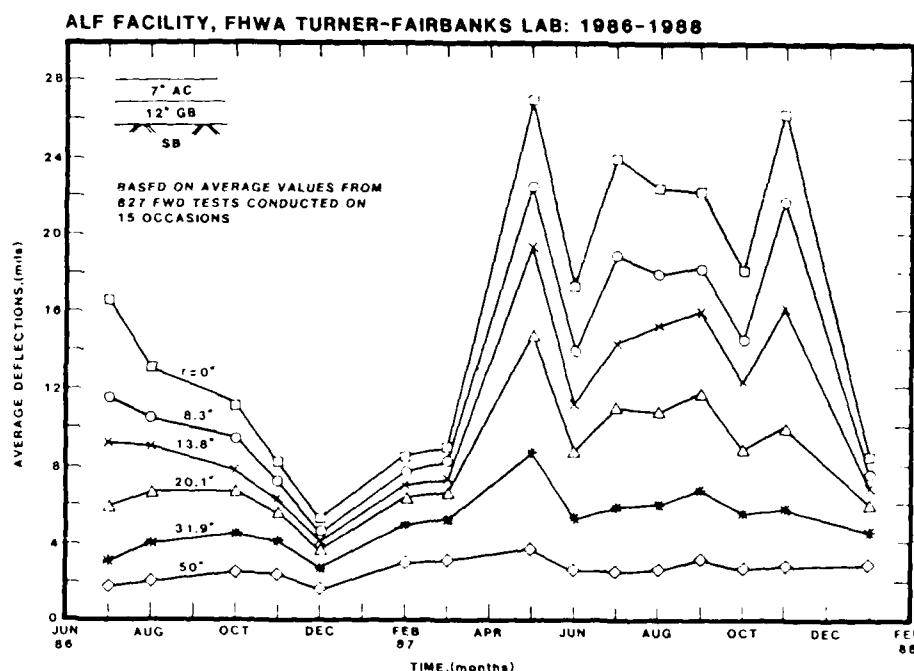


FIG 9 ENVIRONMENTAL INFLUENCE UPON PAVEMENT DEFLECTIONS

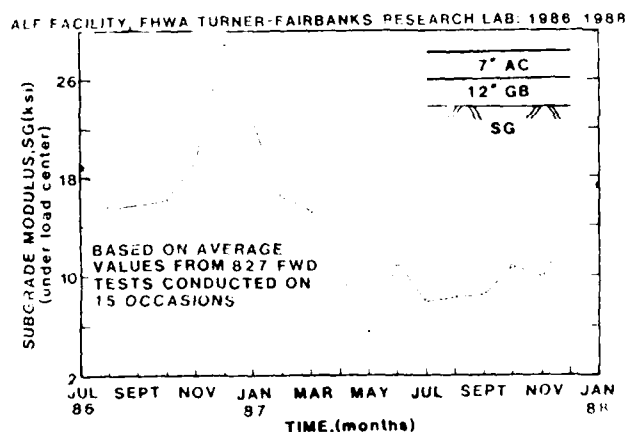


FIG 10 ENVIRONMENTAL INFLUENCE UPON SUBGRADE MODULUS

Unfortunately, while the influence of the environment upon the pavement response is well recognized, a universally accepted procedure for incorporating these factors into the evaluation process is not presently available. Typically, environmental factors are accounted for in the characterization of the various pavement layers. Some procedures, for example, use a different modulus, for each of a number of finite time periods, in the analysis. Others use strength-time relations to arrive at a weighted design modulus value. While still others base the entire evaluation upon a single, generally conservative modulus value.

DEFLECTION TESTING

Numerous nondestructive deflection measuring devices are available for use in pavement structural evaluation work (1, 3, 4, 7, 9, 11, 18, 21). Depending on the type of load applied, these devices can be categorized into five major groups. They are:

1. Static-creep (e.g., Benkelman Beam) and Automated Deflection Beams (e.g., California Traveling Deflectometer),
2. Devices for measuring deflections under a moving wheel load (e.g., Curviameter),
3. Steady-state deflection devices (e.g., Dynaflect, Road Rater),
4. Impulse devices (e.g., Falling Weight Deflectometer or FWD), and
5. Elastic Wave propagation devices.

Of these, the steady-state and impulse load devices use equipment which exert dynamic loads and measure deflections at a number of points on the pavement surface. As a consequence, they are more widely used and preferred in pavement evaluation studies. Elastic wave propagation techniques also make use of dynamic loads but, at present, they are primarily research oriented and not available commercially. The Benkelman Beam and Curviameter measure maximum deflections only.

which limits their use for backcalculation of pavement layer moduli.

Overall, studies have shown that impulse load devices, and in particular FWDs, best simulate the response of pavements under moving wheels (7, 14, 18, 21). In addition, FWDs can produce loads ranging from approximately 3,000 to 24,000 pounds and thus are capable of simulating loading conditions that range from low-volume roads to high-volume, heavy airfield pavements. This is particularly important when dealing with stress dependent materials, especially when the data analysis technique used does not account for non-linearity.

Besides the selection of a testing device, the accurate measurement of deflections and other pavement related data is also critical. As stated earlier, deflection readings and hence moduli are affected by variations in layer thicknesses, material properties (including non-linear behaviour), pavement discontinuities and the presence of a rigid layer. Because of these factors, the differences in deflections from test point to test point within a given pavement section may be quite large. This variability is intrinsic to the pavement and should not be a concern during the testing operations.

It is imperative, however, that layer thicknesses (including depth to bedrock) be established as accurately as possible, since backcalculated moduli are very sensitive to layer thicknesses. This is particularly true for the higher quality pavement materials closer to the surface.

Additionally, with regards to pavement discontinuities, it is also imperative that measurement bias not be built into the deflection testing. If only sound slabs in a highly distressed PCC pavement are tested, for example, one would obviously expect higher effective moduli which are not representative of the overall pavement condition.

In contrast to the above factors, variations in deflection measurements can also occur at each test location. Generally, however, this variability and its impact upon the predicted moduli is very small. Figure 11, for example, shows the distribution of standard deviations for 3059 sets of deflection measurements (each

set comprised of 3 or 5 readings depending on the number of repeat drops) obtained as part of the SHRP (Strategic Highway Research Program) NDT equipment variance study (2). All tests were performed using FWDs (Falling Weight Deflectometer) and included 2 states with different environment and subgrade conditions (Florida and Indiana), 2 pavement types (AC or PCC), 2 or 4 load levels, 3 or 5 repeat drops, 5 full test repetitions, 4 or 5 FWD units and 7 deflection sensors per FWD unit. As can be observed from Figure 11, the variability at each test location is very small, ranging from 0 to 0.24 mils (0 to 6 microns).

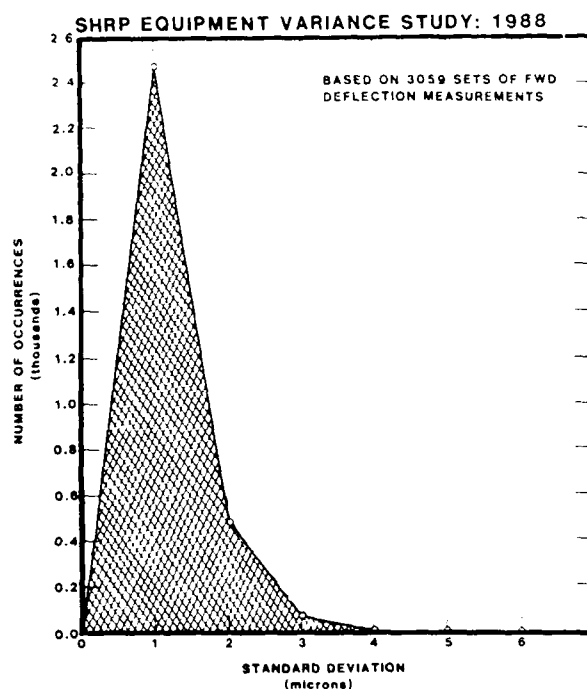


FIG 11 STANDARD DEVIATION DISTRIBUTION FOR FWD NORMALIZED DEFLECTIONS

While not shown in Figure 11, the results of the SHRP study also indicated that (1) test location and pavement type had slight but significant influence upon the deflection variability (i.e., higher variance for Indiana data compared to Florida and for AC pavements compared to PCC); (2) drop height (load level) had a stronger influence (i.e., variability increased as load increased); (3) the FWD units had generally equivalent variances; and (4) the influence of sensor location was more significant and decreased as the sensor distance increased (e.g., 0.9 microns at Sensor 2 and 0.6 microns at Sensor 7).

The number of deflection sensors and their configuration are also important testing considerations. Most backcalculation procedures require that there be as many deflection readings (or more) as there are pavement layers. Otherwise, two or more layers must be combined and treated in the analysis as a composite material. Sensor spacing is also important because deflection basin shapes differ significantly between thin, weak flexible pavements and thick, rigid stiff pavements. This difference is most significant within the first couple of feet; weaker pavements, for example, will have larger deflections over a smaller area when compared to stiffer pavements. Thus, a closer sensor configuration is generally preferred for this type of pavements while larger spacings are recommended for stiffer pavements; i.e., as the distance of the sensors (from the load center) increases, the amount of response measured for the upper pavement layers decreases while that of the subgrade soil increases. In summary, both of these factors are critical because they determine the level of information that is collected for each layer.

A final testing consideration is the environment. As stated earlier, both temperature (seasonal and daily) and moisture variations affect the measured deflections and hence layer moduli for both flexible and rigid pavements. Consequently, it is imperative that careful consideration be given to the time of testing (e.g., day or night, winter or spring, etc.) and that air and pavement temperature (surface and, if possible, vertical temperature profile) be measured. Moisture conditions at the time of testing should also be monitored whenever possible. Ideally, deflection testing (and subsequent analysis) of the pavement in question would be performed at numerous times throughout the year(s) to get an accurate assessment of the environmental influence upon the pavement response. Unfortunately, this is generally not possible due to economic considerations.

ANALYSIS OF DEFLECTION DATA

At present, no analytical solution exists that can determine pavement layer moduli directly from measured surface deflections. As a consequence, a reverse solution is required wherein a set of

"seed" moduli are first assumed and the pavement response (surface deflections) is calculated. The "seed" moduli are then adjusted until a set of modulus is found such that the theoretically predicted deflection basin is equivalent to the measured deflection basin.

Using this concept, numerous analysis solutions have been developed in the last two decades. They range from the empirical approaches; one- or two-layer elastic approximations; linear multi-layer elastic methods; viscoelastic models; elastodynamic procedures; to the more sophisticated finite element solutions (1, 3, 6, 8 to 11, 18, 19, 22 to 25). Of these, the most widely accepted procedures are those based on layered elastic theory concepts. They provide, at the present time, the best compromise between accuracy and practicality.

In turn, many layered elastic solutions have been developed and are currently used by a number of highway agencies, researchers and contractors. Besides the assumptions inherent to layered elastic theory, most of these solutions assume that: (1) the dynamically loadings can be modeled by a pseudo static load uniformly distributed over a circular area; (2) the thickness and the number of layers comprising the pavement system are known; and (3) Poisson's ratio can be estimated. Also, most of these self-iterative procedures make use of computerized elastic layered solutions (CHEVRON, BISAR, ELSYM5, etc.) to backcalculate layer moduli.

There are, however, a number of limitations associated with most of these layered elastic solutions and/or the iterative techniques used which may significantly affect the predicted moduli and lead to inaccurate or erroneous results. They include:

- o Pavements, in general, are not composed of ideal linear elastic materials. In addition to the linear and non-linear elastic responses, most pavement materials exhibit plastic, viscous, viscoelastic and/or viscoplastic responses under load.
- o Many pavement materials are anisotropic and few are homogeneous; e.g., many granular base and subbase materials as well as subgrade soils are

non-linear (stress and/or strain dependent).

- o Material properties vary greatly with time (due to environment, deterioration of pavement layers, etc.) and place; e.g., the modulus of asphaltic concrete materials is highly sensitive to temperature.
- o While layer thicknesses are assumed to be known and exact from construction records or cores, they are generally highly variable in the field.
- o In many cases, the assumption of a semi-infinite subgrade is not valid; i.e., the presence of a rock layer at some finite depth can significantly affect the deflection basin and hence predicted layer moduli.
- o Most procedures are generally applicable to a limited number of layers (typically 3 or 4), thus necessitating the use of equivalent or composite moduli; e.g., two or more layers (say a granular base and subbase) are modeled as a single one.
- o A multi-layer pavement system can have numerous layer moduli combinations that result in the same or similar deflection basin; i.e., there is no unique solution. As a result, the predicted moduli are dependent upon the seed moduli and the allowable range of modulus specified by the user for each pavement layer.
- o Because of the above considerations, the analysis of deflection data requires considerable engineering experience and judgement (for selection of seed moduli and reasonable ranges of moduli) in order to arrive at an acceptable set of layer moduli.
- o If used in the procedure, tolerances (of measured versus predicted deflections) and/or number of iterations specified (by user or fixed in the procedure) can also affect the predicted moduli; e.g., very narrow (stringent) tolerances can prevent the finding of a solution while very large tolerances can result in predicted moduli which are not necessarily the best combination.

- o Depending on many factors such as sensor spacings and environmental conditions, some pavement structures may be very hard to model; e.g., composite pavements (thin AC layer over stiffer PCC), sandwich pavements (an AC or granular material in between two PCC layers), thin layer of a weaker material under thicker PCC layer.

It should be clear from the above discussion that layered elastic solutions are just an approximation of actual in-situ conditions. Nevertheless, they provide the best compromise between accuracy and practicality at the present time.

SUMMARY

The main objective of this paper was to summarize those factors affecting the calculation of effective layer moduli from measured surface deflections. Based upon the experience of the authors coupled with the information available in the literature, numerous factors were identified and grouped into four major categories. They are:

1. Pavement-Subgrade System - random and stratified variations in layer stiffnesses, pavement discontinuities, presence of stiff (rock) layer at shallow depths, and non-linear behaviour of pavement materials and subgrade soils.
2. Environmental Conditions - temperature, moisture, combined effect of temperature and moisture, and seasonal variations.
3. Deflection Testing - testing device and load used, variability of deflection measurements, number of sensors and configuration, pavement considerations, and environmental considerations.
4. Analysis Techniques - analysis solution used and associated limitations.

These factors and their impact upon the measured deflections and backcalculated moduli were discussed. Examples illustrating the influence of many of these factors were also presented. In addition, an over-

view on how each of these factors are incorporated into the overall evaluation process was presented.

DISCLAIMER

The views expressed in this article are exclusively those of the authors and do not reflect the official policy nor views of the agencies referenced herein.

UNITS

To Convert	to	Multiply by
Inch (in)	millimeter (mm)	25.4
Mile (mi.)	kilometer (km)	1.61
Mil	micron	25.4
Pound force per square inch (psi)	kilopascal (kPa)	6.89

REFERENCES

1. "AASHTO Guide for Design of Pavement Structures", American Association of State and Highway Transportation Officials, Washington D.C., 1986.
2. "Analysis of Within Drop Error of Load Cell and Sensor Responses of the FWD", SHRP Technical Report, Strategic Highway Research Program, January 1989.
3. N.A. Ali and N.P. Khosla, "Determination of Layer Moduli Using a Falling Weight Deflectometer", TRB, Transportation Research Record 1117, Washington D.C., 1987.
4. Austin Research Engineers, "Evaluation of Pavement Deflection Measuring Devices, Report No. FHWA-TS-87-208, March 1987.
5. A.J. Bush III and D.R. Alexander, "Pavement Evaluation Using Deflection Basin Measurements and Layered Theory", TRB, Transportation Research Record 1022, Washington D.C., 1986.
6. T.G. Davies and M.S. Mamlouk, "Theoretical Response of Multilayer Pavement Systems to Dynamic Nondes-

tructive Testing", TRB, Transportation Research Record 1022, Washington D.C., 1986.

7. M.S. Hoffman and M.R. Thompson, "Comparative Study of Selected Nondestructive Testing Devices", TRB, Transportation Research Record 852, Washington D.C., 1982.
8. M.S. Hoffman and M.R. Thompson, "Backcalculating Nonlinear Resilient Moduli from Deflection Data", TRB, Transportation Research Record 852, Washington D.C., 1982.
9. S. Husain and K.P. George, "In Situ Pavement Moduli from Dynaflect Deflection", TRB, Transportation Research Record 1043, Washington D.C., 1985.
10. S.W. Lee, et.al., "A Verification of Backcalculation of Pavement Moduli", presented at the 1988 TRB Meeting, Washington D.C., 1984.
11. M.S. Mamlouk, "Use of Dynamic Analysis in Predicting Field Multilayer Pavement Moduli", TRB, Transportation Research Record 1043, Washington D.C., 1985.
12. B.F. McCullough and A. Taute, "Use of Deflection Measurements for Determining Pavement Material Properties", TRB, Transportation Research Record 852, Washington D.C., 1982.
13. Pavement Consultancy Services, "Non-destructive Testing of Subgrade, Base and Subbase Courses, Accelerated Load Facility, FHWA Turner-Fairbanks Research Lab", unpublished reports prepared for Engineering Incorporated, 1986 to 1988.
14. Pavement Consultancy Services, "Non-destructive Evaluation of I-95 CRCP in the Suffolk District", unpublished report prepared for the Virginia Dept. of Highways and Transportation, September 1986.
15. Pavement Consultancy Services, "Non-destructive Evaluation of Interstate Highways in the Staunton District", unpublished report prepared for the Virginia Department of Highways and

Transportation, August 1986.

16. Pavement Consultancy Services, "Delaware Interstate Concrete Pavement Rehabilitation Study", unpublished report prepared for the Delaware Department of Transportation, May 1987.
17. G.R. Rada and M.W. Witczak, "Performance of Cracked and Seated Rigid Airport Pavements", Report No. DOT/FAA/PM-87/4, Washington D.C., April 1987.
18. J.M. Roesset and K.Y. Shao, "Dynamic Interpretation of Dynaflect and Falling Weight Deflectometer Tests", TRB, Transportation Research Record 1022, Washington D.C., 1986.
19. T. Rwebangira, et.al., "Sensitivity Analysis of Selected Backcalculation Procedures", TRB, Transportation Research Record 1117, Washington D.C., 1987.
20. "SHRP-LTPP Manual for FWD Testing - Operational Field Guidelines", Version 1.0, Strategic Highway Research Program, January 1989.
21. O. Tholen, et.al., "Comparison of the Falling Weight Deflectometer with other Deflection Testing Devices", TRB, Transportation Research Record 1007, Washington D.C., 1985.
22. W. Uddin, et.al., "Project Level Structural Evaluation of Pavements based on Dynamic Deflections", presented at the 1985 TRB Meeting, Washington D.C., 1984.
23. W. Uddin, et.al., "Rigid Bottom Considerations for Nondestructive Evaluation of Pavements", TRB, Transportation Research Record 1070, Washington D.C., 1986.
24. P. Ullidtz and R.N. Stubstad, "Analytical-Empirical Pavement Evaluation Using the Falling Weight Deflectometer", TRB, Transportation Research Record 1022, Washington D.C., 1986.
25. G. Wiseman, et.al., "Application of Simplified Layered Systems to NDT Pavement Evaluation", TRB, Transportation Research Record 1022, Washington D.C., 1986.

**Session 9:
Field Instrumentation
Case Studies**

MINNESOTA COLD REGIONS PAVEMENT TEST FACILITY

David E. Newcomb,
Assistant Professor
Richard O. Wolters,
New Technologies Engineer
Steven Lund,
Research Project Engineer

University of Minnesota

Minnesota Department of
Transportation
Minnesota Department of
Transportation

ABSTRACT

The Minnesota Department of Transportation in cooperation with the Federal Highway Administration and the Local Roads Research Board of Minnesota is constructing the Cold Regions Pavement Research Test Facility (CRPRTF). This facility is being built on a 4-km (2.5-mile) portion of Interstate 94 (I-94) in the east-central part of the state.

The CRPRTF will have high-and low-volume traffic test sections as well as nontrafficked test pads. The low-volume sections will be constructed on a parallel access road, and will be trafficked artificially.

Section designs call for the use of portland cement concrete and asphalt concrete surfaces. Different construction techniques will be tried and material problems will be intentionally built into some of the test sections. Special classifications for aggregate surface, base, and subbase materials will be used in the pavement sections.

The natural subgrade in this area is primarily a frost susceptible loam. This combined with shallow water table depths and severe winter temperatures make this an ideal location for frost heave studies. A second type of subgrade will be imported for use in some of the low-volume sections. This soil will be a highly plastic heavy clay.

During the operation of the CRPRTF, information will be obtained on the

and pavement response. This will require instrumentation and data acquisition systems which can endure the harsh weather and severe traffic loading conditions for five to ten years, yet have sufficient sensitivity to give meaningful data.

INTRODUCTION

Background

Much of the nationwide practice of highway pavement design in the U.S. is currently based on the experience of the AASHO Road Test conducted the late 1950's at Ottawa, Illinois. The new American Association of State Highway and Transportation Officials (AASHTO) pavement design guide (1), while introducing many new and needed concepts, still relies primarily on performance equations developed at the Road Test. The limitations for the Road Test results include:

1. Only one subgrade type was present.
2. A narrow range of axle loads and tire pressures were used.
3. Only one climate was represented.
4. Road surface materials were limited to asphalt concrete and portland cement concrete.
5. Twenty years of traffic loading was compressed into two years.

New efforts are underway by the Strategic Highway Research Program and the Federal Highway Administration to study

the materials, design procedures, and construction practices used currently.

The Minnesota Department of Transportation is constructing the Cold Regions Pavement Research Test Facility (CRPRTF) in cooperation with the FHWA and the Local Roads Research Board of Minnesota. This facility will provide an outdoor laboratory in which the traffic loads and environment will actually be those to which a cold regions pavement is subject.

Scope

The CRPRTF will provide researchers the opportunity to investigate the relationships between material properties, construction techniques, design methodologies, traffic loads, environment, pavement responses, and performance in detail. The experiments will include high-volume traffic, low-volume traffic, and no-traffic areas for rigid and flexible pavements as well as aggregate surfaces.

Objective

The primary objective of the facility is to provide findings which will help to develop better fundamental approaches to pavement design, construction, and maintenance.

DESCRIPTION OF FACILITY

Site Layout

The CRPRTF will be located on I-94 approximately 64 km (40 miles) northwest of Minneapolis between the towns of Albertville and Monticello. As shown in Figure 1, the westbound lanes of the interstate highway will serve as the location for the main experiment with the low-volume road portion running parallel. The site also has space for nontrafficked test pads, an instrumentation building, and materials stockpiles.

The topography of the site is relatively flat with only 4.3 m (14 ft) difference in elevation from the east end to the west end. The primary land use in this area is agriculture; and the drainage is relatively poor. A marsh is located about one-fourth of the distance from the western end.

The high-volume portion will contain test sections designed for an expected 10 years of service on the east end and 5 years of service on the west end. The 10-year segment will have approximately 1615 m (5300 ft) of flexible pavements and 732 m (2400 ft) of rigid pavements including transition zones. The 5-year part of the main experiment will have 701 m (2300 ft) of asphalt surface pavements and 549 m (1800 ft) of rigid pavements.

The low-volume traffic experiment will have a total of 15 test sections of which four will be rigid pavements, eight will be flexible pavements, and three will be aggregate surface. Each section in both the main and low-volume road experiments will be approximately 152 m (500 ft) long with about 30 m (100 ft) of transition between them.

Existing Soil Conditions

The natural subgrade in this area is primarily a loam with an AASHTO classification of A-6. There are minor variations of silt and clay present. The R-value of the existing subgrade is on the order of 15 and its resilient modulus is about 83 MPa (12,000 psi) at a deviator stress of 69 kPa (10 psi).

For three of the low-volume road sections, a heavy clay will be imported and placed to a depth of 2 m (6 ft). This clay is expected to have an R-value of about 5 and a resilient modulus of less than 69 MPa (10,000 psi).

A ground water table survey of the area was taken in the summer of 1988. It was found that the depth to ground water varied considerably over the length of the project. The range was from 8 cm (3 in) above the proposed grade to depths of greater than 4.3 m (14 ft). It should be emphasized that this survey was conducted during one of the driest years in the last 50.

TRAFFIC

Expected Traffic

Although the facility will not be located in the coldest possible place in Minnesota, it will be located on one of the highest truck volume routes in the state. The design average daily traffic for this portion of I-94 is 24,200

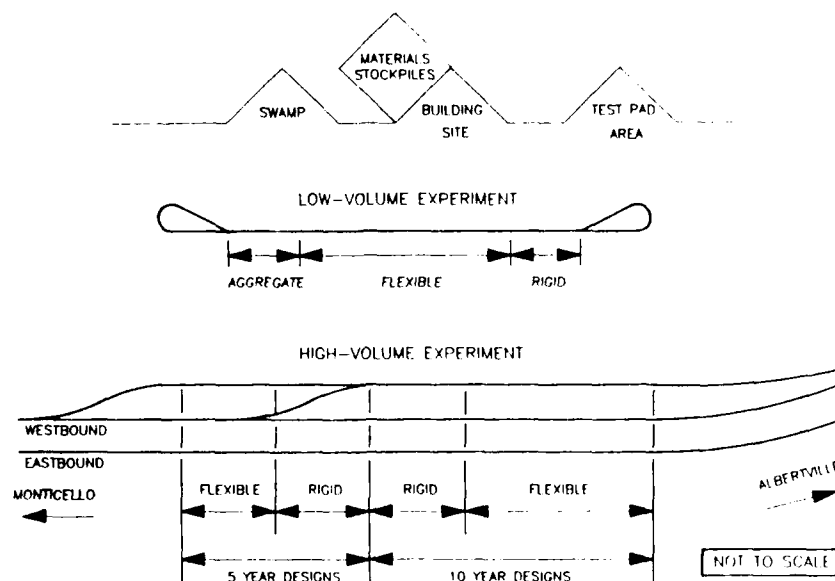


Figure 1. SCHEMATIC LAYOUT OF COLD REGIONS PAVEMENT RESEARCH TEST FACILITY

vehicles with 3200 of these classified as heavy commercial vehicles. For the 5-year sections, this means that about 3.2 million equivalent single axle loads (ESAL) will be experienced by the flexible pavements and 5.1 million ESAL for the rigid pavements. The 10-year flexible pavements can expect 7.2 million ESAL and the rigid pavements will have about 11 million ESAL. The low-volume road portion will be artificially trafficked to a level of about 50,000 ESAL per year.

Traffic Instrumentation

A weigh-in-motion (WIM) system will be located at the beginning of the facility to monitor axle weights continuously or at selected time intervals. There will also be an axle classification system stationed immediately next to the WIM consisting of induction loops to monitor the types of vehicles corresponding to the axle loads. These systems will be installed in the existing roadway, one year prior to the start of operations.

CLIMATE

Weather information for the facility has been compiled by Kersten (2). The weather station nearest the facility is currently located in Buffalo, MN, 18 km (11 miles) to the southwest. The CRPRTF will have its own weather station which

should be operational by the fall of 1989. Some of the available climate data are shown in Figures 2 through 6.

Ambient Temperature

Monthly average, average minimum, and average maximum temperatures for St. Cloud, MN, 48 km (30 miles) to the northwest, are presented in Figure 2. Summertime maximum temperatures as high as 27°C (81°F) can be expected in July; whereas the average minimum temperature for January is -18°C (0°F). The normal range of average monthly temperatures is between -13°C (9°F) and 22°C (71°F).

The accumulation of freezing degree-days for the Minneapolis-St. Paul area (MSP), Buffalo, and St. Cloud is illustrated in Figure 3. The freezing index for Buffalo is about 917°C-days (1650°F-days) in an average year. The distribution of freezing indexes for a 30-year period in St. Cloud is shown in Figure 4. It is expected that the freezing index would be between 1000°C-days (1800°F-days) and 1400°C-days (2600°F-days) for two-thirds of the years.

Precipitation

Average monthly precipitation and snowfall amounts for St. Cloud are given in Figures 5 and 6. The majority of the precipitation occurs from May through September; when more than 50 cm³ (3 in³) can be expected in any given month. From

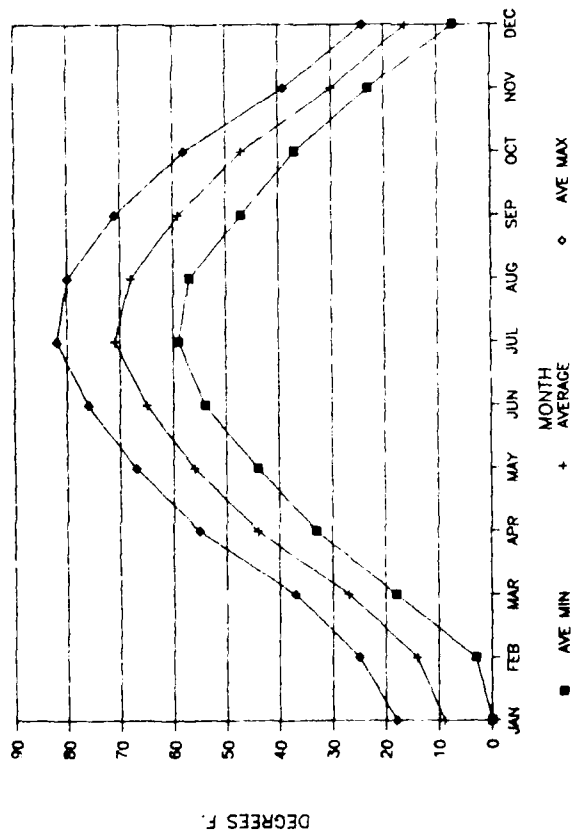


Figure 2. TEMPERATURE AVERAGES FOR ST. CLOUD, MN.

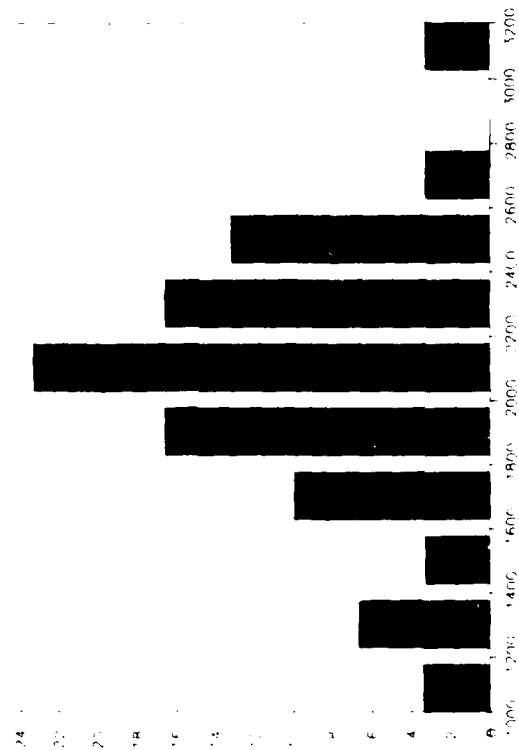


Figure 3. AVERAGE MONTHLY PRECIPITATION FOR ST. CLOUD, MN.

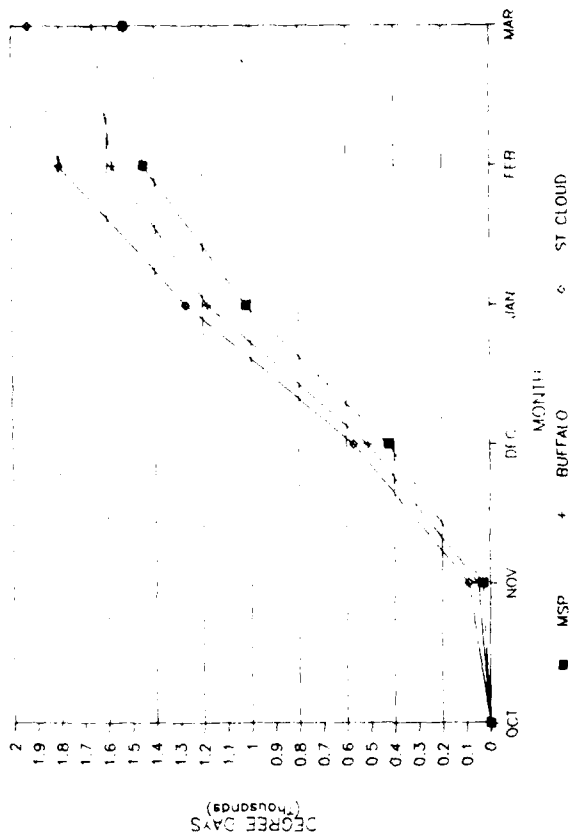


Figure 4. ACCUMULATION OF FREEZING DEGREE-DAYS.

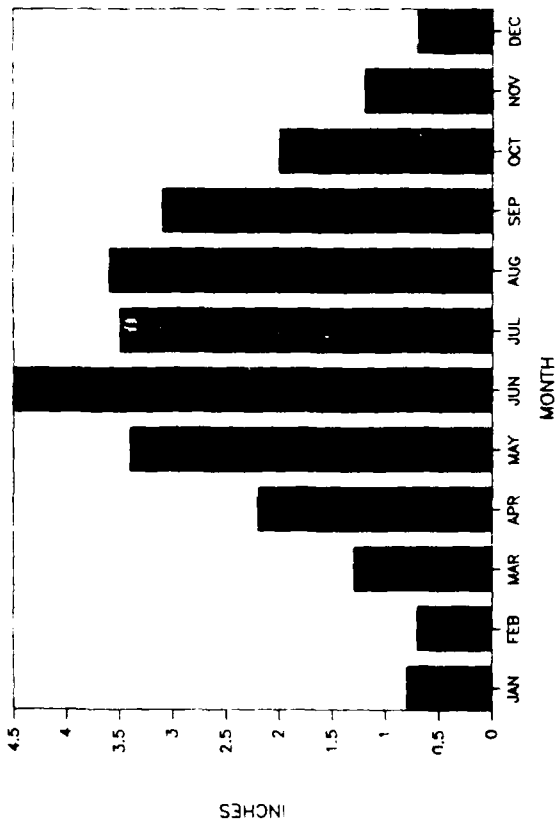


Figure 5. AVERAGE MONTHLY PRECIPITATION FOR ST. CLOUD, MN.

November through March, precipitation is almost exclusively in the form of snowfall, with more than 100 cm³ (6 in³) in any of these months.

Subsurface Temperatures

Ground temperature profiles to a depth of 1.2 m (4 ft) are currently being measured on the existing westbound and eastbound lanes of I-94. Figures 7 through 9 show the temperature measurements for March, July, and November 1988. The spring thaw condition is illustrated in Figure 7; where it can be seen that the subsurface temperatures below 25 cm (10 in) are slightly below 0°C (32°F) and are at 7°C (46°F) near the surface. Figure 8 shows the effect of surface cooling due to precipitation in the summer. The influence of solar gain on a winter day is shown in Figure 9.

Weather Instrumentation

Surface and subsurface environmental conditions will be monitored during the operation of the facility. A weather station to monitor above-ground conditions will be constructed according to Federal Aviation Administration guidelines (3). This will provide information on wind speed and direction, ambient temperature at ground level and at 6.2 m (20 ft), humidity, precipitation, barometric pressure, and solar radiation.

Pavement surface sensors will be installed in the roadway which are capable of detecting surface temperature, the type of water present, and the presence of deicing chemicals. Subsurface temperatures to a depth of 3.7 m (12 ft) will be measured along the length of the facility using thermistor and thermocouple strings. Additionally, pore pressures and drainage quantities in the soils and granular materials will be monitored.

MATERIALS

Materials used in the construction of the pavement sections will be those typically used in pavement construction in Minnesota. It is possible that new types of materials will be tried in the nontrafficked test pads and in future phases of the test facility.

Asphalt Concrete

Some of the bituminous mixtures in the mainline experiment will have problems intentionally designed into them, i.e., high asphalt or air void contents. Also, there will be two asphalts of the same grade and differing temperature susceptibility characteristics used in the mixtures. The aggregate source and gradation will be held constant to the extent possible. The low-volume experiment will have the same bituminous mixture throughout.

Portland Cement Concrete

Normal weight portland cement concrete will be used in the facility. The specifications will call for the use of air entraining which is typical for Minnesota. The maximum size of aggregate particles and gradations will be maintained throughout the length of the sections.

Aggregates

Aggregates for use in surface, base, and subbase layers will be specially produced to provide certain gradation, particle shape, and plasticity characteristics. The special classes of aggregates were developed so that pavement performance characteristics attributable to them could be distinguished. The broad nature of the current Mn/DOT specifications would not necessarily permit this (3). The general requirements for the dense-graded base and surfacing aggregates are listed in Table 1. It is anticipated that a open-graded base aggregate will be added to these.

Two classes of aggregate will be used in the road surface of the low-volume road experiment. Both will have a maximum particle size of 19 mm (0.75 in). Class 1C Sp will have a coarser gradation than Class 1F Sp. The plasticity index (PI) requirement is lower for the Class 1C Sp than for Class 1F Sp. There will not be a requirement for fractured faces for these two classes.

Four classes of aggregate were established for base and subbase materials. Class 3 Sp will have a maximum particle size of 12.5 mm (0.5 in) and a finer gradation than the other base aggregates. Class 4 Sp will have the

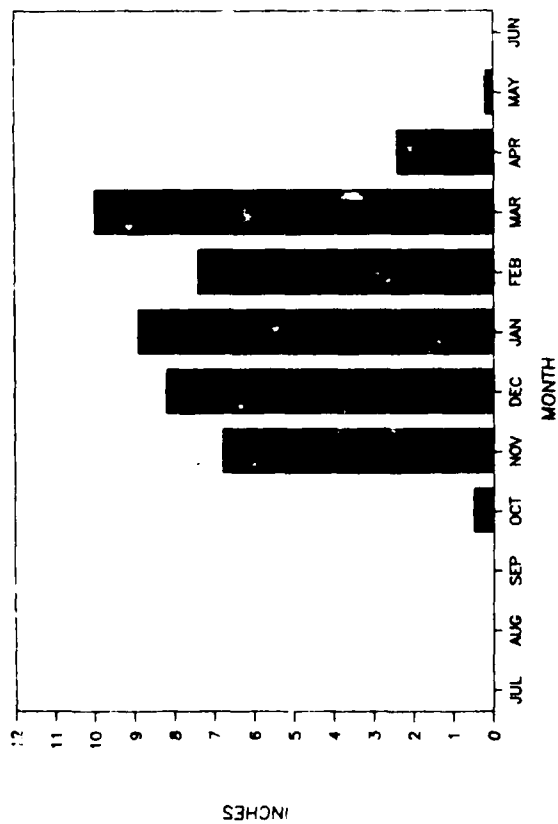


Figure 6. AVERAGE MONTHLY SNOWFALL FOR ST. CLOUD, MN.

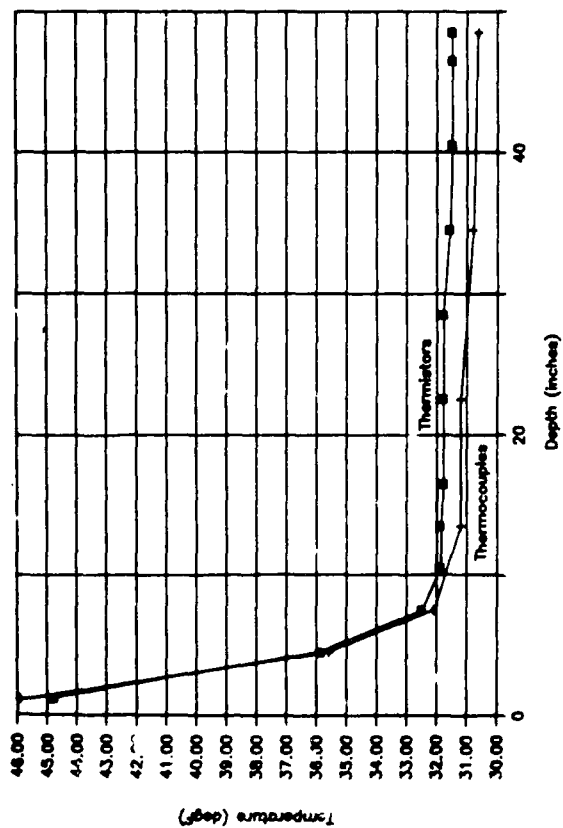


Figure 7. GROUND TEMPERATURE PROFILE, MARCH 17, 1988 (PARTLY CLOUDY, 37°F)

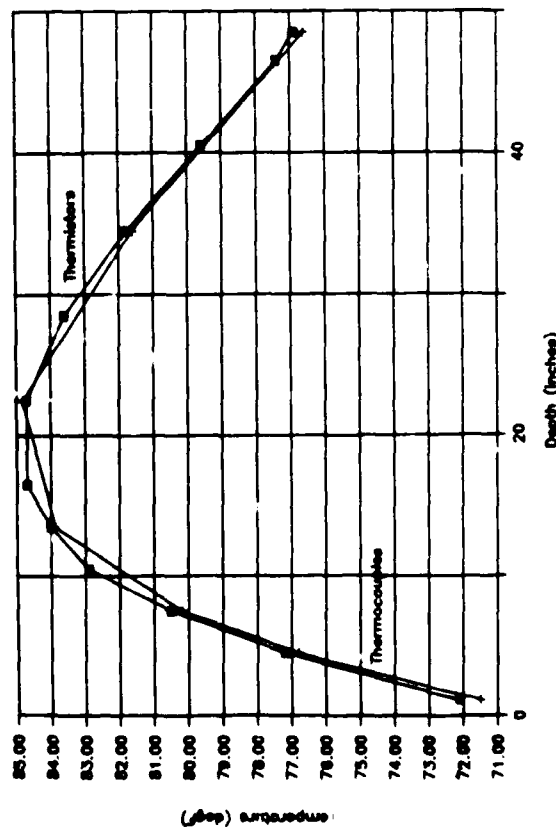


Figure 8. GROUND TEMPERATURE PROFILE, JULY 16, 1988 (LIGHT RAIN, 65°F).

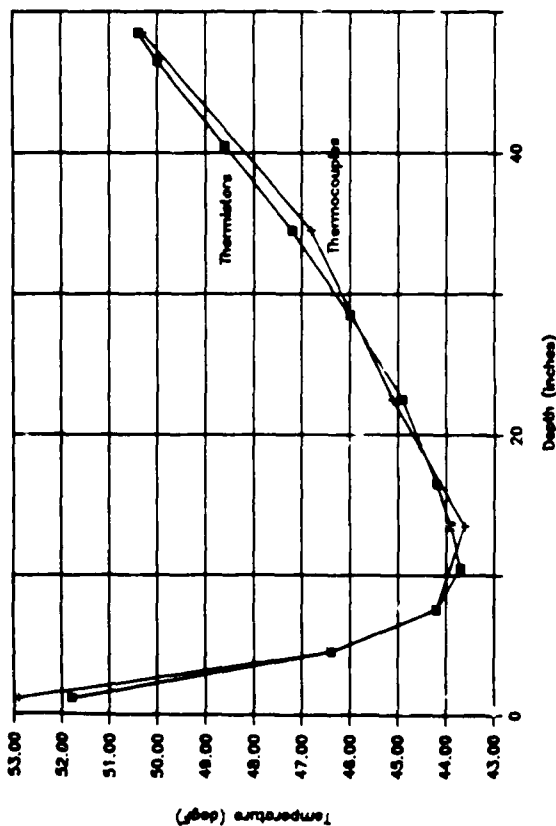


Figure 9. GROUND TEMPERATURE PROFILE, NOVEMBER 9, 1988 (SNOW, 40°F).

Table 1. BASE AND SURFACING AGGREGATE REQUIREMENTS.

Aggregate Class	Primary Function	Maximum Size, in	Fractured Particles	Plasticity	
				LL	PI
1C Sp	Surface	0.75	---	≤35	≤ 6
1F Sp	Surface	0.75	---	≤35	≤12
3 Sp	Base	0.50	---	≤35	≤12
4 Sp	Base	1.50	---	≤35	≤12
5 Sp	Base	1.00	Min	≤25	≤ 6
6 Sp	Base	1.00	Max	≤25	≤ 6

largest maximum size, although the percentage of material passing the 0.075 mm (No. 200) sieve will be of the same order as that for Class 3 Sp. Classes 3 and 4 Sp would be considered "Granular Borrow" and "Select Granular Borrow" materials under the Mn/DOT specifications (3).

Differences in performance due to aggregate shape will be discerned using the Class 5 Sp and Class 6 Sp materials. Class 5 Sp will have a minimum amount of crushed material in it, while Class 6 will contain as much crushed material as possible. Class 5 will also have a finer gradation than Class 6.

EXPERIMENT DESIGN

Although the experiment design for the facility has not been finalized, the information in this section represents the majority of what is planned for the test sections (4,5). It is expected that some changes will be made in order to accommodate such variables as drainable bases.

As mentioned earlier, the mainline test sections on the interstate will be divided into those designed for an expected life of 10 years and those designed for 5 years of service. Both of these will contain cells for rigid and flexible pavements (Table 2). The low-volume road portion will be designed for approximately 50,000 ESAL's per year for a period of 3 years. The low-volume road will have asphalt concrete, portland cement concrete, and aggregate surfaces within its cells (Table 3).

Thickness designs for the flexible pavement sections were done using the Gravel Equivalency approach which is the current Mn/DOT standard. Rigid pavements were designed using Mn/DOT's procedure with refinements to the thicknesses made

by using the AASHTO approach. Aggregate surfaces were designed using the AASHTO low-volume roads procedure.

Mainline Experiment

Ten-Year Designs. Both the flexible and rigid pavement cells for the ten-year designs are located on the eastern portion of the facility as shown in Figure 1. The planned cross-sections for these pavements (10-1 through 10-13) are given in Table 2. It can be seen that this part of the experiment will have four rigid pavement sections and nine flexible pavement sections.

The rigid pavements will all have surface thicknesses of 24 cm (9.5 in) with 13 cm (5.0 in) of subbase materials. Three of these sections (10-1 through 10-3) will have panel lengths of 8.3 m (27 ft) and wire reinforcing. Section 10-4 will have panel lengths of 4.6 m (15 ft). Edge drains will be installed on section 10-2.

Two of the flexible pavement sections (10-6 and 10-10) will have full-depth asphalt concrete surfaces, 30 cm (11.75 in) in thickness. The other asphalt concrete sections will have surface thicknesses of 20 cm (7.75 in) with combined base and subbase thicknesses ranging from 48 cm (19 in) to 71 cm (28 in). The asphalt mixture problems which will be built into the lower bituminous layers are also noted in Table 2. These problems are deviations from target air void and asphalt contents.

Five-Year Designs. This part of the mainline experiment will have four flexible pavement sections and three rigid pavement sections (Table 2). These will be located on the western end of the facility. If and when these fail prior to the failure of the ten-year designs,

Table 2. MAINLINE EXPERIMENT DESIGN.

Sect. No.	Design Life, yr	Surface Type	Surface Thick., in	Base/Subb. Type	Base/Subb. Thick., in	It. Sp., ft or AC char., %
5-1	5	AC	5.75	6 Sp/4 Sp	4/22	----
5-2	5	AC	10.75	----	----	+4•AV
5-3	5	AC	5.75	6 Sp/3 Sp	4/28	+2•AV
5-4	5	AC	5.75	6 Sp	27	+1•AV
5-5	5	PCC	8.50	5 Sp	5	27
5-6	5	PCC	8.50	5 Sp	5	15
5-7	5	PCC	8.50	5 Sp(1)	5	20
10-1	10	PCC	9.50	5 Sp	5	27
10-2	10	PCC	9.50	3 Sp(1)	5	27
10-3	10	PCC	9.50	3 Sp	5	27
10-4	10	PCC	9.50	6 Sp	5	15
10-5	10	AC	7.75	6 Sp/4 Sp	6/16	----
10-6	10	AC	11.75	----	----	+2•AV/-1•AC
10-7	10	AC	7.75	6 Sp/3 Sp	6/19	-1•AC
10-8	10	AC	7.75	5 Sp/4 Sp	6/19	+1•AC
10-9	10	AC	7.75	5 Sp/3 Sp	6/20	+4•AV/-1•AC
10-10	10	AC	11.75	----	----	+2•AV/-1•AC
10-11	10	AC	7.75	6 Sp	19	+2•AV/-1•AC
10-12	10	AC	7.75	5 Sp	23	+1•AC
10-13	10	AC	7.75	3 Sp	28	+2•AV

10 = Edge drains present.

+4•AV = air voids deviation from target

-1•AC = asphalt content deviation from optimum

Table 3. LOW-VOLUME ROAD EXPERIMENT DESIGN.

Sect. No.	Surface Type	Surface Thick., in	Base/Subb. Type	Base/Subb. Thick., in	Subgrade Type
1	ACG	12.00	1F Sp	----	Loam
2	PCC	18.00	1F Sp	----	Loam
3	ACG	24.00	1F Sp	----	Clay
4	AC	3.50	6 Sp/4 Sp	4/20	Clay
5	AC	10.00	----	----	Clay
6	AC	8.50	----	----	Loam
7	AC	3.50	6 Sp	11	Loam
8	AC	3.50	5 Sp	13	Loam
9	AC	5.00	4 Sp	11	Loam
10	AC	5.00	3 Sp	13	Loam
11	AC	3.50	5 Sp/3 Sp	4/12	Loam
12	PCC(1)	6.00	5 Sp	5	Loam
13	PCC(2)	6.00	5 Sp	5	Loam
14	PCC(1)	5.50	5 Sp	5	Loam
15	PCC(1)	7.00	5 Sp	5	Clay

11 = Joint spacing = 15 ft

10 = Joint spacing = 20 ft

traffic will be diverted onto the existing roadway as shown in Figure 1.

The rigid pavements will consist of 22 cm (8.5 in) of portland cement concrete (PCC) over 13 cm (5.0 in) of subbase material. Section M5-5 will have panel lengths of 8.3 m (27 ft) and wire reinforcing. Joint spacings of 4.6 m (15 ft) will be used in Section M5-6. Edge drains will be placed in Section M5-7 which will have panel lengths of 6.2 m (20 ft) with no wire reinforcing.

The flexible pavements portion of the five-year study will have one section of full-depth asphalt concrete consisting of 27 cm (10.75 in). The conventional sections will be composed of 15 cm (5.75 in) of asphalt concrete over combined base and subbase thicknesses of 68 cm (27 in) to 83 cm (32.5 in).

Low-Volume Road (LVR) Experiment

The low-volume road sections are listed in Table 3. These are comprised of aggregate, asphalt, and portland cement concrete surfaced pavements. There will be two types of subgrades present in the LVR portion of the facility. These include the natural subgrade, a loam, and an imported, highly plastic clay. The trafficking of this experiment will most likely be accomplished by means of an operator-driven vehicle.

There will be three aggregate surface sections. These sections were designed using the new AASHTO method for aggregate surface pavements. Section 3 will be a Class 1F Special surface over the clay subgrade.

The eight flexible pavement sections will have surface thicknesses which vary from 9 cm (3.5 in) over granular materials to 27 cm (10.5 in) of full-depth asphalt concrete on the clay subgrade. Two sections will be constructed on the clay subgrade. Combined base and subbase thicknesses range from 28 cm (11 in) to 61 cm (24 in). There will be four sections of portland cement concrete pavements in the LVR. Section 13 will have joint spacing of 6.2 m (20 ft), while the other sections will have 4.6 m (15 ft) panel lengths. One PCC section (15) will be constructed over the clay subgrade. The subbase thickness will be constant in the three rigid pavement sections at 13 cm (5 in).

PAVEMENT RESPONSE AND PERFORMANCE

Pavement Response

The capability to continuously collect pavement response data is being planned for selected test sections in both the Main and Low-Volume Road experiments. Although these sections have yet to be chosen, it is safe to assume that they will include each of the surface types present.

The rigid pavements will be instrumented with strain gages placed in the bottom of the slabs to monitor the amount of curl being experienced due to temperature and moisture variations in the PCC. These strain gages will also provide information regarding the response due to load when traffic passes over the slab in the curled condition. Load transfer from slab to slab will also be monitored. This could possibly be done with the use of pressure cells to measure the load transfer or accelerometers to measure the displacement on both sides of transverse joints. It may be possible to measure the width of joint openings by means of displacement transducers. The stresses in the subbase and subgrade materials will be monitored using pressure cells.

The flexible pavements will be instrumented to monitor the horizontal strains and vertical deflections in the various asphalt layers. Horizontal strains will probably be measured using H-type strain gages; and vertical deflections will be measured with either multi-depth deflectometers or velocity transducers. It may be possible to measure the shear stresses by means of rosette strain gages which are capable of measuring strains in two different directions at once. The stresses in the aggregate and subgrade layers will be measured using pressure cells.

Periodic Monitoring

At various intervals in the lifetimes of the different experiments, evaluations of materials and pavement conditions will be made. These will include destructive and nondestructive materials testing, ride quality assessments, frost heave measurements, and visual surveys.

Material sampling and laboratory testing of the surface, base, and subgrade materials will be accomplished during and

immediately after construction. As time in service passes, materials from different sections will be sampled and tested to ascertain what changes are occurring in the pavement due to traffic and environment. These results will be related to the material properties inferred from the deflection measurements made with the falling weight deflectometer.

Ride quality will most likely be monitored using a profilometer. These measurements will probably be taken on a seasonal basis. This will provide useful information about the effects of frost heave and surface condition on the actual quality of the pavement surface.

Visual surveys will be used to ascertain the overall condition of each test section cell as well as the mode of deterioration in each. This will be related to the primary responses of the pavement and the types of loads being experienced.

CONSTRUCTION SCHEDULE

The construction of this facility will begin in the summer of 1989. During this construction season, the right-of-way for the facility will be purchased. The weigh-in-motion system will be installed on the existing pavement immediately in front of the CRPRTF, and a weather station will be erected. Materials production and stockpiling will begin at this time. Additionally, preliminary investigations of instrumentation will take place.

During the 1990 season, the grading for the entire site will be accomplished. A building will be constructed to house the data acquisition and storage equipment. The pavement test sections will be finished with instrumentation installed in time to open the facility to traffic by the fall of 1990.

SUMMARY

The CRPRTF will not answer all the questions which arise with respect to pavement structures. There are limitations such as only having one type of climate. It will, however, provide a facility at which many of the theories and assumptions used in pavement engineering can be tested. The main features of the

facility include:

1. Two types of aggregate will be placed in the low volume portion.
2. A broad spectrum of traffic will be represented.
3. Three types of surfacing materials will be used.
4. Environmental, load, and pavement response instrumentation will be in place for continuous observations.
5. Periodic materials testing and pavement surveys will be done.
6. Thirty-five or more pavement cross-sections will be in place.
7. Design details and material properties will be varied.

ACKNOWLEDGEMENTS

The authors gratefully acknowledge the contributions of the many individuals on the Task Force and Advisory Committees who have provided direction on the goals and experiment design of the CRPRTF. Thanks are also due the State of Minnesota for providing the funding for the facility. Special recognition is extended to Drs. Witczak and Kersten for providing much of the information presented herein.

REFERENCES

1. AASHTO Guide for the Design of Pavement Structures, American Association of State Highway and Transportation Officials, Washington, DC, 1986.
2. Kersten, M.S., "Cold Regions Pavement Research Test Facility: Climate Summary," Letter Report, Minnesota Dept. of Transportation, Dec. 1988.
3. Witczak, M.W., "Recommended CRPRTF Base and Road Surface Aggregate Classes," Version No. 1, Minnesota Dept. of Transportation, May 1988.
4. Witczak, M.W., "Pavement Test Section Plan - Low Volume Road Site," Version No. 2, Minnesota Dept. of Transportation, Feb. 1989.
5. Witczak, M.W., "Pavement Test Section Plan - I-94 Main Experiment - 5 and 10 Year Design," Version No. 2, Minnesota Dept. of Transportation, Feb. 1989.

FULL SCALE PAVEMENT TEST INTERNATIONAL JOINT RESEARCH

A.-G. Dumont	Project Manager Swiss Federal Institute of Technology Lausanne - Switzerland
R. Addis	Chairman of the analysis subgroup Transport & Road Research Laboratory Crowthorne - United Kingdom

The aim of the OECD project is to improve international coordination and cooperation in the field of full scale testing of pavement structures. Besides an increase in understanding of the behaviour and mechanics of pavements, progress will be made in the standardisation and harmonisation of the equipment, measurements data processing and methods of analysis and interpretation.

The operation, the cost of which is estimated to be 3'800'000.- FF, is being financed by approximately fifteen countries and international organisations.

Three pavement structures will be tested under axle loads of 10 and 11.5 tonnes, on the test machine in Nantes (France). A phase of repair will be undertaken as soon as the weakest structure has reached the end of its life, and the test will be continued until 4 million standard axle loads have been applied. The track has

been fully instrumented so that deformation, deflection and stress at different levels in the pavements will be known at any time. Weather data will be continuously recorded. The recorded data on pavement properties and behaviour will be analysed using models of pavement response and performance.

INTRODUCTION

The OECD (Organisation for Economic Cooperation and Development) brings together 23 countries throughout the world. Its Road Research Programme is aimed at encouraging international cooperation in the field of road construction, safety and traffic on the basis of the coordination of the means of research of different members.

The experiment conducted in Nantes, France, on the LCPC (Laboratoire Central des Ponts et Chaussées) test track is being carried out with the financial and scientific participation of the following OECD countries : Australia, Austria, Belgium, Denmark, Finland, France, Germany, Holland, Italy, Norway, Spain, Sweden, Switzerland, The United States and the European Economic Commission.

The budget for this experiment, known as FORCE (First OECD Road Common Experiment) amounts to 3'800'000.- French francs.

BACKGROUND

The group of experts set up by the OECD in 1983 undertook to compare different types of strain gauges on a common structure and under the effects of the same loads. Thus in April 1984, 10 countries participated at Nardo, Italy in a comparison test which provided some very useful information. In order to continue the work of international collaboration and cooperation of this group, new scientific objectives were established aimed at :

- expanding the range of validity of the results obtained so far and making them available for tests currently in progress or planned.
- increasing our knowledge of the performance and mechanics of pavements.
- progressing with regard to the standardisation and bringing into

line of measuring equipment and techniques and the procedures employed for the processing, analysis and interpretation of data.

- verifying the design and reinstatement techniques at present employed in the different participating countries.
- reactivating the exchange of information in the field of full scale tests.

The test site in Nantes was selected because of the size of the test installation (the largest in the world)

(figure 1) and because of its availability given that the experiment was to be carried out over a 12 month period.

In parallel with the cooperative test a number of countries have started to carry out tests on reproducing similar conditions to those in Nantes on their own installations (materials, structures, loads) with a view to obtaining cross checking information.



Figure 1 LCPC test installation at Nantes

CONDUCT OF TESTS

More than 360 gauges were installed at different levels in each layer when constructing the three pavement structures (figure 2).

STRUCTURE		
I	II	III
6 cm AC	6 cm AC	6 cm AC
	6 cm AC	18 cm cement treated base
30 cm gravel	30 cm gravel	
soil		soil
	soil	

Figure 2 Pavement structures constructed on the site

A number of tests are now being conducted on the materials of these pavements. What were termed "zero" point measurements were first carried out when the load, speed and transverse position parameters were varied as follows :

- Load : 8.2 tonnes to 13.0 tonnes
- Speed : 3 Km/h to 86 Km/h
- Transverse position : -52.5 cm to +52.5cm

The "FATIGUE" phase was then started on carrying out 500 000 applications of a load of 10 tonnes on the inner track and 11.5 tonnes on the outer track of each structure. A comparison of the effect of these loads is to be made. On completion of this phase the weakest structure will be at the end of its life. Maintenance work will then be carried out on providing a strengthening layer of asphalt concrete and the test continued with the "MAINTENANCE" phase consisting this time of 3'000'000 passes of a single 11.5 tonne load.

Different parameters will be measured and analysed throughout the tests. This will be a matter of measuring longitudinal and transverse deformation within and at the base of bound layers (asphalt concrete and cement treated with gravel), vertical deformations and stresses in the unbound layers (soil and sub-base gravel) and surface deflections.

A particular type of sensor was

employed for the measurement of each of the different parameters.

CHOICE OF SENSOR

The result of inquiries concerning the measuring techniques employed in the OECD countries provided the basis for our choice of sensors. We are also aware that site conditions are not always very compatible with the fragile nature of the sensors and it is accordingly better to multiply the number employed so as to ensure that despite losses it will be possible to measure each parameter in a statistically valid way.

Given that only a limited proportion of the budget had been allowed for the sensors we were obliged to reject those that were too expensive despite the fact that their principle of operation and performance was very acceptable.

We decided to employ two different types of sensors for the measurement of both deformation and deflection in order to guard against the general failure of one particular type and so as to be able to compare the results of two different set of measurement.

TYPES OF SENSOR

Horizontal deformation

These sensors are required to measure the horizontal deformation within a layer of material during the application of a load. Strain gauges are employed made up of a thin conductor whose electrical elongation to which it is subject. The unit of measurement amounts to 10^{-6} .

The Nardo experiment confirmed the reliability of sensors in the form of an H of which the active part consists of a strain gauge embedded in a strip of plastic. Two aluminium bars, one secures to each extremity of the gauge ensure that it is properly anchored in the material. More than 120 of this type of sensor, known as the "Type 1", were installed in the structures built on the Nantes test track.

A second model known as "Type 2" was slightly different in that the

gauge was cemented onto an aluminium plate and protected by a resin (figure 3).

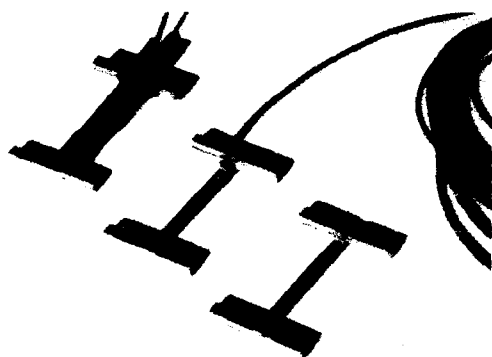


Figure 3 Strain gauge type 2

Care had to be taken to ensure that the aluminium plate was not too stiff since it would then have functioned as a reinforcing element in the pavement layer. This would have resulted in unrealistically low deformation measurements.

Vertical deformation

In the case of granular materials (soil and gravel) we installed sensors designed to measure the relative displacement of two metal plates as shown by figure 4. This displacement is sensed by means of a previously calibrated, short stroke inductive detector (figure 4).

Surface deflection

The surface of pavement is subjected to a vertical displacement as a rolling load passes. The dynamic measurement of this displacement is measured with respect to a metal rod sunk to a depth of 2 to 6 metres where it is considered that there can be no vertical displacement. A sensor secured to the surface layer of the pavement bears on this rod. Two types of sensors are employed.

The type 1 sensor consists of a metal plate fixed to the pavement with the free extremity resting on the rod. Four

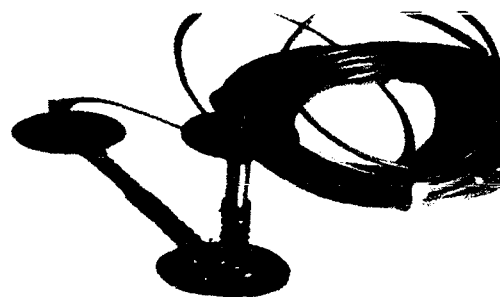


Figure 4 Vertical deformation sensor for use in granular materials

strain gauges mounted on the plate provide a measure of the deflection.

The type 2 sensor differs in that it consists of an inductance, the iron core being secured to the rod and the coil to the pavement.

Vertical stresses

A miniature displacement sensor is mounted between two diaphragms (figure 5). The output signal is measure of the effective displacement from which the soil pressure can be determined on referring to calibration curve.

Temperature

Accurate and regular measurement of the temperature is essential. Most models of the reaction and performance of pavement take account of this parameter.

About a dozen copper-constantan thermo-couples were fitted at different levels in each of the structures. A complete set of temperature readings are taken for each phase of measurements and during the loading phases a set of such readings are taken automatically every hour.



Figure 5 Pressure sensor



Figure 6 Installation of deformation sensors at the base of the asphalt layer

Frost level

The frost level is determined by means of a cryopedometer. This consists of a tube filled with glass balls and fluorescein, the colour of the latter changing down to the frost level.

Hygrometry

The level of the water level is regularly checked by means of a piezometer.

A tensiometer is also to be employed with a view to determine the degrees of saturation of the soil and the movement of water that can take place within it.

INSTALLATION OF SENSORS

All the sensors described above were installed before or during the construction of the pavements.

The installation of the sensors at the interface between two layers is a relatively easy matter (figure 6). Precautions need to be taken however to ensure that the sensor is in the right position and that it is properly protected in connection with the circulation of road construction plant on the site.

The installation of sensors within the granular layers is a more difficult matter (figure 6). Having laid the material it is necessary to excavate a cavity and to place the sensor in the correct position within that cavity on making sure that its "zero setting" has been respected. The excavated material then has to be replaced on respecting the initial conditions as well as possible. In the case of treated gravel this operation has to be carried out quickly so as not to disturb the setting of the cement (figure 7)

INITIAL RESULTS

At the moment when we are just starting to carry out the first measurements we can confirm that the sensors that have been installed in the structures are in good working order. The sensors have been connected to a new data acquisition system which enables us to obtain readings from 32 of them at a time.

CONCLUSIONS

The scale of the OECD experiment led us to choose inexpensive sensors of known reliability. We were accordingly



Figure 7 Installation of vertical deformation sensors

able to install a large number of them and so as to guard against the possibility of one particular type being incompatible with the operating constraints of fatigue testing ring. The large amount of data that we will be able to acquire will also enable us to come to statistically significant conclusions.

REFERENCES

1. Accelerated methods of predicting the life of pavements, OECD, Paris, 1985.
2. Full scale tests on road superstructures, OECD, Paris, 1985.
3. Deformation measurements in hydrocarbon layers, Office fédéral des routes, Berne, 1985.

CASE STUDIES IN APPLICATION OF PAVEMENT INSTRUMENTATION

Ross A. Bentsen, U. S. Army Engineer Waterways Experiment Station
Albert J. Bush III, U. S. Army Engineer Waterways Experiment Station

Two pavement investigations have been performed by the U. S. Army Engineer Waterways Experiment Station which involved the installation of instruments to measure the pavement response to traffic movement and to the operation of pavement nondestructive testing (NDT) devices.

One study was initiated to develop a transfer function correlating the pavement deflection under aircraft loading to the deflection produced by NDT. Velocity transducers were installed in the asphalt surface course of two airfield taxiways to measure pavement deflection beneath a moving aircraft. Tests were conducted with a falling weight deflectometer (FWD) at the same location to produce data for the development of the transfer function.

The second project involved a test road constructed to study the effects of tire pressure on low-speed, low-volume pavement design. Multidepth deflectometers were placed to determine deflections at various depths in the pavement system. Strain gages were placed to measure the tensile strain at the bottom of the asphalt surface course. A weather station has been installed to collect sundry environmental data including the temperatures measured by thermistors at various depths in the AC surface.

This paper will discuss the types of instrumentation used in each project

as well as the methods used in their installation and collection of the data.

AIRCRAFT DEFLECTION TESTING

This project evolved from a Federal Aviation Administration (FAA) request for the development of a transfer function correlating the pavement deflection caused by a moving aircraft to the deflections produced during NDT. The use of NDT for pavement evaluation has become widespread, but no research has been performed which correlated NDT deflections to measured aircraft deflections. The aircraft deflections were produced by a Boeing 727 supplied by the FAA and by smaller trainer aircraft furnished by the U. S. Navy and Air Force.

One requirement in developing a transfer function between the aircraft deflections and the NDT deflections is a thorough knowledge of the pavement properties for the intended test sections. Extensive subsurface investigations were performed for another study in 1987 on specific pavement sections at both Sheppard AFB in Wichita Falls, Texas, and the Naval Air Station at Pensacola, Florida. In order to use the information gained from the previously performed in situ and laboratory tests, the asphalt test sections at

these sites were utilized in the aircraft deflection testing.

A Dynatest FWD was used to perform the NDT for these tests. The FWD determines deflections using seven velocity transducers placed at 1-foot increments away from the 12-inch loading plate. Desiring a similar deflection basin to correlate the aircraft deflections with the NDT deflections, the deflection sensor configuration shown in Figure 1 was designed for data collection using the aircraft's starboard main gear loading. Deflections were measured using eight sensors oriented perpendicular to the direction of aircraft travel. One deflection sensor was positioned at the center line of the gear's two wheels. One sensor was centered under the starboard tire, and one sensor was located at each of the starboard tire edges. Four deflection sensors were placed at 1-foot intervals away from the starboard tire. Deflections were determined in this experiment with a Mark Products L-10B velocity transducer, which has a natural frequency of 4.5 Hz, and was 70 percent critically damped using a 375 ohm shunt resistor. The L-10B has a deflection range of 80 mils.

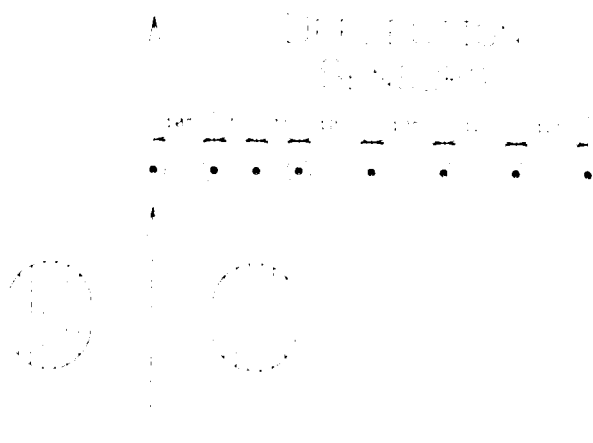


Figure 1. Aircraft Deflection Sensor Configuration

The transducers could not be placed directly on the pavement surface so the gages were installed in 2-inch-diameter holes drilled approximately middepth into the 5-inch asphalt surface course (Figure 2). Saw cuts were used to contain the coaxial cables attached to the transducers and guide them to the data

collection equipment. The bottom of the holes were leveled with a high modulus, high strength epoxy, and the gages were fixed to the hardened epoxy with a thin layer of modeling clay. Deflections greater than 80 mils were anticipated directly under the wheel so the larger holes there were necessary to accommodate a Mark Products L-1U velocity transducer with a natural frequency of 4.5 Hz and a deflection range of 100 mils. It was realized that some elastic deformation of the asphalt surface would be lost by measuring in this manner, but the amount was considered to be negligible.

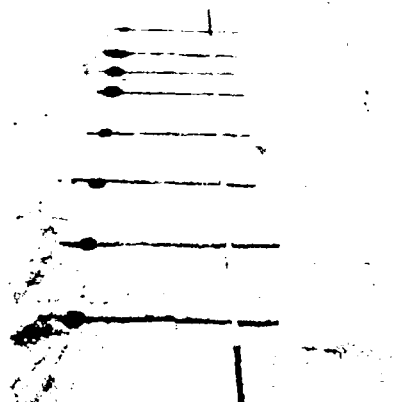


Figure 2. Deflection Sensor Installation

Two operational variables, the speed of the aircraft and the location of the gear loading as it passed over the sensors, would affect the deflection registered by the sensors. Therefore, it was necessary to measure these variables as the aircraft passed through the deflection test section. Target aircraft operating speeds of 5, 12, and 20 knots were used in the data collection, and the precise aircraft speed was determined with infrared light sensors placed sequentially along the direction of aircraft travel (Figure 3). Opposed mode light sensors were used, meaning that movement was detected by a separate transmitter and



Figure 3. Infrared Light Sensor Configuration

receiver. The sensors were made by Banner Engineering Corporation and detect objects using a beam of infrared light about 1/2 inch in diameter with a detecting range between the sensors of 200 feet. The light sensors were installed on adjustable stands in order to detect the aircraft wheel at its center. The transmitters were set up on one side of the taxiway and the receivers on the other. Five light sensors were spaced 4-feet apart. The data from the series of light sensors were used to determine the speed and location of the tire with respect to the deflection sensors. This particular sensor produces a beam narrow enough that the signal from one transmitter is only detected by its respective receiver.

The lateral location of the gear loading as it passed over the deflection sensors was determined by a strip of flour and water paste painted on the downstream side of the deflection sensors (Figure 3). The location of the outboard tire was measured in relation to the first sensor. A measurement of 17 inches, which is half the spacing of the 727 main gear, meant that the gear load was centered over the first sensor.

The signals from the velocity transducers and the infrared light sensors were recorded with two devices--a tape machine and a computer. The direct analog signal was recorded with a

14-track tape machine recording on intermediate band at a tape speed of 3-3/4 inches per second and at a maximum frequency response of 1.25 kHz. The frequency spectrum recorded at this setting was 0 to 200 Hz, and a 14-channel variable gain buffer amplifier was used to record the analog signal approaching the maximum deviation of the tape machine's response. The amplifier was also used to prevent interference between the tape machine and the computer. The computer was used to digitally record the data by converting the signal through a 16-channel multiplexed 12-bit A-D board. The data were recorded at a rate of 1,000 samples per second per channel with a resolution of plus or minus 5 millivolts. Digital gain settings of 1, 2, 4, and 8 allowed the signal to be amplified and recorded at the A-D board's maximum range of plus or minus 10 volts. The amplifiers on both the tape machine and the computer allowed us to record the data at the maximum resolution of each recording device.

The aircraft weight was necessary to correlate the aircraft deflection with the FWD deflection and, in particular, the weight of the gear trafficking the deflection sensors. Each of the aircraft gear was weighed by towing the 727 onto two portable scales with capacities of 70,000 pounds each

(Figure 4). Ramps with no scales used beneath the other gear kept the load fairly balanced. The total weight measured with the scales correlated well with the aircraft weight calculated by the flight engineer so, as the aircraft lost fuel with each successive pass through the test section, the flight engineer's calculated weight was recorded to correlate each aircraft run with the FWD data.

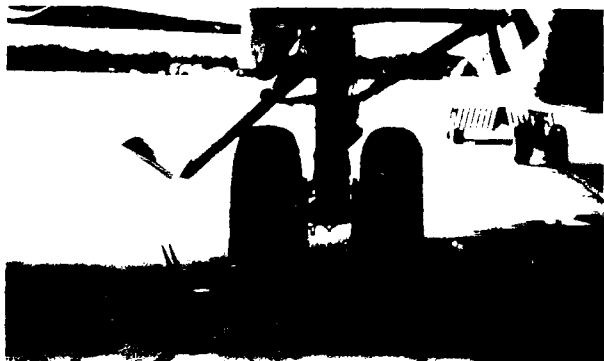


Figure 4. Scales Weighing Aircraft Main Gear

The distance between the nose gear and the main gear is about 63 feet so the data collection for each run was started just after the nose gear had passed through the light sensors. Data collection for each run lasted between 3 and 5 seconds, depending on the aircraft's speed. After each pass of the aircraft, the offset of the outside wheel was measured in relation to the first sensor using the imprint in the flour paste (Figure 5).

After three successful aircraft runs at a given speed, the Dynatest FWD generated deflections at four load levels between 9 and 25 kips (Figure 6). Using the position of the last aircraft run shown in the flour paste, tests were made at the position of the outboard tire and then at the center line of the two tires. Tests were performed directly adjacent to the in-pavement sensors, and the deflection measurements from each load level were collected simultaneously with the FWD sensors and the in-pavement sensors.



Figure 5. Lateral Measurement of Outer Wheel Location



Figure 6. FWD Testing Adjacent to In-Pavement Sensors

To supplement the data that were collected using the B-727, tests were also performed with a Navy A-4 at Pensacola and with an Air Force T-38 at Sheppard. These aircraft were towed through the test section at a target speed of about 10 knots.

Pavement temperatures in the asphalt layer were measured on the quarter hour using three thermistors. The thermistors were placed at the midpoint and at 1 inch from the top and 1 inch from the bottom of the 5-inch asphalt surface.

Unfortunately, results from the deflection testing are unavailable at this time. The correlation between actual aircraft deflections and NDT which will result from the aircraft deflection testing will help determine the validity of current pavement evaluation criteria that are used for

calculating allowable wheel loads on pavements.

TIRE PRESSURE TEST ROAD

The second project which necessitated in-pavement instrumentation involved a test road which had been built to study low-speed, low-volume pavement design. This facility has 15 test sections of various thicknesses of asphalt and granular surface. Each test section has two traffic lanes--one for high-pressure-tired truck traffic and one for low-pressure-tired truck traffic. The two traffic lanes will help determine whether low-volume road pavement thickness depths can be reduced using decreased tire pressures, identify the parameters in the tire/road contact that contribute to road surfacing deterioration, and determine the effects of tire pressure on pavement deterioration during periods of weak subgrade conditions.

Instruments being used in the performance of this testing are multidepth deflectometers (MDDs) which are being used to measure the deflections at various depths in the pavement,

thermistors placed in the asphalt surface to collect temperature data, strain gages installed at the base of the asphalt layer, and a weather station that automatically collects various environmental data.

Three of the asphalt-surfaced sections of the test road have been instrumented with various combinations of MDDs, strain gages, and thermistors (Figure 7). Section 6 has a pavement cross section of 2 inches of asphalt over 2 inches of limestone aggregate and has instruments consisting of a thermistor at the top of the asphalt and a strain gage at the bottom of the asphalt in the high pressure lane. Section 10 has a cross section of 4 inches of asphalt over 4 inches of limestone base and contains strain gages and MDDs in both traffic lanes as well as thermistors at three levels in the AC. Section 12 has a pavement consisting of 5 inches of asphalt over the subgrade and contains an MDD and a strain gage in the high pressure tire lane and thermistors at three levels in the asphalt surface.

The MDD is a series of linear variable differential transformer (LVDT) displacement transducer modules

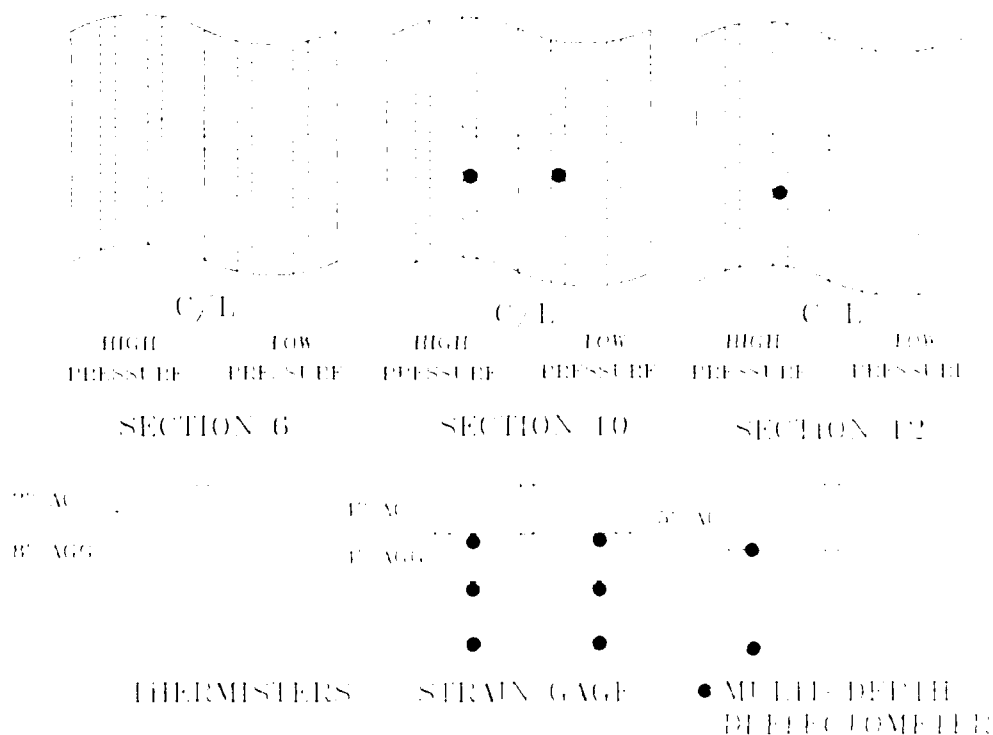


Figure 7. Instruments Installed in Test Road

NO-4214 957

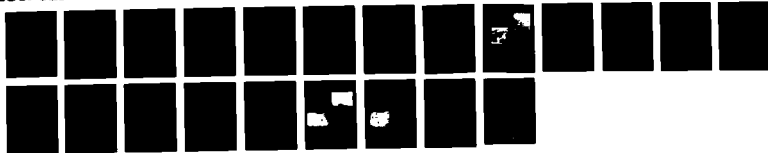
STATE OF THE ART OF PAVEMENT RESPONSE MONITORING
SYSTEMS FOR ROADS AND AIR. (U) COLD REGIONS RESEARCH AND
ENGINEERING LAB MANOVER NN V JANOO ET AL. SEP 89
CRREL-SR-89-23

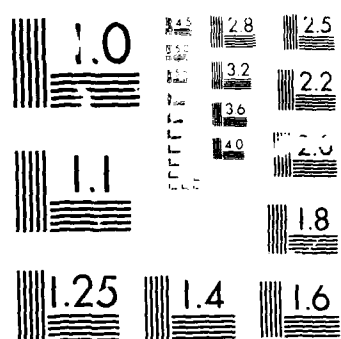
575

F/B 13/2

ML

UNCLASSIFIED





that are installed in a core hole to measure deflection at various depths in the pavement structure. Figure 8 shows the basic components of an MDD module. After the core hole is drilled, a rubber wall enclosure is poured and set to the outside wall. An anchor rod is cemented into the bottom of the core hole. The MDD module is fixed, lowered into the core hole, and tightened against the rubber wall at the desired depth. An interconnecting rod is connected to the anchor rod, and the LVDT is calibrated for deflection measurement. Successive modules are placed and calibrated in this manner. Cable ducting along the outside of the module allows for wires from the LVDT to pass beside the tightened module to the top of the hole.

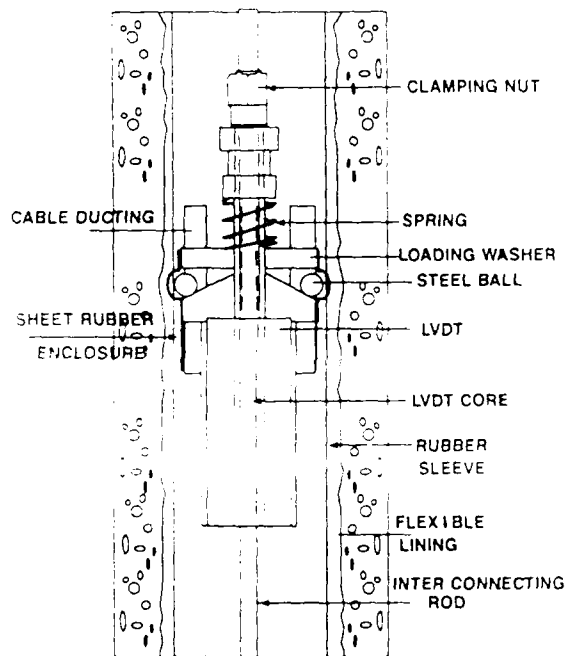


Figure 8. Components of an MDD Module

A typical cross section of an MDD installed in a pavement (Figure 9) shows the anchor cemented at the required depth. The top of the anchor rod contains a snap connector which allows for the MDD modules to be placed and removed from the hole during installation and calibration of the LVDT. After the modules are calibrated and secured in the core hole, the cables from each LVDT are connected to the surface cap. This cap connects to the flat connector cable which is laid on the pavement surface

and leads to the data collection computer. The variability of the module placement allows for deflection measurements to be taken at any depth in a given core hole. This illustration shows MDD modules located in the base course and one of the subbase courses.

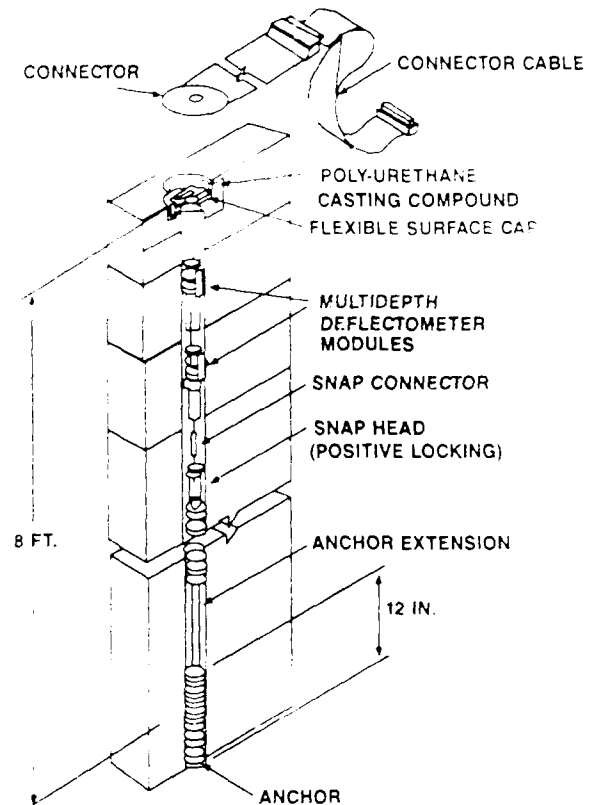


Figure 9. Typical Cross Section of MDD after Installation

Typical results from the MDD installed in Section 10 are illustrated in Figure 10. Section 10 has a pavement cross section of 4 inches of asphalt over 4 inches of limestone base. MDD modules were placed at 4 inches (at the interface of the asphalt and the base), at 10 inches (2 inches into the surface of the subgrade), and at 24 inches (16 inches into the subgrade). This graph shows the effects of depth on deflection as each of the five axles of the high-pressure-tired truck passes over the MDD. This plot shows data with the truck moving at a little over 2 miles per hour.

Figure 11 is a plot of the deflection created by an FWD operating at a load of 9,998 pounds directly adjacent to the MDD in Section 10. The pulse

created by the FWD is detected by each LVDT with the amount of deflection decreasing as the depth of the LVDT is increased.

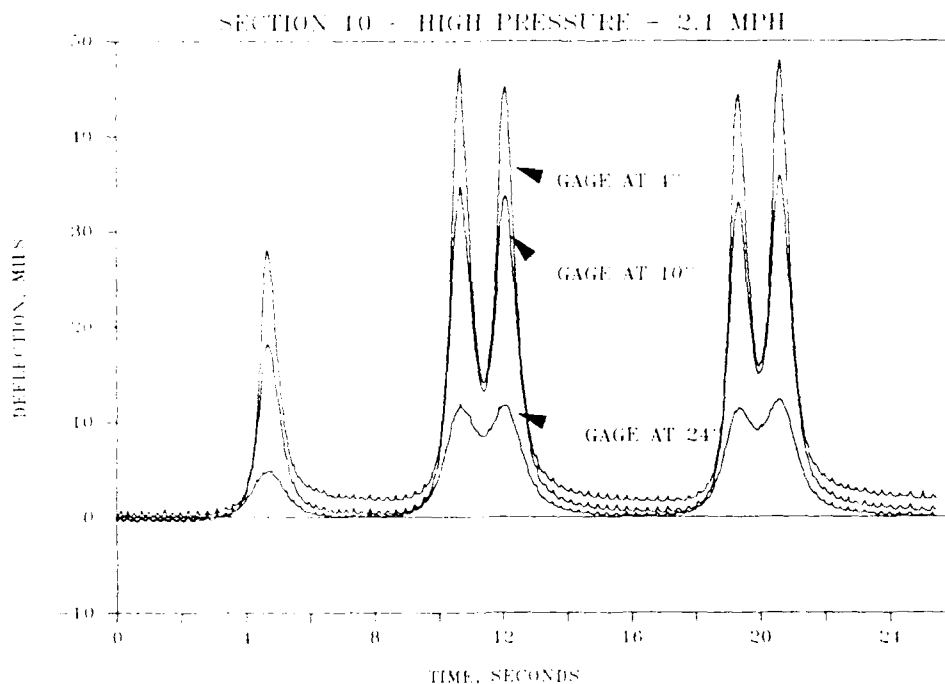


Figure 10. MDD Response to FWD Loading

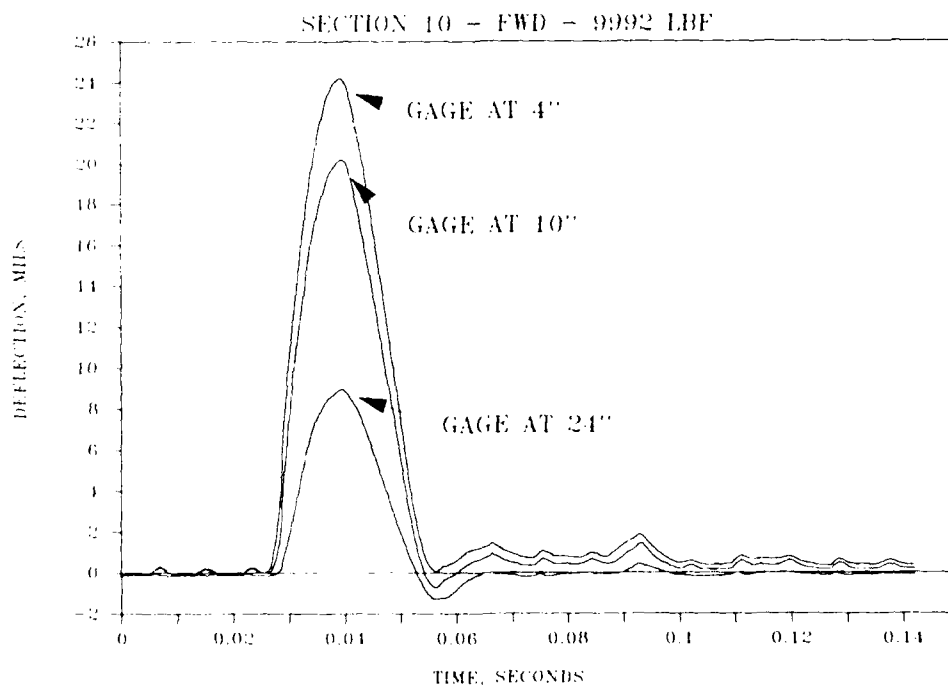


Figure 11. MDD Response to FWD Loading

The effects of speed on the maximum deflection registered by each LVDT are illustrated in Figure 12. The data shown are the deflections from the first loading axle of the high-pressure-tired truck versus speed. As the truck speed is increased, less deflection is measured by each of the LVDTs. The tandem tires of each truck axle are carrying 9,000 pounds. Also illustrated are the maximum deflections at the three depths created by a 9,000-pound drop of the FWD. The deflection created by the FWD is markedly less than that generated by the truck.

Figure 13 shows the responses of both the high-pressure- and low-pressure-tired trucks at varying speeds on the high pressure lane of Section 10. The deflection caused by the high-pressure-tired truck is greater than the low-pressure-tired truck at all three depths. The effect of decreasing deflection with increasing speed is again illustrated.

Two-inch foil-type strain gages were installed on the bottom of cores which were taken from the asphalt surface after its placement. The strip gages were attached to the core using epoxy. The core was then epoxied back into its original core hole in the asphalt surface to perform strain measurements under traffic.

The weather station makes an hourly record of the temperatures registered by the thermistors installed in the AC surface as well as the air temperature, relative humidity, solar radiation, barometric pressure, rainfall, and wind velocity. The data are recorded on a microprocessor contained in the weather station. The microprocessor can then be removed, and the data transferred to a computer for analysis.

ACKNOWLEDGEMENTS

The research presented in this paper was sponsored by the U. S. Department of Transportation Federal Aviation Administration and Federal Highway Administration and the U. S. Department of Agriculture Forest Service.

The testing was performed by personnel of the U. S. Army Engineer Waterways Experiment Station, Vicksburg, Mississippi, and Federal Aviation

Administration Airport Technology Branch, Atlantic City, New Jersey.

The use of commercial products in this research does not constitute a recommendation or an endorsement.

The opinions expressed in this paper are the views of the author and do not represent the views of the Departments of Defense, Transportation, or Agriculture. This paper does not constitute a standard, specification, or regulation. This paper is published with the permission of the Chief of Engineers.

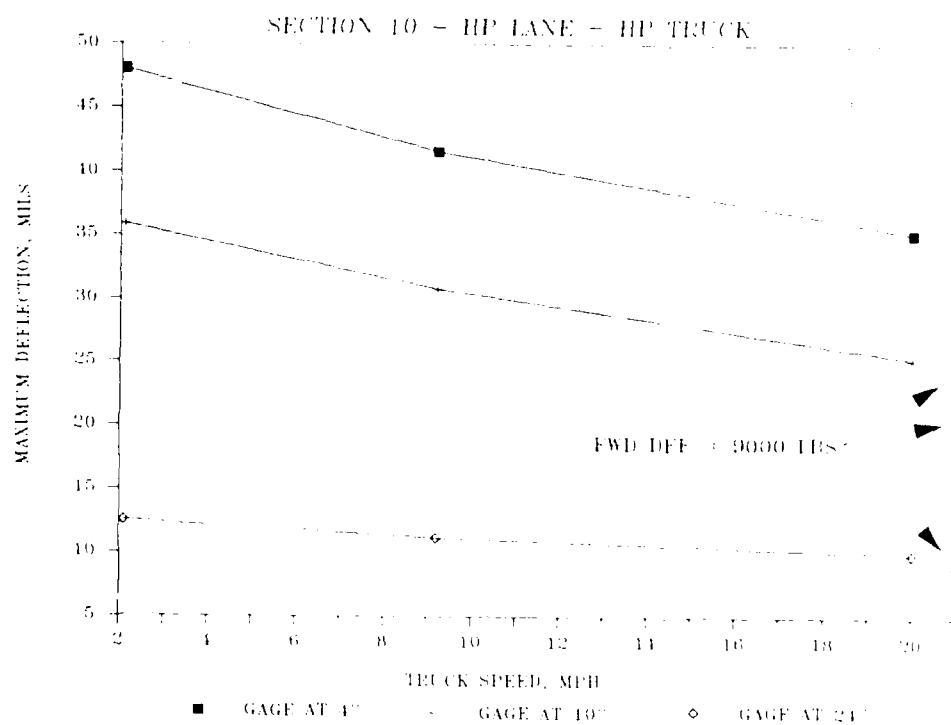


Figure 12. Effect of Speed on MDD Maximum Deflections

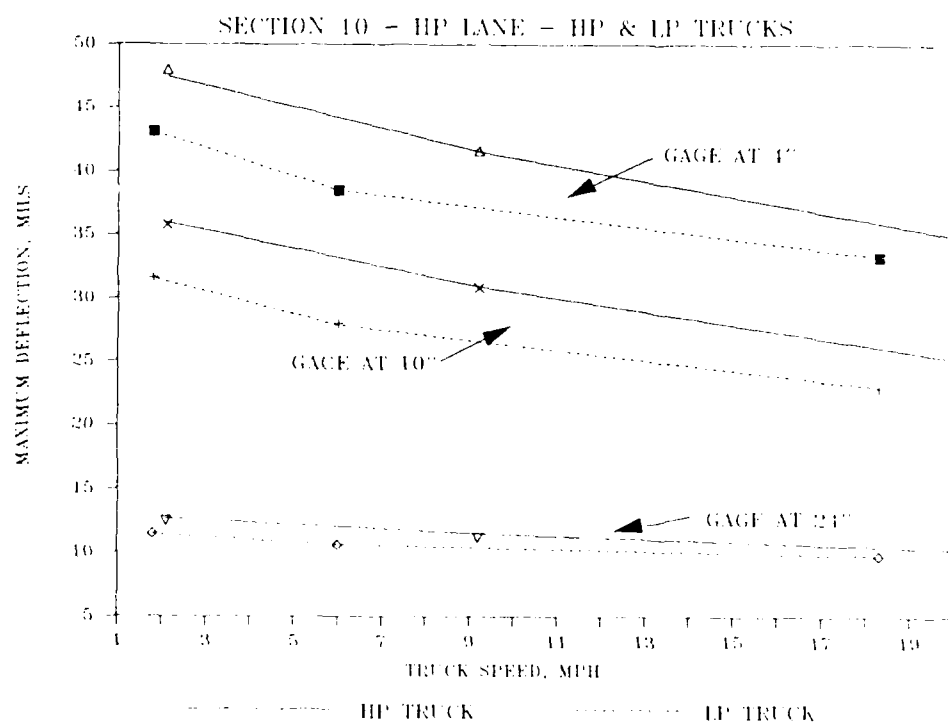


Figure 13. Effect of Speed and Tire Pressure on MDD Maximum Deflections

EXPERIMENT F PAVEMENT INSTRUMENTATION AT TRRL

I. F. Addis

Transport and Road Research
Laboratory
Tring, Hemel Hempstead

ABSTRACT

The Transport and Road Research Laboratory has been involved with the instrumentation of experimental pavements for many years. The experience gained has been used to improve existing gauges, to develop new gauges, and to refine installation techniques. Because of the nature of the paving materials used, the analysis of information derived from pavement instrumentation can be an extremely difficult process. To minimise these difficulties, gauges used have had to be carefully designed, with appropriate attention to accuracy, reliability and installation procedures.

This paper describes briefly the history of pavement instrumentation at TRRL, details the types of gauge currently in use, and indicates new developments in gauges and installation techniques.

Finally, the range of research applications of the instrumentation are described, together with the purposes of these experiments.

INTRODUCTION

During construction, and while in service, a road pavement offers an extremely hostile environment to any instrument from which it is hoped to gain useful information concerning the response of the pavement to loading. Moisture, hot asphalt or bituminous mixes, hard aggregates and construction machinery all carry

significant risk for the survival of gauges either during or after installation. Measurements from a gauge may be sent away in order due to the presence of a storm in the gauge or its cabling, or a mechanical change to either. One of the principal requirements of a gauge designed to measure pavement response, therefore, is that it is robust as well as accurate and reliable.

This paper describes the history, development and application of a range of gauges used by TRRL for the measurement of pavement response.

HISTORY OF PAVEMENT INSTRUMENTATION AT TRRL

A systematic programme of construction of full scale pavement experiments built into the public network began in 1955 and served as the basis for formulation of design standards until about 1960. Some of the later experiments constructed in this series were instrumented with gauges that had been developed in the preceding 10 years for use in controlled full scale experiments at the TRRL site, or in the accelerated pavement testing machine known as Road Machine 1. Better et al (1969) have described the instrumentation of a full scale pavement experiment built in 1968 using gauges whose principles of construction remain virtually unchanged today. Since 1970, however, growths in both the number of commercial vehicles in the national fleet, and the average wearing power of individual vehicles (expressed in terms of equivalent 30kN axles per

vehicles have frequently exceeded forecasts. In response to the need to introduce designs capable of carrying these greatly increased traffic levels, Lowell et al developed an improved methodology for pavement design to allow for the more rapid introduction of improved materials and designs, with an assurance of good performance under heavy traffic. Progress in developing this methodology emphasized the need for pavement testing under controlled accelerated conditions of loading and temperature, in order to improve our understanding of the influence of these parameters on pavement deterioration and to link the results to the variable conditions experienced by a road in service. Of equal importance, from the point of view of pavement instrumentation, the results of controlled accelerated pavement testing are an important input to the refinement of pavement performance models.

The more recent emphasis on controlled testing has prompted a closer look at the design, operation and reliability of the gauges used and the techniques of installation. The remaining sections describe the various types of gauge used, and some recent improvements to their design or installation.

TYPES OF GAUGE USED

Because of the non-linear and visco-elastic nature of many road materials, the response of a pavement to the passage of heavy wheel loads at the surface is a complex process not easily expressed in mathematical terms. For these reasons, much attention has been paid to the development and use of layered elastic response models, in which only the elastic modulus and Poisson's ratio for the constituent materials determine the stresses and strains generated. To validate this approach the stress and/or strain at particular levels in the pavement must be measured; also, these measurements must be supported by an understanding of the variation of modulus of a material with, for example, temperature or moisture content. Generally, these relationships will be determined in laboratory conditions and the results applied to an interpretation of the measured response of the pavement.

At TPRI, most of the instrumentation work has been aimed at the principal responses of the pavement, namely sub-

grade stress and strain, strain at the under-side of the bound layers, and deflection at the surface and within layers. In addition, much attention has been paid to the measurement of pavement temperature.

Subgrade stress

Potter (1972) has described the main requirements of a soil stress gauge in order to have a gauge calibration that does not change with soil modulus. These are: that the modular ratio between gauge and soil should exceed 40:1, that the diameter to thickness ratio should exceed 5:1 and that the central area only of the gauge should be sensitive to applied pressure. Soil stress gauges that satisfy these requirements have been based on a piezo-electric active element (Figure 1)

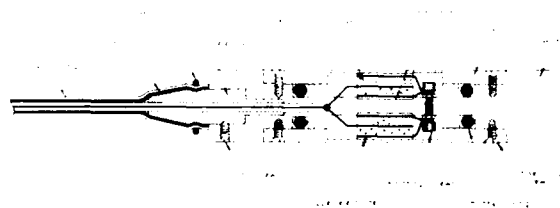


Fig 1. Sectional Elevation of Piezoelectric Gauge (Mk II)

or an inductive displacement transducer (Figure 2). The first of these gauges has

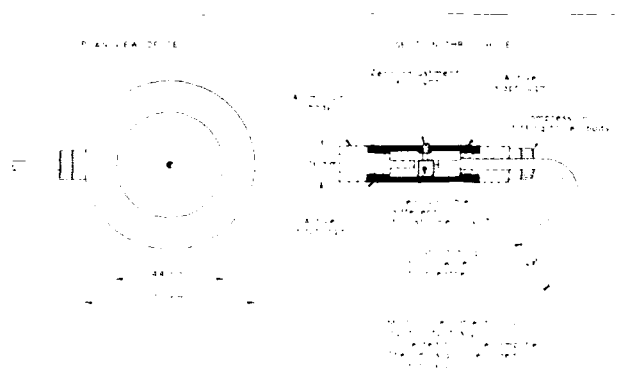


Fig 2. TPRI/LVDT Soil Stress Gauge

proved to be a durable but somewhat expensive instrument, it has been installed in many full scale test pavements. Although having a number of advantages, including high mechanical strength, it has the disadvantage of requiring a charge, rather than voltage, amplifier. This type of amplifier often lacks the stability necessary for accurate measurement, and does not overcome the main disadvantage of this type of gauge, namely that the increase of minute amounts of water reduces the dissipation resistance of both crystals and cable, leading to a loss of charge on the faces of the crystals and inaccuracy in the measurement.

In the second type of gauge, some of these disadvantages have been overcome. The active element of the gauge is now an inductive displacement transducer, operating between diaphragms fixed to each side of an annular section. The overall diameter of the gauge has been reduced to 20mm and the overall thickness to 10mm. The transducer is excited from an AC carrier amplifier system, and provision is made for zero adjustment through the upper active diaphragm. This type of gauge is substantially cheaper to produce than the piezo-electric device and has other advantages brought about by the simplified excitation and recording system.

Both types of gauge are individually calibrated in a pressure chamber. The gauge is immersed in water contained in the chamber and a slowly increasing gas pressure is applied to the chamber. The output from the gauge due to the pressure change is recorded, both as pressure increases and decreases, usually over a range of $\pm 200 \text{ kN/m}^2$.

The installation of either type of gauge in both cohesive and granular soils requires careful attention. Usually, a hole about 10mm in diameter is excavated by hand to the appropriate depth, the gauge is placed in the desired orientation on a small platform of soil, and soil, either minced or sieved depending on it's nature, is returned to the hole and compacted by hand. Although this method of installation has been used for many years, it is clear that the gauge is contained in a "plug" of heavily disturbed soil. It was thought that this may partly account for the relatively wide variations in stress recorded by different gauges in the same pavement under identical loading conditions, and improvements to the method of installation were sought. This resulted

in the development of a gauge which, in the present form, is a self-contained unit which can be used in the field and which need not be connected to any outside cable.

Self-contained gauge

The gauge is self-contained and has been designed to be used in the field to give an instantaneous reading of strain in a variety of orientations. It is shown in Figure 3. It consists of a transducer with flanges attached to the ends of the active displacement transducer, the upper

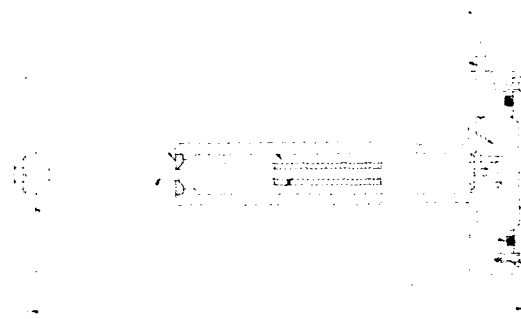


Fig. 3. Soil Strain Gauge

which runs in PTFE bearings, to reduce friction and ensure that the gauge offers little resistance to movements in the direction of measurement. The two anti-phase secondary coils of the transducer are wired to form a half bridge, and movement of the flanges is measured in terms of the out-of-balance voltage generated as the core moves.

Each gauge is calibrated prior to installation in a micrometer, etc. Additional transducers are calibrated with each batch of gauges, and these are subsequently used as standards to check the calibration of the carrier amplifier system before and after a series of tests. The sensitivity of the gauge is unaffected by temperature.

Although the installation process works well in practice, excavation, placement of the gauge and replacement of excavated soil gives rise to doubt that the gauge is in soil truly representative of the whole. A further problem arises because of the need to provide a gauge that is sensitive enough to measure the

small, strong, and resistant to strain pavement, and the hole is filled with a range of sand or gravel. The porous sand supports the soil in the vicinity of the gauge. The sand is then tamped in short segments, each 1/4 in. thick, and careful installation of the gauge hole is maintained with the use of a wedge between the flange and soil, being to ensure no lateral displacement. At this point, the soil is tamped in place and the gauge is driven into the soil. During and after this operation, the gauge is kept in a relatively undisturbed position, with the use of the jacking plate, thus maintaining the proper frame orientation.

The new technique utilizes a jack which acts as a wedge between the new jack, the gauge, and the soil. The first step of the

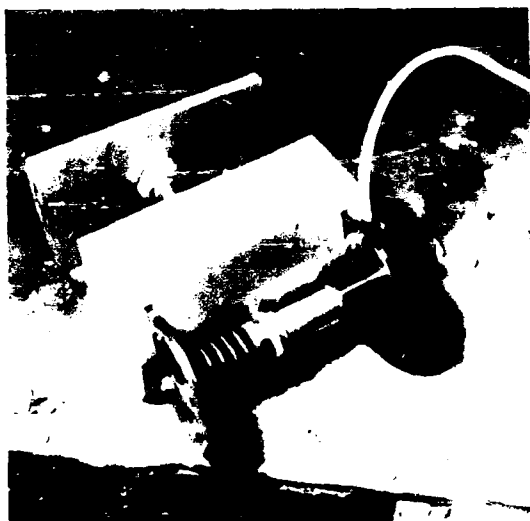


Fig. 4. Strain Gauge Installation (A)

operation is to excavate a hole approximately 1/2 in. in diameter and 1 in. deep. The gauge is then inserted by a distance equal to the hole depth, and the position of the gauge is determined by the flip in direction of the hole. The gauge is then driven into the soil by a screw thread, which is attached to the handle of the jack.

The gauge is then driven into the soil by a screw thread, which is attached to the handle of the jack. The gauge is then driven into the soil by a screw thread, which is attached to the handle of the jack. The gauge is then driven into the soil by a screw thread, which is attached to the handle of the jack. The gauge is then driven into the soil by a screw thread, which is attached to the handle of the jack.

operation is to excavate a hole approximately 1/2 in. in diameter and 1 in. deep. The gauge is then inserted by a distance equal to the hole depth, and the position of the gauge is determined by the flip in direction of the hole.

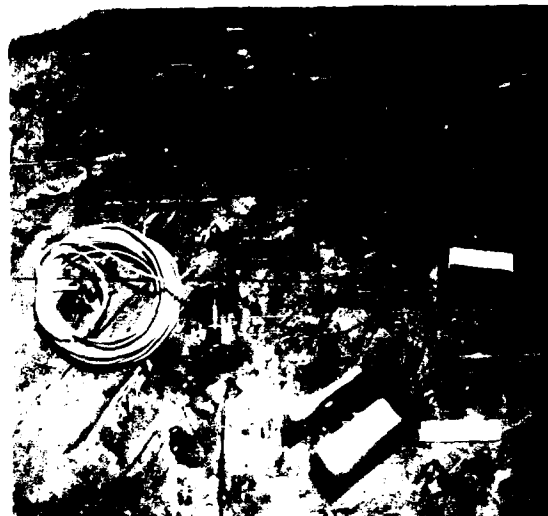


Fig. 5. Components of Gauge Installation

The gauge in the soil is then driven to the required depth in the hole, and the exposed ends of the flange are brought into contact with the vertical face of the soil. A reaction plate is positioned between the jacking plate and the rear face of the hole and the gauge is driven horizontally into the soil by rotating the screw thread. The gauge is then removed and the hole backfilled by hand with sieved or mined soil.

A controlled experiment to quantify improvements due to this method is virtually impossible, but results obtained from gauges installed by this technique appear to show less variability in similar soil than with the previous technique.

The principles of the method have been used for the installation of soil stress gauges, but this is an inherently more difficult exercise because of the need to make a precisely dimensioned, perpendicular hole in a vertically excavated face. However, initial trials have been very encouraging and further work is planned.

Gauges for measuring strain in the base or surface layers.

The gauge is then driven into the soil by a screw thread, which is attached to the handle of the jack. The gauge is then driven into the soil by a screw thread, which is attached to the handle of the jack.

on suitable lower surface, and should be relatively transparent. Therefore, large, round, transparent, and thick (1/2" thick) rings that were thin and relatively stretchable were used and size highly variable (see fig. 1). The rings were of 80/100 mesh size, which allowed the material to be stretched to about the diameter of the ring. The rings were used to stretch the material to the diameter of the ring.

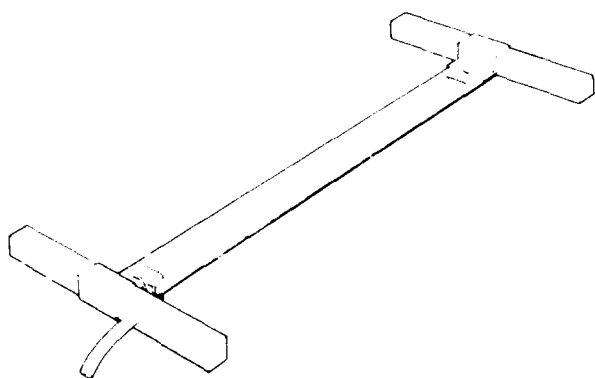


Fig. 1. Aluminum strip strain gauge.

Two of each strain gauge to provide a cross section of the solid material. A resistance foil strain gauge is oriented on the surface of the aluminum strip and is then covered with epoxy resin and covered with V tape to minimize the risk of moisture penetration. The strain gauges are wired with a timer gauge to form a unit bridge. Each gauge can therefore give a output, and a facility gauge can be identified by difference between the two.

Experience with this type of gauge showed that the epoxy resin layer covering the resistance foil was thick enough to be uncomfortable for wearing during handling in other instrumentation, and that the cracking caused by moisture failure of the resistance foil. In a later design, gauges were built using only one foil, thus reducing the overall thickness of epoxy coating. The effect of this last

change was to reduce the thickness of the epoxy coating to 0.001 in. (0.025 mm) and the thickness of the foil to 0.001 in. (0.025 mm).

The first design of the strain gauge was used to measure the strain in the concrete during the curing process. The strain was measured in the concrete during the curing process.

The second design of the strain gauge was used to measure the strain in the concrete during the curing process. The strain was measured in the concrete during the curing process.

The third design of the strain gauge was used to measure the strain in the concrete during the curing process. The strain was measured in the concrete during the curing process.

The fourth design of the strain gauge was used to measure the strain in the concrete during the curing process. The strain was measured in the concrete during the curing process.

Transient pavement deflection

The measurement of transient pavement deflection has always received little attention, because of the problems of determining the present structural condition of a flexible pavement. In the field, a number of devices have been used to measure transient pavement condition, beginning with the beam deflection and moving now to the deflection graphs and falling weight deflectometers. The beam deflection is brought about by the application of a load to the surface of the pavement, and the deflection is measured by the deflection graphs.

However, even a very accurate, after requires a very detailed knowledge of the behavior of the pavement, and this is particularly true of transient deflection. Although it is possible to measure total pavement deflection, it is not possible to measure transient deflection, and this is a knowledge of what is the deflection curve in the pavement layer would be invaluable.

I

I

I

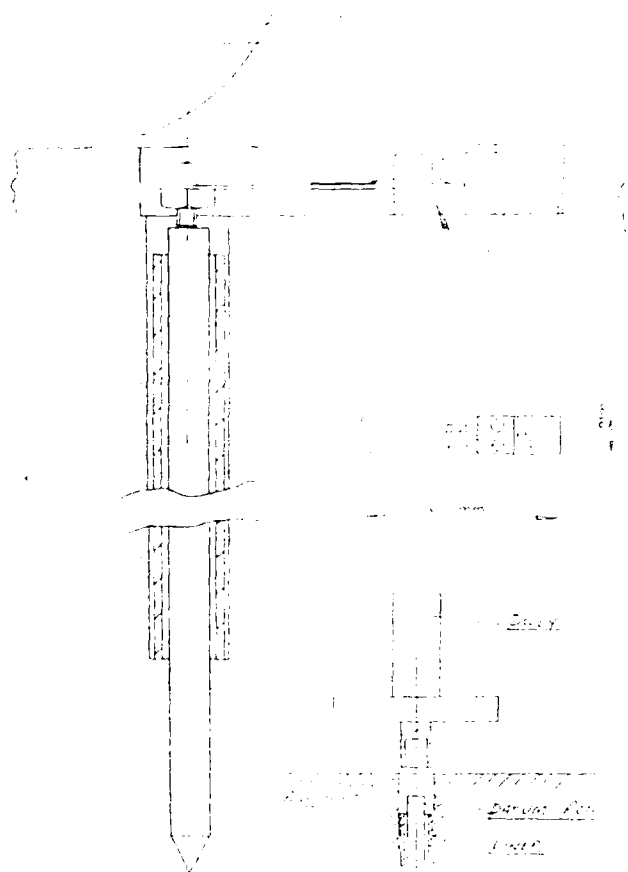


Fig. 8. General arrangement of TRFL deflection stage.

8mm 1/8" stainless steel or brass tube that terminates 25mm below the pavement surface. A 6mm diameter pointed steel rod is cut to length so that when driven securely into the base of the hole, the head of the datum rod is 5mm below the road surface. Some judgement of the nature of the soil is required so that a secure fixing is obtained. A strong cohesive soil will require the datum rod to be driven about 100 - 150mm (4 - 6in) into the soil, whereas a more granular soil will need fixing length of 300mm (12in) or more. Both the lining tube and the datum rod are driven into place using the dolly arrangement shown in Figure 8. To measure deflections in moderately strong cohesive subgrade, the pavement is first drilled until the subgrade is penetrated. The lining tube is then greased and used to bore a hole to the datum level in the soil and finally to remain in place as the

lining tube. Then a strip of the lining tube of a length sufficient to cover the length of the vessel is inserted into the end of the lining tube, and an indicator on which the required depth, the amount of the cavity, is marked free into the lining tube. The lining tube is then inserted into the vessel, and the depth of the cavity is determined, and the lining tube is then removed before.

Calibration of the force transducer is done using a ten-gram weight. The springing of the meter drum leads to a small error in the cantilever arm, at the point where it will make contact with the film. A small fixed weight, both the excitation and signal recording unit, are used in this process so that the complete system is calibrated.

The pothole is now located directly in the center of the TRRI, where "clusters" of holes are located, occupying only a small area of the pavement, approximately 1000 x 1000 mm. It may have been installed in experimental pavements to measure the contribution of layers to total deflection.

Temperature

The measurement of pavement temperature in controlled pavement design experiments is an important but often neglected requirement. All flexible pavements are, to a greater or lesser extent, temperature sensitive, and although the temperature regime to which an in-service pavement is subjected changes continually, the importance of these changes can only be established by close control of temperature during an experiment, only having sufficient information available to make temperature corrections possible. At TRRL accelerated testing of pavements is carried out on pavements whose temperature at a given depth is closely controlled. This is achieved by installing in the pavement many thermocouples, the outputs of which are used to control infra-red heaters. Copper-constantan thermocouples have been used for many years, because of their relatively high output for the temperature ranges involved and for their robust nature. In practice, duplicate thermocouples are installed at a given level in the pavement during construction, but both sets invariably survive the construction process. Although it is relatively cumbersome to record the outputs from thermocouples, they are considered preferable to less robust thermistors.

The latter have, however, been successfully used in cores for placement in the road structure. Thermistor heads piled into holes drilled horizontally into cores extracted from the road have remained active for several years until they failed, probably due to the penetration of moisture into the head.

TYPICAL APPLICATION OF PAVEMENT INSTRUMENTATION

Accelerated testing

In the Pavement Test Facility (PTF) at TRRL, sections of experimental pavement are subjected to controlled, accelerated loading in order to assist the development of pavement design methods and to compare the performance of new designs or materials. Test sections are generally instrumented with some or all of the instruments described in this paper, and the layout of these gauges in the restricted length of a test section is important. It is frequently found that the variability of a given parameter is considerable, even within the relatively short length of 20-30 ft of well-controlled pavement construction used in the PTF. Figure 9 shows the layout of gauges generally used in each section of the PTF.

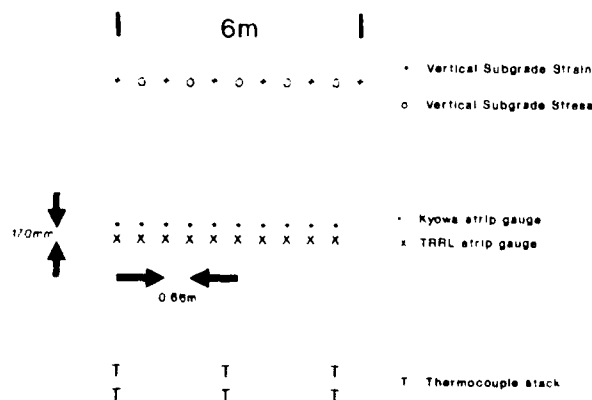


Fig 9. Typical instrumentation layout in PTF

sufficient numbers of gauges are included to allow an average for the whole of the test length to be derived, without including so much instrumentation that the per-

formance of the pavement might be affected. Data from the gauges is collected at the roadside and stored in a data logger. Some on-line data reduction and presentation is undertaken, but in the main, the results are transferred to a main-frame computer for analysis.

Controlled experiments in service track

Research has recently been undertaken into the pavement wear aspects of different wheel and axle groupings, and into the effects of various layouts of pavements. A length of flexible pavement in the TRRL track was instrumented with longitudinal base strain gauges. These were placed on a single line at intervals of 1m (3ft) over a length of 50m (165ft) of the test track. Except for buried thermocouples no other instrumentation was used, since the likely effects of the variables studied would be stronger on the base strain parameter than on other parameters. Temperature, however, would certainly vary over the duration of the experiments and was monitored continuously.

Correlation with other types of gauge

In recent years, a variety of different types of gauge for the measurement of the same parameters of pavement response have been developed by other workers in the field. Under the guidance of the Organisation for Economic Co-operation and Development (OECD) a trial was conducted in 1983 to attempt to correlate measurements from various types of base strain gauge. The TRRL type of gauge was used in this experiment and the results of the trial, reported by OECD, indicate both the advantages and disadvantages of different types of gauge and installation technique. It is hoped that they will offer a basis on which progress may be made towards "standard" types of gauge.

CONCLUSIONS

1. TRRL has developed and is using a full range of gauges for the measurement of pavement response to load.
2. Significant improvements have been made to the installation technique for the soil strain gauge.
3. A simple and reliable gauge for the measurement of the layer deflection in multi-layer pavements has been developed.
4. The gauges have found a number of

applications in controlled accelerated pavement testing, monitoring the condition of full-scale in-service pavements and for other experimental work.

from the text may be reproduced, except for commercial purposes, provided the source is acknowledged.

ACKNOWLEDGEMENTS

The work described in this paper forms part of the programme of the Transport and Road Research Laboratory and the paper is published by permission of the Director.

REFERENCES

Basson J E B, Wijnberger O J and J Skultety 1981. The multi-depth deflectometer: A multistage sensor for the measurement of resilient deflections and permanent deformation at various depths in road pavements. NITRR Report RP/3/81 South Africa. National Institute for Transport and Road Research.

Lister N W and A P Mayo 1970. A gauge for the measurement of transient and long-term displacements in road pavements RRL report LR 252. Crowthorne: Road Research Laboratory.

OECD 1985. Strain measurement in bituminous layers. Complementary Report. Berne Switzerland. Swiss Federal Office of Highways.

Potter J F 1969. Gauge for the measurement of dynamic and long-term strain in soil. RRL Report LR 251 Crowthorne: Road Research Laboratory.

Potter J F 1972. Stresses and strains generated in road structures. In Proceedings of J.B.C.S.A. Conference 1972. pp63-70. London.

Potter J F, Mayhew H C and A P Mayo 1969. Instrumentation of the full-scale experiment on A1 Trunk road at Conington, Huntingdonshire. RRL Report LR 296 Crowthorne: Road Research Laboratory.

Powell W D, Potter J F, Mayhew H C and M E Nunn 1968. The structural design of bituminous roads. TRRL Report LR 1132. Crowthorne: Transport and Road Research Laboratory.

Crown Copyright. The views expressed in this Paper are not necessarily those of the Department of Transport. Extracts

CONSTRUCTION OF FULLY INSTRUMENTED TEST PAVEMENTS IN NORTH CAROLINA

R N (Dick) Stubstad
N Paul Khosla
W Wayne Wynn

Dynatest Consulting, Inc
North Carolina State University
Dynatest Consulting, Inc

ABSTRACT

In the fall of 1988 and spring of 1989, forty-eight pavement test sections were constructed along State Route # 421 Bypass near Siler City, North Carolina, twenty-four sections in each direction of traffic. Various stress and strain gauges, along with other *in situ* measuring devices, were installed in the twenty-four northbound sections during construction.

This paper describes the materials and pavement layer thicknesses composing these pavement sections, as well as the gauges and other measuring devices used along with their method of installation.

Ultimately, the purpose of the project is to provide pavement engineers with important, field-verified information about the relationships between pavement response (in terms of deflections, stresses and strains) and performance (in terms of roughness, fatigue, etc).

Also, back-calculation of moduli and corresponding calculations of theoretical stresses and strains will be conducted using Falling Weight Deflectometer load-deflection data.

Finally, these theoretical values will be compared to the measured values to assess the validity of mechanistic-based pavement evaluation methods and develop new pavement design and performance models for typical materials used in the North Carolina region as well as elsewhere.

INTRODUCTION

During the past decade or two, pavement evaluation and rehabilitation design methods have -- slowly but surely -- changed from being essentially empirical in nature to being mechanistic, or analytical.

Formerly the approach was, in essence, if the deflection of an existing pavement was large, the pavement was "poor". Conversely, if the deflection was small, the pavement was "good". Empirical evidence, generally speaking, supported this logical supposition, mitigated in the more refined empirical approaches by considering the traffic level and even the thickness of the bound (asphalt) layer in the relationships used relating deflection to pavement performance.

In fact, these empirical methods are still in widespread use. An example of such an approach may be found in California Test Method # 356, outlined in detail in *Reference (1)*.

The Benkelman Beam was one of the deflection measuring instruments in common use prior to the introduction of vibratory, and later impulse-type, loading devices. Since these latter devices were capable of measuring the whole deflection "basin", through the use of multiple geophones or sensors, it stands to reason that more "mechanistic" approaches could be used in lieu of the traditional empirical, "center deflection"-based approaches employed earlier.

Many of these new approaches consider the whole deflection basin in an attempt to treat pavements in much the same way as other civil engineering structures are, ie, through the calculation of moduli (or stiffnesses) and critical stresses and strains under the expected traffic loadings.

Of course, the mechanistic component of the new procedures still needs to be supplemented by an empirical component, ie, the relationship(s) between critical stresses and strains and actual, *in situ* pavement performance. Examples of the use of these mechanistic approaches may be found in *References (2), (3) and (4)*.

The question still remains, however, whether the calculated stresses and strains using mechanistic approaches correspond to what actually occurs in the field under traffic loads. If they do, then the mechanistic approaches would appear to be sound. If not, both the mechanistic and empirical components of the new approaches would appear to be in question, although offsetting errors could very well result in more or less "correct" results in terms of expected pavement performance and resulting rehabilitation design.

The question also remains as to how various materials and pavement designs perform under actual traffic loadings, and whether the same general, mechanistic relationships may be used in evaluating a range of pavement types subjected to essentially the same traffic loads.

EXPERIMENTAL DESIGN

Based on the needs arising from the new, mechanistic approaches to pavement evaluation, expected performance and rehabilitation design (as well as new pavement design), the Federal Highway Administration and the North Carolina Department of Transportation have now initiated a full-scale project to investigate the response and performance of a variety of typical pavement types used in the State of North Carolina and elsewhere. The research project is being conducted under the leadership of Dr Paul Khosla, Professor of Civil Engineering at North Carolina State University.

In the experimental design of the project, it was deemed important to

construct as wide a variety of typical pavement sections as possible (though limited to asphalt-surfaced pavements). In addition, each design section was "doubled up" in order to obtain a statistical check on the results along a different stretch of the same highway, in the same direction of traffic.

As a result, twelve pavement section types were constructed, two of each type in two directions of traffic (having different expected traffic loads), for a total of forty-eight sections.

Typical Sections

Typical pavement sections and a table of the actual design thicknesses, etc, are shown in *Figure 1*. As can be seen, all sections have an asphalt concrete (AC) surface course of at least 50 mm (2 in). In most sections, either a layer of asphalt binder and/or asphalt-bound base material underlies the AC surface course. In others, a cement treated base course (CTBC) or aggregate base course (ABC) was placed directly under the 50 mm surface course with no additional AC. Some sections were constructed with at least two asphalt-bound layers in addition to either ABC or CTBC. The subgrade was either compacted natural material (a sandy clay), or lime treated.

Each test section is 300 m (1,000 ft) or more in length. The total length of the experimental project is some 12 km (7-1/2 miles).

Instrumentation

It was decided that, near the center of each of the twenty-four northbound test sections, a site would be prepared during construction allowing for the installation of the following *in situ* instrumentation:

Two subgrade pressure transducers
Two subgrade moisture cells
Two subgrade thermocouples
One base course moisture cell (ABC only)
One base course thermocouple (ABC only)
Three asphalt strain gauges
Three asphalt thermocouples

No instrumentation was planned for the southbound roadway, although the performance of these sections will also be monitored.

TYPICAL SECTION USAGE CHART FOR TYP SEC. NO. 11, 12, 13, & 14 STA 79+71.63 TO STA 542+50 -L-									
STATION TO STATION	TYPICAL SECTION	1-1	H	MB	ABC	CTBC	SUBGRADE STAB	TOTAL DEPTH	TEST NO.
79+71.63 To 99+50	11	2' (C)	3' (C)		8' (C)		Yes	13	-
99+50 To 110+50	11	2' (C)	14' (C)		12' (C)		No	15 1/2	1
110+50 To 121+50	12	2' (C)			12' (C)		Yes	14	2
121+50 To 143+50	11	2' (C)	3' (C)		8' (C)		No	13	3
143+50 To 154+50	11	2' (C)	14' (C)			7 1/2' (C)	No	11	4
154+50 To 165+50	11	2' (C)	14' (C)		8' (C)		Yes	11 1/2	5
165+50 To 176+50	11	2' (C)	3' (C)			5 1/2' (C)	No	10 1/2	6
176+50 To 187+50	13	2' (C)	14' (C)	5 1/2' (C)			No	9	7
187+50 To 201+50	12	2' (C)				7 1/2' (C)	Yes	9 1/2	8
201+50 To 212+50	13	2' (C)	3' (C)	4' (C)			No	9	9
212+50 To 234+50	11	2' (C)	14' (C)			5 1/2' (C)	Yes	9	10
234+50 To 245+50	14	2' (C)		5 1/2' (C)			Yes	7 1/2	11
245+50 To 273+50	13	2' (C)	14' (C)	4' (C)			Yes	7 1/2	12, 13
273+50 To 284+50	14	2' (C)		5 1/2' (C)			Yes	7 1/2	14
284+50 To 300+50	11	2' (C)	14' (C)			5 1/2' (C)	Yes	9	15
300+50 To 318+50	11	2' (C)	3' (C)		8' (C)		No	13	16
318+50 To 330+50	11	2' (C)	14' (C)		8' (C)		Yes	11 1/2	17
330+50 To 379+50	11	2' (C)	14' (C)			7 1/2' (C)	No	11	18
379+50 To 401+50	12	2' (C)				7 1/2' (C)	Yes	9 1/2	19
401+50 To 412+50	13	2' (C)	14' (C)	5 1/2' (C)			No	9	20
412+50 To 441+00	11	2' (C)	3' (C)			5 1/2' (C)	No	10 1/2	21
441+00 To 451+00	13	2' (C)	3' (C)	4' (C)			No	9	22
451+00 To 480+50	11	2' (C)	14' (C)		12' (C)		No	15 1/2	23
480+50 To 491+50	12	2' (C)			12' (C)		Yes	14	24
491+50 To 542+50	11	2' (C)	3' (C)		8' (C)		Yes	13	-

PAVEMENT SCHEDULE

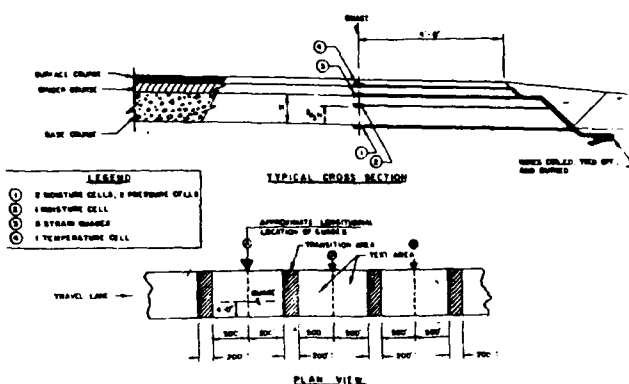
ITEM NO.	DESCRIPTION
(C1)	PROP. APPROX. 1" BITUMINOUS CONCRETE SURFACE COURSE, TYPE 1-1, AT AN AVERAGE RATE OF 110 LBS. PER SQ. YD.
(C2)	PROP. APPROX. 1 1/2" BITUMINOUS CONCRETE SURFACE COURSE, TYPE 1-1, AT AN AVERAGE RATE OF 165 LBS. PER SQ. YD.
(C3)	PROP. APPROX. 2" BITUMINOUS CONCRETE SURFACE COURSE, TYPE 1-1, AT AN AVERAGE RATE OF 110 LBS. PER SQ. YD. IN EACH OF TWO LAYERS.
(D1)	PROP. APPROX. 1 1/2" BITUMINOUS CONCRETE BINDER COURSE, TYPE H, AT AN AVERAGE RATE OF 165 LBS. PER SQ. YD.
(D2)	PROP. APPROX. 3" BITUMINOUS CONCRETE BINDER COURSE, TYPE H, AT AN AVERAGE RATE OF 330 LBS. PER SQ. YD.
(E1)	PROP. APPROX. 4" BITUMINOUS CONCRETE BASE COURSE, TYPE MB, AT AN AVERAGE RATE OF 440 LBS. PER SQ. YD.
(E2)	PROP. APPROX. 5 1/2" BITUMINOUS CONCRETE BASE COURSE TYPE MB, AT AN AVERAGE RATE OF 605 LBS. PER SQ. YD.
(J1)	PROP. 8" AGGREGATE BASE COURSE
(J2)	PROP. 12" AGGREGATE BASE COURSE
(K1)	PROP. 5 1/2" CEMENT TREATED BASE COURSE
(K2)	PROP. 7 1/2" CEMENT TREATED BASE COURSE
(L1)	SUBGRADE TO BE STABILIZED WITH EITHER LIME (18" AT 18 LBS. PER SQ. YD. OR CEMENT (7" AT 48 LBS. PER SQ. YD.) AT LOCATIONS AS DIRECTED BY THE ENGINEER.
(L2)	SUBGRADE TO BE STABILIZED WITH 200 TO 400 LBS PER SQ. YD. OF STABILIZER AGGREGATE MIXED WITH THE TOP 3' OF SUBGRADE SOIL AT LOCATIONS AS DIRECTED BY THE ENGINEER.
(T)	EARTH MATERIAL
(U)	EXISTING PAVEMENT

NOTE. PAVEMENT EDGE SLOPES ARE 1 : 1 UNLESS SHOWN OTHERWISE

NOTE: 1 inch = 25.4 mm ; 1 lb = 0.454 kg ; 1 yd² = 0.836 m²

Figure 1. TYPICAL PAVEMENT SECTIONS AND EXPERIMENTAL DESIGN OF TWENTY-FOUR TEST SECTIONS, NORTH CAROLINA TEST ROAD (SR # 421)

A typical schematic of the placement of the instrumentation is shown in **Figure 2**.



NOTE: 1' = 0.305 m; 1" = 25.4 mm

Figure 2. TYPICAL PLACEMENT OF IN SITU PAVEMENT INSTRUMENTATION

Please note, however, that the placement of the so-called "subgrade" gauges was always made in untreated material. In other words, in cases where the upper 150 - 200 mm (6 - 8 in) of subgrade was lime stabilized, the subgrade instrumentation was placed about 50 mm (2 in) below the treated upper layer of subgrade. If the subgrade was unstabilized, the instrumentation was placed about 50 mm below the top of the subgrade.

Similarly, in cases where more than one layer of asphalt-bound material was placed, whether asphalt surface, binder or base, the asphalt strain gauges were placed at the bottom of the lowest-lying layer of asphalt-bound material.

In selected sections, multi-depth deflectometers (MDDs) will also be installed after completion of the construction (expected completion by the summer of 1989).

SPECIFICATIONS AND INSTALLATION

Except for the MDDs, which will be installed sometime during the summer of 1989, all instrumentation had been installed in all twenty-four test sections prior to March 1989.

Both the soil pressure transducers and the asphalt strain gauges were furnished by Dynatest Consulting, Inc.

These instruments were manufactured by a Dynatest subcontractor in Denmark, FTC ApS. Their design is based on over 20 years of research at the Technical University of Denmark in gauge design, installation and direct experience with a variety of commercial types and new, custom-built gauge designs. The registration equipment for the Dynatest transducers was also furnished by FTC ApS.

The moisture cells were manufactured by Watermark, Type "200-X". These cells measure, in effect, the soil suction from which, coupled with the temperature of the soil, the moisture content can be calculated from a calibration curve. The resistance display unit for the moisture cells is also manufactured by Watermark.

The thermocouple wire was the standard Type "T", cut to length according to the needs of the installation site. The temperature display unit is a "JKT Digi-Sense" type.

All installation was performed by Dynatest personnel, with assistant personnel furnished by North Carolina State University.

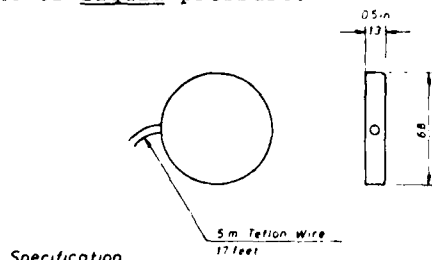
Gauge Specifications

The success of the project will primarily revolve around the efficacy of the soil pressure cells [for measuring vertical subgrade stress] and the asphalt strain gauges [for measuring horizontal strain at the bottom of the asphalt-bound layer(s)]. The correct measurement of these parameters under moving wheel loads has, in the past, often proved to be rather elusive. One example, where asphalt strains were measured by many different strain gauges which produced widely divergent results, was at the Nardo Test Track in Italy (see *Reference 5*).

The Dynatest/FTC Gauges were chosen primarily because they are believed to be very reliable, durable and accurate, even under conditions of varying temperature and modulus of the material in which the gauges are embedded.

The soil pressure cells, called the **SOPT** (**SOil Pressure Transducer**) series, are designed for use in both cohesive and granular materials. This transducer type is based on a new design which yields important advantages over the normal membrane-type pressure cells, in

that the latter type is generally non-linear with respect to the modulus of the soil medium as well as its moisture content and gradation, etc. The sensitivity and linearity problems previously encountered with soil pressure gauges have been virtually eliminated with the SOPT hydraulic pressure design, which utilizes a thin membrane over the entire cell area allowing the measurement of liquid pressure.



Specification

Type	FTC - I	FTC - II
Range	10 - 200 kPa, 15 - 30 psi	100 - 800 kPa, 15 - 120 psi
Cell-material	Pure Titanium	
Coating	Epoxy and Sand	
Temperature	-30 - 150°C	-22 ~ 300°F
Resistance	4x350Ω in full Weston Bridge	
Function	Linear for E-modulus < 500,000 kPa < 70,000 psi	
Output	Reff Calibration chart	
Voltage	up to 12V	
Fatigue-life	More than 3x10 ⁶ cycles	
Service-life	> 36 months	
Time of Delivery	~ 3 months	

Figure 3. DYNATEST/FTC SOIL PRESSURE TRANSDUCER (SOPT)

The SOPT cells are temperature compensated for use in the range of -30° to 150°C (-20° to 300°F). The SOPT model chosen for the present project was the one designed for fine grained soils exhibiting maximum longevity. It is 68 mm (2-11/16") in diameter, and should perform for at least 36 months or 3,000,000 cycles, whichever comes first (see **Figure 3**).

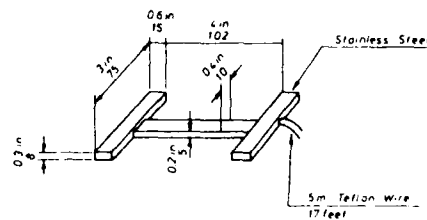
The asphalt strain gauges, called the **PAST** (**PA**vement **ST**rain **T**ransducer) series, are designed to measure horizontal strains at the bottom of either flexible (AC) or rigid (PCC) pavement layers.

A PAST unit is an "H"-type precision strain gauge, some 102 mm (4 in) in length and constructed using materials with a relatively low stiffness, while

at the same time exhibiting very high flexibility and strength. The gauges are protected against mechanical and chemical deterioration by means of a multi-layer coating, allowing them to perform in fatigue up to as many as 100,000,000 loading cycles or 36 months (whichever comes first). The temperature range of the PAST series of gauges is some -30° to 150°C (-20° to 300°F).

The average modulus of the PAST cell body is approximately 2.2 MPa (20 psi). This insures a negligible influence on the surrounding AC or PCC materials, resulting in accurate, non-material or -temperature dependent measurements under virtually all field conditions.

The PAST gauges used in this project are shown in **Figure 4**.



Specifications

Type	FTC II A (asphalt)	
Range	up to 1500 μstrain	
Cell-material	Epoxy - Fibreglass	
Coating	Epoxy - Silicone - PFT - Titanium	
Temperature	-30 ~ 150°C	-22 ~ 300°F
Resistance	120Ω ±10%, GF=2.0	
Voltage	up to 12V (full bridge)	
E-modulus	≈ 320,000 psi	≈ 2200 MPa
Sq-area	≈ 0.5 cm ²	≈ 0.078 sq inch
Fatigue-life	Theoretical up to 10 ⁶ cycles	
Service-life	Typical > 36 months	
Strain force	≈ 110 $\frac{N}{1000 \mu m/m}$	≈ $\frac{24 lbs}{1000 \mu strain}$
Time of Delivery	~ 3 months	

Figure 4. DYNATEST/FTC PAVEMENT STRAIN TRANSDUCER (PAST)

Installation Procedures

The gauges used in the project, except for the MDDs which will be installed after the pavement construction is completed, are normally installed as construction progresses. Needless to say, this did not occur flawlessly for all twenty-four instrumented test sections, given the complexity of the construction process

and some minor (generally short-lived) communication difficulties between the General Contractor, the State of North Carolina, North Carolina State University and Dynatest.

When the first gauges were to be installed in the subgrade (just after fine grading of the subgrade layer), the contractor believed that the University and Dynatest should be notified after placement of the base materials, not before. Thus two of the twenty-four test sections already had a full thickness of base placed by the time Dynatest and North Carolina State University personnel were notified to carry out the first gauge installations.

One of these two "lost" sections was "rescued" by digging through non-compacted base and placing the soil pressure, temperature and moisture transducers and then replacing the same volume of base materials to the same (uncompacted) density. The placement of one of the SOPT transducers is shown in **Figure 5**. The moisture cell and a thermocouple are immediately adjacent to the soil pressure cell shown in the picture.

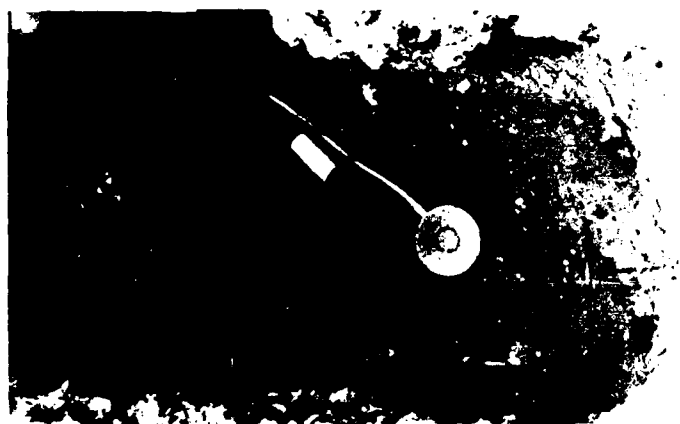


**Figure 5. INSTALLATION
OF SOPT TRANSDUCER IN SUBGRADE**

The remaining SOPT gauges were installed as planned, i.e. before the subgrade was covered and compacted by subsequent layers. Thus all but one of the twenty-four sections now are equipped with two (and in one case, three) installed SOPT units, along with the requisite moisture and temperature sensors.

When it came to the construction of the asphalt layers, essentially the same

difficulties were encountered. The contractor thought that the FAST transducers were to be installed above the asphalt-bound base materials, instead of below. Thus three of the twenty-four test sections are now "lost" as far as measuring asphalt strain goes.



**Figure 6. INSTALLATION
OF PAST TRANSDUCER BELOW ASPHALT**

Everything went smoothly and as planned for the remaining twenty-one sections, where three -- and in several cases four -- PAST gauges were installed at the bottom of the lowest asphalt-bound layer. The placement of one of the PAST transducers is shown in **Figure 6**. The fresh asphalt mix is subsequently placed above the gauges, and compacted along with the rest of the asphalt pavement using normal construction equipment.

Installation Success Rate

As far as is known at the present time, all gauges installed are performing properly. The final "verdict", though, will not be known until the asphalt surface course is placed and field tests are conducted after traffic begins to use the highway.

Consequently, no measurements of actual stresses or strains have been made as of yet. The thermocouples and moisture cells all appeared to read properly a few weeks after installation, and all SOPT and PAST gauges were "zeroed", electronically, as they should be, indicating that they are still functioning as designed.

Planned Field Tests

Two types of field tests are planned after construction has been completed:

1. **FWD Tests**
2. **Moving Wheel Load Tests**

In addition to these two types of tests, the traffic level (passes and weights) will be monitored along the highway, using state-of-the-art technology of weigh-in-motion devices. Further, the longitudinal profile of all sections will be monitored, along with rut depth measurements and periodic surface condition surveys.

Moving wheel load tests will be conducted at various load levels and vehicle velocities. For each test section, the current temperatures and moisture conditions will be measured and recorded, and the stresses and strains measured by the SOPT and PAST transducers will be recorded for each passing (test) wheel load. These tests will be repeated for the various seasonal conditions encountered locally, in central North Carolina.

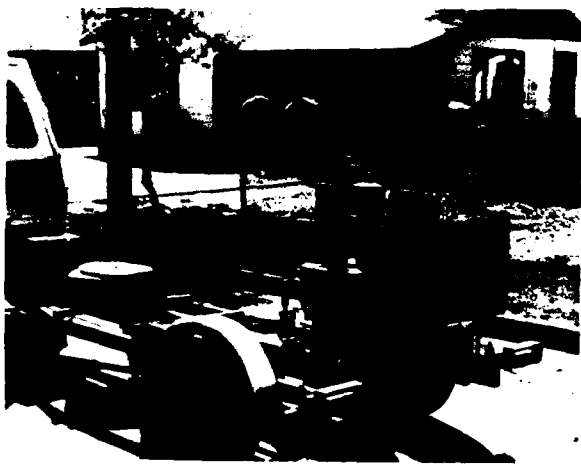


Figure 7. THE NORTH CAROLINA DOT'S DYNATEST 8000 FWD TEST SYSTEM

FWD tests will be conducted at the same time, at several locations at or near the site of the gauge installation. To successfully carry out FWD tests and correctly interpret the FWD load-deflection data, highly accurate and repeatable deflections must be measured along the whole deflection basin. The North Carolina DOT's Dynatest Model 8000 FWD will be used to achieve these aims.

In another paper published in these Proceedings, Richter and Irwin (see **Reference 6**) have indicated that SHRP's Dynatest 8000 FWDs do indeed meet the stringent criteria of $\pm 2\%$ systematic error and ± 2 microns (± 0.04 mils) random error (repeatability), or better. It is believed that the North Carolina DOT's FWD is ideally suited to monitor the structural condition, moduli, etc., of the twenty-four test sections under investigation in this study. The North Carolina FWD is shown in **Figure 7**.

It is not anticipated that stresses and strains will be measured directly under the influence of the FWD, since the placement of the FWD test load is so critical and the transducers themselves are not placed along one vertical column (actually, they are all separated by about two feet, longitudinally). Thus a moving wheel load will invariably pass over the gauges and the peak values will be monitored for all gauges, simultaneously. The stationary FWD cannot perform the same concurrent measurements.

The Dynatest 8000 FWD, on the other hand, will be used to back-calculate the mechanistic properties of the pavement section (ie, moduli values), and appropriate stresses and strains will be calculated using these moduli values in conjunction with the traffic-imposed load levels and wheel configurations. Then, these calculated values will be compared with the measured values, under traffic loads, to see whether they correspond to one another or not.

RESEARCH OBJECTIVES

The main objective of this research project is to develop mechanistic, or analytical procedures and relationships between stress and/or strain levels imposed by traffic and pavement performance in terms of roughness, rutting and surface distress, for a variety of typical North Carolina flexible pavements. Further, the use of the FWD in back-calculating representative moduli values to use in the mechanistic procedures will be investigated.

It is recognized at this point, however, that many pitfalls exist which will need to be closely scrutinized as data is gathered and conclusions made. One of the major problems with back-calculation is the fact that pavement

layers, especially unbound layers, are often non-linear, non-homogeneous, and anisotropic. The use of linear elastic theory in back-calculation, therefore, may result in significant errors in the resulting moduli.

Furthermore, it is by no means certain that elastic layered theory, even if allowances are made for non-homogeneity, anisotropy and non-linearity, is valid for all types of pavements. Elastic theory assumes that pavement layers behave "elastically", in all directions, whether the materials are in tension or compression. For bound materials which are uncracked, this may indeed hold true, but what about granular bases or sandy soils? If elastic theory does not hold true, what kind of mechanistic approach can be proposed instead? These are questions which this research project also hopes to answer, one way or the other.

Field measurements should begin by the Summer of 1989. Subsequently, more published reports on the outcome of the study will be forthcoming, as data is gathered and conclusions drawn.

ACKNOWLEDGMENTS

The authors wish to acknowledge the North Carolina Department of Transportation and the Federal Highway Administration for the HPR funds provided for this full-scale project. North Carolina State University is also acknowledged for their leading roll in conducting the research and providing the Principal Investigator (Dr Paul Khosla) for the project.

Last but not least, the credit for success in the crucial installation phase of the instrumentation goes to the field crew provided by Dynatest (Mr Wayne Wynn and Mr Ismael Collado) and especially to the dedicated and untiring North Carolina State University graduate student, Mr James Trogden, who provided countless hours of day and night "overtime" assistance.

REFERENCES

- (1) CalTrans; "Asphalt Concrete Overlay Design Manual"; CalTrans, Sacramento, California, 1979.
- (2) Ullidtz, P and R N Stubstad; "Analytical - Empirical Pavement Evaluation Using the Falling Weight Deflectometer"; Transportation Research Board, TRP # 1022, Washington D C, 1985.
- (3) Yapp, M, R G Hicks and B Connor; "Development of an Improved Overlay Design Procedure for the State of Alaska"; Vol. II: Final Report, State of Alaska, Department of Transportation and Public Facilities, Fairbanks, Alaska, 1987.
- (4) Finn, R N and C L Monismith; "Asphalt Overlay Design Procedures"; NCHRP Synthesis of Highway Practice # 116, Transportation Research Board, Washington D C, 1984.
- (5) OECD Road Transport Research; "Strain Measurements in Bituminous Layers"; OECD Report by the OECD/12 Scientific Expert Group, Berne, Switzerland, 1985.
- (6) Richter, S A and L H Irwin; "SHRP Prototype Procedures for Calibrating Falling Weight Deflectometers"; Proceedings, State of the Art of Pavement Response Monitoring Systems for Roads and Airfields, CRREL, Hanover, New Hampshire, 1989.

END

FILMED

1-90

DTIC